National Research
Council Canada

Conseil national
de recherches Canada

NRC · CNRC

Canadian Journal of Fisheries and Aquatic Sciences

Journal canadien des sciences halieutiques et aquatiques

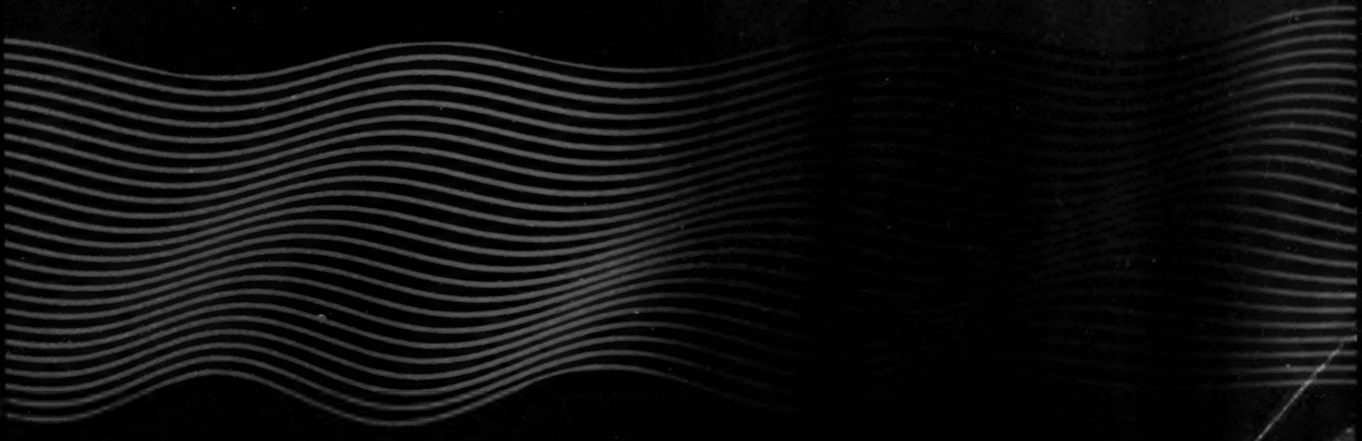

http://cjfas.nrc.ca

http://jcsha.cnrc.ca

ISSN 0706-652X / CJFSDX 59(6) 925–1084 (2002)

The *Canadian Journal of Fisheries and Aquatic Sciences*, previously published as *Contributions to Canadian Biology* 1901–1925, *Contributions to Canadian Biology and Fisheries* 1926–1934, *Journal of the Biological Board of Canada* 1934–1937, and *Journal of the Fisheries Research Board of Canada* 1938–1979, is issued monthly to form annual volumes of 12 numbers plus supplements.

Editorial policy: The Journal publishes original research articles, perspectives (syntheses, critiques, re-evaluations), discussions (comment and reply), and rapid communications. Manuscripts may concern cells, organisms, populations, communities, ecosystems, or processes that affect aquatic systems. They may cover a range of disciplines including biology and ecology of marine and freshwater organisms, limnology, oceanography, physiology, toxicology, genetics, economics, disease, and management. Preference will be given to manuscripts that emphasize understanding of observed phenomena and interpretation of experimental results. The Journal encourages papers that lead from clearly stated purpose or rationale and from testable hypotheses, concepts, or questions to identifiable conclusions or syntheses. Such papers may amplify, modify, question, or redirect accumulated knowledge embodied in contemporary perceptions of a particular state of aquatic sciences. The Journal discourages papers that are essentially descriptive, except in emerging disciplines; have only site-specific or local applications (a certain year, place, taxon, chemical compound, etc.); only confirm previously established principles; or apply standard techniques without breaking new methodological ground.

Manuscripts for publication should be submitted to the Editors, *Canadian Journal of Fisheries and Aquatic Sciences*, Department of Zoology, University of Guelph, Guelph, ON N1G 2W1, Canada (519-824-4120 ext. 2646; fax: 519-767-9798; e-mail: cjfas@uoguelph.ca).

Submissions in either English or French are acceptable. The information must be original, that is, not copyrighted, published, or submitted elsewhere except in abstract form or unless by written consent of the Editor. NRC accepts no responsibility for statements or opinions expressed by a contributor. Acceptance of an advertisement, announcement, or other material does not imply endorsement by either the Journal's Editors or NRC. The use of proprietary names does not imply endorsement of the product or company.

Correspondence concerning accepted manuscripts and corrected proofs should be sent to NRC Research Press, National Research Council of Canada, Ottawa, ON K1A 0R6, Canada (fax: 613-952-7656; e-mail: research.press@nrc.ca).

Instructions to Authors are published once a year in the first issue of each volume. Copies are available from NRC Research Press or at http://cjfas.nrc.ca. The **Publication Policy** of NRC Research Press is available at http://cjfas.nrc.ca.

The National Research Council of Canada accepts no responsibility for statements or opinions expressed by a contributor. Acceptance of an advertisement, announcement, or other material does not imply endorsement by either the Journal's Editors or NRC.

Microfilm: Issues from 1934 through the current volume can be purchased on 16- or 35-mm microfilm. Photocopies of individual articles or issues can be purchased from University Microfilms International, 330 North Zeeb Road, Ann Arbor, MI 48106, U.S.A.

U.S. periodical postage paid at Champlain, N.Y., and at additional mailing offices. Attention U.S. POSTMASTER: Send address changes to **Canadian Journal of Fisheries and Aquatic Sciences**, c/o USACAN Media Distribution Center, P.O. Box 2888, Plattsburg, NY 12901, U.S.A.

Publié sans interruption depuis 1901, le *Journal canadien des sciences halieutiques et aquatiques* a paru sous plusieurs titres : *Contributions to Canadian Biology* 1901–1925, *Contributions to Canadian Biology and Fisheries* 1926–1934, *Journal of the Biological Board of Canada* 1934–1937, et *Journal of the Fisheries Research Board of Canada* 1938–1979. Le Journal paraît tous les mois, formant ainsi un volume de 12 numéros, et offre en plus jusqu'à deux suppléments par année.

Politique éditoriale : On publie, dans le Journal, des articles rendant compte de recherche originale, des perspectives (synthèses, critiques et réévaluations), des discussions (commentaires et réponses) et des communications rapides. Les documents peuvent porter sur les cellules, organismes, populations, communautés, écosystèmes ou processus qui affectent les systèmes aquatiques. Ils peuvent relever de divers domaines y compris la biologie et l'écologie des organismes marins et d'eau douce, la limnologie, l'océanographie, la physiologie, la toxicologie, la génétique, l'économie, la pathologie et la gestion. On accorde la préséance aux articles qui contribuent à la compréhension de phénomènes observés et à l'interprétation de résultats expérimentaux. On invite les auteurs à soumettre des articles ayant des objectifs précis ou relevant d'hypothèses, de concepts ou de questions vérifiables et se terminant par de solides conclusions ou d'utiles synthèses. Ces articles enrichissent, changent, mettent en question ou réorientent les connaissances acquises sur divers aspects des sciences aquatiques. On décourage toutefois la soumission d'articles simplement descriptifs (à moins qu'il ne s'agisse de nouvelles disciplines), d'application très limitée (applicables à une seule année, une seule région ou un seul taxon, portant sur un unique composé chimique, etc.); d'articles qui ne font que reprendre les principes énoncés dans des articles précédents; et d'articles rendant compte de l'application de normes sans gain de méthodologie.

Les auteurs voudront adresser leurs **manuscrits** aux directeurs scientifiques, *Journal canadien des sciences halieutiques et aquatiques*, Department of Zoology, University of Guelph, Guelph, ON N1G 2W1, Canada (519-824-4120 poste 2646; télécopieur : 519-767-9798; courriel : cjfas@uoguelph.ca).

Les contributions peuvent être en anglais ou en français. Elles doivent être originales, c.-à.-d. qu'elles ne doivent pas avoir fait l'objet d'un copyright, avoir été publiées ou soumises ailleurs, sauf sous forme abrégée ou avec le consentement du rédacteur. Le CNRC ne se tient en aucune façon responsable des opinions exprimées par un collaborateur ou des déclarations qui pourrait faire ce dernier. La publication d'annonces publicitaires, d'avis et autres n'implique pas l'endossement de leur contenu par les directeurs du Journal ou du CNRC. L'utilisation des noms de marques de commerce ne signifie aucunement une sanction du produit en question ou de la compagnie qui le fabrique.

La correspondance ayant trait aux manuscrits acceptés et les **épreuves corrigés** doivent être envoyées aux Presses scientifiques du CNRC, Conseil national de recherches du Canada, Ottawa, ON K1A 0R6, Canada (télécopieur : 613-952-7656; courriel : presses.scientifiques@cnrc.ca).

Les Recommandations aux auteurs sont publiées une fois par année dans le premier numéro de chaque volume. Des copies sont disponibles auprès du Bureau de la rédaction aux Presses scientifiques du CNRC ou au http://jcsha.cnrc.ca. **La Politique de publication** est disponible auprès des Presses scientifiques du CNRC ou au http://jcsha.cnrc.ca.

Le Conseil national de recherches du Canada ne se tient en aucune façon responsable des opinions exprimées par un collaborateur ou des déclarations que pourrait faire ce dernier. La publication d'annonces publicitaires, d'avis et autres n'implique pas l'endossement de leur contenu par les directeurs de la Revue ou du CNRC.

Microfilms : On peut acheter sur microfilms de 16 ou 35 mm tous les numéros depuis 1934. Des photocopies d'articles ou de numéros individuels sont aussi en vente auprès de University Microfilms International, 330 North Zeeb Road, Ann Arbor, MI 48106, É.-U.

This Journal is indexed or abstracted in / Cette revue est signalée ou résumée dans
ABSEARCH, Aquatic Sciences and Fisheries Abstracts, Biological Abstracts, Biological & Agricultural Index, CAB Abstracts, Chemical Abstracts, Current Contents, Elsevier BIOBASE, Environmental Abstracts, Environmental Periodicals Bibliography, GEOBASE, GeoRef, Internationale Bibliographie der Zeitschriftenliteratur, Life Sciences Collection, Meteorological and Geoastrophysical Abstracts, Oceanic Abstracts, PASCAL Database, and Science Citation Index.

Volume 59, Number 6, June 2002

Canadian Journal of Fisheries and Aquatic Sciences

Published by the National Research Council of Canada

Volume 59, numéro 6, juin 2002

Journal canadien des sciences halieutiques et aquatiques

Publié par le Conseil national de recherches du Canada

Senior Editor / Directrice scientifique principale Moira M. Ferguson

Editors / Directeurs

Jeffrey A. Hutchings, *Dalhousie University, Halifax*
Pierre Pepin, *Northwest Atlantic Fisheries Centre, DFO/MPO, St. John's, Newfoundland*
W. Gary Sprules, *University of Toronto at Mississauga*

Assistant to the Editors / adjointe aux directeurs scientifiques **Holly Foster**

Associate Editors / directeurs scientifiques associés

M.T. Arts, *Environment Canada, Burlington*
D. Boisclair, *Université de Montréal*
U. Borgmann, *Environment Canada, Burlington*
S.E. Campana, *DFO/MPO, Dartmouth*
R. Carignan, *Université de Montréal*
J.J. Dodson, *Université Laval*
G.T. Evans, *DFO/MPO, St. John's, Newfoundland*
K.T. Frank, *DFO/MPO, Dartmouth*
M.M. Hansen, *Danish Institute for Fisheries Research, Silkeborg, Denmark*
R. Hilborn, *University of Washington*
A. Hontela, *Université du Québec à Montréal*
D.F. Houlihan, *University of Aberdeen*
F.A. Huntingford, *University of Glasgow*
G.S. Jamieson, *DFO/MPO, Nanaimo*
B. Jonsson, *Norwegian Institute for Nature Research, Oslo, Norway*
P. Magnan, *Université du Québec à Trois Rivières*
C.T. Marshall, *Institute of Marine Research, Bergen, Norway*
R.B. Millar, *University of Auckland, New Zealand*
Y.T. Prairie, *Université du Québec à Montréal*
T.J. Quinn II, *University of Alaska–Fairbanks, Juneau, Alaska*
T.P. Quinn, *University of Washington*
R.D. Robarts, *Environment Canada, Saskatoon*
B. Sainte-Marie, *DFO/MPO, Mont-Joli*
D.W. Schindler, *University of Alberta*
R.E.H. Smith, *University of Waterloo*
S.J. Smith, *DFO/MPO, Dartmouth*
W.F. Vincent, *Université Laval*
R.D. Vinebrooke, *University of Regina*
C.J. Walters, *University of British Columbia*
R.D. Ward, *CSIRO Marine Research, Australia*
B. de Young, *Memorial University of Newfoundland*

NRC Research Press / Presses scientifiques du CNRC

Editor-in-chief / directeur général **Bruce P. Dancik**
Assistant Editor-in-chief / directeur général adjoint **Iain E.P. Taylor**

Journals Program / Programme des revues

(Fax / télécopieur : 613-952-7656; e-mail / courriel : research.press@nrc.ca; URL: http://researchpress.nrc.ca)

Director / directrice **Aldyth Holmes**
Business Manager / gestionnaire des affaires **Paul McClymont**
Managing Editor / rédactrice administrative **Cecily M. Pearson (613-993-9099)**
Publication Officers / agentes de publication **Jennifer McColl and Lee Murphy**
Advertising / annonces publicitaires **Judy Gorman (613-993-0151)**
Reprints / tirés à part **Roxanne Landriault (613-990-2254)**
Subscriptions / abonnements **Helen Goulet (613-993-9084)**

© National Research Council of Canada 2002. World rights reserved. No part of this publication may be reproduced, stored, or transmitted in any form or by any means, without the written permission of the publisher, except as stated below.

The National Research Council of Canada grants **permission*** to individuals to make single copies of articles for personal use. Any person may reproduce short excerpts from articles in the journal for any purpose that respects the moral rights of authors, provided that the source is fully acknowledged. As a courtesy, the consent of authors of such material should be obtained directly from the author.

Authorization to reproduce items for other than personal use, as stated above, is granted by the National Research Council of Canada provided that the copyright fee of $7.00 per copy is paid directly to CANCOPY, One Yonge Street, Suite 1900, Toronto, ON M5E 1E5, Canada.

*The above permission does not extend to other kinds of copying, such as copying for general distribution, for advertising, or promotional purposes, for creating new collective works, or for resale. For such copying, arrangements must be made with the publisher, National Research Council of Canada, Ottawa, ON K1A 0R6, Canada.

© Conseil national de recherches du Canada 2002. Tous droits réservés. Il est interdit de reproduire, de sauvegarder ou de transmettre quelque partie de la présente publication dans quelque format ou de quelque façon sans le consentement écrit de l'éditeur, à l'exception des conditions suivantes.

Le Conseil national de recherches du Canada accorde aux particuliers le droit de faire des copies individuelles pour leur usage personnel. Toute personne peut reproduire de courts extraits des articles de la Revue pour autant que les droits moraux de l'auteur soient respectés et que la mention de provenance soit clairement indiquée. Il est de convenance de demander le consentement de l'auteur avant de faire mention de son travail.

On obtiendra l'autorisation de reproduire des articles à d'autres fins que l'usage personnel (tel qu'on l'a décrit ci-dessus) auprès du Conseil national de recherches du Canada pour autant que des redevances de droits d'auteurs de 7,00 $/copie soient versées au CANCOPY, 1, rue Yonge, bureau 1900, Toronto, ON M5E 1E5, Canada.

*La permission ci-dessus ne s'applique pas à la reproduction à grande échelle, telle que la reproduction aux fins de distribution générale, publicitaire ou promotionnelle, de compilation de nouveaux ouvrages collectifs ou de revente. Dans de tels cas, il faudra ratifier une entente particulière avec l'éditeur, le Conseil national de recherches du Canada, Ottawa, ON K1A 0R6, Canada.

Subscription information

The *Canadian Journal of Fisheries and Aquatic Sciences* (ISSN 0706-652X) is published monthly by the National Research Council of Canada. 2002 annual subscription rates (second class postage) for Canada are $732CAN institutional and $227CAN personal, for US & foreign $732US institutional and $227US personal. For air mail add $175US to foreign rate. Canadian customers please include 7% GST (business no. 12149 1807 RT 0275). Subscriptions are entered for the calendar year. Remittances should be made payable to the Receiver General for Canada credit NRC. Price for regular single issues: institutional, $95.00; personal, $30.00. Supplements will be priced separately. Special rates apply to members of Canadian scientific and engineering societies if they subscribe through their respective societies.

There are no refunds on cancelled subscriptions once delivery has begun. Claims for missing issues should be made within four months (N. America) or six months (outside N. America) following the date of publication. The publisher expects to supply missing issues only when losses have occurred in transit and when the reserve stock will permit. For change of address and subscription enquiries: Subscription Office, NRC Research Press, National Research Council of Canada, Ottawa, ON K1A 0R6, Canada; tel.: 613-993-9084; fax: 613-952-7656; e-mail: research.press@nrc.ca.

Microform backfiles are available from UMI, P.O. Box 1346, Ann Arbor, MI 48106-1346, U.S.A., and Micromedia Ltd., 20 Victoria St., Toronto, ON M5C 2N8, Canada.

All issues of the *Canadian Journal of Fisheries and Aquatic Sciences* since 1996 are available on the Web. Pricing information can be found at http://cjfas.nrc.ca.

Renseignements sur l'abonnement

Journal canadien des sciences halieutiques et aquatiques (ISSN 0706-652X) est une publication mensuelle du Conseil national de recherches du Canada. Le prix de l'abonnement annuel au Canada (courrier de deuxième classe) est de 732 $CAN pour les organismes et de 227 $CAN pour les particuliers. À l'étranger (y compris les É.-U.), le prix de l'abonnement est de 732 $US pour les organismes et de 227 $US pour les particuliers. L'expédition par avion exige des frais de 175 $US en sus du prix d'abonnement à l'étranger. Les clients du Canada doivent ajouter la TPS de 7% (numéro d'entreprise 12149 1807 RT 0275). Les abonnements sont pour l'année civile. Tout paiement doit être adressé au Receveur général du Canada, crédit du CNRC. Le prix par numéro est de 95 $ pour les organismes et de 30 $ pour les particuliers. Le prix des hors-série varie. Les membres des sociétés canadiennes de sciences et de génie bénéficient de taux préférentiels en s'abonnant via leurs sociétés respectives.

Aucun remboursement ne sera accordé ni aucune annulation acceptée une fois que les livraisons auront commencé. Les réclamations de numéros manquants devront être soumises dans les quatre mois (Amérique du Nord) ou dans les six mois (à l'extérieur de l'Amérique du Nord) suivant la date de publication. L'éditeur ne fournira de numéros manquants que si le document a été perdu pendant l'expédition et que si le stock le permet. Adressez tout changement d'adresse ou toute question quant à l'abonnement au : Bureau des abonnements, Presses scientifiques du CNRC, Conseil national de recherches Canada, Ottawa, ON K1A 0R6, Canada; téléphone : 613-993-9084; télécopieur : 613-952-7656; courriel : presses.scientifiques@nrc.ca.

On peut obtenir les fichiers rétrospectifs sur **microforme** auprès de UMI, P.O. Box 1346, Ann Arbor, MI 48106-1346, É.-U., et auprès de Micromedia Ltée, 20 rue Victoria, Toronto, ON M5C 2N8, Canada.

À partir de 1996, tous les numéros de *Journal canadien des sciences halieutiques et aquatiques* sont accessibles sur le Web. On trouvera des renseignements sur les tarifs à http://jcsha.cnrc.ca.

EDITORIAL / ÉDITORIAL

It has now been five years since the Editorial Office of the *Canadian Journal of Fisheries and Aquatic Sciences* moved to the University of Guelph. The Journal continues to prosper, and this can be attributed to the fine staff at the University and NRC Research Press, as well as the advice and hard work of our Associate Editors and referees. The Journal is appearing promptly and continues to maintain its excellent international reputation. We thank our authors for sending us manuscripts that are based on excellent quality research of broad significance.

As the Journal enters a second five-year mandate at the University of Guelph, Moira Ferguson will assume the role of Senior Editor. John Roff has elected to "retire" from the Journal so that he may pursue other opportunities in his research. We are grateful for his many years of service with CJFAS—first as a member of the Editorial Board, then as co-Editor for the last five years—and we wish him the very best in his future endeavours.

We have made some alterations to the editorial hierarchy that, we believe, will improve service to our authors and result in an even better Journal for our readers. The fundamental character and scope of the Journal will remain unchanged. Most of the changes will not be apparent to our authors and referees, and will reflect merely changes in the mechanics of manuscript movement to make sure the best-qualified individual oversees each submission. We will make every effort to minimize any impact these changes might have on the smooth and efficient operation of the Editorial Office.

Three very talented individuals will be joining the CJFAS team as Editors on 1 June 2002. Dr. Jeffrey Hutchings, Department of Biology, Dalhousie University, is an evolutionary ecologist with expertise in both freshwater and marine fishes; Dr. Pierre Pepin from the Department of Fisheries and Oceans in St. John's, Newfoundland, works on the ecology of larval marine fishes and biological oceanography, and also has expertise in quantitative fisheries science; Dr. W. Gary Sprules is from the Department of Zoology, University of Toronto at Mississauga, and has expertise in the ecology of invertebrates and freshwater food webs. All three individuals have served CJFAS as Associate Editors and are well acquainted with the editorial scope and policy of the Journal. Their efforts will no doubt provide new perspectives and insights that will enhance the impact and quality of the science published in CJFAS.

As always, we welcome your comments and look forward to continuing to publish the highest quality research in fisheries and aquatic sciences.

Dr. Moira M. Ferguson
Senior Editor, CJFAS

Dr. Bruce Dancik
Editor-in-Chief, NRC Research Press

Il y a maintenant cinq ans que le Bureau de la rédaction du Journal canadien de sciences halieutiques et aquatiques est établi à l'Université de Guelph. Le Journal continue de connaître un grand succès attribuable à la compétence de son personnel, tant à l'Université qu'aux Presses scientifiques du CNRC, de même qu'au dévouement et aux conseils de ses Directeurs scientifiques associés et de ses réviseurs. Le Journal paraît toujours à temps et maintient une excellente réputation internationale. Les auteurs soumettent des manuscrits basés sur de la recherche de toute première qualité et de grand intérêt scientifique.

Maintenant que le Journal inaugure un second mandat de cinq ans à l'Université de Guelph, Moira Ferguson assumera le rôle de Directrice scientifique principale. John Roff a choisi de prendre ses distances du Journal pour consacrer son temps à de nouvelles avenues de recherche. Nous lui sommes redevables des années de dévouement qu'il a consacrées au Journal—d'abord comme membre du Comité de rédaction, puis comme codirecteur scientifique au cours des cinq dernières années—et nous lui souhaitons franc succès dans ses projets.

Nous avons fait quelques changements dans la structure de la direction qui, croyons-nous, amélioreront nos services aux auteurs et produiront un journal de qualité encore supérieure à l'intention de nos lecteurs. Le caractère fondamental et les perspectives du Journal resteront les mêmes. La plupart des changements ne seront pas apparents à nos auteurs ni à nos réviseurs et se refléteront surtout dans le traitement des manuscrits de manière à ce que chaque article soumis soit analysé par la personne la plus compétente. Nous ferons tout notre possible pour que ces changements n'affectent ni la bonne marche, ni l'efficacité du Bureau de la rédaction.

Trois personnes de grand talent se joindront à notre équipe comme Directeurs scientifique le 1er juin 2002. Le professeur Jeffrey Hutchings du département de biologie de l'Université Dalhousie est spécialisé en écologie évolutive des poissons marins et dulcicoles. Monsieur Pierre Pepin du Ministère des pêches et océans à St. John's, Terre-Neuve, étudie l'écologie des larves de poissons marins et l'océanographie biologique et est expert en sciences halieutiques quantitatives. Le professeur W. Gary Sprules du département de zoologie de l'Université de Toronto à Mississauga se spécialise dans l'écologie des invertébrés et les réseaux alimentaires dulcicoles. Les trois ont œuvré comme Directeurs scientifiques associés du Journal et connaissent bien sa politique éditoriale et son optique. Ils apporteront certainement des perspectives et points de vue nouveaux qui amélioreront l'impact et la qualité des contributions scientifiques publiées dans le Journal.

Comme par le passé, nous sollicitons vos commentaires et nous nous engageons à continuer de publier des travaux de la plus haute qualité dans les domaines des sciences halieutiques et aquatiques.

Moira M. Ferguson, Ph.D.
Directrice scientifique principale, JCSHA

Bruce Dancik, Ph.D.
Directeur général, Presses scientifiques du CNRC

RAPID COMMUNICATION / COMMUNICATION RAPIDE

Reconstructing the lives of fish using Sr isotopes in otoliths

Brian P. Kennedy, Andrea Klaue, Joel D. Blum, Carol L. Folt, and Keith H. Nislow

Abstract: For many species, understanding the processes underlying variation in life history strategies is limited by the difficulty of tracking individuals throughout their lives. Within the rapidly expanding field of otolith microchemistry, novel approaches are being combined with state-of-the-art analytical techniques to provide new and valuable information about the environmental history of fishes. However, no approach to date allows the reconstruction of fish movements at high temporal resolution (weeks to months) over relatively small spatial scales (1–10 km). We used micromilling techniques to extract strontium (Sr) isotopic signatures from the otoliths of four returning Atlantic salmon (*Salmo salar*) adults. Distinct Sr isotopic signatures were detectable from four life cycle stages, including prefeeding hatchery development, rearing stream growth, smolt out-migration, and ocean residence. High-resolution analyses of Sr isotope records establish that natal stream signatures are recoverable and show that both site fidelity within the freshwater stage and the timing of migration vary considerably among individuals. Results made possible with this approach provide insight into a long-standing debate on the mobility of salmon during their nonmigratory stage. The ability to resolve flexible behaviors of salmon increases our understanding of their population biology and conservation needs.

Résumé : Chez de nombreuses espèces, la difficulté de suivre les individus tout au cours de leur vie limite la compréhension des processus qui sous-tendent la variation des stratégies de leur cycle biologique. Des méthodes nouvelles dans le domaine en pleine expansion de la micro-chimie des otolithes, combinées à des techniques analytiques toutes récentes, fournissent des informations nouvelles et précieuses sur l'histoire environnementale des poissons. Cependant, aucune technique ne permet actuellement de retracer les déplacements des poissons sur une haute échelle temporelle (semaines à mois), sur une échelle spatiale relativement réduite (1–10 km). Nous avons utilisé des techniques de microfraisage pour extraire les signatures isotopiques de strontium (Sr) des otolithes de 4 saumons altantiques (*Salmo salar*) adultes de retour de la mer. Des signatures distinctes du Sr isotopique dans les otolithes se reconnaissent à quatre stades du cycle, le développement en pisciculture antérieur au début de l'alimentation, la croissance dans le cours d'eau d'élevage, la migration des saumoneaux vers la mer et le séjour en eau salée. L'analyse de haute précision des isotopes de Sr dans les otolithes révèle que la signature du cours d'eau d'origine peut être décelée et démontre que la fidélité au site durant la phase d'eau douce et le calendrier de la migration varient considérablement d'un individu à un autre. Cette méthodologie apporte des perspectives nouvelles dans le vieux débat sur la mobilité des saumons durant leur phase non migratrice. La possibilité de déterminer les comportements flexibles chez les saumons vient améliorer notre compréhension de la biologie des populations et de leurs exigences en vue d'une meilleure conservation.

[Traduit par la Rédaction]

Introduction

The anadromous life cycle of salmon is generally regarded as highly predictable. Spawning adults return to their natal streams, fry hatch and grow in single stream reaches, and migratory smolts travel to the ocean in a relatively synchronized fashion. The classic view of juvenile salmon during their freshwater phase has been that populations comprise territorial individuals that exhibit high site fidelity and rarely move beyond 50 m (Gerking 1959; Rodríguez 2002). These

Received 28 March 2002. Accepted 14 May 2002. Published on the NRC Research Press Web site at http://cjfas.nrc.ca on 24 June 2002.
J16824

B.P. Kennedy,[1] **A. Klaue, and J.D. Blum.** Department of Geological Sciences, University of Michigan, 425 East University Avenue, Ann Arbor, MI 48109, U.S.A.
C.L. Folt. Department of Biological Sciences, Dartmouth College, Hanover, NH 03755, U.S.A.
K.H. Nislow. Northeastern Research Station, USDA Forest Service, Amherst, MA 01003, U.S.A.

[1] Corresponding author (e-mail: bpkenned@umich.edu).

DOI: 10.1139/F02-070

generalizations have formed the conceptual basis for years of work on the population dynamics and life history of salmon (e.g., Hansen and Quinn 1998). They also provide the basis for predominately localized conservation approaches. Relatively little is known about the extent to which individual strategies vary at different life history stages for salmon, or most other fish species, because of difficulties in tracking individuals.

Recent studies suggest that the paradigms of predictability and restricted movement in salmon reflect inherent biases in conventional tagging techniques that focus either on the recaptured, nonmobile fraction of the population or on only fish large enough to receive tags (Gowan et al. 1994). For instance, radiotelemetry has provided compelling evidence that some salmon move more extensively than previously thought during their freshwater phase. However, telemetry cannot be used to study movements of small fish or entire populations (e.g., Gowan et al. 1994). Tracking individual fish of all sizes as they move through river networks would significantly improve our understanding of life history variability, habitat use, and energy and material transport by many fish species.

Our study shows that stable isotopes of strontium (Sr) can be used to discern movements over an individual's life. This information may help to resolve debates over salmonid life history and has valuable management applications. Over 10 million Atlantic salmon (*Salmo salar*) are stocked annually into tributaries of the Connecticut River, U.S.A. Less than 500 return each year. Tracing the lifetime movements of the successful adults would be extremely helpful for guiding restoration and management policies.

Our approach builds upon recent studies using geochemical signatures in fish otoliths, or ear stones, to identify natal stream habitats and the movements of fish from stocked or marked locations (Kennedy et al. 2000; Thorrold et al. 2001). Otoliths are small mineral structures in which increments of calcium carbonate, in the form of aragonite, are accreted daily in thin concentric rings (approximately 1–10 μm). Because the aragonite rings remain unaltered after deposition and can be referenced to specific ages, information recovered at different locations within the otolith can be used to reconstruct events throughout the lifetime of a fish. Changes in the elemental composition across the length of an otolith reflect either changes in the ambient water conditions or, in the case of some trace elements and isotopes, modifications due to the physiological conditions of a fish at a specific time (Kalish 1989; Kennedy et al. 2000).

Despite the remarkable potential of otolith microchemistry, relatively few studies have combined elemental analysis with the unique otolith growth bands to take advantage of the high-resolution chemical information stored within daily otolith increments (Campana and Thorrold 2001, but see Limburg 2001). By analyzing Sr isotopes in otolith increments, we overcome three obstacles that have otherwise prevented the widespread use of other geochemical tracers as population fingerprints. First, elemental concentrations of surface waters often exhibit relatively low spatial variability and comparatively high temporal variability. This can preclude their use as a predictable and unique geographic marker among multiple locations or over long time periods (e.g., Gillanders et al. 2001). Sr isotope ratios of surface waters are based upon the underlying bedrock geology, which can vary significantly even among adjacent watersheds. They also provide extremely stable signatures over seasons and years (Kennedy et al. 2000). Second, elemental markers in otoliths are often correlated with physiological factors experienced by individual fish. This limits their utility in distinguishing populations (e.g., Kalish 1989). In contrast, Sr isotopes are not fractionated biologically and therefore the Sr isotopic composition of an individual's habitat is incorporated directly into calcified tissues without modifications resulting from changes in diet, stress, temperature, or other physiological factors (Kennedy et al. 2000). Third, because of the regulated deposition of aragonite in otoliths, the concentrations of some elements can be extremely low, which effectively constrains their analytical resolution in otolith subsamples. Yet, the high concentration of Sr in otoliths enables elemental analysis of tiny subsamples of otolith material and allows for resolution over comparatively short time intervals.

In this study, we isolated Sr isotopic signatures from otoliths of spawning adult salmon at a resolution that allows us to (*i*) recover natal stream signatures, (*ii*) reconstruct the freshwater movements of Atlantic salmon over relatively small spatial scales (1–10 km) and short time scales (weeks to months), and (*iii*) identify the timing of migration for salmon smolts. We combine micromilling techniques with Sr isotope analysis from otolith increments to address the long-standing hypotheses that juvenile salmon movements are rare and that their timing is predictable. In so doing, we reconstruct the environmental history of individuals and find evidence challenging key aspects of salmon life history paradigms.

Methods

We measured age-specific $^{87}Sr/^{86}Sr$ ratios within the sagittal otoliths of four adult Atlantic salmon, which were captured as they returned to spawn in the Connecticut River. The fish were collected at Holyoke Dam on the Connecticut River in Massachusetts, U.S.A., which is located 140 km upstream of the river mouth and is the first dam encountered by returning salmon. The fish were randomly chosen from a cohort of 154 returning salmon in 1999.

Otoliths were cleaned, mounted, and sanded so that daily increments could be resolved when magnified to 1000× with a Leica® compound scope (Fig. 1). Otolith images were digitized and projected onto a computer monitor so that otoliths could be systematically drilled using a computer-controlled micromill. Otolith subsamples came from drilled paths (40–50 μm) along parallel, concentric growth curves at known distances from the otolith center using a Merchantek® xyz-stage micromill. Powdered aragonite (<25 μg) was carefully transferred to individually labeled, clean Teflon® vessels and gently digested in quartz-distilled concentrated Seastar® HNO_3. Digestion, elemental separation, and Sr isotope analysis were performed using established methods (Kennedy et al. 2000). The solution was dried to completeness and then redissolved in ultra-pure 3N HNO_3. Sr was separated from this solution using Sr-specific cation exchange resin. An aliquot of the Sr solution containing ~20 ng of Sr was evaporated to dryness, transferred onto single tungsten filaments with Ta_2O_5 activator, and loaded

Fig. 1. Atlantic salmon (*Salmo salar*) sagittal otolith. Numbered sections delineate the major life cycle stages within the otolith of an anadromous salmon. Hatchery accretion (marked as 1) is represented at the core of the otolith. Material derived from natal stream(s) and smolt stage (2 and 3, respectively) is deposited around this core. Lastly, the material accumulated in the ocean is located in the outermost region of the otolith (4). Drilling paths were narrow (<50 μm) and contained entirely within distinct life cycle stages.

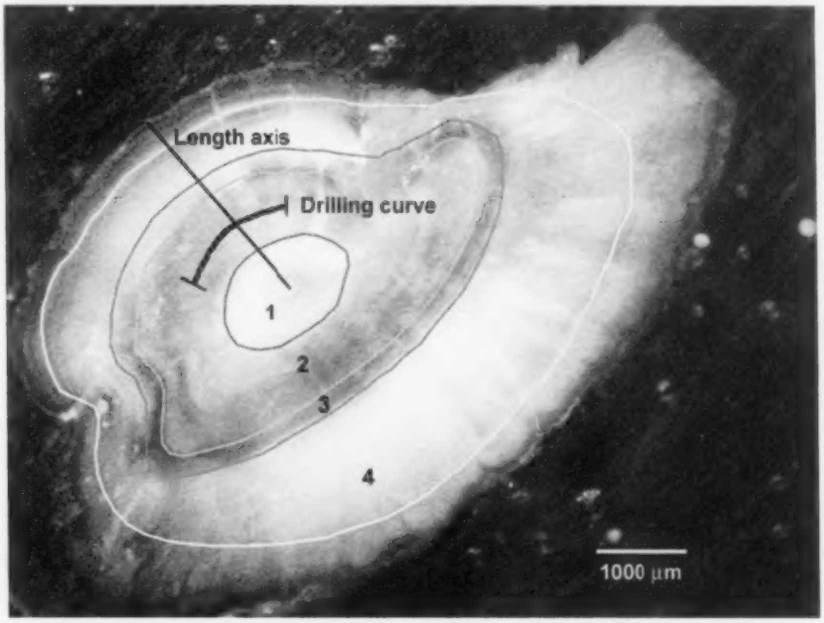

into the mass spectrometer. All Sr isotopic compositions were measured using a Finnegan MAT 262 thermal ionization mass spectrometer. $^{87}Sr/^{86}Sr$ were normalized to $^{86}Sr/^{88}Sr$ = 0.1194. Twenty analyses of a National Institute of Standards and Technology standard reference material (SRM-987) were completed during the 5-month duration of this study and yielded a mean $^{87}Sr/^{86}Sr$ of 0.710250 ± 0.000005 (2 standard errors (SE)).

Changes in the Sr isotope ratios along the accretionary axis of an otolith imply a change in the environment experienced by a fish. To first quantify the precision of replicated Sr isotope measurements for a fish that lived within a single environment, we analyzed otolith increments from one 4-year-old hatchery salmon that had been reared to adulthood at the White River National Fish Hatchery (WRNFH) in Bethel, Vt., U.S.A. Sr isotope ratios in the otolith of this individual served as a control against which we compared the variability of Sr isotope ratios of our field-caught fish.

To identify natal stream signatures and to test for movement during the freshwater phase, we measured the isotopic signatures for these individuals at several points before smoltification. The otolith of a salmon at the time of stocking has a radius of approximately 400 μm. To establish rearing stream signatures, otoliths were drilled sequentially at radial distances between 600 and 1000 μm, representing at least four different time points throughout about 12 months of growth for each individual (first spring–summer to second spring–summer).

Most Atlantic salmon in the Connecticut River basin smolt during their third spring. However, a subset of the population leave their rearing tributaries after only their second spring. Using micromilled otolith increments, we compared the migratory behavior of the returning adult salmon as smolts. Because modern ocean water has a uniform global Sr isotopic signature ($^{87}Sr/^{86}Sr$ = 0.70918), it can provide the most precise marker to date for identifying the incorporation of a marine-derived signature in fish, and hence, the timing and duration of ocean residence.

Results and discussion

Our micromilling technique was successful for characterizing distinct Sr isotopic signatures from the four major stages in the life cycle of adult Atlantic salmon: (1) prefeeding hatchery development (core), (2) rearing-stream growth, (3) smolt out-migration, and (4) ocean residence (Fig. 2). Micromilled otolith subsamples from our control fish, an adult salmon that lived exclusively at WRNFH, displayed very little variability around an average value of 0.71049 ± 0.00002 (SE) (Fig. 2). In contrast, Sr isotope ratios from micromilled otolith subsamples of the returning adult salmon varied significantly. Because all returning salmon were originally spawned in one of five hatcheries, the isotopic signature at the core of their otoliths must match that of prestocked fry from one those hatcheries. The Sr isotopic signatures from the otolith cores of three of the four returning adult salmon were similar to that of hatchery fry sampled at WRNFH (0.7123, 0.7127, 0.7129 vs. 0.7122; Fig. 2), making it their likely source. Since 1996, WRNFH has supplied more than 70% of stocked fry. The fourth fish was probably spawned in one of the two other hatcheries located in central and western Vermont. Those regions are underlain

Fig. 2. Age-specific Sr isotope ratios from adult Atlantic salmon (*Salmo salar*). Signatures are measured along a growth axis for four returning salmon (salmon 1 to salmon 4) and one hatchery fish. The $^{87}Sr/^{86}Sr$ signature is expressed as a function of distance from the center of the otolith and records distinct environments as the otolith accretes increments. Sr isotope ratios of unfed, unstocked fry from the White River National Fish Hatchery (WRNFH, shaded triangle) correspond closely with the values for otolith cores from three of the four salmon. Precise natal stream signatures, identified by boxes, are quantifiable in three of the four individuals. Measurement error is expressed as the standard error of 20 analyses of a National Institute of Standards and Technology standard reference material (SRM-987) throughout the course of this experiment and is represented as the thin horizontal line within the symbol (marked with arrow).

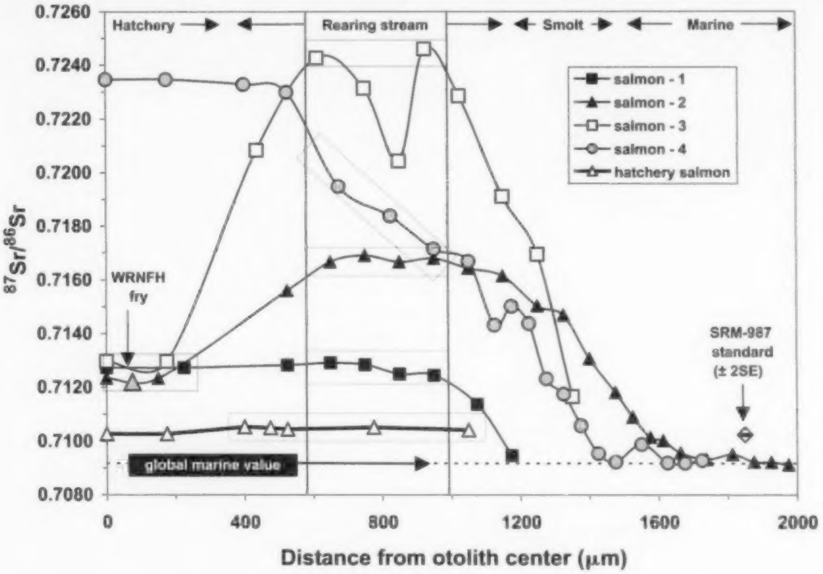

Table 1. Natal stream $^{87}Sr/^{86}Sr$ signatures recovered from freshwater portions of adult otoliths.

Sample	$^{87}Sr/^{86}Sr$	Radius of measurement (μm)	*n*
1	0.71268 (0.00012)	600–1000	4
2	0.71676 (0.00006)	600–1000	4
3	0.72443 (0.00017)	600–1000	2
4	0.71834 (0.00068)	600–1000	3
Hatchery fish	0.71049 (0.00002)	400–1100	5
Range and variability of stream water	0.7107–0.7235 (0.00015)	NA	6
Range and variability of age-0 resident fish	0.7123–0.7285 (0.00005)	NA	17

Note: Sample numbers correspond to fish designations in Fig. 2. Sr isotope ratios are the mean isotopic composition (± standard error (SE)) of micromilled otolith increments taken exclusively from the freshwater portion of each otolith. Mean SE from replicate streamwater and resident fish samples is calculated from the average SE of samples for water (6 sites) and fish (17 sites) throughout Vermont (Kennedy et al. 2000) and expressed here for comparison to the variability from within a single otolith. NA, not applicable.

primarily by old, Cambrian, silicate-bearing rock that yields a high $^{87}Sr/^{86}Sr$ ratio (0.72337) similar to the signature found in the otolith core of this individual (Kennedy et al. 2000).

In two of the four fish, the natal signatures were precise and repeatable throughout the freshwater phase. This is consistent with the hypothesis that Atlantic salmon juveniles undergo restricted movement (i.e., these fish remained in a single stream the entire time). The isotopic signatures of all fish were also statistically distinguishable from one another (Tukey's Honestly Significant Difference, $p < 0.001$; Fig. 2). This indicates that these four salmon were reared in different streams and highlights the promise of this technique for distinguishing among natal sources for mixed fish stocks. The standard error of replicated drilled paths from the freshwater phase for individual fish ranged from 0.008% to 0.023% of the Sr ratio (or ± 0.00006 to 0.00017) (Table 1). The within-stream variability of field-caught fish was slightly larger than the variability we measured for the control hatchery-reared adult. It was comparable to the average within-site variation for water samples collected throughout a growing season (Table 1). Hence, minor fluctuations in a stream water Sr isotopic signature appear to be reflected in the otolith signature.

Counter to the hypothesis of restricted juvenile movement, the other two fish moved significantly among habitats during their freshwater rearing (or natal) phase. The "natal" stream signature for the third fish (salmon 3 in Fig. 2) was interrupted by periodic movements to different habitats. Rapid shifts in the Sr isotope ratios of this fish suggest that it moved extensively at times during the freshwater phase. However, it appears to have returned to the same rearing stream during the summer growing periods. The spacing and timing of the isotopic shift is consistent with an over-wintering movement from a headwater stream in the summer (where it was probably stocked) with a high $^{87}Sr/^{86}Sr$ ratio into a deeper downstream tributary with a lower $^{87}Sr/^{86}Sr$ value. The fourth fish underwent a different movement pattern. Unlike the other three fish, it had no distinguishable natal stream signature (Fig. 2). Instead, the $^{87}Sr/^{86}Sr$ ratios in its otolith decreased with distance from the center of the otolith resulting in isotopic variability during the first year of growth that is four times greater than those of more sedentary individuals (SE = 0.00068 and coefficient of variation = 0.094%). This steady decline is consistent with a pattern of slow progressive movement downstream throughout its two-year freshwater residency.

Scientists know considerably more about variability in migration and breeding dates among salmon populations (Quinn et al. 2000) than in movement during their nonmigratory stage. Retrospective approaches based on otolith microchemistry can be used to examine this variability further by definitively linking individual salmon survival with specific smolting strategies (e.g., Limburg 2001). Sr isotopic values from the outermost otolith increments from all salmon demonstrated the same distinctive trend over time toward the ocean water value (Fig. 2). In two of the four fish, we analyzed multiple subsections of the outer otolith rings to confirm the constancy of this value and found that there was little variability around a distinct modern ocean signature (range = 0.70912–0.70952; Fig. 2). Significant differences in the point at which the different otoliths incorporated a marine signature indicated that individuals smolted at different ages. Based on Sr isotope ratios and confirmed by both age–length analysis and annual checks in the otoliths, salmon-1 migrated to the ocean during its second spring, 1 year earlier than the other three fish.

Despite the increasing research into geochemical signatures and their recognized potential for discerning among populations, many of the assumptions that underlie their successful application in aquatic and fisheries sciences have not been critically assessed (Campana 1999). This study provides additional evidence that Sr isotope ratios (see also Kennedy et al. 2000) are incorporated unchanged from their aqueous environment, and therefore, they circumvent the confounding physiological or structural factors that can complicate the use of alternative elemental or isotopic markers (e.g., Kalish 1989). As a result, we used Sr isotope ratios in the otoliths from four randomly selected adult Atlantic salmon to distinguish hatchery marks, natal stream signatures, interstream movements, and migratory behaviors. Our examination of individual fish revealed clearly that all four fish adopted different strategies over their lives. This high level of variability in salmon life history strategies could not have been described by conventional marking techniques. We suggest that geologically derived fingerprints, like Sr isotopes, yield critical information about the habitat use and conditional behaviors of individuals. When applied to globally imperiled species like Atlantic salmon, this approach may help to inform management practices, which are otherwise limited to static local measures of performance.

Acknowledgements

We would like to thank K. Gillette, M. Novak, J. Revita, and J. Rowan of the U.S. Fish and Wildlife Service for their assistance in acquiring the salmon specimens and K. Lohmann, A. Dutton, and M. Kelley for access to instruments and laboratory assistance. We appreciate the constructive comments of Simon Thorrold and one anonymous reviewer on an earlier draft of the manuscript. The study was supported by grant #NA86FL0538 from the National Oceanic and Atmospheric Administration.

References

Campana, S.E. 1999. Chemistry and composition of fish otoliths: pathways, mechanisms and applications. Mar. Ecol. Prog. Ser. **188**: 263–297.

Campana, S.E., and Thorrold, S.R. 2001. Otoliths, increments, and elements: keys to a comprehensive understanding of fish populations? Can. J. Fish. Aquat. Sci. **58**: 30–38.

Gerking, S.D. 1959. The restricted movement of fish populations. Biol. Rev. Camb. Philos. Soc. **34**: 221–242.

Gillanders, B.M., Sanchez-Jerez, P., Bayle-Sempere, J., and Ramos-Espla, A. 2001. Trace elements in otoliths of the two-banded bream from a coastal region in the south-west Mediterranean: are there differences among locations? J. Fish Biol. **59**: 350–363.

Gowan, C., Young, M.K., Fausch, K.D., and Riley, S.C. 1994. Restricted movement in resident stream salmonids—a paradigm lost? Can. J. Fish. Aquat. Sci. **51**: 2626–2637.

Hansen, L.R., and Quinn, T.R. 1998. The marine phase of the Atlantic salmon (*Salmo salar*) life cycle, with comparisons to Pacific salmon. Can. J. Fish. Aquat. Sci. **55**(Suppl. 1): 104–118.

Kalish, J.M. 1989. Otolith microchemistry: validation of the effects of physiology, age and environment on otolith composition. J. Exp. Mar. Biol. Ecol. **132**: 151–178.

Kennedy, B.P., Folt, C.L., Blum, J.D., and Nislow, K.H. 2000. Using natural strontium isotopic signatures as fish markers: methodology and application. Can. J. Fish Aquat. Sci. **57**: 2280–2292.

Limburg, K. 2001. Through the gauntlet again: demographic restructuring of American shad by migration. Ecology, **82**: 1584–1596.

Quinn, T.P., Unwin, M.J., and Kinnison, M.T. 2000. Evolution of temporal isolation in the wild: genetic divergence in timing of migration and breeding by introduced chinook salmon populations. Evolution, **54**: 1372–1385.

Rodríguez, M.A. 2002. Restricted movement in stream fish: the paradigm is incomplete, not lost. Ecology, **83**: 1–13.

Thorrold, S.R., Latkoczy, C., Swart, P.K., and Jones, C.M. 2001. Natal homing in a marine fish metapopulation. Science (Washington, D.C.), **291**: 297–299.

Sampling variability and the design of bacterial abundance and production studies in aquatic environments

Geneviève M. Carr and Antoine Morin

Abstract: Published data for aquatic bacterial abundance and production in benthic and planktonic environments were collected from the literature to describe relationships between sample means and variances, to explore the factors that affect these relationships, and to estimate the number of samples needed to detect specified differences among means with adequate power. Between 75 and 94% of sample $\log_{10}$(variance) was explained by $\log_{10}$(mean) for both bacterial abundance and production. Differences in mean–variance relationships of bacterial abundance and production due to habitat (river, lake, marine), quantification method, and experimental manipulation (planktonic bacteria) or substrate type (benthic bacteria) were negligible (less than 11% of residual variance from regressions explained). Between 12 and 69 replicates are necessary to detect a 20% difference in means for bacterial abundance and production with a power of 80%. Given the median rate of replication of 3 to 4, the majority of published studies reviewed here are, at best, able to detect differences in means of 50% (planktonic bacterial abundance) or 100% (planktonic production and benthic abundance and production) with 80% power. If effect sizes less than these values are deemed biologically meaningful, then future studies will have to increase sampling effort to enable detection of such differences.

Résumé : Des données sur l'abondance et la production de bactéries benthiques et planctoniques ont été récoltées dans la littérature et analysées pour décrire la relation entre la moyenne et la variance d'échantillonnage, pour examiner les facteurs affectant cette relation, et pour estimer le nombre d'échantillons requis pour détecter une différence entre deux moyennes avec une puissance statistique donnée. Entre 75 % et 94 % de la variabilité du $\log_{10}$ variance peut être attribuée au $\log_{10}$ de la moyenne pour l'abondance et la production des bactéries. Les différences dans les relations entre la moyenne et la variance de l'abondance et la production bactérienne attribuées aux habitats (rivières, lacs, océans), la méthode de quantification et les manipulations expérimentales (bactéries planctoniques) ou le type de substrat (bactéries benthiques) sont négligeables et expliquent moins de 11 % de la variabilité. Les analyses de puissance indiquent que entre 12 et 69 échantillons sont nécessaires pour détecter une différence de 20 % entre deux moyennes d'abondance ou de production bactérienne avec une puissance de 80 %. Puisque la médiane du nombre d'échantillons dans les études utilisées dans cette analyse se situe entre 3 et 4, la majorité de ces études pouvaient au mieux détecter une différence entre les moyennes de 50 % (pour l'abondance de bactéries planctoniques) ou de 100 % (production bactérienne planctonique ou abondance et production bactérienne benthique) avec une puissance de 80%. Il semble donc que si des tailles d'effet plus petites que 50 % sont jugées écologiquement signifiantes, alors les études futures devront utiliser un nombre plus élevé d'échantillons pour les détecter statistiquement.

[Traduit par la Rédaction]

Introduction

Interest in the role of bacteria in mediating fluxes of organic matter and minerals in aquatic environments has mounted in the last three decades as our ability to detect their presence and quantify production has improved (Cole 1999). Recent studies have demonstrated that planktonic bacteria contribute, among other things, to the metazoan food web in pelagic systems (Sherr and Sherr 1988), whereas when attached to benthic surfaces, bacteria play a role in the physical development of complex biofilm communities and also in the cycling of nutrients through these communities (Lock et al. 1984; Stock and Ward 1989). However, because of sampling variability and methodological constraints, field studies of bacteria in aquatic systems require considerable effort that could be minimized by optimizing study designs.

Spatial and temporal variability of bacteria is the most important factor affecting the design of any study that quantifies bacteria in the natural environment. Organisms that are highly variable require large sampling effort to estimate population parameters in space or time. Knowledge of the variability of a population is necessary to design adequate sampling programs that can detect biologically meaningful

Received 15 February 2002. Accepted 23 May 2002. Published on the NRC Research Press Web site at http://cjfas.nrc.ca on 9 July 2002.
J16765

G.M. Carr[1] and A. Morin. Department of Biology, University of Ottawa, 30 Marie Curie, Ottawa ON K1N 6N5, Canada.

[1] Corresponding author (e-mail: gcarr@science.uottawa.ca).

Can. J. Fish. Aquat. Sci. **59**: 930–937 (2002) DOI: 10.1139/F02-072

differences among samples with sufficient power (Peterman 1990). Organisms living in aquatic environments are notoriously variable both in their distribution and in their abundance (Downing 1979; Morin and Cattaneo 1992). To date, there have been no surveys of the variability of abundance and production of aquatic bacteria in either planktonic or benthic environments, despite the increased interest in the role of bacteria in trophic and biogeochemical studies of aquatic ecosystems.

Here, we report on the results of a meta-analysis of published bacterial abundance and production data in benthic and planktonic environments. The goals of this study were (*i*) to quantify the relationship between spatial variance and mean of bacterial measures and (*ii*) to use these relationships to estimate the minimum number of replicates in space necessary to detect differences among means for samples of bacterial abundance and production with adequate power. We report on differences in mean–variance relationships for bacterial abundance and production in marine and freshwater environments, lotic and lentic systems, and benthic versus planktonic habitats. We also examine the effect of quantification techniques and whether experimental manipulation influences mean–variance relationships for bacterial abundance.

Materials and methods

The published literature was searched systematically for values of bacterial cell abundance and production in benthic and planktonic environments of aquatic ecosystems. Because we rely here on the relationship between mean and variance of a sample to describe variability in bacterial populations, we only used estimates of abundance and production that were accompanied by some estimate of variability about the mean (standard deviation, standard error, coefficient of variation, confidence limits). We were specifically interested in estimates of means and variances describing an observation at a single place and time to evaluate spatial variability. Thus, estimates of means and variances that were summaries of multiple sites or multiple sampling efforts over time were not included in this analysis. Studies that collected only one sample from a location and replicated bacterial measures by subsampling were also excluded because the replication technique made it impossible to distinguish between analytical and spatial variability. Abundance and production of planktonic bacteria were expressed volumetrically, whereas estimates for attached bacteria were expressed aerially. In the case of benthic bacteria, we only used estimates of abundance and production that were reported aerially and so in most cases corresponds to attached or periphytic bacteria.

For each study, we recorded the methods used to quantify production and abundance. Production methods consisted of determining incorporation rates of either thymidine (Findlay et al. 1984) or leucine (Smith and Azam 1992). The dominant methods to enumerate bacterial abundance consisted of cell staining and microscopic examination according to the acridine orange direct count (AODC; Hobbie et al. 1977) or 4′,6-diamidino-2-phenylindole (DAPI; Porter and Feig 1980) methods. We also recorded the habitat from which samples were drawn (lake, river, marine) and whether the samples underwent any form of experimental manipulation (planktonic bacteria) or were grown on natural or artificial substrata (benthic bacteria).

The relationship between variance and mean was described by linear regression on $\log_{10}$-transformed variables. Residuals of bacterial abundance relationships were examined by analyses of variance (ANOVAs) for deviations attributable to quantification technique, habitat, and whether the samples had been experimentally manipulated (planktonic bacteria) or whether they were grown on natural or artificial substrata (benthic bacteria).

We quantified the number of replicates per sample needed to detect a difference between two means with an acceptable level of type I (α) and type II (β) error with SYSTAT (version 10, Systat Software Inc., Richmond, Calif., http://www.systat.com). For this, we assumed that statistical comparisons by Student's *t*-tests would be performed using the log-transformed data, and thus, estimated the variance (s^2) of a lognormal distribution as a function of the arithmetic means ($\bar{x}$) for bacterial measures according to the method of Hines and Montgomery (1980), such that

$$s^2 = \ln(10^a\ \bar{x}^{b-2} + 1)$$

where a is the y intercept and b is the slope of $\log_{10}$(mean) – $\log_{10}$(variance) relationships for each bacterial measure. We pooled the variances for the different means and computed the number of replicates needed to achieve 50 and 80% power when type I error is set at 5%.

Results

Our literature search yielded 29 planktonic bacteria studies and 16 benthic bacteria studies. Of these, 22 and 12 studies reported abundance and 11 and 5 studies reported production for planktonic and benthic bacteria, respectively (Table 1). The benthic studies were restricted entirely to river environments; there were some studies that reported bacterial abundance in sediments of other environments (mostly marine) but abundance was expressed volumetrically rather than aerially, and thus could not be compared to other benthic studies. Publication dates for the data collected ranged from 1976 to 2001. Bacterial abundances spanned five orders of magnitude in both planktonic and benthic systems, whereas production spanned four to five orders of magnitude for the same systems. Abundance and production means and variances were all heavily right-skewed; skewness was eliminated by $\log_{10}$ transformations. Median number of replicates for all measures was between three and four (Table 1).

Log_{10}(variance) increased linearly with $\log_{10}$(mean) for abundance and production in benthic and planktonic environments (Fig. 1). Mean bacterial abundance and production explained between 75 and 94% of the variability in variance of a sample with regressions for benthic bacteria explaining more of the variability than planktonic bacteria (Table 2). With the exception of benthic bacterial production, the slopes of the mean–variance relationships were less than two and these differences were statistically significant (Table 2). The slope for benthic bacterial production was not significantly different from two. A slope of two for a mean–variance relationship on a log–log scale indicates the coefficient of variation (CV, standard deviation/mean) is independent of

Table 1. Summary statistics of bacterial production and abundance measures retrieved from literature and used in this study.

	Planktonic bacteria		Benthic bacteria	
Parameter	Abundance (cells·L^{-1})	Production (µg C·L^{-1}·h^{-1})	Abundance (cells·cm^{-2})	Production (mg C·m^{-2}·h^{-1})
Mean	4.50×10^{10}	2.67	2.39×10^{9}	23.8
Median	1.68×10^{9}	0.579	3.69×10^{7}	3.26
Minimum	1.60×10^{7}	0.008	6.25×10^{5}	0.259
Maximum	6.24×10^{12}	38.4	5.51×10^{10}	140
n (observations)	469	199	235	54
Coefficient of variation (mean %)	20.6	35.4	34.5	48.3
Median no. replicates	3	3	3	4
Range of replication	2–16	2–14	2–8	3–5
No. studies	22	11	12	5

Note: Data sources are as follows. Planktonic bacteria: Alldredge et al. (1986); Benner and Biddanda (1998); Benner et al. (1995); Bertilsson and Tranvik (1998); Boon (1994); Bouvy et al. (1998); Bunte and Simon (1999); Carlsson and Caron (2001); Cochlan (2001); Cole and Pace (1995); Edwards (1987); Eisenmann et al. (1999); Ferguson and Rublee (1976); Findlay et al. (1986); Kirchman et al. (2000); Kroer (1993); Langenheder and Jürgens (2001); Lind and Dávalos-Lind (1991); Lindell et al. (1995); Moeseneder and Herndl (1995); Palumbo et al. (1987); Rich et al. (1996); Scavia and Laird (1987); Scavia et al. (1986); Seitzinger and Sanders (1999); Suzuki et al. (1993); Tapper and Hicks (1998); Theil-Nielsen and Søndergaard (1999); Tranvik (1994). Benthic bacteria: Findlay et al. (1993); Freeman and Lock (1995); Geesey et al. (1978); Hudson et al. (1990); Hudson et al. (1992); Kaplan and Bott (1989); Ledger and Hildrew (1998); Lock et al. (1984); Mohamed et al. (1998); Neely and Wetzel (1995); Romaní and Sabater (1997, 1999*a*, 1999*b*); Rosenfeld and Hudson (1997); Sabater and Romaní (1996); Stock and Ward (1989).

Fig. 1. Mean–variance relationships of bacterial abundance (*a* and *b*) and production (*c* and *d*) for planktonic and benthic bacteria. Units for abundance and production are as in Table 1. Fitted lines are linear regressions and correspond to equations in Table 2. Note difference in axis scales between top and bottom panels.

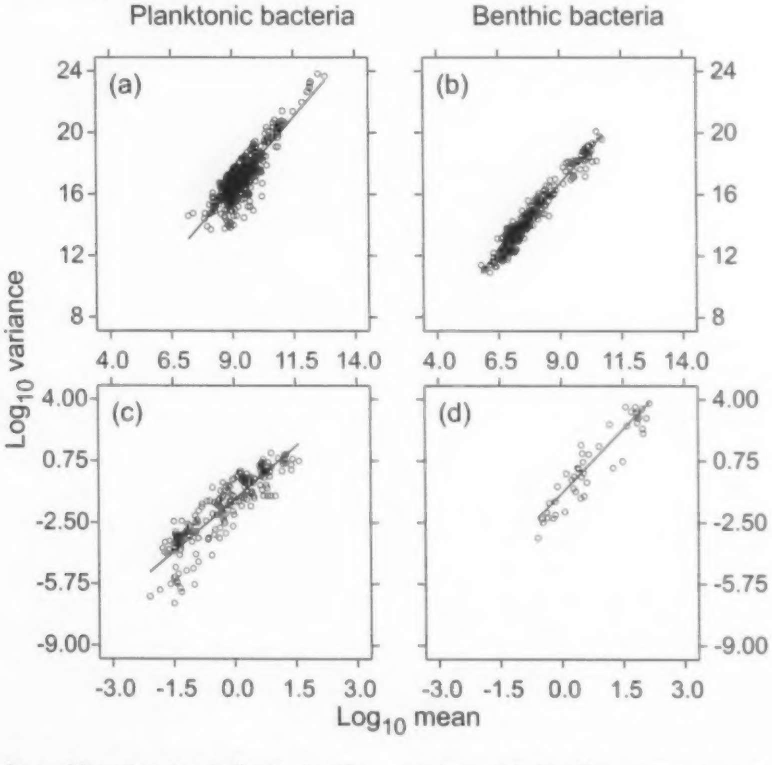

the mean, whereas a slope of less than two indicates that the CV decreases with the mean and a slope of greater than two indicates that the CV increases with the mean.

Coefficients of variation for all bacterial measures varied from a mean of 20.6% (planktonic abundance) to 48.3% (benthic production) (Table 1). Since the slopes of mean–variance relationships were near two, we assumed that the CV was approximately independent of the mean. Following this assumption, a two-way ANOVA showed that log$_{10}$-transformed CVs for benthic bacteria were higher than for planktonic bacteria ($P < 0.001$), that CVs for production estimates were higher than those for abundance estimates

Table 2. Regression statistics for mean ($\bar{x}$) – variance (s^2) relationships for benthic and planktonic bacterial measures (abundance and production).

Dependent variable	Model	r^2	RMS	n	$P_{\beta=2}$
Planktonic bacteria					
$\log_{10}(s^2_{\mathrm{abundance}})$	$-0.235[0.470] + 1.848[0.050] \times \log_{10}(\bar{x}_{\mathrm{abundance}})$	0.746	0.612	469	0.002
$\log_{10}(s^2_{\mathrm{production}})$	$-1.279[0.063] + 1.856[0.068] \times \log_{10}(\bar{x}_{\mathrm{production}})$	0.790	0.716	199	0.036
Benthic bacteria					
$\log_{10}(s^2_{\mathrm{abundance}})$	$0.387[0.233] + 1.811[0.029] \times \log_{10}(\bar{x}_{\mathrm{abundance}})$	0.943	0.274	235	< 0.001
$\log_{10}(s^2_{\mathrm{production}})$	$-0.951[0.148] + 2.247[0.134] \times \log_{10}(\bar{x}_{\mathrm{production}})$	0.843	0.620	54	0.072

Note: Values in square brackets are standard errors (SE) of coefficients. *RMS* denotes the residual mean square of the model. All mean–variance relationships are significant ($P << 0.001$). $P_{\beta=2}$ denotes the probability that slopes (β) are different from 2 as determined by a t-test, where $t = |\beta-2|/\mathrm{SE}_\beta$ and degrees of freedom = $n - 2$.

Fig. 2. Coefficient of variation as a function of mean for (*a*) bacterial production and (*b*) abundance in benthic (solid symbols) and planktonic (open symbols) bacteria. Units for mean production and abundance are as in Table 1.

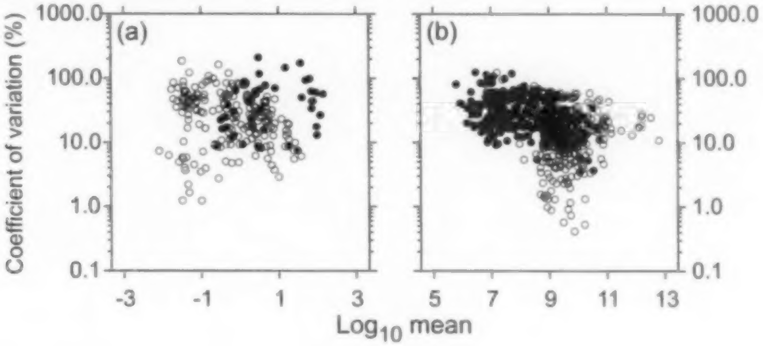

($P < 0.001$), and that there was no interaction between type of bacteria and type of measurement ($P = 0.52$). The effects on CV were small and the ANOVA model explained only 12.7% of the variability in CV. This is evident in Fig. 2, where the scatter of CVs for benthic and planktonic abundance and production measurements is roughly the same, with almost complete overlap of points where the values for the means are of the same order of magnitude.

One-way ANOVAs of the residuals of the mean–variance relationships yielded significant differences among some of the factors examined, but these were mostly negligible in terms of the amount of variation explained. Residuals of mean–variance relationships for bacterial abundance in the plankton differed according to enumeration method (AODC, DAPI; $P = 0.002$; Fig. 3), but this difference explained only 2% of the residual variance and was not significant for benthic bacterial abundance. Thymidine production methods yielded estimates with higher variances than leucine production methods ($P \leq 0.028$) and these differences accounted for 11 and 9% of residual variance for planktonic and benthic bacteria, respectively (Fig. 3). It should be noted that only one study used the leucine incorporation method for benthic production estimates and so this result should be interpreted cautiously. Experimental manipulation of planktonic samples and substrate type (natural or artificial) for benthic samples had no effect on variability of production and abundance estimates ($0.45 \leq P \leq 0.06$; Fig. 3). Habitat explained 2.3 and 6.3% of the residual variance for planktonic abundance and production, respectively ($P \leq 0.005$; Fig. 3). In the case of planktonic abundance, river samples had higher variance than lake and marine samples, whereas marine samples had higher variance than lake samples for planktonic production (rivers could not be evaluated for planktonic production because of a lack of data). We were not able to assess habitat effects for benthic bacteria because all data retrieved from the literature were from river systems.

The number of replicates needed to detect a difference among means with a specific power differed with bacterial measures, such that more samples, on average, would be needed for benthic than planktonic bacteria and for production than abundance measures (Fig. 4). To detect a difference in means of 20% (i.e., $\bar{x}_2/\bar{x}_1 = 1.2$) with a power of 80%, 12 and 23 replicates would be needed for planktonic abundance and production measures, and 42 and 69 replicates would be needed for benthic abundance and production measures, respectively. The number of replicates needed to detect a doubling of means dropped to between three and seven replicates for all bacterial measures (Fig. 4).

Discussion

The relationship between $\log_{10}$(variance) and $\log_{10}$(mean) for aquatic bacteria was linear for both benthic and planktonic abundance and production measures. Similar relationships have been observed for other aquatic biotic variables, including benthic invertebrates in lakes and rivers, freshwater measures of periphyton, lake chlorophyll, and macrophyte biomass (Table 3). Most of these relationships have slopes near to or just below 2, indicating that the CV is independent of the mean or decreases slightly with increasing means

Fig. 3. Mean (±2 standard errors) of residuals of variance–mean models for benthic (solid symbols) and planktonic (open symbols) bacterial production and abundance. Residuals are grouped according to quantification technique (production: thymidine or leucine incorporation rates; abundance: acridine orange direct count (AODC) or 4′,6-diamidino-2-phenylindole (DAPI) enumeration methods), whether the samples underwent any form of manipulation (planktonic bacteria) or whether they were grown on natural or artificial substrata (benthic bacteria), and habitat from which the samples were taken (river, lake, or marine).

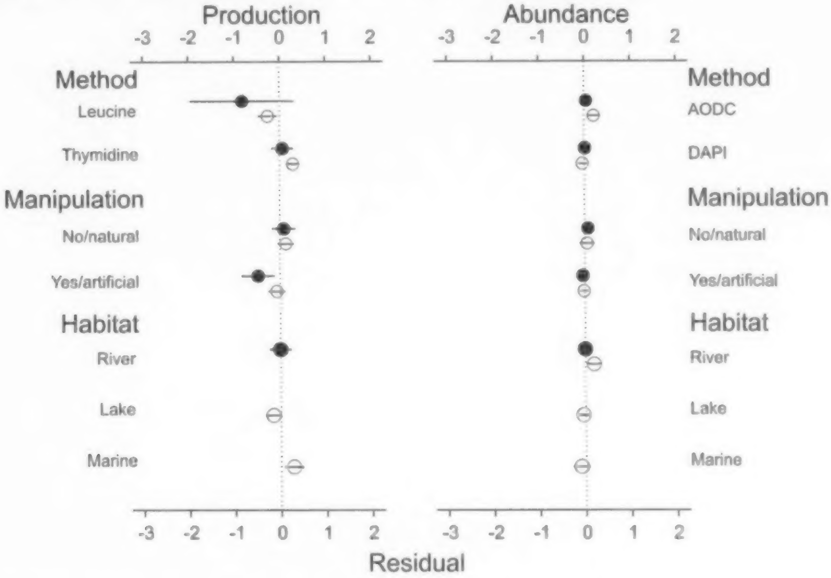

Fig. 4. Number of replicates required per sample to detect predetermined differences between means with a power of (*a*) 50% and (*b*) 80% for planktonic (open symbols) and benthic (solid symbols) bacterial abundance (circles) and production (triangles). The denominator in the ratio of means, $\bar{x}_1$, was set as the median of all published observations for each measure (Table 1). Note scale of *x*- and *y*-axes to maximize separation among points. Between $\bar{x}_2/\bar{x}_1 = 1$ and 2, number of replicates was evaluated for increments of 0.1.

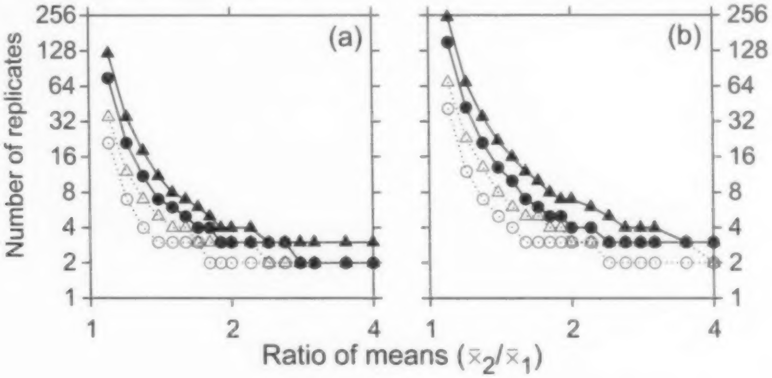

(Table 3). This pattern suggests a nearly universal feature of biotic populations that as measured values increase for a population, the populations become more stable (or less variable).

Several of the above studies included additional factors that improved variance–mean relationships (size of sampler for benthic studies, discharge for river studies), but the improvements to model fit were small relative to the strength of these relationships. We also assessed the influence of several factors on variance–mean relationships for bacterial abundance and production estimates and found that only small amounts of the residual variance could be explained by quantification techniques and habitat. In particular, thymidine incorporation techniques yielded more variable production estimates than leucine in the plankton and the trend was supported with benthic data, despite limited data. The AODC enumeration technique also yielded more variable estimates than DAPI in the plankton, but these differences were very small and not significant for benthic bacteria. Only one study enumerated bacterial abundance by flow cytometry, so we were unable to evaluate if this relatively new technique offers any advantages over traditional

Table 3. Published models predicting variance (s^2) based on means ($\bar{x}$) for different measures of aquatic biota.

Parameter	Model of $\log(s^2)$	r^2	n	Source
Spatial variance				
Abundance, lake benthos	$1.38 + 1.61\log\bar{x}$	0.97	69	1
Abundance, river benthos	$0.482 + 1.386\log\bar{x} + 0.047(\log\bar{x})^2 - 0.384\log(\text{sampler size})$	0.93	1461	2
Abundance, marine benthos	$0.262 + 1.22\log\bar{x}$	0.86	3015	7
Abundance, freshwater periphyton	$5.48 + 1.31\log\bar{x} - 0.26\log(\text{sampler size})$	0.89	55	3
Abundance, benthic bacteria	$0.39 + 1.81\log\bar{x}$	0.94	235	This study
Abundance, planktonic bacteria	$-0.24 + 1.85\log\bar{x}$	0.75	469	This study
Production, freshwater periphyton	$-1.06 + 1.88\log\bar{x}$	0.83	200	3
Production, benthic bacteria	$-0.95 + 2.25\log\bar{x}$	0.84	54	This study
Production, planktonic bacteria	$-1.28 + 1.86\log\bar{x}$	0.79	199	This study
Ash-free dry mass, freshwater periphyton	$-1.56 + 1.91\log\bar{x} + 0.47\log(\text{sampler size})$	0.80	187	3
Biovolume, freshwater periphyton	$-0.78 + 1.72\log\bar{x}$	0.76	94	3
Chlorophyll, freshwater periphyton	$-1.68 + 2.07\log\bar{x} + 0.45\log(\text{sampler size})$	0.84	1193	3
Dry mass, freshwater periphyton	$-0.75 + 1.81\log\bar{x} + 0.26\log(\text{sampler size})$	0.92	57	3
Biomass, macrophytes, lakes	$0.76 + 1.57\log\bar{x} - 0.16\log(\text{sampler size})$	0.95	1200	8
Biomass, macrophytes, rivers	$0.30 + 1.92\log\bar{x}$	0.94	48	4
Temporal variance				
Chlorophyll, seasonal, lakes	$-1.03 + 2.50\log\bar{x}$	0.94	68	5
Chlorophyll, annual, lakes	$-0.53 + 2.10\log\bar{x}$	0.93	47	5
Chlorophyll *a*, seasonal, river	$-1.44 + 2.13\log\bar{x}$	0.54	12	6

Note: Models are separated according to those predicting spatial variability (as in this study) and those predicting temporal variability. Sources are (1) Downing (1979); (2) Morin (1985); (3) Morin and Cattaneo (1992); (4) G.M. Carr, unpublished data; (5) Marshall et al. (1988); (6) Cattaneo and Prairie (1995); (7) Vézina (1988); (8) Downing and Anderson (1985).

microscopic techniques in terms of reducing variance in abundance estimates. Residual variance was not affected by experimental manipulation (planktonic bacteria) or substrata on which the samples were grown (benthic bacteria).

Peterman (1990) highlighted the fact that most studies in the aquatic sciences fail to consider the power of their analyses when a null hypothesis is not rejected, and others have echoed these comments (Osenberg et al. 1994; Steidl et al. 1997). The mean–variance relationships presented here for bacteria are useful in the planning stage of studies where decisions need to be made about sampling effort required to detect significant trends with sufficient power. Our analyses show that between three and seven replicates are usually sufficient to detect a doubling of means for abundance and production in both benthic and planktonic environments with a power of 80%; however, replication rate would need to be increased to detect even a 50% difference in means with the same power. Production estimates need slightly more replicates to detect a specific difference among means than abundance estimates, whereas benthic bacteria need more replication than planktonic bacteria.

Among the studies examined here, the median replication rates for the different bacterial measures would be able to detect, with 80% power, a ratio of means equivalent to approximately 1.6 and 2.0 in the case of planktonic abundance and production and 2.4 and 2.6 in the case of benthic abundance and production, respectively. Thus, approximately half of the planktonic bacteria studies reviewed here would have been unable to detect a 50% difference in mean abundances, and a 100% difference, or doubling, in means could not be detected by approximately half of the benthic bacteria studies and also half the planktonic production studies. Clearly, the power of most studies to detect small differences in means is low and the ability of investigators to detect biologically meaningful trends in the data may be limited by the lack of power of many studies. Failure to consider sampling variance and the power to detect differences in means in the design of studies will inevitably lead to difficulties in interpretation of results.

Acknowledgements

This work was supported by an Ontario Graduate Scholarship to G.M.C. and a Natural Sciences and Engineering Research Council grant to A.M. Discussions with and reviews from J. Houlahan, J. Stephenson, S. Derrane, R. Sommaruga, and one anonymous referee greatly improved the manuscript.

References

Alldredge, A.L., Cole, J.J., and Caron, D.A. 1986. Production of heterotrophic bacteria inhabiting macroscopic organic aggregates (marine snow) from surface waters. Limnol. Oceanogr. **31**: 68–78.

Benner, R., and Biddanda, B. 1998. Photochemical transformations of surface and deep marine dissolved organic matter: effects on bacterial growth. Limnol. Oceanogr. **43**: 1373–1378.

Benner, R., Opsahl, S., Chin-Leo, G., Richey, J.E., and Forsberg, B.R. 1995. Bacterial carbon metabolism in the Amazon River system. Limnol. Oceanogr. **40**: 1262–1270.

Bertilsson, S., and Tranvik, L.J. 1998. Photochemically produced carboxylic acids as substrates for freshwater bacterioplankton. Limnol. Oceanogr. **43**: 885–895.

Boon, P.I. 1994. Discrimination of algal and bacterial alkaline phosphatases with a differential-inhibition technique. Aust. J. Mar. Freshw. Res. **45**: 83–107.

Bouvy, M., Arfi, R., Cecchi, P., Corbin, D., Pagano, M., Saint-Jean, L., and Thomas, S. 1998. Trophic coupling between bacterial and phytoplanktonic compartments in shallow tropical reservoirs (Ivory Coast, West Africa). Aquat. Microb. Ecol. **15**: 25–37.

Bunte, C., and Simon, M. 1999. Bacterioplankton turnover of dissolved free monosaccharides in a mesotrophic lake. Limnol. Oceanogr. **44**: 1862–1870.

Carlsson, P., and Caron, D.A. 2001. Seasonal variation of phosphorus limitation of bacterial growth in a small lake. Limnol. Oceanogr. **46**: 108–120.

Cattaneo, A., and Prairie, Y.T. 1995. Temporal variability in the chemical characteristics along the Rivière de l'Achigan: how many samples are necessary to describe stream chemistry? Can. J. Fish. Aquat. Sci. **52**: 828–835.

Cochlan, W.P. 2001. The heterotrophic bacterial response during a mesoscale iron enrichment experiment (IronEx II) in the eastern equatorial Pacific Ocean. Limnol. Oceanogr. **46**: 428–435.

Cole, J.J. 1999. Aquatic microbiology for ecosystem scientists: new and recycled paradigms in ecological microbiology. Ecosystems, **2**: 215–225.

Cole, J.J., and Pace, M.L. 1995. Bacterial secondary production in oxic and anoxic freshwaters. Limnol. Oceanogr. **40**: 1019–1027.

Downing, J.A. 1979. Aggregation, transformation, and the design of benthos sampling programs. J. Fish. Res. Board Can. **36**: 1454–1463.

Downing, J.A., and Anderson, M.R. 1985. Estimating the standing biomass of aquatic macrophytes. Can. J. Fish. Aquat. Sci. **42**: 1860–1869.

Edwards, R.T. 1987. Production of heterotrophic bacteria inhabiting macroscopic organic aggregates (marine snow) from surface waters. Limnol. Oceanogr. **32**: 221–234.

Eisenmann, H., Burgherr, P., and Meyer, E.I. 1999. Spatial and temporal heterogeneity of an epilithic streambed community in relation to the habitat templet. Can. J. Fish. Aquat. Sci. **56**: 1452–1460.

Ferguson, R.L., and Rublee, P. 1976. Contribution of bacteria to standing crop of coastal plankton. Limnol. Oceanogr. **21**: 141–145.

Findlay, S., Meyer, J.L., and Edwards, R.T. 1984. Measuring bacterial production via rate of incorporation of [^{3}H] thymidine into DNA. J. Microbiol. Methods, **2**: 57–72.

Findlay, S., Carlough, L., Crocker, M.T., Gill, H.K., Meyer, J.L., and Smith, P.J. 1986. Bacterial growth on macrophyte leachate and fate of bacterial production. Limnol. Oceanogr. **31**: 1335–1341.

Findlay, S., Howe, K., and Fontvieille, D. 1993. Bacterial-algal relationships in streams of the Hubbard Brook Experimental Forest. Ecology, **74**: 2326–2336.

Freeman, C., and Lock, M.A. 1995. The biofilm polysaccharide matrix: a buffer against changing organic substrate supply? Limnol. Oceanogr. **40**: 273–278.

Geesey, G.G., Mutch, R., and Costerton, J.W. 1978. Sessile bacteria: an important component of the microbial population in small mountain streams. Limnol. Oceanogr. **23**: 1214–1223.

Hines, W.W., and Montgomery, D.C. 1980. Probability and statistics in engineering and management science. 2nd ed. John Wiley & Sons, New York.

Hobbie, J.E., Daley, R.J., and Jasper, J. 1977. Use of Nuclepore filters for counting bacteria by fluorescence microscopy. Appl. Environ. Microbiol. **33**: 1225–1228.

Hudson, J.J., Roff, J.C., and Burnison, B.K. 1990. Measuring epilithic bacterial production in streams. Can. J. Fish. Aquat. Sci. **47**: 1813–1820.

Hudson, J.J., Roff, J.C., and Burnison, B.K. 1992. Bacterial productivity in forested and open streams in southern Ontario. Can. J. Fish. Aquat. Sci. **49**: 2412–2422.

Kaplan, L.A., and Bott, T.L. 1989. Diel fluctuations in bacterial activity on streambed substrata during vernal algal blooms: effects of temperature, water chemistry, and habitat. Limnol. Oceanogr. **34**: 718–733.

Kirchman, D.L., Meon, B., Cottrell, M.T., Hutchins, D.A., Weeks, D., and Bruland, K.W. 2000. Carbon versus iron limitation of bacterial growth in the California upwelling regime. Limnol. Oceanogr. **45**: 1681–1688.

Kroer, N. 1993. Bacterial growth efficiency on natural dissolved organic matter. Limnol. Oceanogr. **38**: 1282–1290.

Langenheder, S., and Jürgens, K. 2001. Regulation of bacterial biomass and community structure by metazoan and protozoan predation. Limnol. Oceanogr. **46**: 121–134.

Ledger, M.E., and Hildrew, A.G. 1998. Temporal and spatial variation in the epilithic biofilm of an acid stream. Freshwater Biol. **40**: 655–670.

Lind, O.T., and Dávalos-Lind, L. 1991. Production of heterotrophic bacteria inhabiting macroscopic organic aggregates (marine snow) from surface waters. Limnol. Oceanogr. **36**: 1200–1208.

Lindell, M.J., Granéli, W., and Tranvik, L.J. 1995. Enhanced bacterial growth in response to photochemical transformation of dissolved organic matter. Limnol. Oceanogr. **40**: 195–199.

Lock, M.A., Wallace, R.R., Costerton, J.W., Ventullo, R.M., and Charlton, S.E. 1984. River epilithon: toward a structural-functional model. Oikos, **42**: 10–22.

Marshall, C.T., Morin, A., and Peters, R.H. 1988. Estimates of mean chlorophyll-*a* concentration: precision, accuracy, and sampling design. Water Resour. Bull. **24**: 1027–1034.

Moeseneder, M.M., and Herndl, G.J. 1995. Influence of turbulence on bacterial production in the sea. Limnol. Oceanogr. **40**: 1466–1473.

Mohamed, M.N., Lawrence, J.R., and Robarts, R.D. 1998. Phosphorus limitation of heterotrophic biofilms from the Fraser River, British Columbia, and the effects of pulp mill effluent. Microb. Ecol. **36**: 121–130.

Morin, A. 1985. Variability of density estimates and the optimization of sampling programs for stream benthos. Can. J. Fish. Aquat. Sci. **42**: 1530–1534.

Morin, A., and Cattaneo, A. 1992. Factors affecting sampling variability of freshwater periphyton and the power of periphyton studies. Can. J. Fish. Aquat. Sci. **49**: 1695–1703.

Neely, R.K., and Wetzel, R.G. 1995. Simultaneous use of ^{14}C and ^{3}H to determine autotrophic production and bacterial protein production in periphyton. Microb. Ecol. **30**: 227–237.

Osenberg, C.W., Schmitt, R.J., Holbrook, S.J., Abu-Saba, J.E., and Flegal, A.R. 1994. Detection of environmental impacts: natural variability, effect size, and power analysis. Ecol. Appl. **4**: 16–30.

Palumbo, A.V., Bogle, M.A., Turner, R.R., Elwood, J.W., and Mulholland, P.J. 1987. Bacterial communities in acidic and circumneutral streams. Appl. Environ. Microbiol. **53**: 337–344.

Peterman, R.M. 1990. Statistical power analysis can improve fisheries research and management. Can. J. Fish. Aquat. Sci. **47**: 2–15.

Porter, K.G., and Feig, Y.G. 1980. The use of DAPI for identifying and counting aquatic microflora. Limnol. Oceanogr. **25**: 943–946.

Rich, J.H., Ducklow, H.W., and Kirchman, D.L. 1996. Concentrations and uptake of neutral monosaccharides along 140°W in the equatorial Pacific: contribution of glucose to heterotrophic bacterial activity and the DOM flux. Limnol. Oceanogr. **41**: 595–604.

Romaní, A.M., and Sabater, S. 1997. Metabolism recovery of a stromatolitic biofilm after drought in a Mediterranean stream. Arch. Hydrobiol. **140**: 261–271.

Romaní, A.M., and Sabater, S. 1999*a*. Epilithic ectoenzyme activity in a nutrient-rich Mediterranean river. Aquat. Sci. **61**: 122–132.

Romaní, A.M., and Sabater, S. 1999*b*. Effect of primary producers on the heterotrophic metabolism of a stream biofilm. Freshwater Biol. **41**: 729–736.

Rosenfeld, J.S., and Hudson, J.J. 1997. Primary production, bacterial production, and invertebrate biomass in pools and riffles in southern Ontario streams. Arch. Hydrobiol. **139**: 301–316.

Sabater, S., and Romaní, A.M. 1996. Metabolic changes associated with biofilm formation in an undisturbed Mediterranean stream. Hydrobiologia, **335**: 107–113.

Scavia, D., and Laird, G.A. 1987. Bacterioplankton in Lake Michigan: dynamics, controls, and significance to carbon flux. Limnol. Oceanogr. **32**: 1017–1033.

Scavia, D., Laird, G.A., and Fahnenstiel, G.L. 1986. Production of planktonic bacteria in Lake Michigan. Limnol. Oceanogr. **31**: 612–626.

Seitzinger, S.P., and Sanders, R.W. 1999. Atmospheric inputs of dissolved organic nitrogen stimulate estuarine bacteria and phytoplankton. Limnol. Oceanogr. **44**: 721–730.

Sherr, E., and Sherr, B. 1988. Role of microbes in pelagic food webs: a revised concept. Limnol. Oceanogr. **33**: 1225–1227.

Smith, D.C., and Azam, F. 1992. A simple economical method for measuring bacterial protein synthesis rates in seawater using ^{3}H-leucine. Mar. Microb. Food Webs, **6**: 107–114.

Steidl, R.J., Hayes, J.P., and Schauber, E. 1997. Statistical power analysis in wildlife research. J. Wildl. Manag. **61**: 270–279.

Stock, M.S., and Ward, A.K. 1989. Establishment of a bedrock epilithic community in a small stream: microbial (algal and bacterial) metabolism and physical structure. Can. J. Fish. Aquat. Sci. **46**: 1874–1883.

Suzuki, M.T., Sherr, E.B., and Sherr, B.F. 1993. DAPI direct counting underestimates bacterial abundances and average cell size compared to AO direct counting. Limnol. Oceanogr. **38**: 1566–1570.

Tapper, M.A., and Hicks, R.E. 1998. Temperate viruses and lysogeny in Lake Superior bacterioplankton. Limnol. Oceanogr. **43**: 95–103.

Theil-Nielsen, J., and Søndergaard, M. 1999. Production of epiphytic bacteria and bacterioplankton in three shallow lakes. Oikos, **86**: 283–292.

Tranvik, L. 1994. Effects of colloidal organic matter on the growth of bacteria and protists in lake water. Limnol. Oceanogr. **39**: 1276–1285.

Vézina, A.F. 1988. Sampling variance and the design of quantitative surveys of the marine benthos. Mar. Biol. **97**: 151–155.

Is the introduction of benthic species necessary for open-water chemical reconstruction in diatom-based transfer functions?

Aline Philibert and Yves T. Prairie

Abstract: Despite the overwhelming tendency in paleolimnology to use both planktonic and benthic diatoms when inferring open-water chemical conditions, it remains questionable whether all taxa are appropriate and necessary to construct useful inference models. We examined this question using a 75-lake training set from Quebec (Canada) to assess whether model performance is affected by the deletion of benthic species. Because benthic species are known to experience very different chemical conditions than their planktonic counterparts, we hypothesized that they would introduce undesirable noise in the calibration. Surprisingly, such important variables as pH, total phosphorus (TP), total nitrogen (TN), and dissolved organic carbon (DOC) were well predicted from weighted-averaging partial least square (WA-PLS) models based solely on benthic species. Similar results were obtained regardless of the depth of the lakes. Although the effective number of occurrence (*N*2) and the tolerance of species influenced the stability of the model residual error (jackknife), the number of species was the major factor responsible for the weaker inference models when based on planktonic diatoms alone. Indeed, when controlled for the number of species in WA-PLS models, individual planktonic diatom species showed superior predictive power over individual benthic species in inferring open-water chemical conditions.

Résumé : Même si la quasi-totalité des modèles en paléolimnologie utilise à la fois les espèces planctoniques et benthiques pour prédire les conditions physico-chimiques en eaux libres, on pourrait se demander si en effet toutes les espèces sont bien utiles. Afin de pousser d'avantage cette réflexion, nous avons travaillé sur un ensemble de calibration constitué de 75 lacs au Québec (Canada). Tout d'abord nous avons évalué si lors de l'omission des taxons benthiques la performance des modèles était affectée. Comme les taxons benthiques sont connus pour nicher sous des conditions chimiques différentes de celles de leur analogues planctoniques, nous avions la présomption que les taxons benthiques pourraient introduire du bruit de fond dans les modèles. A notre grande surprise, les meilleures prédictions pour le pH, le phosphore total (PT), l'azote total (NT) ou encore le carbone organiques dissous ont été obtenues sur des modèles basés uniquement des espèces benthiques. Même en faisant varier la profondeur des lacs nous avons obtenus les mêmes résultats. Si le nombre d'occurrence effective (*N*2) ou encore la tolérance des espèces influençaient la stabilité de la racine de l'erreur quadratique (en <<jackknife>>), le nombre d'espèces inclues dans le modèle était indéniablement le facteur clé qui était responsable quant à la faiblesse des modèles basés uniquement sur les taxons planctoniques. En effet, pour le même nombre d'espèces inclus dans nos modèles, les espèces planctoniques offrent un potentiel de prédiction supérieur à celui des espèces benthiques.

Introduction

Most recent methodological advances in paleolimnology have focused on methodology for sample collection (Renberg 1981; Glew 1988), chronological techniques (MacDonald et al. 1991), and in particular, statistical modelling (ter Braak and van Dam 1989; Birks et al. 1990; ter Braak and Juggins 1993). Although these have undoubtedly led to significantly better paleoreconstruction models, it is surprising that so few studies have examined some of the more fundamental underpinnings of the paleolimnological approach. For example, accurate estimates of past environmental conditions are based on biological assemblages and assume that we can statistically model the present-day responses of any species in relation to the open-water conditions. Although this assumption is probably correct for many organisms, it is likely inappropriate for organisms adapted to low light conditions or other microhabitats (i.e., inhabiting the hypolimnion or near the sediment–water interface). Because these organisms are essentially sessile, they experience a different range of light intensities depending their depth and the substrate to which they are attached (Vadeboncoeur and Lodge 2000). Moreover, the chemistry of these environments can be notoriously different from that of the mixed layer (Wetzel 1983; Hansson 1992; Blumenshine et al. 1997), and there is little evidence of a good correlation between the chemical conditions of these two environments. This problem is particularly acute with paleolimnological

Received 15 November 2001. Accepted 31 March 2002. Published on the NRC Research Press Web site at http://cjfas.nrc.ca on 12 July 2002.
J16613

A. Philibert[1] and Y.T. Prairie. Département des Sciences Biologiques, Université du Québec à Montréal, UQÀM, P.O. Box 8888, Station Centre-Ville Montréal, QC H3C 3P8, Canada.

[1] Corresponding author (e-mail: alinediatom@yahoo.ca).

DOI: 10.1139/F02-061

calibrations based on diatoms because benthic diatoms often dominate the assemblages in many environments (Cameron et al. 1999; Dixit et al. 1999; Fallu and Pienitz 1999). Nevertheless, most diatom-based transfer functions are based on complete diatom assemblages (pelagic, littoral, or benthic ones), even if the stated purpose is to predict open-water chemical conditions (Siver 1999).

Here, we hypothesize that benthic diatoms are likely to introduce noise in predictive models because of the disparity of nutrient pools (Blumenshine et al. 1997), coupled with the higher degree of variability in the physical and chemical conditions under which benthic algae grow (Wetzel 1983; Burkholder and Wetzel 1990). For example, the nature and distribution of the substratum with respect to light and depth affect the response of benthic algae to changes in water-column nutrients (Vadeboncoeur and Lodge 2000). In addition, fluxes from the sediment can greatly enhance their nutrient supply (Hansson 1992; Scheffer 1998; Siver 1999). Some authors have already argued that it would be more appropriate to base predictive models solely on planktonic species that inhabit the open-water habitat (Bennion 1994; Siver 1999). In particular, Siver (1999) established outstanding models from Connecticut lakes (U.S.A.) solely based on planktonic diatoms for pH, total nitrogen (TN), and specific conductivity. Whether this high performance from using planktonic diatoms alone is a general phenomenon has, however, not been widely tested.

Our main objective in this study was to assess whether the performance of diatom-based inference models can be improved through the deletion of benthic species. First, we tested whether calibration models based solely on planktonic diatoms were able to produce robust and reliable predictions of selected environmental variables in the training set. Second, we compared the predictive power of models based on planktonic species only, benthic species only, and all species combined. Because the relative abundance of planktonic and benthic species is itself a function of lake characteristics, such as lake depth and light penetration, we further examined our hypothesis in shallow and deep lakes separately. In deep lakes ($Z_{\max} > 10$ m) that stratify during summer and where planktonic species are relatively more abundant than benthic species (a mean of 74%), we expect planktonic diatoms to be superior predictors of environmental variables. Conversely, in shallow lakes ($Z_{\max} < 10$ m), we expect benthic taxa to have better predictive power.

In addition to habitat type and depth, we further examined whether other potentially confounding characteristics of the species assemblages could influence the model performance. Therefore, throughout our analyses, we took into account how the model performance varied with the number of taxa included in the model, the effective number of occurrence (*N*2), and the tolerance of each species.

Materials and methods

Study sites

Our calibration set consists of 75 lakes, 40 from Abitibi and 35 from Réservoir Gouin (Haute Mauricie) (Fig. 1). Overall, the study lakes from the two regions are fairly shallow (median maximum depth = 10 m) and small (0.01–2.31 km^2), with watershed areas ranging from 0.09 km^2 to 19.72 km^2. The water chemistry of the lakes is diverse (Table 1). The lakes range from clear to dark, with corresponding dissolved organic carbon (DOC) concentrations between 1.8 and 18.5 mg·L^{-1}. The lakes are mostly dimictic, except for the very shallow lakes, which do not stratify. In Abitibi, lakes range from oligotrophic to eutrophic (2.8–52 μg·L^{-1} total phosphorus, TP), a range that encompasses all of the lakes from Haute Mauricie (4.9–16.5 μg·L^{-1}). Similarly, the lakes in Haute Mauricie are slightly acidic to circumneutral (pH = 5.6–7.0), whereas lakes in Abitibi span a wider pH range (between 4.2 and 8). Climate variables (temperature and precipitation) of the two regions are similar because of their close proximity (for more details, see Philibert and Prairie 2002).

The sampling and measurement of environmental variables, as well as the counting of diatoms, followed standard methods. The taxonomy and nomenclature was primarily based on Krammer and Lange-Bertalot (1986–1991) and Hustedt (1930–1966). The distinction between planktonic and benthic taxa in our data set was, at times, a difficult and somewhat arbitrary task. We based our classification on what is generally accepted in the literature, yet we fully acknowledge that some "ambiguous" algae exist (such as *Aulacoseira subarctica*, *Asterionella formosa*, and *Tabellaria flocculosa*), i.e., those that may have been collected in pelagic zones in one study and referred to as benthic in other areas. On this basis, a maximum of about 7% of the species could be classified as ambiguous, and in these cases, we followed the recommendations of algal taxonomists, including one working on live diatoms from the Haute Mauricie region. Appendix A describes the flora and reports the "pelagic" or "benthic" appellation attributed to species used in this study. A total number of 214 diatom species were identified, of which 47 were classified as planktonic and 167 as benthic (see Appendix A).

Statistical analyses

The training set thus consisted of a total of 214 diatoms collected from 75 lakes for which we measured 18 environmental variables (Table 1; for more details, see Philibert and Prairie 2002). To test whether the three groups of taxa (planktonic, benthic,and combined) conserved the same predictive potential according the maximal depth in lakes, we divided our calibration set of 75 lakes into two classes: shallow and deep. Because the maximum depth in the calibration set ranged from 1 to 34 m, we chose the depth of 10 m as a limit between shallow and deep basins. Thirty-five lakes were classified as shallow lakes, and 40 as deep.

As Wilson et al. (1996) noted, most calibration data sets published to date have chosen their criteria for species deletion according a minimal percentage of abundance and occurrence in lakes, e.g., 1% abundance in at least one lake (Fritz et al. 1993), 2% in at least one lake (Fritz et al. 1991), or 1% in at least three lakes (Wilson et al. 1996). Because our hypotheses concern the effect of both the number of species and the *N*2 on the predictive ability of predictive models, we used the most inclusive criterion, i.e., all taxa with at least 1% abundance in one lake.

Multivariate statistical techniques were used to explore the relationships between environmental variables and diatom taxa and to identify the variables most likely to produce

Fig. 1. Map showing sampling sites in Québec, Canada. Lakes sampled are presented by solid circles.

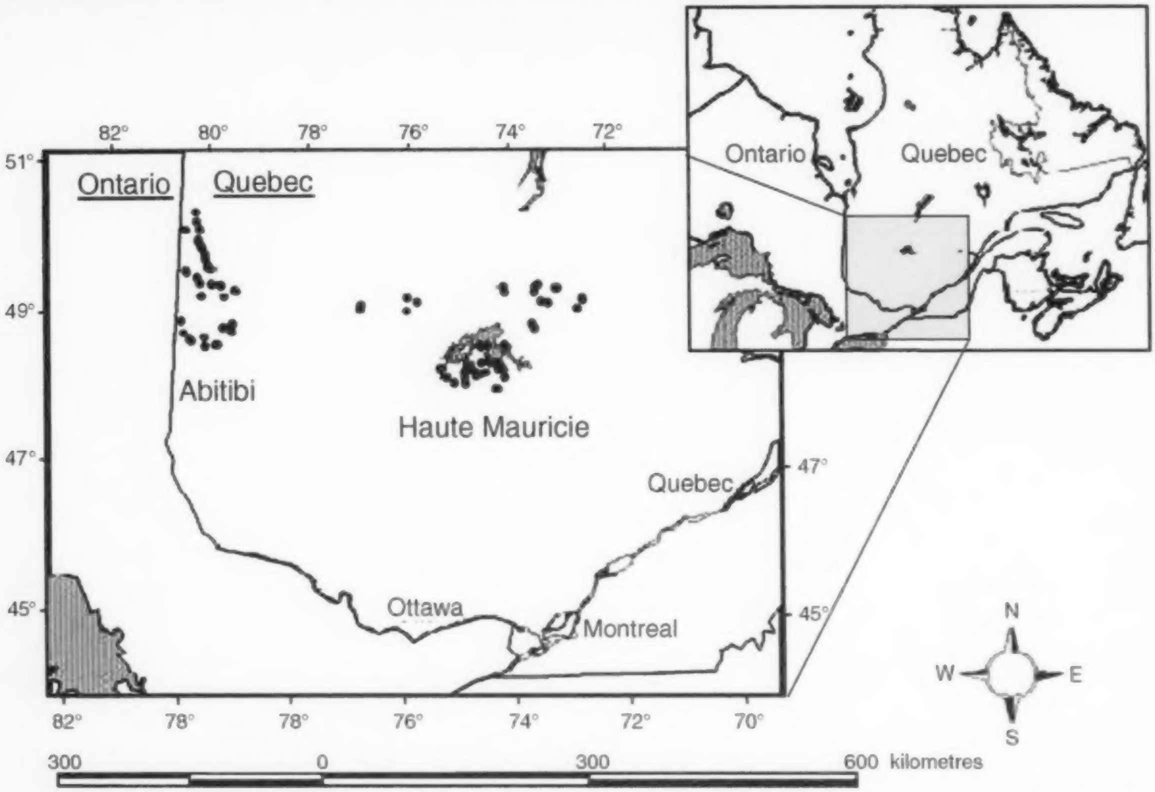

the most reliable inference models. The environmental variables were log-transformed because of their heterogeneous distribution. A canonical correspondence analysis (CCA) with forward selection was carried out to select the environmental variables retained for inference models using CANOCO version 4.0 for Windows (ter Braak and Smilauer 1998). Among the forward-selected variables in which we were interested were pH, TP, TN, and DOC. Before the development of transfer functions, a series of detrended CCA (DCCA), constrained solely to each environmental variable of interest (pH, TP, TN, and DOC), were used to establish the significance of selected variables in the explanation of diatom distributions (ter Braak and Prentice 1988; Birks 1995). Furthermore, this series of DCCA were also performed first to determine the species gradient lengths with respect to the selected variable and then to determine if unimodal, or linear-based, models of reconstruction were most appropriate (Birks 1995, 1998). For each environmental variable retained, a DCCA was done with detrending-by-segments, non-linear rescaling to estimate the lengths of compositional gradients. This was achieved using the computer program CANOCO version 4.0 for Windows (ter Braak and Smilauer 1998). Also, a partial CCA (pCCA) constrained on each variable with or without co-variable was carried out to validate the independent information carried by the individual variables.

Several calibration models assuming a unimodal response between taxa and environmental variables were tested, such as simple weighted-averaging (WA) or inverse deshrinking WA, with or without tolerance downweighting of each taxon (Birks et al. 1990). Weighted-averaging partial least square (WA-PLS) using one or several components was also developed. Linear relationships between organisms and their environment were tested from partial least square calibration models (PLS). On the basis of various simulations and comparisons, the above models were compared to assess which one performed the best for each variable. All unimodal models mentioned earlier and the linear PLS models were carried out using the computer program WACALIB version 3.3 (Line et al. 1994). In all cases, DCCA models included species gradients with lengths superior to 2 standard deviations (SD). Because WA-PLS techniques offered best predictions regardless of the variable, they were used throughout for testing our hypotheses.

We concentrated on statistical requirements for robust models, such as the lowest root mean square error (RMSE). As noted in Birks (1998), model performance statistics such as RMSE are not dependent on the range of the observed environmental gradient, unlike the coefficient of determination (r^2), which measures the strength of the relationship between observed and predicted values (Birks 1998). Apparent RMSE were used when testing the effect of lake depth because the combination of only 47 taxa in smaller subsets of lakes (shallow and deep) rendered jackknife procedures highly unstable.

When we performed tests to control for the influence of

Table 1. Summary of the ranges of environmental variables for both study regions (Abitibi and Haute Mauricie).

Variables	Minimum	Maximum	Mean	Median	SD
LAT (°N)	47.80	49.70	48.68	48.79	0.48
LON (°W)	–73.32	–79.47	–77.13	–78.68	2.23
ALT (m)	280.00	558.00	377.0	366.0	71.41
LA (km^2)	0.01	2.38	0.32	0.28	0.34
DA (km^2)	0.09	21.68	2.64	1.75	3.33
DA/LA	1.90	48.76	11.64	8.79	10.22
DA/VOL	0.24	28.56	3.84	2.58	4.38
T_w (year)	0.08	5.70	1.11	0.77	1.04
Z_{max} (m)	1.00	34.00	10.69	10.00	6.75
Z (m)	1.44	10.10	4.03	3.66	1.96
Secchi (m)	0.25	6.62	2.78	2.43	1.54
DOC (mg·L^{-1})	1.75	16.72	7.98	6.70	3.89
TP (μg·L^{-1})	2.75	30.50	10.28	9.00	5.89
TN (μg·L^{-1})	79.00	1489.50	249.2	286.31	20.80
NO_3^{2-} (μg·L^{-1})	0.45	146.00	9.70	4.89	17.95
NH_4 (μg·L^{-1})	3.50	657.00	20.31	8.84	75.13
pH	4.16	8.00	6.30	6.39	0.76
Alkalinity (μeq·L^{-1})	4.30	2495.00	191.93	57.30	362.00
Chl *a* (μg·L^{-1})	1.10	32.90	3.71	2.50	4.23
Ca^{2+} (mg·L^{-1})	0.24	16.66	2.57	1.63	2.94
Mg^{2+} (mg·L^{-1})	0.18	3.46	0.62	0.44	0.55

Note: SD, standard deviation; latitude, LAT; longitude, LON; altitude, ALT; lake area, LA; drainage area, DA; volume, VOL; residence time, T_w; maximal depth, Z_{max}; mean depth, Z; Secchi depth, Secchi; dissolved organic carbon (DOC), total phosphorus, TP; total nitrogen, TN; nitrates, NO_3^{2-}; ammonium, NH_4; chlorophyll *a*, Chl *a*; calcium, Ca^{2+}; magnesium, Mg^{2+}; fraction of incident light, LUM.

the total number of species, the tolerance of species, or the effective number of occurrences or Hill's *N*2 (Hill 1973), we focused our analyses on pH as the main environmental variable. Because of the large and more even pH span between 4 and 8.5, we were able to use jackknife measures of fit and precision and compared our results with other similar studies (Birks 1994; Wilson et al. 1996). All tests performed to assess which factors influence the most diatom distribution and model performance were done using a SAS/IML implementation of the WA-PLS algorithm (Y.T. Prairie, unpublished). The WA species tolerance was calculated following weighted averaging. The *N*2 can be considered as the effective number of occurrences of each species. It includes both the occurrences of species and the relative abundances in all lakes within the training set (Hill 1973). *N*2 is the inverse of the Simpson index.

Results

General relationships

Among the CCA forward-selected variables were pH, total phosphorus (TP), total nitrogen (TN), and dissolved organic carbon (DOC). After a series of constrained DCCAs, the variables pH, TP, TN, and DOC were selected as significant environmental variables ($p < 0.05$) that were likely the best predictors of species change. That was done for the three taxa groupings (planktonic, benthic, and all species) and on all classes of lake depths (shallow, deep, and the whole set of 75 lakes).

Planktonic, benthic, or both?

For all environmental variables retained, we were able to develop significant predictive WA-PLS models (3 components) using only planktonic species, only benthic species, or by combining all diatoms (Table 2). However, their predictive power differed greatly. Surprisingly, using only planktonic diatoms systematically produced the worst models with RMSE significantly larger than those of either only benthic or all taxa models (*F* test on the ratio of the residual variances, $p < 0.05$). The best models were invariably produced when all taxa were included, although their predictive power was statistically indistinguishable from models based on benthic species only (*T* test, $p < 0.05$). This same trend was observed for all four environmental variables (pH, TP, TN, and DOC). Independently of the species grouping included in WA-PLS models, pH was the best-predicted environmental variable.

The influence of the species number

The large variability in the number of species (planktonic or benthic) included in our predictive models made it difficult to separate the effect of the number of species from the effect of the type of taxa considered. Indeed, we identified 47 planktonic and 167 benthic diatoms. Using the complete set (all diatoms), we examined how species number influences prediction by successively deleting species at random and re-estimated a WA-PLS model at each model reduction. For pH models, the greatest lost of predictive power occurred when the number of species was below 120 (Fig. 2), providing a preliminary threshold value when species deletion is carried at random regardless of species characteristic. We then repeated the same exercise for each group of dia-

Table 2. Weighted-averaging partial least square models (WA-PLS) based on three groups of diatoms: planktonic, benthic, and all taxa.

	Performance	PH (units)	TP ($\mu g \cdot L^{-1}$)	TN ($\mu g \cdot L^{-1}$)	DOC ($mg \cdot L^{-1}$)
Training set (*n* = 75)					
Planktonic	r^2	0.66*	0.65*	0.82	0.64*
	RMSE	0.44*	3.74*	77.43*	2.32*
Benthic	r^2	0.92	0.82	0.88	0.86
	RMSE	0.21	2.51	61.81	1.45
All taxa	r^2	0.94	0.92	0.93	0.89
	RMSE	0.18	1.65	49.38	1.28
Deep lakes (*n* = 42)					
Planktonic	r^2	0.89	0.48*	0.77*	0.60*
	RMSE	0.24*	1.97*	37.34*	14.36*
Benthic	r^2	0.93	0.92	0.89	0.91
	RMSE	0.18	0.74	25.28	6.87
All taxa	r^2	0.96	0.81	0.92	0.83
	RMSE	0.14	1.11	21.54	9.24
Shallow lakes (*n* = 35)					
Planktonic	r^2	0.68*	0.89	0.79*	0.79*
	RMSE	0.46*	3.86*	1.94*	1.94*
Benthic	r^2	0.96	0.91	0.96	0.96
	RMSE	0.16	2.13	0.82	0.82
All taxa	r^2	0.95	0.97	0.95	0.95
	RMSE	0.18	1.11	0.92	0.92

Note: WA-PLS were executed for pH, total phosphorus (TP), total nitrogen (TN), and dissolved organic carbon (DOC) predictions in the training set of 75 lakes, deep lakes (*n* = 42) and shallow lakes (*n* = 35). Apparent root mean square error (RMSE) and r^2 accounted for the robustness and the reliability of these models. Number of components = 3. Asterisks (*) indicate significant differences between r^2 and RMSE of planktonic algae and the two other groups.

Fig. 2. Plot of root mean square error of prediction $\mathrm{RMSE}_{\mathrm{jackknife}}$ for pH generated randomly from different numbers of species with regard to the type of taxa (planktonic or (and) benthic diatoms). Data sets were generated at 20-species intervals using a random number generator without replacement, performed 10 times for each interval. The mean of $\mathrm{RMSE}_{\mathrm{jackknife}}$ from the 10 runs and corresponding to a certain number of species is represented by each solid square in the plot.

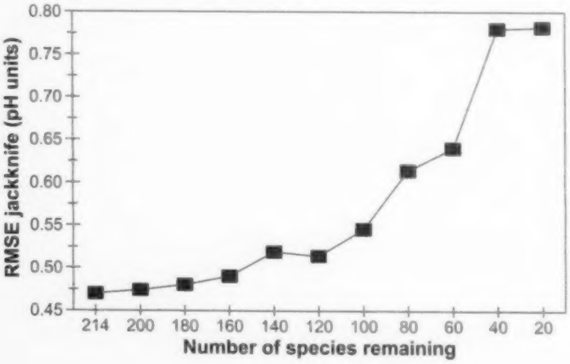

Fig. 3. Plot of root mean square error of prediction $\mathrm{RMSE}_{\mathrm{jackknife}}$ for pH generated randomly from different numbers of species with regard to the type of taxa (planktonic or (and) benthic diatoms). Data sets were generated at 47 species and 5-species intervals using a random number generator without replacement, performed 10 times for each interval. The mean of $\mathrm{RMSE}_{\mathrm{jackknife}}$ from the 10 runs is indicated by the number of species corresponding. All taxa merged together, planktonic species, and benthic species are represented by squares, solid ovals, and solid triangles, respectively.

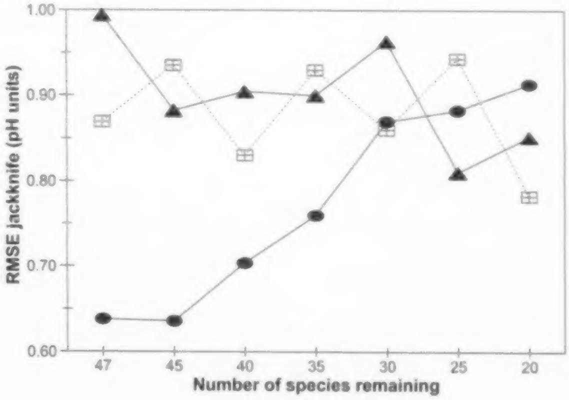

toms separately. For a given number of species (starting with 47, the total number of planktonic species) included in the models, planktonic diatoms yielded the better predictive potential (lowest $\mathrm{RMSE}_{\mathrm{jackknife}}$) in comparison to benthic species, except when the number of species dropped below 25 (Fig. 3). The same trend was obtained for all of the other three variables (TP, TN, and DOC). This is an important result as it argues that the higher performance of benthic taxa is essentially a species number phenomenon. Although each individual planktonic species carries more predictive information when controlled for the number of species (Fig. 3),

Fig. 4. Plot showing the variation of the root mean square error $\mathrm{RMSE}_{\mathrm{jackknife}}$ for pH when the effective number of occurrence (*N*2) changes. We successively deleted species (*a*) with the lowest *N*2 number or (*b*) with the highest *N*2 number. At each *N*2 number, the number of species remaining in the weighted-averaging partial least square (WA-PLS) models was reported. In *a*, when the deletion criterion was at *N*2 = 2, all taxa having an *N*2 strictly inferior to 2 were eliminated. In *b*, when the deletion criterion was at *N*2 = 2, all taxa having an *N*2 superior or equal to 2 were eliminated. $\mathrm{RMSE}_{\mathrm{jackknife}}$ values and the number of species are represented by solid squares and solid triangles, respectively.

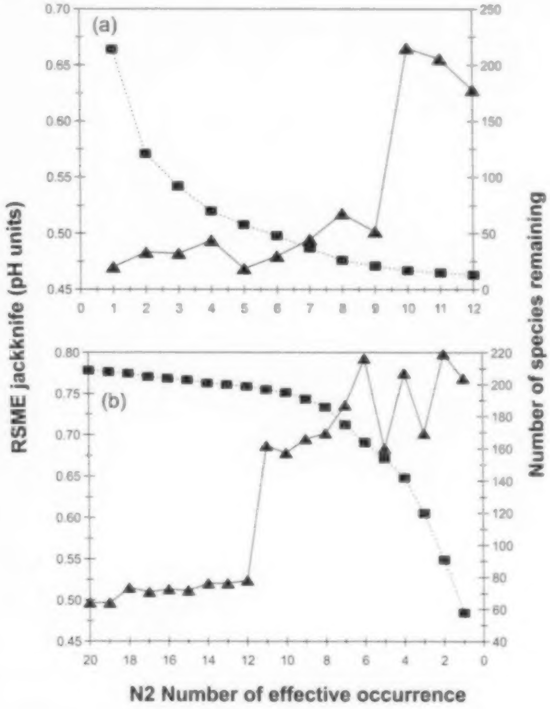

Fig. 5. Plot showing the variation of the weighted-averaging partial least square (WA-PLS) models root mean square error $\mathrm{RMSE}_{\mathrm{jackknife}}$ for pH when the species tolerance changes. We successively deleted species (*a*) with lowest pH tolerance or (*b*) with the highest pH tolerance. In *a*, when the deletion criterion was at tolerance = 2, all taxa having a pH tolerance strictly inferior to 2 were eliminated. In *b*, when the deletion criterion was at 2, all taxa having a pH tolerance superior or equal to 2 were removed. $\mathrm{RMSE}_{\mathrm{jackknife}}$ values and the number of species are represented by solid squares and solid triangles, respectively.

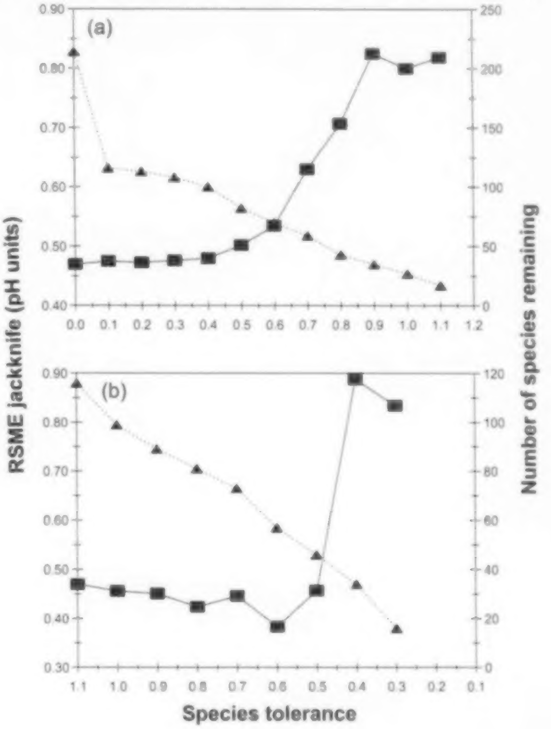

the more numerous benthic taxa collectively generated better models (Table 2). It is therefore not surprising that the best models are achieved when all species are combined (Table 2).

The role of depth

Planktonic species dominate in deep lakes and comprise an average of 88% of the diatoms relative abundance. Conversely, benthic species represent 59% of the total abundance in shallow basins. Models built for deep lakes ($Z_{\max} >$ 10 m) use apparent RMSE and r^2 indices because of the smaller number of lakes in models when separating the calibration set of 75 lakes into deep and shallow lakes. Benthic taxa and the group with all taxa combined produced significantly better predictions than planktonic ones for TP, TN, and DOC concentrations (higher r^2 and lower RMSE; Table 2). For pH, although the predictive power was not significantly different between groups of taxa, planktonic algae still produced the largest RMSE. The variable pH was the best-predicted variable independent of habitat type. The predictive power was statistically indistinguishable between models based on benthic taxa or on all taxa combined.

For shallow lakes ($Z_{\max} <$ 10 m), benthic taxa and the group using all taxa produced significantly stronger predictions (lower RMSE) than planktonic diatoms for pH, TN, and DOC (Table 2). Using only planktonic species systematically produced the largest RMSE. Regardless of the group of taxa, pH and DOC concentrations tended to be best predicted. Regardless of the depth of lakes, the deletion of benthic diatoms significantly diminished the predictive power in our WA-PLS models. The similarity of the patterns in both deep and shallow lakes suggests that lake depth does not modulate the relative importance of benthic or planktonic algae on model performance, again pointing to a species number phenomenon.

Species rarity: the role of the effective number of occurrence (*N*2)

Planktonic taxa were most abundant in 70% of the lakes. Dominant taxa included *Asterionella formosa*, *Aulacoseira subarctica*, *Cyclotella bodanica* var. *lemanica*, C. *stelligera*, and *Tabellaria flocculosa*. The most widely represented benthic taxa were *Brachysira brebissonnii*, *Eunotia bilunaris*, *E. incisa*, and *Frustulia rhomboides*. Hill's *N*2, an index of evenness that takes into account both the number of occurrences and the relative abundance, gave higher weights to the following taxa: *Cyclotella stelligera*, *Tabellaria flocculosa*, *Aulacoseira italica* var. *subarctica*, *Achnanthes minutissima*, *Cyclotella bodanica* var. *lemanica*, *Brachysira brebissonnii*, and *Frustulia rhomboides* var. *saxonica*. Sixty species may be considered as rare, with a low *N*2 number of 1 (see Appendix A). Because *N*2 between planktonic and benthic diatoms was significantly different (*T* test, $p < 0.05$), we tried to assess the influence of selected species deletion criteria on the WA-PLS pH model. This test was done by varying the *N*2 for individual taxa to be included in the predictive model. We tested the influence of the *N*2 on the performance of models by first successively deleting species with the lowest *N*2 and, conversely, successively deleting those with the largest *N*2 values.

The lowest $\mathrm{RMSE}_{\mathrm{jackknife}}$ occurred when all 214 taxa were included in the WA-PLS pH model ($\mathrm{RMSE}_{\mathrm{jackknife}} = 0.47$, $r^2_{\mathrm{jackknife}} = 0.60$) (Fig. 4*a*). The same observations were reported in Birks (1994) and Wilson et al. (1996) when using WA and $\mathrm{WA}_{(\mathrm{tol})}$ (weighted by species tolerance) models based on pH. Even if the deletion of species having $N2 < 2$ corresponded to a substantial species loss, the $\mathrm{RMSE}_{\mathrm{jackknife}}$ underwent very little change. There was a region of stability where the $\mathrm{RMSE}_{\mathrm{jackknife}}$ remained only slightly affected, when taxa having *N*2 from 1 to 9 were eliminated from the WA-PLS pH model. However, the number of species remaining in our models dropped abruptly in this range from 214 to 48 species and dropped under the critical number of species ($n \sim 120$) when $N2 > 3$ (Fig. 4*b*).

Our second numerical experiment, where species with the largest *N*2 were first eliminated, also yielded interesting results. As before, the lowest $\mathrm{RMSE}_{\mathrm{jackknife}}$ occurred when all taxa were included in the WA-PLS pH model (Fig. 4*a*). The $\mathrm{RMSE}_{\mathrm{jackknife}}$ varied only slightly between the deletion criteria of $N2 = 20$ and 12, probably because it corresponded to a minimal loss of species (only 15 species were eliminated). A rapid rise of $\mathrm{RMSE}_{\mathrm{jackknife}}$ occurred with taxa having an *N*2 lower than 11. The number of species remaining was therefore greater than the critical number required for the relative stability of the $\mathrm{RMSE}_{\mathrm{jackknife}}$ ($n \sim 120$ species). The deletion of species presenting an *N*2 inferior to 11 continued to decrease the predictive ability of our WA-PLS models. Very similar trends were observed for TP, TN, and DOC when we tested *N*2.

Species tolerance

Even if the average tolerance of planktonic and benthic diatoms for pH was similar (*T* test, $p < 0.05$), the distribution was different between both groups and was especially asymmetric for benthic taxa. Indeed, 40% of benthic taxa had a tolerance close to zero vs. 20% of planktonic species. We tried to assess whether the deletion of high tolerance species would improve the model performance. We calculated tolerance only for species with *N*2 higher than 3 to get relevant tolerance estimates. *Cymbella microcephala*, *Pinnularia braunii*, *Eunotia polyglyphis*, and *Aulacoseira perglabra* were the wider tolerance species for pH (see Appendix A), whereas *Tabellaria ventricosa*, *Fragilaria brevistriata*, *Eunotia linearis*, and *Navicula cryptotenella* had narrow pH tolerances. To vary the species tolerance for pH included in WA-PLS models, we first deleted species with the lowest tolerance for pH followed by species with the highest tolerance. The lowest $\mathrm{RMSE}_{\mathrm{jackknife}}$ occurred when all taxa were included in the WA-PLS pH model (Fig. 5*a*). However, even if analyses were done under the critical number of species (~120), there was a clear region of stability where deleting species with tolerance smaller than 0.6 pH units had little impact on the predictive power of the model. Beyond the lower tolerance limit of 0.6 pH units, the number of species dropped under 60 and the residual error rose.

In our next numerical experiment, higher pH tolerant species were eliminated first (Fig. 5*b*). Although small in magnitude, there is a trend for a decreasing $\mathrm{RMSE}_{\mathrm{jackknife}}$ when species of high tolerance are removed up to an upper tolerance limit of about 0.6. Past this threshold value, the number of species remaining was very small (less than 40) and the prediction error consequently rose very rapidly. The best model (in an absolute sense) was achieved when species of WA tolerances of 0.6 or greater were removed.

Discussion

Contrary to our expectations, pelagic taxa, i.e., those diatoms that are in direct contact with the measured environmental characteristics of interest, are less apt to yield powerful predictive models than benthic ones. This was true for all variables considered in this study. However, once we accounted for the number of species, we found that planktonic algae showed the best predictive power. Therefore, although each individual planktonic species brings more useful information into the predictive model than individual benthic species, the latter group nevertheless produced better models because the benthic habitat harbours a much richer and diverse diatom flora than the water column. This also explains why combining all taxa regardless of their habitat produces yet better models, with the lowest $\mathrm{RMSE}_{\mathrm{jackknife}}$.

Siver (1999) successfully developed transfer functions based solely on planktonic diatoms but restricted his analysis to lakes ($n = 46$) with greater than 50% planktonic diatoms. Unfortunately, he did not test whether including benthic taxa as well could develop even more effective models. To our knowledge, no other study examined this question of the effect of species deletion on the basis of habitat type (planktonic and (or) benthic) on model performance.

The results presented here indicate that benthic algae do respond, directly or indirectly, to changes in open-water chemistry. However, for pH and nutrients, particularly phosphorus, the open-water environment can have concentrations an order of magnitude lower than that experienced at the sediment–water interface, where benthic taxa live. One could argue that the benthic and planktonic habitats being physically juxtaposed (Blumenshine et al. 1997), they must show some chemical correspondence even if the strength of the planktonic–benthic coupling may vary among systems, depending on topography and depth. This planktonic–benthic coupling also generates the potential for several modes of interaction. For example, some studies also demonstrated that benthic algae are competitively depressed by planktonic ones (shading) in eutrophic lakes, suggesting a negative and indirect relation between benthic and pelagic processes (Hansson 1988). Regardless that the exact mechanism by which benthic algae respond to changes in open-water chemistry is not clear, our results suggest links between benthic and planktonic diatom communities with the environmental variables selected.

The deletion of rare species (with low *N*2 number) apparently had little impact on the performance in the WA-PLS pH model. In the training set, most species with low *N*2 number also had very low relative abundance in each sample site (significant correlation = 0.4, $p < 0.05$) and probably had very little weight in our WA-PLS pH models. Nevertheless, the plateau observed where the removal of species with $N2 < 9$ had little effect on model performance is surprising, particularly in light of the large number of species that this represents (only about 50 species are left at $N2 < 9$). Birks (1994) showed results similar to ours with little change in $\mathrm{RMSE}_{\mathrm{jackknife}}$ between *N*2 of 1 and 15. In contrast, the plateau was much narrower in Wilson et al. (1996), where WA and $\mathrm{WA}_{(\mathrm{tol})}$ models were approximately constant only within *N*2 values of 1 to 3, perhaps because the parameters (optima and tolerances) of these rare species are necessarily poorly estimated. The rapid rise in the $\mathrm{RMSE}_{\mathrm{jackknife}}$ observed after deleting species with *N*2 higher than 9 is likely due to the too low number of species remaining in our models ($n < 21$ species).

The experiment where species with a large *N*2 number were first deleted was also quite informative. First, very ubiquitous taxa (*N*2 higher than 11) apparently do not reduce the robustness of prediction by introducing noise in the calibration. Second, the sharp rise in $\mathrm{RMSE}_{\mathrm{jackknife}}$ when the *N*2 lower limit reached 11 was not a species number effect because very few species were in fact lost. This suggests that the few species that were lost in that removal procedure were indeed very important, although probably not related to their *N*2 values. Clearly, the effective number of occurrence *N*2 is not key to the predictive importance of a taxon.

Is tolerance an important attribute?

Our observation that deleting species of narrow tolerances did not degrade the model until too few species remained is an important result because it contravenes some fundamentals behind the paleolimnological approach, i.e., that species with a narrow environmental niche are particularly important. In our data set, as in many others, taxa with narrow tolerances are often rare taxa, and one can therefore question whether the estimated tolerance is small because the species is truly confined to specific environmental conditions or because the tolerance was so poorly estimated. Statistically, given two species of identical tolerance but of differing rareness, the probability, by chance, that the "rare" species will be deemed of narrower tolerance than its "frequent" counterpart is much greater than the reverse. However, in our case, the distinction is actually of little practical value because (*i*) the relation between rarity and tolerance is likely to remain in future data sets as well and (*ii*) our study clearly shows that no predictive power is lost when 75% of the species (those with the lowest tolerance) are removed. We suggest that rare species have poorly estimated optimas and that this may explain the reason why they are not very useful in predictive models. The reverse experiment (deleting wide tolerance species first) is incongruous with the first in that it showed essentially the same results: most species are not important to the prediction and their importance does not appear to be related to their tolerances. The only difference is that species with wide tolerances were shown to actually hinder predictive success or robustness; by deleting highest pH tolerant species, we obtained the lowest $\mathrm{RMSE}_{\mathrm{jackknife}}$ of all (0.38 pH units). Combining these two numerical experiments on species tolerances clearly cast some doubt on the long-held view that species tolerance is a key attribute in inference models.

The different findings of this study are puzzling. On the one hand, the relative performance of benthic vs. planktonic diatoms suggests that the more species included in the model, the more information is bundled in the model and the better is its predictive power. On the other hand, our species deletion experiments clearly show that most are useless in the models and that some actually hinder their performance. Although their ability to hinder performance seems related to their ubiquity, their importance cannot be attributed to either their effective occurrence or their tolerance, at least in our data set. Very similar conclusions based on an entirely different modeling approach were reached by Racca et al. (2002). However, the question remains entirely open as to what characteristics of a species make it important in a predictive model. Until this question is answered, our recommendation at this point is that the safest procedure is unfortunately to include every taxon. From an ecological point of view, including all species would capture all of the ecological signal and would ensure the best possible analogues in downcore reconstructions.

Acknowledgments

This paper was made possible through the support of the Network of Centres of Excellence–Sustainable Forest Management (SFM–NCE). We thank Dr. Richard Carignan (University of Montreal) for sharing the water chemistry data and Serge Paquet (University of Quebec in Montreal) for recommendations in the classification of benthic vs. planktonic species. Also, we acknowledge Marlène Le Bel, Alexandre Soucisse, and Dany Diotte for assistance in the field.

References

Bennion, H. 1994. A diatom–phosphorus transfer function for shallow, eutrophic ponds in southeast England. Hydrobiologia, **275/276**: 391–410.

Birks, H.J.B. 1994. The importance of pollen and diatom taxonomic precision in quantitative palaeoenvironment reconstructions. Rev. Paleobot. Palynol. **83**: 107–117.

Birks, H.J.B. 1995. Quantitative paleoenvironmental reconstructions. *In* Statistical modeling of Quaternary science data: technical guide 5. *Edited by* D. Maddy and J.S. Brew. Quaternary Research Association, Cambridge, England. pp. 161–264.

Birks, H.J.B. 1998. Numerical tools in paleolimnology progress potentialities and problems. J. Paleolimnol. **20**: 307–332.

Birks, H.J.B., Line, J.M., Juggins, S., Stevenson, A.C., and ter Braak, C.J.F. 1990. Diatoms and pH reconstructions. Philos. Trans. Rev. Soc. Lond. B, **327**: 263–278.

Blumenshine, S.C., Vadeboncoeur, Y., Lodge, D.M., Cottingham, K.L., and Knight, S.E. 1997. Benthic–pelagic links: responses of benthos to water-column nutrient enrichment. J. North Am. Benthol. Soc. **16**: 466–479.

Burkholder, J.M., and Wetzel, R.G. 1990. Alkaline phosphatase and algal biomass on natural and artificial plants: re-evaluation of the role of macrophytes as a phosphorus source for epiphytes. Limnol. Oceanogr. **35**: 736–746.

Cameron, N.G., Birks, H.J.B., Jones, V.J., Berge, F., Catalan, J., Flower, R.J., Garcia, J., Kawecka, B., Koinig, K.A., Marchetto, A., Sanchez-castillo, P., Sisko, M., Solovieva, N., Stefkova, E., and Toro, M. 1999. Surface-sediment and epilithic diatom pH calibration sets for remote European mountain lakes (AL: PE Project) and their comparison with the Surface Waters Acidification Programme (SWAP) calibration set. J. Paleolimnol. **22**: 291–317.

Dixit, S.S., Smol, J.P., Charles, D.F., Hughes, R.M., Paulsen, S.G., and Collins, G.B. 1999. Assessing water quality changes in the lakes of the northeastern United States using sediment diatoms. Can. J. Fish. Aquat. Sci. **56**: 131–152.

Fallu, M.A., and Pienitz, R. 1999. Diatomées lacustres de Jamésie–Hudsonie (Québec) et modèle de reconstitution des concentrations de carbone organique dissous. Ecoscience, **6**(4): 603–620.

Fritz, S.C., Juggins, S., Battarbee, R.W., and Engstrom, D.R. 1991. Reconstruction of past changes in salinity and climate using a diatom-based transfer function. Nature (London), **352**: 706–708.

Fritz, S.C., Juggins, S., and Battarbee, R.W. 1993. Diatom assemblages and ionic characterization of freshwater and saline lakes of the Northern Great Plains, North America: a tool for reconstructing past salinity and climate fluctuations. Can. J. Fish. Aquat. Sci. **50**: 1844–1856.

Glew, J.R. 1988. A new trigger mechanism for sediment samplers. J. Paleolimnol. **2**: 241–243.

Hansson, L.A. 1988. Effects of competitive interactions on the biomass development of planktonic and periphytic algae in lakes. Limnol. Oceanogr. **33**(1): 121–128.

Hansson, L.A. 1992. Factors regulating periphytic algal biomass. Limnol. Oceanogr. **37**: 322–328.

Hill, M.O. 1973. Diversity and eveness-unifying notation and its consequences. Ecology, **54**(2): 427–432.

Hustedt, F. 1930–1966. Die Kieselalgen : Deutschland, Österreich und der Schweiz unter Berückischtigung der übrigen Länder Europas sowie der augrendenzenden Meeresgebiete. Teil 1 (1930, pp. 920), 2 (1959, pp. 845), 3 (1961–1966, pp. 816), Ottokoeltz Science Publishers, Koenigstein, Germany. Reprinted 1991.

Krammer, K., and Lange-Bertalot, H. 1986–1991. Bacillariophyceae. Süsswasserflora von Mitteleuropa. Band 2(1–4). Vols. 1–4. Gustav Fischer Verlag Publisher, Stuttgart, Germany.

Line, J.M., ter Braak, C.J.F., and Birks, H.J.B. 1994. WACALIB 3.3, a computer program to reconstruct environmental variables from fossil assemblages by weighted averaging and to derive sample-specific errors of prediction. J. Paleolimnol. **10**: 147–152.

MacDonald, G.M., Beukens, R.P., and Kieser, W.E. 1991. Radiocarbon dating of limnic sediments: a comparative analysis of discussion. Ecology, **72**: 1150–1155.

Philibert, A., and Prairie, Y.T. 2002. Diatom-based transfer functions in western Quebec lakes (Abitibi and Haute Mauricie): the possible role of epilimnetic CO_2 concentration in influencing diatom assemblages. J. Paleolimnol. In press.

Racca, J.M.J., Wild, M., Birks, H.J.B., and Prairie, Y.T. 2002. Separating wheat from chaff. Diatom selection using an artificial neuronal network pruning algorithm. J. Paleolimnol. In press.

Renberg, I. 1981. Improved methods for sampling, and varve counting of varved lake sediments. Boreas, **10**: 255–258.

Scheffer, M. 1998. Ecology of shallow lakes. Chapman and Hall, London.

Siver, P. 1999. Development of paleolimnological inference models for pH, total phosphorus and specific conductivity based on planktonic diatoms. J. Paleolimnol. **21**: 45–59.

ter Braak, C.J.F., and Juggins, S. 1993. Weighted averaging partial least squares regression (WA-PLS): an improved method for reconstructing environmental variables from species assemblages. Hydrobiologia, **269/270**: 485–502.

ter Braak, C.J.F., and Prentice, I.C. 1988. A theory of gradient analysis. Adv. Ecol. Res. **18**: 271–317.

ter Braak, C.J.F., and Smilauer, P. 1998. CANOCO reference manual and user's guide to Canoco for Windows: software for canonical community ordination. Version 4. Microcomputer Power, Ithaca, N.Y.

ter Braak, C.J.F., and van Dam, H. 1989. Inferring pH for diatoms: a comparison of old and new calibration methods. Hydrobiologia, **178**: 209–223.

Vadeboncoeur, Y., and Lodge, D.M. 2000. Periphyton production on wood and sediment: substratum-specific response to laboratory and whole-lake nutrient manipulations. J. North Am. Benthol. Soc. **19**(1): 68–81.

Wetzel, R.G. 1983. Limnological analyses. Spring-Verlag, New York.

Wilson, S.E., Cumming, B.F., and Smol, J.P. 1996. Assessing the reliability of salinity inference models from diatom assemblages: an examination of a 219-lake data set from western North America. Can. J. Fish. Aquat. Sci. **53**(7): 1580–1594.

Appendix A

Table A1. Description of the flora. The appellation (planktonic or benthic) attributed to species used in this study is also reported.

Diatom flora	Species number	Occurrence Abitibi	 Gouin	pH optima	Hill's $N2$	Minimal, %	Maximal, %	Tolerance pH	Type of species
Achnanthes 1, not identified	2	—	1	6.48	1	1	1	—	Benthic
Achnanthes biasolettiana (Grunow) Cleve and Grunow	1	1	—	7.28	1	2.84	2.84	—	Benthic
Achnanthes bioretii Germain	3	2	—	6.08	2	1.26	1.43	—	Benthic
Achnanthes carissima (Lange-Bertalot) Lange-Bertalot and Krammer	4	—	1	6.71	1	1.17	1.17	—	Benthic
Achnanthes catenata Bily and Marvan	5	2	—	6.00	1.8	1.2	2.44	—	Benthic
Achnanthes flexella var. *alpestris* Brun	6	3	—	6.35	2.8	1	2	0.37	Benthic
Achnanthes flexella var. *flexella* (Cleve) Cleve-Euler	7	1	—	7.80	1	1.2	1.2	—	Benthic
Achnanthes joursacense Heribaud	8	1	—	6.75	1	2.33	2.33	—	Benthic
Achnanthes kriegeri Krasske	9	—	1	6.51	1	2.08	2.08	—	Benthic
Achnanthes lanceolata var. *rostrata* (Oestrup) Lange-Bertalot	10	1	2	6.71	1.7	1.29	10.56	0.13	Benthic
Achnanthes minutissima var. *affinis* (Lange-Bertalot) L.B. and K.	11	—	1	6.33	1	1.79	1.79	—	Benthic
Achnanthes minutissima var. *minutissima* Kützing	12	24	17	6.72	19.6	1	26.95	0.99	Benthic
Achnanthes oblongella Oestrup	13	2	—	5.95	2	1.26	1.71	—	Benthic
Achnanthes pusilla (Grunow) De Toni	14	3	—	7.04	2.5	1.27	4.96	0.26	Benthic
Achnanthes ventralis (Krasske) Lange-Bertalot	15	4	—	7.45	1.9	1.11	9.59	0.58	Benthic
Achnanthes ziegleri Lange-Bertalot	16	2	—	7.73	1.9	2.62	3.73	—	Benthic
Actinella punctata Lewis	17	5	—	5.20	3.4	1.43	6.91	0.92	Benthic
Amphicampa hemicyclus (Ehrenberg) Karsten	18	6	—	5.58	3.4	1.48	16.59	0.64	Benthic
Amphipleura pellucida (Kützing) Kützing	19	1	—	7.28	1	1.65	1.65	—	Benthic
Amphora ovalis (Kützing) Kützing	20	7	—	6.80	6.5	1	2.11	0.42	Benthic
Amphora pediculus var. *pediculus* (Kützing) Cleve	21	1	—	8.01	1	2.99	2.99	—	Benthic
Amphora thumensis (Mayer) Cleve	22	1	—	8.01	1	1	1	—	Benthic
Anomoeoneis aponina Kützing	23	—	2	5.91	1.7	1.1	2.53	—	Benthic
Anomoeoneis I Brébisson	24	—	1	6.48	1	1.57	1.57	—	Benthic
Anomoeoneis follis (Ehrenberg) Cleve	25	1	—	5.94	1	3.33	3.33	—	Benthic
Anomoeoneis serians (Brébisson) Cleve	26	1	—	5.21	1	1.19	1.19	—	Benthic
Anomoeoneis vitrea (Grunow) Ross	27	—	1	6.72	1	1.31	1.31	—	Benthic
Asterionella formosa Hassall	28	12	29	6.08	12.9	1.05	49.08	0.74	Benthic
Aulacoseira 1, not identified	29	3	—	5.70	2.5	1.29	5.25	0.37	Planktonic
Aulacoseira 2, not identified	30	4	—	6.00	3.4	1.18	3.46	0.19	Planktonic
Aulacoseira alpigena (Grunow) Krammer	31	—	17	6.47	9.7	1	18.56	0.41	Planktonic
Aulacoseira ambigua (Grunow) Simonsen	32	11	—	6.47	4.1	1	33.52	1.07	Planktonic
Aulacoseira distans var. *distans* (Ehrenberg) Simonsen	33	13	9	6.53	10.4	1	39.56	0.92	Planktonic
Aulacoseira distans var. *humilis* Cleve-Euler	34	14	—	6.34	7.8	1.27	19.35	0.66	Planktonic
Aulacoseira distans var. *nivalis* (W.Smith) Haworth	35	2	—	6.60	1.9	3.04	4.65	—	Planktonic
Aulacoseira distans var. *nivaloides* Camburn	36	11	—	5.98	6.4	1	17.61	0.65	Planktonic
Aulacoseira distans var. *tenella* (Nygaard) Florin	37	20	12	6.17	11.1	1	63.51	0.83	Planktonic
Aulacoseira italica var. *subarctica* (O.Müller) Simonsen	38	6	32	6.51	20.6	1.84	44.42	0.40	Planktonic
Aulacoseira italica var. *tenuissima* (Grunow) Simonsen	39	2	—	7.00	1.6	2.18	6.28	—	Planktonic
Aulacoseira lacustris (Grunow) Krammer	40	1	—	4.16	1	4.85	4.85	—	Planktonic
Aulacoseira lirata (Ehrenberg) Ross	41	10	15	6.20	14.6	1.48	46.68	0.67	Planktonic

Table A1 *(continued)*.

Diatom flora	Species number	Occurrence		pH optima	Hill's *N2*	Minimal, %	Maximal, %	Tolerance pH	Type of species
		Abitibi	Gouin						
Aulacoseira lirata var. *biseriata* (Grunow) Haworth	42	2	—	5.49	1.5	1.41	4.95	—	Planktonic
Aulacoseira nygaardii Camburn	43	5	—	5.33	4.5	1	3.27	0.98	Planktonic
Aulacoseira perglabra (Oestrup) Haworth	44	10	6	5.32	5.1	1	47.05	1.97	Planktonic
Aulacoseira perglabra var. *floriniae* Camburn	45	4	—	5.74	2	1.43	20.44	0.30	Planktonic
Aulacoseira tenuior (Grunow)	46	4	1	5.89	4.4	1	2.52	0.48	Planktonic
Brachysira brebissonii 1, not identified	47	19	13	6.07	17.7	1.08	15.96	0.51	Planktonic
Brachysira brebissonii 3, not identified	48	1	—	5.94	1	7.1	7.1	—	Benthic
Brachysira procera Lange-Bertalot	49	2	—	6.30	1.9	1.16	1.77	—	Benthic
Brachysira styriaca (Grunow) Hustedt	50	2	—	6.46	1.8	1.29	2.66	—	Benthic
Brachysira vitrea (Grunow) Ross	51	14	—	6.78	6.8	1	19.59	0.95	Benthic
Caloneis silicula (Ehrenberg) Cleve	52	—	1	6.54	1	1.32	1.32	—	Benthic
Cocconeis placentula var. *euglypta* Ehrenberg	53	1	—	7.40	1	1	1	—	Benthic
Cyclotella antiqua W. Smith	54	1	—	7.40	1	1.46	1.46	—	Benthic
Cyclotella bodanica Grunow	55	2	—	6.89	1.6	2.96	8.37	—	Planktonic
Cyclotella bodanica var. *lemanica* (O.Müller) Bachmann	56	11	25	6.63	18	1.28	39.32	0.52	Planktonic
Cyclotella comensis Grunow	57	—	8	6.39	5.9	1.49	9.4	0.41	Planktonic
Cyclotella distinguenda Hustedt	58	—	1	6.28	1	1	1	—	Planktonic
Cyclotella gamma Skvortow	59	1	—	7.80	1	1	1	—	Planktonic
Cyclotella glomerata Bachmann	60	—	3	6.43	1.2	1.44	41.02	0.06	Planktonic
Cyclotella meneghiniana Kützing	61	4	1	6.69	3.6	1	4.52	0.57	Planktonic
Cyclotella michiganiana Skvortzow	62	7	—	7.08	4.6	1	11.75	0.69	Planktonic
Cyclotella ocellata Pantocsek	63	5	6	6.73	6.4	1	6.86	0.32	Planktonic
Cyclotella pseudostelligera 1, not identified	64	7	1	6.32	6	1.11	11.09	0.75	Planktonic
Cyclotella pseudostelligera 3, not identified	65	5	—	7.06	3.2	1.06	10.47	0.46	Planktonic
Cyclotella rossii Håkansson	66	—	3	6.74	2.4	2.09	5.86	0.03	Planktonic
Cyclotella stelligera 1, not identified	67	13	25	6.49	21.8	1	34.24	0.56	Planktonic
Cyclotella stelligera 3, not identified	68	1	—	6.12	1	5.56	5.56	—	Planktonic
Cyclotella stelligeroides Hustedt	69	2	—	6.26	1.3	4.86	28.5	—	Planktonic
Cymbella aequalis W. Smith	70	1	—	6.95	1	4.66	4.66	—	Planktonic
Cymbella cesatii (Rabenhorst) Grunow	71	1	—	7.57	1	1.13	1.13	—	Benthic
Cymbella delicatula Kützing	72	2	—	7.58	1.1	1.2	21.85	—	Benthic
Cymbella gaeumannii Meister	73	10	—	5.62	7.5	1	3.95	0.62	Benthic
Cymbella gracilis (Ehrenberg) Kützing	74	6	3	6.17	8.7	1	1.88	0.53	Benthic
Cymbella hebridica (Grunow) Cleve	75	8	1	5.18	3	1	16.46	1.07	Benthic
Cymbella incerta (Grunow) Cleve	76	5	—	6.39	4.5	1.2	3.33	0.44	Benthic
Cymbella microcephala Grunow	77	7	1	6.53	4.9	1	7.8	1.47	Benthic
Cymbella minuta Hilse	78	1	—	4.54	1	1.24	1.24	—	Benthic
Cymbella naviculiformis Auerswald	79	1	—	6.59	1	1.01	1.01	—	Benthic
Cymbella silesiaca Bleisch	80	4	5	6.31	4.1	1	9.14	0.46	Benthic
Denticula elegans Kützing	81	3	—	7.30	2.4	3.84	17.52	0.36	Benthic
Diploneis elliptica (Kützing) Cleve	82	—	1	6.71	1	1.17	1.17	—	Benthic
Diploneis modica Hustedt	83	3	—	6.59	2.9	1.05	1.65	0.29	Benthic
Diploneis ovalis (Hilse) Cleve	84	3	—	7.16	2.7	1	2.33	0.11	Benthic

Diploneis puella (Schumann)	85	2	—	6.74	1.8	1.06	2.1	—	Benthic
Eunotia arculus (Grunow) Lange-Bertalot	86	—	1	5.90	1	1.36	1.36	—	Benthic
Eunotia arcus Ehrenberg	87	1	—	6.95	1	1.55	1.55	—	Benthic
Eunotia bidentula Schumann	88	7	—	4.66	6.3	1	3.22	0.36	Benthic
Eunotia bilunaris (Ehrenberg) Mills	89	10	—	5.20	4.9	1.05	17.04	0.96	Benthic
Eunotia bilunaris var. *mucophyla* Lange-Bertalot and Nörpel	90	6	12	6.01	15.6	1	2.49	0.69	Benthic
Eunotia carolina Patrick	91	1	—	5.21	1	1.9	1.9	—	Benthic
Eunotia elegans Oestrup	92	—	1	6.33	1	1	1	—	Benthic
Eunotia exigua (Brébisson) Rabenhorst	93	5	2	5.93	5.4	1	2.38	0.86	Benthic
Eunotia exigua var. *bidens* Hustedt	94	—	2	6.36	2	1	1.11	—	Benthic
Eunotia faba Ehrenberg	95	2	4	5.85	3.7	1.12	4.47	0.94	Benthic
Eunotia flexuosa (Brébisson) (Kützing)	96	1	1	6.65	2	1	1	—	Benthic
Eunotia glacialis Meister	97	—	2	6.63	1.9	1.05	1.75	—	Benthic
Eunotia hemicylcus (Ehrenberg) Ralfs	98	—	1	6.34	1	1	1	—	Benthic
Eunotia implicata Nörpel et al.	99	2	—	6.56	1.9	1.05	1.46	—	Benthic
Eunotia incisa Gregory	100	7	13	6.14	14.9	1	5.38	0.48	Benthic
Eunotia linearis Okuno	101	—	4	6.31	3.8	1	1.7	0.21	Benthic
Eunotia meisteri Hustedt	102	1	1	6.68	1.9	1.11	1.85	—	Benthic
Eunotia microcephala Krasske	103	2	—	5.66	2	1.48	2.47	—	Benthic
Eunotia minor (Kützing) Grunow	104	1	2	5.38	2.7	1	1.98	0.86	Benthic
Eunotia naegelii Migula	105	—	1	6.40	1	1.63	1.63	—	Benthic
Eunotia nymanniana Grunow	106	2	—	5.15	1.9	1	1.48	—	Benthic
Eunotia paludosa Grunow	107	5	2	6.43	3.7	1	7.88	0.73	Benthic
Eunotia pectinalis (Dillwyn) Rabenhorst	108	—	9	6.38	7.3	1.08	3.5	0.35	Benthic
Eunotia pectinalis var. *ventralis* (Ehrenberg) Hustedt	109	7	—	5.18	3.7	1	13.37	0.90	Benthic
Eunotia pirla Carter	110	4	—	4.73	3.6	1	2.72	0.35	Benthic
Eunotia polyglyphis Grunow	111	5	—	6.67	2.5	1	7.06	1.19	Benthic
Eunotia praerupta Ehrenberg	112	2	—	7.05	1.4	1	5.32	—	Benthic
Eunotia pyramidata Hustedt	113	—	2	5.98	2	1	1.28	—	Benthic
Eunotia rhomboidea Hustedt	114	8	—	4.84	5.3	1.11	6.68	0.40	Benthic
Eunotia rhynchocephala Krasske	115	4	—	5.64	4	1	1.29	0.38	Benthic
Eunotia schwabei Krasske	116	—	3	6.37	2.9	1	1.42	0.26	Benthic
Eunotia seminulum (Nörpel) Lange-Bertalot	117	—	1	6.61	1	1.28	1.28	—	Benthic
Eunotia septentrionalis Oestrup	118	2	—	5.34	1.9	1.17	1.9	—	Benthic
Eunotia serra Ehrenberg	119	3	1	5.60	3.6	1	2.06	1.13	Benthic
Eunotia serra var. *diadema* (Ehrenberg) Patrick	120	—	1	6.22	1	1.48	1.48	—	Benthic
Eunotia subarcuatoides Alles et al.	121	1	5	5.99	6	1.23	1.52	0.65	Benthic
Eunotia sudetica O. Müller	122	2	—	4.95	1.9	1.4	2	—	Benthic
Eunotia tenera W. Smith	123	16	—	6.74	9.9	1	16.09	0.61	Benthic
Fragilaria brevistriata 1, not identified	124	7	—	6.73	4.9	1.91	13.89	0.78	Benthic
Fragilaria brevistriata 2, not identified	125	2	—	7.96	1.6	4.56	15.17	—	Benthic
Fragilaria brevistriata 3 Grunow	126	4	5	6.67	6.1	1	6.87	0.16	Benthic
Fragilaria capucina Desmazières	127	4	—	5.44	3.2	1.26	4.44	0.67	Benthic
Fragilaria constricta Ehrenberg	128	4	—	4.99	3	2.54	11.11	0.31	Benthic
Fragilaria constricta var. *stricta* Cleve	129	1	2	6.60	2.8	1.26	2.71	0.24	Benthic
Fragilaria construens var. *binodis* (Ehrenberg) Grunow	130	13	4	6.89	8.8	1	17.88	0.86	Benthic
Fragilaria construens var. *construens* (Ehrenberg) Grunow	131	1	1	7.04	1	1.91	1.91	1.06	Benthic
Fragilaria construens var. *spiranum* (Ehrenberg) Grunow	132	—	1	6.74	1.4	1.95	8.47	—	Benthic

Table A1 (*concluded*).

Diatom flora	Species number	Occurrence		pH optima	Hill's *N*2	Minimal, %	Maximal, %	Tolerance pH	Type of species
		Abitibi	Gouin						
Fragilaria construens var. *venter* (Ehrenberg) Grunow	133	3	11	6.27	7.7	1	21.64	—	Benthic
Fragilaria crotonensis Kitton	134	—	1	6.40	1	3.18	3.18	—	Planktonic
Fragilaria exigua Grunow	135	—	1	6.74	1	2.49	2.49	—	Benthic
Fragilaria fasciculata (Agardh) Lange-Bertalot	136	4	2	5.73	5.2	0.84	2.37	0.78	Benthic
Fragilaria inflata Pantocsek	137	1	—	5.44	1	1.51	1.51	—	Benthic
Fragilaria inflata var. *istranii* Pantocsek	138	1	—	7.30	1	2.22	2.22	—	Benthic
Fragilaria intermedia Grunow	139	5	—	7.24	3.1	1.23	7.86	0.36	Benthic
Fragilaria lapponica Grunow	140	1	—	5.39	1	2.94	2.94	—	Benthic
Fragilaria lata (Cleve-Euler) Renberg	141	9	—	6.65	7.2	1	4.38	1.16	Benthic
Fragilaria nanana Lange-Bertalot	142	5	—	6.41	4.3	2.38	6.05	0.81	Benthic
Fragilaria pinnata Ehrenbert	143	—	2	6.69	3.5	1.68	39.99	—	Benthic
Fragilaria pinnata var. *pinata* Ehrenberg	144	10	—	7.19	2	1	1.1	0.46	Benthic
Fragilaria pseudoconstruens Marciniak	145	—	1	6.44	1	1.03	1.03	—	Benthic
Fragilaria vaucheriae (Kützing) Petersen	146	—	1	6.51	1	10.57	10.57	—	Benthic
Fragilaria virescens var. *exigua* Grunow	147	15	—	5.90	7.6	1.44	38.15	0.59	Benthic
Fragilaria 1, not identified	148	—	1	6.28	1	1	1	—	Benthic
Frustulia rhomboides 1, not identified	149	—	2	6.16	16.1	1	13.57	—	Benthic
Frustulia rhomboides 3, not identified	150	—	24	6.28	1.8	1.26	2.32	0.35	Benthic
Frustulia rhomboides var. *amphipleuroides* (Grunow) De Toni	151	1	—	4.60	1	1.23	1.23	—	Benthic
Frustulia rhomboides var. *crassinervia* (Brébisson) Ross	152	24	—	5.47	2	1.3	1.36	1.02	Benthic
Frustulia rhomboides var. *saxonica* (Rabenhorst) De Toni	153	2	—	4.59	17.6	1	7.14	—	Benthic
Gomphonema 1, not identified	154	1	—	6.80	1	1.17	1.17	—	Benthic
Gomphonema angustatum Agardh	155	—	2	6.37	1.9	1	1.73	—	Benthic
Gomphonema gracile Ehrenberg	156	4	3	6.78	6.7	1	2.05	0.61	Benthic
Gomphonema parvulum (Kützing) Kützing	157	2	—	6.67	2	1.46	1.63	—	Benthic
Gomphonema subtile Ehrenberg	158	2	—	6.93	1.6	1.11	3.1	—	Benthic
Navicula 1, not identified	159	4	—	7.46	3.4	1	4.08	0.37	Benthic
Navicula 2, not identified	160	3	—	6.73	2.7	1	2.13	0.58	Benthic
Navicula brachysira Brébisson	161	4	—	5.86	3.5	1.01	2.82	0.43	Benthic
Navicula bulnheimii Grunow	162	—	1	6.95	1	1.44	1.44	—	Benthic
Navicula cocconeiformis Gregory	163	3	—	6.57	2.8	1	1.61	0.63	Benthic
Navicula cryptocephala Kützing	164	2	—	7.31	1.7	1	2.6	—	Benthic
Navicula cryptotenella Lange-Bertalot	165	4	—	7.31	3.2	1	4.26	0.23	Benthic
Navicula diluviana Krasske	166	2	—	7.95	1.7	5.28	13.18	—	Benthic
Navicula indifferens Hustedt	167	—	1	6.40	1	1.41	1.41	—	Benthic
Navicula kuelbsii Lange-Bertalot	168	—	1	6.71	1	1.56	1.56	—	Benthic
Navicula laevissima Kützing	169	9	—	6.45	7.1	1.2	4.88	0.90	Benthic
Navicula leptostriata Jørgensen	170	4	—	6.10	3.9	1.05	1.55	0.88	Benthic
Navicula mediocris Krasske	171	5	—	6.12	4.7	1.05	2	0.41	Benthic
Navicula molestiformis Hustedt	172	—	3	6.24	2.8	1.4	2.61	0.28	Benthic
Navicula pupula Kützing	173	9	1	6.73	9	1	3.1	0.61	Benthic
Navicula radiosa Kützing	174	7	4	6.71	8.2	1	4.96	0.63	Benthic
Navicula scutiformis Grunow	175	—	1	6.43	1	1.09	1.09	—	Benthic

Navicula seminuloides Grunow	176	3	—	6.37	2.9	1.05	1.65	0.75	Benthic
Navicula seminulum Grunow	177	1	—	6.09	1	1.26	1.26	—	Benthic
Navicula soehrensis var. *muscicola* (Petersen) Krasske	178	—	1	6.43	1	1.82	1.82	—	Benthic
Navicula stroemii Hustedt	179	1	—	7.30	1	1.48	1.48	—	Benthic
Navicula subatomoides Hustedt	180	6	3	6.50	8.1	1	2.43	0.84	Benthic
Navicula subtilissima Cleve	181	9	2	5.40	1.8	1.08	53.57	0.52	Benthic
Navicula viridula (Kützing) A94	182	1	—	7.80	1	1.68	1.68	—	Benthic
Neidium ampliatum (Ehrenberg) Krammer	183	10	1	5.09	7.8	1	5.56	0.74	Benthic
Neidium iridis (Ehrenberg) Cleve	184	9	—	5.04	3.3	1.05	11.52	1.02	Benthic
Nitzischia minutula Grunow	185	11	—	6.46	7.4	1.06	7.08	0.68	Benthic
Nitzschia fonticola Grunow	186	7	1	6.35	6.1	1	5.13	1.19	Benthic
Pinnularia 1, not identified	187	3	—	4.91	2.5	2.26	7.38	0.34	Benthic
Pinnularia biceps Gregory	188	—	1	6.40	1	2.24	2.24	—	Benthic
Pinnularia braunii (Grunow) Cleve	189	14	—	5.30	5.2	1	24.75	1.34	Benthic
Pinnularia divergens W. Smith	190	—	2	6.52	1.4	1.03	4.72	—	Benthic
Pinnularia gibba Ehrenberg	191	12	1	5.81	9.4	1	6.42	1.02	Benthic
Pinnularia interrupta W. Smith	192	3	—	6.00	2.6	1	3.32	0.93	Benthic
Pinnularia maior (Kützing) Rabenhorst	193	5	3	6.50	7.8	1	1.55	0.58	Benthic
Pinnularia mesolepta (Ehrenberg) W. Smith	194	—	1	6.54	1	6.98	6.98	—	Benthic
Pinnularia microstauron 1 Ehrenberg	195	5	1	5.84	5.2	1	2.67	1.15	Benthic
Pinnularia microstauron 2 Ehrenberg	196	11	—	5.63	10	1	2.88	0.77	Benthic
Pinnularia schoenfelderii Krammer	197	—	3	6.54	1.7	1.24	8.3	0.06	Benthic
Pinnularia viridis (Nitzsch) Ehrenberg	198	4	—	5.24	3.2	1.01	3.5	1.03	Benthic
Stauroneis agrestis Petersen	199	6	—	5.70	5.4	1	2.4	1.03	Benthic
Stauroneis anceps Ehrenberg	200	—	2	6.58	1.9	2.5	3.49	—	Benthic
Stauroneis gracilis Ehrenberg	201	—	1	6.54	1	3.21	3.21	1.13	Benthic
Stauroneis phoenicenteron (Nitzsch) Ehrenberg	202	9	1	6.04	8	1	3.44	—	Benthic
Stauroneis producta Grunow	203	—	1	5.90	1	1.8	1.8	—	Benthic
Stephanodiscus niagarae Ehrenberg	204	1	—	7.30	1	2.59	2.59	—	Benthic
Tabellaria binalis Ehrenberg	205	—	2	6.11	2	1	1.03	0.32	Planktonic
Tabellaria fenestrata (Lyngbye) Kützing	206	—	22	6.47	11.2	1	15.96	0.70	Planktonic
Tabellaria flocculosa 1 (Roth) Kützing	207	10	—	5.96	7.9	1	3.52	0.29	Planktonic
Tabellaria flocculosa 2 (Roth) Kützing	208	3	—	5.22	2.1	1	4.2	0.54	Planktonic
Tabellaria flocculosa 3 var. *linearis* Koppen	209	15	34	6.29	20.9	1	46.82	0.30	Planktonic
Tabellaria flocculosa 4 (Roth) Kützing	210	7	—	4.98	5.9	1	3.21	—	Planktonic
Tabellaria flocculosa Small (Roth) Kützing	211	—	1	6.26	1	33.4	33.4	0.33	Planktonic
Tabellaria quadrisepta Knudson	212	—	9	6.29	6.7	1	3.71	0.93	Planktonic
Tabellaria ventricosa Kützing	213	23	—	5.79	5.4	1.07	9.54	0.15	Planktonic
Tabellaria ventricosa Small Kützing	214		10	6.37	13.8	1	9.88	—	Planktonic

Hypoxia-based habitat compression in the Neuse River Estuary: context-dependent shifts in behavioral avoidance thresholds

Lisa A. Eby and Larry B. Crowder

Abstract: Anthropogenic activities in estuarine watersheds alter physical and chemical characteristics of these ecosystems. Increased nutrient loading and changes in hydrology affect oxygen budgets and subsequently alter the spatial and temporal extent of hypoxia. We used classification and regression tree analyses to examine behavioral avoidance thresholds over a range of dissolved oxygen concentrations. In an examination of 10 fish species, all avoided areas with dissolved oxygen concentrations of <2.0 mg·L^{-1}. Our data suggest that the dissolved oxygen avoidance threshold expressed by fish may be context-dependent. Specifically, the spatial extent of hypoxia significantly affected avoidance thresholds. Fish may occupy poorer quality habitat (areas with lower dissolved oxygen levels) as conditions worsen and the size of the oxygenated refuge shrinks. When the entire estuary is oxygenated, fish utilize all depths. During hypoxic episodes, fish are restricted to oxygenated, shallow, warmer areas. This habitat compression may result in higher densities and greater overlap with potential competitors and predators. Hypoxic zones alter habitat use and may increase bioenergetic costs, potentially resulting in sublethal effects, i.e., decreased growth and condition, on the estuarine fish community.

Résumé : Dans les bassins hydrographiques des estuaires, l'activité humaine modifie les caractéristiques physiques et chimiques de l'écosystème. La charge accrue de nutriments et les changements hydrologiques affectent les bilans d'oxygène et, en conséquence, modifient la répartition spatiale et temporelle de l'hypoxie. Des arbres de classification et de régression (CART) nous ont permis d'étudier les seuils d'évitement comportemental sur une gamme étendue de concentrations d'oxygène dissous. Les 10 espèces de poissons testées ont toutes évité les zones de concentration d'oxygène $<2{,}0$ mg·L^{-1}. Nos données nous laissent croire, cependant, que les seuils d'évitement des concentrations d'oxygène observés chez les poissons varient selon les conditions locales. En particulier, la répartition spatiale de l'hypoxie affecte significativement les seuils d'évitement. Les poissons peuvent occuper des habitats de qualité inférieure (zones où les concentrations d'oxygène sont faibles) lorsque les conditions se détériorent et que la taille des refuges oxygénés rétrécit. Lorsque tout l'estuaire est oxygéné, les poissons occupent toutes les profondeurs. Durant les périodes d'hypoxie, les poissons sont restreints aux zones oxygénées, peu profondes et chaudes. Une telle compression de l'habitat peut entraîner un accroissement des densités et un chevauchement plus important avec les compétiteurs et les prédateurs potentiels. La présence de zones hypoxiques modifie l'utilisation de l'habitat et peut faire augmenter les coûts métaboliques, ce qui peut entraîner des effets sublétaux chez la communauté des poissons de l'estuaire, tels qu'une croissance réduite et une condition physique diminuée.

[Traduit par la Rédaction]

Introduction

Human activities in and near coastal zones are modifying physical and chemical characteristics in estuaries. Anthropogenic changes in temperature, velocity, salinity, depth, dissolved oxygen concentrations, sedimentation, and nutrient loading are all common in U.S. estuaries (e.g., review in Day et al. 1989). Given these and other recent alterations, it is important to determine how anthropogenic changes to hydrologic characteristics in coastal areas influence habitat use by estuarine fishes. Not only does one need to know the fishes' physiological limits to these environmental variables, but also the costs associated with sublethal effects of these changes. For example, higher stream current velocity increases foraging rates for drift-feeding fishes, but also imposes additional energetic costs. Foraging models that incorporate these conflicting energetic considerations have successfully predicted habitat use in the lab (Tyler and Gilliam 1995) and in the field (e.g., Hughes and Dill 1990). In southeast U.S. estuaries, increased nutrient loading and changes in hydrology affect oxygen budgets of estuaries and may increase the temporal and spatial extent of hypoxic zones (areas with dissolved oxygen concentrations <2 mg·L^{-1}). Remaining in hypoxic conditions is physiologically costly (e.g., Stewart et al. 1967; Bejda et al. 1987), so fish move out of these conditions both in the laboratory (Wannamaker and Rice 2000) and in the field (e.g., Pihl et al. 1991; Howell and Simpson 1994).

There are known costs to remaining in hypoxic waters, so movement by fishes has been considered strictly a physio-

Received 6 November 2001. Accepted 15 April 2002. Published on the NRC Research Press Web site at http://cjfas.nrc.ca on 11 July 2002.

L.A. Eby[1,2] and L.B. Crowder. Duke University Marine Lab, Beaufort, NC 28516–9721, U.S.A.

[1] Corresponding author (e-mail: lisa.eby@asu.edu).

[2] Present address: Wildlife Biology Program, The University of Montana, Missoula, MT 59812-0576, U.S.A.

DOI: 10.1139/F02-067

logical response. However, because external conditions (i.e., temperature, prey availability, and predation risk) also influence behavior, behavioral avoidance of low oxygen concentrations may be context-dependent. Many studies define hypoxia at 2.0 mg·L^{-1} as a threshold for fish movement (e.g., Pihl et al. 1991, 1992). There is some evidence that this threshold may not be universal (NRC 2001), instead fish response may differ across system, species, or time of year. For example, in Long Island Sound, New York, finfish and squid responded to dissolved oxygen levels of 3.0 mg·L^{-1} (Howell and Simpson 1994). Previous studies have demonstrated confounding factors such as interaction of temperature and oxygen preferences (Coutant 1987; Schurmann et al. 1991) and potential increases in prey vulnerability in hypoxic areas (Pihl et al. 1992) as two conditions that may alter behavioral avoidance of hypoxic waters. The importance of context-dependency in explaining community structure and interactions has been demonstrated in other systems (e.g., Menge et al. 1994). Similarly, the influence of external factors on behavior is ubiquitous and has been well described particularly in studies of habitat selection (e.g., Sih 1980; Lima and Dill 1990). The presence of predators is a common factor that alters habitat use of young-of-the-year freshwater fish, often restricting them to complex, vegetated habitat (e.g., Mittlebach 1986; Turner and Mittlebach 1990; Persson 1993).

Changes in fish distribution, specifically the temporary restriction of fish to oxygenated habitat, in response to hypoxic zones has been demonstrated in several estuarine systems, e.g., Chesapeake Bay (Pihl et al. 1991), Long Island Sound (Howell and Simpson 1994), Gulf of Mexico (Stuntz et al. 1983), and Neuse River Estuary (Lenihan et al. 2001). However, few studies have focused on how habitat restriction in response to hypoxia may influence metabolic costs, feeding rates, and species interactions (although see Breitburg 1992). Habitat restriction is potentially costly, such as in cases where piscivores restrict small fish to the littoral, vegetated habitat, leading to increased competition among prey fish in refuge (Mittlebach 1988; Turner and Mittlebach 1990). Depending on the structural complexity and prey resources within the refuge, this habitat restriction may alter competitive interactions and thus result in changes in diet and decreases in growth rates for disadvantaged species (e.g., Persson and Eklov 1995).

Our objective was to examine the role of hypoxia in altering fish distributions in the Neuse River Estuary. In this paper we examined species-specific differences in thresholds for avoidance of hypoxia, determined whether these thresholds are context-dependent, and examined how avoidance of hypoxic zones influences habitat use and the potential for species interactions. First, we compared the level of dissolved oxygen that excludes fish from an area for 10 common estuarine species. Although most species avoid hypoxia, previous field and lab studies suggest possible species-specific differences in sensitivity to low dissolved oxygen concentrations (Pihl et al. 1991; Wannamaker and Rice 2000).

Second, we examined whether avoidance thresholds for low dissolved oxygen concentrations were context-dependent. We determined thresholds for each sampling date for three abundant species (croaker *Micropogonias undulatus*, spot *Leiostomus xanthurus*, and blue crab *Callinectes sapidus*) and examined four alternative hypotheses regarding the influence of month, temperature, oxygen range, and spatial extent of hypoxia (Table 1). First, we hypothesized that dissolved oxygen thresholds may decrease through the season as fish acclimate and become less sensitive to low dissolved oxygen concentrations as exposure increases. Second, avoidance thresholds may increase with water temperatures because warmer water holds less oxygen (lower percentage saturation) and increases fish metabolic rates. Third, thresholds may be higher if there is a wide range of dissolved oxygen concentrations (i.e., 1.0 to 8.0 mg·L^{-1}) to choose from versus a narrower range consisting of primarily unfavorable levels between 1.0 and 3.0 mg·L^{-1}. Fourth, thresholds may be linked to the size of the hypoxic zone. As the areal extent of the hypoxic region increases, the size of the oxygenated refuge decreases. Crowding may force fish to move into areas with lower dissolved oxygen concentrations than they would otherwise use (Table 1).

Finally, we began to explore how hypoxia influences habitat use and potential species interactions. For example, fish respond to small temperature gradients by moving toward preferred temperatures (Magnuson et al. 1979). We hypothesized that expected relationships between spot, croaker, and blue crab abundance and temperature or depth gradients will be disrupted by hypoxia because of habitat restriction. Spot and croaker are ubiquitous and abundant species inhabiting coastal waters in the southeastern U.S. They are both demersal with similar seasonal distributions and life histories and so are potential competitors (Parker 1971). In the Neuse River Estuary, blue crabs are also very abundant and share many of the same prey taxa as spot and croaker (Virnstein 1977; Gee et al. 1985). Kneib (1982) found that larger blue crab actively fed on coastal fish. Because of the potential for competition and predation, we hypothesized that during periods of extensive hypoxia, habitat compression would result in higher levels of overlap, potentially intensifying interactions among these species.

Methods

Study site

The Neuse River Estuary is the major southern tributary of North Carolina's Pamlico Sound (Fig. 1). It is shallow with an average depth of about 3.5 m and maximum depth of about 7 m. Freshwater inflow and wind energy dominate the hydrography of the system. The estuary drains a watershed of about 16 000 km^2 and receives substantial nutrient loading from a number of sources, including agricultural runoff, industrial discharge, and wastewater from municipal treatment plants (Paerl and Pinckney 1996). Nutrients reach the estuary through discharge from the upper Neuse River, its tributaries, streams, rainfall, and groundwater. Annually, about 70% of nutrient input originates from diffuse, nonpoint sources such as surface runoff, rainfall, and groundwater. Point sources, attributed to wastewater treatment plants and industrial discharges, account for the remaining 30% (Paerl and Pinckney 1996). High primary production and subsequent increased flux of organic carbon to bottom waters increases oxygen demand. This high oxygen demand in the bottom water combined with a stratified water column results in hypoxic conditions.

Table 1. Alternative hypotheses for differences in avoidance thresholds for each date.

Independent variable	Relationship	Mechanism
Month	–	Fish may become less sensitive to hypoxia across the season as exposure increases.
Average temperature	+	Fish may become more sensitive to lower oxygen conditions as temperature increases because warmer waters hold less oxygen and fish metabolic rates increase.
Oxygen range	+	Fish may have stronger preferences for higher oxygen levels (>6.0 $mg \cdot L^{-1}$) than marginal habitat (2.0–4.0 $mg \cdot L^{-1}$).
Percent of study area hypoxic	–	As the areal extent of the hypoxic zone increases, the size of the oxygenated refuge decreases and fish are forced to use areas with lower dissolved oxygen levels.

Fig. 1. Neuse River Estuary, N.C., study area (inset of the U.S. east coast). The two sets of dots represent fixed grids that were randomly subsampled; upstream (1997 through 1999) and downstream (1998 and 1999).

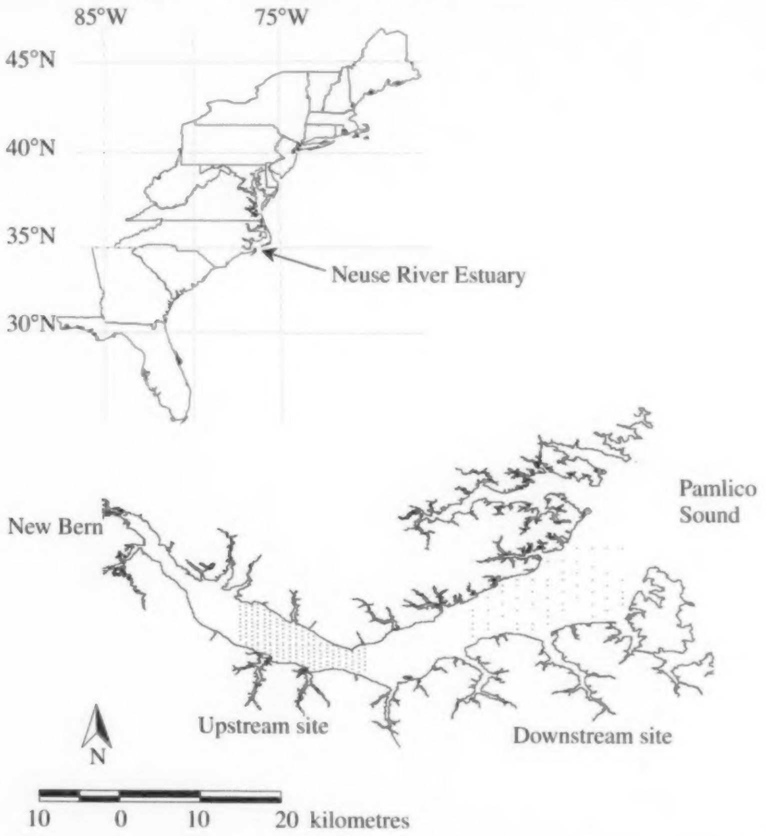

This estuary provides critical habitat for juvenile and adult fish. The Neuse River fish community consists of many species, including spot, croaker, menhaden (*Brevoortia tyrannus*), bay anchovy (*Anchoa mitchilli*), alewife (*Alosa pseudoharengus*), blueback herring (*Alosa aestivalis*), striped mullet (*Mugil cephalus*), pinfish (*Lagodon rhomboides*), southern flounder (*Paralichthys lethostigma*), sheepshead minnow (*Cyprinodon variegatus*), mummichog (*Fundulus heteroclitus*), and Atlantic silversides (*Menidia* sp.) (Nelson et al. 1991). These estuarine waters are also fishing grounds for the two most economically important species in the state, blue crabs and shrimp.

We chose two study sites because of the potential for different dynamics in water quality conditions above and below the narrow turn in the river at Cherry Point (Luettich et al. 2000). The upstream sampling site spanned about 88 km^2, whereas the downstream study site encompassed about 200 km^2 (Fig. 1).

Sample collection and processing

We collected water quality and fish samples in the upstream study site biweekly from June through October 1997 and in both the upstream and downstream site at least monthly from May through October in 1998 and 1999 (Fig. 1). We trawled during the day for 2 min at 2.5–3.5 knots (covering about 0.18 km) using a 9-m mongoose trawl (48-mm-mesh wings and body with a 12.8-mm-mesh tail bag) from the R/V *Susan Hudson*, a 19-m Duke University

Marine Lab research vessel. Trawl duration was standardized, so distance trawled did not vary much between sites or among dates. We mapped a fixed grid across the sampling area (Fig. 1) and randomly subsampled it throughout the season. Neighboring stations were about 0.5–0.75 km apart at the upstream site and 1.0–2.0 km apart downstream. We sampled about 32 stations on each date. All fish landed were identified to species and counted. Catches were reported in catch per unit effort (CPUE) calculated as individuals/100 m trawled. We determined geographic position and speed over ground with a Garmin Geopositioning System (GPS; Garmin, Kansas), and then estimated distance trawled from tow times and ground speed of the boat.

We profiled the water column before and after each trawl with a portable conductivity, temperature, and depth (CTD) probe (SeaBird Electronics, Inc., Bellevue, Wash.). The CTD sampled at 8 readings/s, so water quality data were averaged into 0.25-m depth intervals. We used measurements from the bottom 0.25 m of the water column to characterize bottom conditions. Because mongoose trawls fish from the bottom 1 m of the water column, we compared fish data to measurements averaged over the bottom metre. If we trawled through an environmental gradient (e.g., if depth or dissolved oxygen differed by more than 2 m or 2.0 $mg \cdot L^{-1}$ between the CTD casts at the beginning and end of the trawl), then we used station information to characterize water quality but did not include those trawl catches in analyses.

Hypoxic zone calculations

To estimate the extent of the hypoxic zone within the study areas, we entered bottom water measurements (0.25 m) into a geographical information system (ArcView; ESRI, Calif.). We took two depth profiles (one at both the beginning and end of each trawl), so for each sampling period we had between 60 and 80 profiles within the study area. We interpolated environmental data in ArcView Spatial Analyst using the inverse distance weighting subroutine. The number of pixels in the interpolated map that were less than 2.0 $mg \cdot L^{-1}$ was divided by the total number of pixels in the study area to determine percentage of study area that was hypoxic during a given sampling period.

Species-specific threshold comparisons

Classification and regression tree (CART) analysis is a nonparametric stepwise splitting procedure that predicts one variable as a function of other categorical and continuous variables. The method begins with a single cluster of values of the dependent variable and searches the candidate set of predictor variables for the best way to split the cluster into two clusters. Each predictor is tested by sorting all of the n cases on the predictor and examines all $n - 1$ points at which to split the data. For each possible split, the within-cluster sum of squares is computed about the mean of the cluster. This is done for every possible split based on every predictor. The split that is chosen is the predictor value that yields the smallest overall within-cluster sum of squares (Clark and Pregibon 1992).

To determine an avoidance threshold for what dissolved oxygen concentrations exclude fish from an area, we performed a CART analysis with presence–absence fish data and dissolved oxygen concentration. These thresholds were examined using the entire data set (all sampling dates from 1997–1999, $N = 1233$ stations) separately for 10 different species (blue crab (*Callinectes sapidus*), shrimp (*Penaeus* spp.), croaker (*Micropogonias undulates*), spot (*Leiostomus xanthurus*), menhaden (*Brevoortia tyrannus*), silver perch (*Bairdiella chrysoura*), southern flounder (*Paralichthys lethostigma*), hogchoker (*Trinectes maculatus*), weakfish (*Cynoscion regalis*), and pinfish (*Lagodon rhomboids*).

Focal-species threshold comparisons

To evaluate the hypotheses presented in Table 1 and examine whether avoidance thresholds for dissolved oxygen are context-dependent, we performed CART analyses with spot, croaker, and blue crab presence–absence data separately on each sampling date for which hypoxia was present ($N = 22$ sampling dates with hypoxia). For each sampling date, we sampled about 32 stations (range 28–40). Sampling dates when the entire study area was well oxygenated were excluded from this analysis. Then using a general linear model, these CART thresholds (for each date) were modeled as a function of month, average temperature, dissolved oxygen gradient, and percent of study area with hypoxic bottom waters.

Electivity calculations

We calculated electivity for four different dissolved oxygen ranges, 0.0–2.0 $mg \cdot L^{-1}$, 2.0–4.0 $mg \cdot L^{-1}$, 4.0–6.0 $mg \cdot L^{-1}$, and 6.0–10.0 $mg \cdot L^{-1}$ to examine potential for a preference of a particular dissolved oxygen level. We were specifically interested in the midrange (2.0–4.0 $mg \cdot L^{-1}$) because fish are found in these dissolved oxygen levels in the field, but those remaining in waters with these dissolved oxygen levels may incur metabolic costs (e.g., Brett 1979). We calculated a general electivity index (EI) to measure preference for a particular dissolved oxygen range using Jacobs' (1974) modification of Ivlev's electivity index (1961):

$$(1) \qquad \mathrm{EI} = (A - B)/((A + B) - 2AB)$$

where A is the proportion of fish found in a particular habitat (i.e., dissolved oxygen concentrations between 2.0 and 4.0 $mg \cdot L^{-1}$), and B is the proportion of the total area in the environment of that particular type. Thus, we compared the proportion of fish found in each dissolved oxygen category versus the availability of area within the particular category. Although Ivlev's electivity index was derived to quantify selectivity in diets (Ivlev 1961), it has since been modified (Jacobs 1974) and used for quantifying preferences in habitat selection (e.g., Copp 1992; Wilkins and Myers 1992). This selectivity index ranges from –1 to +1. Values greater than zero mean that the habitat type was used in greater proportion than availability (i.e., it was "preferred"). Values less than zero mean the habitat type was used in a smaller proportion than its availability, and a value of zero indicates that the type was used in proportion equal to its availability. This assumes that fish have equal access to all habitat types. Therefore we constrained our analyses to the upstream site and species (blue crab, spot, and croaker) where this assumption is met. Populations of these three species are distributed throughout the entire upstream study site before hypoxic zones form.

Focal-species habitat use changes

We focused on blue crabs, spot, and croaker for our distribution analyses because they are demersal species, captured well by bottom trawls, and abundant throughout the sampling season. Our data are spatially dependent and delta distributed (thus, cannot be transformed to mimic normal data), so we used a Mantel test to examine the relationship between abundance and environmental variables. Partial Mantel tests allow for the calculation of partial correlation coefficients, which indicate the strength of the correlation between two distance matrices, once the effects of the other variables have been taken into account (Legendre and Fortin 1989; Legendre 1993). This test works by computing the relationship between difference matrices. The entries in the matrices are actually differences measured between individual points. For these analyses, matrices consist of pairwise differences in physical distance, temperature, salinity, depth, dissolved oxygen, and catch at sampling stations. The null hypothesis is that the observed relationship between difference matrices could have been obtained by any random arrangement. We used code originally developed by Manly (1991).

This test allowed us to examine relationships between fish catches, environmental variables (depth, dissolved oxygen, salinity, temperature), and space. We used partial Mantel tests to examine which environmental variables explained a significant portion of the variance in fish distributions. For each species, we conducted analyses for each date separately (from June 1997 to October 1999). Also, we included croaker and blue crab CPUE as predictor variables in the Mantel runs with spot CPUE as the dependent variable to determine if there is more overlap between spot and croaker or spot and blue crab in the presence of hypoxic zones. Significant positive results from partial Mantel tests indicate a relationship between the difference matrices. To examine the direction of the trends between CPUE and the environmental variables, we plotted the raw data.

In addition, we examined how hypoxic zones influenced the depth distribution of three focal species with categorical and regression trees. We predicted spot, croaker, and blue crab catch versus depth to determine if there were consistent changes in the depth limit of each species for dates with different spatial extents of hypoxia.

Results

Range of environmental conditions

We sampled the same depth range over every sampling period. The mean depth sampled was 3.5 m (range 1.0–7.3 m). Temperature showed a seasonal cycle that was consistent among years with mean temperatures around 20°C in May, peaking around 28–30°C in July and August, and decreasing again to about 18–20°C by October (Fig. 2*a*). Salinity varied dramatically among years and seasons. Within any given month, the bottom water of the upstream site was fresher than the downstream site, but seasonal and interannual trends were similar at the two sites. In both 1997 and 1998, the lowest salinities occurred in the spring and the estuary became more saline as the summer progressed. In the fall of 1999, hurricanes dropped about a metre of rainfall in the watershed over a 3-week period (Paerl et al. 2001), and this large influx of freshwater pushed most of the salt water out of the estuary (Paerl et al. 2001; Fig. 2*b*).

Dissolved oxygen concentrations in the Neuse River Estuary were spatially and temporally dynamic within each year. Hypoxia formed most often in the deeper upstream portion of the estuary but at times extended throughout the estuary. Hypoxic bottom waters were intermittently present throughout the entire sampling season, from May until October. In 1997, hypoxia was spatially widespread in the upstream sampling. In 1998, however, the system rarely experienced large zones of bottom water hypoxia until September. In 1999 intermittent, widespread hypoxia was again present, until the hurricanes freshened the system. At the upstream site, an average of 28, 6, and 17% of the study area was hypoxic during the 1997, 1998, and 1999 field seasons, respectively. The largest hypoxic zone that our upstream site experienced was in August 1999, when 67% of the study site was hypoxic, but in both 1997 and 1999, we commonly mapped hypoxic zones that were from 20 to 40% of the study area. At the downstream site, hypoxic zones were less common and less extensive, with an average of 3 and 5% of the study area (maximum areas were 15% for 1998 and 22% for 1999) hypoxic during the 1998 and 1999 field season (Fig. 2*c*).

Species-specific thresholds

We examined avoidance thresholds for dissolved oxygen level of 10 different species (Fig. 3). Dissolved oxygen concentrations where the data set was split for presence–absence data were between 2 and 3 $mg \cdot L^{-1}$ for most fish species (weakfish, 2.1 $mg \cdot L^{-1}$; blue crab, 2.3 $mg \cdot L^{-1}$; shrimp, 2.2 $mg \cdot L^{-1}$; croaker, 2.3 $mg \cdot L^{-1}$; spot, 2.3 $mg \cdot L^{-1}$; menhaden, 2.6 $mg \cdot L^{-1}$; southern flounder, 2.6 $mg \cdot L^{-1}$; and hogchoker, 3.0 $mg \cdot L^{-1}$). Because of constraints associated with precisely measuring dissolved oxygen concentrations in the field and a survey not being able to fill every 0.1 $mg \cdot L^{-1}$ bin for analyses, small differences of ≤ 0.5 $mg \cdot L^{-1}$ in avoidance thresholds between many of the species should not be interpreted as biologically significant. Pinfish (4.1 $mg \cdot L^{-1}$) and silver perch (4.2 $mg \cdot L^{-1}$) had the highest dissolved oxygen avoidance thresholds (Fig. 3).

Focal-species threshold comparisons

Spot, croaker, and blue crab were abundant over the entire sampling season every year. This allowed us to evaluate if month, temperature, oxygen availability, or extent of hypoxia (Table 1) explained any of the variability in dissolved oxygen thresholds (CART splits) for each date. Overall correlation coefficients among predictor variables were low (Pearson's correlation coefficients <0.23), except extent of hypoxia was correlated with oxygen range (Pearson's correlation coefficient = –0.48). Extent of hypoxia explained a significant amount of the variance in the splits for spot (p = 0.02) and croaker (p = 0.01). There was a decrease in the CART dissolved oxygen threshold with increasing size of hypoxic zone (Fig. 4). In other words, the smaller the oxygenated refuge area, the lower the low oxygen threshold. No variables were significant in the analyses of dissolved oxygen thresholds for blue crab.

Fig. 2. (*a*) Mean and standard deviation for temperature (°C) for both the upstream and downstream study areas during sampling each month. (*b*) Monthly mean and standard deviation for salinity (‰) for the two study areas. (*c*) Scatterplots represent monthly mean and standard deviation in dissolved oxygen concentration (mg·L^{-1}) averaged over the study areas for each month. Columns represent the average proportion of the study area with hypoxic bottom waters on the sampling dates. Black diamonds and bars and gray squares and bars represent data from the upstream and downstream study areas, respectively.

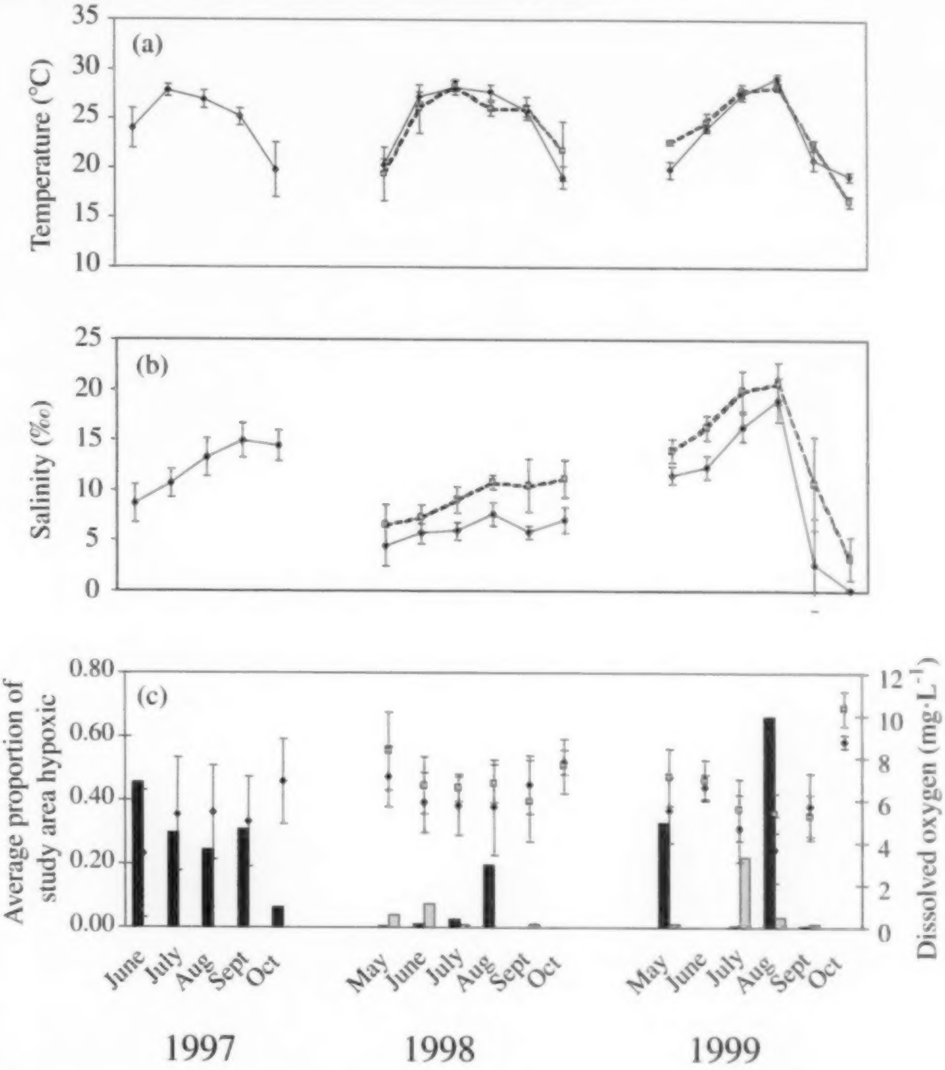

Spot, croaker, and blue crab all had similar patterns in their electivity index for the four different dissolved oxygen categories (Table 2). Electivity indices were negative for areas with dissolved oxygen concentrations between 0.0 and 2.0 mg·L^{-1}, indicating that habitat was used to a lesser extent than its availability, supporting the result that all three species avoided hypoxic waters. The dissolved oxygen range 2.0–4.0 mg·L^{-1} was also used in a smaller proportion than its availability (Table 2). Although indices for the 4.0–6.0 mg·L^{-1} dissolved oxygen range were around –0.30, the variation was large and standard deviations encompassed zero implying no preference or that the habitat was used in proportion to availability. The only dissolved oxygen ranges that were used in a greater proportion than their availability were in the dissolved oxygen range of 6.0–10.0 mg·L^{-1} (Table 2).

Focal-species habitat use changes

Our methodology of examining four variables on each sampling date requires multiple tests. For each species and site, we observed significant results more often than expected by chance. At each site (upstream and downstream), there were 4 variables and 19 dates, therefore 3.8 significant tests are expected by chance at the 0.05 level. There were between 9 and 15 significant tests for any particular species

Fig. 3. Catch per unit effort (CPUE, number/100 m trawled) vs. dissolved oxygen concentration (mg·L^{-1}) for the entire Neuse River Estuary data set (N = 1233 stations). Vertical lines represent data splits from categorical and regression tree analyses. Splits for presence–absence data were around 2.0 mg·L^{-1} for most fish.

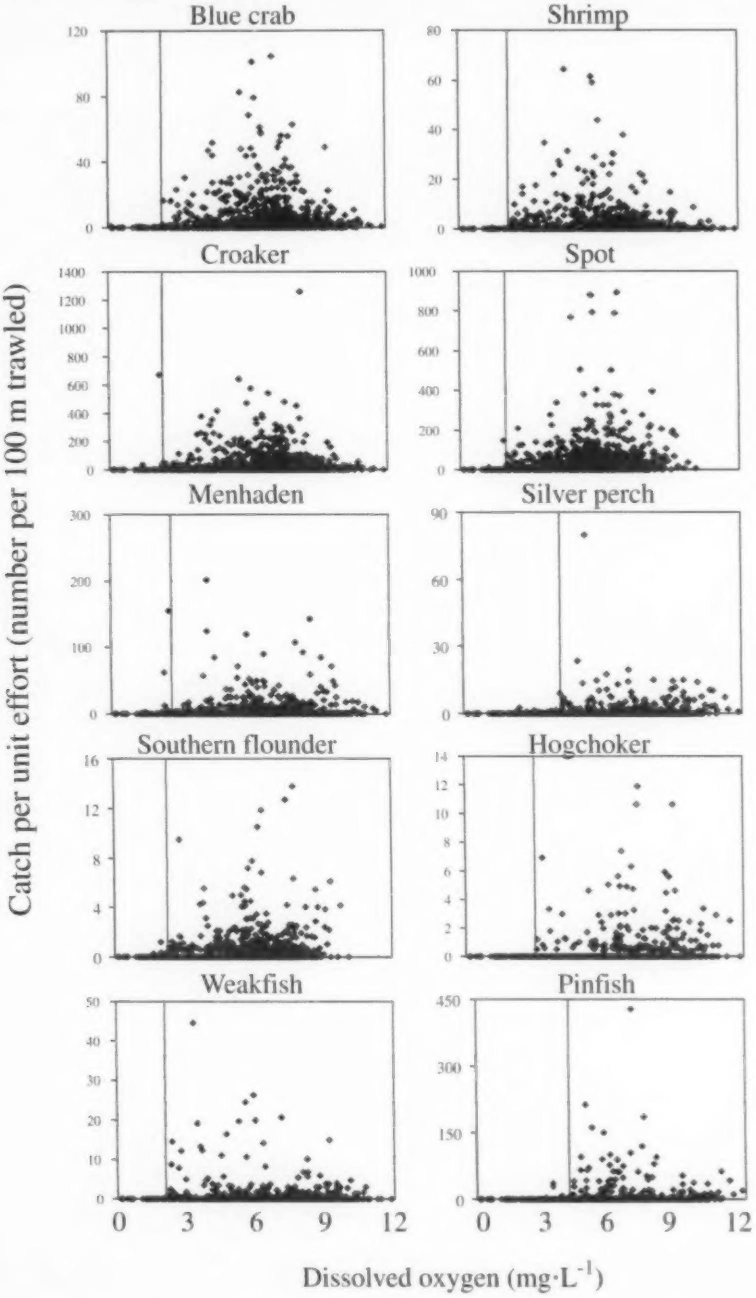

and site (see Appendix A). Our goal was to examine the patterns in which variables and dates were significant.

We expected demersal species to be distributed along temperature and depth gradients throughout the summer. In addition, we were expecting salinity to explain variance in blue crab distributions in the fall. When the estuary was oxygenated, we commonly found fish throughout the entire study area. There were no consistent seasonal trends in which environmental variables were significant ($p < 0.05$; Table 3). Depth and temperature were common significant variables for all three species. Temperature and depth were the most common variables explaining Atlantic croaker distributions.

Fig. 4. Avoidance threshold for dissolved oxygen (DO) concentrations (from CART results) for each sampling date vs. percent of the study area that was hypoxic that same date ($N = 22$). This relationship is significant for both spot (*Leiostomus xanthurus*) ($p = 0.02$) and croaker (*Micropogonias undulates*) ($p = 0.01$).

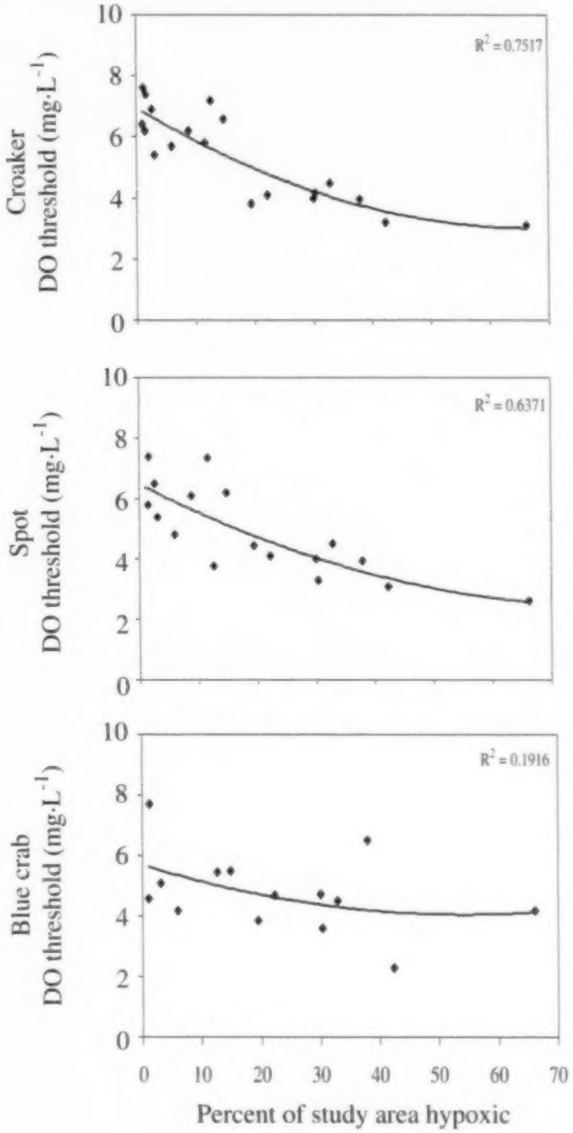

Table 2. Jacobs' electivity indices (EI) for four different dissolved oxygen ranges ($mg \cdot L^{-1}$) calculated for spot (*Leiostomus xanthurus*), croaker (*Micropogonias undulates*), and blue crab (*Callinectes sapidus*).

	0–1.9	2.0–3.9	4.0–5.9	≥6.0
Spot				
Jacobs' EI				
Mean	–0.96	–0.58	–0.30	0.58
SD	0.19	0.46	0.55	0.38
Croaker				
Jacobs' EI				
Mean	–0.94	–0.60	–0.30	0.58
SD	0.28	0.42	0.57	0.36
Blue crab				
Jacobs' EI				
Mean	–0.98	–0.71	–0.30	0.60
SD	0.08	0.37	0.56	0.40

Note: Electivity indices were calculated for each date and then averaged across the sampling dates. SD, standard deviation.

Croakers were either distributed across the depth range and depth was not significant or depth was significant and croaker catches were highest in the shallower waters, between 1 and 4 m deep. Generally the highest fish catches were found between 27°C and 29°C. In all years, croaker catches were higher at the fresher end of the salinity range in the spring and summer. Spot were also typically distributed across the entire depth range. When depth was significant, spring and summer catches were higher in shallow waters, whereas fall catches were higher in the deeper waters. Spot distributions tended towards 28°C. Dissolved oxygen concentration was a significant predictor variable for spot (with a positive relationship) even when the entire estuary was oxygenated, because spot catches were often highest in the highest dissolved oxygen concentrations. Temperature and depth were also significant in explaining variances in blue crab catch, with the highest catches typically found in the warmer, shallow waters. During oxygenated periods, significant environmental variables explained very little of the variance (partial R^2s ≤ 0.05).

Fish and crab distributions changed consistently during periods of extensive hypoxia, however. To examine how use of the estuary varies with size of the hypoxic zone, we initially compared consecutive sampling days with different levels of hypoxia to demonstrate distribution shifts. For example, in September of 1997, the first sampling period had large hypoxic zones covering 42% of the bottom waters in the study area, whereas on the second sampling date, 10 days later, the hypoxic zone was less than half this size. Results from CART analyses of splits in the depth distribution for spot, croaker, and blue crab were 2.0, 1.5, and 1.5 m during the first hypoxic sampling and 3.1, 3.5, and 3.3 m for the second, more oxygenated sampling period. This trend of restricting fish to shallow waters as hypoxia increases was evident when all data are included in the analysis. There was a significant relationship between the extent of hypoxia on the limit of blue crab ($p < 0.001$) and croaker ($p = 0.017$) depth distributions. The same trend was apparent for spot depth distributions but was not significant ($p = 0.151$; Fig. 5).

This hypoxia-driven habitat shift concentrated fish in shallow waters that were often warmer than the average estuarine temperature. The highest catches of spot and croaker were typically between 27–28°C, whereas during periods with large hypoxic zones, the entire oxygenated area was between 29–30°C. This trend of fish residing in warmer temperatures during periods of extensive hypoxia was reflected in the Mantel's results. In August, when hypoxic zones were common and large, temperature was a positive significant predictor variable with the highest catches being in the warmer

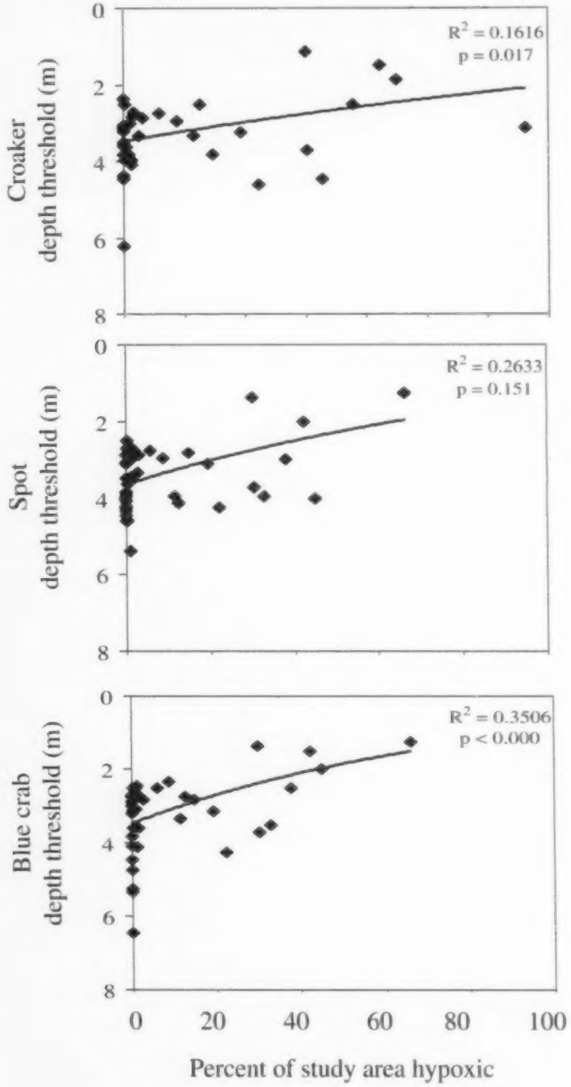

Fig. 5. Depth cutoffs from CART results for each sampling date vs. percent of study area hypoxic. There is a significant relationship between the extent of hypoxia on the limit of blue crab (*Callinectes sapidus*) ($p < 0.001$) and croaker (*Micropogonias undulates*) ($p = 0.017$) depth distributions. The same trend is apparent for spot (*Leiostomus xanthurus*) depth distributions but is not significant ($p = 0.151$).

waters (Table 3). These results imply that fish were either using areas of warmer temperatures for faster growth in late summer or getting pushed into warmer temperatures because of habitat loss. To investigate these alternatives, we examined the amount of variance explained in the catch data (partial *R*s) by temperature. Partial *R*s (ρR) associated with temperature were 2 to 10 times higher for blue crab (no hypoxia, $\rho R = 0.023$; hypoxia present, $\rho R = 0.274$) and croaker (no hypoxia, $\rho R = 0.05$; hypoxia present, $\rho R = 0.1$) during extensive hypoxia. In addition, temperature was only a significant variable explaining spot distributions when hypoxia was present. Fish appear to be restricted to warmer areas and not choosing warmer waters.

There was high overlap between spot and croaker distributions within our study area. At the upstream site, croaker distribution was a significant predictor of spot distribution from June through October in all years. The variance in spot catch explained by croaker catch was consistently higher than any environmental parameter (mean $\rho R^2 = 0.3$; range 0.01–0.95). At the downstream site, relationships between spot and croaker were significant in June, July, and August in 1998 and 1999 (mean $\rho R^2 = 0.3$). There was no trend in overlap with habitat loss. In contrast, blue crab catch was rarely a significant predictor of spot catch and only occurred when on average 33% of the study area was hypoxic.

Discussion

All the fish and crustacean species we examined avoided hypoxic areas. All species moved from deep hypoxic waters to shallow oxygenated areas during hypoxic episodes. When shallow areas became hypoxic during occasional seiching events (Luettich et al. 2000), fish were isolated in pockets of oxygenated water. When dissolved oxygen levels increased in deeper portions of the estuary, fish and crustaceans moved back into these areas, broadening their distribution.

All species we examined were excluded from dissolved oxygen concentrations below 2.0 mg·L^{-1}. In our study, croaker and hogchoker avoidance thresholds were 2.0 mg·L^{-1}, but results from studies in other systems indicate that these species may be more sensitive to hypoxia (Pihl et al. 1991). Whether this is due to differences between systems or populations is unknown. In addition, more research is required to determine whether pinfish and silver perch actually have higher dissolved oxygen thresholds than other species. In laboratory experiments, pinfish demonstrated preferences for dissolved oxygen levels up to 6.0 mg·L^{-1} (Wannamaker and Rice 2000). Pinfish prefer vegetated bottom and sea grass habitats (e.g., Coen et al. 1981), which are rare and primarily found in the shallowest waters in the Neuse River Estuary. Our field results cannot discount the alternative that this bias in their distribution towards very shallow waters, where hypoxic conditions rarely occurred, may have resulted in the higher avoidance threshold.

Of the four hypotheses posed regarding context dependency, only the areal extent of hypoxia was supported by our analyses. Spot, croaker, and blue crab were consistently excluded from areas with dissolved oxygen concentrations of ≤2.0 mg·L^{-1}. This suggests a fixed, physiological, lower threshold near 2.0 mg·L^{-1}. However, when we examined these data by date, spot, croaker, and blue crab had different avoidance thresholds depending on the external conditions in the estuary. Analyses supported the hypothesis that spatial extent of hypoxia (or conversely the area of the oxygenated refuge habitat) is affecting avoidance thresholds. With a small hypoxic area (<20%) spot and croaker had avoidance thresholds between 4 and 5 mg·L^{-1}, which may imply a preference for dissolved oxygen levels higher than 2.0 mg·L^{-1}. Fish may be forced to occupy poor quality habitat as conditions worsen and the oxygenated refuge area shrinks. One possible mechanism may be that as fish are crowded into oxy-

Table 3. Results of partial Mantel tests of spot, croaker, and blue crab catch per unit effort data versus environmental factors by month.

	May	June	July	August	September	October
Hypothesis:	*T, D, S*	*T, D*	*T, D,* DO	*T, D,* DO	*T, D, S,* DO	*T, D, S,* DO
Spot						
Upstream	DO (1999)	*D* (1999)	DO (1998, 1999)	*D* (1997) *T* (1998, 1999) DO (1999)	*T* (1997) *D* (1998, 1999) DO (1998)	*S* (1998, 1999) *D* (1998)
Downstream	DO (1998) *D* (1998)	*D* (1998) *T* (1998) *S* (1998)	*D* (1998)	DO (1998)	*S* (1998) DO (1998) *T* (1999)	
Croaker						
Upstream		*D* (1999)	DO (1998)	*T* (1997, 1998) *S* (1999)	*D* (1998, 1999) *S* (1999)	*S* (1999)
Downstream	*S* (1999)	*T* (1998)	*D* (1998)	*T* (1998, 1999)	*S* (1998) *D* (1998) DO (1998)	
Blue crab						
Upstream		*S* (1999) *D* (1999)		*T* (1998, 1999) *D* (97, 99) DO (1997)	*T* (1997) *S* (1997) *D* (1998)	*T* (1999) *D* (1999)
Downstream	*T* (1998, 1999) *S* (1998, 1999)	*D* (1998)	*D* (1999) *T* (1999) *S* (1999)	*T* (1998, 1999)	*D* (1998) *T* (1998) *S* (1999)	

Note: Only significant predictor variables ($p < 0.05$) are shown in the table. The year(s) for which the variable was significant is (are) indicated in parentheses. Appendix A contains partial Mantel test statistics (ρR^2s) for blue crab (*Callinectes sapidus*), spot (*Leiostomus xanthurus*), and croaker (*Micropogonias undulates*) for every sampling date. DO, dissolved oxygen concentration; *S*, salinity; *T*, temperature; *D*, depth.

genated refuges, antagonistic interactions or competition may force them into waters with lower dissolved oxygen concentrations than they may prefer. This has been demonstrated in other systems where the presence of both inter- and intra-specific competitors can qualitatively alter how species rank habitats in terms of foraging profitability and force disadvantaged individuals into less profitable habitats (Werner and Hall 1979).

The three focal species used area with dissolved oxygen range of 2.0 to 4.0 mg·L^{-1} in a lower proportion than what was available. Preferences for dissolved oxygen concentrations above 2.0 mg·L^{-1} have also been reported in laboratory choice experiments (6.0 mg·L^{-1} versus 4.0 mg·L^{-1} or 4.0 mg·L^{-1} versus 2.0 mg·L^{-1}) for several species (spot, white mullet (*Mugil curema*), croaker, and pinfish; Wannamaker and Rice 2000). Therefore, preference for higher dissolved oxygen concentrations suggests that there may be physiological or ecological costs associated with reducing their avoidance thresholds to 2.0 mg·L^{-1}. Studies of largemouth bass, *Micropterus salmoides*, demonstrated lower food conversion efficiency and maximum growth rates for fish held in dissolved oxygen concentrations between 2.0 and 4.0 mg·L^{-1} versus fish held in well-oxygenated waters (Stewart et al. 1967). Similar decreases in maximum growth rate have been seen in other species, including juvenile *Cyprinus carpio* and *Oncorhynchus kisutch* (review in Brett 1979).

Behavioral models and experimental work have demonstrated that over short time frames behavioral decisions can be predicted from cost–benefit ratios taking factors such as foraging returns, bioenergetic constraints, and predation risks into account (e.g., Crowder and Magnuson 1983; Turner and Mittelbach 1990). If fish use areas with higher metabolic costs (dissolved oxygen concentrations of 2.0–4.0 mg·L^{-1}), there must be a tradeoff or cost to remaining in the oxygenated refuge once it shrinks to a certain size. Examination of changes in habitat use present several possibilities. First, extensive hypoxic zones typically restricted fish to shallow, warmer waters. Although optimal temperatures are not known for these species, horizontal displacement may shift fish distributions into potentially more costly environments. Second, shallow margins of the estuary may not have the same level of prey resources as the greater depths, particularly early in the growing season (Sullivan and Gaskill 1999). Third, during periods of habitat compression, juvenile fish will be in higher densities and also have greater overlap with the distribution of blue crab. Our analyses indicate that when the estuary is well-oxygenated, blue crab and juvenile fish have different distributions, but during periods of extensive hypoxia their overlap increases to the point where the distribution of spot is significantly predicted by the distribution of blue crabs. Juvenile spot and small blue crab consume the same prey items when alone; their combined presence has been shown to enhance feeding of spot (Martin et al. 1989). Although blue crabs infrequently feed on live fish, restriction of both fish and crabs to the usable habitat will increase encounters and harassment, as well as potential predation risk on juvenile fish.

Our expectation that the focal demersal species (spot, croaker, and blue crab) distribute themselves towards particular temperatures or depths was only weakly supported. A larger geographical scale (i.e., larger range in the environmental variables) may demonstrate stronger preferences that were not apparent here (as in Rose and Leggett 1989, for example). These species generally used the entire estuary when it was well oxygenated. When hypoxia was extensive, fish were restricted to the oxygenated shallows, decreasing the limits of their depth distribution and compressing their habitat.

Our hypothesis that spot and croaker would partition the habitat when the estuary was well oxygenated but overlap during extensive hypoxia was not supported. Partial Mantel results suggested high overlap between spot and croaker distributions within the study areas, regardless of areal extent of hypoxia. The study area is at a mid-salinity range within the estuarine system, where the ranges of these species overlap. There was no spatial separation within the study area, but interannual differences in salinity were reflected in the variation of the dominant fish species among sampling years. Spot was most abundant in 1997 and 1999 when spring and summer salinities averaged 13‰ and 17‰, whereas croaker was dominant in 1998 (average salinity 8‰ for spring and summer), implying some partitioning at a scale larger than the study area.

All fish and crustacean species that we captured moved out of hypoxic waters. Dead fish are infrequently taken in trawls. Thus, direct effects of hypoxia on motile species in these systems are minor. Habitat selection in these intermittently hypoxic estuaries goes from being a balance of multiple factors (abiotic influences and biotic interactions) to achieve the best growth rate to primarily being influenced by one limiting factor (dissolved oxygen) as spatial extent of the low oxygen zones increases. Behavioral avoidance of hypoxic zones is context-dependent, depending on the extent of hypoxia. Hypoxia-derived habitat compression forces fish into depressed dissolved oxygen levels, potentially exposing them to increased metabolic costs and intensifying species interactions. Anthropogenic activities that increase the temporal or spatial extent and intensity of intermittent hypoxia in systems that experience historic, natural hypoxia may have important sublethal effects on the fish community.

Acknowledgements

We would like to acknowledge David Lewis, Andy Read, and Pete Peterson for insightful comments of this manuscript. Also, we would like to thank everyone who worked with us in the field since 1997, including Catherine McClellum, Shae Keller, Paula Gillikin, Kristin TePas, Daniel Waples, Hazel Richmond, Shabeen Alley, Carrie Selberg, Sharleen Johnson, Katie Barnas, Rebecca Goldman, Julia Whitcomb, Damon Gannon, Kevin Craig, and many student volunteers. A special thanks is extended to the crew of the R/V *Susan Hudson*, Tim Boynton, Lanier Mitchum, Huey Willis, and Jeffrey Priddy. This work was funded by grants from Environmental Protection Agency (Grant #R26100-01-0), Water Resource Research Institute (Project #50220), NOAA North Carolina Sea Grant (Project R/MRD-37), and the J.F. Allen Award from the American Fisheries Society (to L.A. Eby). Although the research described in this article has been funded in part by the United States Environmental Protection Agency through (Grant #R26100-01-0) to Drs. Larry Crowder and Andrew Read, it has not been subjected to the Agency's required peer review and policy review and therefore does not necessarily reflect the views of the Agency and no official endorsement should be inferred.

References

Bejda, A.J., Studholme, A.L., and Olla, B.L. 1987. Behavioral responses of red hake, *Urophycis chuss*, to decreasing concentrations of dissolved oxygen. Environ. Biol. Fishes, **19**: 261–268.

Breitburg, D.L. 1992. Episodic hypoxia in Chesapeake Bay: interacting effects of recruitment, behavior, and physical disturbance. Ecol. Monogr. **62**: 525–546.

Brett, J.R. 1979. Environmental factors and growth. *In* Fish physiology. Vol. VIII. *Edited by* W.S Hoar, D.J. Randall, and J.R Brett. Academic Press, Inc., New York. pp. 632–637.

Clark, L.A., and Pregibon, D. 1992. Tree-based models. *In* Statistical models. *Edited by* J.M. Chambers and T.J. Hastie. S. Wadsworth and Brooks, Pacific Grove, Calif. pp. 377–419.

Coen, L.D., Heck, K.L., and Abele, L.G. 1981. Experiments on competition and predation among shrimps of seagrass meadows. Ecology, **62**: 1484–1493.

Copp, G.H. 1992. Comparative microhabitat use of cyprinid larvae and juveniles in a lotic floodplain channel. Environ. Biol. Fishes, **33**: 181–193.

Coutant, C.C. 1987. Thermal preference: when does an asset become a liability? Environ. Biol. Fishes, **18**: 161–172.

Crowder, L.B., and Magnuson, J.J. 1983. Cost–benefit analysis of temperature and food resource use: a synthesis with examples from the fishes. *In* Behavioral energetics: the cost of survival in vertebrates. *Edited by* W.P. Aspey and S.I. Lustick. Ohio State University Press, Columbus. pp. 189–221.

Day, J.W., Jr., Hall, C.A.S., Kemp, W.M., and Yanez-Arancibia, A. (*Editors*). 1989. Estuarine ecology. John Wiley and Sons, Inc., New York. pp 512–542.

Gee, J.M., Warwick, R.M., Davey, J.T., and George, C.L. 1985. Field experiments on the role of epibenthic predators in determining prey densities in an estuarine mudflat. Estuar. Coast. Shelf Sci. **21**: 429–448.

Howell, P., and Simpson, D. 1994. Abundance of marine resources in relation to dissolved oxygen in Long Island Sound. Estuaries, **17**: 394–402.

Hughes, N.F., and Dill, L.M. 1990. Position choice by drift-feeding salmonids: model and test for arctic grayling (*Thymallus arcticus*) in subartic mountain streams, interior Alaska. Can. J. Fish. Aquat. Sci. **47**: 2039–2048.

Ivlev, V.S. 1961. Experimental ecology of the feeding of fishes. Yale University Press, New Haven, Conn.

Jacobs, J. 1974. Quantitative measurement of food selection, a modification of the forage ratio and Ivlev's electivity index. Oecologia, **14**: 413–417.

Kneib, R.T. 1982. The effects of predation by wading birds (*Ardeidae*) and blue crabs (*Callinectes sapidus*) on the population size structure of the common mummichog, *Fundulus heteroclitus*. Estuar. Coast. Shelf Sci. **14**: 159–165.

Legendre, P. 1993. Spatial autocorrelation: trouble or new paradigm? Ecology, **74**: 1659–1673.

Legendre, P., and Fortin, M.J. 1989. Spatial pattern and ecological analysis. Vegetatio, **80**: 107–138.

Lenihan, H.S., Peterson, C.H., Byers, J.E., Grabowski, J.H., Thayer, G.H., and Colby, D.R. 2001. Cascading of habitat degradation: oyster reefs invaded by refugee fishes escaping stress. Ecol. Appl. **11**: 764–782

Lima, S.L., and Dill, L.M. 1990. Behavioural decisions made under risk of predation: a review and prospectus. Can. J. Zool. **68**: 619–640.

Luettich, R.A., Martens, C.S., McNinch, J.E., Paerl, H.W., Pinckney, J.L., Peterson, C.H., Alperin, M., and Wells, J.T. 2000. Neuse Modeling and Monitoring (MODMON) technical report. Water Resources Research Institute, Raleigh, N.C.

Magnuson, J.J., Crowder, L.B., and Medvick, P.A. 1979. Temperature as an ecological resource. Am. Zool. **19**: 331–343.

Manly, B.F.J. 1991. RT: a program for randomization testing. Version 1.02. Western EcoSystems Technology, Inc., Cheyenne, Wyo.

Martin, T.H., Wright, R.A., and Crowder, L.B. 1989. Non-additive impact of blue crabs and spot on their prey assemblages. Ecology, **70**: 1935–1942.

Menge, B.A., Berlow, E.L., Blanchette, C.A., Navarrete, S.A., and Yamada, S.B. 1994. The keystone species concept: variation in interaction strength in a rocky intertidal habitat. Ecol. Monogr. **64**: 249–286.

Mittlebach, G.G. 1986. Predation-mediated habitat use: some consequences for species interactions. Biol. Fish. **16**: 159–169.

Mittlebach, G.G. 1988. Competition among refuging sunfishes and effects of fish density on littoral zone invertebrates. Ecology, **69**: 614–623.

National Research Council (NRC). 2001. Clean coastal waters: understanding and reducing the effects of nutrient pollution. National Academy Press, Washington, D.C.

Nelson, D.M., Irlandi, E.A., Settle, L.R., Monaco, M.E., and Coston-Clements, L.C. 1991. Distribution and abundance of fishes and invertebrates in southeast estuaries. ELMR Rep. No. 9. NOAA/NOS Strategic Environmental Assessments Division, Rockville, Md.

Paerl, H.W., and Pinckney, J.L. 1996. Hypoxia, anoxia, and fish kills in relation to nutrient loading in the Neuse River estuary: why was 1995 a "bad" year? *In* Water wise. Vol. 4, No. 2. May 1996. UNC Sea Grant Program, Raleigh, N.C.

Paerl, H.W., Bales, J.W., Ausley, L.W., Buzzelli, C.P., Crowder, L.B., Eby, L.A., Fear, J.M., Go, M., Peierls, B.L., Richardson, T.L., and Ramus, J.S. 2001. Ecosystem impacts of three sequential hurricanes (Dennis, Floyd, and Irene) on the United States' largest lagoonal estuary, Pamlico Sound, N.C. Proc. Nat. Acad. Sci. **98**: 5655–5660.

Parker, J.C. 1971. The biology of spot, *Leiostomus xanthurus*, and Atlantic croaker, *Micropogonus undulatus*, in two Gulf of Mexico nursery areas. Texas A&M University Sea Grant Publication TAMU-SG-71-210, May 1971.

Persson, L. 1993. Predator-mediated competition in prey refuges: the importance of habitat dependent prey resources. Oikos, **68**: 12–22.

Persson, L., and Eklov, P. 1995. Prey refuges affecting interactions between piscivorous perch (*Perca fluviatilis*) and juvenile perch and roach (*Rutilus rutilus*). Ecology, **76**: 70–81.

Pihl, L., Baden, S.P., and Diaz, R.J. 1991. Effects of periodic hypoxia on distribution of demersal fish and crustaceans. Mar. Biol. **108**: 349–360.

Pihl, L., Baden, S.P., Diaz, R.J., and Schaffner, L.C. 1992. Hypoxia-induced structural changes in the diet of bottom-feeding fish and crustacea. Mar. Biol. **112**: 349–361.

Rose, G.A., and Leggett, W.C. 1989. Interactive effects of geophysically forced sea temperatures and prey abundance on mesoscale coastal distributions of a marine predator, Atlantic cod (*Gadus morhua*). Can. J. Fish. Aquat. Sci. **46**: 1904–1913.

Schurmann, H., Steffensen, J.F., and Lomholt, J.P. 1991. The influence of hypoxia on the preferred temperature of rainbow trout, *Oncorhynchus mykiss*. J. Exp. Biol. **157**: 75–86.

Sih, A. 1980. Optimal behavior: can foragers balance two conflicting demands? Science (Washington, D.C.), **210**: 1041–1043.

Stewart, N.E., Shumway, D.L., and Doudoroff, P. 1967. Influence of oxygen concentration on the growth of juvenile largemouth bass. J. Fish. Res. Board Can. **24**: 475–494.

Stuntz, W.E., Sanders, N., Leming, T.D., Baxter, K.N., and Barazotto, R.M. 1983. Area of hypoxic bottom water found in northern Gulf of Mexico. Coastal Oceanogr. Climatol. News, **4**: 37–38.

Sullivan, E.T., and Gaskill, D. 1999. Effects of anoxia on the value of bottom habitat for fisheries production in the Neuse River Estuary. Final Report for Fisheries Resource Grant 98 EP-04, Department of Marine Fisheries, Morehead City, N.C.

Turner, A.M., and Mittelbach, G.G. 1990. Predator avoidance and community structure: interactions among piscivores, planktivores, and plankton. Ecology, **71**: 2241–2254.

Tyler, J.A., and Gilliam, J.F. 1995. Ideal free distributions of stream fish: a model and test with minnows (*Rhinicthys atratulus*). Ecology, **76**: 580–592.

Virnstein, R.W. 1977. The importance of predation by crabs and fishes on benthic infauna in the Chesapeake Bay. Ecology, **58**: 1199–1217.

Wannamaker, C.M., and Rice, J.A. 2000. Effects of hypoxia on movements and behavior of selected estuarine organisms from the southeastern United States. J. Exp. Biol. Ecol. **249**: 145–163.

Werner, E.E., and Hall, D.J. 1979. Foraging efficiency and habitat switching in competing sunfishes. Ecology, **60**: 256–264.

Wilkins, H.K.A., and Myers, A.A. 1992. Microhabitat utilisation by an assemblage of temperate Gobiidae (Pisces: Teleostei). Mar. Ecol. Prog. Ser. **90**: 103–112.

(Appendix A follows.)

Appendix A

Table A1. Results from partial Mantel tests (ρR^2) for blue crab (*Callinectes sapidus*), spot (*Leiostomus xanthurus*), and croaker (*Micropogonias undulates*) from the upstream study site.

	Blue crab				Spot				Croaker			
	T	*S*	DO	*D*	*T*	*S*	DO	*D*	*T*	*S*	DO	*D*
8/01/1997[a]												
p				0.000								
ρR^2				0.186								
8/15/1997												
p								0.001	0.040			
ρR^2								0.187	0.088			
8/24/1997												
p			0.026									
ρR^2			0.054									
9/11/1997												
p	0.010				0.048							
ρR^2	0.527				0.175							
9/21/1997												
p		0.009										
ρR^2		0.066										
10/23/1997												
p												
ρR^2												
5/10/1998												
p												
ρR^2												
6/21/1998												
p												
ρR^2												
7/19/1998												
p							0.005				0.034	
ρR^2							0.161				0.039	
8/16/1998												
p	0.000				0.019				0.037			
ρR^2	0.453				0.131				0.156			
9/05/1998												
p				0.003			0.046	0.005				0.028
ρR^2				0.082			0.009	0.027				0.064
9/23/1998												
p												
ρR^2												
10/22/1998												
p								0.036				0.006
ρR^2								0.085				0.088
5/14/1999												
p							0.023					
ρR^2							0.073					
6/18/1999												
p		0.027		0.021				0.000				0.000
ρR^2		0.036		0.022				0.119				0.101
7/18/1999												
p							0.045					
ρR^2							0.066					
8/19/1999												
p	0.005			0.044	0.005		0.023			0.037		
ρR^2	0.140			0.032	0.174		0.075			0.028		
9/23/1999												
p								0.049		0.043		0.001
ρR^2								0.024		0.030		0.152
10/21/1999												
p	0.019			0.002		0.039				0.028		
ρR^2	0.029			0.205		0.045				0.146		

Note: Only significant results are presented. DO, dissolved oxygen concentration; *S*, salinity; *T*, temperature; *D*, depth.

[a] Dates given as month/day/year.

Table A2. Results from partial Mantel tests for blue crab (*Callinectes sapidus*), spot (*Leiostomus xanthurus*), and croaker (*Micropogonias undulates*) from the downstream study site.

	Blue crab				Spot				Croaker			
	T	*S*	DO	*D*	*T*	*S*	DO	*D*	*T*	*S*	DO	*D*
4/30/1998[a]												
p							0.008					
ρR^2							0.055					
5/14/1998												
p								0.040				
ρR^2								0.022				
5/28/1998												
p	0.013	0.018										
ρR^2	0.067	0.038										
6/10/1998												
p				0.009				0.004				
ρR^2				0.060				0.070				
6/25/1998												
p					0.001	0.033			0.024			
ρR^2					0.134	0.064			0.030			
7/09/1998												
p				0.004				0.019				0.006
ρR^2				0.043				0.028				0.070
7/23/1998												
p				0.017								
ρR^2				0.037								
8/06/1998												
p	0.041						0.042		0.036			
ρR^2	0.022						0.050		0.048			
8/20/1998												
p												
ρR^2												
9/17/1998												
p	0.002			0.004			0.012					0.000
ρR^2	0.019			0.048			0.038					0.130
9/17/1998												
p												
ρR^2												
9/30/1998												
p						0.014	0.000				0.002	
ρR^2						0.036	0.186				0.127	
10/15/1998												
p	0.035					0.001					0.023	
ρR^2	0.068					0.121					0.058	
5/27/1999												
p	0.003	0.027							0.039	0.050		
ρR^2	0.343	0.063							0.060	0.034		
6/27/1999												
p												
ρR^2												
7/22/1999												
p	0.020	0.014										
ρR^2	0.110	0.045										
8/23/1999												
p	0.017								0.041			
ρR^2	0.273								0.078			
9/27/1999												
p		0.016			0.023							
ρR^2		0.068			0.214							
10/28/1999												
p												
ρR^2												

Note: Only significant results are presented. DO, dissolved oxygen concentration; *S*, salinity; *T*, temperature; *D*, depth.
[a]Dates given as month/day/year.

Resistance to three pathogens in the endangered winter-run chinook salmon (*Oncorhynchus tshawytscha*): effects of inbreeding and major histocompatibility complex genotypes

Kristen D. Arkush, Alan R. Giese, Holly L. Mendonca, Anne M. McBride, Gary D. Marty, and Philip W. Hedrick

Abstract: We have carried out the first major infectivity trial to examine differential genetic resistance in fish for pathogens. We used captive-bred, endangered winter-run chinook salmon (*Oncorhynchus tshawytscha*) to determine resistance to three pathogens: the bacterium, *Listonella* (*Vibrio*) *anguillarum*, infectious hematopoietic necrosis virus (IHNV), and *Myxobolus cerebralis*, the parasite that causes whirling disease. We compared resistance to these three pathogens between inbred and outbred salmon and between siblings that were heterozygous or homozygous for a class II gene in the major histocompatibility complex (MHC). In two of five different comparisons, we found significant genetic effects on disease resistance. First, MHC heterozygotes had a higher survival than MHC homozygotes when exposed to IHNV and the selection disadvantage of homozygotes was estimated to be 8.5%. Second, outbred fish had a higher resistance (or lower infection severity) than inbred fish when exposed to *M. cerebralis*. Using a quantitative genetics approach, it appears that there are slightly more than three gene equivalents segregating that would result in no resistance to *M. cerebralis* when homozygous. Overall, our investigation suggests that pathogen susceptibility in the winter-run chinook salmon will increase if further genetic variation is lost in this endangered species.

Résumé : Nous avons mis sur pied le premier test d'infectivité à grande échelle qui vérifie la résistance génétique différentielle des poissons aux pathogènes. Des saumons quinnat (*Oncorhynchus tshawytscha*) élevés en captivité et appartenant à la race menacée à montaison hivernale ont servi à tester la résistance à trois pathogènes : la bactérie *Listonella* (*Vibrio*) *anguillarum*, le virus de la nécrose hématopoïétique infectieuse (IHNV) et *Myxobolus cerebralis*, le parasite qui cause la maladie du tournis. Nous comparons la résistance à ces trois pathogènes chez des saumons consanguins et non consanguins et chez des frères et sœurs hétérozygotes ou homozygotes pour un gène de classe II du complexe majeur d'histocompatibilité (MHC). Dans deux de cinq comparaisons, il y a des effets génétiques significatifs sur la résistance à la maladie. D'abord, les hétérozygotes MHC ont une meilleure survie que les homozygotes lors d'une exposition au IHNV et le désavantage sélectif des homozygotes est estimé à 8,5 %. Ensuite, les poissons non consanguins ont une plus forte résistance (ou leur infection est moins sévère) que les poissons consanguins lors d'expositions à *M. cerebralis*. Une approche génétique quantitative laisse croire qu'il y a un peu plus de trois ségrégations d'équivalents-gènes qui causent l'absence de résistance à *M. cerebralis* en condition homozygote. En résumé, notre étude indique que la susceptibilité aux pathogènes chez le saumon chinook à montaison hivernale risque de s'accroître s'il se perd encore plus de variation génétique chez cette espèce menacée.

[Traduit par la Rédaction]

Introduction

Among the major threats to endangered species are habitat alteration and destruction, overharvesting, and the biotic effects of introduced competitors and predators. In recent years, it has become widely recognized that endangered species may be also threatened by exposure to pathogens (e.g., Lafferty and Gerber 2002), many of them exotic and novel to the endangered species. Here we define pathogens broadly to include viruses, bacteria, protozoa, and helminthes, all of which can cause a reduction in fitness to the host. In endangered species, a pathogen introduced from another more

Received 15 November 2001. Accepted 17 April 2002. Published on the NRC Research Press Web site at http://cjfas.nrc.ca on 15 July 2002.
J16616

K.D. Arkush, H.L. Mendonca, and A.M. McBride. Bodega Marine Laboratory, University of California–Davis, Bodega Bay, CA 94923, U.S.A.
A.R. Giese and P.W. Hedrick.[1] Department of Biology, Arizona State University, Tempe, AZ 85287, U.S.A.
G.D. Marty. Department of Anatomy, Physiology, and Cell Biology, School of Veterinary Medicine, University of California–Davis, Davis, CA 95616, U.S.A.

[1] Corresponding author (e-mail: philip.hedrick@asu.edu).

DOI: 10.1139/F02-066

common species, particularly if the endangered species has low resistance, may result in final decline to extinction.

Resistance of a host to pathogens often has an important genetic component. In particular, genes in the major histocompatibility complex (MHC) (Edwards and Hedrick 1998) play an important role in disease resistance to pathogens in vertebrates (Hedrick and Kim 2000). For example, the MHC in humans has been shown to be important in resistance to HIV (human immunodeficiency virus), hepatitis, and malaria. Resistance to HIV and hepatitis in humans appears to be higher for MHC heterozygotes than for homozygotes (Thurz et al. 1997; Carrington et al. 1999). Further, susceptibility to HIV may be the result of a single amino acid change in a MHC molecule (Gao et al. 2001), suggesting that the role of small changes in the MHC may be important.

In endangered species, the level of genetic variation in the MHC, and other genes that may influence host resistance, may be lower because of past or present small population size, than more common species. This may make endangered species even more susceptible to the effects of pathogens than common species that have large, stable population sizes, which generally have greater genetic variation. In the small populations of endangered species, there may also be a higher frequency of inbreeding, a factor that results in an increase in homozygosity for all loci. There is evidence that inbred animals within a population may have higher susceptibility to pathogens than outbred individuals (Coltman et al. 1999; P.W. Hedrick et al. 2001*b*).

The annual number of spawning adults of the endangered winter-run chinook salmon, *Oncorhynchus tshawytscha*, from the Sacramento River, California, drainage has declined from over 100 000 in 1969 to about 200 in 1991. As a result of the low spawning adult numbers, the U.S. Fish and Wildlife Service (USFWS) has been successfully releasing young fish since 1991 to increase the survival of eggs and juveniles compared to those in the natural population and to provide protection from any catastrophic event in the mainstem Sacramento River impacting juveniles (Hedrick et al. 1995, 2000*a*, 2000*b*). In addition, refuge populations were established at Bodega Marine Laboratory (BML) and the California Academy of Sciences Steinhart Aquarium in case the natural run became extinct. The population at BML was also established as a genetic broodstock to provide progeny for release if the natural numbers and those from the supplementation program were inadequate.

Here we investigated genetic resistance of winter-run chinook salmon produced from the broodstock at BML to three different pathogens (a bacterium, a virus, and a myxozoan parasite). All of these pathogenic agents are associated with debilitating and (or) deadly infections in salmonids. Moreover, these pathogens have either caused mortality in winter-run chinook salmon captive broodstock or in wild fish. Our specific goals were to determine if resistance in winter-run chinook salmon to the three pathogens (*i*) differed between heterozygotes and homozygotes at a MHC gene and (*ii*) differed between inbred and outbred individuals.

Methods

Pathogens

The bacterium used, *Listonella* (*Vibrio*) *anguillarum*, is one causative agent of vibriosis, a disease characterized by a hemorrhagic septicemia. This bacterium is found worldwide and is a significant pathogen of salmonids (Egidius 1987). Wild populations of salmon are susceptible to *L. anguillarum*, but more significant infections occur in cultured salmon, especially coho (*Oncorhynchus kisutch*), chinook (*O. tshawytscha*), and sockeye (*Oncorhynchus nerka*) (Evelyn 1971).

The virus used, infectious hematopoietic necrosis virus (IHNV), is the type species of the newly recognized genus *Novirhabdovirus* in the family Rhabdoviridae (Walker et al. 2000), infects young trout and certain Pacific salmon species, causing an acute, systemic, and often virulent disease (Wolf 1988). IHNV causes epizootics among wild and cultured salmonid fish and is considered the most important viral pathogen affecting salmonids in North America (Wolf 1988; Leong and Fryer 1993).

The other pathogen, *Myxobolus cerebralis*, is a myxozoan parasite that causes whirling disease. Whirling disease has been detected in salmonid populations from 23 states in the United States (Hedrick et al. 1998), and the negative and serious impacts of the disease on wild populations of resident salmonids in the intermountain regions have been documented (Nehring and Walker 1996). Recently, R.P. Hedrick et al. (2001) demonstrated that two anadromous species, chinook and steelhead (*Oncorhynchus mykiss*), are highly susceptible to infection and disease, and predicted that severe and negative impacts at the population level might occur if these species are exposed at early life stages to high levels of *M. cerebralis*.

Fish spawning matrix and early rearing

The fish used in the this experiment were progeny from captive-reared winter-run chinook salmon of brood years 1994 and 1995 held at BML. Maturing fish were determined by the use of ultrasonography and if gamete maturation was evident, fish were immediately moved into fresh water. Once in fresh water, feeding was discontinued and the salinity was increased to 10 ppt for two hours twice a week as a prophylactic treatment for the prevention of fungal infections (e.g., *Saprolegnia* spp.). Maturing fish were manually palpated 1–2 times weekly while anesthetized with methane tricaine sulfonate (MS-222, Argent Chemical Laboratories, Redmond, Wash.) at a concentration of 100 $\mathrm{mg \cdot L^{-1}}$.

On date of spawning, crosses were made such that both full-sib inbred progeny (inbreeding coefficient $f = 0.25$, see Hedrick 2000) and corresponding outbreds ($f = 0$) could be created from the same female, i.e., eggs from one female were divided and one half of the eggs was fertilized with milt from a full sib and the other half with milt from an unrelated male. In addition, a number of parents were selected so that their progeny would segregate for heterozygotes and homozygotes at the class II MHC locus examined by Kim et al. (1999). Genotypes were scored using SSCP (single-strand conformation polymorphism) as described by Kim et al. (1999). As a result, 15 families, five of which had both inbred and outbred progeny, were used (for details on the family and genotype of the parents of the captive broodstock progeny, see Table 1).

Onts-wr1, *Onts-wr2*, *Onts-wr3*, and *Onts-lfl* (referred to as alleles 1, 2, 3, and 4, respectively) were found in frequencies of 0.839, 0.097, 0.058, and 0.007 for the pooled 1991–

Table 1. The family and pit-tag numbers of winter-run chinook salmon captive broodstock parents and their major histocompatibility complex (MHC) genotypes used in spawning matrix.

	Female			Male		
Family	Family	Number	Genotype	Family	Number	Genotype
1 Inbred	7G	010885367	13	7G	010873564	11
1 Outbred	7G	010885367	13	9H	010563778	11
2 Inbred	9H	011320859	11	9H	010563778	11
2 Outbred	9H	011320859	11	12E	010635809	11
3 Inbred	12E	011107514	12	12E	010635809	11
3 Outbred	12E	011107514	12	15B	011121815	11
4 Inbred	9G	010323571	11	9G	011316869	11
4 Outbred	9G	010323571	11	15B	011121815	11
5 Inbred	11H	011021052	11	11H	010599560	11
5 Outbred	11H	011021052	11	7G	010887631	11
7	21N	010638829	12	7D	011016868	11
8	7G	010632781	11	9F	010563606	12
9	11H	010869589	11	9F	010563606	12
10	9F/H	011361370	12	7D	011016868	11
11	8G	010867285	14	7D	011016868	11
12	18O	010867557	22	9F	010563606	12
13	8E/G	010866086	14	7D	011016868	11
14	9H	011289549	13	7D	011016868	11
15	14N	010890790	13	9H	010563326	11
16	14H	011097372	11	5D	011008519	13

Note: Inbred families are those from matings of full siblings (from the same parental family) and outbred families are those from matings of unrelated individuals The MHC alleles 1, 2, 3, and 4 are *Onts-wr1*, *Onts-wr2*, *Onts-wr3*, and *Onts-lf1*, respectively, as given in Kim et al. (1999).

1994 samples (Kim et al. 1999). The most frequent of these alleles, allele 1, differed from alleles 2, 3, and 4 by 4, 5, and 4 amino acids, respectively, in the region of the antigen binding site that was sequenced (65 amino acids). In other words, even though there was generally not very much divergence between these alleles compared to that in some mammalian studies, heterozygotes containing allele 1 and the other alleles differed by approximately 6.7% in their amino acids in that region. Also note that because allele 1 is in high frequency, it is present at least once in all the crosses and many of the rare genotypes are not represented.

Eggs were harvested using standard hatchery practice. Following fertilization, the eggs were rinsed twice and then treated with an iodophor (Argentyne, Argent Chemical Laboratories, Redmond, Wash.) solution at 100 ppm for 15 min. Next, the eggs were again rinsed twice and loaded into standard Heath incubation trays receiving well water. Water temperature was maintained at 10–11°C and hatching typically began 30–35 days after fertilization. Two or three days after fertilization, the eggs were treated with formalin (Paracide/F, Argent Chemical Laboratories, Redmond, Wash.) at 1667 ppm for 15 min per Heath stack, three times weekly. At strong eye-up (when both eyes were visible in the egg), the eggs were "shocked" by water agitation. After at least 2 days, the eggs were counted and the unfertilized eggs removed for disposal.

After hatching, the sac-fry remained in the trays in the stacks until most of the yolk-sac had been absorbed and then transferred to aerated 33 cm × 33 cm × 45.7 cm aquaria supplied with chilled, recirculated well water. The fish were fed daily on the hour initially, and then reduced to 6–7 feedings per day on a commercially available formulation (BioOregon, Warrenton, Oreg.). The fish were maintained in these aquaria and grown out until transferred into the containment facility for the pathogen exposure trials.

Exposure protocols

Listonella (Vibrio) anguillarum

Listonella anguillarum, strain VA-32, used in this study was obtained from rainbow trout in Norway (originally provided by Tore Håstein). To obtain large cultures for experimental exposures, frozen aliquots of VA-32 were inoculated into 500 mL of tryptic soy broth (TSB) in replicate flasks for 16 h and incubated with shaking at 20–22°C. The broth cultures were examined by wet mount, Gram stain, and slide agglutination tests prior to use to confirm the presence of the bacterium (Thoesen 1994). Levels of bacteria in the broth cultures were estimated by optical density and later confirmed by plate count analysis (Gould et al. 1979).

The concentrations of bacteria producing approximately 50% mortality in each test were determined by LD_{50} studies prior to the initiation of each challenge. For the exposures, 50 mL of a $1 \times 10^{-2.5}$ dilution of the bacterial culture in broth was used as the inoculum. The bacterial suspension was added to 17.4 L of aerated, static well water at 14.5°C in each replicate tank of 30 fish requiring challenge; after 30 min the water flow to each tank was resumed. Challenges were conducted on three separate occasions because of tank space limitations. Numbers of fish per family group varied, so some families were divided into three replicate tanks of fish exposed to *L. anguillarum*, while others were divided into two replicates. The final dose titration was 2.77×10^8 (inbred vs. outbred challenge #1), 1.20×10^9 (inbred vs. outbred challenge #2), and 6.64×10^8 (heterozygous vs. homozygous) colony forming units (CFU) per tank. A control group per family was treated similarly but with uninoculated broth. Fish were monitored throughout the day, and mortalities were removed and recorded in the morning, midday, and late afternoon and put into plastic bags, labeled, and placed on ice (the same procedure was followed for IHNV-exposed fish). Each fish was necropsied by standard procedures to determine the presence of the bacterial pathogen, using specific hyperimmune rabbit serum (Thoesen 1994).

At 21 days after challenge with the bacteria, all remaining fish were euthanized with an overdose of MS-222, counted, and weighed. For both the surviving and dead individuals exposed to either *L. anguillarum* or IHNV, fin clips were taken from families 1, 3, 7, 8, 9, 10, 11, 12, 13, 14, 15, and 16 so that MHC genotypes could be determined.

Infectious hematopoietic necrosis virus

IHNV strain SRCV (Sacramento River chinook virus) used in this study was originally isolated from adult chinook salmon in central California. The virus was propagated in the chinook salmon embryo cell line CHSE-214, as previously described (Arkush et al. 1989). Viral concentrations yielding approximately 50% mortality in each test were determined by LD_{50} studies prior to the initiation of each challenge. For the exposures, two replicate groups of 30 fish each per treatment (e.g., inbred or outbred for family groups 1–5) per family group were placed in a 2-L plastic container containing 1.7 L of aerated fresh water at 12°C. This container in turn was placed in a 10-L bucket containing 5 L of 12°C fresh water to help maintain temperature in the exposure vessel. To each of the two replicate groups of either inbred or outbred fish, 17 mL of cell culture supernatant containing 3.2×10^7 $TCID_{50}$ (50% tissue culture infective dose) IHNV·mL^{-1} was added and the fish were maintained in this system for 1 h (for a final concentration of 3.2×10^5 $TCID_{50}$ IHNV·mL^{-1} exposure water). One group of 30 fish each per inbred and outbred groups per family was treated similarly except that they received cell culture supernatant alone. At the end of the exposure period, fish were netted out of the plastic containers and placed in 58-L aquaria supplied with flow-through fresh water at 12°C. All mortalities were examined by standard necropsy procedures and tissue samples were processed for detection of the virus (Thoesen 1994). At 21 days postexposure, all remaining fish were euthanized as previously described, counted, and weighed.

Myxobolus cerebralis

Fish from families 1–5 (both inbred and outbred) were transported to the University of California–Davis containment facility for acclimation (because only two of these families were segregating for the MHC locus, the sample size was too small to examine the effect of MHC heterozygosity). They were held in 17-L tanks supplied with aerated, flow-through well water at 15°C and maintained on a commercial ration (BioOregon) at 2% body weight per day. Immediately prior to the exposure, fish were randomly divided into three tanks per treatment (inbred or outbred) per family group (two tanks for challenge and one for control), 30 fish per tank. For the exposures, 30 fish were collected from a given treatment (inbred or outbred) per family group and held in a plastic container with 1 L aerated well water. To each vessel, 20 mL of water containing 75 000 triactinomyxons of *M. cerebralis* were added to replicate exposed groups (exposure rate of approximately 2500 triactinomyxons per fish), while the control group received 20 mL of water alone. Triactinomyxons of *M. cerebralis* used were produced from laboratory populations of oligochaetes infected with spores isolated from fish as previously described (Andree et al. 1998). Infected rainbow trout from the California Department of Fish and Game, Mt. Whitney, Calif., were the original source of spores for oligochaete infection in the lab (Modin 1998). The exposures were maintained for two hours. At the end of the challenge, water flow to the tank was resumed such that the internal vessel filled and allowed the fish to move freely into the 15-L tank and the plastic containers were removed.

The fish were fed at 2% body weight per day and all tanks were checked twice daily for mortalities. Seventy-eight days postexposure, the fish were euthanized as previously described, then measured and weighed, fin-clipped, and fixed whole in 10% neutral buffered formalin. Histological specimens were processed for standard paraffin embedding, sectioning, and staining with hematoxylin and eosin (Humason 1979). Cartilaginous tissue in each section was examined for the presence of *M. cerebralis* and associated lesions and scored on a scale of 0 (none) to 4 (severe) as described previously (Hedrick et al. 1999). The pathologist examined the fish and assigned severity scores without knowing the genetic status of the fish.

Genotype identification of offspring

As stated above, the parental MHC genotypes were determined using the approach of Kim et al. (1999). For the offspring, caudal fin clips (5 mm^2) were excised at the time of mortality or at the termination of the exposure experiments. Fin clips were stored in TEN buffer [10 mM Tris (pH 8), 1 mM ethylenediamine tetra-acetic acid (EDTA), 150 mM NaCl] at −20°C. DNA from a portion of each fin clip (1 mm^2) was extracted as described in Banks et al. (2000) and stored frozen at −20°C after extraction. The plates were thawed at room temperature and then centrifuged at 593 × *g* for 5 min at 4°C.

Amplification primers for the MHC class II *B1* chinook salmon exon were taken from Miller et al. (1997) and a clamp was constructed similar to that described by Miller and Withler (1997). The sense strand (5′-CCG ATA CTC CTC AAA GGA CCT GCA-3′) was synthesized, 5′-HEX labeled and HPLC (high pressure liquid chromatography) purified by Integrated DNA Technologies, Inc. (IDT, Coralville, Iowa). The antisense strand had a 40-nucleotide GC-clamp attached to the 5′ end (5′-GCC CGC CCC CGC CGC CCA GCC CGC GCC CCG CGC CGC CCG CGG TCT TGA CTT G[A/C]T CAG TCA-3′, GC-clamp in bold) and was synthesized and polyacrylamide gel electrophoresis (PAGE)-purified by IDT, Inc. These primers amplified a 257-bp PCR (polymerase chain reaction) product.

PCR reaction components were: 1 mM $MgCl_2$, 0.1 mM dNTP, 0.3 µM each PCR primer, 0.5 U *Taq* DNA polymerase (Promega, Madison, Wis.), and 1× *Taq* DNA polymerase buffer (Promega) containing 10 mM Tris–HCl (pH 9.0), 50 mM KCl, and 0.1% Triton®X-100. DNA (4 µL supernatant from Chelex extractions) was added to the PCR mix to obtain a 20-µL final reaction volume. The PCR cycling program consisted of 35 cycles of 94°C for 1 min, 55°C for 2 min, and 72°C for 2 min, with an initial denaturation step of 94°C for 4 min and a final elongation step of 72°C for 7 min. PCR was performed in a PTC-225 DNA Engine Tetrad.

To determine genotypes, denaturing gradient gel electrophoresis (DGGE) was performed using the DCode™ universal mutation detection system (Bio-Rad, Hercules, Calif.). Acrylamide gels (8%, 16 cm × 16 cm format, 1-mm spacers) were cast for parallel gradients using the gradient delivery system (model 475, Bio-Rad) according to manufacturer's directions such that an increasing gradient was formed between the top (30%) and the bottom (45%) of the gel. An equal volume of 2× gel loading dye (0.05% bromophenol blue, 70% glycerol) was added to the nondenatured PCR products and then they were loaded (3 µL) onto the preheated (56°C) gel into wells created by a 52-well sharkstooth comb (manufactured by CBS Scientific Company, Inc., Del Mar, Calif., to be used with the Bio-Rad DCode™ system). Gels were run in 1× Tris–acetate EDTA (TAE) buffer at 80 V for 16–18 h at 56°C. Gel sandwiches were then scanned on an FMBIO® fluorescent imaging system (ReadImage v1.5, Analysis v8.0, MiraiBio Inc., Alameda, Calif.) at 585 nm.

Although the PCRs amplify a 257-bp product for all samples, allele types with the same length but different nucleotide sequences could be differentiated using DGGE based on the sequence-dependent melting behavior of DNA, thereby circumventing the need for sequencing all samples for genotypic information. Known parental genotypes representing the allele types expected in the progeny (see Table 1 and Note) were used as standards and offspring were scored manually relative to the parental genotypes.

Statistical analyses

During the exposure trials, offspring from the same family were subdivided into multiple aquaria. We used *G* tests of heterogeneity with Bonferroni adjustments for multiple comparisons to support lumping of data within families (Sokal and Rohlf 1995). In two cases, these tests were statistically significant ($\alpha < 0.05$) and those data were excluded from further analysis. The data excluded were from the Family 5 inbred fish for the *L. anguillarum* and IHNV trials. In the case of the *L. anguillarum* trial, a single aquarium was clearly anomalous, and only those data were removed. In the case of the IHNV trial, no clear anomaly was evident, so all of the data were excluded. All other data were grouped by family.

For each of the three pathogens, we tested for differences in susceptibility to disease between homozygous and heterozygous fish and between inbred and outbred fish, and for effects of the MHC genotype. For the *L. anguillarum* and IHNV trials we first applied Mantel–Haenszel tests to look for overall effects, then used *G* tests for heterogeneity on individual families to elucidate patterns underlying the tests for overall significance (Agresti 1996). Only mortalities from which we were able to reisolate the pathogen (either *L. anguillarum* or IHNV) were considered in the statistical analyses, thus providing the most conservative comparison.

For the *M. cerebralis* trials, we used logistic regression to test for differences in severity of infection, as measured by the relative number of *Myxobolus*-associated lesions in head and spinal tissues. The severity of infection for an individual fish was summarized in two ways. First, the maximum (MAX) score for any given tissue was used as a proxy for overall infection level, and second, the scores for all tissues were summed (SUM). Results based on these two summary measures were essentially identical, and we report results from the more conservative analysis of MAX scores. To facilitate comparisons to the other two pathogens (binary response variable: survival), we re-analyzed the *M. cerebralis* data using the binary response variable of presence or absence of infection. Re-analysis in this way did not change the conclusions regarding *M. cerebralis*.

Logistic regression analyses were applied by using backward stepwise regression with an elimination criterion of $\alpha >$ 0.05. A likelihood-ratio test was applied to assay the effect of heterozygosity, inbreeding, and MHC genotype. Analyses were carried out in Excel (Microsoft Corp.) and JMP (SAS Institute Inc., Cary, N.C.).

When outbred fish had a higher resistance than inbred fish when exposed to a pathogen, we first evaluated this effect by comparing the mean values of resistance for inbred ($\overline{w}_{\mathrm{I}}$) and outbred ($\overline{w}_{\mathrm{N}}$) fish as the ratio $\overline{w}_{\mathrm{I}}/\overline{w}_{\mathrm{N}}$. This effect can be further evaluated by standardizing it by the level of inbreeding in the inbred offspring. A general standardization approach is to estimate the number of lethal equivalents (Hedrick and Kalinowski 2000)

$$2B = -\frac{2\ln(\overline{w}_{\mathrm{I}}/\overline{w}_{\mathrm{N}})}{f}$$

where $2B$ here is the number of genes in the genome that when made homozygous (by inbreeding) would result in a resistance of 0.

Results

In the *L. anguillarum* and IHNV exposure trials, only dead fish from which we were able to reisolate the respective pathogen were included in the analyses. Overall recovery rates for *L. anguillarum* and IHNV were 94.8% and 100%, respectively. Among all of the fish in the control groups in the trials (798 and 514 total for *L. anguillarum* and IHNV, respectively), only four fish died during the experiment. Re-isolation of either *L. anguillarum* or IHNV was attempted from these control subjects (depending on the exposure trial), but all cultures were negative.

Effects of MHC heterozygotes versus homozygotes

The results are given as the survival rates for the MHC heterozygotes and homozygotes when exposed to *L. anguillarum* and IHNV (Table 2) and as the difference between the two categories of genotypes in the proportion of survival (Fig. 1). There was no difference in overall survival of different MHC genotypes with exposure to *L. anguillarum*. In five families, heterozygotes had higher survival than homozygotes (the difference in Family 16 was statistically significant); in five families homozygotes had higher survival than heterozygotes. There was a significant overall difference in survival of MHC heterozygotes and homozygotes upon exposure to IHNV, with higher survival for heterozygotes than homozygotes for seven of the 10 families (Table 2; Fig. 1).

Table 2. Survival or disease resistance and sample sizes (*N*) for salmon heterozygous (Het) and homozygous (Hom) for a major histocompatibility complex (MHC) class II gene exposed to the two pathogens, *Listonella anguillarum* and IHNV (infectious hematopoietic necrosis virus).

	Listonella anguillarum					IHNV				
	N		Survival			*N*		Survival		
Family	Het	Hom	Het	Hom	*P*	Het	Hom	Het	Hom	*P*
1	57	58	0.61	0.60	0.907	29	32	0.93	0.78	0.090
3	63	71	0.43	0.42	0.944	32	27	0.75	0.78	0.802
7	48	43	0.35	0.37	0.859	31	29	0.77	0.59	0.116
8	40	49	0.25	0.35	0.320	27	33	0.89	0.76	0.182
9	40	50	0.33	0.34	0.881	25	35	0.72	0.69	0.775
10	51	37	0.39	0.27	0.231	24	35	0.88	0.80	0.444
11	52	33	0.29	0.24	0.640	38	23	0.79	0.83	0.726
12	—	—	—	—	—	30	30	0.77	0.80	0.754
13	—	—	—	—	—	33	27	0.76	0.59	0.172
14	47	47	0.17	0.28	0.214	30	34	0.97	0.85	0.108
15	46	46	0.50	0.57	0.531	—	—	—	—	—
16	49	39	0.82	0.62	0.036	—	—	—	—	—
Total	493	473	0.58	0.59	0.833	299	305	0.82	0.75	0.022

Note: *P* values for individual families are *G* tests for heterogeneity (df = 1), whereas *P* values for the combined data (Total) are Mantel–Haenszel tests (df = 1) with the data stratified by family. For families 12 and 13 exposed to *L. anguillarum*, there were some unexpected genotypes given the parental genotypes, so these families were not included. Families 15 and 16 were not exposed to IHNV.

The overall survivals of MHC heterozygotes and homozygotes were 0.82 and 0.75, respectively. Further, there was no evidence for an effect of specific MHC genotypes (11, 12, 13, 14, or 22) in any of the trials for either *L. anguillarum* or IHNV (results not shown).

Effects of inbreeding versus outbreeding

There was no overall difference in survival between outbred ($f = 0$) and inbred ($f = 0.25$) individuals when exposed to either *L. anguillarum* or IHNV (Table 3; Fig. 2), although outbred progeny in Family 1 had a 36% higher survival than inbred progeny when exposed to *L. anguillarum*.

On the other hand, inbreeding affected both the probability of infection (Table 3; Fig. 2) and the severity of infection (Table 4) in the *M. cerebralis* trials. For the *M. cerebralis* trials, four of five families provided evidence for an effect of inbreeding on severity of infection, as did the analysis of all families together (Table 4). Similar results were obtained when probability of infection, rather than level of severity, was used as the response variable (compare Tables 3 and 4). These results were also consistent, whether MAX or whether SUM scores were analyzed.

Discussion

We examined the genetic resistance of winter-run chinook salmon to three different important salmonid pathogens, and in two cases, we found significant genetic effects on disease resistance. First, MHC heterozygotes had a higher survival (0.82) than MHC homozygotes (0.75) when exposed to IHNV (there was no significant effect for MHC heterozygotes versus homozygotes for *L. anguillarum*). The extent of differential selection of viability for IHNV can be estimated if these values are standardized so the relative survival of heterozygotes is unity and the relative survival of the homozygotes is $1 - s$, where s is the selection coefficient (Hedrick 2000). In this case, the estimate of s is 0.085. This estimate is based on a sample of genotypes that closely reflects that encountered in natural populations. That is, in the study here, 96%

Fig. 1. Difference in survival between major histocompatibility complex (MHC) heterozygotes and homozygotes after exposure to (*a*) *Listonella anguillarum* and (*b*) infectious hematopoietic necrosis virus (IHNV) for the 10 families segregating for the MHC locus, where * indicates $P < 0.05$.

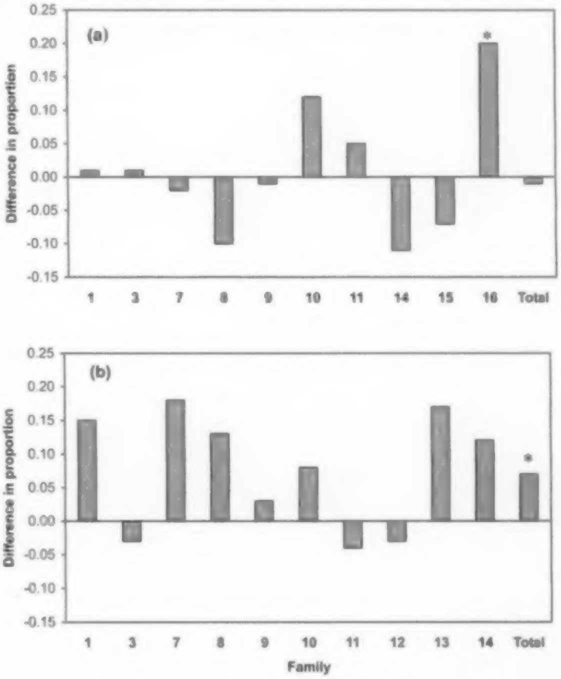

Table 3. Survival or disease resistance and sample sizes (*N*) for outbred (Out) and inbred (In) salmon exposed to one of three pathogens, *Listonella anguillarum*, IHNV (infectious hematopoietic necrosis virus), or *Myxobolus cerebralis*.

	Listonella anguillarum					IHNV					*Myxobolus cerebralis*				
	N		Survival			*N*		Survival			*N*		Resistance		
Family	Out	In	Out	In	*P*	Out	In	Out	In	*P*	Out	In	Out	In	*P*
1	115	107	0.61	0.45	0.017	61	59	0.85	0.80	0.420	60	55	0.97	0.84	0.014
2	59	60	0.37	0.38	0.906	60	60	0.87	0.80	0.326	58	51	0.91	0.59	<0.001
3	134	128	0.43	0.48	0.338	59	58	0.76	0.78	0.866	58	54	0.71	0.31	<0.001
4	132	138	0.30	0.33	0.683	60	58	0.57	0.69	0.166	58	60	0.81	0.62	0.019
5	125	59	0.34	0.29	0.448	60	—	0.73	—	—	30	31	0.60	0.61	0.918
Total	565	492	0.41	0.40	0.489	300	235	0.76	0.77	0.941	264	251	0.82	0.59	<0.001

Note: *P* values for individual families are *G* tests for heterogeneity (df = 1) whereas *P* values for the combined data (Total) are Mantel–Haenszel tests (df = 1) with the data stratified by family.

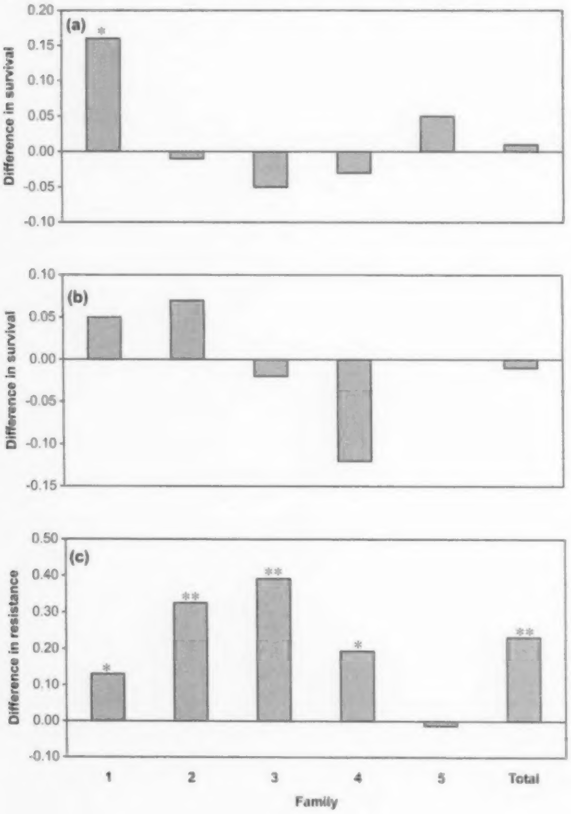

Fig. 2. Difference in survival or resistance between outbred and inbred fish after exposure to (*a*) *Listonella anguillarum*, (*b*) IHNV (infectious hematopoietic necrosis virus), and (*c*) *Myxobolus cerebralis* for the five families with both inbred and outbred offspring, where * indicates $P < 0.05$ and ** indicates $P < 0.001$.

of the homozygotes were 11, and using the allele frequencies from Kim et al. (1999), it is expected that 98% of the homozygotes in the wild population would be 11. Similarly, 84% of the heterozygotes here were 12 or 13, and it is expected that 92% of the heterozygotes in the wild population would be 12 or 13.

To our knowledge, there are only two other studies that have investigated the role of specific MHC genotypes in disease resistance in fish. P.W. Hedrick et al. (2001*b*) carried out a smaller study examining resistance to the fluke *Gyrodactylus* in topminnows and found that "homozygotes for a MHC gene had lower (although statistically nonsignificant) survival when infected with flukes than did heterozygotes". On the other hand, Langefors et al. (2001) found an association of high resistance in Atlantic salmon to the bacterium *Aeromonas salmonicida* with a class II allele but did not find an association with heterozygosity.

Second, outbred fish had a higher resistance (or lower infection severity) than inbred fish when exposed to *M. cerebralis* (there was no significant effect for inbred versus outbred for either *L. anguillarum* or IHNV). We can evaluate this effect by comparing the mean values of resistance to *M. cerebralis* for inbred ($\overline{w}_I$) and outbred ($\overline{w}_N$) fish, and the ratio here is $\overline{w}_I/\overline{w}_N = 0.55/0.82 = 0.67$, a large reduction in the value for inbreds as compared to outbreds. This can be further evaluated by estimating the number of lethal equivalents (2*B*) (Hedrick and Kalinowski 2000). In this case,

$$2B = -\frac{2\ln(0.55/0.82)}{0.25} = 3.20$$

or there are slightly over three genes (or a larger number of genes each with a smaller effect) that would result in no resistance when homozygous. Although there are a number of other studies that have shown greater susceptibility to pathogens in inbred than in outbred individuals (see P.W. Hedrick et al. 2001*b* for references), this is the first demonstration of higher susceptibility in inbred salmon.

The three pathogens chosen are important in a number of salmonids. Both IHNV and *M. cerebralis* have been detected in Sacramento River drainage stocks and have been associated with mortality (Ross et al. 1960; Modin 1998). No mortality events associated with *L. anguillarum* have been documented, but the bacterium is of concern in the production of anadromous salmonids for supplementation strategies and thus hatchery-origin stocks are vaccinated against the disease prior to release. For the winter-run chinook salmon captive broodstock program, all fish are vaccinated prior to seawater acclimation.

As early as 1960, IHNV epizootics were reported in young chinook salmon cultured at Coleman National Fish Hatchery (CNFH) located on Battle Creek, a tributary of the

Table 4. Proportions of outbred and inbred salmon in each level of infection severity after exposure to *Myxobolus cerebralis*.

			Severity					
Family		*N*	0	1	2	3	4	*P*
1	Outbred	60	0.97	0.03	0.00	0.00	0.00	0.033
	Inbred	55	0.84	0.09	0.04	0.04	0.00	
2	Outbred	58	0.91	0.03	0.05	0.00	0.00	<0.001
	Inbred	51	0.59	0.16	0.24	0.02	0.00	
3	Outbred	58	0.71	0.12	0.10	0.07	0.00	<0.001
	Inbred	54	0.31	0.17	0.39	0.13	0.00	
4	Outbred	58	0.81	0.03	0.09	0.07	0.00	0.034
	Inbred	60	0.62	0.08	0.23	0.07	0.00	
5	Outbred	30	0.60	0.20	0.13	0.07	0.00	0.881
	Inbred	31	0.61	0.19	0.16	0.03	0.00	
Total	Outbred	264	0.82	0.06	0.08	0.04	0.00	<0.001
	Inbred	251	0.55	0.13	0.22	0.06	0.00	

Note: The severity levels are 0, no lesions; 1, minimal; 2, mild; 3, moderate; 4, severe and the *P* values are from logistic regression.

Sacramento River near Red Bluff, Calif. (Ross et al. 1960; Parisot and Pelnar 1962). At that time, mortalities only occurred in chinook salmon, while juvenile steelhead and Kamloops trout at the same facility survived, suggesting some mechanism of host resistance or virus strain virulence differences. In one study of sockeye salmon, for example, McIntyre and Amend (1978) demonstrated that heritability of tolerance to IHNV was approximately 30%, although the virus strain was not identified and tolerance was not evaluated in the adult offspring. Since its first description, various IHNV isolates have been identified. Host and environmental factors affect the virulence of IHNV strains (see LaPatra 1998 for review), and even the evolution of viral genetic heterogeneity has been described (Anderson et al. 2000).

More recently, IHNV has been re-isolated from both wild and hatchery-propagated chinook salmon, including fall, late-fall, and winter-run adults (J. Scott Foott, U.S. Fish and Wildlife Service, California–Nevada Fish Health Center, 24411 Coleman Fish Hatchery Road, Anderson, CA 96007, U.S.A., personal communication). The virus is considered well established in the upper Sacramento River because of the overlap of the four adult chinook salmon runs, perhaps resulting in co-evolutionary processes between the virus and host. Indeed, investigators were unable to transmit IHNV from infected hatchery-propagated fall-run chinook salmon to natural chinook salmon collected from the Sacramento River. Yet our results demonstrate that modest host genetic selection can result in increased susceptibility to the disease and subsequent mortality. This could have broader, negative implications for wild winter-run chinook, particularly if the population is subjected to further reproductive constraints such that the proportion of MHC homozygotes increases. Our findings are further supported by the work of Palti et al. (2001) who demonstrated that polymorphism of the MHC class II beta-chain intron could be linked to IHNV resistance in backcrosses of rainbow trout and cutthroat trout (*Oncorhynchus clarki*).

At CNFH, *M. cerebralis* was detected in hatchery-reared steelhead in the mid-1980s (Modin 1998). The USFWS fish health policy led to the destruction of one brood year of steelhead at that facility (J. Scott Foott, U.S. Fish and Wildlife Service, California–Nevada Fish Health Center, 24411 Coleman Fish Hatchery Road, Anderson, CA 96007, U.S.A., personal communication). Since 1990, *M. cerebralis* has not been detected in any juvenile production group at CNFH (pepsin–trypsin digest method) following closure of a *M. cerebralis*-positive, private processing facility in the upper drainage (Modin 1998). Both field observations and experimental exposures indicate that there is a range in susceptibility to whirling disease among salmonids (Hedrick et al. 1999; Thompson et al. 1999). Following experimental infections a range of host responses ensue, from suspended parasite development in Arctic grayling (*Thymallus arcticus*) to extensive replication resulting in crippling disease in rainbow trout (Hedrick et al. 1999). Even among chinook salmon strains there is a range of responses to the parasite, suggesting that genetic variation of the host could be a key component of susceptibility (R.P. Hedrick et al. 2001). Indeed, our results demonstrate that within a given strain (winter-run) there is a significant genetic influence in the development of whirling disease, and it can be detected in a single generation of full-sib mating.

In mammals, all the major genes in the MHC appear to be clustered in one small linkage group (Edwards and Hedrick 1998). However, in fishes, the class I MHC genes (primarily involved in recognition of intracellular pathogens, like viruses) and the class II MHC genes, such as the one that we investigated (primarily involved in recognition of extracellular pathogens, like bacteria), appear unlinked (Hansen et al. 1999; Sato et al. 2000). Even the class II genes in some fishes appear to be in two linkage groups (Sato et al. 2000). However, there is no published evidence that the class II genes in salmonids are in two linkage groups and the identity, number, and expression of class II genes in salmonids, beyond the gene that we have examined, is uncertain (Grimholt et al. 1994; Miller et al. 1997).

Relevant to our finding of a difference in survival between class II MHC heterozygotes and homozygotes only for IHNV is that genes unlinked to the class II locus, or linked but in linkage equilibrium with the class II locus, may influence pathogen resistance. As a result, the signal from examining MHC genetic variation at a single gene influencing pathogen resistance would be expected to be less in fish than in mammals because of the lower level of linkage disequilibrium expected (because of the lower linkage discussed above). Although it might be expected a priori that resistance for the class II locus would be more likely for the bacterium *L. anguillarum*, it is possible that all expressed class II loci are not linked in salmonids, suggesting that this expectation may not always be valid. Further, the association of resistance to a virus related to class II genotypes is not unexpected, and for example, has been found in humans for hepatitis (Thurz et al. 1997) and salmonids for IHNV (Palti et al. (2001).

The extent of variation at the class II MHC gene that we have examined (Kim et al. 1999) is lower than has been generally found for class II MHC genes in other organisms (e.g., Gutierrez-Espeleta et al. 2001; P.W. Hedrick et al. 2001*a*). As a result, one may expect that the potential differential selection for resistance to different pathogens may be less in winter-run chinook than for these other organisms. Although this may be a general trend, in some cases even a single amino-acid change or the right type in the right position in the MHC molecule may result in a differential level of resistance (Gao et al. 2001). Further, as pointed out by Hedrick and Kim (2000), there are a number of other difficulties that may be encountered when trying to estimate the selective effects for pathogen resistance on MHC (and on different levels of inbreeding). Despite these difficulties, the present study illustrates the advantage of large-scale experiments and the usefulness of using more than one pathogen when examining resistance.

Overall, we have shown that the endangered winter-run chinook salmon appears to be genetically susceptible to the detrimental effects of pathogens. If there were further losses of genetic variation because of continued small population size in winter-run, then one would predict both a higher level of homozygosity at MHC genes and higher levels of inbreeding. As a result, the pathogens that we have examined, and potentially others that may infect winter-run, may cause in a decline in the number of winter-run chinook salmon and an additional extinction threat to this critically endangered species.

Acknowledgements

This research was conducted under a permit from the National Marine Fisheries Service and was funded in part by grants from the U.S. Fish and Wildlife Service. Further support for this work was provided by funds from the California Department of Water Resources (contract 4600000804). We appreciate the work of Karen Parker in initially determining the genotypes of the potential parental fish. We are indebted to Leslie Hain, Brian Mulvey, and Julie Zerr for broodstock husbandry and spawning, and assistance in conducting the pathogen challenges. Ron Hedrick and Terry McDowell kindly provided the *M. cerebralis* triactinomyxons and assisted in the whirling disease experiments. This is contribution 2157, Bodega Marine Laboratory, University of California–Davis.

References

Agresti, A. 1996. An introduction to categorical data analysis. John Wiley and Sons, Inc., New York.

Anderson, E.D., Engelking, H.M., Emmenegger, E.J., and Kurath, G. 2000. Molecular epidemiology reveals emergence of a virulent infectious hematopoietic necrosis (IHN) virus strain in wild salmon and its transmission to hatchery fish. J. Aquat. Anim. Health, **12**: 85–99.

Andree, K.B., MacConnell, E., and Hedrick, R.P. 1998. A nested polymerase chain reaction for the detection of genomic DNA of *Myxobolus cerebralis* in rainbow trout *Oncorhynchus mykiss*. Dis. Aquat. Org. **34**: 145–154.

Arkush, K.D., Bovo, G., DeKinkelin, P., Winton, J.R., Wingfield, W.H., and Hedrick, R.P. 1989. Biochemical and antigenic properties of the first isolates of infectious hematopoietic necrosis virus from salmonid fish in Europe. J. Aquat. Anim. Health, **1**: 148–153.

Banks, M.A., Rashbrook, V.K., Calavetta, M.J., Dean, C.A., and Hedgecock, D. 2000. Analysis of microsatellite DNA resolves genetic structure and diversity of chinook salmon (*Oncorhynchus tshawytscha*) in California's Central Valley. Can. J. Fish. Aquat. Sci. **57**: 915–927.

Carrington, M., Nelson, G.W., Martin, M.P., Kissner, T., Vlahov, D., Goedert, J.J., Kaslow, R., Buchbinder, S., Hoots, K., and O'Brien, S.J. 1999. *HLA* and HIV-1: heterozygote advantage and *B*35-Cw*04* disadvantage. Science (Washington, D.C.), **238**: 1748–1752.

Coltman, D.W., Pilkington, J.G., Smith J.A., and Pemberton, J.M. 1999. Parasite-mediated selection against inbred Soay sheep in a free-living, island population. Evolution, **53**: 1259–1267.

Edwards, S., and Hedrick, P.W. 1998. Evolution and ecology of MHC molecules: from genomics to sexual selection. Trends Ecol. Evol. **13**: 305–311.

Egidius, E. 1987. Vibriosis: pathogenicity and pathology. A review. Aquaculture, **67**: 15–28.

Evelyn, T.P.T. 1971. First records of vibriosis in Pacific salmon cultured in Canada, and taxonomic status of the responsible bacterium, *Vibrio anguillarum*. J. Fish. Res. Board Can. **28**: 517.

Gao, X., Nelson, G.W., Karacki, P., Martin, M.P., Phair, J., Kaslow, R., Goedert, J.J., Buchbinder, S., Hoots, K., Vlahov, D., O'Brien, S.J, and Carrington, M. 2001. Effect of a single amino acid change in MHC class I molecules on the rate of progression to AIDS. N. Engl. J. Med. **344**: 1668–1675.

Gould, R.W., Antipa, R., and Amend, D.F. 1979. Immersion vaccination of sockeye salmon (*Oncorhynchus nerka*) with two pathogenic strains of *Vibrio anguillarum*. J. Fish. Res. Board Can. **36**: 222–225.

Grimholt, U., Olasker, I., de Vries Lindstrom, C., and Lie, O. 1994. A study of variability in the MHC class II β1 and class I α2 domain exons of Atlantic salmon (*Salmo salar*) Anim. Genet. **25**: 147–153.

Gutierrez-Espeleta, G.A., Hedrick, P.W., Kalinowski, S.T., Garrigan, D., and Boyce, W.M. 2001. Is the decline of desert bighorn sheep from infectious disease the result of low MHC variation? Heredity, **86**: 439–50.

Hansen, J.D., Strassburger, P., Thorgaard, G.H., Young, W.P., and Du Pasquier, L. 1999. Expression, linkage and polymorphism of MHC-related genes in rainbow trout, *Oncorhynchus mykiss*. J. Immunol. **163**: 774–786.

Hedrick, P.W. 2000. Genetics of populations. 2nd ed. Jones and Bartlett, Boston, Mass.

Hedrick, P.W., and Kalinowski, S. 2000. Inbreeding depression and conservation biology. Annu. Rev. Ecol. Syst. **31**: 139–162.

Hedrick, P.W., and Kim, K.J. 2000. Genetics of complex polymorphisms: Pathogens and maintenance of the major histocompatibility complex variation. *In* Evolutionary genetics:

from molecules to morphology. *Edited by* R.S. Singh and C.B. Krimbas. Cambridge University Press, Cambridge. pp. 204–234.

Hedrick, P.W., Hedgecock, D., and Hamelberg, S. 1995. Estimation of effective population size in winter-run chinook salmon. Conserv. Biol. **9**: 615–624.

Hedrick, P.W., Hedgecock, D., Hamelberg, S., and Croci, S.J. 2000*a*. The impact of supplementation in winter-run chinook salmon on effective population size. J. Hered. **91**: 112–116.

Hedrick, P.W., Rashbrook, V.K., and Hedgecock, D. 2000*b*. Effective population size in returning winter run chinook salmon. Can. J. Fish. Aquat. Sci. **57**: 2368–2373.

Hedrick, P.W., Parker, K.M., and Lee, R. 2001*a*. Genetic variation in the endangered Gila and Yaqui topminnows: microsatellite and MHC variation. Mol. Ecol. **10**: 1399–1412.

Hedrick, P.W., Kim, K.J., and Parker, K.M. 2001*b*. Parasite resistance and genetic variation in the endangered Gila topminnow. Anim. Conserv. **4**: 103–109.

Hedrick, R.P., El-Matbouli, M., Adkison, M.A., and MacConnell, E. 1998. Whirling disease: re-emergence among wild trout. Immun. Rev. **166**: 365–376.

Hedrick, R.P., McDowell, T.S., Gay, M., Marty, G.D., Georgiadis, M.P., and MacConnell, E. 1999. Comparative susceptibility of rainbow trout (*Oncorhynchus mykiss*) and brown trout (*Salmo trutta*) to *Myxobolus cerebralis* the cause of salmonid whirling disease. Dis. Aquat. Org. **37**: 173–183.

Hedrick, R.P., McDowell, T.S., Mukkatira, K., Georgiadis, M.P., and MacConnell, E. 2001. Susceptibility of three species of anadromous salmonids to experimentally induced infections with *Myxobolus cerebralis*, the causative agent of whirling disease. J. Aquat. Anim. Health, **13**: 43–50.

Humason, G. 1979. Animal tissue techniques. Freeman, San Francisco.

Kim, J.T., Parker, K.M., and Hedrick, P.W. 1999. MHC differentiation in Sacramento River chinook salmon. Genetics, **151**: 1115–1122.

Lafferty, K.D., and Gerber, L. 2002. Good medicine for conservation biology: the intersection of epidemiology and conservation theory. Conserv. Biol. **16**: 593–604.

Langefors, A., Lohm, J., Grahn, M., Andersen, O., and von Schantz, T. 2001. Association between major histocompatibility complex class IIB alleles and resistance to *Aeromonas salmonicida* in Atlantic salmon. Proc. R. Soc. Lond. Ser. B Biol. Sci. **268**: 479–493.

LaPatra, S.E. 1998. Factors affecting pathogenicity of infectious hematopoietic necrosis virus (IHNV) for salmonid fish. J. Aquat. Anim. Health, **10**: 121–131.

Leong, J.C., and Fryer, J.L. 1993. Viral vaccines for aquaculture. Annu. Rev. Fish Dis. **3**: 225–240.

McIntyre, J.D., and Amend, D.F. 1978. Heritability of tolerance for infectious hematopoietic necrosis in sockeye salmon (*Oncorhynchus nerka*). Trans. Am. Fish. Soc. **107**: 305–308.

Miller, K.M., and Withler, R.E. 1997. *Mhc* diversity in Pacific salmon: population structure and transspecies allelism. Hereditas, **127**: 83–95.

Miller, K.M., Withler, R.E., and Beacham, T.D. 1997. Molecular evolution at Mhc genes in two populations of chinook salmon *Oncorhynchus tshawytscha*. Mol. Ecol. **6**: 937–954.

Modin, J. 1998. Whirling disease in California: a review of its history, distribution, and impacts, 1965–1997. J. Aquat. Anim. Health, **10**: 132–142.

Nehring, R.B., and Walker, P.G. 1996. Whirling disease in the wild: the new reality in the intermountain west. Fisheries (Bethesda), **21**: 28–32.

Palti, Y., Nichols, K.M., Waller, K.I., Parsons, J.E., and Thorgaard, G.H. 2001. Association between DNA polymorphisms tightly linked to MHC class II genes and IHN virus resistance in backcrosses of rainbow and cutthroat trout. Aquaculture, **194**: 283–289.

Parisot, T.J., and Pelnar, J. 1962. An interim report on Sacramento River chinook disease: a virus-like disease of chinook salmon. Prog. Fish-Cult. **24**: 51–55.

Ross, A.J., Pelnar, J., and Rucker, R.R. 1960. A virus-like disease of chinook salmon. Trans. Am. Fish. Soc. **89**: 160–163.

Sato, A., Figueroa, F., Murray, B.W., Malaga-Trillo, E., Zaleska-Rutczynska, Z., Sultmann, H., Toyosawa, A., Wedekind, C., Steck, N., and Klein, J. 2000. Nonlinkage of major histocompatibility complex class I and class II loci in bony fishes. Immunogenetics, **51**: 108–116.

Sokal, R.R., and Rohlf, F.J. 1995. Biometry. 3rd ed. W.H. Freeman and Co., New York.

Thoesen, J.C. (*Editor*). 1994. Suggested procedures for the detection and identification of certain finfish and shellfish pathogens. 4th ed. Version 1. Fish Health Section, American Fisheries Society, Bethesda, Md.

Thompson, K.G., Nehring, B.R., Bowden, D.C., and Wygant, T. 1999. Field exposure of seven species or subspecies of salmonids to *Myxobolus cerebralis* in the Colorado River, Middle Park, Colorado. J. Aquat. Anim. Health, **11**: 312–329.

Thurz, M.R., Thomas, H.C., Greenwood, B.M., and Hill, A.V.S. 1997. Heterozygote advantage for HLA class-II type in hepatitis B virus infection. Nat. Genet. **17**: 11–12.

Walker, P.J., Benmansour, A., Calisher, C.J., Dietzgen, R., Fang, R.X., Jackson, A.C., Kurath, G., Leong, J.C., Nadin-Davies, S., Tesh, R.B., and Tordo, N. 2000. Family Rhabdoviridae. *In* The Seventh Report of the International Committee for Taxonomy of Viruses. Springer-Verlag, New York. pp. 563–583.

Wolf, K. 1988. Infectious hematopoietic necrosis. *In* Fish viruses and fish viral diseases. *Edited by* K. Wolf. Cornell University Press, Ithaca. pp. 83–114.

A flexible maximum likelihood approach for fitting growth curves to tag–recapture data

Geoff M. Laslett, J. Paige Eveson, and Tom Polacheck

Abstract: We describe a novel maximum likelihood method for fitting general growth curves to tag–recapture data. The growth model allows for the asymptotic length and the time to tagging to vary from individual to individual, with other parameters being fixed. Unlike the Fabens approach, we do not take differences to fit the parameters, but instead model the joint density of the release and recapture lengths. We simulate data to examine the bias and precision of the estimated parameters obtained using our fitting method. We include simulations for which the time to tagging model is incorrect, but find that the growth curve is usually still fitted with small bias. Furthermore, we introduce a new growth curve that allows for different growth rates for juveniles and adults. The new growth curve needs sufficient data coverage before and after the transition from juvenile to adult for all parameters to be estimated precisely. We illustrate the method on real data by fitting this new growth curve to southern bluefin tuna tag–recapture data.

Résumé : On trouvera ici une méthode nouvelle de vraisemblance maximale pour ajuster les courbes générales de croissance à des données de marquage et de recapture. Le modèle de croissance permet d'inclure des variations individuelles dans la longueur asymptotique et l'âge au marquage, tous les autres paramètres étant fixes. Au contraire de la méthode de Fabens, nous n'utilisons pas les différences pour ajuster les paramètres, mais nous modélisons la densité conjointe des longueurs au marquage et à la recapture. Une simulation des données permet de déterminer l'erreur et la précision des paramètres estimés par notre méthode d'ajustement. Dans des simulations où le modèle de l'âge au marquage est incorrect, la courbe de croissance s'ajuste néanmoins avec de faibles erreurs. De plus, nous présentons une nouvelle courbe de croissance qui permet de tenir compte de l'existence de taux différents de croissance pour les jeunes et les adultes. La nouvelle courbe de croissance nécessite une gamme suffisante de données d'avant et d'après la transition de jeune à adulte pour pouvoir estimer les paramètres avec précision. L'ajustement de la nouvelle courbe de croissance à des données de marquage et de recapture du thon rouge du Sud donne une illustration concrète du fonctionnement de la méthode.

[Traduit par la Rédaction]

Introduction

Understanding how fish grow is a fundamental component of fish biology, and quantitative information on growth is critical to the stock assessment process. However, it is not only mean growth that is important to characterize, but also the variability among individuals. One of the primary sources of information used for estimating the growth rates of fish comes from tagging studies. In these studies, the length of a fish is measured and recorded when the fish is released and recaptured. The times of release and recapture are also recorded so that the time at liberty is known. The estimation of growth rates from these data presents a difficult challenge for several reasons: there are only two measurements per fish, the age at first release is not precisely known, and fish vary in their growth from individual to individual.

Despite these obvious difficulties, several efficient methods of estimating growth curves from tag–recapture data have been developed (e.g., Fabens 1965; Francis 1988; Palmer et al. 1991). The estimation process involves determining both an appropriate parametric form for the growth curve and a reliable statistical procedure for fitting the data to the growth curve. The determination of the appropriate curve is often an iterative process using standard statistical model selection criteria. Nonparametric estimation of growth from tag–recapture data is generally not feasible because of the paucity and structure of the data. In any case, parametric models can provide insights into the underlying functional processes and allow for direct comparison of growth curves across time and space or between different populations or species. Moreover, differences among individuals can be captured by modeling some of the growth parameters as random variables.

A wide variety of parametric models has been used to model fish growth, with the von Bertalanffy (VB) growth model being the most ubiquitous. However, the generalized von Bertalanffy, the Richards, the Gompertz, and the logistic models have all been advocated (see Schnute 1981). In fact, any cumulative statistical distribution scaled by an asymptotic length could be used, although the growth curve preferably should have a biological motivation. Almost all modeling of

Received 6 June 2001. Accepted 8 May 2002. Published on the NRC Research Press Web site at http://cjfas.nrc.ca on 12 July 2002.
J16395

G.M. Laslett.[1] CSIRO Mathematical and Information Sciences, Private Bag 10, Clayton South MDC, Clayton, Victoria 3169, Australia.
J.P. Eveson and T. Polacheck. CSIRO Marine Research, G.P.O. Box 1538, Hobart, Tasmania 7001.

[1] Corresponding author (e-mail: Geoff.Laslett@csiro.au).

DOI: 10.1139/F02-069

fish growth has been based on modeling the growth rate as a continuous, smooth, monotonically decreasing function of age. However, recent analyses of growth in southern bluefin tuna (SBT) suggest that there is a marked change in the growth process somewhere during the transition from the juvenile to subadult part of the life cycle (Anonymous 1994; Hearn and Polacheck 2002). Hearn and Polacheck (2002) suggest this might also be a feature in other tuna species. In the SBT case, growth has been modeled as a two-stage process in which growth in each stage follows a different VB curve, with a discontinuity in the growth rates at the transition point between the two. However, Hearn and Polacheck (2002) identify problems both with the biological interpretation of this model and in statistically fitting it. Thus there is a need, at least in the case of SBT, for alternative growth models that can adequately represent the complex pattern of growth.

A large body of scientific literature exists on the statistical estimation of growth curves from tag–recapture data. The most widely used approach in fisheries' research has been the one developed by Fabens (1965). However, this approach does not take into account variability among individuals in their growth curves, cannot be applied to the full range of potential growth models, and is not asymptotically consistent (Maller and de Boer 1988). Extensions to the Fabens approach that can accommodate individual variability in growth within a VB model framework have been developed by Sainsbury (1980) and Hampton (1991), but these methods still bear some of the limitations of a Fabens-type approach. James (1991) and Wang (1998) have developed fitting procedures based on estimating equations as a statistically rigorous alternative to Fabens' method, but again there are problems in applying the estimating equations approach to more complicated growth models. As such, there remains a need for a flexible estimation method that can be adopted to a wide range of alternative growth models, that can accommodate individual variability in the growth parameters, and that can provide a statistical basis for selecting the most appropriate and parsimonious model.

In the current paper, we develop an alternative maximum likelihood approach for estimating growth curves from tag–recapture data that is based on estimating the joint density of tag and recapture lengths rather than modeling growth increments. This method allows for individual variability in growth by having selected parameters considered as random effects. Standard statistical tests based on likelihood theory and Akaike's information criteria (Akaike 1974) may be used to compare and select among alternative models. Although Wang et al. (1995) have proposed a similar approach, our method requires less restrictive assumptions and can easily be applied to a wide range of growth curves. Furthermore, we have developed a new growth curve that can accommodate a marked change in the growth pattern at some point in the life cycle. We apply our estimation method along with the proposed new growth curve to tag–recapture data for SBT.

Methods

The joint density of tag and recapture lengths for a general growth model

In this section, we derive the joint density of tag and recapture lengths for a single fish. This is formulated in terms of a general model for fish growth in which the asymptotic length varies from fish to fish. Other parameters are fixed. The joint density is needed for maximum likelihood fitting of the growth model and inference about its relative fit.

In tag–recapture studies, a fish is tagged at time t_1 with length l_1 and is recaptured at time t_2 with length l_2. We know that fish growth during the very early stages of life (e.g., during the egg and larval stages) follows a different process from subsequent growth. However, we do not have data with which to model this initial growth. We define t_0 to be the time at which a fish would have had length 0 if we were to project its postlarval growth trajectory backwards. We acknowledge that t_0 is a theoretical value with no real biological interpretation.

Let $A = t_1 - t_0$, then A varies from fish to fish, partly because the fish are spawned at different times (which results in t_0 varying between fish) and partly because there may be several tagging expeditions (so that t_1 varies). For convenience, we will refer to A simply as the age at tagging, keeping in mind that it is age relative to t_0, not relative to birth.

We assume that a generic growth function $f(t)$ is available, where $f(t)$ is a monotone increasing function of time, t. It approaches 1 as $t \to \infty$ and is 0 when t is t_0. The growth of each fish follows the form of $f(t)$, although with individual variations.

The assumed growth curve for the fish is

$$(1) \qquad l(t) = L_\infty f(t;A,\theta)$$

where L_∞ (the asymptotic length) is random from fish to fish with mean μ_∞ and variance σ^2_∞, A is random from fish to fish with density $p(\cdot)$, θ is a vector of fixed unknown parameters, and t is real time. For example, for the von Bertalanffy model,

$$f(t;A,\theta) = \begin{cases} 1 - \exp(-k(A + t - t_1)) & \text{if } t > t_1 - A \\ 0 & \text{otherwise} \end{cases}$$

so $\theta = \{k\}$ has only one component. Let $\delta t = t_2 - t_1$ be the time increment between tagging and recapture. To analyze tag–recapture data, we need the familiar equations

$$f(t_1;A,\{k\}) = 1 - \exp(-kA)$$

$$f(t_2;A,\{k\}) = 1 - \exp(-k(A + \delta t))$$

James (1991), Palmer et al. (1991), and Wang et al. (1995) have all discussed the estimation of von Bertalanffy parameters from tag–recapture data using this style of model. Our aim is to show that parameter estimation is still feasible for more complex and realistic growth models $f(\cdot)$ in eq. 1.

In this article, we assume that L_∞ and A are both random variables. Models in which either L_∞ or A are the same unknown constants for all fish are implausible, and models for which L_∞ and A are different constants are overparameterized, so ours is the simplest realistic assumption. We denote random variables by capital letters. We follow James (1991), Palmer et al. (1991), and Wang et al. (1995) in assuming that L_∞ and A are independent. We have no evidence to the contrary.

We assume for convenience that L_∞ has a normal distribution. Intuitively, this seems reasonable, and we have no data to refute it. We also assume that measurements are taken at times t_1 and t_2 (with $t_1 < t_2$), so that

$$(2) \qquad l_1 = l(t_1) + \epsilon_1$$

$$(3) \qquad l_2 = l(t_2) + \epsilon_2$$

where ϵ_1 and ϵ_2 represent measurement error. They are also normally distributed with mean 0 and variance σ^2 and are independent from fish to fish. We assume also that ϵ_1 and ϵ_2 are independent of L_∞ and A.

We are now in a position to derive the joint distribution of l_1 and l_2. For the moment, we argue conditional upon a known value of A, say $A = a$. Then l_1 and l_2 are both the sum of normal random variables and hence are themselves normal. Their first and second moments are

$$\mu_1(a) = E(l_1|a) = \mu_\infty f_1$$

$$\mu_2(a) = E(l_2|a) = \mu_\infty f_2$$

$$\sigma_1^2(a) = \mathrm{Var}(l_1|a) = \sigma_\infty^2 f_1^2 + \sigma^2$$

$$\sigma_2^2(a) = \mathrm{Var}(l_2|a) = \sigma_\infty^2 f_2^2 + \sigma^2$$

$$\mathrm{Cov}(l_1, l_2|a) = \sigma_\infty^2 f_1 f_2$$

$$\rho(a) = \mathrm{Corr}(l_1, l_2|a) = \frac{\sigma_\infty^2 f_1 f_2}{\sigma_1(a)\,\sigma_2(a)}$$

where $f_1 = f(t_1; a, \theta)$ and $f_2 = f(t_2; a, \theta)$. Clearly, l_1 and l_2 are joint normal with conditional density

$$(4) \qquad h(l_1, l_2|a) = \frac{1}{2\pi\sigma_1(a)\sigma_2(a)\sqrt{1-\rho(a)^2}} \exp\left\{-\frac{q_{12}(a)}{2(1-\rho(a)^2)}\right\}$$

where

$$q_{12}(a) = \frac{(l_1-\mu_1(a))^2}{\sigma_1(a)^2} - 2\rho(a)\frac{(l_1-\mu_1(a))(l_2-\mu_2(a))}{\sigma_1(a)\,\sigma_2(a)} + \frac{(l_2-\mu_2(a))^2}{\sigma_2(a)^2}$$

If A is random, the unconditional joint density of l_1, l_2 is

$$(5) \qquad h(l_1, l_2) = \int_0^\infty h(l_1, l_2|a)p(a)\mathrm{d}a$$

There are several points to note. First, the joint density (eq. 5) involves a single integral, whereas Wang et al. (1995) have a double integral. Second, $l_2 < l_1$ is allowed, whereas Wang et al. (1995) do not allow it. Third, a more complex model for the measurement error may be desirable and can easily be incorporated. For example, in the case of SBT, recapture lengths are measured by fishermen and scientists, but tag lengths are measured by scientists only. The fishermen are believed to be less precise. Hence it may be desirable to structure the measurement errors so that $\mathrm{Var}(\epsilon_2) > \mathrm{Var}(\epsilon_1)$ when l_2 is measured by fishermen. Fourth, correlation between ϵ_1 and ϵ_2 may also be allowed for very easily, although it is likely to be poorly identified. Finally, conditioning on nonlinear components to simplify the analysis of partially nonlinear models has a long history in statistics. A seminal paper is Halperin (1963).

The joint density for zero measurement error

It is useful to have a special formula for $h(l_1, l_2)$ when $\sigma^2 = 0$, because it is not immediately clear what eq. 5 reduces to. We first look at the von Bertalanffy model. It is possible then to calculate exactly what A must be if l_1, l_2, and k are known: it is

$$(6) \qquad a^* = -\frac{1}{k}\log\left(\frac{l_2-l_1}{l_2-dl_1}\right)$$

where $d = \exp(-k(t_2 - t_1))$. Arguing from first principles, we obtain

$$(7) \qquad h_0(l_1, l_2) = \frac{1}{\sigma_\infty f_2^*}\phi\left(\frac{l_2/f_2^* - \mu_\infty}{\sigma_\infty}\right)p(a^*)\frac{1}{k}\left\{\frac{1}{l_2-l_1} - \frac{d}{l_2-dl_1}\right\}$$

where $f_2^* = f(t_2; a^*, \theta)$ and $\phi(\cdot)$ is the standard normal density. If $l_2 \le l_1$, then $h_0(l_1, l_2)$ is set to 0.

For general log-concave growth curves, the formula is

$$(8) \qquad h_0(l_1, l_2) = \frac{1}{\sigma_\infty f_2^*}\phi\left(\frac{l_2/f_2^* - \mu_\infty}{\sigma_\infty}\right)p(a^*)\frac{\partial a^*}{\partial l_1}$$

suggesting that an explicit formula for a^* in terms of l_1 and l_2 is needed for each model. However, it is easy to prove that

$$\frac{1}{f_2^*}\frac{\partial a^*}{\partial l_1} = \left(l_2\frac{\partial f_1^*}{\partial a^*} - l_1\frac{\partial f_2^*}{\partial a^*}\right)^{-1}$$

so we really only need to differentiate $f(t; a, \theta)$ with respect to a and evaluate it at (t_1, a^*) and (t_2, a^*). Note that a^* is the solution to $f_1/l_1 = f_2/l_2$, which may need to be solved numerically. A growth curve $f(t)$ is log-concave if $\log f(t)$ is concave: that is, any straight line joining two points on the curve $\log f(t)$ lies on or beneath the curve. Many of the commonly used simple growth curves are log-concave. For several examples, we confirmed numerically that $h(l_1, l_2)$ converges to $h_0(l_1, l_2)$ as $\sigma^2 \to 0$.

Numerical computation of the integral

Computation of the integral in eq. 5 is not straightforward. When maximizing a likelihood, the integral needs to be computed separately for each fish at each step of the likelihood maximization. If there are 1000 fish in the study, and the likelihood optimization routine takes 500 steps to find the optimal parameters, the integral will need to be computed 500 000 times. For large-scale applications, a fast and accurate quadrature method is required. We used Gauss–Hermite integration after using a robust search method to locate the approximate maximum of the integrand. For details, refer to Appendix A.

A new growth curve: the von Bertalanffy with logistic growth rate parameter

Extensive tagging studies of southern bluefin tuna were undertaken during the 1960s and 1980s. This large database has enabled researchers to examine the adequacy of the von Bertalanffy growth curve, which has traditionally been the standard for this species. As noted in the Introduction, recent analyses suggest that a more complex model incorporating a two-stage growth process is required (Hearn and Polacheck 2002).

Wang (1998) has proposed the following generalization of the von Bertalanffy growth curve. Suppose a fish has length 0 at time t_0. Then the growth rate at time t is given by

$$l'(t) = (L_\infty - l(t))k(t)$$

where $k(t)$, the function that controls the growth rate, may depend on time. The solution is

$$l(t) = L_\infty(1 - \exp(-K(t_0,t)))$$

where $K(t_0,t) = \int_{t_0}^{t} k(u)\mathrm{d}u$. Hearn and Polacheck (2002) argue that for SBT $k(t)$ should be a constant value, k_1 say, for juvenile tuna and a lower value, k_2, for adult tuna. Thus $k(t)$ is a step function

$$(9)\qquad k(t) = \begin{cases} k_1 & \text{for } t < t_0 + \alpha \\ k_2 & \text{otherwise} \end{cases}$$

In this model, α is the age at which juveniles become adults, denoted by t^* in Hearn and Polacheck (2002). The Hearn and Polacheck model is slightly more general than this, but the extra generality is only mildly supported by the data.

The step function (eq. 9) seems harsh from a biological viewpoint. We would at least like to allow for the possibility of a slower transition between juvenile and adult growth. In addition, the step function may cause problems for statistical analysis. For example, the likelihood in Hearn and Polacheck's (2002) analysis has two modes, which might be caused by the step function.

We propose instead modeling $k(t)$ by a logistic curve:

$$(10)\qquad k(t) = k_1 + (k_2 - k_1)\frac{1}{1 + \exp(-\beta(t - t_0 - \alpha))}$$

For $t \ll t_0 + \alpha$, $k(t) \approx k_1$, and for $t \gg t_0 + \alpha$, $k(t) \approx k_2$. As t increases, $k(t)$ makes a smooth transition from k_1 to k_2. The rate of transition is governed by β, being sharper for larger β. As $\beta \rightarrow \infty$, eq. 10 reduces to the step function given in eq. 9. An advantage of the logistic form is that it can be explicitly integrated, yielding the growth curve

$$l(t) = L_\infty\left[1 - \mathrm{e}^{-k_2(t-t_0)}\left\{\frac{1 + \mathrm{e}^{-\beta(t-t_0-\alpha)}}{1 + \mathrm{e}^{\beta\alpha}}\right\}^{-(k_2-k_1)/\beta}\right]$$

if $t \geq t_0$. Of course, $l(t) = 0$ if $t < t_0$. In the notation of eq. 1, $\theta = \{k_1, k_2, \alpha, \beta\}$ has four components, in contrast to the ordinary von Bertalanffy curve, which has one. We propose calling this the von Bertalanffy growth curve with logistic growth rate and abbreviating it as the "VB log k" model. The traditional von Bertalanffy curve is recouped if $k_1 = k_2 = k$. Note that the VB log k model is not a member of the Schnute (1981) class.

The VB log k model could be further generalized to three or more phases in growth, reflecting different growth conditions for multiple life stages. It is also possible to generalize the von Bertalanffy by using a logistic rate $k(t)$ on the length scale: $l(t) = L_\infty(1 - \mathrm{e}^{-k(t)(t-t_0)})$. However, this model does not have a simple growth rate interpretation, so we leave it for future investigation.

Estimation

Wang et al. (1995) suggest that a gamma distribution be used for $p(\cdot)$, the distribution of A, although we prefer the lognormal. In fact, an advantage of our approach is that any well-behaved parametric model for A can be adopted. Once the models for A and growth $f(t)$ have been decided upon, the unknown parameters can be estimated by maximizing the log-likelihood

$$\sum_{i=1}^{n} \log h(l_{1i}, l_{2i})$$

where n is the number of fish, and (l_{1i}, l_{2i}) are the two measurements for fish i. A numerical optimization algorithm with bound constraints is needed to fit the model.

After successfully maximizing the log-likelihood, the user may wish to estimate the realized values of A and L_∞ for each fish. One way to do this is to calculate the estimated posterior distribution using Bayes' theorem.

Thus, for a given fish, we can calculate

$$p(A = a \mid l_1, l_2) = \frac{h(l_1, l_2 \mid a)p(a)}{h(l_1, l_2)}$$

by plugging in the maximum likelihood estimates of the unknown parameters. This distribution gives the plausible range of values of A compatible with the data l_1 and l_2. Of course, calculating this conditional distribution might be practical if there are only a few fish, but often there are hundreds. The user really requires a single summary statistic for each fish. The mean would probably be chosen, although other summary statistics, such as the median, mode, trimmed mean, and so on, could be used if desired. The mean requires a one-dimensional integration. It is worth noting that the mode of A given l_1 and l_2 is already determined for each fish if the method outlined in Appendix A for calculating the likelihood is followed. Typically, we find little difference between the mean and the mode.

Similarly, we can calculate $q(L_\infty|l_1, l_2)$, the density of the the asymptotic length given the data. In practice, we would probably use the mean of $q(L_\infty|l_1, l_2)$ as a point estimate of the asymptotic length for a particular fish. The direct approach yields a double integral, but this can be avoided by exploiting the joint normality of L_∞, l_1, and l_2 when a is known. The formula is

$$(11)\qquad E(L_\infty \mid l_1, l_2) = \frac{\int_0^\infty E(L_\infty|l_1, l_2, a)\; h(l_1, l_2|a)p(a)\mathrm{d}a}{h(l_1, l_2)}$$

where

Table 1. Mean parameter estimates (and standard deviations) from applying our new estimation method to simulated von Bertalanffy data.

Distribution of A			Mean growth parameter estimates (standard deviation)				Mean parameter estimates for A (standard deviation)			
True	Assumed	σ	μ_∞	σ_∞	k	σ	u	v	σ_c	p
LogN(0.5,0.5)	LogN(u,v)	0	100.3 (1.8)	5.0 (0.4)	0.50 (0.02)	0.01(0.02)[a]	0.50 (0.06)	0.50 (0.04)		
		0	99.9 (0.8)	5.0 (0.2)	0.50 (0.01)	—[b]	0.50 (0.03)	0.50 (0.03)	—	—
LogN(0.5,0.5)	LogN(u,v)	2	100.1 (2.2)	4.7 (1.0)	0.50 (0.04)	2.0 (0.2)	0.50 (0.06)	0.50 (0.04)	—	—
LogN(0.5,0.5)	LogN(u,v)	4	99.7 (3.0)	4.3 (2.2)	0.51 (0.05)	3.9 (0.4)	0.49 (0.08)	0.50 (0.04)	—	—
Multimodal	Gaus.Mixt.(u,v,σ_c,p)	2	100.0 (3.3)	5.1 (1.1)	0.50 (0.05)	2.1 (0.5)	1.1 (0.06)	2.1 (0.14)	0.20 (0.03)	0.80 (0.05)
Multimodal	LogN(u,v)	2	100.6 (2.9)	4.8 (1.1)	0.49 (0.04)	2.0 (0.2)	0.21 (0.05)	0.31 (0.03)	—	—

Note: For each model, we ran 100 simulations with 100 recaptures per simulation. Data were generated with $L_\infty \sim N(100, 25)$ and $k = 0.5$. Times at liberty were taken to be $\Gamma(1,1)$ distributed. The standard deviation of the measurement error, σ, was varied, as was the distribution on the true and assumed age at tagging A. LogN(u,v) denotes a lognormal with mean u and standard deviation v on the log scale; Gaus.Mixt.(u,v,σ_c,p) denotes a Gaussian 2-component mixture with means u and v, common standard deviation σ_c, and proportion p belonging to the first component.

[a] Parameters were estimated using likelihood for measurement error and setting lower bound on σ at 0.001.

[b] Parameters were estimated using likelihood for no measurement error.

$$(12)\quad E(L_\infty | l_1, l_2, a) = \mu_\infty + \frac{\sigma_\infty^2}{\sigma^2 + \sigma_\infty^2 (f_1^2 + f_2^2)} (f_1(l_1 - \mu_\infty f_1) + f_2(l_2 - \mu_\infty f_2))$$

Thus, the conditional means $E(L_\infty | l_1, l_2)$ can be calculated by substituting eq. 12 into eq. 11 and using one-dimensional integration. It is reassuring to note that this yields the correct result when $\sigma^2 = 0$, in which case $l_1 = L_\infty f_1$ and $l_2 = L_\infty f_2$, and it is readily checked that $E(L_\infty | l_1, l_2, a) = L_\infty$. Of course, the bivariate conditional distribution $p(A, L_\infty | l_1, l_2)$ could also be calculated, although there seems little point.

Results

Simulated data

To test our proposed model fitting procedure and its generality, we carried out a number of simulations. We generated growth data according to various models, looking at the effect of different growth curves, different distributions on the age at tagging, and different amounts of measurement error.

Initially, we considered the traditional von Bertalanffy (VB) curve. In all model runs, L_∞ was taken to be normally distributed with mean 100 and standard deviation 5, and k was taken to be 0.5, such that 95% of the average maximum length was achieved by age 6. The times at liberty were generated according to a $\Gamma(1,1)$ distribution, which was chosen to be representative of tagging studies in which most recaptures occur quickly and subsequently decrease (in this case, 63% within the first year and 95% within 3 years).

At first, ages at tagging, A, were generated according to a lognormal distribution with mean and standard deviation on the log scale of 0.5 and 0.5, respectively (which we will denote by $A \sim \text{LogN}(0.5,0.5)$). This gives a positively skewed distribution with a mode around 1.5 years of age. The effect of varying the amount of measurement error was investigated by setting σ equal to 0, 2, and 4 in different simulations. For each situation, 100 simulations using a sample size of 100 recaptures per simulation were carried out.

We now summarize the results from the above simulations. The parameter estimates obtained using the new estimation method were all unbiased, except for a slight underestimation of the variability in L_∞ as the measurement error increased (Table 1, rows 1 to 4). Otherwise, the effect of increasing the measurement error was only to increase the standard deviation of the parameter estimates. Note that in the case of zero measurement error, we ran simulations using both the likelihood based on the joint density developed for measurement error (eq. 5) and the likelihood based on the joint density for no measurement error (eq. 8). The two methods gave comparable estimates (Table 1, rows 1 and 2).

With such a small sample size and relatively short times at liberty, there is not much information on older fish with which to discern the distribution of L_∞. Hence, it is not too surprising that the variability in L_∞ is slightly biased; perhaps more surprising is that the mean value is estimated correctly. Increasing the sample size from 100 to 500 or, alternatively, changing the distribution on the times at liberty to be uniform on [1,7] eliminated the slight bias in the standard deviation of L_∞ when σ was equal to 4.

For many studies, the ages at tagging may not follow a simple distributional form. For example, in the case of SBT, fish spawn from October to April, and tagging is performed most commonly during January. This results in a multimodal distribution for the release ages. Thus, it is important that our estimation method works for a variety of distributions for A. We generated values for A that we believe are representative of the real ages at tagging for SBT using the following steps. Firstly, from the true tagging data for SBT, we took a random sample of 100 fish and retained their release date and integer age (an integer age had been assigned to each fish based on its release length, and this age is likely to be accurate for young fish). Next, we generated a "birth date" for each fish from a normal distribution with a mean of zero (representative of January 1) and a standard deviation of 1.5 months (so that roughly 95% of the birth dates fell between October 1 and April 1). Lastly, we calculated a release age for each fish by taking its integer age (in years) and adding the difference between its release date and birth date (expressed in decimal years).

The distribution of release ages generated in the above manner has distinct modes at ages 1 and 2 and is clearly not lognormal (Fig. 1). A Gaussian mixture model appears to be an appropriate choice. Thus, we applied our estimation method to simulated data that included such ages at tagging assuming that they follow a two-component Gaussian mixture distribution with means u and v, a common standard deviation σ_c, and a proportion p belonging to the first component. We again generated times at liberty according to a $\Gamma(1,1)$ distribution, and tag and recapture lengths according to a VB curve with $k = 0.5$ and L_∞ random normal with mean 100 and standard deviation 5. The standard deviation of the measurement error was taken to be 2. The mean parameter estimates for L_∞, k, and σ were unbiased (Table 1, second last row), which shows that the method works even for fairly complex distributions for A.

To investigate the robustness of our method to the distribution assumed for A, we reran the above simulations assuming a lognormal distribution for A. Again, the growth parameter estimates were unbiased (Table 1, last row). In this case, the lognormal distribution gave a fair approximation to the true distribution of A, as shown in Fig. 1 where the fitted lognormal curve is overlaid on the histogram of release ages. In most situations, the researcher will have some information about the release ages, and the method appears to be quite robust provided a reasonable distribution for A is chosen. For example, in the above simulations, we could have chosen the gamma distribution instead of the lognormal and achieved equally good results.

Fig. 1. Histogram of simulated realistic ages at tagging for southern bluefin tuna, scaled such that the total area of the bars is one. The line shows the fitted probability density function (pdf) assuming a lognormal distribution.

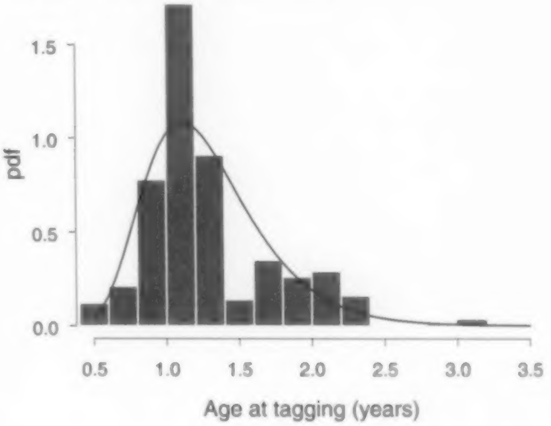

One of the advantages of our estimation method is its ability to generalize to a wide range of growth curves. To illustrate this, we ran simulations on growth data generated from a logistic curve, a generalized von Bertalanffy (GVB) curve, as well as a von Bertalanffy curve with a logistic growth rate (VB log k, as described in the Methods section). The logistic curve can be expressed as

$$(13)\qquad l(t) = L_\infty(2(1 + \exp(-k(t - t_0)))^{-1} - 1)$$

parameterized such that $l(t) = 0$ when $t = t_0$ and $l(t)$ approaches L_∞ as $t \to \infty$. The equation for a GVB curve is

$$(14)\qquad l(t) = L_\infty(1 - \exp(-k(t - t_0)))^r$$

for $r > 0$. Note that the logistic and GVB curves are both special cases of the Richards' growth curve. In our simulations for all models, we took L_∞ to be normally distributed with mean 100 and standard deviation 5, A to be LogN(0.5, 0.5), the times at liberty to be $\Gamma(1,1)$, and σ to be 2.

For the logistic curve, we set $k = 0.5$, and for the GVB curve, we set $k = 0.5$ and $r = 2$. These two curves have a slower rate of growth than the VB curve, and the GVB curve has an inflection point at age $\log(2)/0.5 \approx 1.4$ (Fig. 2a). For the logistic and GVB models, we ran 100 simulations with 100 recaptures per simulation. For both models, all parameter estimates were accurate with the exception of σ_∞, which shows a small negative bias and larger variability (Table 2). As with our simulations for the VB model, this is not surprising because we are generating data that has very little information on older fish. We illustrate a typical simulated data set for the logistic model along with the true curve (Fig. 2b). The asymptotic length is not reached until approximately age 10 but there is little data exceeding age 6. Still, μ_∞ is estimated very accurately and with more extensive data coverage, σ_∞ would be estimated with greater accuracy and precision as well.

For the VB log k model, we set $k_1 = 0.8$, $k_2 = 0.3$, $\alpha = 1.5$, and $\beta = 4$, giving a fairly rapid reduction in growth rate from about age 0.5 to age 2.5 (Fig. 3). To avoid identifiability problems, we did not optimize over β because β appears to be highly correlated with k_1 and k_2. Furthermore, we increased the sample size to 500 recaptures in each of the 100 model runs because the data are otherwise insufficient to discriminate between likelihoods for many sets of parameter values. Even for this more complex growth model, the parameter estimates were accurate and unbiased (Table 3, row 1).

The necessity to fix β can be relaxed if the data are more comprehensive such that there is sufficient information before and after the transitional stage in the growth rate; however, care must still be used. We increased α to 2.5 so

Table 2. Mean parameter estimates (and standard deviations) from applying our new estimation method to simulated logistic and generalized von Bertalanffy (GVB) growth curves.

	Mean growth parameter estimates (standard deviation)					Mean parameter estimates for *A* (standard deviation)	
Growth curve	μ_∞	σ_∞	k	r	σ	$\mu_{\log A}$	$\sigma_{\log A}$
Logistic	100.0 (2.9)	4.2 (1.5)	0.50 (0.03)	—	2.0 (0.2)	0.51 (0.07)	0.49 (0.03)
GVB (r = 2)	100.2 (3.3)	4.4 (1.3)	0.50 (0.05)	2.1 (0.6)	2.0 (0.2)	0.49 (0.15)	0.50 (0.07)

Note: For each model, we ran 100 simulations with 100 recaptures per simulation. Data were generated assuming $L_\infty \sim N(100,25)$, $k = 0.5$, age at tagging $A \sim \text{LogN}(0.5,0.5)$ and $\sigma = 2$. Times at liberty were taken to be $\Gamma(1,1)$ distributed.

Fig. 2. (*a*) Comparison between the von Bertalanffy (VB), logistic, and generalized von Bertalanffy (GVB) growth curves with $L_\infty = 100$ and $k = 0.5$ for all curves and $r = 2$ for the GVB curve. (*b*) A typical simulated data set to which we are fitting the logistic growth curve.

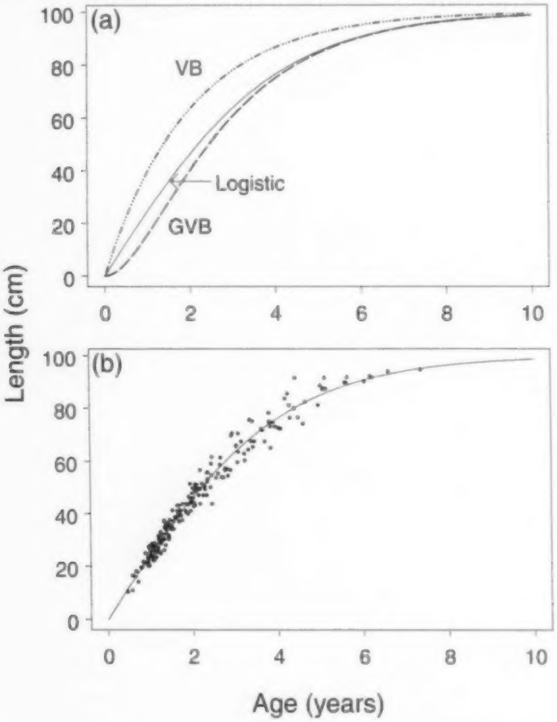

Fig. 3. (*a*) Logistic growth rate with $k_1 = 0.8$, $k_2 = 0.3$, $\alpha = 1.5$, and $\beta = 4$. (*b*) von Bertalanffy curve with logistic growth rate (parameters as above) and $L_\infty = 100$.

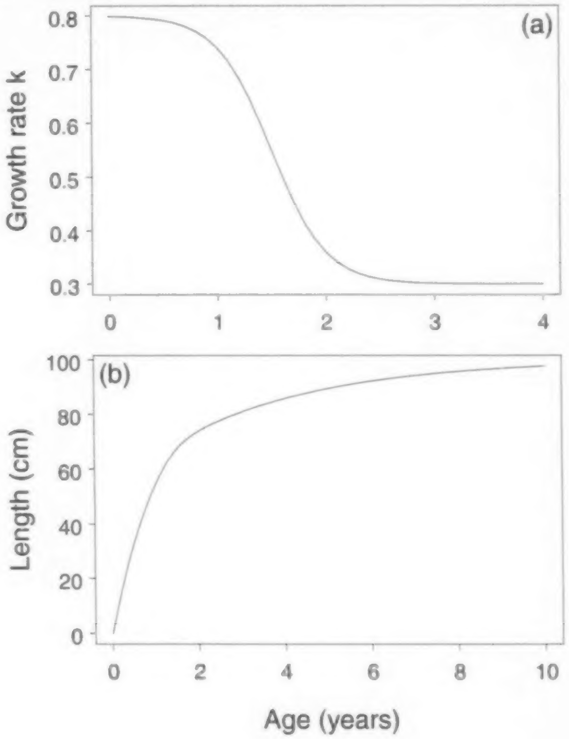

that there was more data before the transition and also changed the times at liberty to be uniform over the interval [1,7] and then ran simulations in which β was allowed to vary. In several data sets, either β, k_1, or k_2 converged to one of its set bounds. Nevertheless, for the 82 of the 100 model runs in which this did not occur, the mean estimates for the parameters were good (Table 3, row 2). Note that the coefficient of variation in β is much larger than in any of the other parameters.

SBT tag–recapture data

To illustrate the method on real data, we used tag–recapture data from SBT that were released in the 1980s. A total of 1412 recaptures were included in the analysis. The times at liberty ranged from 270 days (an imposed minimum to remove the effects of seasonal growth) to 4356 days (12 years), with 95% of the returns occurring in the first 3 years.

We began by using our method to fit the standard von Bertalanffy growth curve. We assumed that the ages at tagging followed a lognormal distribution, because our simulations in the previous section using release ages generated from the SBT tagging data indicated this was a reasonable assumption. Furthermore, we assumed that the measurement errors in release and recapture lengths, ϵ_1 and ϵ_2, were normally distributed with mean = 0 and common variance σ^2. We proceeded to make the model more complex by fitting the VB log k growth curve, leaving all other assumptions the same. Finally, we fit both the VB and the VB log k growth curves incorporating a more complicated error structure in which the error variance in recapture lengths differed according to the measurer, scientific staff or fishermen.

Table 3. Mean parameter estimates (and standard deviations) from applying our new estimation method to simulated von Bertalanffy logistic *k* growth data.

			Mean growth parameter estimates (standard deviation)							Mean parameter estimates for *A* (standard deviation)	
d*t*	*n*	α	μ_∞	σ_∞	k_1	k_2	α	β	σ	$\mu_{\log A}$	$\sigma_{\log A}$
Γ(1,1)	100	1.5	99.7	5.0	0.81	0.31	1.5	4[a]	2.0	0.50	0.50
			(2.2)	(0.4)	(0.06)	(0.04)	(1.1)		(0.1)	(0.05)	(0.02)
Unif(1,7)	82[b]	2.5	100.4	5.0	0.83	0.30	2.4	4.3	1.9	0.48	0.51
			(2.1)	(0.3)	(0.08)	(0.09)	(0.3)	(1.8)	(0.4)	(0.08)	(0.02)

Note: We ran *n* simulations with 500 recaptures per simulation. Data were generated with $L_\infty \sim N(100,25)$, $k_1 = 0.8$, $k_2 = 0.3$, $\alpha = 1.5$ or 2.5 (as specified in the table), and $\beta = 4$, age at tagging $A \sim \text{LogN}(0.5,0.5)$, and $\sigma = 2$. The distribution on the times at liberty, d*t*, was varied from a gamma distribution (Γ(1,1)) to a uniform distribution (Unif(1,7)).

[a] Fixed at 4 to avoid identifiability problems.

[b] Of the 100 simulations, 82 did not have identifiability problems in which β, k_1, or k_2 converged to a set bound.

Table 4. Parameter estimates from applying our estimation method to 1980s southern bluefin tuna tag–recapture data ($n = 1412$).

		Parameter estimates											
Growth curve	Error structure	μ_∞	σ_∞	k_1	k_2	α	β[a]	$\mu_{\log A}$	$\sigma_{\log A}$	σ	σ_f	–log likelihood	AIC
VB	Simple	160.6	8.8	0.28	—	—	—	0.55	0.17	3.9	—	9633.1	19 278.2
VB	Sci./Fish.	162.0	7.1	0.27	—	—	—	0.56	0.18	2.9	4.2	9611.3	19 236.6
VB log*k*	Simple	188.2	10.9	0.22	0.16	3.0	30	0.58	0.16	3.7	—	9609.7	19 237.4
VB log*k*	Sci./Fish.	186.6	9.3	0.22	0.17	2.9	30	0.58	0.18	2.6	4.1	9585.7	19 191.4

Note: Negative log-likelihood values and Akaike's information criteria (AIC) are also given. Results are for the von Bertalanffy (VB) and von Bertalanffy logistic *k* (VB log *k*) growth curves with both simple and measurer-dependent (Sci./Fish.) error structures.

[a] β constrained to be ≤30.

Scientists measured all release lengths so there was no need to make this distinction for ϵ_1. In particular,

$$\text{var}(\epsilon_1) = \sigma^2$$

$$\text{var}(\epsilon_2) = \begin{cases} \sigma^2 & \text{if measured by a scientist} \\ \sigma^2 + \sigma_f^2 & \text{if measured by a fisherman} \end{cases}$$

For a given growth curve (either the VB or VB log *k*), the estimates of the growth parameters were very similar regardless of the error structure assumed (Table 4). However, the fits were significantly better when the measurer-dependent error structure was included, as indicated by the smaller Akaike information criteria (AIC) values (Table 4). This suggests that the more complex error structure is a worthwhile addition as it explains a significant amount of the residual variation.

Both of the VB log *k* models gave a significantly improved fit compared with the VB model with an equivalent error structure. Again this is indicated by the smaller AIC values. The mean fitted curves for the VB and VB log *k* models with measurer-dependent error variance are very similar up until about age 7, at which point the VB log *k* curve becomes progressively higher than the VB curve (Fig. 4). To further compare and evaluate these models, we calculated residuals for the fitted recapture lengths (Fig. 5). To calculate these fitted values requires a realized value of *A* and L_∞ for each fish, which we estimated using the procedures described in the Methods section (under Estimation). Briefly, for each fish we calculated the mean of the posterior distribution for *A* and for L_∞ given the fish's release length and recapture length. Two features of the residual plots are worth noting. First, the improved fit of the VB log *k* model over the VB model is apparent in the residuals for large fish. We see that the mean asymptotic length is being underestimated in the VB model. Second, the reason for incorporating a measurer-dependent error structure seems clear because the residuals are markedly smaller for lengths measured by scientists than for those measured by fishermen.

Approximate errors for the parameter estimates can be obtained by inverting the observed information matrix $\{\partial^2 l/\partial p_i \partial p_j\}$, where *l* is the maximum log-likelihood and *p* is the vector of parameters. Parameters on the boundary of the parameter space must be regarded as fixed. We used this method for the VB log *k* model with simple error structure (Table 4, row 3). The estimates 0.220 of k_1 and 0.163 of k_2 have standard errors of 0.011 and 0.013, respectively, with correlation 0.918. Thus the estimate of $k_1 - k_2$ is 0.057 with standard error 0.017, confirming that k_1 and k_2 are significantly different and that a simple VB model is inadequate. Similarly, for the VB log *k* model with measurer-dependent error variance (Table 4, row 4), the estimate of $k_1 - k_2$ is 0.053 with standard error 0.019, leading to the same conclusion.

For the VB log *k* models, β, the parameter that governs the rate at which the growth rate changes was optimized at a set upper bound of 30. This means an almost instantaneous switch in growth rate from k_1 to k_2 at age α. However, in the previous section we saw that the estimate of β can be high even if the true value of β is low when the data coverage is inadequate. To check this, we ran a number of simulations of 1400 fish with parameters close to those for the fitted VB

Fig. 4. Mean growth curves for the 1980s southern bluefin tuna tag–recapture data. The solid line is the von Bertalanffy fit and the broken line is the von Bertalanffy logistic *k* fit, both from models incorporating a measurer-dependent error structure. The dotted vertical line shows the estimated transition point, α, for the von Bertalanffy logistic *k* model.

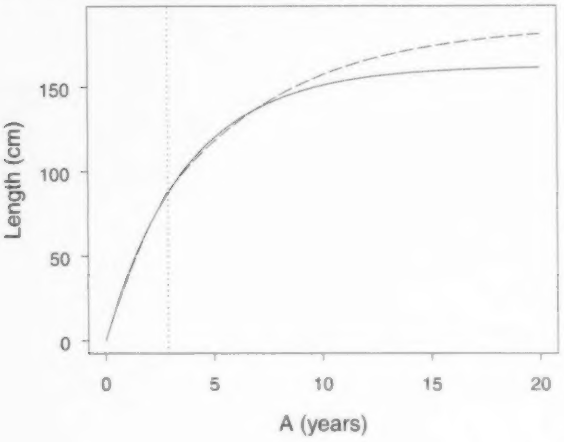

log *k* model with simple error structure (Table 4, row 3), but with $\beta = 3$. The times at liberty were sampled from the observed times. We found that β was estimated correctly more than half the time, but converged to 30 (the upper bound) in the remaining runs. The other parameters were all estimated with minimal bias and good precision regardless of the estimate of β. Hence, we cannot be certain of the rate of transition between the phases, but we expect the other parameter estimates to be unaffected.

Discussion

The results from this paper show that the maximum likelihood method we propose for fitting growth models to tag–recapture data is a viable alternative to the methods already in existence. By modeling the joint density of l_1 and l_2, we avoid the inconsistency problems that result from applying Fabens' method. However, in return, we must model the distribution of *A*.

Wang (1998) has recommended fitting growth models using first-order estimating equations. This appears attractive because it also is statistically rigorous, yet it avoids the need to model *A*. We therefore consider this method more closely for our own situation. James (1991) has described the method for the von Bertalanffy model, but it may be extended to other more realistic models following the principles outlined by Wang (1998). For the VB log *k* model, let

$$S(t_1, t_2) =$$

$$k_2(t_2 - t_1) + \frac{k_2 - k_1}{\beta}[\log(1 + e^{-\beta(t_2 - t_1 - \alpha)}) - \log(1 + e^{\alpha\beta})]$$

and

$$\eta(t_1, t_2, l_1, l_2) = l_2 - l_1 - (\mu_\infty - l_1)(1 - e^{-S(t_1, t_2)})$$

Fig. 5. Residuals between the actual and fitted recapture lengths for (*a*) the von Bertalanffy model and (*b*) the von Bertalanffy logistic *k* model fit to the 1980s southern bluefin tuna tag–recapture data. Both models incorporate a measurer-dependent error structure; the pluses indicate length measurements made by fishermen, whereas the open circles indicate length measurements made by scientists.

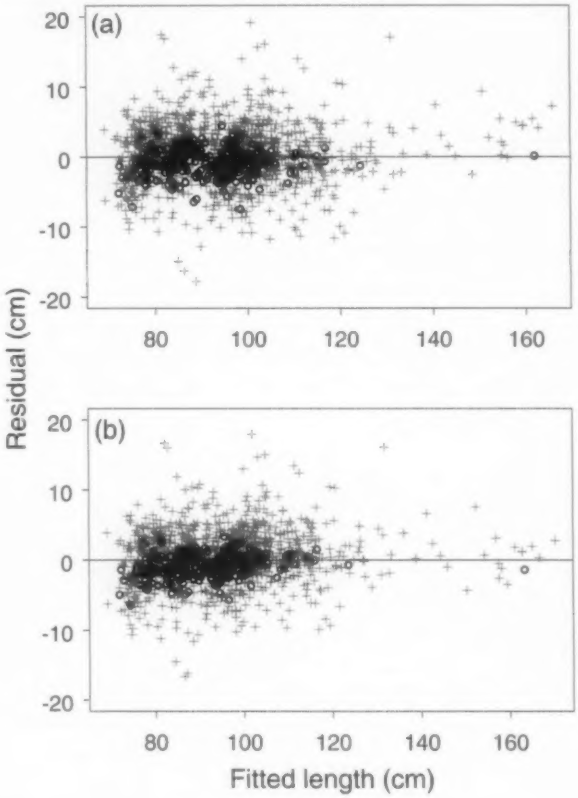

For fish *i*, let $S_i = S(t_{1i}, t_{2i})$ and $\eta_i = \eta(t_{1i}, t_{2i}, l_{1i}, l_{2i})$. The five unknown parameters $\{\mu_\infty, k_1, k_2, \alpha, \beta\}$ may be estimated by solving the five nonlinear equations

$$\sum_{i=1}^{n} \eta_i = 0; \quad \sum_{i=1}^{n} \frac{\partial S_i}{\partial k_1}\eta_i = 0; \quad \sum_{i=1}^{n} \frac{\partial S_i}{\partial k_2}\eta_i = 0;$$

$$\sum_{i=1}^{n} \frac{\partial S_i}{\partial \alpha}\eta_i = 0; \quad \sum_{i=1}^{n} \frac{\partial S_i}{\partial \beta}\eta_i = 0$$

We attempted to solve these equations for the 1980s tagging data using commercial routines, with starting values near the maximum likelihood estimates for the VB log *k* model with simple error structure. We obtained $\hat{\mu}_\infty = 164.5$, $\hat{k}_1 = 0.265$, $\hat{k}_2 = 0.263$, $\hat{\alpha} = -0.606$, and $\hat{\beta} = 12.5$. These are suspiciously close to a simple VB solution. Suppose that $\tilde{k}$ and $\tilde{\mu}_\infty$ are the solutions of the simple VB estimating equations. It is then easy to show that setting $k_1 = k_2 = \tilde{k}$, $\alpha = 0$, $\beta \to \infty$, and $\mu_\infty = \tilde{\mu}_\infty$ will solve the VB log *k* estimating equations—in fact, α and β merely need to satisfy $\sum_{i=1}^{n} \zeta_i \eta_i = 0$, where $\zeta_i = \log(1 + e^{-\beta(t_{2i} - t_{1i} - \alpha)})$, so other combinations of α and

β may suffice. Hence, a simple VB model always provides one solution. It is possible that the equations have other solution classes, but the existence of a simple VB solution is already an unsatisfactory feature.

There are other problems with these estimating equations: they do not yield estimates of σ_∞ and the residual variance parameters, and there is no way of estimating and testing for structure in the residual variation. These problems might be solved by moving to second-order estimating equations. However, we recommend staying with maximum likelihood, at least until the estimating equations approach is better understood.

Although the literature on fitting growth models to tag–recapture data is vast, most methods in existence bear some limitation: they do not allow for individual variability in growth, are restrictive in the way in which individual variability can be incorporated, give inconsistent parameter estimates, are inflexible in the error structures that can be assumed, or are not easily generalized to growth functions other than the von Bertalanffy. Our proposed maximum likelihood method appears to overcome these weaknesses.

In the case of a random L_∞, our method can easily be generalized to any growth function. This was suggested in the derivation of the likelihood, which used a generic growth function, $f(t)$, and illustrated in our simulations using a range of growth functions.

Although we only allowed for individual variability in growth through a random asymptotic length, the likelihood equations can be derived for other random effects. For example, in the von Bertalanffy model, we might want to assume a random k parameter instead. We can adapt the argument presented in the Methods section and condition on both A and k, but a double integration is now required and would be time-consuming computationally. Alternatively, we can use modified Sheiner–Beal linearization to make the model linear in its random effects (Jones 1993, chapt. 7). If these are Gaussian, we avoid any integration problems, even where L_∞ and k are both random. However, we concur with the arguments summarized in the discussion of Wang et al. (1995) that reject the need for letting both k and L_∞ vary.

As a final point, the VB log k growth curve that we proposed shows potential as a growth curve for modeling SBT and other large pelagic species. The improved fit from applying this model compared with the simple von Bertalanffy lends support to the idea of a two-stage growth process for SBT.

Acknowledgements

We are grateful to the scientists and crew who participated in the SBT tagging operations and especially to the Australian and Japanese fishers who returned tags along with recapture length measurements. We would also like to thank Dr. Mark Palmer for providing several useful comments on a draft of this manuscript. Lastly, we wish to acknowledge the Fisheries Research and Development Corporation (FRDC) for their funding contribution to this project.

References

Akaike, H. 1974. A new look at the statistical model identification. IEEE Trans. Automated Control, **AC-19**: 265–289.

Anonymous. 1994. Report of the southern bluefin tuna trilateral workshop. Hobart, Australia, January/February 1994.

Brent, R.P. 1973. Algorithms for minimization without derivatives. Prentice-Hall, Englewood-Cliffs, N.J.

Fabens, A.J. 1965. Properties and fitting of the von Bertalanffy growth curve. Growth, **29**: 265–289.

Francis, R.I.C.C. 1988. Maximum likelihood estimation of growth and growth variability from tagging data. N.Z. J. Mar. Freshw. Res. **22**: 42–51.

Halperin, M. 1963. Confidence interval estimation in non-linear regression. J. R. Stat. Soc. B, **25**: 330–333.

Hampton, J. 1991. Estimation of southern bluefin tuna *Thunnus maccoyii* growth parameters from tagging data, using von Bertalanffy models incorporating individual variation. Fish. Bull. U.S. **89**: 577–590.

Hearn, W.S., and Polacheck, T. 2002. Estimating growth rate changes of southern bluefin tuna from tag-return data. Fish. Bull. In press.

James, I.R. 1991. Estimation of von Bertalanffy growth curve parameters from recapture data. Biometrics, **47**: 1519–1530.

Jones, R.H. 1993. Longitudinal data with serial correlation: a state-space approach. Chapman and Hall, London.

Maller, R.A., and de Boer, E.S. 1988. An analysis of two methods of fitting the von Bertalanffy curve to capture–recapture data. Aust. J. Mar. Freshw. Res. **39**: 459–466.

Palmer, M.J., Phillips, B.F., and Smith, G.T. 1991. Application of nonlinear models with random coefficients to growth data. Biometrics, **47**: 623–635.

Sainsbury, K.J. 1980. Effect of individual variability on the von Bertalanffy growth equation. Can. J. Fish. Aquat. Sci. **37**: 241–247.

Schnute, J. 1981. A versatile growth model with statistically stable parameters. Can. J. Fish. Aquat. Sci. **38**: 1128–1140.

Wang, Y-G. 1998. Growth curves with explanatory variables and estimation of the effect of tagging. Aust. N.Z. J. Stat. **40**: 299–304.

Wang, Y-G., Thomas, M.R., and Somers, I.F. 1995. A maximum likelihood approach for estimating growth from tag–recapture data. Can. J. Fish. Aquat. Sci. **52**: 252–259.

Appendix A

We discuss the efficient and accurate numerical computation of the integral in eq. 5. Denote the integrand by

$$g(a) = h(l_1, l_2|a)p(a)$$

for given l_1 and l_2. Note that $g(a)$ is proportional to the conditional distribution of A given l_1 and l_2. Consideration of several examples with A lognormal suggests that $g(a)$ is often unimodal and nearly Gaussian in appearance. We can exploit this observation to integrate $g(a)$ efficiently. We first need to find the mode and spread of $g(a)$. After considerable experimentation, we decided on the following scheme.

1. Use an efficient and robust search method (e.g., Brent's method) to locate the maximum of $g(a)$ (Brent 1973, chapt. 5). This is best done on the log scale, because $g(a)$ is approximately Gaussian near its maximum and hence approximately quadratic on the log scale. Denote the location of the maximum by μ_g.
2. Estimate the standard deviation of $g(a)$ by

$$\sigma_g = \sqrt{-1 / z''(\mu_g)}$$

where $z(a) = \log g(a)$. A simple way of calculating $z''(\mu_g)$ is to fit a quadratic to $\log g(a)$ in the neighbourhood of μ_g.

Once we have good estimates of μ_g and σ_g, we can use any accurate quadrature method to calculate eq. 5. We preferred to use Gauss–Hermite integration because it does not require many function evaluations. Define $g(a) = 0$ for $a < 0$. Thus

$$\begin{aligned} h(l_1, l_2) &= \int_0^\infty g(a)\mathrm{d}a \\ &= \int_{-\infty}^\infty g(a)\mathrm{d}a \\ &= \sqrt{2}\,\sigma_g \int_{-\infty}^\infty g(\sqrt{2}x\,\sigma_g + \mu_g)\mathrm{d}x \\ &\approx \sqrt{2}\,\sigma_g \sum_{k=1}^m w_k \mathrm{e}^{x_k^2} g(\sqrt{2}x_k\sigma_g + \mu_g) \end{aligned}$$

where x_k $(k = 1, 2, ..., m)$ and w_k $(k = 1, 2, ..., m)$ are the abscissae and weights of m-point Gauss–Hermite quadrature. Note that $\sum_{k=1}^m w_k = \sqrt{\pi}$ for any m, so that the above version of Gauss–Hermite quadrature is exact if $g(a)$ is proportional to a Gaussian density with mean μ_g and standard deviation σ_g. For a 20-point quadrature, the composite factors $w_k \mathrm{e}^{x_k^2}$ range from 0.491 to 0.899, whereas the weights w_k range from 0.462 down to 2.23×10^{-13}. Hence it is best to use the composite factors $w_k \mathrm{e}^{x_k^2}$ directly. Experimentation with this integration scheme confirmed that it is very accurate provided good values of μ_g and σ_g have been found.

For maximum likelihood estimation, $\log h(l_1, l_2)$ is required rather than $h(l_1, l_2)$. A stable method of computing this is

$$\begin{aligned} (15)\quad \log h(l_1, l_2) & \\ &= \log g(\mu_g) + \log \int_0^\infty \exp(\log g(a) - \log g(\mu_g))\mathrm{d}a \\ &= \log g(\mu_g) + \log \int_{-\infty}^\infty z_0(a)\mathrm{d}a \\ &\approx \log g(\mu_g) + \log \sigma_g \\ &\qquad + \log \sum_{k=1}^m w_k \mathrm{e}^{x_k^2} \{\sqrt{2}z_0(\sqrt{2}x_k\sigma_g + \mu_g)\} \end{aligned}$$

where $z_0(a) = \exp(\log g(a) - \log g(\mu_g))$ if $a \geq 0$ and is 0 otherwise. In $z_0(a)$, $\log g(a)$ is computed directly, not by taking logs of exponentials. Thus $\log g(a) = \log h(l_1, l_2|a) + \log p(a)$, where

$$\begin{aligned} \log h(l_1, l_2|a) = &- \log(2\pi) - \log \sigma_1(a) - \log \sigma_2(a) \\ &- 0.5\log(1 - p(a)^2) - \frac{q_{12}(a)}{2(1 - p(a)^2)} \end{aligned}$$

and if $p(a)$ is lognormal with parameters $\mu_{\log A}$ and $\sigma_{\log A}$,

$$\begin{aligned} \log p(a) = -0.5\log(2\pi) - \log \sigma_{\log A} - \log a \\ - 0.5(\log a - \mu_{\log A})^2/\sigma_{\log A}^2 \end{aligned}$$

Computation of $\log g(a)$ rather than $g(a)$ avoids overflow problems: a value of $g(a)$ of e^{-1000} may be truncated to 0 on a computer, but $\log g(a) = -1000$ is computed very accurately. In $z_0(a)$, $\log g(a) - \log g(\mu_g)$ is computed before exponentiating. Also, $z_0(\mu_g) = 1$ at μ_g and $0 \leq z_0(a) \leq 1$ for all a, so that the sum in eq. 15 and its log may be computed accurately for any set of parameters. If $g(a)$ is proportional to a Gaussian curve with mean μ_g and standard deviation σ_g ($\sigma_g \ll \mu_g$), then

$$\sum_{k=1}^m w_k \mathrm{e}^{x_k^2} \{\sqrt{2}z_0(\sqrt{2}x_k\sigma_g + \mu_g)\} = \sqrt{2\pi} \approx 2.5066$$

However, when fitting the model in row 1 of Table 4, for example, we found that this quantity varied between about 1.8 and 3.5, so that approximating $g(a)$ by a Gaussian curve (a common statistical procedure, sometimes called Laplace's approximation) is not accurate.

When the measurement error is small, $g(a)$ can exhibit a very small spread. In this case, Gauss–Hermite integration is particularly useful because it makes use of the mode and spread of the distribution. However, precise values of these parameters are required in order to achieve accurate integration. Occasionally, we have encountered situations in which A given l_1 and l_2 is not unimodal. This seems to occur when A has a complicated distribution or when the growth curve is complex and the measurement error is substantial. We have found that Simpson's rule or the extended trapezoidal rule is satisfactory under such circumstances, although it tends to be slower than Gauss–Hermite integration.

Long-term response of periphyton and macrophytes to reduced municipal nutrient loading to the Bow River (Alberta, Canada)

Al Sosiak

Abstract: The biomass of periphyton and aquatic macrophytes (*Potamogeton vaginatus* and *Potamogeton pectinatus*) in the Bow River was sampled over 16 years to assess the response of these plants to improved phosphorus (1982–1983) and nitrogen removal (1987–1990) at Calgary's two municipal wastewater treatment plants. These improvements in treatment reduced total phosphorus loading to the Bow River by 80%, total ammonia loading by 53%, and nitrite + nitrate loading by 50%. No change in periphytic biomass was detected after enhanced phosphorus removal where total dissolved phosphorus (TDP) in river water remained relatively high (10–33 $\mu g \cdot L^{-1}$). However, periphytic biomass declined at sites further downstream with TDP < 10 $\mu g \cdot L^{-1}$. Regression analysis predicted that nuisance periphyton biomass (>150 $mg \cdot m^{-2}$) occurred at TDP > 6.4 $\mu g \cdot L^{-1}$ (95% confidence interval: 1.9–7.6 $\mu g \cdot L^{-1}$). Macrophyte biomass was inversely correlated with discharge and was lower during high-discharge years. Biomass also declined following enhanced nutrient removal, with the greatest decrease following reduced nitrogen discharge. These results provide the first evidence for a response of periphyton and aquatic macrophytes to enhanced nutrient removal from municipal wastewater.

Résumé : La biomasse du périphyton et des macrophytes aquatiques (*Potamogeton vaginatus* et *Potamogeton pectinatus*) a été mesurée sur une période de 16 ans dans la rivière Bow pour déterminer la réaction de ces plantes à l'amélioration du retrait du phosphore (1982–1983) et de l'azote (1987–1990) par les deux usines municipales de traitement des eaux usées de Calgary. Ces améliorations de traitement ont réduit l'apport de phosphore total à la rivière Bow de 80 %, celui de l'ammoniaque total de 53 % et celui des nitrites + nitrates de 50 %. Aucun changement n'a pu être détecté dans la biomasse du périphyton après le retrait amélioré du phosphore lorsque la concentration de phosphore dissous total (TDP) est demeurée relativement élevée (10–33 $\mu g \cdot L^{-1}$) dans l'eau de la rivière. Cependant, la biomasse du périphyton a baissé à des sites plus en aval où la concentration de TDP était < 10 $\mu g \cdot L^{-1}$. Une analyse de régression permet de prédire que la biomasse de périphyton qui est considérée nuisible (>150 $mg \cdot m^{-2}$) apparaît aux concentrations de TDP > 6,4 $\mu g \cdot L^{-1}$ (intervalle de confiance de 95 % : 1,9–7,6 $\mu g \cdot L^{-1}$). La biomasse des macrophytes est en relation inverse avec le débit et est plus faible les années de fort débit. La biomasse a aussi diminué après le retrait plus efficace des nutriments; la diminution la plus importante s'est produite à la suite de la réduction de l'apport d'azote. Ces résultats constituent les premières indications que le périphyton et les macrophytes aquatiques réagissent à un retrait plus efficace des nutriments dans les eaux usées municipales.

[Traduit par la Rédaction]

Introduction

Nutrients from municipal wastewater discharges have caused eutrophication of lakes and rivers across Canada. To reduce this nutrient discharge, tertiary treatment has been installed at municipal wastewater treatment plants (WWTPs) serving about 34% of the Canadian population (Chambers et al. 1997). Reductions in phosphorus loading from municipal wastewater have controlled or reversed eutrophication in various Canadian lakes (reviewed in Chambers et al. 1997). However, there have been fewer studies of the response of aquatic plants in flowing water to reduced municipal nutrient loading. Although the response of periphyton to nutrient enrichment has been examined in stream channel experiments (Bothwell 1989; Horner et al. 1990), no studies appear to have evaluated the response of periphyton to reduced municipal loading in natural stream ecosystems. Chambers (1993) found no evidence of reduced growth of aquatic macrophytes in the South Saskatchewan River owing to reduced municipal phosphorus loading from Saskatoon. Terrell and Canfield (1996) reported similar findings after the elimination of both phosphorus and nitrogen discharge from a WWTP to a cove on a Florida river.

Received 23 October 2001. Accepted 17 May 2002. Published on the NRC Research Press Web site at http://cjfas.nrc.ca on 25 July 2002.
J16580

A. Sosiak. Science and Standards Division, Alberta Environment, Room 301, 2938 11 St. NE, Calgary, AB T2E 7L7, Canada (e-mail: Al.Sosiak@gov.ab.ca).

The Bow River is a major tributary of the Saskatchewan–Nelson river system, which originates in the Rocky Mountains of southwestern Alberta, Canada. Nutrient levels are low (Table 1) and little growth of submersed macrophytes occurs upstream from the two WWTP outfalls in Calgary (M1, Fig. 1). However, lush growth of periphyton, giant pondweed (*Potamogeton vaginatus*), and sago pondweed (*Potamogeton pectinatus*) occurred downstream of the WWTP outfalls in coarse gravel to cobble substrate

DOI: 10.1139/F02-071

Table 1. Physical,[a] chemical, and biological characteristics of selected Bow River sampling sites, May–October 1979–1996.

Variable	Units	Bowness		Stier's Ranch		Ronalane	
		Mean	Range	Mean	Range	Mean	Range
Depth	m	0.64	—	0.65	—	NA	—
Width	m	122	—	59	—	NA	—
Current velocity	$m \cdot s^{-1}$	1.3	—	2.6	—	NA	—
Duration of ice cover[b]	days	148	October 22 – May 2	Rarely freezes	—	136	October 15 – April 20

Variable	Units	Bowness		Stier's Ranch		Ronalane	
		Median	Range	Median	Range	Median	Range
Bed material size	mm	100	—	14	14–300[c]	18	—
Daily mean discharge	$m^3 \cdot s^{-1}$	96.7	39.1–387	95.8	43.9–450	57.7	12.2–817
Ammonia, total as N	$mg \cdot L^{-1}$	0.02	0.01–0.10	0.20	0.02–1.50	0.05	0.01–0.26
Nitrite + nitrate, dissolved as N	$mg \cdot L^{-1}$	0.030	0.003–0.100	0.680	0.180–2.00	0.03	0.003–0.98
Nitrogen, total as N	$mg \cdot L^{-1}$	0.22	0.02–2.32	1.28	0.50–5.76	0.53	0.20–7.81
Phosphorus, total dissolved as P	$mg \cdot L^{-1}$	0.003	0.003–0.040	0.026	0.003–0.280	0.011[d]	0.003–0.090
Phosphorus, total as P	$mg \cdot L^{-1}$	0.008	0.003–0.121	0.049	0.006–0.350	0.030	0.007–0.645
Silica, reactive	$mg \cdot L^{-1}$	3.10	2.10–4.59	2.80	0.01–5.50	0.60	0.01–5.10
Turbidity	NTU	1.8	0.2–8.0	3.7	0.3–45.0	8.5	0.5–520
Water temperature	°C	12.5	0.8–18.2	13.0	2.8–21.0	17.0	1.4–25.1
Macrophyte biomass	$g \cdot m^{-2}$	Absent	—	425.5	0–3897[c]	69.9	—
Periphytic Chl *a*	$mg \cdot m^{-2}$	25.1	0.7–233.2	152.4	3.4–889.7	79.5	3.9–493.3

Note: NA, not available; NTU, nephelometric turbidity units.

[a] Source: River Engineering Branch, Alberta Environment, 9th Floor, 9820-106 Street, Edmonton, AB T5K 2J6, Canada.

[b] Source: Kellerhals et al. (1972).

[c] Range at macrophyte sampling sites M1–M8.

[d] Median TDP concentration following enhanced phosphorus removal (1990–1996): 0.005 $mg \cdot L^{-1}$.

(Table 1) (Charlton et al. 1986). Drifting aquatic macrophytes and algae clogged intakes for irrigation systems, interfered with boating and angling (Alberta Environment 1979) and caused low levels of dissolved oxygen at night (Cross et al. 1986). Few submersed macrophytes were found downstream from Carseland (Fig. 1), except below the Bassano Reservoir, during a basin-wide survey by Alberta Environment (AENV) (A. Sosiak, unpublished data).

In 1982–1983, the City of Calgary installed chemical phosphorus removal at both the Bonnybrook (near site M2, Fig. 1) and the Fish Creek WWTPs (site M5, Fig. 1; new total phosphorus (TP) approval limit: 1 $mg \cdot L^{-1}$) and later added biological removal. During the next 6 years, macrophyte biomass declined at some sampling sites, but periphytic biomass did not change significantly (Sosiak 1990). Although phosphorus levels had been reduced, there was concern that ammonia in the Bow River could reach toxic levels with the rapid population growth that has occurred in Calgary (Fig. 2). The City of Calgary then also decreased ammonia and nitrate discharge to the Bow River from both WWTPs by modifications to the activated sludge process (1987), increased aeration (1990), and biological nitrogen removal (in stages beginning in 1990). The Bonnybrook WWTP (alone) must comply with a new ammonia limit of 5 $mg \cdot L^{-1}$ during July–September and 10 $mg \cdot L^{-1}$ during other months.

Aquatic macrophyte and periphytic biomass, as dry weight and chlorophyll *a* (Chl *a*), respectively, were sampled over 16 years by AENV to determine the long-term response of these aquatic plants in the Bow River to reduced nutrient discharge from the WWTPs in Calgary. In this paper, I first evaluate changes in nutrients and aquatic plant biomass following enhanced phosphorus removal and then the response to both phosphorus and nitrogen removal. I then develop predictive equations for aquatic plant biomass.

Materials and methods

Sampling sites and methods

Grab samples for chemical constituents and field measurements (dissolved oxygen, pH, conductivity, temperature) were collected at least monthly at four sites upstream from WWTP discharge in Calgary and at four sites downstream from WWTP discharge during 1979–1996 (Fig. 1). The site at Stier's Ranch was the first fully mixed location downstream from the WWTP discharge. The site at Cluny was only sampled during 1985–1996. Most sites were long-term river monitoring sites (LTRN) sampled by AENV for a wide range of variables; however, two headwater sites were sampled by Environment Canada. During 1980–1986, the duration and frequency of periphyton sampling varied each year among sites (*n* = 6–22). After 1986, periphyton at all sites and other variables at Bowness and Stier's Ranch were only sampled during May–October (*n* = 6), the time period when shoreline areas at all sites are always ice free. Single composite samples of surficial sediments were collected each fall from sites at Bowness, Stier's Ranch, and Ronalane during

Fig. 1. Bow River sampling sites in Alberta, Canada.

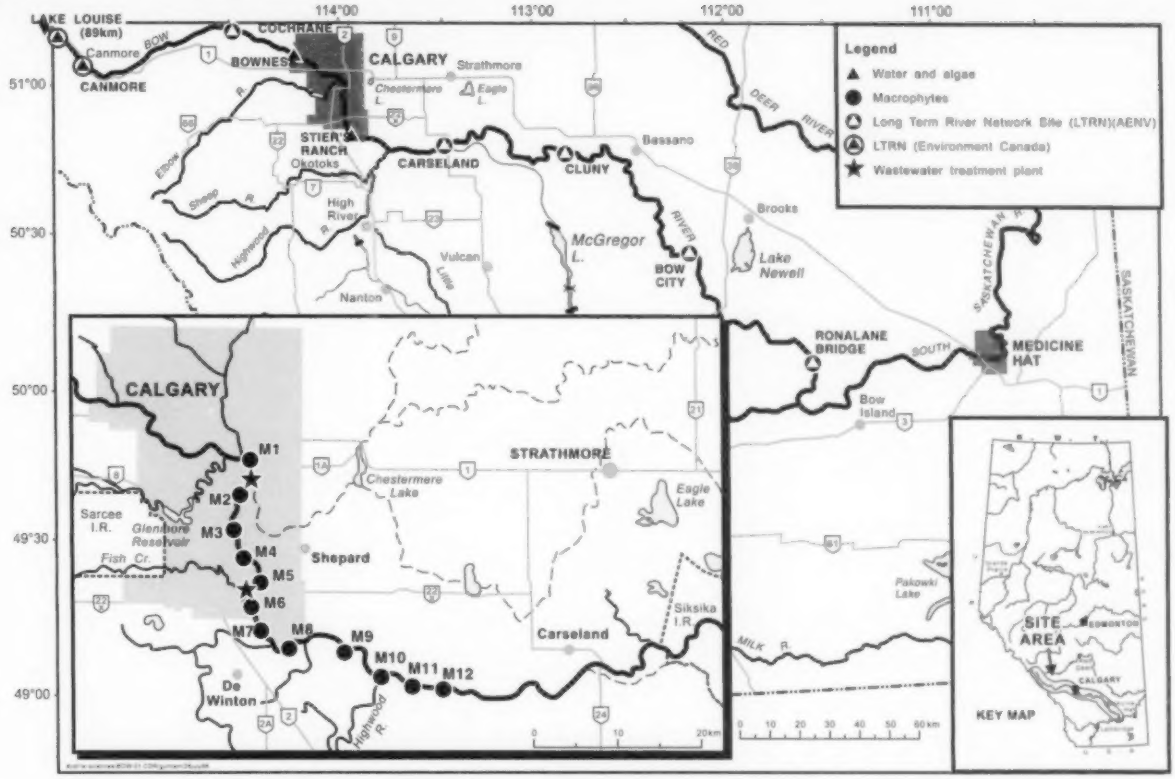
LAKE LOUISE (89km)
Canmore
CANMORE
BOW
COCHRANE
BOWNESS
CALGARY
Strathmore
Chestermere L.
Eagle L.
STIER'S RANCH
Okotoks
CARSELAND
CLUNY
Bassano
Elbow R.
Sheep R.
Highwood R.
High River
Vulcan
Nanton
Little
McGregor L.
RED DEER RIVER
Brooks
RIVER
BOW CITY
Lake Newell
RONALANE BRIDGE
SOUTH
SASKATCHEWAN R.
MEDICINE HAT
SASKATCHEWAN
Bow Island
Pakowki Lake
MILK R.
114°00
113°00
112°00
111°00
51°00
50°30
50°00
49°30
49°00
Legend
Water and algae
Macrophytes
Long Term River Network Site (LTRN)(AENV)
LTRN (Environment Canada)
Wastewater treatment plant
STRATHMORE
Chestermere Lake
Eagle Lake
Sarcee I.R.
Glenmore Reservoir
Fish Cr.
Shepard
Siksika I.R.
Carseland
De Winton
Highwood R.
M1
M2
M3
M4
M5
M6
M7
M8
M9
M10
M11
M12
0 10 20km
0 10 20 30 40 50 60km
SITE AREA
EDMONTON
CALGARY
KEY MAP

1981 and 1987–1996 using an airlift sampler (Cross et al. 1986), which used nitrogen gas pulsation to suspend fine sediments from the mainly cobble and boulder riverbed. Sediment samples were analyzed for forms of phosphorus but not nitrogen.

Mean daily discharge on sampling days and monthly mean discharges were provided by the Water Survey of Canada from stage recorders on the Bow River at Lake Louise (Water Survey of Canada Station No. 05BA001), Banff (05BB001), Ghost Dam (05BE006), Bearspaw (05BH008), Calgary (05BH004), Carseland (05BM002), Bassano Dam (05BM004), and near the mouth of the river (05BN012). Because there is no flow gauge immediately below Calgary, daily and monthly discharges were calculated from the sum of discharges in the Bow River at Calgary, the Elbow River below Glenmore Dam (05BJ001), Fish Creek at Priddis (05BK001), and City of Calgary WWTP return flows minus diversion to the Western Headworks Canal (05BM003) plus the Highwood River near the mouth (05BL024) for macrophyte sites below the Highwood River.

Epilithon (periphyton growing on stones or similar objects) was routinely sampled during 1980–1996 from Bowness to Ronalane (Fig. 1), a distance of 371 km. The routine sampling site for periphyton upstream from the WWTP discharge at Bowness (sampled in 1980, 1981, and 1993) was moved 5 km downstream in 1983 to Bowness Park (Fig. 1), where all other variables were sampled during 1979–1996. During 1980–1983, all periphytic samples for Chl *a* analysis were collected by brushing 9–12 rocks of known surface area, randomly collected from areas at wading depth, and filtering a single subsample of slurry through a glass fiber filter (Whatman GF/C). The surface area of these rocks was determined so that results could be expressed per unit area. The material retained on the filter was covered with anhydrous magnesium carbonate and stored at –4°C. During 1984–1996, periphyton samples were collected from nine rocks by scraping a 4-cm^2 area delimited by a template with a scalpel. Three samples, each a composite of material from three rocks, were collected per site on each sampling date and analyzed separately. Additional periphytic samples were collected for species identification using the same method monthly during 1981 and 1982 and quarterly in 1994.

In early September 1981–1996, five aquatic macrophyte samples were randomly collected from right and left bank sites at 12 shoreline sampling locations located from 2.5 km upstream to 33.0 km downstream of both municipal plants (Fig. 1). Sites were spread over 50.3 km, or 69% of the macrophyte distribution (A. Sosiak, unpublished data). Previous studies indicated that maximum biomass occurred in mid- to late September (Charlton et al. 1986). Plants within a 30.48 × 30.48 cm frame were uprooted and collected in a 3-mm-mesh sampling net. In the laboratory, debris was removed and samples less than 200 g wet weight were oven-

Fig. 2. Combined mass load of TP, nitrate, and total ammonia contributed to the Bow River from the Calgary WWTPs compared with the City of Calgary's population, 1979–1997. Circles, TP; triangles, NO_3-N; squares, NH_3-N; diamonds, Calgary's population.

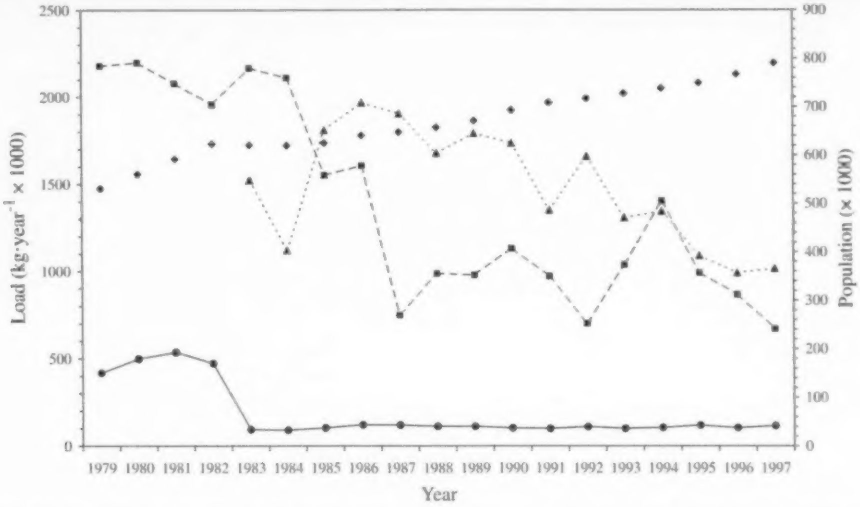

dried at 105°C for 24 h. Samples over 200 g were centrifuged for 1 min to remove excess moisture and then weighed and converted to dry weight by dividing wet weight by 7.73 (Charlton et al. 1986). This conversion factor was periodically verified.

Sample analysis

Analytical techniques and detection limits for all variables tested statistically in this study are given in Table D1.[1] Chemical constituents were analyzed at the Water Quality Laboratory of Environment Canada in Calgary during 1979–1984. After this laboratory was relocated in 1984, all chemical constituents sampled by AENV were analyzed by Chemex Labs Alberta, Inc., of Calgary (now Maxxam Analytics, Inc.). In all years, periphytic pigments were extracted in 90% acetone at the Monitoring Branch, AENV laboratory in Edmonton, homogenized, and analyzed using spectrophotometry with corrections for total pheophytin.

The City of Calgary (C. Collins, Bonnybrook Wastewater Treatment Plant, 4302-15th St. SE, Calgary, AB T2G 3M8, Canada, personal communication) provided census data and nutrient discharge estimates for both municipal WWTPs during 1979–1997. Nitrate was not measured at the City of Calgary laboratory before 1983.

Periphytic species were identified and counted as single-celled individuals, filaments, or colonies and biomass estimates were prepared by Dr. M. Agbeti of Bio-Limno Research and Consulting (Edmonton, Alta.). Aliquots of diluted samples were allowed to settle overnight in sedimentation chambers. A minimum of 500 algal cells or colonies was counted for each sample using an inverted microscope. Algal wet biomass was calculated from recorded abundance and published cell biomass values from other rivers.

Data analysis

The water quality data collected in this study were often not normally distributed and exhibited significant seasonality, serial correlation, and flow dependency. Accordingly, nonparametric statistical methods that compensate for these factors were used in all analyses except regression following procedures in the water quality statistics package WQHYDRO (Aroner 1995). Trend analysis was used to determine whether water chemistry changed significantly following enhanced nutrient removal and whether macrophyte and periphytic biomass declined as anticipated.

Except for macrophytes, which were only sampled once per year, time periods before and after changes in wastewater treatment were first tested for seasonality using the Kruskal–Wallis test for seasonality. Step trend analysis was then used to test whether enhanced phosphorus and nitrogen removal at the WWTPs resulted in immediate incremental changes in plant biomass and other variables. Data with significant seasonal variation were tested for step trends using the seasonal Wilcoxon–Mann–Whitney test (time intervals in Table 2), and changes in medians were calculated using the seasonal Hodges–Lehman estimator. For data without significant seasonal variation, the Anderson–Darling analysis of variance, followed by an experimentwise Kruskal–Wallis multiple comparison test, was used to test step trends. The Anderson–Darling analysis of variance is not adversely affected by differences in variance between samples, which often occurred in these data.

All variables were then tested for monotonic trends, or gradual increasing or decreasing biomass or concentration, following the installation of enhanced phosphorus removal in 1982–1983. Data with significant seasonal variation were tested for monotonic trends using the seasonal Kendall test, with correction for significant serial correlation as required. Serial correlation, or correlation between consecutive observations, was tested using Kendall tau correlation analysis on a time series with trend and seasonality removed. Data that did not display significant seasonal variation were tested for

---

[1] Copies may be purchased from the Depository of Unpublished Data, CISTI, National Research Council of Canada, Montreal Road, Ottawa, ON K1A 0S2, Canada.

Table 2. Incremental changes (step trends) in selected variables in the Bow River after the installation of enhanced phosphorus and nitrogen removal at Calgary WWTPs.

	Significant change in discharge, biomass, or concentration[a]						
Site	Discharge ($m^3 \cdot s^{-1}$)	Macrophyte biomass ($g \cdot m^{-2}$)[b]	Periphytic Chl *a* ($mg \cdot m^{-2}$)	TP ($mg \cdot L^{-1}$)	TDP ($mg \cdot L^{-1}$)	Ammonia ($mg \cdot L^{-1}$)	Nitrite + nitrate ($mg \cdot L^{-1}$)
Changes after the installation of enhanced phosphorus removal[c]							
Bowness, macrophyte site 1	–6.20	NS	NS[d]	NS	+0.002	NA	NS
Stier's Ranch, macrophytes (sites 2–12)	–11.85	RB: –177 LB: –273	NS	–0.188	–0.144	+0.150	NS
Carseland	–12.60	—	NS	–0.117	–0.110	–0.035	NS
Bow City	–21.63	—	NS	–0.108	–0.028	NS	NS
Ronalane	–20.35	—	NS	–0.046	–0.021	NS	NS
Changes after enhanced nitrogen removal[e]							
Bowness, macrophyte site 1	+18.95	+72.6	NS	NS	NS	–0.005	+0.013
Stier's Ranch, macrophytes (sites 2–12)	+16.70	RB: –329 LB: –354	NS	NS	NS	–0.073	–0.229
Carseland	+26.15	—	–82.08	–0.005	–0.005	–0.030	–0.210
Cluny	+21.60	—	–97.46	NS	–0.005	NS	–0.132
Bow City	+34.95	—	–15.03	NS	–0.004	–0.005	NS
Ronalane	+19.72	—	–47.41	NS	–0.003	NS	NS

Note: Bowness site is upstream from the Calgary WWTPs and the other sites are downstream. NS, not significant; NA, data not tested because of change in detection limits; RB, right bank facing downstream; LB, left bank facing downstream.

[a] Seasonal or nonseasonal Hodges–Lehmann estimator.

[b] Median of estimates from sites with significant change in biomass.

[c] Intervals tested: macrophytes, 1981–1982 versus 1983–1989; discharge and chemistry, 1979–1982 versus 1983–1985.

[d] Site 05BH0110 at Bowness; flow-adjusted and tested 1980, 1981 versus 1993.

[e] Intervals tested: macrophytes, 1983–1989 versus 1990–1996; discharge and chemistry, 1983–1988 versus 1989–1996.

monotonic trends using the Mann–Kendall test. Sen slopes were calculated to provide an estimate of the approximate magnitude of significant monotonic trends.

Intermediate trend statistics were calculated for monthly median values and then combined in an annual statistic. A χ^2 test of trend homogeneity was used to ensure that monthly trends followed one consistent direction over the year. Where trends were not homogeneous, trend tests were calculated just for the May–October time period, which had consistent homogeneity of trends. As recommended by Ward et al. (1990), a 0.10 level of significance was used in all trend analysis.

Previous work (Chambers et al. 1991) found that current velocity was an important factor regulating macrophyte biomass in the Bow River. Since there was a small but significant increase in discharge at the macrophyte sampling sites during 1983–1996, which could scour macrophytes and partially account for declining biomass, macrophyte data were also adjusted for discharge and again tested for trends. Macrophyte biomass (dependent variable) each year was flow-adjusted by robust regression (Aroner 1995) against total discharge over the season (independent variable), and residuals from the model with the best fit were tested for trends. This procedure is based on the assumption that variations in discharge do not appreciably affect the physiological response of macrophytes to nutrients and other variables. Periphytic Chl *a* from the old sampling site at Bowness was also flow-adjusted to compensate for the large variation in discharge during the three years (1980, 1981, and 1993) that this site was sampled. Variables were not otherwise flow-adjusted prior to analysis.

Spearman rho rank correlation was used to determine whether periphytic Chl *a* and macrophyte biomass were significantly correlated with physical and chemical variables. Results for the various sites from Bowness to Ronalane were merged for correlation and regression analysis. Maximum periphytic Chl *a* during May–October 1980–1996 was correlated with the median concentration of other variables sampled during the same time period. Median macrophyte biomass from the different sites each year ($n = 5$) (1981–1996) was combined and correlated with median chemistry from Bowness (macrophyte site 1), Stier's Ranch (sites 2–10), or Carseland (sites 11 and 12) and total discharge during the macrophyte growing season (May–September). To rigorously evaluate effects of discharge on maximum periphytic Chl *a*, this variable was correlated with total May–October discharge, median discharge on sampling days, and, as an index of scouring potential, the number of days each season that discharge was high enough to initiate bed movement. Bed mobility threshold flows were calculated by River Engineering Branch, AENV, using Shield's mobility number (Shields 1936) for five sites from Bowness to Bow City with sufficient bed material information. To eliminate spurious correlation due to significant mutual correlation among three variables, partial Spearman rank correlation coefficients between macrophyte biomass and chemical variables were calculated as required.

Step-up linear multiple regression analysis ($\alpha = 0.05$) (SYSTAT version 8.0) was then used to determine the relationship between aquatic plant biomass, physical variables, and nutrients. Maximum periphytic Chl *a* and macrophyte biomass were regressed against May–October (medians) of all variables that were significantly correlated with biomass.

All chemical data, except the various forms of nitrogen during regression with periphytic Chl *a*, were transformed to natural logarithms (ln) to normalize the distribution of each

Table 3. Significant monotonic trends in periphytic Chl *a*, and physical and chemical variables in the Bow River during 1983–1996.

	Sen slope (units/year) for significant trends (seasonal Kendal tau test, except as indicated[a])							
Site	Discharge ($m^3 \cdot s^{-1}$)	Periphytic Chl *a* ($mg \cdot m^{-2}$)	TP ($\mu g \cdot L^{-1}$)	TDP ($\mu g \cdot L^{-1}$)	Total ammonia ($\mu g \cdot L^{-1}$)	Nitrite + nitrate ($\mu g \cdot L^{-1}$)	TN ($\mu g \cdot L^{-1}$)	Reactive silica ($\mu g \cdot L^{-1}$)
Lake Louise	NS	—	NS	NS	–<0.01[a]	+0.50	+2.62	NS
Canmore	NS	—	–<0.20	–0.25	–1.96	+2.43	+4.55	+28.95
Cochrane	+1.452	—	NS	NS	–<0.01	+2.40	–4.88	NS
Bowness	+1.901	NS	NS	+<0.01	–<0.01[a]	+2.11	–13.09	+42.67
Stier's Ranch	+2.098	NS	NS	NS	–10.01	–47.27	–54.44	+62.65
Carseland	+4.012	–11.066	NS	–0.61[a]	–2.50	–39.81	–59.41	+92.99
Cluny	NS	–7.904[a]	NS	–0.70	NS	–21.31	–30.22	+78.08
Bow City	+4.417	–2.033[a]	NS	–0.67[a]	NS	NS	–23.27	NS
Ronalane	+2.991	–5.281[a]	NS	–0.73	NS	NS	–16.35	NS

Note: The Bowness site is upstream from the Calgary WWTPs and the other sites are downstream. NS, not significant.
[a]Kendal tau test (nonseasonal).

Fig. 3. TP in surficial sediments in the Bow River, 1981–1996. WWTP notation illustrates the location of the discharge from WWTPs between the Bowness and Stier's Ranch sites.

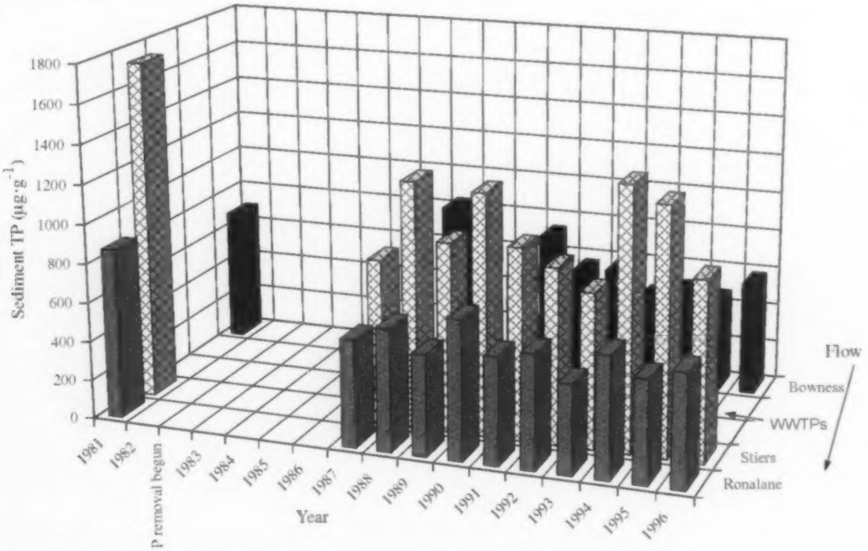

variable. Macrophyte biomass was transformed to ln + 1 to allow for zeros, and periphytic Chl *a* was transformed using the Box–Cox transformation ($Y^{0.25}$). Normal-probability plots of residuals were inspected for linearity to determine if the assumption of normality was satisfied. Plots of residuals against predicted values were inspected for randomness to determine if the assumption of constant variance was satisfied. One outlier was removed from the macrophyte analysis. Variance inflation factors (VIF) for each independent variable were calculated to ensure that none were significant in the multiple regression equation due to appreciable multicollinearity (VIF > 10) with other independent variables and were thus redundant.

The best multiple regression equation for periphyton was then used to predict the concentration of total dissolved phosphorus (TDP) and nitrite + nitrate that caused nuisance periphytic biomass in the Bow River, here defined as maximum periphytic Chl *a* exceeding 150 $mg \cdot m^{-2}$, as recommended by Welch et al. (1988). To estimate 95% confidence intervals (CI) for these threshold concentrations, the confidence region for biomass was inverted to calculate the range of values for [TDP], and then [nitrite + nitrate], that could plausibly correspond to a periphytic Chl *a* of 150 $mg \cdot m^{-2}$. A TDP:TP regression equation was then developed to permit comparison with other TP criteria (Dodds et al. 1997).

Results

Phosphorus

Both [TP] and [TDP] declined during 1989–1996 at Canmore, perhaps due to improved municipal treatment at Banff in 1989. Furthermore, there was a slight increase in TDP at Bowness. Otherwise, there were no significant monotonic trends in phosphorus detected at any of the four sites upstream from the municipal outfalls in Calgary (Tables 2 and 3).

TP loading to the Bow River from the two WWTPs in Calgary decreased by 80% after enhanced phosphorus re-

Fig. 4. TDP during May–October at selected sites: (*a*) Stier's Ranch, (*b*) Cluny, (*c*) Bow City, and (*d*) Ronalane. Bars in boxes are medians, tops and bottoms of boxes represent the 25th and 75th percentiles, and whiskers represent the 10th and 90th percentiles (values outside these percentiles plotted). In some cases, the medians coincide with the 25th percentile. Numbers above bars present sample size.

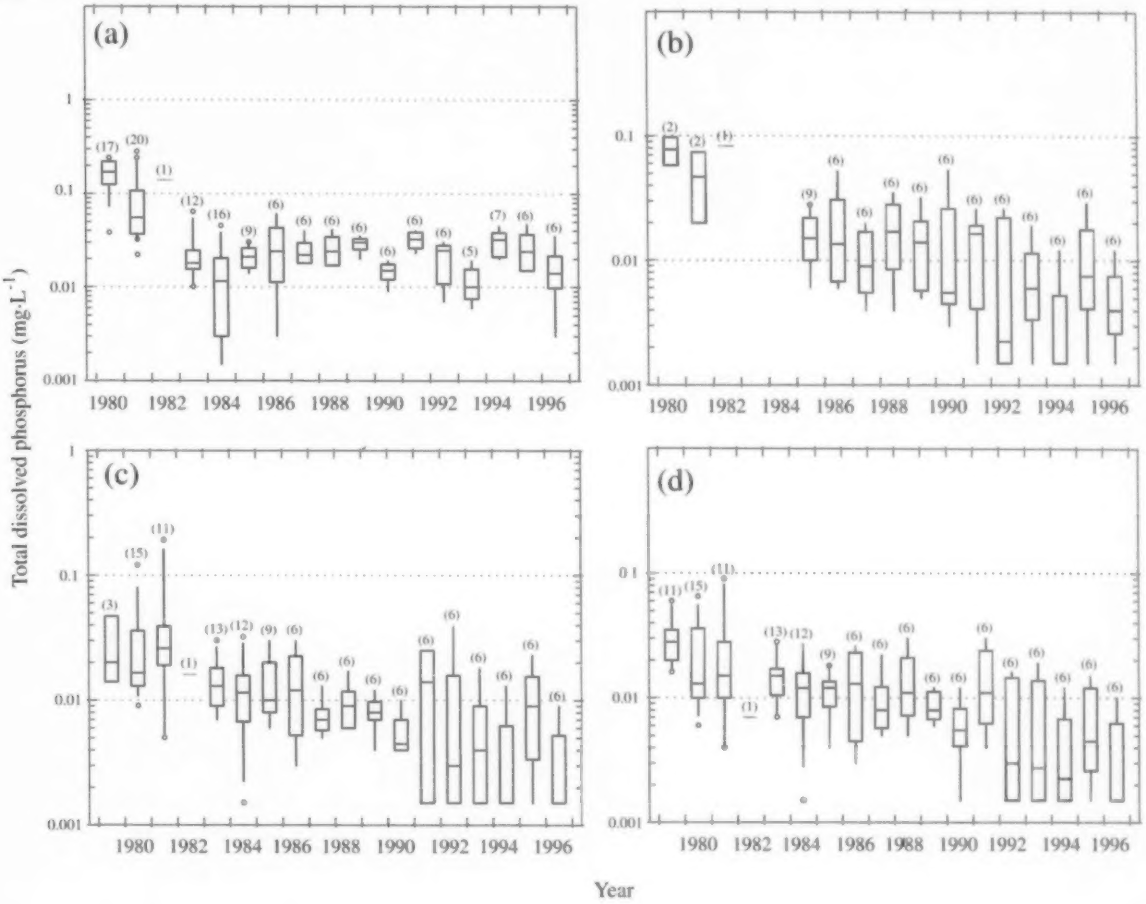

moval was installed in 1982–1983 (Fig. 2). Both [TP] and [TDP] decreased significantly in the Bow River after 1982–1983 at all sites downstream from Calgary (Table 2). TP declined in fine surficial river sediments from 1981 to 1987 at two of these sites (Stier's Ranch and Ronalane) but not upstream from the WWTPs, at Bowness (Fig. 3).

Median [TDP] (May–October) decreased 67% from 55 $\mu g \cdot L^{-1}$ in 1981 to 18 $\mu g \cdot L^{-1}$ in 1983 immediately downstream from Calgary (Stier's Ranch) but remained between 10 and 33 $\mu g \cdot L^{-1}$ (Fig. 4*a*), the highest in the basin. While there was no trend in median TDP at Stier's Ranch after 1983, TDP declined thereafter at the four sites further downstream (Table 3) and was below 10 $\mu g \cdot L^{-1}$ after 1991 at the three lower sites (Cluny, Bow City, and Ronalane) (Figs. 4*b*–4*d*). Median TDP (May–October) at Ronalane after 1991 ($<5\ \mu g \cdot L^{-1}$) was at least 70% lower than in 1981 (15 $\mu g \cdot L^{-1}$).

Nitrogen

Ammonia loading to the Bow River from the two WWTPs in Calgary was relatively steady from 1979 to 1984 and then declined by 53% over the next 3 years with improved treatment, with the greatest decrease in 1987 (Fig. 2). During May–October 1980–1989, median [total ammonia] was highest in the Bow River downstream from Calgary (Stier's Ranch), generally 0.2–0.3 $mg \cdot L^{-1}$, but thereafter the median declined there the most (step trend, Table 2). After 1989, median [total ammonia] was 0.11–0.28 $mg \cdot L^{-1}$ at Stier's Ranch (Fig. 5*a*), 0.01–0.06 $mg \cdot L^{-1}$ at Carseland, and $\leq 0.04\ mg \cdot L^{-1}$ at all other sites.

Municipal nitrate loading to the Bow River peaked in 1986 and then gradually declined by 50% between 1986 and 1996 (Fig. 2). Median [nitrite + nitrate] in the Bow River downstream from Calgary (Stier's Ranch) peaked in 1985 at 1.2 $mg \cdot L^{-1}$ (Fig. 5*b*) and then both nitrite + nitrate and ammonia declined significantly ($P < 0.05$, monotonic trend, Table 3) at Stier's Ranch and Carseland. No significant monotonic trends in nitrite + nitrate were detected further downstream at Bow City and Ronalane. After 1989, median [nitrite + nitrate] was 0.41–0.81 $mg \cdot L^{-1}$ at Stier's Ranch and Carseland and $\leq 0.5\ mg \cdot L^{-1}$ at all other sites. Although me-

Fig. 5. (*a*) Total ammonia and (*b*) nitrite + nitrate during May–October at Stier's Ranch.

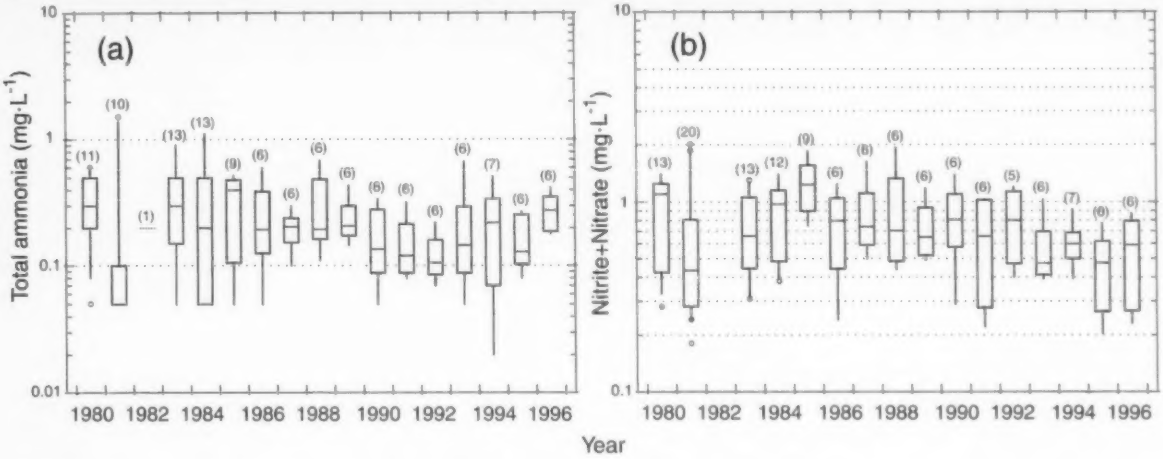

Fig. 6. Discharge on sampling days during May–October at Stier's Ranch.

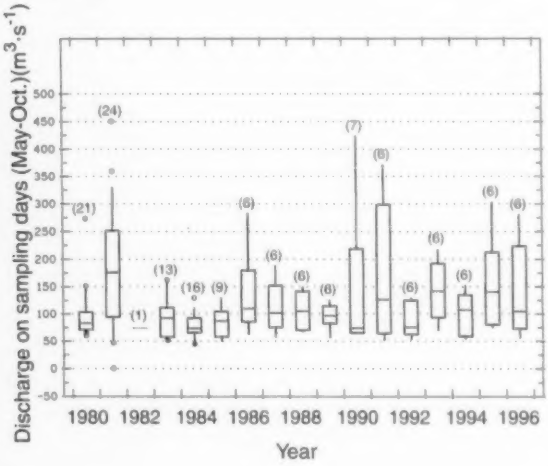

dian biologically available N:P ratios (as (NO_2 + NO_3 + NH_4 + NH_3)/TDP) generally ranged from 6 to 12 before 1983 at all sites downstream from Calgary, most N:P ratios were well above 20 at these sites after 1989.

Discharge

On average, the highest river discharge during the study period occurred in 1981 (Fig. 6), before enhanced nutrient removal was installed. However, discharge high enough to initiate bed movement (≥413 $m^3·s^{-1}$ at Stier's Ranch) occurred at regular intervals throughout the study period. Such discharge occurred on fewer days in the reach that includes Stier's Ranch (11 days in 1981, 1986, 1990, and 1995), in the main area of macrophyte growth, than at other sites on the lower Bow River (Carseland, Cluny, Bow City: 188–438 days during May–October 1980–1996, except 1983, 1984, and 1987). The lowest discharge occurred during a drought in 1984 and 1985. Following this drought, increasing trends in discharge were detected over the entire year during 1983–1996 at every site except Lake Louise, Canmore, and Cluny (Table 3).

Reactive silica, temperature, and turbidity

Median [reactive silica] was relatively high (May–October median >2.0 $mg·L^{-1}$) from the headwaters of the Bow River to Stier's Ranch, and there were increasing trends in silica at most sites between Canmore and Cluny (Table 3). Median [reactive silica] was much lower at the two sites furthest downstream (Bow City and Ronalane), often below 0.5 $mg·L^{-1}$, but no trends in silica were detected at these sites. Significant declining trends in water temperature were detected only at two sites (Cluny and Bow City) after 1983. No trends in turbidity were detected at any sites.

Periphytic Chl *a* and algal species composition

No significant step trend in periphytic Chl *a* was detected at any site during the 3 years (1983–1985) following the installation of enhanced phosphorus removal (Table 2). Furthermore, there was no change in Chl *a* 3 years before and after the change in sampling method in 1984. Accordingly, there was no indication that this change in sampling method biased results.

There was no monotonic trend in periphytic Chl *a* detected during 1983–1996 upstream from the WWTP discharge at Bowness or downstream at Stier's Ranch. However, this variable gradually declined (monotonic trend) during 1983–1996 at all four downstream sites (Carseland, Cluny, Bow City, and Ronalane) (Table 3; Fig. 7).

Algal species were only identified during 3 years (Fig. 8), but the available data suggest that the species composition of the periphyton has changed since enhanced nutrient removal was installed. The abundance (cells per unit area) of cyanobacteria and diatoms declined significantly since 1980–1981 at two of three sites with declining trends in periphytic Chl *a* (Bow City and Ronalane). Furthermore, the abundance of chlorophyta declined significantly at Stier's Ranch. Although *Cladophora* or *Stigeoclonium* were dominant chlorophyta at all sites from Stier's Ranch to Ronalane in 1980 and 1981

Fig. 7. Trend plots of periphytic Chl *a* during 1983–1996 at selected sites: (*a*) Carseland, (*b*) Cluny, (*c*) Bow City, and (*d*) Ronalane. Sen slope represented by a horizontal line.

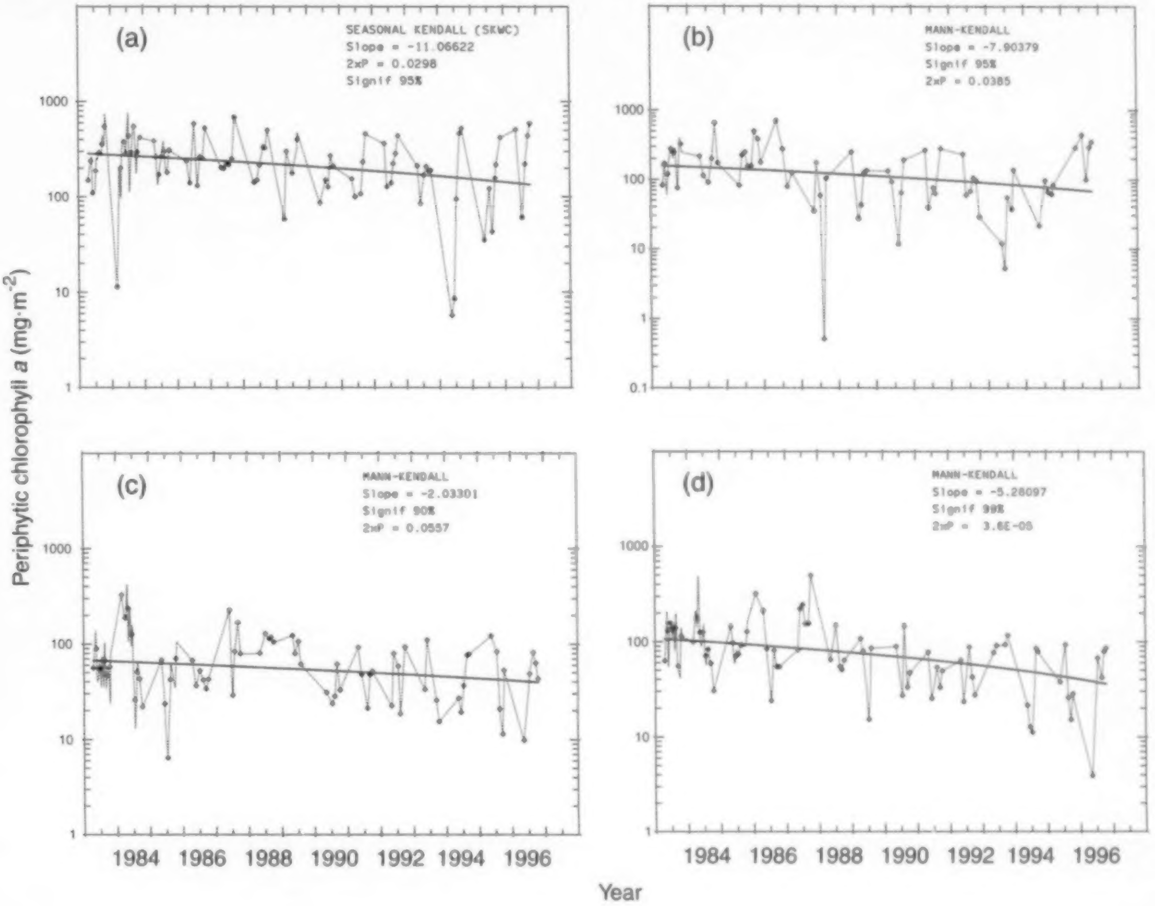

(Charlton et al. 1986), these taxa were not found at any site in 1994. Periphytic algal species composition and biomass estimates in 1994 are given in Table D2.[1]

Biomass estimates (μg·cm^{-2}) were only available for May–October 1994 (n = 3 per site) but indicate that biomass was then primarily diatoms at these sites, although cyanobacteria and green algae were also abundant at some sites.[1] Cyanobacteria (primarily *Phormidium*) were especially numerous (cells per unit area) at Carseland in 1994 (Fig. 8), but cyanobacterial biomass was at most 23% of the periphyton, and median Chl *a* was lower at this site in 1994 than in 1981 and 1982 (Fig. 7*a*).

Macrophyte biomass

Macrophyte biomass declined significantly after 1983 at all of the sites along the right bank (facing downstream) and all but one of the monitoring sites on the other bank of the river (monotonic trends, Fig. 9). Biomass was highest along the right bank in the plumes from the two WWTPs, which both discharge along this side of the river. Furthermore, significant declines in biomass were still detected at nearly half of these sites ($P < 0.10$, n = 9) after the data were flow-adjusted to eliminate any influence of an increasing discharge trend.

Macrophyte biomass declined significantly at some sites (n = 8) over 7 years (1983–1989) after enhanced phosphorus removal was installed at the WWTPs. However, the greatest decrease in biomass (n = 20) (Table 2), especially at sampling sites M10–M12 (Fig. 1), occurred at all sites during declining nitrogen but stable phosphorus levels (1990–1996) (Table 3). Macrophyte biomass was negligible at the upstream control site (site 1) during periodic visits from 1981 to 1989 (Fig. 9). However, biomass and nitrite + nitrate increased at this site after 1989, in spite of an increase in discharge (Table 2), which presumably increased scouring.

The species composition of the macrophyte community was not routinely recorded throughout the entire study. However, periodic observations indicated that *P. vaginatus* remained dominant after 1983 at sites 1–8, and either *P. vaginatus* or *P. pectinatus* was dominant at sites 9–12, as in 1981 and 1982 (Charlton et al. 1986) before enhanced nutrient removal was installed. *Zannichellia palustris* and

Fig. 8. Cell counts for periphyton at five sites on the Bow River, 1980, 1981, and 1994: Bowness (1) (different sampling location at Bowness in 1994 than in 1980 and 1981), Stier's Ranch (2), Carseland (3), Bow City (4), and Ronalane (5).

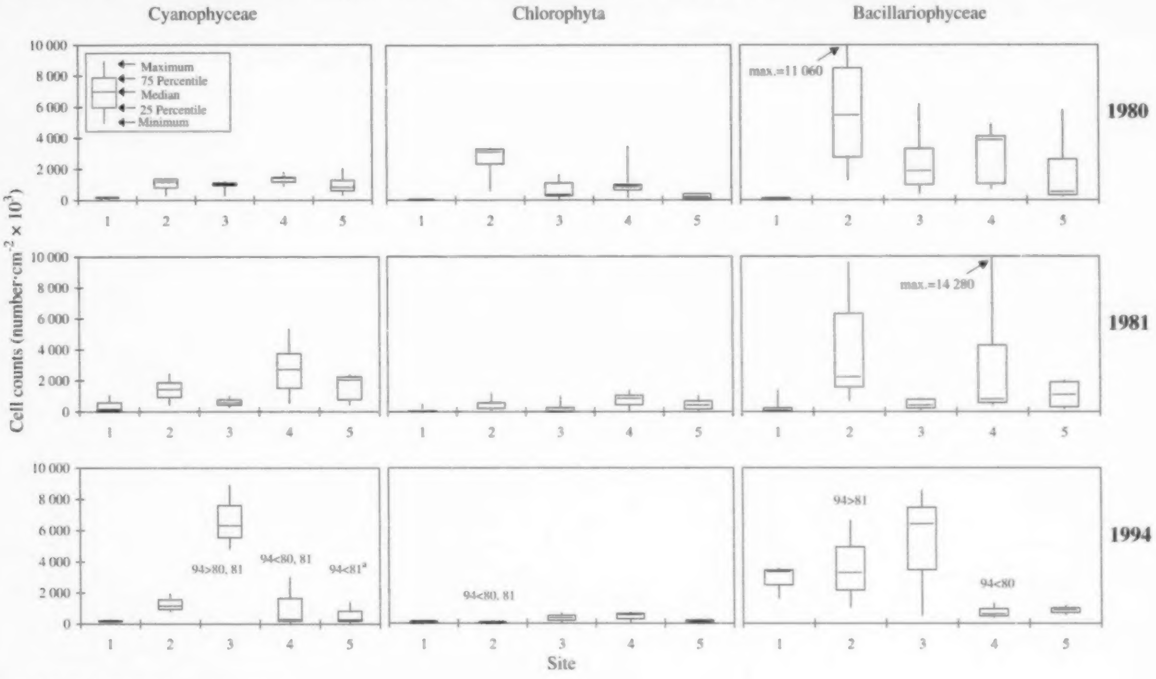

[a]Statistically significant differences between samples

Table 4. Correlation between aquatic plant biomass and physical and chemical variables in the Bow River.

	Spearman rank correlation (rho)[a,b] between plant biomass and other variables[c]							
Variable	Season discharge	Turbidity	Water temperature	TP	TDP	TN	Ammonia	Nitrite + nitrate
Maximum periphytic Chl *a*	–0.009	**–0.337**	–0.112	**0.414**	**0.636**	**0.717**	**0.544**	**0.662**
Fall macrophyte biomass	**–0.577**	0.046	**0.195**	**0.398**	**0.294**	**0.393**	**0.174**	**0.251**

[a]Bold values are statistically significant ($P < 0.10$, two-tailed test).

[b]Partial Spearman rank correlation used to eliminate spurious correlation where the tested variable, biomass, and a third variable were all significantly correlated.

[c]May–October medians.

Potamogeton crispus also occurred infrequently in sheltered areas.

Correlation and predictive equations for biomass

Maximum periphytic Chl *a* was strongly correlated with total nitrogen (TN), TDP, and nitrite + nitrate and correlated to a lesser extent with ammonia and TP (Table 4) but was not significantly correlated with temperature or discharge ($P > 0.699$) evaluated using three different methods ($\rho \le -0.044$). There was a negative correlation between periphytic Chl *a* and turbidity.

The following multiple regression equation indicates that median TDP ($P = 0.001$) with nitrite + nitrate ($P < 0.001$) explained 55% of the variability in maximum periphytic Chl *a*: maximum periphytic Chl *a* ((mg·m^{-2})$^{0.25}$) = 4.590 + 1.397 nitrite + nitrate (mg·L^{-1}) + 0.274 TDP (ln mg·L^{-1}); $r^2 = 0.55$, $n = 90$. Independent variables in the periphyton and macrophyte equations have been arranged in declining order of statistical significance, as indicated by t values. Other independent variables were not statistically significant.

To solve the multiple regression equation for TDP at nuisance periphytic biomass, [nitrite + nitrate] was first set at 0.211 mg·L^{-1}. This was the [nitrite + nitrate] at a maximum periphytic Chl *a* of 150 mg·m^{-2}, as predicted by a regression equation (maximum periphytic Chl *a* ((mg·m^{-2})$^{0.25}$) = 2.979 + 2.600 nitrite + nitrate – 0.6199 nitrite + nitrate^2 (mg·L^{-1}); $r^2 = 0.56$, $n = 90$). Similarly, [TDP] of 4.8 μg·L^{-1} was used to solve the multiple regression equation for nitrite + nitrate (where maximum periphytic Chl *a* ((mg·m^{-2})$^{0.25}$) = 5.389 + 0.1084TDP – 0.0459TDP^2 (ln mg·L^{-1}); $r^2 = 0.45$, $n = 90$). The multiple regression equation was then used to predict that nuisance levels of maximum periphytic Chl *a* will occur at a median [TDP] of 6.4 μg·L^{-1} (CI: 1.9–7.6 μg·L^{-1}) and a median [nitrite + nitrate] of 0.267 mg·L^{-1} (CI: 0.090–

Fig. 9. Macrophyte biomass in the Bow River, 1981–1996: (*a*) right bank and (*b*) left bank, both facing downstream. *Significant declining trend; NS, not significant; fac, flow-adjusted concentration; black bars indicate zero values.

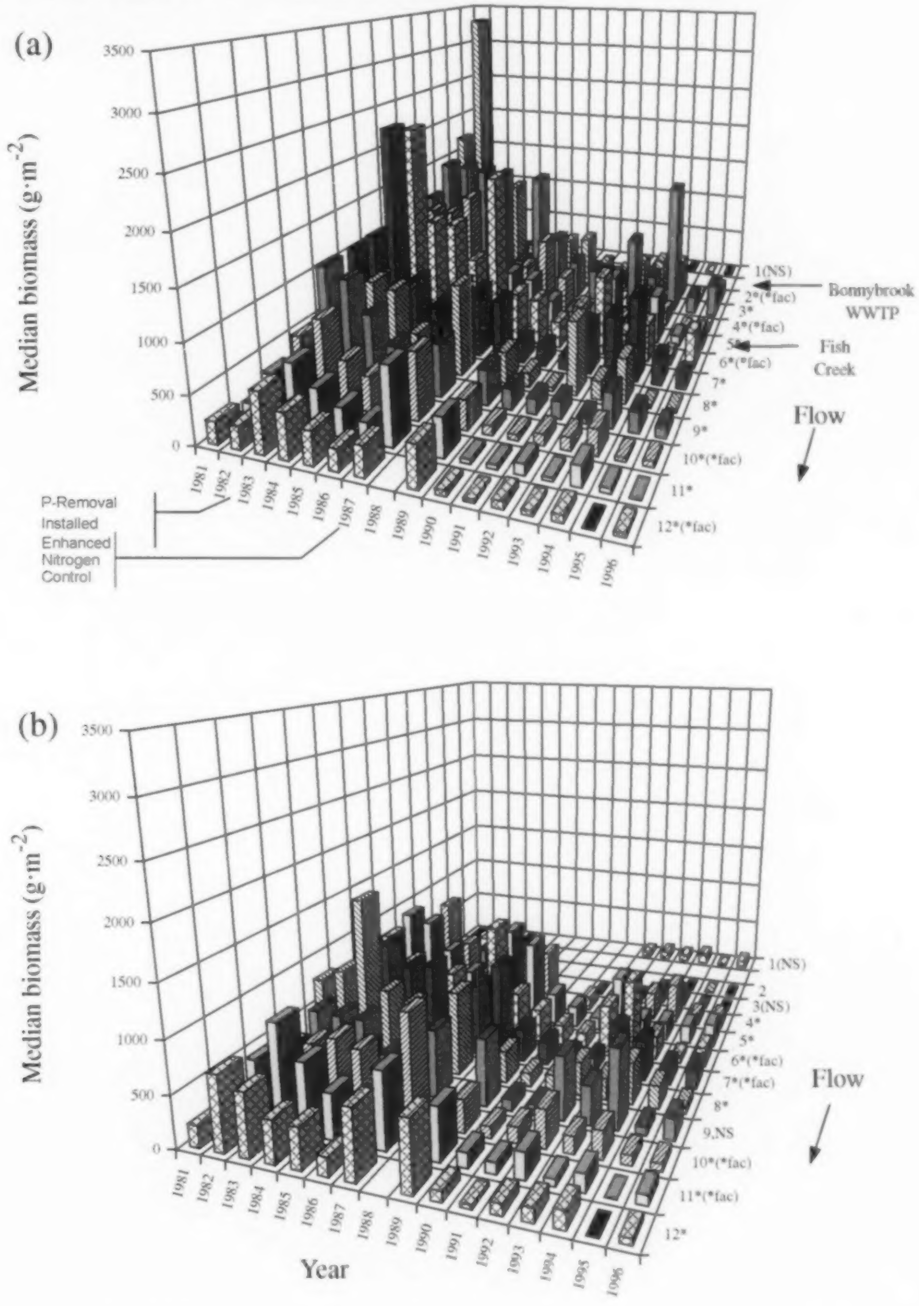

0.302 mg·L^{-1}). This median [TDP] is equivalent to a median [TP] of 18 μg·L^{-1} (where TDP (ln mg·L^{-1}) = –0.3268 + 1.169TP (ln mg·L^{-1}); $r^2 = 0.86$, $n = 90$).

With any discharge correlation eliminated, macrophyte biomass was most strongly correlated with TP and TN but was also significantly correlated with TDP, nitrite + nitrate, ammonia, and water temperature (Table 4). Macrophyte biomass was negatively correlated with discharge.

The following equation indicates that discharge ($P < 0.001$), nitrite + nitrate ($P < 0.001$), TDP ($P < 0.001$), and water temperature ($P = 0.031$) explained 57% of the variability in macrophyte biomass: macrophyte biomass (ln + 1 g·m^{-2}) =

44.596 – 1.909 discharge (ln m^3) + 0.754 nitrite + nitrate (ln $mg \cdot L^{-1}$) + 0.622 TDP (ln $mg \cdot L^{-1}$) + 1.722 temperature (ln °C); $r^2 = 0.57$, $n = 294$.

Discussion

Periphyton

After 1983, the lower Bow River was phosphorus limited and the biomass of periphyton (mainly diatoms) decreased where [TDP] declined below 10 $\mu g \cdot L^{-1}$. Although there have been various enrichment studies in stream channels and in situ, declining periphytic biomass has not been previously reported following controls on phosphorus discharge to a river. The regression equation developed for the Bow River predicted that nuisance levels of maximum periphytic Chl *a* of 150 $mg \cdot m^{-2}$ will occur at the relatively low median TDP of 6.4 $\mu g \cdot L^{-1}$ (1.9–7.6 $\mu g \cdot L^{-1}$). This TDP would be equivalent to about 18 $\mu g \cdot L^{-1}$ TP, well below the 30 $\mu g \cdot L^{-1}$ that Dodds et al. (1997) found would prevent the same maximum periphytic Chl *a*, based on an analysis of results from 200 different sites or rivers from North America, Europe, and New Zealand. However, Chételat et al. (1999) found that nutrient-enriched sites on 13 rivers in Ontario and Quebec had higher periphytic Chl *a* and were usually dominated by *Cladophora* at TP over about 20 $\mu g \cdot L^{-1}$.

Periphytic biomass in the Bow River decreased at TDP similar to levels that have limited growth in experimental stream systems. Bothwell (1989) found that there was a linear increase in the biomass of diatom mats where 1–30 µg soluble reactive phosphorus (SRP)·L^{-1} was added to water in stream channels containing 1.3–2.4 $\mu g \cdot L^{-1}$. Similarly, Horner et al. (1990) reported increased periphytic biomass accrual in laboratory streams containing ≤2 $\mu g \cdot L^{-1}$ to which an additional 15 µg SRP·L^{-1} was added and further increases due to improved nutrient uptake at higher water velocity up to 60 $cm \cdot s^{-1}$. Subsequent work with a calibrated model of channel periphyton accrual has shown that biomass declined only after SRP was reduced below 10 $\mu g \cdot L^{-1}$ (Walton et al. 1995).

Although SRP is widely used in eutrophication studies, TDP was measured in the current study because previous work in the Bow River (Cross et al. 1986) and elsewhere (Bradford and Peters 1987) determined that this was the best indicator of biologically available phosphorus, based on algal assays. In the Bow River, SRP was 0.65 of TDP in summer and 0.78 of annual average TDP (Cross et al. 1986).

During the same time period, there was no significant change in periphytic biomass at an upstream control site (Bowness) or at higher median [TDP] (10–33 $\mu g \cdot L^{-1}$) at Stier's Ranch, where no trend in TDP was detected after 1983. TDP at Stier's Ranch was probably still sufficient for a high rate of periphyton growth. Bothwell (1989) calculated that a maximum areal biomass occurred at an additional 28 µg SRP·L^{-1} (about 36 µg TDP·L^{-1} in the Bow River) and found that periphytic biomass was not phosphorus limited at higher [SRP] (>30–50 $\mu g \cdot L^{-1}$).

Although there was little change in TP loading from Calgary's municipal plants after 1983, a large decline in [TDP] in the lower Bow River occurred after 1989. The reasons that TDP declined in the lower Bow River after 1989 are not known. The Town of High River ceased discharge of wastewater to the Bow River basin in September 1989, but this source contributed only 2408 kg in 1990, or just 2.3% of the combined annual loading from Calgary WWTPs.

There was no evidence that variables other than phosphorus caused the observed decline in periphytic biomass. Wellnitz et al. (1996) reported that the addition of nitrate increased the biovolume of periphyton in Rocky Mountain streams, while the addition of phosphorus alone increased periphytic Chl *a*, ash-free dry mass, and cell density. In the Bow River, periphytic Chl *a* was positively correlated with ammonia and nitrite + nitrate. However, in spite of decreased nitrogen loading from Calgary, no monotonic trends in these forms of nitrogen were detected at two sites with declining periphytic biomass (Bow City and Ronalane). Absence of trends in these variables suggests that municipal loading of nitrogen had less impact at these sites, as nitrogen is lost along the river by denitrification and biological uptake upstream. Although reactive silica at Bow City and Ronalane often fell below levels that limit diatom abundance in lakes (0.5 $mg \cdot L^{-1}$; Wetzel 1983), no trends in silica were detected at these sites.

Similarly, none of the physical variables included in this analysis appeared to account for the decline in periphytic biomass. Although season discharge was significantly correlated with periphytic biomass at some sites (Carseland, Bow City, and Ronalane alone), this relationship was not statistically significant overall. Presumably, the characteristics of individual sites, such as slope, bed mobility, and algal species composition, influence the degree to which biomass is affected by discharge. Furthermore, although positive trends in discharge were detected at Bowness and Stier's Ranch, trends in periphytic biomass were not detected at these sites. Chételat et al. (1999) found no relationship between periphyton biomass and water velocity over the range 10–107 $cm \cdot s^{-1}$ in 13 Ontario and Quebec rivers.

Some authors have reported light limitation of periphytic biomass (Kjeldsen 1996) and community structure (Wellnitz et al. 1996) in streams, but Bothwell (1988) found that seasonal variation in solar insolation had no effect on growth rate at lower nutrient levels. Although solar insolation was not measured in the lower Bow River, there have been no changes in riparian vegetation or turbidity that could account for declining periphytic biomass.

There has been no evidence to date of decreased secondary production following the decline in macrophyte and periphytic biomass in the Bow River downstream from Calgary. No year-to-year trends were detected in the zoobenthic community in annual monitoring at Cochrane, Carseland, or Ronalane during 1983–1987 (Anderson 1991). Furthermore, the condition of trout (estimated weight of 500-mm trout) collected just downstream from Calgary during 1988–1992 did not decrease after enhanced nutrient removal was installed (Table D3).[1] Since no change in periphytic biomass has been detected immediately downstream from Calgary, changes in higher trophic levels would not be expected there. However, declining invertebrate and fish production may occur over time further downstream where periphytic biomass has declined.

Changes in sampling methods or frequency do not appear to account for declining trends in periphytic biomass or nutrients. Periphytic Chl *a* did not change significantly from

1983 to 1984, when the sampling method to remove periphyton from rocks was changed, and a single sampling method was used during 1984–1996 when declining trends were detected at sites along the lower Bow River. Furthermore, Charlton (1986) did not find any significant difference between the two sampling methods in periphytic Chl *a* collected from various habitats in the Muskeg River, except in very shallow areas (<15 cm depth). However, the change to a scraping method may have reduced the diversity of algal species sampled on rocks that were not smooth (Aloi 1990) compared with results before 1984. Trends in periphytic biomass and phosphorus were also present when only the May–October data were tested. Accordingly, the analysis was not affected by changes in the duration of sampling at some sites.

Macrophytes

Macrophyte biomass in the Bow River greatly declined over 14 years following the installation of enhanced nutrient removal at Calgary WWTPs, especially at sampling sites furthest downstream. The greatest decrease in macrophyte biomass occurred during 1990–1996 following decreases in nitrogen loading from wastewater and declining nitrogen (total ammonia $<0.2\ \mathrm{mg \cdot L^{-1}}$, nitrite + nitrate $<0.8\ \mathrm{mg \cdot L^{-1}}$) but stable TDP in river water at Stier's Ranch. These results and the regression analysis indicate that macrophyte growth was limited more by the availability of nitrogen than of phosphorus, but both nutrients influenced growth.

The regression analysis suggests that discharge had a stronger influence than nutrients on macrophyte biomass in the Bow River. Furthermore, discharge was high enough to initiate brief periods of bed movement and presumably scouring in the area of macrophyte growth during 3 years under enhanced nutrient removal (1983–1996). Chambers et al. (1991) found that macrophyte biomass at sites on the Bow River decreased with increasing current velocity within the weed bed over the range of 0.01 to 1 $\mathrm{m \cdot s^{-1}}$ and was rare at speeds over 1 $\mathrm{m \cdot s^{-1}}$. However, it would be difficult and impractical to manage macrophyte growth in the Bow River through manipulation of discharge without also controlling nutrient loading. Higher discharge could be used to scour macrophytes, but higher discharge could adversely affect other users of the Bow River. Furthermore, significant macrophyte growth occurred prior to the installation of nutrient removal during 1981 (range of macrophyte biomass: 31–1114 $\mathrm{g \cdot m^{-2}}$), when median river discharge was very high.

The reason that macrophyte biomass declined following a decrease in nitrogen loading cannot be determined from the available data, but depletion of nitrogen in river sediments could be an important factor. Aquatic macrophytes in lakes and rivers derive more of their phosphorus and nitrogen supply from sediments through their roots than from the water column (reviewed in Chambers et al. 1989), even in coarse river sediments. Chambers and Prepas (1994) found that nitrogen concentrations in porewater and sediments downstream from a WWTP discharge were greatest at sites with the highest open-water concentrations and highest macrophyte biomass. Since river water can strongly influence riverbed concentration, it is postulated that the nitrogen pool in the bed of the Bow River declined along with the concentration in river water. Rapid depletion of nitrogen in the bed of the Bow River may have caused nitrogen limitation in sediments.

Other studies have found that aquatic macrophytes are more apt to be limited by their supply of nitrogen rather than of phosphorus. Macrophyte growth in lakes was not stimulated by the addition of phosphorus in studies reviewed by Barko et al. (1991), but treatment with nitrogen enhanced the biomass of water hyacinth (*Eichhornia crassipes*) in a lake (Carignan et al. 1994). Feijoo et al. (1996) found a positive correlation between biomass of the submersed macrophyte *Egeria densa* and nitrogen in stream water and sediments. Barko et. al (1991) concluded that pools of exchangeable nitrogen in lake sediments are smaller, more rapidly depleted, and more likely to limit production of submersed macrophytes than pools of phosphorus. In contrast, Carr and Chambers (1998) found that the biomass of *P. pectinatus* in the South Saskatchewan River below Saskatoon was related to sediment phosphorus but not nitrogen concentration, and biomass in their artificial streams did not respond to additional nitrogen alone. The fine-textured sediments in their artificial streams (Carr and Chambers 1998) and the South Saskatchewan River may retain an adequate supply of nitrogen more readily than the rocky substrate typical in the Bow River, although in the same basin.

In addition to reduced municipal discharge, nitrogen loading to the Bow River was also reduced when two fertilizer plants ceased discharge in 1987 and 1990. These two plants contributed about 7128 kg unionized $\mathrm{ammonia \cdot annum^{-1}}$ and 13 976 kg $\mathrm{nitrate \cdot annum^{-1}}$ in 1988–1989 (Nahulak and Kabat 1990). However, these industrial loads were only 0.7 and 0.8%, respectively, of the annual municipal loading from Calgary.

Few other studies have monitored the response of aquatic macrophytes to a reduction in nutrient loading from municipal wastewater. Terrell and Canfield (1996) found that large reductions in nitrogen and phosphorus loading from municipal wastewater did not control filamentous algae or submersed vegetation in a cove of the productive Crystal River in Florida, and further nutrient control was not recommended. Chambers (1993) concluded that a decline in percent cover of pondweed (including *P. pectinatus* and *P. vaginatus*) in the South Saskatchewan River was primarily a result of high flow rather than the installation of enhanced phosphorus removal at the WWTP at Saskatoon. In contrast, declining trends in macrophyte biomass in the Bow River were still significant at nearly half of the sites after data were adjusted to eliminate the influence of river discharge.

The biomass of aquatic macrophytes (including the species dominant in the Bow River) also declined in the Highwood River downstream from High River 1 year after the discharge of all treated wastewater ceased in 1989 (fig. 7.3-2 in Golder Associates 1995). Before 1989, dissolved oxygen levels declined to 3.6 $\mathrm{mg \cdot L^{-1}}$ (lower in the mixing zone) due to nocturnal respiration by aquatic macrophytes in this river, leading to fish kills. Since then, dissolved oxygen has been no lower than 6.3 $\mathrm{mg \cdot L^{-1}}$ in hourly monitoring throughout the summers of 1990–1997.

Studies elsewhere have found no evidence for nutrient limitation of macrophyte growth in running water. Kern-Hansen and Dawson (1981) reported no correlation between macrophyte biomass and either water or sediment nutrient concentration in 19 Danish streams. Canfield and Hoyer (1988) found that aquatic macrophytes in relatively productive streams in Florida were limited by shading rather than nutrient supply. Unlike most of these Florida streams, the channel of the Bow River at the macrophyte sampling sites is wide (59 m at Stier's Ranch), with little shading from riparian vegetation at most sites. Accordingly, shading by riparian vegetation is unlikely to have reduced macrophyte biomass at these sites. Furthermore, no trends in turbidity were detected during this study.

Management implications

The results of this study suggest that nuisance growth of aquatic plants caused by municipal loading can be managed through the control of nutrient discharge to some rivers. The response of specific aquatic plant communities to reduced nutrient loading will depend on the species composition of these communities, substrate characteristics, and whether nutrients in sediments and water still exceed levels required for optimal growth. In the Bow River, aquatic macrophyte biomass decreased following a reduction in nitrogen loading which resulted in river median total ammonia of 0.11–0.28 $mg \cdot L^{-1}$ and nitrite + nitrate of 0.47–0.81 $mg \cdot L^{-1}$. Periphytic biomass decreased in the Bow River where TDP in river water was reduced below 10 $\mu g \cdot L^{-1}$ but not at higher TDP (10–33 $\mu g \cdot L^{-1}$).

Acknowledgements

I thank all technical and professional staff of the Water Management Division, AENV, who assisted in the sampling of the Bow River during this program. Hal Hamilton and Shirley Charlton were responsible for the design and supervision of the sampling program before 1987. Bridgette Halbig and Doreen LeClair assisted in data compilation and report preparation. Monique Richard, Eugene Welch, Dave Trew, and Water Quality Section, AENV, staff provided valuable comments on the manuscript. Michelle Hiltz of the Alberta Research Council provided extensive advice on multiple regression analysis. Peter Ehlers of the Department of Mathematics and Statistics, University of Calgary, also provided advice on regression analysis and kindly did the calculations that allowed me to assign CIs to nutrient level predictions.

References

Alberta Environment. 1979. South Saskatchewan River basin eutrophication control study. Interim report. Water Quality Control Branch, Pollution Control Division. *Available from* Alberta Government Library, 6th Floor, 9920-108 Street, Edmonton, AB T5K 2M4, Canada.

Aloi, J.E. 1990. A critical review of recent freshwater periphyton field methods. Can. J. Fish. Aquat. Sci. **47**: 656–670.

Anderson, A.M. 1991. An overview of long-term zoobenthic monitoring in Alberta rivers (1983–1987). Environmental Quality Monitoring Branch, Environmental Assessment Division, Alberta Environment. *Available from* Alberta Environment Library, 6th Floor, 9920-108 Street, Edmonton, AB T5K 2M4, Canada.

Aroner, E.R. 1995. WQHYDRO. Version 2010. Water quality/hydrology/graphics/analysis system. P.O. Box 18149, Portland, Oreg.

Barko, J.W., Gunnison, D., and Carpenter, S.R. 1991. Sediment interactions with submersed macrophyte growth and community dynamics. Aquat. Bot. **41**: 41–65.

Bothwell, M.L. 1988. Growth rate responses of lotic periphytic diatoms to experimental phosphorus enrichment: the influence of temperature and light. Can. J. Fish. Aquat. Sci. **45**: 261–270.

Bothwell, M.L. 1989. Phosphorus-limited growth dynamics of lotic periphytic diatom communities: areal biomass and cellular growth rate responses. Can. J. Fish. Aquat. Sci. **46**: 1293–1301.

Bradford, M.E., and Peters, R.H. 1987. The relationship between chemically analyzed phosphorus fractions and bioavailable phosphorus. Limnol. Oceanogr. **32**: 1124–1137.

Canfield, D.E., Jr., and Hoyer, M.V. 1988. Influence of nutrient enrichment and light availability on the abundance of aquatic macrophytes in Florida streams. Can. J. Fish. Aquat. Sci. **45**: 1467–1472.

Carignan, R., Neiff, J.J., and Planas, D. 1994. Limitation of water hyacinth by nitrogen in subtropical lakes of the Parana floodplain (Argentina). Limnol. Oceanogr. **39**: 439–443.

Carr, G.M., and Chambers, P.A. 1998. Macrophyte growth and sediment phosphorus and nitrogen in a Canadian prairie river. Freshwater Biol. **39**: 525–536.

Chambers, P.A. 1993. Nutrient dynamics and aquatic plant growth: the case of the South Saskatchewan River. NHRI Contribution No. 93001. Environment Canada, Saskatoon, Sask.

Chambers, P.A., and Prepas, E.E. 1994. Nutrient dynamics in riverbeds: the impact of sewage effluent and aquatic macrophytes. Water Res. **28**: 453–464.

Chambers, P.A., Prepas, E.E., Bothwell, M.R., and Hamilton, H.R. 1989. Roots versus shoots in nutrient uptake by aquatic macrophytes in flowing waters. Can. J. Fish. Aquat. Sci. **46**: 433–439.

Chambers, P.A., Prepas, E.E., Hamilton, H.R., and Bothwell, M.L. 1991. Current velocity and its effect on aquatic macrophytes in flowing water. Ecol. Appl. **1**: 249–257.

Chambers, P.A., Allard, M., Walker, S.L., Marsalek, J., Lawrence, J., Servos, M., Busnarda, J., Munder, K.S., Adare, K., Jefferson, C., Kent, R.A., and Wong, M.P. 1997. Impacts of municipal wastewater effluents on Canadian waters: a review. Water Qual. Res. J. Can. **32**: 659–713.

Charlton, S.E.D. 1986. The ecology of five rivers. Ph.D. thesis, University of Alberta, Edmonton, Alta.

Charlton, S.E.D., Hamilton, H.R., and Cross, P.M. 1986. The limnological characteristics of the Bow, Oldman and South Saskatchewan rivers (1979–82). Part II. The primary producers. Pollution Control Division, Alberta Environment, Edmonton, Alta. *Available from* Alberta Government Library, 6th Floor, 9920-108 Street, Edmonton, AB T5K 2M4, Canada.

Chételat, J., Pick, F.R., Morin, A., and Hamilton, P.B. 1999. Periphyton biomass and community composition in rivers of different nutrient status. Can. J. Fish. Aquat. Sci. **56**: 560–569.

Cross, P.M., Hamilton, H.R., and Charlton, S.E.D. 1986. The limnological characteristics of the Bow, Oldman and South Saskatchewan rivers (1979–82). Part I. Nutrient and water chemistry. Pollution Control Division, Alberta Environment, Edmonton, Alta. *Available from* Alberta Government Library, 6th Floor, 9920-108 Street, Edmonton, AB T5K 2M4, Canada.

Dodds, W.K., Smith V.H., and Zander, B. 1997. Developing nutrient targets to control benthic chlorophyll levels in streams: a case study of the Clark Fork River. Water Res. **31**: 1738–1750.

Feijoo, C.S., Momo, F.R., Bonetto, C.A., and Tur, N.M. 1996. Factors influencing biomass and nutrient content of the submersed macrophyte *Egeria densa* Planch. in a pampasic stream. Hydrobiologia, **341**: 21.

Golder Associates. 1995. Proposed Little Bow Project/Highwood Diversion Plan Environmental Impact Assessment. Vol. 3. Environmental assessment. *Prepared for* Alberta Public Works, Supply and Services, Civil Projects Division, Edmonton, Alta.

Horner, R.R., Welch, E.B., Seeley, M.R., and Jacoby, J.M. 1990. Responses of periphyton to changes in current velocity, suspended sediment and phosphorus concentration. Freshwater Biol. **24**: 215–232.

Kellerhals, R., Neill, C.R., and Bray, D.I. 1972. Hydraulic and geomorphic characteristics of rivers in Alberta. Research Council of Alberta, River Engineering and Surface Hydrology Report 72.1. *Available from* Alberta Government Library, 6th Floor, 9920-108 Street, Edmonton, AB T5K 2M4, Canada.

Kern-Hansen, U., and Dawson, F.H. 1981. The standing crop of aquatic plants of lowland streams in Denmark and the inter-relationships of nutrients in plant, sediments and water. *In* Proceedings EWRS 5th Symposium on Aquatic Weeds, Amsterdam, Netherlands. pp. 143–150. (Cited in Chambers et al. 1989.)

Kjeldsen, K. 1996. Regulation of algal biomass in a small lowland stream: field experiments on the role of invertebrate grazing, phosphorus and irradiance. Freshwater Biol. **36**: 535–546.

Nahulak, W.M., and Kabat, Z.A. 1990. Industrial wastewater discharges to the Bow River. Water Quality Branch, Standards and Approvals Division, Alberta Environment, Edmonton, Alta. *Available from* Alberta Government Library, 6th Floor, 9920-108 Street, Edmonton, AB T5K 2M4, Canada.

Shields, A. 1936. Anwendung der Aehnlichkeitsmechanik und der Turbulenzforschung auf die Geschiebebewegung. Mitteilungen der Preussischen Versuchsanstalt für Wasserbau und Schiffbau, Heft **26**, Berlin.

Sosiak, A.J. 1990. An evaluation of nutrients and biological conditions in the Bow River, 1986 to 1988. Environmental Assessment Division, Alberta Environment, Calgary, Alta. *Available from* Alberta Government Library, 6th Floor, 9920-108 Street, Edmonton, AB T5K 2M4, Canada.

Terrell, J.B., and Canfield, D.E., Jr. 1996. Evaluation of the effects of nutrient removal and the "Storm of the Century" on submersed vegetation in Kings Bay – Crystal River, Florida. Lake Reservoir Manage. **12**: 394–403.

Walton, S.P., Welch, E.B., and Horner, R.R. 1995. Stream periphyton response to grazing and changes in phosphorus concentration. Hydrobiologia, **302**: 31–46.

Ward, R.C., Loftis, J.C., DeLong, H.P., and Bell, H.F. 1990. Ground water quality data analysis protocol. J. Water Pollut. Control Fed. **60**: 1938–1945.

Welch, E.B., Jacoby, J.M., Horner, R.R., and Seeley, M.R. 1988. Nuisance biomass levels of periphytic algae in streams. Hydrobiologia, **157**: 161–168.

Wellnitz, T.A., Rader, R.B., and Ward, J.V. 1996. Importance of light and nutrients in structuring an algal community in a Rocky Mountain stream. J. Freshwater Ecol. **11**: 399–412.

Wetzel, R.G. 1983. Limnology. 2nd ed. Saunders College Publishing, Philadelphia, Pa.

Hydrological and trophic characteristics of tuna habitat: consequences on tuna distribution and longline catchability

Arnaud Bertrand, Erwan Josse, Pascal Bach, Philippe Gros, and Laurent Dagorn

Abstract: We studied relationships between tropical tunas (albacore (*Thunnus alalunga*), bigeye (*Thunnus obesus*), and yellowfin (*Thunnus albacares*)) and their biotic and abiotic environments through simultaneous acoustic observations of tunas and their prey, experimental longline catch, and oceanographic data in French Polynesia. Vertical habitat limits were estimated based on temperature and dissolved oxygen at capture data. We then studied tuna–micronekton relationships to better understand how tuna occupy the pelagic space. At a regional scale, tunas were more abundant in areas rich in prey with favourable hydrological conditions. Inside such areas, at the scale of a longline set, however, the longline catches were maximal only when prey were not distributed in dense patches (except for yellowfin tuna). We interpreted this result by considering that areas with high prey abundance attract tunas, but at a small scale, if prey are patchy distributed, tunas are more inclined to feed on them rather than on longline baits. The effect of patches on yellowfin tuna catch per unit effort (CPUE) does not appear likely because this species also feeds on the mixed layer, where patch density was very low. Not only hydrological characteristics, but also prey density and prey patch characteristics, should be taken into account for interpreting longline CPUE data.

Résumé : Nous étudions les relations liant les thons tropicaux (germon (*Thunnus alalunga*), thon obèse (*Thunnus obesus*), et thon à nageoires jaunes (*Thunnus albacares*)) à leurs environnements biotique et abiotique. Pour ce faire, nous avons réalisé simultanément, en Polynésie Française, des observations acoustiques des thons et de leurs proies, des pêches à l'aide d'une palangre instrumentée et des mesures hydrologiques. Des limites d'habitat vertical des thons calculées sur la base de données de température et d'oxygène dissous sont proposées. Nous étudions ensuite les relations thons–micronecton afin de mieux comprendre la stratégie d'occupation de l'espace des thons. A une échelle régionale, les thons sont plus abondants dans des zones riches en proies avec des conditions hydrologiques favorables. Cependant, à l'intérieur de telles zones, les captures sont maximales lorsque les proies ne sont pas distribuées sous forme de patchs (sauf pour le thon à nageoires jaunes). Nous interprétons ces résultats en considérant que les zones de fortes abondances en proies attirent les thons mais, qu'à une échelle fine, si les proies sont distribuées sous la forme de patchs denses, les thons s'en nourrissent préférentiellement, au détriment des appâts de la palangre. Ces patchs ne semblent pas influencer les prises par unité d'effort (PUE) des thons à nageoires jaunes, probablement parce que cette espèce se nourrit également dans la couche homogène où la densité en patchs est très faible. Les caractéristiques hydrologiques, mais également la densité en proies et leur type de distribution, devraient donc être pris en compte pour l'interprétation des données de PUE.

Introduction

The influence of oceanographic features (mainly temperature and oxygen) on tuna distribution has been the focus of several reviews (e.g., Sharp 1978; Sund et al. 1981; Brill 1994). The distribution of tunas has also been linked to forage availability (Sund et al. 1981). These results are not surprising considering the elevated metabolic rates of tropical tunas (Olson and Boggs 1986). Studying the relations binding tunas to their biotic and abiotic environments is difficult, as it is necessary to simultaneously observe tunas, their prey, and the physicochemical conditions. This is especially true when using fishing data, because observations are biased by accessibility and catchability. Longline catch per unit of effort (CPUE) values are not necessarily good indices of tuna distribution or abundance. Hook depths must coincide with the vertical distribution of tunas, which is not always the case (Hanamoto 1987; Boggs 1992; Hampton et al. 1998). Similarly, micronekton (i.e., tuna prey) observations or biomass estimations are known to be biased when using pelagic

Received 27 March 2001. Accepted 31 March 2002. Published on the NRC Research Press Web site at http://cjfas.nrc.ca on 18 July 2002.
J16286

A. Bertrand[1] **and P. Bach.** Institut de recherche pour le développement (IRD), rue jean Monnet, BP 171, 34207 Sète CEDEX, France.
E. Josse. IRD, BP 70, 29280 Plouzané, France.
P. Gros. Institut français de recherche pour l'exploitation de la mer (IFREMER), BP 21105, F 44311 Nantes CEDEX 03, France.
L. Dagorn. IRD, c/o Hawaii Institute of Marine Biology, P.O. Box 1346, Coconut Island, Kaneohe, Hawaii 96744, U.S.A.

[1] Corresponding author (e-mail: Arnaud.Bertrand@ird.fr).

DOI: 10.1139/F02-073

Fig. 1. Position of longline and hydrological stations (crosses), zones defined from habitat characterization of hydrologic features (horizontal lines), and micronekton distribution (shaded areas) (from Bertrand et al. 1999*b*, 2000). Mean temperature (*T*, bold line) and dissolved oxygen (thin line) profiles calculated by 10 m strata are plotted for each zone hydrological zone.

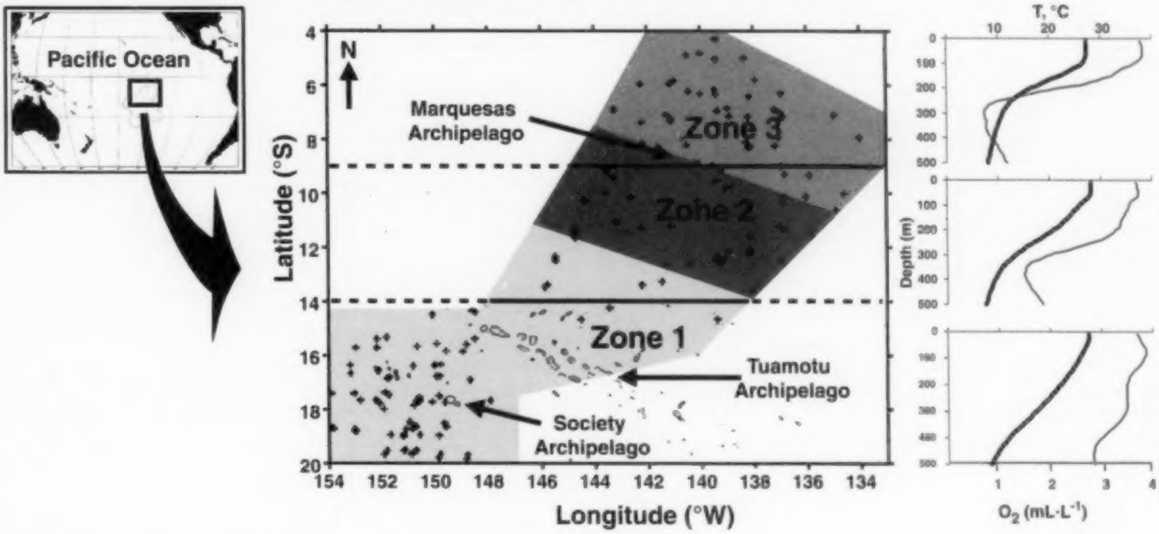

trawls (Power 1996). However, recent developments in acoustic survey technologies have made it possible to simultaneously observe both tunas (Bertrand et al. 1999*a*; Bertrand and Josse 2000; Josse and Bertrand 2000) and their prey (Marchal and Lebourges 1996; Bertrand et al. 1999*b*), independent of any fishing activity.

Describing a biological system requires an appropriate choice of scales of observation. This choice is difficult because the populations and the ecosystems cannot be described by a single scale (Levin 1992). We chose to describe the pelagic habitat at two scales: (*i*) a regional scale, i.e., the northern part of the French Polynesian Exclusive Economic Zone (EEZ); and (*ii*) a finer (local) scale, i.e., the scale of a longline set. The regional scale allowed the description of the broad outlines of the biotic and abiotic conditions as well as the general relationships between members of the pelagic ecosystem. This was necessary before investigating smaller-scale relationships, in particular, fishing gear – predator – prey interactions.

Using simultaneous acoustic data (on both tunas and their prey), experimental longline data, and hydrological data collected during the ECOTAP Program (a joint scientific project between IRD (Institut de recherche pour le développement), IFREMER (Institut français de recherche pour l'exploitation de la mer), and SRM (Service des ressources marines) to study the distribution and behaviour of subsurface tunas in French Polynesia), we developed a schematic model of the relationships between adult tropical tunas, i.e., albacore tuna (*Thunnus alalunga*), bigeye tuna (*Thunnus obesus*), yellowfin tuna (*Thunnus albacares*), and their environment at regional and local scales. First, we defined a volume of suitable habitat for tunas based on temperature and dissolved oxygen (DO) conditions. We combined these results with acoustic prey observations to interpret the vertical and horizontal distributions of tunas observed from acoustics and longline experiments. At a finer scale (the scale of a longline set), the fishing-independent observations of tunas from acoustics allowed us to determine which environmental factors most influenced longline catchability. We specifically attempted to determine if the abundance and spatial distribution of prey modified the attraction of tunas to baited longline hooks.

Material and methods

The data were collected on board the IRD R/V *Alis* (28 m long) during experiments carried out in the French Polynesia exclusive economic zone (EEZ), between 4°S and 20°S latitude and between 134°W and 154°W longitude in the vicinity of the Society, Tuamotu, and Marquesas Archipelagos, from July 1995 to August 1997 (Fig. 1).

Instrumented longline fishing experiments

Because of the expanse of the study area and logistic constraints, fishing sets were distributed continuously along a transect in such a way that the largest possible ocean surface could be sampled. A total of 80 000 hooks were deployed during 163 fishing operations (Fig. 1). The longline was instrumented with hook timers and time–depth recorders (Boggs 1992) to estimate both time and depth of capture using a model developed by Bach et al. (1996). The gear was generally set early in the morning (between 04:00 and 07:00) and retrieved in the afternoon (between 13:00 and 15:00). Typically, longlines were used to fish down to a depth of 500 m, except in the Marquesas where the presence of deoxygenated waters justified a reduction in the maximum fishing depth.

Acoustic data measurements

Acoustic data were collected from diurnal rectangular surveys above the longline or from rectangular or straight surveys at night between each fishing operation. These data were collected with a Simrad EK500 (version 4.01; Kongsberg Simrad AS, Kongsberg, Norway) echosounder connected to a 38 kHz, split-beam, hull-mounted Simrad ES38B transducer (beam angle 6.9° at –3 dB), with a 1-ms pulse duration. The water column was sampled to a depth of 500 m. Acoustic and navigation data were stored on a PC using Simrad Subsea EP500 software. The on-axis and off-axis calibration was performed using a 60 mm copper sphere and a standard procedure (Foote et al. 1987). Acoustic measurements were recorded so as to observe both tunas by echo-counting and their prey by echo-integration.

Individual target echoes were selected using the trace-tracking procedure of the EP500. The criteria used to select individual tuna targets were described by Bertrand and Josse (2000). Direct in situ species recognition was not possible. A –70 dB threshold was applied on integration data. All prey echo types were coded as described by Bertrand et al. (1999*b*), who showed that the acoustic back-scattered energy by the surface unit (s_a) can be considered representative of micronektonic fish and squid biomass. For some analyses, the s_a was classified into three categories: low, medium, high.

Hydrological measurements

Physicochemical measurements were carried out near the experimental longline. Temperature, salinity, and DO profiles were determined using a Seacat SBE 19 (Seabird Electronics, Inc., Bellevue, Wash.) from the surface to a depth of 600 m.

Large-scale characterization of the pelagic habitat

Using multivariate analysis, Bertrand et al. (1999*b*, 2000) have defined two typologies of the study area based on hydrological and micronekton characteristics according to acoustic and pelagic trawl data. Based on hydrologic features, we divided the northern part of the Polynesian EEZ into three zones (Fig. 1). The first one (zone H1), located south of 14°S, was characterized by a mixed layer of about 50 m, with temperature slowly decreasing from this layer down to 500 m. The DO concentration was high throughout the vertical section. The second zone (zone H2), between 9°S and 14°S, presented a 60-m mixed layer, below which a weak thermocline was present between 170 m and 320 m and a weak oxycline (3.3 mL·L^{-1} to 1.5 mL·L^{-1}) between 200 m and 350 m. The third zone (zone H3), north of 9°S, presented a strong thermocline and oxycline between 100 m and 250 m with an average, minimum DO concentration of 0.8 mL·L^{-1} (values lower than 0.1 mL·L^{-1} were sometimes observed).

In French Polynesia, the micronekton is mainly composed of a vertically migrating multispecies community dominated in weight by lanternfishes (myctophids). The mesopelagic fishes are distributed either in scattering layers with other prey species or in dense, quasimonospecific patches (Bertrand 1999). We described this prey community according to their overall biomass and the number of dense patches. The characterization of the micronekton distribution allowed us to divide the study area into three zones quite similar to the hydrologic ones (Fig. 1). The first micronekton zone (zone M1), located south of 13°S, was characterized by a very low overall biomass and a small number of micronekton patches. The second zone (zone M2), located mainly between 8°S and 13°S, corresponded to a weak convergence. This zone presented the highest overall biomass and numbers of micronekton patches. In the third zone (zone M3), located north of the Marquesas Archipelago, the micronekton biomass was moderate in comparison to the whole study area, while micronekton patches were not numerous. It must be noted that when the type of zone, i.e., micronektonic or hydrologic, is not indicated in the text, the results are valid for both types.

Table 1. Average weight of tuna caught by experimental longline and temperature and dissolved oxygen concentrations below which less than 2.5% of the fish were caught.

Species	Average weight (kg)	*T*, °C	O_2, mL·L^{-1}
Bigeye	31.4 (SD = 14.8)	8 (*n* = 271)	0.6 (*n* = 251)
Albacore	20.7 (SD = 3.2)	10 (*n* = 511)	1.5 (*n* = 475)
Yellowfin	29.1 (SD = 12.5)	10.5 (*n* = 191)	1.0 (*n* = 174)

Note: SD, standard deviation; *n*, sample size.

Definition of an index for the "habitat volume"

Bertrand et al. (2000) defined a volume of tuna habitat based on temperature and dissolved oxygen, which are the main hydrologic parameters used by previous workers to describe the distribution of tunas (Hanamoto 1987; Cayré and Marsac 1993; Brill 1994). For each parameter and each species, we measured a threshold value below which less than 2.5% of experimental longline catches were made (Table 1). For each observation site and each species, we then defined a habitat depth matching the shallowest depth associated with the temperature or the DO thresholds (Fig. 2). For statistical purposes, we classified into four categories the vertical habitat range of the three tuna species individually and pooled. In this last case, the calculation of the range of habitat takes account of the species proportion as determined by catches.

Environmental correlates with tuna distribution

We used four methods to identify the environmental factors (a selection is presented in Table 2) that are correlated with variations in tuna CPUEs and (or) of the acoustic tunas densities.

Correlation analyses

Correlation analyses using the "Desco" procedure of the SPAD 3.5 software (CISIA-CERESTA, Montreuil CEDEX, France) were used to analyze the global linear effect linking tuna abundance and distribution to the environmental factors. This procedure allows the characterization of continuous variables by other continuous variables using correlation, by the category of the nominal variables using mean comparisons, and by nominal variables using the Fisher statistics.

General linear models

General linear models (GLM) (SAS Institute Inc., Cary, N.C.) were used to estimate CPUEs and tuna acoustic densities from environmental parameters. Deviates were assumed normal.

Fig. 2. Latitudinal display of the theoretical habitat limits for bigeye (*Thunnus obesus*, BET), albacore (*Thunnus alalunga*, ALB), and yellowfin (*Thunnus albacores*, YFT) tuna. The limits of the three hydrological zones are indicated, and the mean depth of catches (with standard error) are also plotted species by species for each zone (except for albacore in zone 3 as only 5 fish were caught).

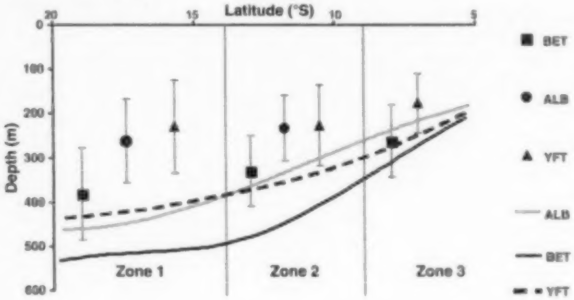

Table 2. Descriptors of the environment used in the analyses.

Variable code	Description	Type
Lat.	Latitude	C
Zone M	Belonging to one of the three micronektonic zones	N
Zone H	Belonging to one of the three hydrological zones	N
SAT	Presence–absence of micronekton patches	N
RALB, RBET, RYFT, RTUNA	Category of hydrological habitat range for the three tuna species individually and pooled	N
$s_a$log	log(s_a+1) total diurnal	C
s_aNlog	log(s_a+1) total nocturnal	C
s_a	Category of s_a diurnal	N
s_aN	Category of s_a nocturnal	N

Note: N, categorical variable; C, continuous variable; s_a, acoustic backscattering energy by surface unit; RALB, range of albacore vertical habitat; RBET, range of bigeye vertical habitat; RYFT, range of yellowfin vertical habitat; RTUNA, range of pooled tunas vertical habitat.

Robust regressions

Descriptors retained by GLM were independently studied to better understand the highlighted relations, mainly in each micronektonic zone. For that purpose, we used the least trimmed squares (LTS) regression (S-PLUS 4.5 Software, MathSoft Inc., Cambridge, Mass.) to minimize the effect of outlying points, which are almost always present in data resulting from in situ observations. Bias corrected confidence intervals (BC_α, Efron 1987) were calculated on regression parameters by bootstrapping with 1000 replications. In some cases, a robust regression was not a relevant tool because of the strong proportion of zeros in the data. The model could thus only capture the alignment of these values on the x axis. As the number of null values was independent of $\log(s_a + 1)$, they were withdrawn from analyses in these cases.

Influence of micronekton patches

Micronekton is distributed in scattering layers and dense patches. When large prey patches were observed during a survey, they contributed to the major part of the prey density, i.e., the prey density was correlated to the number and the size of prey patches. When only small patches were observed, prey density was not correlated to the number of prey patches. The structure of the prey environment, mainly the presence or absence of dense patches of myctophids, may influence the presence and (or) the catch of tunas. To clarify this point, we measured longline CPUEs and tuna acoustic densities for each of the three categories of micronekton abundance (low, medium, high) in presence and in absence of prey patches. We also calculated the corresponding standard deviations.

Results

Tuna distribution

The relationship between the zonal distribution of tuna CPUEs (all species pooled) and acoustic densities of tunas (Table 3) was linear ($R^2 = 0.996$, $p < 0.01$). This result suggests that our experimental longline tuna CPUEs can be considered as an index of relative abundance at a regional scale. Our experimental catches can be considered less biased than commercial ones because the whole range of tuna habitat was sampled as far as possible.

Tuna CPUEs were significantly higher in zone 2 than in the two other zones (Kruskal–Wallis test, $p < 0.01$), with about 2 tunas per 100 hooks. In zone 1, tuna abundance was intermediate compared to the whole study area, with 1.3 tuna per 100 hooks. Lastly, the lowest CPUEs were observed in zone 3, with 0.8 tuna per 100 hooks. The results are different if we consider CPUEs by species. Albacore tuna were caught with similar CPUEs in zones 1 and 2 and were almost absent in zone 3. Bigeye tuna CPUEs were significantly higher in zone 2 (Kruskal–Wallis test, $p < 0.01$) than in the other zones, which were not significantly different between each other (Kruskal–Wallis test, $p > 0.05$). Yellowfin tuna CPUEs were similar in zones 2 and 3 and very low in zone 1 (Table 3).

By weighting the CPUEs by the volume of corresponding potential habitat, we transform an index of abundance into an index of density (expressed in a number of fish per 100 hooks per 100 m of habitat) (Table 4). The distributions then appear different. These densities were proportionally lower in zone 1 for each of the three species. Bigeye tuna were captured with identical CPUEs per unit of volume in zones 2 and 3. Yellowfin tuna density was highest in zone 3, whereas albacore tuna presented the highest CPUEs with respect to the volume of habitat in zone 2.

Environmental correlates with tuna distribution

Correlation analyses

Results of the correlation analysis can be synthesized as follows. At a total study area scale, tuna CPUE were positively correlated with zone 2, where micronekton abundance was maximum. At a zone scale, tuna CPUEs (all species together and for each species) were positively correlated with the abundance of micronekton and the presence of patches in zone M1 and zone M3. In zone M2, where prey abundance was maximal, tuna acoustic densities and CPUEs were also

Table 3. Catch per unit effort (in number of fish per 100 hooks) of tuna caught using instrumented longlines related to the hydrologic zone (zone H, first number) and micronekton zone (zone M, second number) and of acoustic densities of tuna (number of fish per square kilometre) corresponding to the micronektonic zone.

Zone	Acoustic densities	All tunas	Albacore	Bigeye	Yellowfin
Total	1.33	1.40	0.73	0.39	0.28
Zone 1	1.33	1.25 / 1.38	0.90 / 1.00	0.26 / 0.30	0.09 / 0.09
Zone 2	1.87	2.05 / 1.94	1.05 / 0.88	0.60 / 0.58	0.40 / 0.48
Zone 3	0.69	0.84 / 0.84	0.02 / 0.03	0.36 / 0.38	0.45 / 0.43

Table 4. Density indices (catch per unit effort over the habitat range) of tuna caught by the instrumented longline (in number of fish per 100 hooks per 100 m depth) by hydrologic zone.

Zone	Bigeye	Albacore	Yellowfin
Zone H1	0.05 (503)	0.21 (428)	0.02 (413)
Zone H2	0.13 (451)	0.35 (301)	0.12 (332)
Zone H3	0.13 (263)	0.01 (223)	0.18 (251)

Note: Mean depth of habitat (m) in parentheses.

maximal. However, inside this zone, albacore and bigeye tuna CPUEs were negatively correlated with the micronekton abundance (negative correlations also between albacore tuna CPUEs and the presence of patches), whereas the correlation was positive for yellowfin tuna CPUEs.

GLM

Models were fitted to tuna acoustic densities and CPUEs for all tuna pooled and individually for yellowfin and albacore tunas (Table 5). No model could be fitted for bigeye tuna. In all cases, the best models were additive with interaction between the diurnal acoustic back-scattering energy (s_a) and either the micronektonic zone (zone M) or the range of the albacore vertical habitat (RALB). The categories of the albacore vertical habitat followed the latitudinal evolution of the habitat volume: RALB1 (0–290 m), located north of 9°S; RALB2 (0–340 m), located between 9°S and 12°30′S; RALB3 (0–410 m), located between 12°30′S and 15°30′S; and RALB4 (>410 m), located south of 15°30′S.

The fitting of the analysis of variance model led to estimates of tuna acoustic densities or the tuna CPUEs (Y):

$$E(Y_{i,j,k}) = \mu_{i,j} = \mu + \alpha_{i,j},$$

where i is the micronektonic zone or the class of habitat range; j is the acoustic back-scattering energy (s_a); and k is the number of observations corresponding of the (i, j) combination. The term μ is the general mean of the population, and α is the interaction term. We used least-square mean fitting to estimate the CPUEs or the tuna acoustic density for each class of variable (Fig. 3).

Results can be synthesized as follows. In zones M1 and M2, observed tuna acoustic densities appeared maximal when the micronekton abundance was medium. The whole tuna CPUEs decreased as micronekton biomass increased in zone M2 and less markedly in zone M1. These results were driven by the albacore data, the most commonly caught species in these zones. Conversely, the CPUE of all tunas increased with the micronekton biomass in zone M3, where yellowfin tuna represent 50% of catches. These results highlight both zone and species effects.

Table 5. Goodness-of-fit parameters of the analysis of variance model fitted for tuna catch per unit effort (CPUE) and tuna acoustic density.

CPUE or tuna density	Tested effect	df	R^2	P level
Tuna acoustic density (n = 93)	Zone M·s_a	8	0.20	*
All tuna (n = 121)	Zone M·s_a	8	0.18	**
Albacore (n = 125)	RALB·s_a	10	0.44	**
Yellowfin (n = 125)	Zone M·s_a	8	0.24	**

Note: s_a, acoustic back-scattering energy; zone M, micronektonic zone; RALB, range of albacore's vertical habitat; n, total number of observations; df, degrees of freedom; *, $P < 0.05$; **, $P < 0.01$.

Robust regressions

The results of the variance analysis show that the best models are additive models with interaction between acoustic back-scattering energy (s_a) and the micronektonic zone for bigeye and yellowfin tunas or the range of habitat for albacore tuna. Robust regressions were computed between the tuna acoustic densities or the CPUEs and the micronekton abundance (s_a). These regressions were adjusted by zone and for the whole study area when species were considered separately. The observation of the CPUEs or scatterplots of acoustic density of tunas according to the s_a and the first attempts at adjustment showed that the relationship between the two types of data was not linear; a logarithmic curve better fit the data. A logarithmic transformation of the explanatory variable ($\log(x + 1)$) was thus made to approach a linear relation.

The results of the robust regressions did not highlight relations between the tuna acoustic densities and the diurnal micronekton abundance (s_a) (Table 6). The expectancy of the tuna acoustic density at a given site was the arithmetic mean of abundance in the zone, with no effect of the s_a. In zone M3, the robust regression was not fully relevant because of the strong proportion of null values. The CPUEs of all tunas were negatively correlated with the diurnal micronekton abundance in zones M1 and M2. This result is doubtful in zone M1, as each species considered individually did not show such correlation (Table 6). Total albacore tuna CPUEs were negatively correlated with the micronekton abundance. This trend was significant for habitat range 2 (zone 2) and not significant for the range 3 (which presents few observations, zones 1–2) and was not observed for range 4 (zone 1).

Fig. 3. Catch per unit effort (CPUE, in number per 100 hooks) least-square mean evolution of tuna acoustic densities (*a*), all tunas (*b*), albacore (*Thunnus alalunga*, ALB) (*c*), and yellowfin tuna (*Thunnus albacores*, YFT) (*d*) (in number per km²) according to the categories of the acoustic back-scattering energy (s_a) by micronektonic zone (zone M1 (solid circles), zone M2 (solid squares), zone M3 (solid triangles)) or by hydrological habitat range for albacore (*c*): RALB1 (solid diamonds), RALB2 (solid circles), RALB3 (solid squares), RALB4 (solid triangles). The standard deviation is plotted for each value.

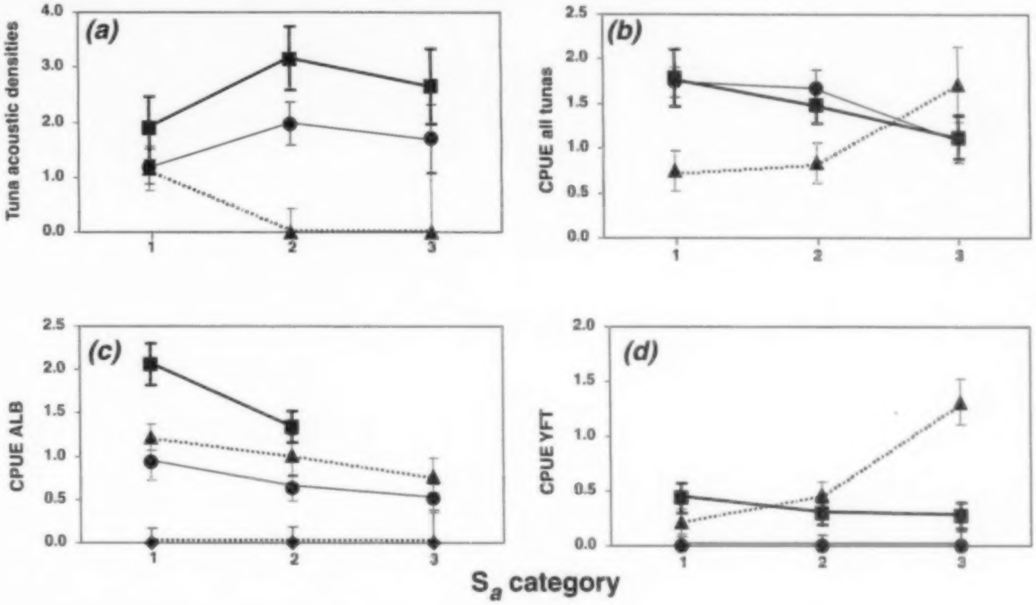

In the areas where albacore tuna were present, CPUEs and micronekton abundances were negatively correlated especially where micronekton was very abundant. The LTS regressions are of poor relevance with bigeye tuna CPUE data because of the numerous zero values. Nevertheless, in zone 2, the robust regression displayed a clear negative slope. Yellowfin tuna was the only species not presenting any negative correlation but a positive trend (but nonsignificant) in each case.

Influence of micronekton patches

Results (Table 7) show that the coefficients of variation of CPUEs between samplings are very high. This result is not surprising taking into account the low number of samples and the nature of the data (the catch of one tuna may notably change the results). Thus, these results are only additional information to reinforce the previous analyses.

In the absence of micronekton patches, for example, when prey were in scattering layers only, tuna acoustic densities were positively correlated with the density of micronekton; an opposite trend was observed mainly when prey were distributed in patches. However, this last trend was much less marked than the one observed for tuna CPUEs. In the absence of micronekton patches, CPUEs did not show any clear relationship with the overall micronekton density. It should nevertheless be noted that the highest tuna CPUEs were associated with high densities of micronekton distributed in scattering layers; the trend was opposite when micronekton was patchy in distribution. It is important to recall that during the day, if patches were present and of significant size, they contributed to the majority of the total micronekton density. So when patches were present, the value of s_a was correlated with the size and the number of patches. Very high tuna CPUEs were thus observed when micronekton was distributed in scattering layers, whereas the CPUEs were low in the presence of large dense patches. These results also applied at the species level to bigeye and albacore tunas, even if, in the absence of prey patches, the maximum CPUEs were not associated with the strongest

Table 6. Sign of the slope of the robust regression between the tuna acoustic densities and catch per unit effort (CPUE) according to the log($s_a$diurnal +1) for the whole study area and by micronektonic zone.

CPUE or tuna abundance	Total	Zone M1	Zone M2	Zone M3
Tuna acoustic density		0	0	0
All tuna		(–)	(–)	0
Bigeye	0	0	(–)	0
Yellowfin	0		0	0
CPUE	**Total**	**RALB2**	**RALB3**	**RALB4**
Albacore	(–)	(–)	0	0

Note: In the case of albacore, CPUEs are represented according to the range of albacore vertical habitat (RALB) categories 2, 3, and 4. 0, nonsignificant slope; (–), slope significantly negative. The shaded boxes are those for which the strong proportion of null values makes the robust regression less relevant.

Table 7. Tuna acoustic densities and catch per unit effort (CPUE) for all tunas and by species (ALB, albacore; BET, bigeye; YFT, yellowfin) according to the category of the diurnal s_a and of the presence or the absence of micronekton patches (SAT) (*n*, number of observations; cv, coefficient of variation, in %). The trend of the relation binding the tuna densities or CPUE with the diurnal s_a is also represented.

	SAT	s_a1	s_a2	s_a3	Trend
Tuna acoustic density	**Absent**	1.18 (n: 50, cv: 88)	1.38 (n: 37, cv: 128)	1.64 (n: 13, cv: 81)	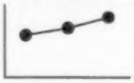
	Present	1.80 (n: 4, cv: 143)	1.46 (n: 15, cv: 77)	1.35 (n: 6, cv: 41)	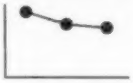
CPUE Tuna	**Absent**	1.64 (n: 51, cv: 84)	1.22 (n: 36, cv: 85)	2.05 (n: 13, cv: 83)	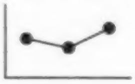
	Present	2.44 (n: 4, cv: 60)	1.59 (n: 15, cv: 39)	0.90 (n: 12, cv: 76)	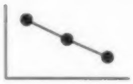
CPUE ALB	**Absent**	0.91 (n: 51, cv: 105)	0.56 (n: 36, cv: 124)	0.74 (n: 13, cv: 89)	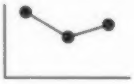
	Present	1.71 (n: 4, cv: 92)	0.83 (n: 15, cv: 75)	0.38 (n: 12, cv: 99)	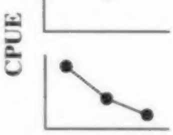
CPUE BET	**Absent**	0.52 (n: 51, cv: 139)	0.36 (n: 36, cv: 123)	0.33 (n: 13, cv: 85)	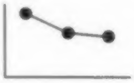
	Present	0.59 (n: 4, cv: 121)	0.50 (n: 15, cv: 100)	0.27 (n: 12, cv: 109)	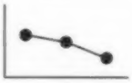
CPUE YFT	**Absent**	0.21 (n: 51, cv: 154)	0.31 (n: 36, cv: 183)	0.98 (n: 13, cv: 202)	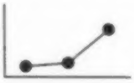
	Present	0.10 (n: 4, cv: 115)	0.25 (n: 15, cv: 98)	0.24 (n: 12, cv: 121)	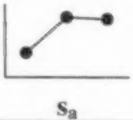

micronekton densities. Conversely, yellowfin tuna present a different pattern: CPUEs did not tend to decrease in the presence of micronekton patches.

Discussion

Habitat limits of tropical tunas

Longline catches rely on the behaviour of fishes to be attracted by the longline baits and might represent biased observations of the fishes' vertical distribution. Considering also that longline data represent fish depth at only one instant in time, they should be considered with caution but should not be rejected as they also provide large samples of indirect observations (indirect as the fish have to behave to be caught, then to be observed) that can provide reliable trends. Such a large database thus represents valuable information on tuna vertical distribution. We already know that bigeye tuna tracked with sonic transmitters in French Polynesia (Josse et al. 1998; Dagorn et al. 2000) moved in hydrological conditions consistent with the proposed level values, as shown by a comparative study (Bach et al. 2002). More direct observations of vertical movements through electronic tags should be developed, especially for yellowfin and albacore tunas.

By definition, the limit values calculated for temperature and DO are not lethal limits as some fish were caught beyond those levels. They also do not correspond to "comfort limits" sensu stricto. For instance, bigeye tuna are able to forage in very deep waters where they tolerate very low temperatures and sometimes low DO concentrations. Archival tagging shows that bigeye tuna can temporarily dive deeper than 1000 m at a temperature of 3°C (J. Hampton, Secretariat of the Pacific Community, BP D5, 98848 Nouméa CEDEX, Nouvelle Calédonie, personal communication). In such conditions, bigeye tuna need to make brief upward excursions (Holland et al. 1992; Dagorn et al. 2000) to increase muscle temperature (Holland et al. 1992). These deep waters might, therefore, not correspond to physiologically comfortable areas for bigeye tuna, but they occupy these waters for foraging activities. In fact, inside limits, tunas are likely to adopt depths where prey are present rather than depths of preferred temperature or DO. We consider that the vertical extent of tuna habitat is limited by the parameter that first goes over its threshold: temperature, DO, or prey biomass. Therefore, the threshold values proposed here can be considered as vertical habitat limits. These limits are in agreement with those proposed in the literature (Sharp 1978; Holland et al. 1990; Brill 1994) for bigeye and albacore tunas. However, our temperature-at-capture data for yellowfin tuna show contrasting results to those observed in previous studies. Several ultrasonic tagging experiments (Holland et al. 1990; Block et al. 1997; Brill et al. 1999) have shown that during the daytime, yellowfin tuna usually swim within or immediately below the mixed layer in warm water usually between 17.5°C and 26°C. In fact, yellowfin tuna have been observed diving into very cold waters beneath the thermocline (as cold as 7°C, Block et al. 1997), but those dives were not numerous and were usually very short in duration, and we do not know the reasons for those dives. In contrast, our data show that more than 80 individuals (45% of our database) were caught at temperatures below 17.5°C (with a minimum of 10°C), which is very cold for this species. More than the absolute water temperature, the temperature gradient (Cayré and Marsac 1993) is a key factor in determining the vertical swimming behaviour of this species. Comparing vertical movements of small yellowfin tuna tracked in the northern extreme of their range in the eastern Pacific (Block et al. 1997) and large individuals tracked near the Hawaiian islands, Brill et al. (1999) found similar time-at-temperature distributions for the two groups when temperature was expressed relative to the surface-layer temperatures, despite very different environments. All fish spent most of their time in water temperatures no lower than 8°C below the surface layer temperature. Surprisingly, in our study, 100 individuals (56% of our database) were caught at depths where the water temperature was more than 8°C below the mixed layer temperature (with a maximum of 18.6°C difference).

Our data lead to two possible interpretations that we express as questions. (*i*) Do deep longlines attract yellowfin tuna to deeper and colder waters, modifying their natural vertical distribution? Are yellowfin more inclined to bite longline hooks when making some rapid dives to depths with marginal temperature and DO levels than when swimming in more comfortable conditions? (*ii*) Do yellowfin tuna exhibit deeper and cooler vertical distributions in offshore areas of French Polynesia than those observed in other oceanic areas?

The first interpretation is not in accordance with previous comparisons between ultrasonic telemetry data and longline catch data. Ultrasonic telemetry and depth-of-capture data near the main Hawaiian Islands showed similar depth distributions for yellowfin tuna (Holland et al. 1990; Boggs 1992; Brill et al. 1999), while Bach et al. (2002) found similar results for bigeye tuna in French Polynesia. However, by setting the gear deeper than the assumed preferred depth stratum for yellowfin tuna, our longline experiments might have provided biased results of yellowfin tuna depth distribution as individuals might have been attracted by deep baits. The second interpretation might also be valid, as all the ultrasonic telemetry data on yellowfin tuna in tropical waters have been collected in coastal areas. Our knowledge of yellowfin tuna vertical dynamics might only correspond to an inshore behaviour, whereas yellowfin tuna in some offshore waters might exhibit a different vertical swimming behaviour notably because of different prey communities. For instance, it should be noted that in French Polynesia, yellowfin tuna feed on the mixed layer and on a deeper sound-scattering layer (SSL), as shown by stomach content analyses (Bertrand 1999), which also explains the high variance of our depth-of-capture data. Further ultrasonic telemetry experiments on yellowfin tuna in offshore areas are therefore clearly needed to clarify the moment-to-moment vertical movements that they use to exploit those two layers and, therefore, their depth and temperature distributions.

Tuna catches and environment

As stated above, vertical and horizontal limits of tuna habitat depend on the trophic and hydrologic conditions. In the study area, catches of albacore tuna were highest, followed by bigeye tuna. CPUEs and acoustic tuna densities were higher in zone 2 where the hydrologic conditions did not prevent the tunas (mainly albacore and bigeye tuna) from exploiting abundant deep prey. North of the Marquesas Islands, in zone 3, tuna abundance was lower. This may be a function of the very low occurrence of albacore tuna. Despite a rather low prey biomass, tuna abundance in zone 1 was fairly high compared with what would be expected based on analysis of commercial-catch data (Fonteneau 1997).

Albacore distribution

Catch rates of albacore tuna were very low in zone 3. Low albacore abundance close to the equator is typical, as those from the northern and southern hemispheres are assumed to come from two distinct populations with very limited exchanges (Sund et al. 1981; Kimura et al. 1997). It appears that the hydrological conditions (i.e., the vertical range of habitat) close to the equator prevent them from occupying such areas. The CPUEs were quite similar in zones 1 and 2, whereas the prey environments were different: zone 1 had a large vertical range of habitat with scattered prey, and in zone 2, the vertical range of habitat was lower but prey were much more abundant and distributed in dense patches. The dense patches in zone 2 are likely to concentrate albacore tuna.

Bigeye tuna

Bigeye tuna is the most tolerant species with respect to hydrological constraints. In zone 1, bigeye tuna were located in deep strata presumably to forage on SSL organisms (Dagorn et al. 2000). In zone 3, where the micronekton density was moderate, CPUEs were slightly higher than in zone 1. Perhaps this is because more hooks are concentrated in the waters occupied by this species in zone 3, whereas in zone 1, mainly the deep hooks caught this species. Bigeye tuna

CPUEs were significantly higher in zone 2 where the micronekton was abundant.

Commercial catch analyses (Fonteneau 1997) show very low bigeye tuna catch rates in zone 1, contrary to our experimental catches. As Hanamoto (1987) showed, commercial longline catches reflect the real distribution of tunas only in areas where fishing depth overlaps habitat depth. A biomass of bigeye tuna is located south of the classical fishing ground but is only accessible to longlines set deeper than the classic "deep" ones. It could correspond to a "cryptic" biomass as defined by Fonteneau et al. (1998).

In the same way, Fréon and Misund (1999) showed that bigeye tuna catches are high in areas where deep waters are deoxygenated, "as if this species was taking advantage of its physiological capabilities for limiting competition with other tuna species". Although this assumption is consistent, it is necessary to be careful when using solely commercial catches to describe tuna distribution. The presence of hypoxic deep waters can lead bigeye tuna to be shallower and more accessible to fishing gears (purse seine and longline) and increases the CPUE. In zone 3 where an oxycline (and a thermocline) is present, bigeye tuna are distributed in a depth stratum, which coincides with the depth of the "deep" commercial longlines (i.e., about 250 m). This may explain why most longliners catch bigeye tuna in this area. Conversely, where no oxygen gradients are present (in zone 1, for instance), during the day bigeye tuna are distributed deeper than the depth strata sampled by the "deep" commercial longlines. Strong DO gradients cause the apparent abundance of bigeye to appear higher than in areas with weak oxycline. Consequently, sampling the whole tuna habitat range allows better understanding of tuna spatial occupation and calls into question the role imputed to the oxygen gradients. Therefore, high bigeye tuna catches in areas where deep waters are deoxygenated are probably due more to an increase in bigeye accessibility to the fishing gear that to the total bigeye abundance.

Yellowfin tuna

Yellowfin tuna catches were deeper than expected, considering our knowledge of this species (see the previous section on habitat limits). Yellowfin tuna are less tolerant of low temperatures and low DO concentrations than bigeye tuna, which explains why catches of this species were shallower than those of bigeye tuna regardless of the zone. It also should be noted that the theoretical vertical range of yellowfin tuna habitat is greater than that for albacore in zones 2 and 3 because of a higher tolerance of this species for low DO concentrations. Yellowfin tuna CPUEs were always positively correlated to the micronekton abundance. Despite a lower prey abundance in zone 3 than in zone 2, CPUEs were similar in those two zones. The overall micronekton richness of zone 2 contributed to the increase in the presence of yellowfin tuna in the zone. The lower micronekton abundance found in zone 3 was compensated for by the fact that more prey were distributed toward the surface and thus were more accessible to yellowfin tuna.

Environment and tuna catchability

Tunas and micronekton abundances were maximal in zone 2. Inside this zone, however, albacore and bigeye tuna CPUEs were negatively correlated with prey abundance. Thus, relationships differ according to the scale of observations. This apparent contradiction results from the effect of catchability.

Catchability is a key parameter for abundance estimates. Until now, tuna catchability was principally studied in the horizontal plane and was related to abiotic parameters (Maury et al. 2001). Several studies (Hanamoto 1987; Brill 1994; Hampton et al. 1998) pointed out that bigeye tuna catchability increases with the use of deep longlines, as observed in our work. These studies related catchability to hydrological factors. Few investigators have studied the influence of both the range of habitat and prey availability. Podesta et al. (1993) indicated that swordfish (*Xiphias gladius*) catchability with a longline increases close to thermal fronts, but that CPUE variability cannot be interpreted and must be a function of unmeasured parameters. These authors considered the frontal zone to be areas where prey were abundant, but they did not consider the patchiness of the prey community. Prey distribution is likely to play an important role in the distribution of a fish, its feeding behaviour, and consequently, its catchability by a longline.

To analyze the factors influencing tuna catchability according to the species and the environmental conditions, we compared the influence of the environmental parameters on the tuna acoustic densities as well as on the longline catches. It should be noted that each method alone did not always give definitive results because of the low number of observations and the strong occurrence of null values. However, the results of the various methods were sufficiently similar to validate our conclusions.

Tuna acoustic densities

Acoustic surveys allowed us to observe the presence of tunas independently of catchability. Results did not show clear relationships between tuna acoustic densities and the micronekton abundance inside each zone. Bertrand and Josse (2000) assumed that tuna acoustic counting was negatively biased in the presence of micronekton patches. Such bias can partly explain our results, and we can therefore assume that the density of tunas was underestimated when dense prey patches were present. The lack of a trend could also be linked to the complex pattern of interactions between predators and prey. Predators tend to congregate where prey are abundant. On the other hand, mobile prey tend to avoid areas of high predator density, as stated by Rose and Leggett (1990). These authors showed that at large scales, predator and prey densities are positively correlated. As the scale decreases and approaches the aggregation scale, the strength of the correlation decreases and becomes nonsignificant. Finally, at scales smaller than this dimension, predator and prey densities are negatively correlated. Our results agree with this scheme, as we observed a positive correlation between prey and tuna abundances at the scale of the study area and no correlation at the scale of the acoustic survey. Swartzman et al. (1999) indicated that correlation between zooplanktivorous fishes and their prey was more linked to the patch density than to total prey biomass. They observed a spatial correlation even at a small scale. However, they noted that in the case of piscivorous fish, the proximity between predators and prey might be more difficult to demon-

Fig. 4. Schematic representation of the distribution and catchability of (*a*) albacore (*Thunnus alalunga*), (*b*) bigeye (*Thunnus obesus*), and (*c*) yellowfin tuna (*Thunnus albacares*) in French Polynesia.

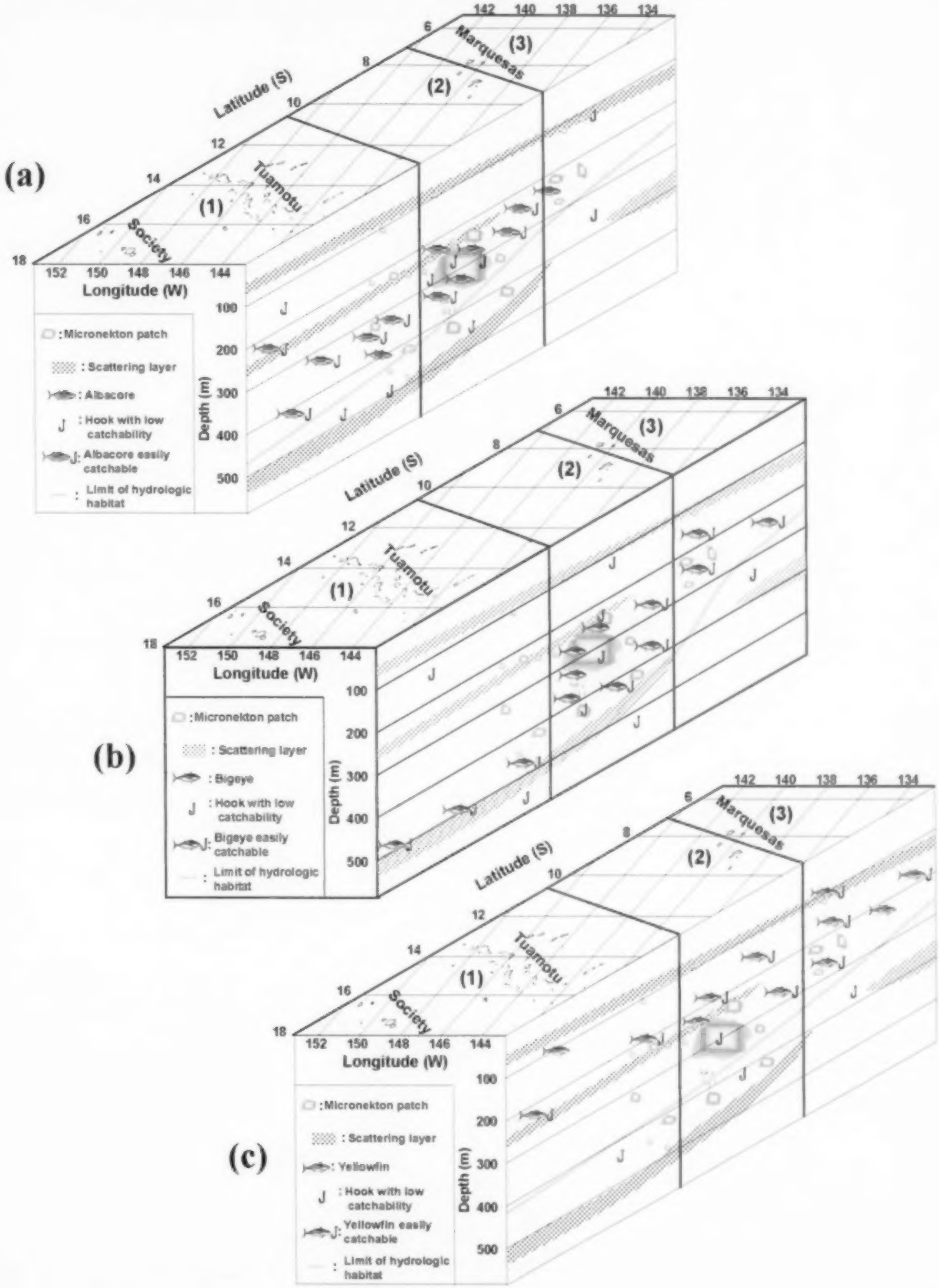
(a)
Latitude (S)
6
8
10
12
14
16
18
142
140
138
136
134
Marquesas
Tuamotu
Society
(1)
(2)
(3)
152
150
148
146
144
Longitude (W)
Depth (m)
100
200
300
400
500
: Micronekton patch
: Scattering layer
: Albacore
J : Hook with low catchability
J: Albacore easily catchable
: Limit of hydrologic habitat
(b)
: Bigeye
J: Bigeye easily catchable
(c)
: Yellowfin
J: Yellowfin easily catchable

strate at small scales than for planktivorous fish because fish are more mobile than zooplankton.

Tunas

Despite having highest CPUEs in zone 2, albacore and bigeye tuna CPUEs calculated at a set scale showed a negative correlation with prey abundance and (or) the presence of prey patches. This negative relationship was not observed in the other zones. The difference could come from albacore and bigeye tunas displaying different motivations to attack the longline baits when they are inside or outside of dense prey patches (Figs. 4*a*, 4*b*). These tunas are likely to be attracted by prey patches during the daytime to feed on them. However, in zone 1, where prey patches are small and not very dense, they can still be inclined to attack baits, as large immobile bait might still represent a good target compared with mobile and disperse live prey. On the other hand, in large, dense patches like those found in zone 2, their motivation to attack baits might be reduced because they focus on very dense prey, with increased foraging success. Such results are in agreement with Swartzman et al. (1999), who highlighted the importance of the prey distribution with respect to the total biomass of prey. As assumed by Bertrand (1999), it is likely that tunas in a low state of repletion (i.e., hungry) attack the longline baits, whereas those inside dense prey patches might be quickly satiated and soon cease searching for food. This suggests that above a certain threshold of prey density, a dense prey patch leads to lower catchability: tunas are present in the area but are not motivated to attack the baited hooks.

Yellowfin tuna (Fig. 4*c*) showed trends similar to the two other species in zones 1 and 3 but differed from them in zone 2 as the correlation between CPUEs and prey abundances remained positive, even at a small scale. Yellowfin tuna feed on organisms of the mixed layer as well as on organisms of deeper SSL, whereas albacore and bigeye tunas mainly feed on the deep SSL and not in the mixed layer. We can therefore assume that as for albacore and bigeye tunas, yellowfin tuna might be less attracted by longline baits when feeding in very dense prey patches in deep waters of zone 2. However, a large proportion of yellowfin tuna also forage in the mixed layer, where the prey density is lower, which limits the possible competition between prey and baits. Therefore, because yellowfin tuna feed in two different depth strata with different prey densities, the competition between prey and baits in deep patches of zone 2 is probably not sufficient to decrease the yellowfin tuna CPUEs, as for the other species.

In conclusion, the simultaneous observations of the biotic and abiotic pelagic habitat and tunas provided new insights into the characteristics of the tuna–environment relationships. For each tuna species, a range of vertical habitat was defined depending on the vertical hydrological characteristics. Combined with the observations of prey, especially their accessibility by each species, we could better understand the strategy used by each species to occupy the pelagic environment. We highlighted the importance of the scale of observations and the role of prey in studying tuna catchability with a longline. On a regional scale, tuna CPUE and prey abundance appeared to be positively correlated. On a finer scale, i.e., at a longline-set scale, it seems that above a certain threshold of prey patch density, tunas might prefer to feed on prey rather than on dispersed baits and might become satiated, reducing their motivation toward baits. Longline catch rates are thus higher in areas of high prey density (zone 2), but at a small scale inside such areas, very dense patches might reduce the catchability of albacore and bigeye tunas. As yellowfin tuna also forage on the scattered prey in the superficial layers, the competition between prey in deep, dense patches and baits does not affect the CPUE of this species as it does for the other species in zone 2. Prey patch characteristics should therefore be taken into account for resource management and when interpreting longline CPUEs.

Acknowledgements

The Government of French Polynesia supported this research. The authors wish to thank the officers and crew of the R/V *Alis* for their kind assistance during experiments. Sincere thanks are extended to all of our colleagues from SRM, IFREMER, and IRD, who worked with us during the ECOTAP program. We are also grateful to Richard Brill, François Gerlotto, Gordon Swartzman, and referees for very helpful comments. Dean Grubbs is warmly thanked for revising the English of this paper.

References

Bach, P., Wendling, B., Abbes, R., and Josse, E. 1996. Characteristics of albacore (*Thunnus alalunga*) catches achieved by experimental fishing with an instrumented longline in the French Polynesia EEZ. *In* 6th South Pacific Albacore Research (SPAR) Workshop, Rarotonga, Cook Islands, 5–7 March 1996. *Available from* P. Bach, IRD, rue Jean Monnet, BP 171-34207 Sète Cedex, France (e-mail: Bach@mpl.ird.fr).

Bach, P., Dagorn, L., Bertrand, A., Josse, E., and Misselis, C. 2002. Acoustic telemetry versus instrumented longline fishing for studying the vertical distribution of pelagic fish: the example of the bigeye tuna (*Thunnus obesus*) in French Polynesia. Fish. Res. In press

Bertrand, A. 1999. Le système (thon–environnement) en Polynésie Française : caractérisation de l'habitat pélagique, étude de la distribution et de la capturabilité des thons, par méthodes acoustiques et halieutiques. Thèse de Doctorat de l'ENSAR, Rennes, N° d'ordre: 99–31, N° série: H43.

Bertrand, A., and Josse, E. 2000. Acoustic estimation of longline tuna abundance. ICES J. Mar. Sci. **57**: 919–926.

Bertrand, A., Josse, E., and Massé, J. 1999*a*. *In situ* acoustic target-strength measurement of bigeye (*Thunnus obesus*) and yellowfin tuna (*Thunnus albacares*) by coupling split-beam echosounder observations and sonic tracking. ICES J. Mar. Sci. **56**: 51–60.

Bertrand, A., Le Borgne, R., and Josse, E. 1999*b*. Acoustic characterisation of micronekton distribution in French Polynesia. Mar. Ecol. Prog. Ser. **191**: 127–140.

Bertrand, A., Misselis, C., Josse, E., and Bach, P. 2000. Caractérisation hydrologique et acoustique de l'habitat pélagique en Polynésie Française : conséquences sur les distributions horizontale et verticale des thonidés. *In* Les espaces de l'Halieutique, Actes du quatrième Forum Halieumétrique. *Edited by* D. Gascuel, A. Biseau, N. Bez, and P. Chavance. Coll. colloques et séminaires, IRD, Paris. pp. 55–74.

Block, B.A., Keen, J.E., Castillo, B., Dewar, H., Freund, E.V., Marcinek, D.J., Brill, R.W., and Farwell, C. 1997. Environmental preferences of yellowfin tuna (*Thunnus albacares*) at the northern extent of its range. Mar. Biol. **130**: 119–132.

Boggs, C.H. 1992. Depth, capture time, and hooked longevity of longline-caught pelagic fish: timing bites of fish with chips. Fish. Bull. **90**: 642–658.

Brill, R.W. 1994. A review of temperature and oxygen tolerance studies of tunas pertinent to fisheries oceanography, movement models and stock assessments. Fish. Oceanogr. **3**: 204–216.

Brill, R.W., Block, B.A., Boggs, C.H., Bigelow, K.A., Freund, E.V., and Marcinek, D.J. 1999. Horizontal movements and depth distribution of large adult yellowfin tuna (*Thunnus albacares*) near the Hawaiian Islands, recorded using ultrasonic telemetry: implications for the physiological ecology of pelagic fishes. Mar. Biol. **133**: 395–408.

Cayré, P., and Marsac, F. 1993. Modelling the yellowfin tuna (*Thunnus albacares*) vertical distribution using sonic tagging results and local environmental parameters. Aquat. Living Resour. **6**: 1–14.

Dagorn, L., Bach, P., and Josse, E. 2000. Movement patterns of large bigeye tuna (*Thunnus obesus*) in the open ocean determined using ultrasonic telemetry. Mar. Biol. **136**: 361–371.

Efron, B. 1987. Better bootstrap confidence intervals. J. Am. Stat. Assoc. **82**: 171–185.

Fonteneau, A. 1997. Atlas of tropical tuna fisheries: world catches and environment. ORSTOM, Paris, France.

Fonteneau, A., Gascuel, D., and Pallarés, P. 1998. Vingt-cinq ans d'évaluation des ressources thonières de l'Atlantique : quelques réflexions méthodologiques. *In* ICCAT Symposium de Sao Miguel, June 1996. *Edited by* J.S. Beckett. ICCAT, Coll. Vol. Sci. Pap., Vol. L(2). pp 523–561.

Foote, K.G., Knudsen, H.P., Vestnes, D.N., MacLennan, D.N., and Simmonds, E.J. 1987. Calibration of acoustic instruments for fish density estimation: a practical guide. ICES Coop. Res. Rep. **144**.

Fréon, P., and Misund, O.A. 1999. Dynamics of pelagic fish distribution and behaviour: effects on fisheries and stock assessment. Blackwell Science, London.

Hampton, J., Bigelow, K., and Labelle, M. 1998. A summary of current information on the biology, fisheries and stock assessment of bigeye tuna (*Thunnus obesus*) in the Pacific Ocean, with recommendations for data requirements and future research. Tech. Rep. Secretariat of the Pacific Community (SPC) Oceanic Fisheries Programme 36, Noumea, New Caledonia.

Hanamoto, E. 1987. Effect of oceanographic environment on bigeye tuna distribution. Bull. Jpn. Soc. Fish. Oceanogr. **51**: 203–216.

Holland, K.N., Brill, R.W., and Chang, R.K.C. 1990. Horizontal and vertical movements of yellowfin and bigeye tuna associated with Fish Aggregating Devices. Fish. Bull. **88**: 493–507.

Holland, K.N., Brill, R.W., Chang, R.K.C., Sibert, J.R., and Fournier, D.A. 1992. Physiological and behavioural thermoregulation in bigeye tuna (*Thunnus obesus*). Nature (London), **358**: 410–412.

Josse, E., and Bertrand, A. 2000. *In situ* acoustic target strength measurements of tuna associated with a fish aggregating device in French Polynesia. ICES J. Mar. Sci. **57**: 911–918.

Josse, E., Bach, P., and Dagorn, L. 1998. Simultaneous observations of tuna movements and their prey by sonic tracking and acoustic surveys. Hydrobiologia, **371/372**: 61–69.

Kimura, S., Nakai, M., and Sugimoto, T. 1997. Migration of albacore, *Thunnus alalunga*, in the North Pacific Ocean in relation to large oceanic phenomena. Fish. Oceanogr. **6**: 51–57.

Levin, S.A. 1992. The problem of pattern and scale in ecology. Ecology, **73**: 1943–1967.

Marchal, E., and Lebourges, A. 1996. Acoustic evidence for unusual diel behaviour of a mesopelagic fish (*Vinciguerria nimbaria*) exploited by tuna. ICES J. Mar. Sci. **53**: 443–447.

Maury, O., Gascuel, D., Marsac, F., Fonteneau, A., and De Rosa, A.L. 2001. Hierarchical interpretation of nonlinear relationships linking yellowfin tuna (*Thunnus albacares*) distribution to the environment in the Atlantic Ocean. Can. J. Fish. Aquat. Sci. **58**: 458–469.

Olson, R.J., and Boggs, C.H. 1986. Apex predation by yellowfin tuna (*Thunnus albacares*): independent estimates from gastric evacuation and stomach contents, bioenergetics, and cesium concentrations. Can. J. Fish. Aquat. Sci. **43**: 1759–1775.

Podesta, G.P., Browder, J.A., and Hoey, J.J. 1993. Exploring the association between swordfish catch rates and thermal fronts on U.S. longline grounds in the Western North Atlantic. Continental Shelf Res. **13**: 253–277.

Power, J.H. 1996. Simulations of the effect of advective–diffusive processes on observations of plankton abundance and population rates. J. Plankton Res. **18**: 1881–1896.

Rose, G.A., and Leggett, W.C. 1990. The importance of scale to predator–prey spatial correlation: an example of Atlantic fishes. Ecology, **71**: 33–43.

Sharp, G.D. 1978. Behavioral and physiological properties of tunas and their effects on vulnerability to fishing gear. *In* The physiological ecology of tunas. *Edited by* G.D. Sharp and A.E. Dizon. Academic Press, Inc., San Diego, Calif. pp. 397–449.

Sund, P.N., Blackburn, M., and Williams, F. 1981. Tunas and their environment in the Pacific Ocean: a review. Oceanogr. Mar. Biol. Annu. Rev. **19**: 443–512.

Swartzman, G., Brodeur, R., Napp, J., Hunt, G., Demer, D., and Hewitt, R. 1999. Spatial proximity of age-0 walleye pollock (*Theragra chalcogramma*) to zooplankton near the Pribilof Islands, Bering Sea, Alaska. ICES J. Mar. Sci. **56**: 545–560.

The accuracy of alternative stochastic growth rate estimates for salmon populations

Richard A. Hinrichsen

Abstract: The accuracies of four alternative estimators of stochastic growth rate for salmon populations are examined using bootstrapping. The first estimator is based on a stochastic Leslie matrix model that uses age-specific spawner counts. The other three estimators use spawner counts with limited age-structure information: a Botsford–Brittnacher model method and two diffusion approximation methods, namely, the least squares approach of Dennis and the robust approach of Holmes. Accuracy of the estimators was quantified using median bias and interquartile ranges of the stochastic growth rate estimates. The Botsford–Brittnacher estimator was found to be unreliable due to large bias. Of the remaining estimators, the stochastic Leslie approach tended to produce the most reliable estimates but had the greatest data demands. With severe lognormal measurement error, the Dennis estimators produced less biased estimates than the other methods, but precision of the stochastic growth rate was generally highest using the stochastic Leslie estimator.

Résumé : Une technique de bootstrap a permis d'examiner la précision de quatre estimateurs de la croissance stochastique des populations de saumons. Le premier estimateur est basé sur un modèle de matrice de Leslie stochastique qui utilise les dénombrements des reproducteurs à chacun des âges. Les trois autres estimateurs utilisent des dénombrements de reproducteurs avec une connaissance limitée de la structure en âge: une méthode basée sur le modèle de Botsford–Brittnacher et deux modèles d'approximation de la diffusion, la méthode des moindres carrés de Dennis et la méthode robuste de Holmes. La précision est calculée à partir de l'erreur médiane et les étendues inter-quartiles des estimés du taux de croissance stochastique. L'estimateur de Botsford–Brittnacher s'est révélé peu fiable à cause de l'erreur importante qui lui est associée. Des autres estimateurs, la méthode stochastique de Leslie a tendance à produire les estimés les plus fiables, mais c'est celle qui exige le plus grand nombre de données. En présence d'importantes erreurs de mesure lognormales, les estimateurs de Dennis produisent des estimés moins erronés que les autres méthodes, mais la précision du taux de croissance stochastique est généralement plus grande lorsqu'on utilise l'estimateur stochastique de Leslie.

[Traduit par la Rédaction]

Introduction

Recently, two approaches have been used to estimate levels of risk to threatened and endangered salmon stocks: the Botsford–Brittnacher model and a modified Dennis model. The Botsford–Brittnacher model was developed for a viability analysis of the winter run of chinook salmon (*Oncorhynchus tshawytscha*) (Botsford and Brittnacher 1998); its estimation method requires spawner counts and average age distribution of recruits. A Dennis-style model was developed for a viability analysis of many Columbia Basins salmon populations; it requires only spawner abundances and maximum age of recruits (Holmes 2001). The primary use of these models was to produce extinction probability estimates, which are unreliable for many reasons, including extremely poor precision (Ludwig 1999; Fieberg and Ellner 2000; Coulson et al. 2001). Inherent in each of these models, however, is a measure of trend in population numbers called stochastic growth rate, which is biologically useful and can be estimated reliably in some cases. Stochastic growth rate, denoted μ, is the asymptotic instantaneous rate of increase in the mean natural log of population abundance, a quantity that is defined for a large class of linear population growth models (Tuljapurkar and Orzack 1980; Caswell 2000). Alternative stochastic growth rate estimators, applied to sums of spawner abundances rather than population abundances (which are unavailable), are the focus of this paper.

The Botsford–Brittnacher and Dennis estimators of stochastic growth rate require only limited age-structured data, which can be a virtue because yearly age-specific spawner data are often lacking. For example, because of a paucity of age-structured data, recruitment cannot be estimated for many stocks in the Columbia Basin, rendering spawner–recruitment models useless. However, in rare cases, age-specific spawner data are available. Thus, I develop a third method, a stochastic Leslie matrix model approach that uses age-specific spawner data.

The stochastic Leslie matrix model is used to address two open questions. Which stochastic growth rate estimator is best when age-specific spawner data are poor or lacking? How much accuracy is gained by knowing the age structure of the spawners? To answer these questions, I use a Monte Carlo approach (in this case, bootstrapping). The stochastic Leslie matrix model is used to generate synthetic spawner

Received 15 October 2001. Accepted 8 May 2002. Published on the NRC Research Press Web site at http://cjfas.nrc.ca on 15 July 2002.
J16567

R.A. Hinrichsen. Hinrichsen Environmental Services, 4608 Union Bay PL NE, Seattle, WA 98105-4027, U.S.A. (e-mail: hinrich@seanet.com).

DOI: 10.1139/F02-065

trajectories to which alternative stochastic growth rate estimators are applied. This yields many replications of the estimators from which two measures of accuracy, bias and dispersion, are calculated. Estimators yielding parameter estimates with relatively low bias and dispersion are preferable. Similar evaluations of accuracy have been used for population growth rate estimates in marine mammals (Barlow 1990; Caswell et al. 1998) and demographic parameter estimates of humpback whales (Barlow and Clapham 1997).

The objective of this investigation is to evaluate the accuracy of alternative estimators of stochastic growth rate for endangered and threatened salmon populations. This is a crucial step in selecting an estimator to gauge the relative risk of decline for a number of listed salmon populations in the Columbia Basin and elsewhere.

Materials and methods

To compare the accuracy of different stochastic growth rate estimators, a way to generate synthetic data sets is needed. There are two approaches to this problem: resample the set of real data or draw samples from an assumed probability model that represents the underlying population process (perhaps estimated by real data). I use the former approach in which data are resampled, freeing the analysis from more stringent assumptions about the underlying population process.

Data

The data used are age-specific spawner series reconstructed for four Snake River stream-type chinook index stocks (Beamesderfer et al. 1997). These index stocks are Johnson Creek (Johnson), Bear Valley Creek/Elk Creek (Bear), Sulphur Creek (Sulphur), and Marsh Creek (Marsh). I chose these stocks for several reasons: their listing under the U.S. Endangered Species Act, which made an analysis of stochastic growth rate useful; their limited influence by hatchery spawners, which would otherwise further complicate the analysis; and their age-specific spawner data, which are needed for specifying an empirical age-structured model used to evaluate accuracies of estimators. These data have been used to evaluate the effect of dams on the productivity of Snake River stream-type chinook populations (Schaller et al. 1999). I did not use data previous to brood year 1980 because this earlier time window includes effects of an ocean regime shift, dam construction, and harvest, which make the assumption of stationarity of the recruits-per-spawner process untenable.

Stochastic Leslie matrix model

The general model that both the Botsford–Brittnacher and Dennis models approximate is a density-independent model that uses current spawners to project future spawners. It is of the form

$$(1) \qquad S_t = \sum_{a=a_1}^{a_2} \phi_{t-a,a} S_{t-a}$$

where S_t is the number of spawners at time t, a_1 is the youngest age at return, a_2 is the oldest age at return, and $\phi_{t-a,a}$ represents the number of adult progeny (recruits) in year t produced per spawner returning in year $t - a$. As such, $\phi_{t-a,a}$ includes the effects of age-specific fecundity, survival, and maturity schedule. It is convenient to define $\boldsymbol{\varphi}_t = [\phi_{t,a_1}, \phi_{t,a_1+1}, \ldots, \phi_{t,a_2}]'$, which is a k vector ($k = a_2 - a_1 + 1$) of age-specific recruits-per-spawner ratios. Unless otherwise noted, the k vector stochastic process described by $\boldsymbol{\varphi}_t$ is assumed to be independent over time, i.e., $\Pr\{\phi_{t+h,a} \le y | \phi_{t,a}\} = \Pr\{\phi_{t+h,a} \le y\}$ for all time increments, denoted h ($h > 0$), ages, denoted a ($a_1 \le a \le a_2$), and levels of $\phi_{t+h,a}$, denoted y, and it is assumed to be stationary.

For convenience, I write eq. 1 in matrix model form:

$$(2) \qquad \mathbf{S}_t = \mathbf{A}_{t-1}\mathbf{S}_{t-1}$$

where $\mathbf{S}_t$ is an a_2 vector of spawner counts $[S_t, S_{t-1}, \ldots, S_{t-a_2+1}]'$, and $\mathbf{A}_t$ is an $a_2 \times a_2$ matrix

$$(3) \qquad \mathbf{A}_t = \begin{bmatrix} 0 & \ldots & \phi_{t-a_1+1,a_1} & \ldots & \phi_{t-a_2+1,a_2} \\ 1 & 0 & 0 & \ldots & 0 \\ 0 & 1 & 0 & & \\ \vdots & & 1 & \ddots & \vdots \\ 0 & \ldots & & 1 & 0 \end{bmatrix}$$

which is a time-dependent Leslie matrix in canonical form (Leslie 1948). When comparing models using asymptotic theory, it will be convenient to work with the running sum of spawners up to the maximum age at return,

$$(4) \qquad R_t = \mathbf{1}'\mathbf{S}_t = \sum_{i=0}^{a_2-1} S_{t-i}$$

where $a_2 \le t$ and $\mathbf{1}$ is an a_2 vector with all entries equal to 1.

The model described by eq. 2 is used extensively to simulate spawner trajectories. At every time step of the simulation, the joint empirical distribution functions of the age-specific recruits-per-spawner ratios is sampled and inserted into the Leslie matrix, $\mathbf{A}_t$, to generate spawners abundance at the next time step. The set of observed age-specific recruits-per-spawner ratios is

$$(5) \qquad \phi_{t,a} = \frac{S_{t+a,a}}{S_t}$$

where $S_{t+a,a}$ represents the number of spawners in year $t + a$ of age a. Assuming that there are n brood years for which spawners counts were taken, $1 \le t \le n - a$ in eq. 5. By assumption, the stochastic process described by $\boldsymbol{\varphi}_t$ is stationary, making the probability distribution function of $\boldsymbol{\varphi}_t$, denoted by F_t, identical at each time t; therefore, F_t can be labeled F (i.e., the subscript t can be dropped). Consequently, each observed $\boldsymbol{\varphi}_t$, whose elements are defined by eq. 5, is a random sample from F. By assumption, the random sample is independent. These independent and identically distributed samples are used to form the empirical distribution function, denoted $\hat{F}$, which is an estimate the true distribution function F (Efron and Tibshirani 1993). In computer simulations, I make extensive use of the "plug-in principle", whereby $\hat{F}$ is used in place of the unknown F for simulating the spawner abundances over time. For sampling, this amounts to the resampling the observed $\boldsymbol{\varphi}_t$ with replacement. Resampling takes place at two different levels in simulations: (*i*) at the population projection level, to specify the matrix in eq. 3 at each time step, so that sample paths of spawners can be produced (for the stochastic Leslie matrix and Botsford–Brittnacher methods only); and (*ii*) at the bootstrapping level, to generate bootstrap data sets from which bootstrap replications of the stochastic growth rate estimates can be obtained for each method. Resampling at level (*i*) is described in the section "Stochastic growth rate estimation", and resampling at level (*ii*) is described in the section "Bias and dispersion estimation".

It turns out that for each of the index stocks, the first age at return for females is $a_1 = 4$ and last age at return is $a_2 = 5$. Therefore, $\mathbf{A}_t$ will be a 5 × 5 matrix, and $\mathbf{S}_t$ will be a 5 vector. In the simulation description below a variable with a "~" over it will represent a simulated quantity.

Stochastic growth rate

For a large class of density-independent population growth models, it is possible to define the rate of increase in mean $\ln(R_t)$, also known as the stochastic growth rate (for spawners, not population abundance), denoted μ. It is guaranteed to exist under quite general conditions, which are assumed to hold in this paper. Two important conditions are that the underlying process is density-independent and the age-specific spawner-to-recruit ratios form a stationary time series (Tuljapurkar 1989).

Stochastic growth rate estimation

For the stochastic Leslie matrix model, I used simulation to estimate stochastic growth rate. The alternative approach of using Tuljapurkar's approximation was not used because, although it is useful for theoretical calculations, it can fail when projection matrix entries (in my case, the age-specific spawner–recruit ratios) have large variances (Caswell 2000). For the salmon populations in this study, variability in first row matrix entries was very high: only the Johnson index stock contained age-specific recruits-per-spawner ratios with coefficients of variation (CVs) less than 1. Simulations were conducted as follows:

(1) Generate a series of age-specific spawner–recruit vectors of length 101 by selecting at random with replacement from the observed vectors from 1980–1994. Label this series $\tilde{\boldsymbol{\varphi}} = \{\tilde{\boldsymbol{\varphi}}_0, \tilde{\boldsymbol{\varphi}}_1, \ldots, \tilde{\boldsymbol{\varphi}}_{100}\}$.

(2) Set the initial simulated spawner vector $\tilde{\mathbf{S}}_4 = [\tilde{S}_4, \tilde{S}_3, \tilde{S}_2, \tilde{S}_1, \tilde{S}_0]'$ in eq. 2 to the spawners counts in the run reconstruction corresponding to years 1995–1999, yielding $\tilde{S}_i = S_{1995+i}$ (i = 0, 1, 2, 3, 4). Note that the initial time subscript for the simulated spawner vector is $t = 4$.

(3) Set the nonzero entries of the first row of the projection matrix $\tilde{\mathbf{A}}_4$ to $\tilde{\phi}_{0,5}$ and $\tilde{\phi}_{1,4}$. This fully specifies the initial projection matrix for the simulations, $\tilde{\mathbf{A}}_4$. Set the simulated time index to $t = 5$.

(4) Use eq. 2 along with the simulated values of the projection matrix and the current spawner vector, to find the next spawner vector, namely, $\tilde{\mathbf{S}}_t = \tilde{\mathbf{A}}_{t-1}\tilde{\mathbf{S}}_{t-1}$.

(5) Fully specify the matrix $\tilde{\mathbf{A}}_t$ by setting the nonzero entries of the first row to $\tilde{\phi}_{t-4,5}$ and $\tilde{\phi}_{t-3,4}$. Increment the simulation time index t to $t + 1$.

(6) Repeat steps 4 and 5 until 100 simulated values of the spawner series are obtained, namely, $\tilde{S}_5, \tilde{S}_6, \ldots, \tilde{S}_{104}$.

This algorithm simulates a spawner series that preserves important characteristics of the original run reconstruction data. First of all, correlations between the age-specific recruits-per-spawner ratios, $\phi_{t,4}$ and $\phi_{t,5}$, will be preserved since, for each simulation year, they will be drawn from the same retrospective brood year. The year-to-year variation in these ratios will also be preserved. Except for later distributional assumptions for measurement error, the simulation is distribution-free, since it is a data resampling procedure: no assumptions were made about the form of the distributions of age-specific recruits-per-spawner ratios. Thus, in the end, each future 100-year simulation will be representative of the stochastic age-structured process described by the retrospective age-specific spawner data.

In each simulation of an index stock, N = 5000 100-year sequences of simulated spawners are generated. The stochastic Leslie estimation method (denoted SL) for the stochastic growth rate proceeds by first calculating the following sequence:

$$\text{mean}\{\ln(\tilde{R}_t)\} = \sum_{i=1}^{N} \ln(\tilde{R}_t^i)/N \tag{6}$$

where the superscript i indexes the simulation. The stochastic Leslie estimate, $\hat{\mu}_{\text{SL}}$, is then the slope of the least squares line of mean$\{\ln(\hat{R}_t)\}$ vs. t ($5 \leq t \leq 104$).

Botsford–Brittnacher model

The Botsford–Brittnacher estimation method (denoted BB) is similar to the stochastic Leslie matrix method, but uses less information; it assumes that average age distribution of recruits is known (but the year-to-year changes in the distribution are not) and that

$$\phi_{t,a} = p_a E_t \tag{7}$$

where p_a is the average fraction of recruits that return at age a, and E_t (cohort replacement rate) represents recruits-per-spawner for spawners in brood year t. Using these definitions in eq. 1 produces

$$S_t = p_{a_1} E_{t-a_1} S_{t-a_1} + p_{a_1+1} E_{t-(a_1+1)} S_{t-(a_1+1)} + \ldots + p_{a_2} E_{t-a_2} S_{t-a_2} \tag{8}$$

where $a_2 + 1 \leq t \leq n$.

To obtain a stochastic growth rate estimate using the Botsford–Brittnacher method, the cohort replacement rates must be estimated, but this presents difficulties. Obtaining these estimates by inputting spawner numbers and average distribution of ages of return into eq. 8 and then solving for E_t leads to an infinite number of solutions when there are multiple ages of recruits. Moreover, if some of the cohort replacement rates were specified so that the problem had a unique or least squares solution, there would be no guarantee that the cohort replacement rates would be positive. Botsford and Brittnacher's solution was to assume for the sake of estimation that all of the recruits returned at a fixed age, a_m, the age at which the greatest fraction of recruits return (modal age). Using this convenient assumption, which I also employ, gives unique and positive replacement rates estimates:

$$(9) \qquad \hat{E}_t = S_{t+a_m}/S_t$$

For all stocks analyzed in this paper, $a_m = 5$.

The stochastic growth rate estimate is obtained through simulation, which is the same as the simulation for the stochastic Leslie matrix model except that the estimated age-specific recruits-per-spawner ratios are replaced by

$$(10) \qquad \hat{\phi}_{t,a} = \hat{p}_a \hat{E}_t$$

As with the stochastic Leslie matrix model, the simulation is carried out a total of $N = 5000$ times to get single estimates of $\hat{u}_{\mathrm{BB}}$, where the subscript BB denotes that the Botsford–Brittnacher estimator was used.

Dennis model

In many analyses, age-specific spawner data are unavailable or unreliable so that the SL and BB methods cannot be used. The approach of Dennis et al. (1991) solves this problem by using theoretical results concerning Leslie matrices, which indicate that under certain assumptions that the natural logarithm of total population size can be approximated by a Wiener process with drift (Tuljapurkar and Orzack 1980; Heyde and Cohen 1985; Tuljapurkar 1989). The population matrices, $\mathbf{A}_t$, in eq. 3 are in Leslie matrix form, so the theoretical asymptotic results apply to eq. 2. As t becomes large, the theory tells us that $\ln(R_t)$ will have an approximate normal distribution with mean of $\ln(R_{a_2}) + \mu t$ and variance $\sigma^2 t$, where R_{a_2} is the initial running sum of spawners. The Dennis approach is to apply this asymptotic result over the entire data set, yielding

$$(11) \qquad \ln(R_t/R_{t-1}) = \mu + \varepsilon_{t-1}$$

where ε_t is assumed to be a normal deviate with mean 0 and variance σ^2.

There are apparent difficulties with this approximation, even if R_t represented total population size instead of a running sum of spawners (Caswell 2000). However, the Weiner process with drift can do a reasonably good job of approximating an age-structured stochastic process (Lande and Orzack 1988). Just as Dennis et al. (1991) did, I ignore the difficulties of the diffusion approximation and obtain the estimates of μ by treating eq. 11 as a least squares regression model. Note, however, running sums of spawners are used in place of the Dennis et al. (1991) total population abundances, therefore $\ln(R_t/R_{t-1})$ $(a_2 + 1 \le t \le n)$ are the values of the dependent variable in the regression. The least squares regression estimate is labeled $\hat{\mu}_{\mathrm{DN}}$. (The subscript DN denotes estimates derived using the Dennis least squares regression approach). As an alternative estimation method, the Dennis–Holmes technique (DH), also called the slope-based method, was used as well (Holmes 2001). In this method, the stochastic growth rate estimate is

$$(12) \qquad \hat{\mu}_{\mathrm{DH}} = \text{slope of the regression line of } \text{mean}[\ln(R_t/R_{t-\tau})] \text{ vs. } \tau$$

where $\tau = 1, 2, 3, 4, 5$ and the least squares regression line in eq. 12 has an intercept of zero. Holmes (2001) found that the slope-based method was robust to large, erratic measurement error in the spawner series; however, it was unclear whether it performed better than the least squares estimator (DN).

Bias and dispersion estimation

To estimate bias and dispersion of stochastic growth rate estimates, I used bootstrapping. Bootstrap samples of age-specific recruits-per-spawner vectors, $\boldsymbol{\varphi}^* = (\boldsymbol{\varphi}_1^*, \boldsymbol{\varphi}_2^*, \ldots, \boldsymbol{\varphi}_{15}^*)$, were obtained by drawing at random with replacement from the set of 15 observed $\boldsymbol{\varphi}_r$. The star notation indicates that $\boldsymbol{\varphi}^*$ is not the original (actual) data set, but a resampled version of the actual data set $\boldsymbol{\varphi}$. A total of $B = 5000$ bootstrap samples, denoted $\boldsymbol{\varphi}^{*1}, \boldsymbol{\varphi}^{*2}, \ldots, \boldsymbol{\varphi}^{*B}$, were drawn for each of the index stocks. Corresponding to each bootstrap sample of recruits per spawner, $\boldsymbol{\varphi}^{*b}$, is a spawner bootstrap sample, $\mathbf{S}^{*b}$, of size $n = 20$, which is needed as input for the Botsford–Brittnacher and two Dennis-type estimators. To ensure a correspondence between $\boldsymbol{\varphi}^{*b}$ and $\mathbf{S}^{*b}$, they were both determined by the same age-specific spawner series generated during the last 20 years of a single 100-year simulation of the stochastic Leslie matrix model.

The bootstrapped data sets were used in place of the actual data set in the estimation process for the stochastic growth rate, yielding $B = 5000$ bootstrap replications for each of the estimates. This process was carried out for each of the four index stocks.

With the $B = 5000$ bootstrap replications of the parameter estimates in hand, I next estimated bias and dispersion of the estimates. Accuracy of the estimates produced by different estimators was depicted using boxplots of the replications. The median bias for stochastic growth rate was estimated as

$$(13) \qquad \text{bias}(\hat{\mu}) = \text{median}(\hat{\mu}^*) - \hat{\mu}_{\mathrm{SL}}$$

respectively, where median($\hat{\mu}^*$)is the sample median of the bootstrap replications of $\hat{\mu}$ (used to represent the stochastic growth rate estimate obtained by any of the four estimators). I used median bias instead of mean bias because outliers can make the mean a misleading measure of central tendency. $\hat{\mu}_{\mathrm{SL}}$ was used in the right-hand side of eq. 13 because it is the plug-in estimate of μ, obtained by using the empirical distribution, $\hat{F}$, in place of the true (unknown) distribution function, F, in the stochastic Leslie matrix model simulations. For evaluating dispersion of an estimate, the bootstrap estimate of interquartile range (IQR) was used:

$$(14) \qquad \text{IQR}(\hat{\mu}) = \hat{q}^*_{0.75} - \hat{q}^*_{0.25}$$

where $\hat{q}^*_p$ is the pth quantile of the bootstrap replications of $\hat{\mu}$. IQR was used instead of standard error because it could be more accurately estimated and was less sensitive to outliers.

Estimators with relatively small bias and dispersion will be preferred to those with large bias and dispersion. A rule of thumb is that biases greater than 25% standard error are considered statistically important (Efron and Tibshirani 1993). Because standard error was not used, I modified this rule by considering biases greater than 19% IQR statistically important. This corresponds to the usual standard error rule when the underlying sampling distribution is normal.

The number of bootstrap replications, $B = 5000$, and the number of trajectories simulated for the SL and BB estimators, $N = 5000$, were deemed sufficient for this numerical exercise, because, at these resampling sizes, using different

Table 1. Stochastic growth rate estimates, median bias, and interquartile range when serial independence is assumed for the recruits-per-spawner ratios.

	Estimate				Median bias				Interquartile range			
Stock	SL	BB	DN	DH	SL	BB	DN	DH	SL	BB	DN	DH
Johnson	0.02	0.04	0.01	0.00	0.00	0.04	0.00	0.00	0.06	0.07	0.07	0.07
Bear	0.06	0.07	0.02	–0.01	–0.01	0.08	0.00	0.00	0.10	0.12	0.12	0.13
Sulphur	0.11	0.12	0.04	–0.01	0.00	0.19	0.00	0.00	0.12	0.22	0.17	0.18
Marsh	0.00	0.01	–0.01	–0.05	–0.01	0.13	0.01	0.01	0.14	0.20	0.17	0.19

Note: SL = stochastic Leslie method, BB = Botsford–Brittnacher method, DN = Dennis method, DH = Dennis–Holmes method. SL is the plug-in estimate.

random seeds for the computer runs yielded minute changes in estimates, median bias, and IQR.

Measurement error

To examine the robustness of the four stochastic growth rate estimators to measurement error, I perturbed the bootstrap spawner data sets with independent lognormal measurement errors that are unbiased in mean (Hilborn and Starr 1984). The perturbed age-specific bootstrap spawner data sets were constructed as follows.

$$S^{**}_{t,a} = S^{*}_{t,a}\exp(x_t - \sigma^2_x/2) \tag{15}$$

where x_t is a normally distributed random variable with mean zero and variance σ^2_x. These perturbed bootstrap data sets (indicated by the superscript "**") were used in place of the actual bootstrap data sets for input into the four alternative estimators to generate replications of the stochastic growth rate estimates influenced by measurement error. To obtain estimates of bias and dispersion of the stochastic growth rate estimates when measurement error is present, the replications were used in eqs. 13 and 14, respectively.

To see how the accuracy of the estimates changed with increasing levels of measurement error, bootstrap bias and interquartile range were estimated as a function of the measurement error standard deviation parameter, σ_x = 0, 0.2, 0.4, 0.6, 0.8, 1. I used these six levels of measurement error because they cover a wide range of possibilities. At the most extreme value of measurement error variance ($\sigma^2_x = 1$), 10% of spawner numbers are greater than 218% of their true value, and 10% are less than 17% of their true value.

Serial dependence sensitivity

The resampling approaches outlined above assumed that there was no serial dependence in the series of age-specific recruits-per-spawner vectors. However, it is certainly possible that serial dependence arises from environmental drivers such as climate effects. In fact, one of the index stocks, Sulphur, showed strong autocorrelation in its retrospective recruits-per-spawner ratios (r = 0.96). Therefore, I conducted a sensitivity analysis to show how the estimators perform when the assumption of independence in the recruits-per-spawner ratios was violated. To do this, I used a Markov resampling technique (Rajarshi 1990). The Markov process had two discrete states: recruits per spawner at or below the median, and recruits per spawner above the median. Bootstrap data sets were generated from the Markov process that used fixed transition probabilities between these two states.

Define

$$y_t = I(\phi_{t,4} + \phi_{t,5} - M) \tag{16}$$

where $I()$ is the indicator function that returns the value 1 if its argument is positive and 0 otherwise, and M is the median of the retrospective recruit-per-spawner ratios. The transition probabilities of interest are the probability that two adjacent recruit per spawner ratios cross the median, $p_{\text{cross}} = \Pr\{y_{t+1}(1 - y_t) + (1 - y_{t+1})y_t = 1\}$ and the probability that they fail to cross the median, $1 - p_{\text{cross}}$. The probability p_{cross} was estimated from the retrospective data using the formula

$$\hat{p}_{\text{cross}} = \sum_{t=1}^{14} \{y_{t+1}(1 - y_t) + (1 - y_{t+1})y_t\} / 14 \tag{17}$$

Note that when there is no serial dependence, one expects $\hat{p}_{\text{cross}}$ to be equal to 0.5. For the Sulphur index stock, $\hat{p}_{\text{cross}}$ = 0.27, so crossings are about half as frequent as expected from a series with no serial dependence.

To generate a synthetic series of age-specific spawner–recruit vectors while preserving first-order serial dependence, I sampled the Markov process implied by the estimated crossing probabilities. The algorithm is as follows.

(1) Divide the retrospective age-specific recruits-per-spawner ratios into two groups: $\boldsymbol{\varphi}^{+}$, which contains all the vectors yielding recruits per spawner greater than M, and $\boldsymbol{\varphi}^{-}$, which contains the remaining recruits-per-spawner vectors.

(2) Set $t = 0$. Initialize the first recruits-per-spawner vector, $\tilde{\boldsymbol{\varphi}}^{\text{MR}}_0$, in the sequence to the one observed in 1994 (the most recent), where the MR superscript indicates Markov resampling.

(3) If $\tilde{\boldsymbol{\varphi}}^{\text{MR}}_t$ lies in $\boldsymbol{\varphi}^{-}$, generate a random number between 0 and 1. If the number is less than $\hat{p}_{\text{cross}}$, set $\tilde{\boldsymbol{\varphi}}^{\text{MR}}_{t+1}$ to a recruits-per-spawner vector that is randomly selected (with replacement) from $\boldsymbol{\varphi}^{+}$; otherwise, select it from $\boldsymbol{\varphi}^{-}$. If $\tilde{\boldsymbol{\varphi}}^{\text{MR}}_t$ lies in $\boldsymbol{\varphi}^{+}$, follow the same procedure, but substitute $1 - \hat{p}_{\text{cross}}$ for $\hat{p}_{\text{cross}}$.

(4) Increment t by 1 and return to step 3. Continue in this way until the series of vectors, $\tilde{\boldsymbol{\varphi}}^{\text{MR}} = \{\tilde{\boldsymbol{\varphi}}^{\text{MR}}_0, \tilde{\boldsymbol{\varphi}}^{\text{MR}}_1, \dots, \tilde{\boldsymbol{\varphi}}^{\text{MR}}_{100}\}$, is obtained.

To obtain the plug-in estimate of stochastic growth rate that incorporates this serial dependence, the series $\tilde{\boldsymbol{\varphi}}^{\text{MR}}$ was used in place of step 1 of the algorithm described in the section "Stochastic growth rate estimation". As before, the plug-in estimator is the slope of the least squares line of mean$\{\ln(\tilde{R}_t)\}$ vs. t ($5 \le t \le 104$). To calculate bias, this plug-in estimate was used in place of $\hat{\mu}_{\text{SL}}$ in eq. 13. (By definition, $\hat{\mu}_{\text{SL}}$ is not the plug-in estimate when a Markov process is assumed, because $\hat{\mu}_{\text{SL}}$ is calculated by treating recruits-per-spawner ratios as if they were serially independent.) For estimating median bias and IQR under the alternative as-

Fig. 1. The effect of estimation method on the accuracy stochastic growth rate (μ) estimators for (*a*) Johnson, (*b*) Bear, (*c*) Sulphur, and (*d*) Marsh index stocks. The estimators used were based on the stochastic Leslie matrix model approach (SL), Botsford–Brittnacher model approach (BB), Dennis approach applied to the running sum of spawners (DN), and Dennis–Holmes approach (DH). In the boxplots, the horizontal line within the box indicates the median; the box encompasses 75% of the 5000 bootstrap replications, and the whiskers are drawn to the nearest value not beyond 1.5 × (interquartile range) from the quartiles. The dashed horizontal line through each plot indicates the best estimate of the true parameter value from the stochastic Leslie matrix model.

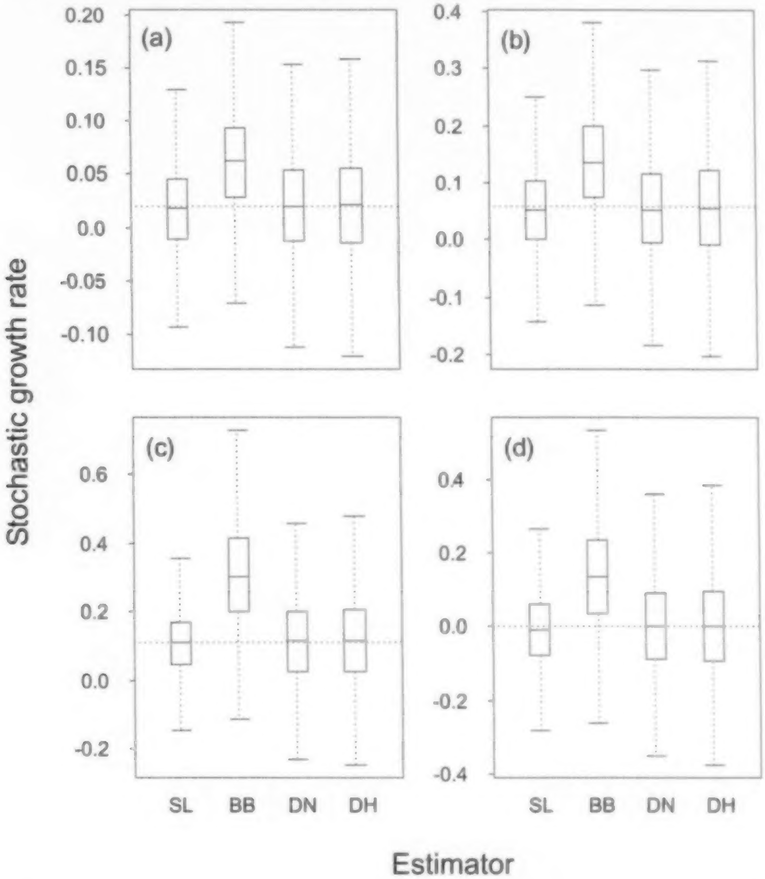

sumption of serially dependence, bootstrap replications were obtained by applying the alternative estimators to the bootstrap data sets generated using Markov resampling.

Results

Stochastic growth rate estimates

In several instances, the stochastic growth rate estimates varied widely among the four techniques used (Table 1), thus stressing the need for a detailed comparison of accuracy. For the Sulphur index stock, the stochastic growth rate estimate varied from $\hat{\mu}_{DH} = -0.01$ to $\hat{\mu}_{BB} = 0.12$.

Accuracy of estimates

The bootstrap bias and IQR calculated for the different stochastic growth rate estimators indicate clear differences in accuracy (Table 1). These differing accuracies are starkly illustrated by boxplots of the bootstrap replications (Fig. 1).

The Botsford–Brittnacher estimator was found to be unreliable due to large bias, which was 60–88% of IQR (exceeding the 19% cutoff). The remaining estimators yielded small bias (less than 7% of IQR). The dispersions of the estimates (as measured by IQR) were smallest for the SL method. DN produced IQRs of the estimates that were 115–140% of those produced by the SL method. The IQRs of the estimates produced by BB and DH tended to be higher than those produced by DN.

Measurement error

For the DN and DH estimators, biases in the estimate of stochastic growth rate changed very little as σ_x increased from zero to one; in contrast, for the SL and BB estimators, biases showed a marked increase with measurement error (Fig. 2). The two Dennis model estimators are more robust to measurement error because they smooth out measurement errors in spawner counts by using running sums, while the SL and BB estimators rely on individual age-specific

Fig. 2. The influence of lognormal measurement error on the median bias of the stochastic growth rate estimates for (*a*) Johnson, (*b*) Bear, (*c*) Sulphur, and (*d*) Marsh index stocks. The biases are shown for the stochastic Leslie SL (squares), Botsford–Brittnacher BB (circles), Dennis DN (triangles), and Dennis–Holmes DH (diamonds) estimators. The dashed horizontal line marks zero bias.

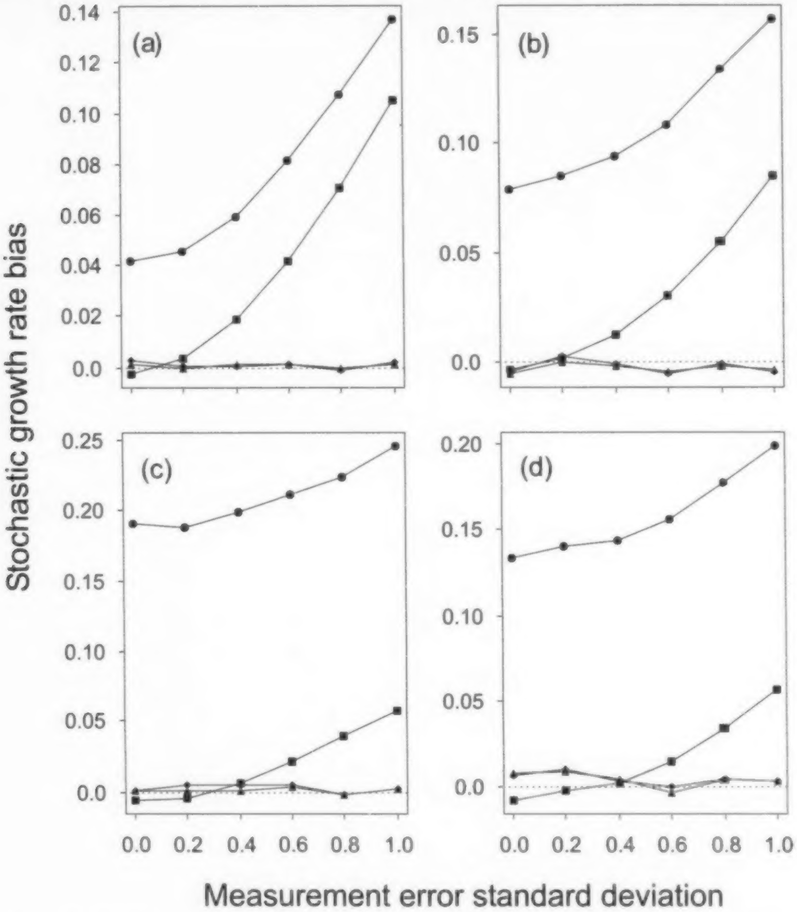

spawner counts, which can be highly corrupted. When a corrupted spawner count is introduced into the SL or BB method, it results in an extreme recruits-per-spawner ratio, which is misinterpreted as a rare event; these tend to move the estimate of stochastic growth rate upward (Caswell 2000). Regardless of the level of measurement error, IQR of the stochastic growth rate tended to be smallest for the SL method and largest for the BB method, and the DN method produced IQRs that were smaller than those produced by the DH method (Fig. 3).

Serial dependence

Incorporating serial dependence in the recruits-per-spawner ratios by using Markov resampling had a small effect on the plug-in estimates of stochastic growth rate (Table 2). Except for the Sulphur index stock, IQR did not change substantially for any of the alternative estimators. For Sulphur, the SL IQR grew by 50%, most likely due to the strong serial dependence in recruits per spawner, which reduces precision by lowering the effective degrees of freedom. The crossing probability estimates, $\hat{p}_{\text{cross}}$, were 0.36, 0.43, 0.27, and 0.50 for Johnson, Bear, Sulphur, and Marsh, respectively. Bias estimates hardly changed, nor did the ranking of the estimation methods by IQR averaged over the four index stocks.

Discussion

The analysis of the statistical characteristics of stochastic growth rate estimates for threatened salmon populations show vivid differences in performance among the four estimators used. Although each method has its weakness, the poorest performance was shown by the BB method, the estimation method for the Botsford–Brittnacher model, even though it had greater data requirements than the two Dennis model estimators. The stochastic growth rate estimates produced by BB were positively biased for all of the four index stocks analyzed, sometimes severely. This occurred not because the Botsford–Brittnacher model is defective, but because it is difficult to estimate. To obtain estimates for the

Fig. 3. The influence of lognormal measurement error on the interquartile range of the stochastic growth rate estimates for (*a*) Johnson, (*b*) Bear, (*c*) Sulphur, and (*d*) Marsh index stocks. The interquartile ranges are shown for the stochastic Leslie SL (squares), Botsford–Brittnacher BB (circles), Dennis DN (triangles), and Dennis–Holmes DH (diamonds) estimators.

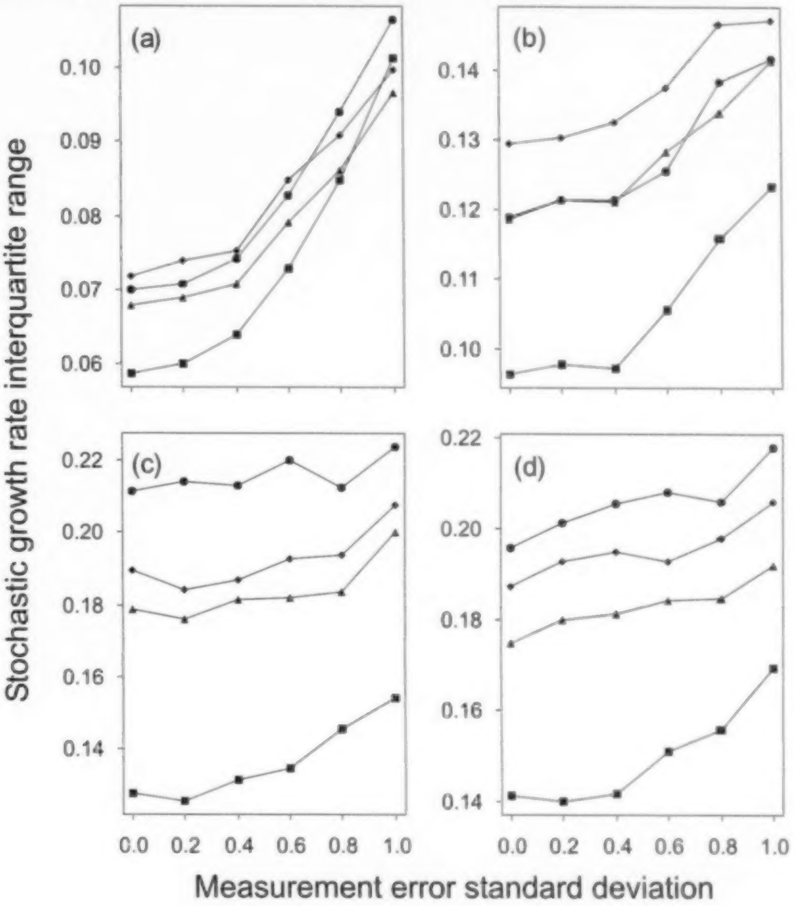

Table 2. The plug-in estimates of stochastic growth rate and the median bias and interquartile range of the alternative estimators when a first-order Markov process is used to simulate serial dependence in the recruits per spawner.

		Median bias				Interquartile range			
Stock	Plug-in estimate	SL	BB	DN	DH	SL	BB	DN	DH
Johnson	0.02	0.01	0.04	0.00	0.00	0.07	0.08	0.08	0.08
Bear	0.07	0.00	0.08	–0.01	0.00	0.10	0.12	0.12	0.14
Sulphur	0.10	0.03	0.19	0.01	0.01	0.18	0.23	0.21	0.23
Marsh	0.02	–0.01	0.13	0.01	0.00	0.14	0.19	0.17	0.18

Note: SL = stochastic Leslie method, BB = Botsford–Brittnacher method, DN = Dennis method, DH = Dennis–Holmes method.

cohort replacement rates, the data were treated as though the age at return for the four index populations was fixed. This dubious technique was described by Botsford and Brittnacher (1998) for modeling the endangered winter-run chinook salmon population in the Sacramento Basin. Because the BB stochastic growth rate estimates are highly biased, are no more precise than the Dennis model estimators, and require more data than the Dennis model estimators (they require the average age distribution of recruits), there appears to be no reason to use the Botsford–Brittnacher estimator. As for the two Dennis estimators, the DH estimates of stochastic growth rate were no more robust to measurement error than the DN estimates. Therefore, using the slope-based estimates as Holmes (2001) suggests appears to offer no distinct advantage over the DN method.

The loss of precision caused by ignoring age-structured data can be large. The IQRs produced by DN were 15–40% higher than those using SL, the stochastic Leslie model method. Therefore, if it is available and measurement error is not too great, age-structured spawner data should be used. On the other hand, severe measurement error can cause the SL method to produce large upward biases in the stochastic growth rate compared to the Dennis estimators. Thus, if measurement error is important, then the SL stochastic growth rate estimate should be corrected for bias if possible or checked against a more robust estimate.

The stochastic growth rates for the index stocks (based on any of the estimators examined in this paper) indicate very different rates of growth than those given by Kareiva et al. (2000) in their Leslie matrix analysis of population growth rates. Kareiva et al. (2000) produced growth rate estimates of –0.20, –0.21, –0.38, and –0.37 compared to estimates based on the stochastic Leslie matrix model of 0.02, 0.06, 0.11, and 0 for Johnson, Bear, Sulphur, and Marsh index stocks, respectively. Like the approaches examined in this paper, the Kareiva et al. (2000) analysis was density-independent; however, it used data from brood years 1990–1999 only, ignoring years of high productivity in the early 1980s. The severe population decline indicated by the Kareiva et al. (2000) matrix analysis is not evident when the spawner data of 1980–1999 are used instead.

The estimators analyzed in this paper rely on the important assumption of stationarity of population growth rate. For salmon, nonstationarity has emerged as an important issue because of the existence of low-frequency ocean regime shifts (Beamish et al. 1999). These shifts, which occur on a decadal time scale (shifts occur approximately every 30 years), can have a large effect on ocean survival of salmon stocks (Hare et al. 1999). However, modeling effects of regime shifts proves difficult because predictions of the timing of regime shifts and their survival effects are highly uncertain.

Density independence is another critical assumption. Because fisheries models almost always include density dependence in recruitment, the class of density-independent models examined in this paper will undoubtedly receive special scrutiny and skepticism among fisheries biologists. I believe such skepticism is healthy and justified, because including density dependence can profoundly influence estimates of population growth. In fact, using a time window that reached back to 1952, Deriso et al. (2001) found significant density-dependent effects for several Snake River stream-type chinook stocks. However, data from the last 20 years for these stocks show little evidence supporting a density-dependent model (Kareiva et al. 2000).

For assessing the accuracy of stochastic growth rate estimators, I have opted for the approach of resampling data rather than sampling from a hypothetical probability model to generate synthetic data sets (Press et al. 1992). I use this approach because it has the advantage of applying less stringent distributional assumptions. Using the alternative approach of specifying a hypothetical model has important difficulties: parameter values are arbitrary (if data are not used for their estimation), and the model may be easily misspecified. Both of these difficulties are illustrated in the work of Holmes (2001), who specified a salmon population matrix to test the Holmes–Dennis approach. All of the vital rates were assumed to be correlated at 0.99 (arbitrary) and all individuals in the class "egg to end of age 2" move to the class "age 2 to age 3" in a single year (a model misspecification). The resampling approach, however, is not without the usual difficulty of generating low values of dispersion because rare events (such as extremely large recruits per spawner that are possible when sampling from the usual lognormal distribution) are underrepresented. However, low dispersion will occur for all estimators, and it is the relative dispersion (relative efficiency) that is of primary interested here.

There are important unknowns that hamper estimation of stochastic growth rate for many Columbia Basin salmon populations. Chief among them is the contribution of the progeny of hatchery-reared spawners to recruitment in wild populations. If the contribution (whether large or zero) is not properly accounted for, trends in wild salmon populations will be masked, regardless of estimator chosen. To illustrate why this is, suppose that a large total recruitment per wild spawner is evident in the retrospective spawner series. If hatchery-reared spawners are as effective at producing adult progeny as wild fish, then the large total recruitment per wild spawner could have been due to a large input of hatchery-reared spawners one generation ago, even though the trend in wild population abundance was downward. At the other extreme, if hatchery-reared spawners produce no adult progeny (recruits), then a large total recruitment per wild spawner indicates a clear upward trend in wild population abundance. An effective experiment aimed at estimating the relative reproductive effectiveness of hatchery-reared spawners will require considerable ingenuity and commitment (Goodman 2001) and is crucial in reliably estimating trends in populations in which hatchery-reared spawner abundance is large.

In assessing the extinction risks of salmon stocks throughout the Columbia Basin, the National Marine Fisheries Service (NMFS) has broadly applied a single stochastic growth rate estimator to all of the stocks that are part of 12 evolutionary significant units (ESUs) listed as threatened or endangered under the U.S. Endangered Species Act (Cumulative Risk Initiative 2000). The broad assessment represents, for the first time, a synthesis and analysis that presents trends in a standardized way. However, this type of uniform analysis has come at a price. First, applying the Dennis model estimator to populations rich in age-structured data (such as the Snake River stream-type chinook) ignores important information and therefore yields a less accurate estimator. This paper shows that the loss of accuracy from using Dennis model shortcut in data-rich situations can be great. In fact, because of the large errors of estimating stochastic growth rate, the primary goal of NMFS in their broad analysis, identifying the stocks with greatest population decline, may be thwarted. A one-size-fits-all approach is not needed to compare risk. As I have shown, stochastic growth rate can be estimated in data-poor situations where only spawner counts and maximum age at return are known, or in data rich situations where age structure of recruits is known as well. Because drawing inferences about population growth is often difficult due to high variability, the choice of estimator ought not be based on what is simplest to implement or what may be uniformly applied, but on what yields the most accurate, and hence informative, result.

Acknowledgements

This study was funded by the U.S. Department of Energy, Bonneville Power Administration Contract No. 00004031. I thank Tom Cooney, Eli Holmes, Charlie Paulsen, and two anonymous referees for their suggestions and comments on earlier drafts of this paper.

References

Barlow, J. 1990. A birth-interval model for estimating cetacean reproductive rates for resighting data. Rep. Int. Whal. Comm. (Spec. Issue), **12**: 155–160.

Barlow, J., and Clapham, P.J. 1997. A new birth-interval approach to estimating demographic parameters of humpback whales. Ecology, **78**: 535–546.

Beamesderfer, R.C.P., Petrosky, C.E., Schaller, H.A., and Langness, O. 1997. Spawner-recruit data for spring and summer chinook salmon populations in Idaho, Oregon, and Washington. *In* Plan for Analyzing and Testing Hypotheses (PATH): report of retrospective analysis for fiscal year 1997. *Compiled and Edited by* D.R. Marmorek and C. Peters. ESSA Technologies Ltd., Vancouver, B.C.

Beamish, R.J., Noakes, D.J., McFarlane, G.A., Klyashtorin, L., Ivanov, V.V., and Kurashov, V. 1999. The regime concept and natural trends in the production of Pacific salmon. Can. J. Fish. Aquat. Sci. **56**: 516–526.

Botsford, L.W., and Brittnacher, J.G. 1998. Viability of Sacramento River winter-run chinook salmon. Conserv. Biol. **12**: 65–79.

Caswell, H. 2000. Matrix population models. 2nd ed. Sinauer Associates, Sunderland, Mass.

Caswell, H., Brault, S., Read, A.J., and Smith, T.D. 1998. Harbor porpoise and fisheries: an uncertainty analysis of incidental mortality. Ecol. Appl. **8**: 1226–1238.

Coulson, T., Mace, G.M, Hudson, E., and Possingham, H. 2001. The use and abuse of population viability analysis. Trends Ecol. Evol. **16**: 219–221.

Cumulative Risk Initiative. 2000. A standardized quantitative analysis of risks faced by salmonids in the Columbia River Basin. Cumulative Risk Initiative, Northwest Fisheries Science Center, NMFS–NOAA, 2725 Montlake Boulevard East, Seattle, Wash.

Dennis, B., Munholland, P.L, and Scott, J.M. 1991. Estimation of growth and extinction parameters for endangered species. Ecol. Monogr. **61**: 115–143.

Deriso, R.B., Marmorek, D.R., and Parnell, I.J. 2001. Retrospective patterns of differential mortality and common year-effects experienced by spring and summer chinook salmon (*Oncorhynchus tshawytscha*) of the Columbia River. Can. J. Fish. Aquat. Sci. **58**: 2419–2430.

Efron, B., and Tibshirani, R.J. 1993. An introduction to the bootstrap. Chapman & Hall/CRC, New York.

Fieberg, J., and Ellner, S.P. 2000. When is it meaningful to estimate an extinction probability? Ecology, **81**: 2040–2047.

Goodman, D. 2001. Managing Columbia Basin salmon: the facts, the questions, and the data. *In* What we don't know about Pacific Northwest fish runs. Proceedings of the Portland State University Salmon Symposium, Portland, Oreg., 7–8 July 2000. *Edited by* P. Koss and M. Katz. Portland State University, Portland, Oreg. pp. 5–23.

Hare, S.R., Mantua, N.J., and Francis, R.C. 1999. Inverse production regimes: Alaska and West Coast Pacific salmon. Fisheries (Bethesda), **24**: 6–14.

Hilborn, R., and Starr, P.J. 1984. Making stock-recruitment work. *In* Proceedings of the workshop on stream indexing for salmon escapement estimation. *Edited by* P.E.K. Symons and M. Waldichuck. Can. Tech. Rep. Fish. Aquat. Sci. No. 1326. pp. 227–244.

Heyde, C.C., and Cohen, J.E. 1985. Confidence intervals for demographic projections based on products of random matrices. Theor. Popul. Biol. **27**: 120–153.

Holmes, E.E. 2001. Estimating risks in declining populations with poor data. Proc. Natl. Acad. Sci. U.S.A. **98**: 5072–5077.

Kareiva, P., Marvier, M., and McClure, M. 2000. Recovery and management options for spring/summer chinook salmon in the Columbia River Basin. Science (Washington, D.C.), **290**: 977–979.

Lande, R., and Orzack, S.H. 1988. Extinction dynamics of age-structured populations in a fluctuating environment. Proc. Natl. Acad. Sci. U.S.A. **85**: 7418–7421.

Leslie, P.H. 1948. Some further notes on the use of matrices in population mathematics. Biometrika, **35**: 213–245.

Ludwig, D. 1999. Is it meaningful to estimate a probability of extinction? Ecology, **80**: 298–310.

Press, W.H., Teukolsky, S.A., Vetterling, W.T., and Flannery, B.P. 1992. Numerical recipes in FORTRAN. Cambridge University Press, New York.

Rajarshi, M.B. 1990. Bootstrap in Markov-sequences based on estimates of transition density. Ann. Inst. Statist. Math. **42**: 253–268.

Schaller, H.A., Petrosky, C.E., and Langness, O.P. 1999. Contrasting patterns of productivity and survival rates for stream-type chinook salmon (*Oncorhynchus tshawytscha*) populations of the Snake and Columbia rivers. Can. J. Fish. Aquat. Sci. **56**: 1031–1045.

Tuljapurkar, S.D. 1989. An uncertain life: demography in random environments. Theor. Popul. Biol. **35**: 227–294.

Tuljapurkar, S.D., and Orzack, S.H. 1980. Population dynamics in variable environments. I. Long-run growth rates and extinction. Theor. Popul. Biol. **18**: 314–342.

Nutrient, chlorophyll, and water clarity relationships in Florida's nearshore coastal waters with comparisons to freshwater lakes

Mark V. Hoyer, Thomas K. Frazer, Sky K. Notestein, and Daniel E. Canfield, Jr.

Abstract: Models relating chlorophyll to nutrients and Secchi depth to chlorophyll using data from nearshore coastal waters of Florida were successfully developed. The models suggest that phosphorus is the primary limiting factor for phytoplankton in the nearshore coastal waters of Florida and that total phosphorus concentration accounts for 81% of the variance in chlorophyll concentration. The models also show that chlorophyll is the dominant factor determining Secchi depth in nearshore coastal waters of Florida and that chlorophyll concentrations account for 68% of the variance in Secchi depth. Thus, these models are robust and should be useful for eutrophication management of Florida's coastal marine systems. The models developed with data from nearshore coastal waters of Florida are similar to models developed for freshwater lakes in Florida, but the amount of chlorophyll per unit of phosphorus and Secchi depth per unit of chlorophyll are both significantly less for marine samples. This suggests that the chlorophyll to biovolume ratios in the nearshore coastal waters of Florida are less than in freshwater systems of Florida. Therefore, nutrient to chlorophyll and chlorophyll to Secchi depth models developed for freshwater systems are probably ill suited for use in Florida's marine systems.

Résumé : Nous avons élaboré des modèles efficaces qui relient la chlorophylle aux nutriments et la profondeur de Secchi à la chlorophylle à l'aide de données récoltées dans les eaux côtières près du littoral de la Floride. Les modèles indiquent que le phosphore est le principal facteur limitant du phytoplancton dans ces eaux et que la concentration de phosphore total explique 81 % de la variance de la concentration de chlorophylle. De plus, la chlorophylle est le facteur principal qui détermine la profondeur de Secchi et les concentrations de chlorophylle expliquent 68 % de la variance de la profondeur de Secchi. Ces modèles s'avèrent donc robustes et devraient être utiles pour gérer l'eutrophisation des systèmes marins côtiers de la Floride. Les modèles élaborés à partir de données provenant des eaux côtières près du littoral de la Floride sont semblables à ceux qui ont été créés pour les lacs d'eau douce de la Floride, mais la quantité de chlorophylle par unité de phosphore et la profondeur de Secchi par unité de chlorophylle sont significativement moins grandes en milieu marin. Il semble donc que les rapports entre la chlorophylle et le biovolume sont plus petits dans les eaux marines côtières de la Floride que dans les milieux d'eau douce du même état. En conséquence, les modèles élaborés en eau douce, qui mettent en relation les nutriments et la chlorophylle ainsi que la chlorophylle et la profondeur de Secchi, s'appliqueront assez mal aux systèmes marins de la Floride.

[Traduit par la Rédaction]

Introduction

Strong relationships between phosphorus, chlorophyll, and water clarity have been observed and reported for freshwater systems around the world (e.g., Sakamoto 1966; Brown et al. 2000). Moreover, there has been a suite of both small- and large-scale experiments implicating phosphorus as the primary nutrient limiting primary production in many, if not most, freshwater systems (see e.g., Schindler 1975). The generality of the relational data coupled with the experimental findings has lead to the development of empirical loading models to predict in-lake phosphorus concentrations as a function of annual phosphorus load, adjusting for differences in lake morphometry and hydraulic residence time (e.g., Vollenweider 1976; Canfield and Bachmann 1981). These models have been the principle tools of lake managers concerned with eutrophication issues over the last 30 years.

With regard to lakes, phosphorus concentrations are typically calculated with phosphorus loading models, and the calculated phosphorus concentrations are, in turn, used in regression models to estimate chlorophyll concentrations. As chlorophyll concentrations are, in many cases, strongly related to water clarity as measured by Secchi depth, the chain of relations allows for a determination of how much nutrient needs to be controlled to achieve a specified reduction in chlorophyll and concomitant increase in water clarity. This general approach has been successful in eutrophication management for many lakes in both Europe and North America (e.g., OECD 1982; Cooke et al. 1993), although it has not been widely applied to the management of coastal marine systems.

Eutrophication of estuaries and coastal waters is, relative

Received 23 October 2001. Accepted 23 May 2002. Published on the NRC Research Press Web site at http://cjfas.nrc.ca on 25 July 2002.
J16584

M.V. Hoyer,[1] T.K. Frazer, S.K. Notestein, and D.E. Canfield, Jr. Department of Fisheries and Aquatic Sciences, University of Florida, Gainesville, FL 32653, U.S.A.

[1] Corresponding author (e-mail: mvhoyer@ufl.edu).

DOI: 10.1139/F02-077

to lakes, a recent problem (Smith et al. 1999; Cloern 2001), though global in scope (Nixon 1995). The possibility of applying an empirically based modeling approach to marine systems to facilitate nutrient-related management strategies was first considered by Vollenweider (1992), and the development of such a modeling framework was a major recommendation of a recent U.S. national nutrient assessment workshop (U.S. EPA 1996). Meeuwig et al. (2000) subsequently used a total phosphorus mass balance model and a total phosphorus and chlorophyll model to accurately predict chlorophyll concentrations in 19 Finnish estuaries. Similar success was had using data from 15 estuaries in Prince Edward Island (Meeuwig 1999). These studies clearly suggest a potential for the use of empirically based models that predict the consequences of increased nutrient loading to estuaries and coastal marine waters. Unfortunately, there are a limited number of such models in existence.

A major objective of this work was to develop nutrient–chlorophyll and chlorophyll – water clarity models using broad-scale survey data collected from nearshore coastal waters around Florida. Because research on the eutrophication of freshwater systems is well advanced compared with that of marine systems, we also compared the models that we developed with existing freshwater models to determine if freshwater models could be applied to coastal systems.

Methods

Between October 2000 and July 2001, surface water (0.5 m) samples were collected on three separate dates (for most sites) from 300 sites located around the entire coast of Florida (Fig. 1). All sampling sites were located within 10 km of shore and some were within the intercoastal waterways of Florida. On each date and at each sampling station, dissolved oxygen concentration ($mg \cdot L^{-1}$), temperature (°C), and salinity (‰) were measured in situ with a hand-held meter (model 85; Yellow Springs Instrument Company Inc., Yellow Springs, Ohio). Water clarity was also measured on each visit with a Secchi disk (m), and the actual water depth was recorded.

Surface water samples were collected in acid-cleaned bottles and transported on ice to the laboratory where they were analyzed for total phosphorus ($\mu g \cdot L^{-1}$), total nitrogen ($\mu g \cdot L^{-1}$), chlorophyll ($\mu g \cdot L^{-1}$), and color (Pt-Co units). Following persulfate digestion (Menzel and Corwin 1965), total phosphorus concentrations were determined using the procedures of Murphy and Riley (1962). Total nitrogen concentrations were determined from whole water samples by oxidizing water samples with persulfate and determining nitrate-nitrogen concentrations with a Bran-Luebbe (Houston, Tex.) autoanalyzer with a cadmium column reduction method (APHA 1989). Surface water chlorophyll concentrations were measured by filtering water through a 47-mm type A/E glass-fiber filter (Pall Corporation, Ann Arbor, Mich.) in the field. Subsequently, filters were stored over silica gel desiccant and then frozen before analysis. Chlorophyll was extracted with a hot ethanol method described by Sartory and Grobbelarr (1984), and chlorophyll concentrations were determined spectrophotometrically (Method 10200 H; APHA 1989). Color was determined spectrophotometrically on filtered water samples (APHA 1989).

Of the total 300 sites, 259 were sampled on three different dates, 35 were sampled on only two dates, and six sites were sampled on four dates. All data were averaged by site and the means were used for model development. All data were $\log_{10}$-transformed before statistical analyses to accommodate heterogeneity of variance (Snedecor and Cochran 1967). Computations were performed with the aid of a statistical software package (SAS Institute 2000), and statements of statistical significance imply $p < 0.05$ unless otherwise stated.

Results and discussion

The 300 sites sampled for this project covered almost all of the nearshore coastal waters around Florida (Fig. 1). All of the sites were within about 10 km of land with an average depth of 4.6 m (Table 1). The average salinity at the sites was 32‰, and average salinity was less than 10‰ at only 5 of the 300 sites. Samples were collected during both winter (2000) and summer (2001) periods, and as expected, there was a wide range in average temperatures among the sites (14.6–27.5°C). Mean oxygen concentrations were always greater than 4.4 $mg \cdot L^{-1}$. Color was generally low, averaging only 8 Pt-Co units, especially when compared with an average color of 44 Pt-Co units reported by Brown et al. (2000) for 360 Florida lakes. Secchi depth readings averaged 2.1 m and also exceeded the average of 1.9 m reported by Brown et al. (2000) for 354 Florida lakes. Total phosphorus and total nitrogen concentrations averaged 25 $\mu g \cdot L^{-1}$ and 309 $\mu g \cdot L^{-1}$, respectively (Table 1), which is less than the averages of 37 $\mu g \cdot L^{-1}$ and 690 $\mu g \cdot L^{-1}$ reported for Florida lakes (Brown et al. 2000). Chlorophyll concentrations averaged 3.7 $\mu g \cdot L^{-1}$, which was also less than the average of 23 $\mu g \cdot L^{-1}$ reported for Florida lakes (Brown et al. 2000).

Total phosphorus alone accounted for 81% of the variance in chlorophyll concentrations of nearshore coastal Florida waters, whereas nitrogen alone accounted for only 44% of the variance in chlorophyll concentrations (Table 2). These percentages are similar to those reported for Florida lakes (Table 2), where total phosphorus alone accounted for 76% of the variance in chlorophyll concentrations and total nitrogen accounted for only 46% of the variance in chlorophyll concentrations. Thus, the phosphorus–chlorophyll models presented for Florida's nearshore coastal waters (Table 2) are as robust as those developed for lakes and suggest that phosphorus accounts for more variance in chlorophyll than in nitrogen in both systems. Although nitrogen has been shown to limit algal populations in both freshwater and coastal systems (Elser et al. 1990; Downing 1997), the data presented here suggest that phosphorus is the primary nutrient limiting algal populations among the 300 nearshore coastal locations sampled in this study. We recognize, however, that some of these 300 stations may at some times be limited by nitrogen. Nevertheless, phosphorus explains most of the variance in chlorophyll concentrations among all 300 sites.

Chlorophyll accounted for 68% of the variance in Secchi depth for Florida's nearshore coastal waters, whereas color accounted for only 45% of the variance in Secchi depth (Table 2). Color has the potential to impact water clarity more in Florida lakes than in coastal waters because color values are generally higher in the lakes, as we indicated earlier. Therefore, to compare chlorophyll–Secchi and color–Secchi

Fig. 1. Location of 300 Florida nearshore coastal sites sampled three times between October 2000 and July 2001. The approximate center of Florida, U.S.A., is located at longitude 81°46′W and latitude 28°59′N.

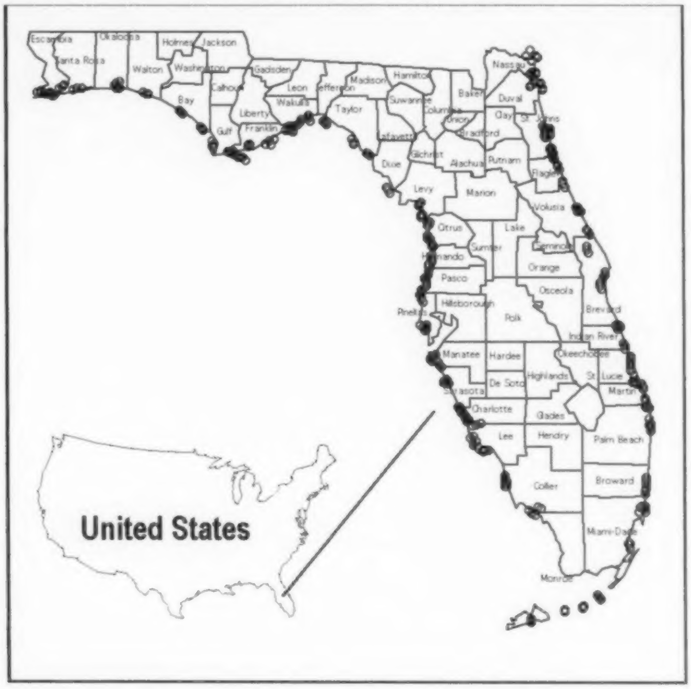
Escambia
Okaloosa
Holmes
Jackson
Santa Rosa
Walton
Washington
Gadsden
Calhoun
Bay
Leon
Jefferson
Madison
Hamilton
Wakulla
Liberty
Taylor
Suwannee
Columbia
Baker
Nassau
Duval
Gulf
Franklin
Lafayette
Union
Clay
St. Johns
Bradford
Gilchrist
Alachua
Putnam
Dixie
Flagler
Levy
Marion
Volusia
Citrus
Lake
Sumter
Seminole
Hernando
Orange
Pasco
Osceola
Pinellas
Hillsborough
Polk
Brevard
Indian River
Manatee
Hardee
Okeechobee
Highlands
St. Lucie
Sarasota
De Soto
Martin
Charlotte
Glades
Lee
Hendry
Palm Beach
Collier
Broward
Miami-Dade
Monroe
United States

Table 1. Mean, standard error, and minimum and maximum values for nine physical and chemical parameters estimated for 300 nearshore sites in the coastal waters around Florida.

Parameter	No. samples	Mean	Standard error	Minimum	Maximum
Depth (m)	300	4.6	0.2	0.5	17.7
Salinity (‰)	300	32.8	0.3	0.5	40.9
Temperature (°C)	300	21.4	0.2	14.6	27.5
Oxygen ($mg \cdot L^{-1}$)	300	6.9	0.1	4.4	22.7
Total phosphorus ($\mu g \cdot L^{-1}$)	300	25	1	3	122
Total nitrogen ($\mu g \cdot L^{-1}$)	300	309	10	93	1337
Chlorophyll ($\mu g \cdot L^{-1}$)	300	3.7	0.2	0.2	28.2
Secchi (m)	253	2.1	0.1	0.6	7.3
Color (Pt-Co units)	300	8	1	0	92

relationships for the nearshore coastal waters of Florida and Florida lakes, we selected a set of Florida lakes (n = 297) that averaged color values less than 32 Pt-Co units. We selected a maximum of 32 Pt-Co units for the lake data because 97.5% of the nearshore coastal sites had color values less than 32 Pt-Co units. As in the nearshore coastal sites, chlorophyll accounted for 72% and color accounted for 49% of the variance in Secchi depth among the 297 Florida lakes with color values less than 32 Pt-Co units. Thus, chlorophyll – water clarity models (Table 2) for nearshore coastal waters are as robust as those developed for lakes, and chlorophyll accounts for more variance in Secchi depth than does color.

The similarity in the relationships above for coastal marine and freshwater lakes (see Table 2) is intriguing. The data indicate clearly that phosphorus in both nearshore coastal waters and lakes of Florida accounts for most of the variance in chlorophyll concentrations and suggest that phosphorus is likely the primary nutrient limiting phytoplankton production in both. Canfield (1983) and Brown et al. (2000) have previously stated that phosphorus is the primary limiting nutrient in Florida lakes, and as the total nitrogen to total phosphorus ratio moves below 10, nitrogen may become limiting. It is generally assumed, however, that nitrogen is the primary limiting nutrient for phytoplankton production in most coastal waters (Downing 1997). There are few empirical data or direct experimental results to corroborate this for Florida's coastal environment, and the data reported here suggest otherwise.

Although the nature of the relationship between total phosphorus and chlorophyll is similar for both freshwater lakes and coastal marine waters in Florida (slopes and r^2 values are about the same), we observed that the intercept in

Table 2. Empirical models and summary statistics describing the association of annual average nutrient and chlorophyll concentrations, Secchi depth and chlorophyll, and color (Pt-Co) and total phosphorus values using data from the nearshore coastal waters of Florida and Florida freshwater lakes (Brown et al. (2000) and M.V. Hoyer, unpublished data).

Model	*N*	*F*	$p > F$	r^2
Florida nearshore coastal waters				
$\log_{10}\text{CHL} = -1.13 + 1.17\log_{10}\text{TP}$	300	1297	<0.01	0.81
$\log_{10}\text{CHL} = -2.99 + 1.38\log_{10}\text{TN}$	300	209	<0.01	0.41
$\log_{10}\text{Secchi} = 0.48 - 0.48\log_{10}\text{CHL}$	253	544	<0.01	0.68
$\log_{10}\text{Secchi} = 0.55 - 0.41\log_{10}\text{Color}$	253	212	<0.01	0.45
$\log_{10}\text{Secchi} = 1.04 - 0.59\log_{10}\text{TP}$	253	393	<0.01	0.61
Brown et al. (2000) for Florida lakes				
$\log_{10}\text{CHL} = -0.37 + 1.05\log_{10}\text{TP}$	533	1712	<0.01	0.76
$\log_{10}\text{CHL} = -2.42 + 1.21\log_{10}\text{TN}$	533	444	<0.01	0.46
Florida freshwater lakes with average color <32 Pt-Co units				
$\log_{10}\text{Secchi} = 0.65 - 0.43\log_{10}\text{CHL}$	297	789	<0.01	0.72
$\log_{10}\text{Secchi} = 0.76 - 0.43\log_{10}\text{Color}$	297	106	<0.01	0.26
$\log_{10}\text{Secchi} = 0.88 - 0.48\log_{10}\text{TP}$	296	270	<0.01	0.47

Note: CHL, chlorophyll ($\mu g \cdot L^{-1}$); TP, total phosphorus ($\mu g \cdot L^{-1}$); TN, total nitrogen ($\mu g \cdot L^{-1}$); Secchi, Secchi depth (m).

the resultant regression equations appeared different for the two system types. Analysis of covariance shows that indeed both the slopes and the intercept for these relations are different. Importantly, the intercept for nearshore coastal waters was much less than the respective intercept in the lake model. To examine this difference further, we plotted the maximum and the mean chlorophyll response equations published by Brown et al. (2000) on the total phosphorus and chlorophyll data collected for both studies (Fig. 2). All of the nearshore coastal data fall well below the maximum response equation, and all but five sites fall well below the mean response equation. Thus, although the amount of variance in chlorophyll concentrations accounted for by total phosphorus is similar, it appears that the amount of chlorophyll per unit of phosphorus is much less in the nearshore coastal water than in the freshwater lakes of Florida.

In freshwater lakes, when the chlorophyll response per unit of phosphorus is below published averages, researchers often suggest that nitrogen may be the nutrient most limiting chlorophyll concentrations and note that this usually occurs when the total nitrogen to total phosphorus ratio (by weight) falls below 10 (e.g., Sakamoto 1966; Smith 1982). As marine scientists and oceanographers typically prefer to examine molar ratios of nitrogen to phosphorus, we note that atomic N to P ratios less than 16 (equivalent to 7 by weight) are generally considered nitrogen limited in marine systems (e.g., Heckey and Kilham 1988; Downing 1997). To further examine the relationship between and nitrogen and phosphorus for the nearshore coastal waters of Florida, we plotted total phosphorus ($\mu g \cdot L^{-1}$) against total nitrogen ($\mu g \cdot L^{-1}$) and placed a line on the graph representing a total nitrogen to total phosphorus ratio of 10 by weight (Fig. 3). The vast majority of the sites have annual average total nitrogen to total phosphorus ratios greater than 10 and almost all would exceed a ratio of 7, suggesting as do the models (Table 2), that phosphorus may be the primary limiting nutrient for phytoplankton at most sites. The high N to P ratios do not explain, however, why the chlorophyll yield per unit of phosphorus is so low (Fig. 2).

Fig. 2. Relations between total phosphorus and chlorophyll for 300 nearshore Florida coastal sites (solid circles) and 533 Florida lakes (open circles, Brown et al. 2000). The uppermost regression line is the maximum chlorophyll response to phosphorus reported for Florida lakes (Brown et al. 2000). The other two lines represent the linear regressions for each data set. Analysis of covariance indicates that both the slopes and the intercepts of these regressions are significantly different ($p = 0.05$).

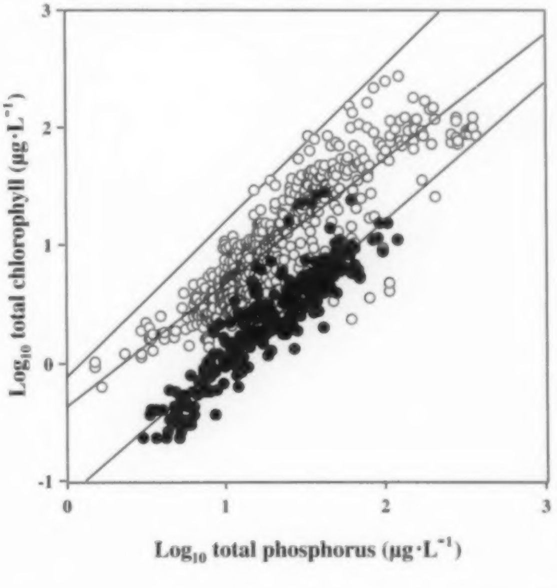

High concentrations of inorganic suspended solids and color can cause light limitation and have been shown to suppress chlorophyll concentrations per unit of phosphorus in freshwater lakes (Hoyer and Jones 1983; Brown et al. 2000). The impacts of the inorganic suspended solids and color, however, generally occur at higher chlorophyll concentrations, resulting in extremely low Secchi depths. This was not

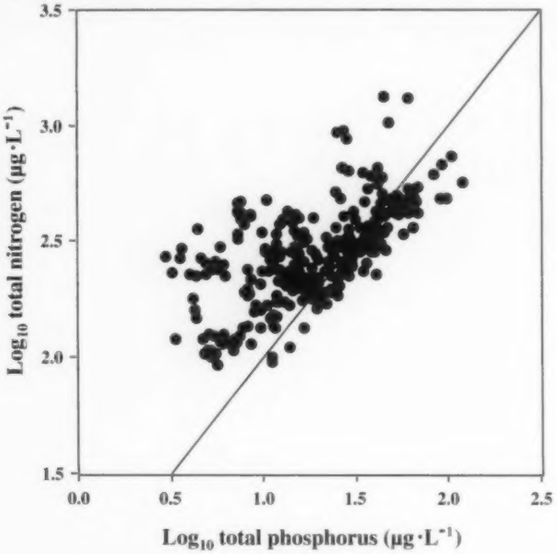

Fig. 3. Relation between total phosphorus and total nitrogen for the nearshore coastal waters of Florida. The line represents the ratio of total nitrogen to total phosphorus (by weight).

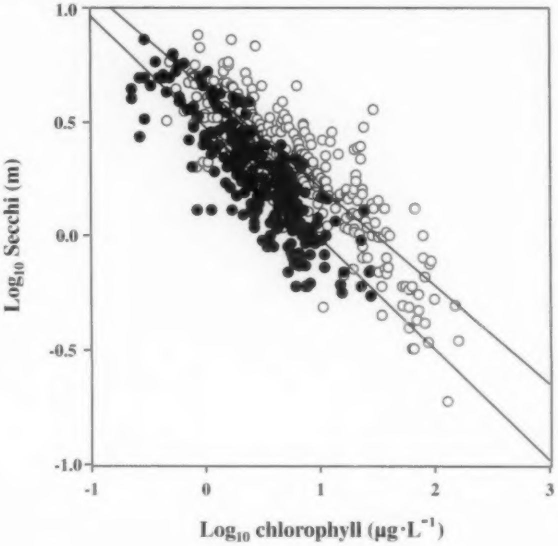

Fig. 4. Relations between chlorophyll and Secchi depth for 300 nearshore Florida coastal sites (solid circles) and 297 Florida lakes with color values less than 32 Pt-Co units (open circles; M.V. Hoyer, unpublished data). The two lines represent the linear regressions for each data set. Analysis of covariance indicates that both the slopes and the intercepts of these regressions are significantly different ($p = 0.05$).

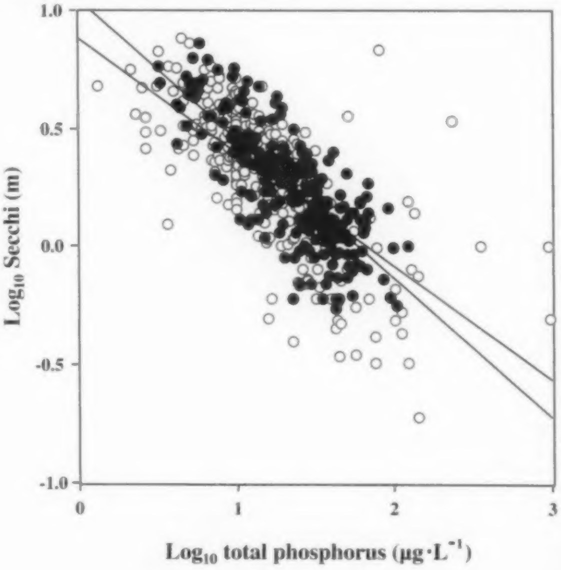

Fig. 5. Relations between total phosphorus and Secchi depth for 300 nearshore Florida coastal sites (solid circles) and 297 Florida lakes with color values less than 32 Pt-Co units (open circles; M.V. Hoyer, unpublished data). The two lines represent the linear regressions for each data set. Analysis of covariance shows that both the slopes and the intercepts of these regressions are not significantly different ($p = 0.05$).

observed in the nearshore coastal data reported here. The average Secchi depth for all 300 sites was 2.1 m (Table 1), and color values for all 300 sites averaged only 8 Pt-Co units. Thus, it is highly unlikely that inorganic suspended solids or color could be suppressing the amount of chlorophyll per unit of phosphorus in the nearshore coastal waters of Florida.

A high flushing rate of freshwater aquatic systems impacts chlorophyll concentrations by washout or removal of phytoplankton before algal standing crop reaches levels determined by concentrations of limiting nutrients (Swanson and Bachmann 1976; Soballe and Kimmel 1987). High flushing has also been shown to suppress algal biomass in the York River estuary (Sin et al. 1999) and the Hudson River estuary (Howarth et al. 2000). A mechanism explaining this suggests that water from springs or rainfall with few or no algal cells needs time for the algal cells to grow and exploit available nutrients in the water. Thus, as the water ages, algal cells eventually reach a level where some nutrient or other factor limits further growth. Bioassays from 20 Florida rivers suggest that it takes from 3 to 7 days to reach this level (Canfield and Hoyer 1988). All of the sites for this study are considerably distant from the headwaters of any river or spring run (Fig. 1). The sites also have an average salinity of 32‰, suggesting that freshwater has mixed with marine water and that the water we sampled probably had 3–7 days for algal populations to reach some level determined by nutrients or some other limiting factor. Therefore, it is unlikely that flushing rates are suppressing the chlorophyll per unit of phosphorus in the nearshore coastal waters of Florida.

Zooplankton and shellfish have both been shown to decrease chlorophyll concentrations in lakes and estuaries (Quiros 1990; Meeuwig et al. 1998). Thus, differential levels of top-down control on algal populations are another possible explanation for the low chlorophyll concentrations per

Table 3. Frequency distributions for the ratio of chlorophyll ($\mu g \cdot L^{-1}$) to volatile suspended solids ($mg \cdot L^{-1}$) for three different Florida gulf coast saltwater habitats (T.K. Frazer, unpublished data), three different freshwater habitat types (Kings Bay/Crystal River, Florida (Hoyer et al. 2001), and Lake Istokpoga and Lake Hatchineha, Florida (Lamb 2000)), and 53 Missouri reservoirs (Hoyer and Jones 1983).

		Percentiles				
System	No. samples	10%	25%	50%	75%	90%
Saltwater						
Marsh	14	0.1	0.2	0.3	0.5	0.9
Estuary	40	0.1	0.1	0.4	0.7	1.5
Gulf	26	0.1	0.2	0.3	0.4	0.9
Freshwater						
Kings Bay	217	2.3	3.4	5.3	7.7	10.7
Lake Istokpoga	288	1.8	2.7	3.5	5.0	6.7
Lake Hatchineha	334	3.5	4.4	5.8	8.1	11.1
Missouri reservoirs	53	2.1	3.8	4.8	5.8	7.5

unit of phosphorus observed in nearshore coastal waters. The whole body of nearshore coastal chlorophyll data, however, is suppressed below that of Florida lakes (Fig. 2) per unit of phosphorus, suggesting that if top-down control is occurring than it is occurring around the whole state of Florida. This would be inconsistent with areas that are devoid of shellfish or areas in the nearshore coastal waters that have large populations of planktivores (Florida Marine Research Institute 2001) that would minimize any impacts of zooplankton grazing. These areas should then have higher chlorophyll per unit of phosphorus, which is not observed in any of the 300 nearshore coastal sites.

As nitrogen, suspended solids, color, flushing rate, or top-down control are not likely factors responsible for the suppression of chlorophyll per unit of phosphorus in the nearshore coastal waters of Florida, other alternatives must be explored. One possible hypothesis to explain the relatively low chlorophyll yield per unit phosphorus is that the chlorophyll per unit biomass of algal cells is less in nearshore coastal waters than in lakes of Florida. The use of chlorophyll as an indicator of algal biomass can be problematic, however, because the ratio of chlorophyll to biomass or biovolume varies among species, systems, and environmental conditions (Heyman and Lundgren 1988; White et al. 1988; Kalchev et al. 1996). Nevertheless, if the chlorophyll to biomass ratio in nearshore coastal waters of Florida is significantly less than the chlorophyll to biomass ratio in freshwater lakes, this may explain the low yields of chlorophyll per unit of phosphorus in nearshore coastal waters (Fig. 2), and we can still assert that phosphorus is likely the primary limiting factor for phytoplankton in the nearshore coastal waters. On the other hand, if the chlorophyll to biomass ratios in nearshore coastal waters is the same as those in lakes, then some other factor is needed to explain the suppression of chlorophyll per unit phosphorus.

To examine this possibility further, we compared the models relating Secchi depth to chlorophyll for nearshore coastal waters and freshwater lakes (Table 2). An analysis of covariance shows that both the slope and intercept are significantly different. Looking at the plotted data for both systems (Fig. 4), it is easy to see that the Secchi depth per unit of chlorophyll in the nearshore coastal waters is less than that in Florida lakes. If the chlorophyll to biomass ratio was the same for both systems, then the Secchi depths per unit of chlorophyll should overlap considerably because the algal populations are the dominant factors determining water clarity in both systems (Table 2).

Following similar logic, we compared the models relating Secchi depth to total phosphorus for nearshore coastal waters and freshwater lakes (Table 2). An analysis of covariance shows that both the slope and intercept are not significantly different. Looking at the plotted data for both systems (Fig. 5), it is easy to see that the Secchi depth per unit of phosphorus in the nearshore coastal and Florida lakes overlap almost completely. Assuming algal cells are the dominate factor determining Secchi depth in both systems and that phosphorus is the primary limiting factor, which we discussed earlier, then Secchi depth per unit of phosphorus should exhibit considerable overlap. If some other factor (other than phytoplankton) was suppressing Secchi depth in nearshore coastal waters, then the Secchi depths per unit of phosphorus in the coastal waters should be suppressed similar to the Secchi – chlorophyll models (Fig. 4). These data strongly suggest that the chlorophyll to biomass ratio of algal cells in nearshore coastal waters is less than that in freshwater lakes.

Additional data provide further support that chlorophyll to biomass ratios in nearshore coastal waters are less than in Florida lakes. Suspended solids and chlorophyll data, both from marine and freshwater systems, are provided in Table 3. The median values for the ratio of chlorophyll to volatile suspended solids in saltwater marsh, estuary, and gulf coast habitats were 0.3, 0.4, and 0.3, respectively (T.K. Frazer, unpublished data). The median values for the same ratio in four freshwater systems (Kings Bay, Florida (Hoyer et al. 2001), Lake Istokpoga, and Lake Hatchineha, Florida (Lamb 2000)) and 53 Missouri reservoirs (Hoyer and Jones 1983) are much higher at 5.3, 3.5, 5.8, and 4.8, respectively. The difference is large enough that the upper 90th percentile for the marine data does not overlap with the lower 10th percentile of the freshwater data (Table 3).

Many factors could impact the ratio between chlorophyll and volatile suspended solids, especially the presence of organic matter other than algal cells. However, chlorophyll and color account for a large percent of Secchi depth variance in both nearshore coastal waters and lakes (Table 2), and the presence of other organic substances would probably weaken those relations. In addition, Kings Bay, Lake Istokpoga, and Lake Hatchineha are shallow systems with abundant aquatic macrophytes, suggesting that the water column could have additional organics other than algal cells, which would only tend to lower the chlorophyll to volatile solids ratio for these freshwater systems. For the Missouri reservoirs, Jones and Hoyer (1982) showed a strong relation between volatile suspended solids and chlorophyll. These findings, and those above, all support the hypothesis that the chlorophyll to algal biomass ratio in the nearshore coastal waters is much less than that in Florida lakes.

Finally, we observed that average chlorophyll to biovolume ratios appear to be less in marine systems than in Florida lakes. Phlips et al. (1999) reported the seasonal average chlorophyll to biovolume ratios for four sites in Florida

Bay, sampled in four different seasons for 5 years. The average for these data was 0.0036 mg chlorophyll$\cdot$mm^{-3} with a range of 0.0014 to 0.0076 mg chlorophyll$\cdot$mm^{-3}. Similar to these values, Tolstoy (1979) reported the chlorophyll to biovolume ratios for four marine systems from the literature that averaged 0.0034 mg chlorophyll$\cdot$mm^{-3} with a range of 0.0019 to 0.0063 mg chlorophyll$\cdot$mm^{-3}. These average values are both less (by over 25%) than the average chlorophyll to biovolume ratio of 0.0049 mg chlorophyll$\cdot$mm^{-3} reported for data from 165 Florida lakes (Canfield et al. 1985) and lend further support to the hypothesis above.

In conclusion, it appears that the general principles applied successfully to the control of eutrophication in freshwaters can be applied to coastal marine systems in Florida. In this study, we successfully developed models relating chlorophyll to nutrients and Secchi depth to chlorophyll using data from nearshore coastal waters of Florida. The models suggest that phosphorus is often the primary limiting factor for phytoplankton production in the nearshore coastal waters of Florida and that phosphorus can account for 81% of the variance in chlorophyll concentrations. The models also show that chlorophyll is the dominant factor determining Secchi depth in nearshore coastal waters of Florida and that chlorophyll can account for 68% of the variance in Secchi depth. Thus, these models are robust and should be useful for eutrophication management of marine systems.

The eutrophication models that we developed using data from nearshore coastal waters of Florida are similar to models developed for freshwater lakes in Florida, but the amount of chlorophyll per unit of phosphorus and Secchi depth per unit of chlorophyll are both significantly less. This suggests that the chlorophyll to biovolume ratios in the nearshore coastal waters of Florida are less than those in freshwater systems of Florida. Therefore, chlorophyll to phosphorus and Secchi depth to chlorophyll models developed for freshwater systems are probably ill suited for use in marine systems. Freshwater models used for prediction in nearshore coastal systems would overestimate chlorophyll based on phosphorus concentrations and overestimate Secchi depth based on chlorophyll concentrations.

Acknowledgments

This article is Journal Series No. R-08677 of the Florida Agricultural Experiment Station. We thank David Girardin (St. John's River Water Management District) and Fred Vose (Florida Marine Research Institute) for supplying boats and assistance in collecting some samples. We thank Rebecca Varner, David Gietbrock (Florida LAKEWATCH), and others for collecting samples around the coast of Florida. We thank Mary Stonecipher and others for laboratory analyses. We thank Roger Bachmann for comments on an early draft of this manuscript. Dr. Jessica Meeuwig and an anonymous reviewer added significantly to the strength of the final manuscript. This project was funded, in part, by the Southwest Florida Water Management District via the Surface Water Improvement and Management Program and the Coastal River Basin Board and the State of Florida Water Quality Assurance Trust Fund.

References

American Public Health Association (APHA). 1989. Standard methods for the examination of water and wastewater. 17th ed. American Public Health Association, Washington, D.C.

Brown, C.D., Hoyer, M.V., Bachmann, R.W., and Canfield, D.E., Jr. 2000. Nutrient–chlorophyll relationships: an evaluation of empirical nutrient–chlorophyll models using Florida and northern temperate lake data. Can. J. Fish. Aquat. Sci. **57**: 1574–1583.

Canfield, D.E., Jr. 1983. Prediction of chlorophyll a concentrations in Florida lakes: the importance of phosphorus and nitrogen. Water Res. Bull. **19**(2): 255–262.

Canfield, D.E., Jr., and Bachmann, R.W. 1981. Prediction of total phosphorus concentrations, chlorophyll *a*, and Secchi depths in natural and artificial lakes. Can. J. Fish. Aquat. Sci. **38**: 414–423.

Canfield, D.E., Jr., and Hoyer, M.V. 1988. Nutrient assimilation capacity of the Little Wekiva River. Final Report. City of Altamonte Springs, Altomonte Springs, Florida.

Canfield, D.E., Jr., Linda, S.B., and Hodgson, L.M. 1985. Chlorophyll–biomass–nutrient relationships for natural assemblages of Florida phytoplankton. Water Resour. Bull. **21**: 381–391.

Cloern, J.E. 2001. Our evolving conceptual model of the coastal eutrophication problem. Mar. Ecol. Prog. Ser. **210**: 223–253.

Cooke, G.D., Welch, E.B., Peterson, S.A., and Newroth, P.R. 1993. Restoration and management of lakes and reservoirs. 2nd ed. CRC Press, Inc., Boca Raton, Fla.

Downing, J.A. 1997. Marine nitrogen: phosphorus stochiometry and the global N:P cycle. Biogeochemistry, **37**: 237–252.

Elser, J.J., Marzolf, E.R., and Goldman, C.R. 1990. Phosphorus and nitrogen limitation of phytoplankton growth in the freshwaters of North America: a review and critique of experimental enrichments. Can. J. Fish. Aquat. Sci. **47**: 1448–1477.

Florida Marine Research Institute. 2001. Status and trends 2001 report—Florida's inshore and nearshore species. Florida Fish and Wildlife Conservation Commission, Florida Marine Research Institute, Education and Information Program, St Petersburg, Fla.

Hecky, R.E., and Kilham, P. 1988. Nutrient limitation of phytoplankton in freshwater and marine environments: a review of recent evidence on the effects of enrichment. Limnol. Oceanogr. **33**: 796–822.

Heyman, U., and Lundergren, A. 1988. Phytoplankton biomass and production in relation to phosphorus—some conclusions from field studies. Hydrobiologia, **170**: 211–227.

Howarth, R.W., Swaney, D.P., Butler, T.J., and Marino, R. 2000. Climate control on eutrophication of the Hudson River estuary. Ecosystems, **3**: 210–215.

Hoyer, M.V., and Jones, J.R. 1983. Factors affecting the relation between phosphorus and chlorophyll *a* in midwestern reservoirs. Can. J. Fish. Aquat. Sci. **40**: 192–199.

Hoyer, M.V., Frazer, T.K., Canfield, D.E., Jr., and Lamb, J.M. 2001. Vegetation evaluation in Kings Bay/Crystal River. Final Report. Southwest Florida Water Management District, Surface Water Improvement and Management Department, Tampa, Fla.

Jones, J.R., and Hoyer, M.V. 1982. Sportfish harvest predicted by summer chlorophyll *a* concentration in midwestern lakes and reservoirs. Trans. Am. Fish. Soc. **111**: 176–179.

Kalchev, R.K., Beshkova, M.B., Boumbarova, C.S., Tsvetkova, R.L., and Sais, D. 1996. Some allometric and non-allometric relationships between chlorophyll-a and abundance variables of phytoplankton. Hydrobiologia, **341**: 235–245.

Lamb, J.M. 2000. Wind-induced sediment resuspension in relation to varying submerged macrophyte coverage in two shallow Florida lakes (Lake Istokpoga and Lake Hatchineha). M.S. thesis, University of Florida, Gainesville, Fla.

Meeuwig, J.J. 1999. Predicting coastal eutrophication from land-use: an empirical approach to small non-stratified estuaries. Mar. Ecol. Prog. Ser. **176**: 231–241.

Meeuwig, J.J., Rasmussen, J.B., and Peters, R.H. 1998. Turbid waters and clarifying mussels: their moderation of empirical chl:nutrient relations in estuaries in Prince Edward Island, Canada. Mar. Ecol. Prog. Ser. **171**: 139–150.

Meeuwig, J.J., Kauppila, P., and Pitkanen, H. 2000. Predicting coastal eutrophication in the Baltic: a limnological approach. Can. J. Fish. Aquat. Sci. **57**: 844–855.

Menzel, D.W., and Corwin, N. 1965. The measurement of total phosphorus in seawater based on the liberation of organically bound fractions by persulfate oxidation. Limnol. Oceanogr. **10**: 280–282.

Murphy, J., and Riley, J.P. 1962. A modified single solution method for the determination of phosphate in natural waters. Anal. Chim. Acta, **27**: 31–36.

Nixon, S.W. 1995. Coastal marine eutrophication: a definition, social causes, and future concerns. Ophelia, **41**: 199–219.

Organisation for Economic Cooperation and Development (OECD). 1982. Eutrophication of waters: monitoring, assessment and control. Organisation for Economic Cooperation and Development, Paris.

Phlips, E.J., Badylak, S., and Lynch, T.C. 1999. Blooms of the picoplanktonic cyanobacterium Synechoccus in Florida Bay, a subtrophical inner-shelf lagoon. Limnol. Oceanogr. **44**: 166–1175.

Quiros, R. 1990. Factors related to variance of residuals in chlorophyll – total phosphorus regressions in lakes and reservoirs of Argentina. Hydrobiologia, **200/201**: 343–355.

Sakamoto, M. 1966. Primary production by phytoplankton community in some Japanese lakes and its dependence on lake depth. Arch. Hydrobiol. **62**: 1–28.

Sartory, D.P., and Grobbelarr, J.U. 1984. Extraction of chlorophyll *a* from freshwater phytoplankton for spectrophotometric analysis. Hydrobiologia, **114**: 117–187.

SAS Institute. 2000. JMP Statistics and Graphics Guide. SAS Institute, Inc., Cary, N.C.

Schindler, D.W. 1975. Whole-lake eutrophication experiments with phosphorus, nitrogen and carbon. Ver. Int. Ver. Theor. Angew. Limnol. **19**: 3221–3231.

Sin, Y.S., Wetzel, R.L., and Anderson, I.C. 1999. Spatial and temporal characteristics of nutrient and phytoplankton dynamics in the York River estuary, Virginia: analyses of long-term data. Estuaries, **22**: 260–275.

Smith, V.H. 1982. The nitrogen and phosphorus dependence of algal biomass in lakes: an empirical and theoretical analysis. Limnol. Oceanogr. **27**(6): 1101–1112.

Smith, V.H., Tillmen, G.D., and Nekola, J.C. 1999. Eutrophication: impacts of excess nutrient inputs on freshwater, marine and terrestrial ecosystems. Environ. Pollut. **100**: 179–196.

Snedecor, G.W., and Cochran, W.G. 1967. Statistical methods. 6th ed. Iowa State University Press, Ames, Iowa.

Soballe, D.M., and Kimmel, B.L. 1987. A large-scale comparison of factors influencing phytoplankton abundance in rivers, lakes and impoundments. Ecology, **68**: 1943–1954.

Swanson, C.D., and Bachmann, R.W. 1976. A model of algal exports in some Iowa Streams. Ecology, **57**: 1076–1080.

Tolstoy, A. 1979. Chlorophyll *a* in relation to phytoplankton volume in some Swedish lakes. Archiv. Hydrobiol. **85**: 133–151.

United States Environmental Protection Agency (U.S. EPA). 1996. National nutrient assessment workshop. Proceedings, December 4–6, 1995, USEPA 822-R-96-004. Office of Water, U.S. Government Printing Office, Washington, D.C.

Vollenweider, R.A. 1976. Advances in defining critical loading levels of phosphorus in lake eutrophication. Mem. Ist. Ital. Idrobiol. **33**: 53–83.

Vollenweider, R.A. 1992. Coastal marine eutrophication: principles and control. *In* Marine coastal eutrophication. The response of marine transitional systems to human impacts: problems and perspectives for restoration. *Edited by* R.A. Vollenweider, R. Marchetti, and R. Viviani. Science of the Total Environment 1992, Elsevier Science, Amsterdam, The Netherlands.

White, E.G., Payne, G., and Pickmore, S. 1988. A limitation to the usefulness of chlorophyll a as a biomass indicator in eutrophication studies. Verh. Internat. Verein. Limnol. **23**: 598–601.

Characterizing catch variability in a multispecies fishery: implications for fishery management

J.A.E. van Oostenbrugge, E.J. Bakker, W.L.T. van Densen, M.A.M. Machiels, and P.A.M. van Zwieten

Abstract: Exploiting several fish species simultaneously reduces variability in daily catches. The reduction depends on the number of species, the catch-frequency distributions of individual species, and the level of co-occurrence of species in the catch. We explore theoretically the reduction of variability (coefficient of variation; CV) in the total catch by combining the distributions of daily catches of individual fish species, including zero catches, into a total catch frequency distribution. Theoretical findings are tested with an example from a stationary lift-net fishery for schooling small pelagic species around Ambon Island in the Central Moluccas, Indonesia. This fishery catches over 30 species, all with high daily variability (CV = 2.2–13.4). The reduction of variability in the total catch (CV = 1.7) is a result of the dominance and independent occurrence of the three main species. We conclude that in this fishery the information value of the total catch as an indicator of the catches of the individual species is low.

Résumé : L'exploitation simultanée de plusieurs espèces de poissons peut réduire la variabilité des captures journalières. L'importance de cette réduction dépend du nombre d'espèces, de la distribution de fréquence des espèces dans la récolte et du niveau de la co-occurrence des espèces dans la récolte. Nous examinons en théorie la réduction de la variabilité (coefficient de variation; CV) dans les captures totales en combinant les distributions des captures journalières d'espèces particulières, incluant les captures nulles, dans la distribution de fréquence des captures totales. Un exemple tiré d'une pêche commerciale à carrelet de petits poissons pélagiques vivant en bancs près de l'Îsle Amboine (Moluques, Indonésie) permet de tester les résultats théoriques. Les récoltes incluent plus de 30 espèces de poissons, chacune avec une variabilité journalière élevée (CV = 2,2–13,4). La réduction de la variabilité dans la capture totale (CV = 1,7) est le résultat de la dominance et de l'occurrence indépendante des trois espèces principales. Dans cette pêche commerciale, la valeur prédictive de la capture totale comme indicateur de la capture des espèces particulières est basse.

[Traduit par la Rédaction]

Introduction

Together with the mean catch, variability in catch rate is one of the primary characteristics of a fishery, affecting many aspects of its functioning, such as its economy and the different options for its management (Platteau and Abraham 1987; van Oostenbrugge et al. 2001). Total variability in catch rate is determined by trends, cyclic patterns, persistence, and "random variation". Random variation on a daily scale causes what we may call basic uncertainty and is the result of small-scale spatial and temporal patterns of fish abundance on the fishing ground and the inability of fishers to respond accurately to such patterns.

Basic uncertainty is intrinsic to a fishery and its magnitude depends on the type of ecosystem, the state of the stocks, and the scale of the fishing operation (van Densen 2001). Variability in daily catches made by individual fishing units, expressed as the coefficient of variation (CV), can be used as a standardized measure of basic uncertainty. For instance, the typical variability in daily catch for fisheries using gill nets and small-scale purse seines on the nonschooling cichlids of Lake Malombe in Burundi is CV = 0.7–0.8 (van Zwieten et al. 2002). The variability in daily catch for the small-scale purse-seine fishery targeting schooling pelagic species in the coastal waters around Ambon Island in the Central Moluccas, Indonesia, is extremely high (CV = 3.1) and only a small proportion can be explained by external factors such as time trends and effects of the lunar cycle (van Oostenbrugge et al. 2001).

For individual species, variability in the catch depends on the dispersion (spatial pattern) of the targeted fish species, their temporal dynamics (dispersal) in relation to the scale of operation of the fishery, and the fishers' strategy. The variability in the total catch of a combination of species is inevi-

---

Received 29 January 2002. Accepted 27 May 2002. Published on the NRC Research Press Web site at http://cjfas.nrc.ca on 25 July 2002.
J16737

J.A.E. van Oostenbrugge,[1] M.A.M. Machiels, and P.A.M. van Zwieten. Fish Culture and Fisheries Group, Wageningen Institute of Animal Science, Wageningen University and Research Centre, P.O. Box 338, 6700 AH, Wageningen, The Netherlands.
E.J. Bakker. Mathematical and Statistical Methods Group, Department of Plant Sciences, Wageningen University and Research Centre, P.O. Box 9101, 6700 HB, Wageningen, The Netherlands.
W.L.T. van Densen. Netherlands Institute for Fisheries Research P.O. Box 68, 1970 AB IJmuiden, The Netherlands.

[1] Corresponding author (e-mail: hans.vanoostenbrugge@alg.venv.wau.nl).

DOI: 10.1139/F02-078

tably lowered compared with the variability in catches of the individual species because of statistical averaging (Doak et al. 1998). Since, with a few exceptions, all tropical fisheries are multispecies fisheries, the variability in the total catch is reduced compared with the variability in catches of individual species. This reduction is important for the fishers as well as for the managers, as the variability in the catches influences the economic uncertainty for the fishers and their ability to perceive differences that affect the functioning of the fishery and its management. Moreover, the reduced variability in the total catch can conceal decreases in catches of individual species and possible overfishing. However, the extent to which the variability is lowered depends on the number of species caught, the characteristics of their individual catch-frequency distributions (CFDs), and the level of their co-occurrence.

The effect of catching a multitude of species on the variability in the total catch is to a large extent comparable to the statistical effects of diversification as discussed in other fields of science. In economics the effect of diversification is well known as the "portfolio effect" and is widely used in the literature on both investment and livelihood diversification (Ellis 1998). In ecology, discussions on the statistical inevitability of stability–diversity relationships have received wide attention (Doak et al. 1998; Lehman and Tilman 2000). However, these discussions do not deal with a problem specific to small-scale multispecies fisheries: the large proportion of zero catches. In particular, small-scale fishers targeting schooling fish hardly ever catch more than a few schools per daily trip; therefore, subsequent catches of individual species include a large number of zero values (e.g., van Oostenbrugge et al. 2002). The probability of co-occurrence of species as well as the correlation in nonzero catches affect the covariance in catches of species; therefore, the reduction of variability is more complex than described in the literature. Because of this, earlier studies of variability in catches omitted zero values (Blanchard and Boucher 2001).

In this study, we first elaborate theoretically how variability is reduced by combining the different frequency distributions of daily catch per species, including zero catches. Subsequently, the theoretical results are tested with a stationary medium-scale lift-net fishery that uses light to attract small pelagic species in the coastal waters around Ambon Island. This fishery is known for its very high variability in daily catches and its low probability of nonzero catch for all species combined ($p = 0.55$) (van Oostenbrugge et al. 2002). In the Discussion we elaborate on the ecological reasons for typical species compositions and the consequences for the management of multispecies fisheries.

Materials and methods

Model

Depending on the size of the spatial window of operation for a fisher and the dispersion and dispersal of his target, the proportion of zero catches in daily catches can be considerable. In these cases, the CFD can be described as a combination of the probability of encountering and capturing a school (p) and a continuous distribution, representing the size of the nonzero catch. The mean, variance, and CV of the size of the catch of species i, including zero catches, are given by

$$(1) \qquad E(G_i) = p_i\mu_i$$

$$(2) \qquad \mathrm{Var}(G_i) = p_i[(1 - p_i)\mu_i^2 + \sigma_i^2]$$

and

$$(3) \qquad \mathrm{CV}(G_i) = \sqrt{\frac{\mathrm{CV}_i^2 + 1 - p_i}{p_i}}$$

where G_i is the size of the catch of species i (usually on a 1-day fishing trip), p_i is the probability of capture of species i, μ_i is the mean size of the nonzero catch of species i, σ_i is the standard deviation of the nonzero catch of species i, and CV_i is the CV of the size of the nonzero catch of species i (σ_i/μ_i). With decreasing p_i the ratio between $\mathrm{CV}(G_i)$ and CV_i increases and the variability in the total catch becomes larger (Fig. 1). If p_i is equal to unity, then $\mathrm{CV}(G_i)$ and CV_i are the same. Because of the lognormal CFD and the high probability of zero catches, estimators of the mean and variance from the delta distribution might be more efficient in the case of small sample sizes (Pennington 1996). These estimators are not used, as they are less straightforward and present difficulties when covariance in a multispecies context is considered.

If we combine two species (i and j), the total catch size can be calculated as $G = G_i + G_j$. Its mean ($E(G)$) and variance ($\mathrm{Var}(G)$) can be calculated as

$$(4) \qquad E(G) = E(G_i) + E(G_j) = p_i\mu_i + p_j\mu_j$$

and

$$(5) \qquad \mathrm{Var}(G) = \mathrm{Var}(G_i) + \mathrm{Var}(G_j) + 2\mathrm{Cov}(G_i,G_j)$$

in which $\mathrm{Cov}(G_i,G_j)$ is the covariance between G_i and G_j. Thus, the variability in the catch of the two species combined is calculated as

$$(6) \qquad \mathrm{CV}(G) = \frac{\sqrt{\mathrm{Var}(G_i) + \mathrm{Var}(G_j) + 2\mathrm{Cov}(G_i,G_j)}}{E(G_i) + E(G_j)}$$

In the simplest situation, i.e., that the two species caught have equal CFDs (p_i, μ_i, σ_i, and thus $E(G_i)$ and $\mathrm{Var}(G_i)$) and the two species are caught independently, so $\mathrm{Cov}(G_i,G_j) = 0$, eq. 6 is reduced to

$$(7) \qquad \mathrm{CV}(G) = \frac{1}{\sqrt{2}} \times \mathrm{CV}(G_i)$$

If the CFDs differ between the two species, as they will in practice, the resulting CV is influenced by the characteristics of the CFDs of the individual species and will be determined mostly by the species with a high mean catch and (or) a high variance (eq. 6). We show the changes in variability of the total catch, as a fraction of the variability in the catch of species i, in relation to the characteristics of the CFDs of two independently occurring species (i and j; Fig. 2). In Fig. 2 the effect of differences in each of the characteristics of the CFDs (p_i, μ_i, σ_i) is shown, whereas all other characteristics are kept constant and the same for the two species. When the CFDs of the two species are the same, the variability in the

Fig. 1. Mean, standard deviation (SD), and coefficient of variation in the total catch (CV_{tot} = SD/mean) in relation to the probability of capture (p). The mean and standard deviation of nonzero catches are constant: $\mu_{nonzero} = 1$, $\sigma_{nonzero} = 2$.

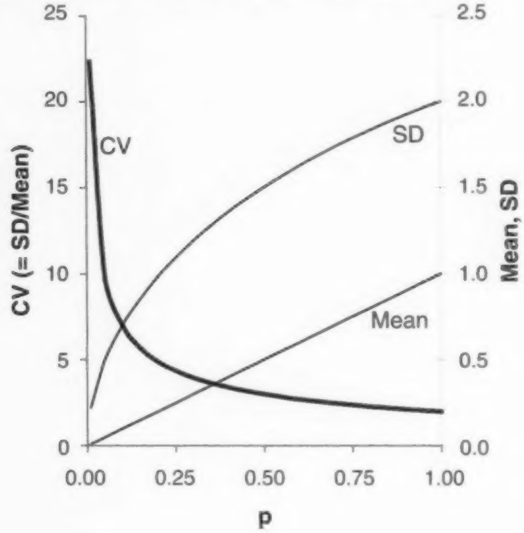

total catch is reduced by a factor $1/\sqrt{2}$, as was shown before (eq. 7). Differences in individual characteristics have particular effects: (*i*) Probability of capture (p) (Fig. 2*a*): the influence of a species with a low p value on the variability in the total catch is low compared with that of a species with a larger p value, because a lowered p value reduces the variance and mean catch, including zero values (eq. 6). Therefore, the smaller p_j is compared with p_i, the more the CV of the total catch (CV_{tot}) resembles the variability in the catch of species i. Conversely, the larger p_j is compared with p_i, the more CV_{tot} resembles the variability in the catch of species j. Because CV_i increases with decreasing p_i (Fig. 1), CV_{tot} becomes smaller relative to CV_i. (*ii*) Mean nonzero catch (μ) (Fig. 2*b*): CV_{tot} increases with decreasing μ_j (eq. 6); conversely, if μ_j is much larger than μ_i, the reduction in CV_{tot} relative to CV_i can be substantial. (*iii*) Standard deviation (σ) (Fig. 2*c*): with decreasing σ_j compared with σ_i, CV_{tot} becomes smaller; conversely, with increasing σ_j compared with σ_i, CV_{tot} becomes larger (eq. 6). Although the magnitude of the effect on total variability differs for other values of the characteristics illustrated (Fig. 2), the effect itself does not. In conclusion, we can state that the variability in the total catch will resemble the variability in the most common species in the catch with the largest standard deviation, while the large variability of rare species hardly contributes to the reduction in variability in the total catch of both species.

When the species are not caught independently, the covariance between the catches of the species affects the reduction of variability as well. To show this, we will consider the specific situation that the CFDs of the two species have the same characteristics ($\mathrm{Var}(G_i)$ and $E(G_i)$). In that case, eq. 6 reduces to

$$(8) \qquad CV(G) = \frac{\sqrt{2\mathrm{Var}(G_i) + 2\mathrm{Cov}(G_i, G_j)}}{2E(G_i)}$$

If the species are highly correlated and thus $\mathrm{Cov}(G_i,G_j)$ is close to $\mathrm{Var}(G_i)$, then $CV(G)$ will approximate $CV(G_i)$. If G_i and G_j are not highly correlated, then $CV(G)$ will be considerably smaller than $CV(G_i)$. $CV(G_i)$ can even become zero if $\mathrm{Cov}(G_i,G_j) = -\mathrm{Var}(G_i)$, a perfect negative correlation between G_i and G_j. In such an extreme situation, G_i is low whenever G_j is high and vice versa. Because the CFD of the individual species (i and j) includes zero catches (eqs. 1 and 2) it can be shown that

$$(9) \qquad \mathrm{Cov}(G_i,G_j) = p_i[(p_{j|i} - p_j)\,\mu_i\mu_j + p_{j|i} r \sigma_i \sigma_j]$$

where $p_{j|i}$ is the conditional probability of capture of species j, given the capture of species i, and r is the correlation coefficient of nonzero catches of species i and j. When species i and j are caught independently of each other, $p_{j|i} = p_j$ and $r = 0$. When species i and j are caught alternately, $p_{j|i} = 0$, so the total variance is reduced by a constant, which is affected by the probability of capture and the mean nonzero catch of both species.

When there are more than two, say n, species, and $G_{tot} = \sum_{i=1}^{n} G_i$, then

$$(10) \qquad CV(G_{tot}) = \frac{\sqrt{\sum_{i=1}^{n} \mathrm{Var}(G_i) + \sum_{i=1}^{n} \sum_{j \neq 1} \mathrm{Cov}(G_i, G_j)}}{\sum_{i=1}^{n} E(G_i)}$$

The reduction of variability is governed here by three factors that influence each other: (1) the total number of species caught, (2) the CFDs of the individual species, and (3) the homogeneity of species composition in subsequent catches, expressed as the covariance between individual species.

When CFDs are equal and the catches of any pair of species are independent, the variability in the total catch can be given by

$$(11) \qquad CV(G_{tot}) = \frac{1}{\sqrt{n}} \times CV(G_i)$$

This means that when a large number of independently occurring species are combined, $CV(G_{tot})$ approaches zero.

In real-life situations this total reduction of variability does not occur, as the CFDs of species caught by multispecies fisheries vary, which makes calculating the reduction in variability highly complex. Doak et al. (1998) tried to simplify this situation in their discussion of the relation between species diversity and the temporal stability of ecosystems. They assumed that the CVs for all species were similar and that species varied independently. Further, they assumed that the relative abundance of each subsequent species declined exponentially by rank number, so that (Doak et al. 1998)

$$(12) \qquad m_i = m_1 \times e^{-a(i-1)}$$

Fig. 2. Isopleth diagrams of CVs of the total catch of two species relative to the CV of species *i* (CV_{tot}/CV_i) in relation to the probability of capture of the two individual species (p_i, p_j) (*a*), the mean nonzero catch of the two individual species (μ_i, μ_j) (*b*), and the SDs of the nonzero catches of the two individual species (σ_i, σ_j) (*c*). The two species were independently caught, and the parameters that are not included in the graphs are constant and the same for the two individual species and are indicated below the graph.

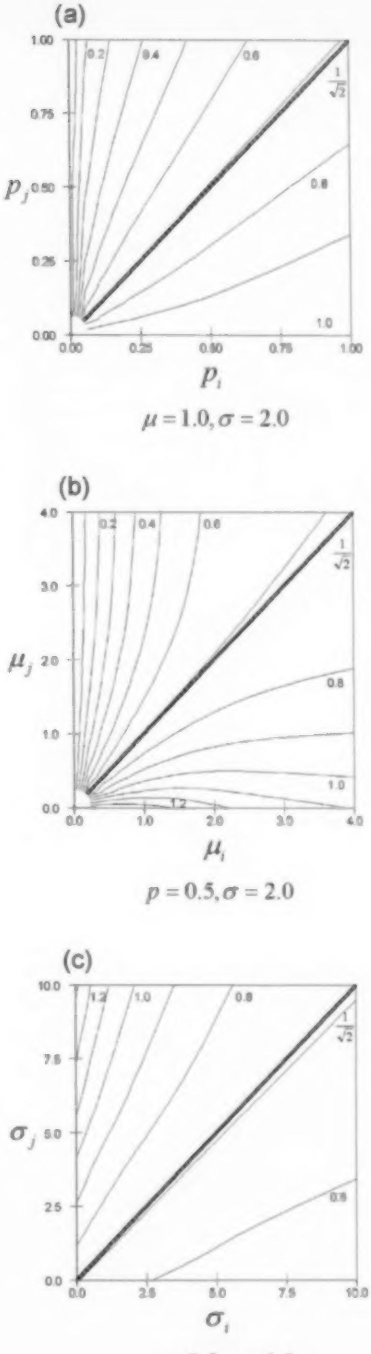

$\mu = 1.0, \sigma = 2.0$

$p = 0.5, \sigma = 2.0$

$p = 0.5, \mu = 1.0$

When applied to the problem of a reduction of variability in a multispecies catch, these parameters signify the following: m_1 is the relative abundance of the most common species, *i* is the species rank when species are ranked according to their relative importance to the total weight of the catch, and *a* is a coefficient that indicates the rate of decline in the relative importance of each subsequent species, or the coefficient of abundance inequality (CAI). Using eq. 12 we can rewrite eq. 10 as (eq. 3 in Doak et al. 1998)

$$(13)\quad CV(G_{tot}) = CV(G_1) \times \left[\frac{(1 - e^{-a})(1 + e^{-an})}{(1 + e^{-a})(1 - e^{-an})}\right]^{1/2}$$

where we can see that the reduction in CV is asymptotic and that with a larger value of *a*, i.e., a greater relative importance of the most abundant species, the maximum reduction in CV that can be attained is lowered (Fig. 3*a*).

Finally, if the CFDs of all species are equal, but the level of co-occurrence between species varies, eq. 10 reduces to

$$(14)\quad CV(G_{tot}) = \frac{\sqrt{n\mathrm{Var}(G_i) + 2\sum_{i=1}^{n}\sum_{j\neq 1}\mathrm{Cov}(G_i, G_j)}}{nE(G_i)}$$

$CV(G_{tot})$ is equal to $CV(G_i)$ if all catches have a perfect positive correlation, i.e., $\mathrm{Cov}(G_i,G_j) = \mathrm{Var}(G_i)$ for all *i*,*j*. In that case, no reduction in CV would be attained by catching more than one species (Fig. 3*b*). $CV(G_{tot})$ is zero in the case of the most negative covariance between the species, so the total catch is constant.

Study site

The research was conducted on a pelagic fishery with lift nets, located in two areas on the southeastern and eastern sides of Ambon Island (Fig. 4). Baguala Bay (3°38′S, 128°17′E) has a total surface area of approximately 17 km² and Haruku Strait (3°35′S, 128°20′E) has a total surface area of approximately 38 km². With water depths not more than 200 m in the mouth of Baguala Bay and in the western part of Haruku Strait (approximately 10 km²), these areas are suitable for a lift-net fishery from stationary anchored platforms.

The coastal lift-net fishery for small pelagic species around Ambon and Lease islands has regional importance. In 1995, the 326 lift-net units contributed 21% of the total catch of coastal fisheries in the Central Moluccas (Anonymous 1981–1997). In addition to human consumption, a large proportion of the 3600 t of mainly anchovies and sardines caught was used as live bait for the offshore pole-and-line fishery for skipjack tuna (*Katsuwonus pelamis*). The tuna fishery represented 12% of the total weight and 29% of the total value of the catch from the Central Moluccas in 1995. Price differences among species caught by the lift-net fishery are negligible,

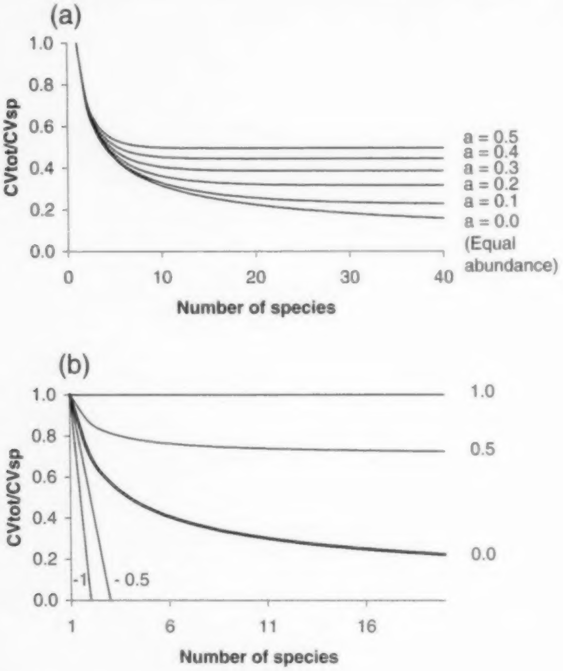

Fig. 3. CV of total catch relative to the CV of the individual species (CV_{tot} / CV_{sp}) resulting from a combination of *n* distributions with equal CVs and varying coefficients of abundance inequality (CAIs; i.e., the decrease in abundance of individual species with increasing rank (eq. 12)) (*a*) and varying covariance (*b*). The line with $a = 0$ denotes a situation in which all species are equally abundant. With increasing CAI, the abundances of individual species are more unequal and the species that occur most often are more important (eq. 13). Adapted from Doak et al. (1998). Numbers in *b* are correlation coefficients (*r*).

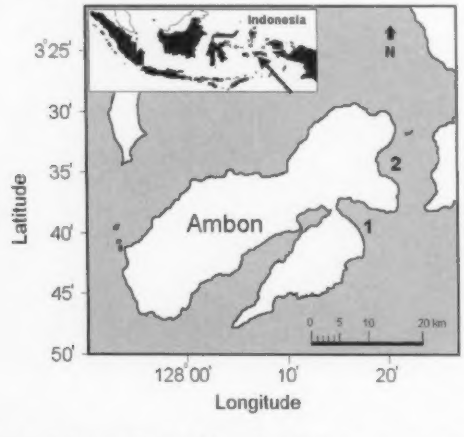

Fig. 4. Ambon and Lease islands showing the locations of Baguala Bay (1) and Haruku Strait (2).

as most of the catch is sold as live bait at a constant price, and market prices of the species caught are similar.

The lift-net units in the Central Moluccas consist of a square wooden platform about 200 m^2 in area mounted on an anchored body. A square lift net is attached under the platform. The surface area of the net opening is equal to the size of the platform; the net has a mesh size of around 3 mm. The stationary lift-net units are operated during 1-night trips made by the crew to and from the platform. The fishing process consists of two phases. First, small pelagic fish are attracted to the unit using all lamps on the platform. When the fishers conclude from direct observation that enough fish have clustered under the platform, all lamps are slowly extinguished except for one in the centre of the unit. Fish concentrate around it and are caught by lifting the net using windlasses, each operated by one of the two to six fishers working on the unit. In this way up to three hauls are made per night. The variability in total catch per night of individual lift-net units is large: CV = 2.5. Only 55% of the trips result in a catch, and only nonzero catches still show large variability: CV = 1.7.

Data collection

A sampling program was carried out from mid-September 1998 (the end of the southeast monsoon) to February 1999. Samples of fish weighing 0.5–4 kg were taken three times a week from 06:30 to 07:30 as the fishers landed their nightly catches at the main landing site in each of the two areas. One to four samples were taken per day, depending on the number of landings. In addition, the total catch was recorded either by counting the baskets (18 kg) when the fish were landed or asking the fishers about the number of buckets (4 kg) sold when the fish were sold as live bait at sea. All small pelagic species (e.g., sardines, anchovies, sprats) were identified to species following Whitehead (1985); juveniles of larger pelagic species such as scads, mackerels, and tunas were identified to genus. All demersal fish were grouped into one category ("other").

Testing the model

Probability of capture (*p*), mean catch per day (μ; $kg \cdot day^{-1}$), standard deviation (σ; kg), and variability (CV), both including and excluding zero catches, were calculated for all individual species caught. Total zero catches included both hauls when no catch was made and cases when no haul was made, usually because the amount of fish attracted under the lift-net platform was negligible. No distinction could be made between these two situations and thus it was not known whether total zero catches were real zero values or low values. Because this distinction is important in terms of the characteristics of the CFD, all total zero catches were excluded from the data set; *p* is therefore the conditional probability of catching a certain species when the total catch is larger than zero.

To test whether pairs of species occurred independently in daily catches, a χ^2 test was used to test the proportion of catches in which a pair of species occurred together against the theoretical probability of co-occurrence of the two species. This theoretical probability was based on the probabilities of occurrence of the two individual species.

Finally, the effects of the characteristics of the CFDs of individual species and the level of co-occurrence among species on the reduction of variability in the total catch were

Table 1. Species composition of lift-net catches from Baguala Bay and Haruku Strait, Ambon Island, Central Moluccas, Indonesia, with descriptive statistics for each species taken from nonzero catches.

	% of total weight	*p*	Mean weight (kg)	CV (nonzero catch)
Sardines				
Ambligaster clupeoides	<0.1	0.02	1.6	0.7
Ambligaster sirm	1.3	0.14	10.4	4.3
Dussumieria elopsoides	0.3	0.03	10.7	1.9
Escualosa sp.	<0.1	0.01	1.5	1.2
Herklotsichthys quadrimaculatus	35.0	0.73	53.4	1.9
Ilisha sp.	<0.1	0.02	7.5	1.4
Sardinella albessa	0	0.01	0.7	0.7
Sardinella atricauda	0.3	0.14	1.9	1.5
Sardinella fimbriata	0.8	0.14	6.5	1.9
Sardinella gibbosa	0.2	0.01	39.9	
Sardinella melanura	5.0	0.48	11.7	1.9
Spratelloides delicatulus	0.2	0.12	1.5	3.1
Spratelloides gracilis	<0.1	0.04	0.5	1.8
Anchovies				
Encrasicholina devisi	19.9	0.32	70.5	2.5
Encrasicholina heteroloba	1.7	0.18	10.5	2.5
Encrasicholina punctifer	23.6	0.22	122.0	2.1
Stolephorus commersonii	0.2	0.10	1.7	1.6
Stolephorus indicus	1.4	0.14	11.0	1.3
Stolephorus waitei	<0.1	0.02	1.3	1.3
Thrissa baelama	1.9	0.31	7.1	3.4
Thrissa setirostris	0.2	0.07	4.0	1.9
Other species				
Atherina spp.	0.7	0.27	2.8	1.8
Auxis spp.	0.2	0.06	3.3	1.5
Caesio spp.	0.4	0.07	5.4	2.0
Decapterus spp.	1.9	0.06	38.1	2.7
Rastrelliger spp.	3.0	0.39	8.5	3.9
Selar spp.	<0.1	0.11	0.3	1.5
Sphyraena sp.	0.1	0.02	3.2	1.3
Other	1.7	0.63	3.1	2.1

examined. This was done by composing the catch by sequentially adding individual species. After a new species was added, p, μ, σ, and CV were calculated for the new combination of species. The theoretical CV of the combination was calculated as well, based on eq. 6 and the characteristics of the CFDs of the individual species, assuming total independence of all fish species. The actual reduction of variability was compared with the theoretical reduction. This exercise was done twice: (1) species were sorted in descending order according to the CV of their individual catches; (2) species were sorted in descending order according to how much of the variance in the total catch they accounted for.

The ranking for the second exercise was based on a forward regression analysis in which the amount of variance accounted for in the total catch was assessed. The model was implemented by using the REG procedure of SAS software (SAS Institute Inc. 1989).

Results

In total, 180 nonzero catches were used for the analyses, with a mean weight of 112 $\text{kg}\cdot\text{trip}^{-1}$. The variability in total daily nonzero catches was large (CV = 1.7) and the catch-frequency distribution was highly positively skewed.

Approximately 30 different small pelagic species were identified in the catches, together with a multitude of demersal species that represented only 1.7% of the total catch (Table 1). The maximum number of species found in a single catch was only 12, and more than 75% of the catches contained fewer than 7 species (mean = 4.7 $\text{species}\cdot\text{catch}^{-1}$).

Assuming equal, independent occurrence and equal CFDs of all 30 species, the variability per species would be equal to the variability of the total nonzero catch (CV = 1.7), increased by a factor $\sqrt{30}$ (eq. 11), leading to a CV of 9.1. However, the relative importance of the individual species' weights varied markedly and decreased exponentially if species were ranked according to relative catch weight (CAI = 0.25, r^2 = 0.97) (Table 1). One sardine species (*Herklotsichthys quadrimaculatus*) and two anchovy species (*Encrasicholina devisi*, *Encrasicholina punctifer*) were dominant, contributing almost 80% of the total weight of all individual catches combined. Moreover, more than 90% of all catches contained at least one of these three species. Because of the skewed species composition, many species with small mean catches had only a small effect on the reduction of variabil-

Fig. 5. CVs of the total catch (+) and the catches of separate species including nonzero catches (●) and total catches per species (▽). The small graphs exemplify time series of species with extreme CFDs in the left or right part of the main graph, indicated by the broken line and arrows, which are caught either always in low numbers (left) or occasionally in high numbers (right).

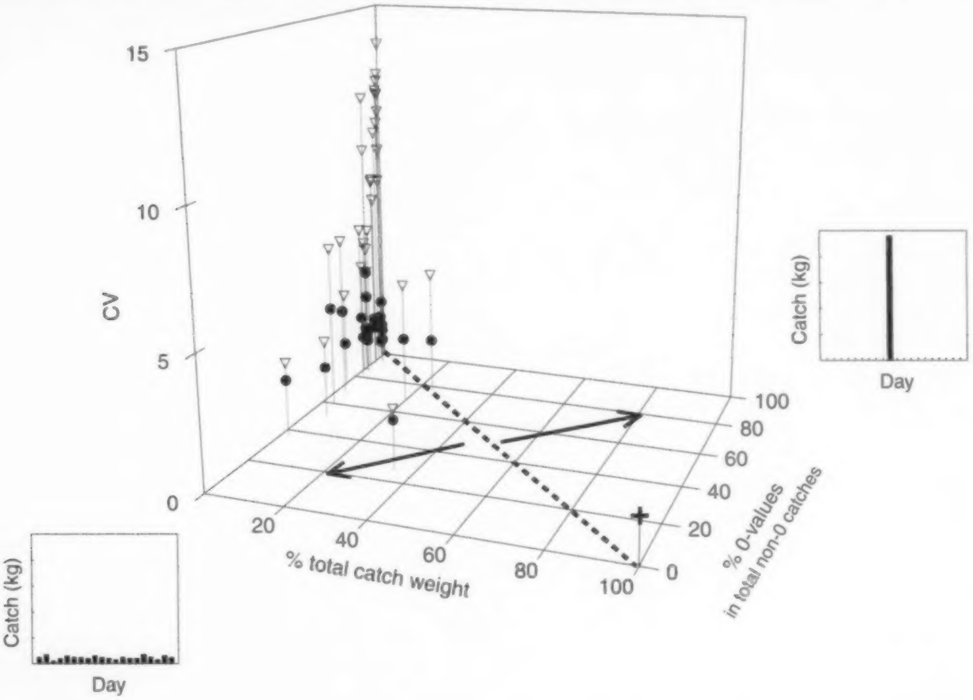

ity (see also Fig. 2), and the total reduction of variability was lower than it would have been if the mean catches of all species had been similar (Fig. 3*a*). Assuming equal variability for all species and a known CAI (0.25), the variability in the individual species would be a CV of 4.7 according to eq. 10, much lower than in the case of complete similarity in the characteristics of the CFDs of all species.

Neither estimate fit the actual data because the variability in each of the species differed as well, with CVs ranging between 2.27 and 13.42 (mean = 7.6, SD = 3.24; Table 1; Fig. 5). This large difference in CVs was mainly due to the large differences in p values among species, which ranged from 0.01 to 0.73, as the CVs of nonzero catches of individual species were much less variable, ranging from 0.73 to 4.26 (mean = 1.9, SD = 0.87). This marked difference in the CFDs of individual species is illustrated by the main three species.

Although the sardine *H. quadrimaculatus* was caught frequently ($p = 0.73$), it contributed only 35% to the total weight of the overall catch, as the average weight of nonzero catches of this species was small (53 kg). The catch variability for *H. quadrimaculatus* was only slightly larger (CV = 2.27) than that for the total nonzero catches (CV = 1.66).

The two anchovy species were more concentrated in the catches. They were caught less frequently ($p = 0.31$ for *E. devisi*; $p = 0.21$ for *E. punctifer*) than *H. quadrimaculatus*. However, their contribution to the overall catch weight (20% for *E. devisi*; 24% for *E. punctifer*) was relatively large in view of their probability of capture, as their mean individual nonzero catch was high (mean weight was 70 kg for *E. devisi* and 122 kg for *E. punctifer*). Because of their large proportion of zero catches, the variability in their individual catches was large (CV = 4.73 and 4.79, respectively).

Most of the other species were more evenly distributed among catches relative to their contribution to the overall catch weight. Despite the low variance in nonzero catches of these species, the variability in their individual catches was large because of the high proportion of zero catches.

Since many of the species with small mean catches had little influence on the reduction in variability, the correlation between the occurrences of different species was of little importance. Only 42 of the total of 435 possible combinations of species occurred more frequently than that based on their individual p values ($\chi^2 < 0.05$). Moreover, in only three cases did this involve one of the four main species (Fig. 6). The two most important species with high co-occurrence, *H. quadrimaculatus* and *S. melanura*, were found together in 43% of daily catches. This was more than expected from their individual p values by a factor of 1.24. In only one case, two species (*E. punctifer* and *S. melanura*) excluded each other. The number of significant correlations in the occurrences of individual species was larger than could be explained by mere chance ($p < 0.05$).

Because of the limited importance of co-occurrence, the reduction in CV could be estimated accurately, based on the mean catch and variability of individual species, assuming

Fig. 6. Co-occurrence of individual species in the catch. Species numbers on the *x* and *y* axes correspond to those listed at the right. –, significantly low co-occurrence ($p < 0.05$); ○, independent occurrence; +, significantly high co-occurrence. Species are sorted according to mean weight in the catches.

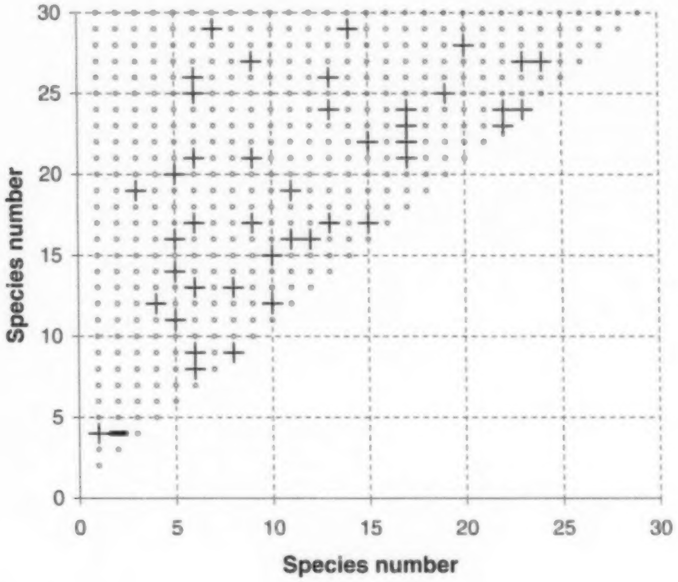

Number	Species
1	*Herklotsichthys quadrimaculatus*
2	*Encrasicholina punctifer*
3	*Encrasicholina devisi*
4	*Sardinella melanura*
5	*Rastrelliger spp.*
6	*Thrissa baelama*
7	*Decapterus spp.*
8	*Others*
9	*Encrasicholina heteroloba*
10	*Stolephorus indicus*
11	*Ambligaster sirm*
12	*Sardinella fimbriata*
13	*Atherina spp.*
14	*Caesio spp.*
15	*Dussumieria elopsoides*
16	*Sardinella atricauda*
17	*Thrissa setirostris*
18	*Sardinella gibbosa*
19	*Auxis spp.*
20	*Spratelloides delicatulus*
21	*Stolephorus commersonii*
22	*Ilisha sp.*
23	*Sphyraena sp.*
24	*Leiognatidae*
25	*Ambligaster clupeoides*
26	*Selar spp.*
27	*Stolephorus waitei*
28	*Spratelloides gracilis*
29	*Escualosa sp.*
30	*Sardinella albessa*

total independence of occurrence (Fig. 7). The variability based on the combined catches correlated almost perfectly with the estimated variability ($r^2 > 0.98$).

When the species were sorted in descending order according to the variability in their individual catches and then combined, the probability of occurrence of the combination increased approximately linearly. Adding the three main species (23, 24, and 30 in Fig. 7*a*) did not affect this pattern. These three species had a large effect on the shape of the curve representing the total weight of the combined species, as was shown before.

The addition of the first 20 species caused a decrease in variability (CV) from 13.4 to 2.9. The absolute effect of the three main species (*H. quadrimaculatus*, *E. devisi*, *E. punctifer*) was small, because at the point where they were added (after species 22 in Fig. 7*c*), the combination of the first 22 species already had a high probability of occurrence ($p = 0.77$) and a weight that was not much lower than that of the species added. However, these three species did have a relatively large effect on the reduction in CV, because the addition of *H. quadrimaculatus* (species 30), for example, reduced the variability of the combination by 27%, from CV = 2.3 to CV = 1.7 (Fig. 7*c*).

The forward regression analysis showed that the combination of the three main species (*H. quadrimaculatus*, *E. devisi*, *E. punctifer*) caused over 90% of the variation in the total catch (Table 2). As a result, these three species also caused the main reduction in variability of the daily catches (Fig. 7*d*). After these species were added, CV = 2.0. Although numerous other species exhibited large variability, they added little to the probability of capture or the weight of the catch, or therefore to the reduction of variability in the total catch (17%, from CV = 2.0 to CV = 1.7).

Discussion

This study shows that the reduction of variability in the day-to-day catch in a multispecies fishery is mainly caused by (*i*) the weight composition of the total catch, (*ii*) the variability in individual species, and (*iii*) their co-occurrence in the catch. As the variability in daily catches of individual species and the reduction of variability in the total catches by individual species can be used as statistical descriptors of the three characteristics of a multispecies fishery, these descriptors can be used to compare multispecies fisheries. We have shown that multispecies fisheries vary in the way in which variability is reduced as a result of the three characteristics of the species composition in the catch, and we will now elaborate on this. Next we discuss the ecological and technical factors influencing the reduction of overall catch variability due to individual species. Finally, we will discuss the consequences of these characteristics in terms of the information value of the total catch and of the catches of individual species for detecting trends and consequently for the management of multispecies fisheries.

The weight composition of the catch is one of the key characteristics of species composition and is of major importance for maximizing the reduction of the variability in the

Fig. 7. Catch characteristics (*a* and *b*) of individual species and combined species and actual and theoretical values of the variability in the catch of individual species and combined species (*c* and *d*). The order in which the species are combined is based on the variability in individual species (*a* and *c*) and the reduction of the variation in the total catch in a regression model (*b* and *d*) (see the text). Theoretical variability values are calculated assuming total independence of the occurrence of the different species. The CVs of species included (*c* and *d*) correspond to those in Table 1; rank numbers of species included in *b* and *d* correspond to those in Table 2. +, catch weight of individual species; ---, catch weight of combined species; △, variability of individual species; ●, actual value of variability of combined species; —, theoretical value of variability of combined species; ○, probability of occurrence of individual species; the thick line shows the probability of occurrence of combined species.

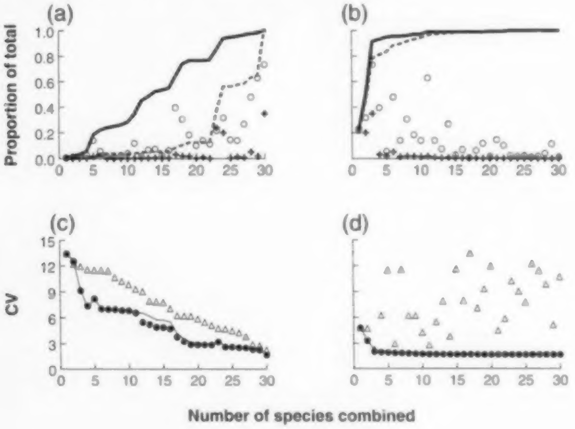

Table 2. Regression analysis of daily catches of species with total daily catches, using forward regression.

Step	Species	Model R^2	F
1	*Encrasicholina punctifer*	0.36	98.2
2	*Encrasicholina devisi*	0.64	140.1
3	*Herklotsichthys quadrimaculatus*	0.94	883.3
4	*Rastrelliger* spp.	0.96	61.0
5	*Decapterus* spp.	0.97	94.2
6	*Sardinella melanura*	0.98	68.7
7	*Ambligaster sirm*	0.99	92.8
8	*Thrissa baelama*	0.99	88.6
9	*Encrasicholina heteroloba*	1.00	154.2
10	*Stolephorus indicus*	1.00	106.4
11	Other	1.00	152.9
12	*Sardinella fimbriata*	1.00	43.8
13	*Caesio* spp.	1.00	42.7
14	*Atherina* spp.	1.00	44.7
15	*Dussumieria elopsoides*	1.00	60.4
16	*Thrissa setirostris*	1.00	51.5
17	*Sardinella gibbosa*	1.00	68.8
18	*Auxis* spp.	1.00	63.1
19	*Spratelloides delicatulus*	1.00	71.4
20	*Ilisha* sp.	1.00	116.7
21	*Sardinella atricauda*	1.00	115.5
22	*Stolephorus commersonii*	1.00	188.9
23	*Sphyraena* sp.	1.00	191.7
24	Leiognatidae	1.00	134.7
25	*Ambligaster clupeoides*	1.00	62.1
26	*Escualosa* sp.	1.00	61.9
27	*Stolephorus waitei*	1.00	96.4
28	*Spratelloides gracilis*	1.00	144.8
29	*Selar* spp.	1.00	513.0
30	*Sardinella albessa*	1.00	—

Note: Model R^2 is the correlation coefficient between daily catches of the combined species after the *i*th species was added and total catches ($p \ll 0.01$ for all combinations noted here).

total catch. For different fisheries, species composition can range from one dominant species combined with a few others that occur rarely, to a multitude of species that occur in almost equal proportions in the catch. The reduction of variability is greater in the latter situation than in the former. Because only a few species form the major part of the catch in most fisheries (Table 3), judging from the reduction of variability, the fisheries are much less "multispecies" than the total number of species suggests. Therefore, in characterizing a multispecies fishery it is better to indicate the size of the contribution of the most important (e.g., four) species to the catch than to indicate just the number of species.

Besides its relative importance, the variance of the individual species in the catch also affects the reduction of variability. Differences in variance are due to either the difference in the probability of capture or the variance of nonzero catches. In the absence of high co-occurrence, the effect of differences in the variance of individual species is smaller than the effect of equal relative differences in the mean catch (eq. 10). Thus, only large differences in variance of important species will have a significant effect on the variability of the total catch, as exemplified by the large variation in the two main anchovy species in the fishery analysed here.

Although the co-occurrence of species in the catch has a negligible effect on the reduction of variability in the total catch in the Ambon Island fishery, it could have a large effect in other multispecies fisheries: variability will be lower when the overall co-occurrence of species in the catch is low and higher when the overall co-occurrence is high. However, general effects on the reduction of variability are hard to state, as in many fisheries individual species may show high co-occurrence, whereas the co-occurrence between groups of species with high co-occurrence may be low. The relative importance of the groups, then, will have a large influence on the reduction of variability.

All characteristics of species composition of the catch result from the interaction between ecological factors affecting the standing-stock biomass, the distribution and dispersal of species, and the technical characteristics of the fishery, particularly its scale of operation and local knowledge of the distribution patterns of the fish. The characteristics of the CFDs of individual species can be explained by the distribution patterns of the species, the scale of operation of the fisheries, local knowledge, and the catchability coefficient relative to the fishing gear used. The large proportion of zero catches, which caused the large variability in the catch that was found for all species in our example from Ambon Island, was a result of the aggregated distribution of the target species at the small spatial scale of operation of the fishery

Table 3. Examples of multispecies fisheries/sampling techniques, total number of taxa caught, numbers of the most important taxa that make up more than 75% of the weight of the total catch, and the fit and parameters of an exponential regression ($y = m_1 \times e^{-a(i-1)}$) fit to the distribution of the relative weight of the species ranked according to the relative importance of that species (Doak et al. 1998).

		No. of taxa		Parameter			
Fishing gear used	System and location	Total	75%	m_1	a	r^2	Reference
Gill net	Lagdo Reservoir, Cameroon	37	5	15.4	0.23	0.98	Postma and van der Knaap 1999
	Piracicaba River, Brazil	22	4	22.2	0.31	0.97	Silvano and Begossi 2001
Intake screen of power station	Severn Estuary, England	16	3	23.8	0.36	0.97	Potter et al. 2001
Trawl	Gulf of Thailand, Thailand	39	6	14.5	0.19	0.97	Pauly 1979
		39	9	11.6	0.14	0.96	
		39	10	11.6	0.13	0.98	
		39	8	10.6	0.12	0.98	
	Algarve coast, Portugal	46	6	12.6	0.20	0.98	Monteiro et al. 2001
	Great Barrier Reef, Australia	51	18	7.1	0.07	0.97	Wassenberg et al. 1998
		51	18	6.6	0.07	0.97	
Trap	Coral reefs, Lesser Antilles	59	16	8.1	0.09	0.93	Gobert 2000
		62	23	7.1	0.08	0.95	
		90	18	6.0	0.06	0.96	
		111	20	7.5	0.09	0.91	
		84	21	21.2	0.28	0.96	

and the inability of the fishers to predict fish distribution. All of the small pelagic fish caught are schooling species (Whitehead 1985). In fact, the variability in the catch per individual species calculated here is not even as high as it is in reality. As only 55% of trips result in a catch and we do not know the reason for the zero values (no haul or zero catch in the haul), the variability of the individual species in catches may well be much higher than is estimated here. For fisheries that operate on a larger scale and species with a more uniform distribution, one would expect variability to be lower than for the fishery described here.

Differences in other characteristics of species composition, such as the number of species and the distribution of relative abundances of individual species, are much more difficult to explain from differences in ecological and technical factors. For instance, Hubbell (2001) explains differences in the distribution of relative abundances of individual species in divergent ecosystems as being population processes such as ecological drift, stochastic limited dispersal, and random speciation, but his explanation is highly complex.

The co-occurrence of species in the catch depends on interactions among species and interactions between species and their environment at the scale of operation of the fishery. If the environment at the scale of operation of the fishery is highly structured, governing the dispersion of many species, e.g., on coral reefs, co-occurrence of species in the catch that use the same habitat will be high and co-occurrence of species that use different habitats will be low. Moreover, within similar habitats species might show different levels of co-occurrence depending on interspecific relations, such as predator–prey relations, schooling, or even territorial behaviour.

The small-scale light-attraction fishery around Ambon Island is a typical example of a fishery that targets species which mostly occur independently. This is because, at the scale of operation of the fishery, the homogeneous environment places no restrictions on the distribution of the species caught (Rosa and Laevastu 1960; Longhurst 1971). Furthermore, the schools of fish will show little or no avoidance behaviour, as all species are pelagic planktivores at the size range at which they are caught (Whitehead 1985), and occupy similar niches. The high and low co-occurrences in the catch are probably due to preferences in schooling behaviour. Some species might systematically form mixed-species schools, whereas others might not, owing to differences in size (Freon and Misund 1999; J.A.E. van Oostenbrugge, unpublished data).

When fishers are able to adjust their effort according to the distribution of individual species or groups of species, they can influence the characteristics of species composition and the reduction of variability by altering their fishing strategy (Laloe and Samba 1991). This can be used for income stabilization or maximization, and depends largely on differences in the prices of individual species.

The variability in catch rates has important consequences for the functioning of the fishery with regard to the uncertainty of the fishers' income, the perception of the state of the fishery by its participants, and its management. Variability determines the number of fishing days needed to allow spatial differences in catch rates to be perceived, which is important for effective allocation of fishing effort. This will be difficult in fisheries with high variability in catch rates, such as the fishery analysed here (van Oostenbrugge et al. 2001). Besides these effects for fishers, large variability in catches might also restrict the options for (co-)management of the resource. It will be hard to convince fishers of the need for restrictive management measures in such a situation, as the effect of measures will be difficult to perceive within the time window of a fisher's active life. Assuming a fishing year of 250 days, the variance in daily catches in the lift-net fishery around Ambon Island causes random variability of at least $CV = 2.4/\sqrt{250} = 0.15$ in the average yearly catch of a fisher, which is high compared with other fisheries (van Densen 2001). For individual species this variability is even higher and could be even larger than a CV of 1.0 on an annual basis.

This having been said, one would think that both fishers and fisheries authorities would benefit from a large reduction of the variability in catch rates in multispecies fisheries. To a certain extent this is true, as the reduction of variability stabilizes the fishers' income at a level at which exploitation of the fishery is economically feasible. Moreover, the reduction of variability makes spatial and temporal patterns in total catch rates easier to perceive. However, this improved perception of trends in the total catch rate is no guarantee of a better insight into the fishery if information is needed at the species level, because trends in the total catch can have little value for indicating trends in the catches of individual species and the status of their stocks.

One of the major problems of managing multispecies fisheries is that the total catch can remain constant in situations of increasing effort, whereas large species with low resilience and low productivity could be heavily overfished and the species composition in the catch could change to small species with high resilience and high productivity (Welcomme 1999). In other words, the problem is the low co-occurrences in catches of individual species over long time periods. To recognise overexploitation, fishers and managers thus need to have information on catches of single species or groups of species so that they can see changes in species composition. In cases of high co-occurrence of species, perceiving trends in catches of individual species is easy, as they are reflected in trends in the total catch. Moreover, managers could choose one of the species with high co-occurrence as an indicator species and restrict monitoring to this species. However, if the species occur independently or show low co-occurrence, perceiving trends in individual species will be difficult; therefore, the use of indicator species will make no sense. In these situations information on catch rates of individual species should be available to allow differences in species composition and the status of stocks to be detected.

Acknowledgements

The present study was carried out as part of the Dutch–Indonesian research program on resource use in the coastal zones of the Moluccas, a co-operative project between Universitas Pattimura and Lembaga Ilmu Pengetahuan Indonesia (LIPI)-Ambon (Indonesia) and Wageningen University and the Research Centre, Nijmegen University, and the Institute of Cultural Anthropology, Leiden University (Holland). The Royal Dutch Academy of Sciences is thanked for financial support (grant No. 95-btm-11). LIPI-Ambon and the fisheries department of Universitas Pattimura are acknowledged for their cooperation and advice. We also thank Maya Manuputty, Anneke van den Oever, Jan Jaap Poos, Gyzlah Sahertian, and Sam Tumuly for their assistance in the field and with data entry. Special thanks go to Leo Nagelkerke for his valuable comments on drafts of this paper.

References

Anonymous. 1981–1997. Buku Tahunan Statistik Perikanan Tahun 1980–1996 (Annual fisheries report Moluccas). Provincial Fisheries Department, Ambon, Moluccas, Indonesia.

Blanchard, F., and Boucher, J. 2001. Temporal variability of total biomass in harvested communities of demersal fishes. Fish. Res. **49**: 283–293.

Doak, D.F., Bigger, D., Harding, E.K., Marvier, M.A., O'Malley, R.E., and Thomson, D. 1998. The statistical inevitability of stability–diversity relationships in community ecology. Am. Nat. **151**: 264–276.

Ellis, F. 1998. Household strategies and rural livelihood diversification. J. Dev. Stud. **35**: 1–38.

Freon, P., and Misund, O.A. 1999. Dynamics of pelagic fish distribution and behaviour: effects on fisheries and stock assessment. Fishing News Book Ltd., Farnham, U.K.

Gobert, B. 2000. Comparative assessment of multispecies reef fish resources in the Lesser Antilles. Fish. Res. **44**: 247–260.

Hubbell, S.P. 2001. The unified neutral theory of biodiversity and biogeography. Princeton University Press, Princeton, N.J.

Laloe, F., and Samba, A. 1991. A simulation model of artisanal fisheries of Senegal. ICES Mar. Sci. Symp. No. 193. pp. 281–286.

Lehman, C.L., and Tilman, D. 2000. Biodiversity, stability, and productivity in competitive communities. Am. Nat. **156**: 534–552.

Longhurst, A.R. 1971. The clupeoid resources of the tropical seas. Oceanogr. Mar. Biol. Annu. Rev. **9**: 349–385.

Monteiro, P., Araujo, A., Erzini, K., and Castro, M. 2001. Discards of the Algarve (southern Portugal) crustacean trawl fishery. Hydrobiologia, **449**: 267–277.

Pauly, D. 1979. Theory and management of tropical multispecies stocks: a review with emphasis on the Southeast Asian demersal fisheries. ICLARM studies and reviews 1, International Center for Living Aquatic Resources, Manila.

Pennington, M. 1996. Estimating the mean and variance from highly skewed marine data. Fish. Bull. **94**: 498–505.

Platteau, J.P., and Abraham, A. 1987. An inquiry into quasi-credit contracts: the role of reciprocal credit and interlinked deals in small-scale fishing communities. J. Dev. Stud. **23**: 461–490.

Postma, D.J., and van der Knaap, M. 1999. Developments in the fishery of Lagdo Reservoir, Cameroon. *In* Fish and fisheries of lakes and reservoirs in Southeast Asia and Africa. *Edited by* W.L.T. van Densen and M.J. Morris. Westbury Academic & Scientific Publishing, Otley, U.K. pp. 311–326.

Potter, I.C., Bird, D.J., Claridge, P.N., Clarke, K.R., Hyndes, G.A., and Newton, L.C. 2001. Fish fauna of the Severn Estuary: Are there long-term changes in abundance and species composition and are the recruitment patterns of the main marine species correlated? J. Exp. Mar. Biol. Ecol. **258**: 15–37.

Rosa H., Jr., and Laevastu, T. 1960. Comparison of biological and ecological characteristics of sardine and related species—a preliminary study. *In* Proceedings of a World Scientific Meeting on the Biology of Sardine and Related Species. *Edited by* H. Rosa and G. Murphy. Food and Agriculture Organisation, Rome.

SAS Institute Inc. 1989. SAS/STAT© user's guide. Version 6. Vol. 2. SAS Institute Inc., Cary, N.C.

Silvano, R.A.M., and Begossi, A. 2001. Seasonal dynamics of fishery at the Piracicaba River (Brazil). Fish. Res. **51**: 69–86.

van Densen, W.L.T. 2001. On the perception of time trends in resource outcome: its importance in fisheries co-management, agriculture and whaling. PhD. thesis, Twente University, Enschede, The Netherlands.

van Oostenbrugge, J.A.E., van Densen, W.L.T., and Machiels, M.A.M. 2001. Risk aversion in allocating effort in a highly uncertain coastal fishery for pelagics, Moluccas, Indonesia. Can. J. Fish. Aquat. Sci. **58**: 1683–1691.

van Oostenbrugge, J.A.E., Poos, J.J., van Densen, W.L.T., and Machiels, M.A.M. 2002. In search of a better unit of effort, differentiation of platform size and lamp type and variability in catch rates by a lift-net fishery for small pelagics (Central Moluccas, Indonesia). Fish. Res. In press.

van Zwieten, P.A.M., Njaya, F. and Weyl, O.L.F. 2002. Effort development and the decline of the fisheries of Lake Malombe: does environmental variability matter? *In* Management, co-management or no-management? Major dilemmas in the sustainable utilisation of SADC freshwater fisheries. *Edited by* E. Jul-Larsen, J. Kolding, R. Overå, J. Raakjær Nielson, and P.A.M. van Zwieten. FAO Fisheries Technical Paper 462(2). FAO, Rome.

Wassenberg, T.J., Burridge, C.Y., Connell, M., and Gribble, N. 1998. A validation of short-duration scientific tows as a representation of long commercial-length tows: comparing the catch rates, size composition and species composition of prawn trawler bycatch in the far northern Great Barrier Reef, Australia. Fish. Res. **36**: 35–46.

Welcomme, R.L. 1999. A review of a model for qualitative evaluation of exploitation levels in multi-species fisheries. Fish. Manag. Ecol. **6**: 1–19.

Whitehead, P.J.P. 1985. Clupeoid fishes of the world. FAO species catalogue. Vol. 7. Food and Agriculture Organisation, Rome.

Effects of food and cover on the growth, survival, and movement of cutthroat trout (*Oncorhynchus clarki*) in coastal streams

Shelly M. Boss and John S. Richardson

Abstract: To examine the extent to which stream-resident coastal cutthroat trout (*Oncorhynchus clarki*) are limited by food and cover, we manipulated these two factors in a 2 × 2 design using enclosures containing 1-year-old trout in two streams. During summer, fish receiving food additions experienced an average growth rate of 1.73% body mass·day^{-1} compared with a rate of 0.022 for unfed fish (ambient food supply only), indicating marked food limitation. The addition of cover decreased mortality by approximately 50% in one stream, but survival was high both with and without cover in the other. There was no interaction of food and cover on growth or survival. Emigration rates were low and were not strongly affected by either factor. We also used mark–recapture modeling to examine whether the 48% greater mass of fed fish at the end of the experiment improved survival over winter. Fed fish were still 46% larger than unfed fish by the next spring, but overwinter survival was not explained by body size. Our results show that, during summer, food availability can limit trout growth, and cover, by mediating predation, can limit survival.

Résumé : Afin de déterminer dans quelle mesure le gîte et la nourriture peuvent être des facteurs limitants pour les truites fardées côtières (*Oncorhynchus clarki*) habitant les cours d'eau de la côte, nous avons établi un plan d'expérience de type 2 × 2 pour manipuler ces facteurs dans des enclos contenant des poissons de 1 an dans deux cours d'eau. En été, les poissons qui ont reçu des suppléments de nourriture avaient un taux de croissance moyen de 1,73 % de la masse totale·jour^{-1}, alors que les poissons qui n'ont eu accès qu'à la nourriture ambiante avaient un taux de 0,022, ce qui indique que la nourriture est un facteur limitant important. L'addition de gîtes a réduit la mortalité d'environ 50 % dans un des cours d'eau, mais, dans l'autre, la survie est restée élevée avec ou sans les gîtes additionnels. Il n'y a pas eu d'effet combiné de la nourriture et du gîte sur la croissance ou la survie. Les taux d'émigration étaient bas et n'étaient pas affectés ni par l'un, ni par l'autre des facteurs. Une modélisation de type marquage–recapture nous a permis de voir si la masse accrue de 48 % à la fin de l'expérience chez les poissons nourris en supplément augmentait leur survie en hiver. Les poissons nourris avaient une masse supérieure de 46 % à celle des poissons non nourris le printemps suivant, mais la survie à l'hiver n'était pas reliée à la taille des poissons. Nos résultats indiquent qu'en été la disponibilité de la nourriture peut limiter la croissance des truites fardées et que le gîte peut limiter la survie en affectant la prédation.

[Traduit par la Rédaction]

Introduction

Resource availability has long been recognized as playing a central role in limiting, and possibly regulating, populations. Food and cover (i.e., a habitat feature that provides protection from predators, competitors, or unfavorable environmental conditions) are often cited as critical resources for stream-dwelling salmonid fishes. Both are thought to strongly influence patterns of individual survival, growth, and habitat selection and, hence, population abundance or biomass (Chapman 1966; Bjornn and Reiser 1991). Laboratory studies have demonstrated how the availability of food and cover can mediate foraging rate – predation risk trade-offs (e.g., Grand and Dill 1997) or rates of emigration (Wilzbach 1985; Mesick 1988). However, most field studies that have linked food or cover to demographic measures are correlative (see Fausch et al. 1988; Poff and Huryn 1998) or have manipulated only a single variable. Few field manipulations have incorporated proper controls and replication (except see Gowan and Fausch 1996), and none have addressed the precise interplay between these two factors, perhaps in part due to the logistic difficulties inherent in performing stream experiments. Thus, the relative values of food and cover, and how they interact to limit fish production, have not yet been well quantified.

Food limitation of stream salmonids has been inferred from several lines of indirect evidence. Positive correlations between food supply and fish abundance, biomass, or growth rates during summer have been commonly noted (e.g., Wilzbach et al. 1986; Ensign et al. 1990). Similar trends have been found in studies that have increased primary and secondary production through nutrient additions (e.g., Deegan and Peterson 1992; Slaney and Ward 1993). Cover

Received 17 October 2001. Accepted 9 May 2002. Published on the NRC Research Press Web site at http://cjfas.nrc.ca on 25 July 2002.
J16575

S.M. Boss[1,2] and J.S. Richardson. Department of Forest Sciences, University of British Columbia, Vancouver, BC V6T 1Z4, Canada.

[1] Corresponding author (e-mail: sboss@ualberta.ca).

[2] Present address: Department of Biological Sciences, University of Alberta, Edmonton, AB T6G 2E9, Canada.

DOI: 10.1139/F02-079

Table 1. Comparison of stream characteristics, experimental details, and enclosure characteristics of East and Spring creeks.

	East Creek	Spring Creek
Stream characteristics		
Gradient of study reach (%)	1.9	1.8
Elevation (m)	154	160
Experimental details		
No. of replicates	12	4
Start date – end date	8 Aug. – 16 Sept.	28 Aug. – 16 Sept.
Duration (days)	40	20
No. of fish per enclosure	5	10
Mean temperature (°C)	15.1 (range = 12.6–17.2)	NA
Enclosure characteristics		
Mean wetted width (m) (mean ± SE)	2.24±0.05	3.25±0.29
Mean depth (cm) (mean ± SE)	12.09±0.22	15.5±1.44
Velocity ($m \cdot s^{-1}$)	<0.14	<0.10
Substrate size (% distribution ± SE)		
Sand and silt (<2 mm)	6.3±1.3	70±10.8
Gravel (2–64 mm)	70.3±3.0	26.3±9.7
Cobble (64–130 mm)	22.3±3.7	3.75±1.3

Note: NA, not available (temperature logger in Spring Creek was lost); SE, standard error.

may influence survival by protecting fish from their predators and by providing refuge from high water velocities. Many studies have demonstrated a positive correlation between the abundance of salmonids and the amount of in-stream physical structure (e.g., Fausch et al. 1988; Roni and Quinn 2001). The association of fish with in-stream structure, however, may simply reflect habitat preferences and does not provide sufficient evidence that cover improves survival.

Previous experiments have provided insight into the role of food (Mason 1976) or cover (Gowan and Fausch 1996) separately but have only partially addressed the interaction of these resources (Wilzbach et al. 1986). Evidence of density dependence in individual growth rates (e.g., Jenkins et al. 1999) and increased growth and survival of salmon from direct addition of food (Mason 1976) provides strong support for a food-limitation hypothesis. Field and artificial stream experiments have reported conflicting results when testing for the effect of cover on survival (Lonzarich and Quinn 1995; Gowan and Fausch 1996) and growth (Harvey 1998; Sundbaum and Näslund 1998). Quantifying the effects of food and cover on growth, survival, and migration requires experimental manipulation in the field.

In addition, linking summer growth to other measures of individual performance, such as overwinter survival, may further clarify the role of summer resources for fish. A pattern of improved winter survival with increasing size has been found for several species of stream salmonids, including trout (e.g., Mason 1976; Hutchings 1994; Smith and Griffith 1994). Thus, factors limiting growth during summer may impact individuals and populations through both immediate and delayed mechanisms.

Resident (i.e., nonanadromous) coastal cutthroat trout (*Oncorhynchus clarki*) are common in small streams of the Pacific Northwest. We tested how and to what extent food, cover, and the interaction of the two affect cutthroat trout during summer. We experimentally manipulated the supply of food and cover within enclosures containing individually marked trout in two natural streams. We predicted that (*i*) food addition would affect individuals primarily through increased growth, (*ii*) cover addition would primarily increase survival, and (*iii*) both would decrease emigration. To determine whether differences in body size (in this study due to experimentally altered phenotypes) result in differential growth or survival over winter, experimental trout were recaptured over winter following their release from enclosures.

Materials and methods

Study area

Research was conducted at the Malcolm Knapp Research Forest (49°16′N, 122°34′W) within the Coastal Western Hemlock (*Tsuga heterophylla*) biogeoclimatic zone of British Columbia, Canada. Two streams, East Creek and Spring Creek (Table 1), with unexploited populations of resident coastal cutthroat trout were selected that contained suitable reaches for installing experimental enclosures. Resident cutthroat trout are the only species of fish within the study reaches. East Creek is a second-order stream and is a tributary to Spring Creek, a third-order stream; the study reaches were separated by approximately 0.5 km of stream. The surrounding western hemlock, western redcedar (*Thuja plicata*), and Douglas-fir (*Pseudotsuga menziesii*) forests were harvested for the second time in the mid-1970s and replanted with Douglas-fir. The current streamside forest is dominated by Douglas-fir, with sparse red alder (*Alnus rubra*), salmonberry (*Rubus spectabilis*), and western redcedar in riparian zones.

Summer experiment

During August and September of 1997, we performed a factorial experiment in East and Spring creeks with two levels of food and cover. The four treatments were (*i*) control (no food or cover added), (*ii*) food addition, (*iii*) cover addition, and (*iv*) both food and cover added. Each treatment was replicated four times (three in East Creek and one in Spring Creek). Groups of individually marked 1-year-old cutthroat trout were introduced into 9-m-long enclosed reaches of stream. Enclosures were randomly assigned treatments within each stream, except in one case where a single enclosure, with a 40-cm-deep undercut bank, was restricted to either a cover or a food and cover treatment. Due to the intensive setup necessary, we first installed enclosures in East Creek and began the experiment and then constructed the Spring Creek enclosures. This resulted in the experiment running for 40 days in East Creek and 20 days in Spring Creek (Table 1).

The food addition treatment consisted of live mealworms (larval *Tenebrio molitor*). Daily rations were 16% of the biomass of all fish per enclosure. In East Creek, we adjusted rations at the midpoint of the experiment to account for increased biomass due to fish growth. Food was dispensed over 12 h by automatic conveyor belt style feeders attached to the upstream fence of the enclosure. This slow, haphazard introduction of food mimics how fish would encounter natural prey falling from riparian vegetation. A cover structure consisted of a 25.4 cm × 2.54 cm × 1.8 m wooden plank tied to the top of two cinder blocks. In East Creek, each enclosure assigned a cover treatment received three plank – cinder block structures, and in Spring Creek, which at the time of setup was twice the wetted width, each received six. Fish readily used the structures as cover and as foraging stations throughout the experiment.

The reaches selected for enclosure locations were low in structural complexity and had relatively homogeneous widths and depths (Table 1). Although rarely necessary, any structure present, such as boulders or small wood, was removed. Two fences installed across the width of the stream enclosed each reach. Enclosure fences were 4-mm wire mesh attached to an 81.3-cm-high wooden frame supported by steel reinforcing rods, with the bottom board of each fence buried in the substrate. To control for differing light levels among enclosures, any shrubs overhanging the stream were tied back.

Each enclosure had an upstream and downstream emigration trap fitted onto the fences. Traps were 28 × 28 × 28 cm and had a 2-cm-wide v-notched entrance; two flexible plastic strips extended from both sides of the v and met at the center of the entrance. Fish could exit the enclosure into a trap, which then held the fish until checked.

Fish marking and monitoring

Baited minnow traps and some electrofishing were used to collect the study fish from their respective streams. Fork length (millimetres) and mass (nearest 0.01 g) were measured for all fish. Five size-classes of 1-year-old cutthroat trout were used: (*i*) 68–72, (*ii*) 73–76, (*iii*) 7–80, (*iv*) 81–84, and (*v*) 85–88 mm for East Creek and (*i*) 74–78, (*ii*) 79–82, (*iii*) 83–86, (*iv*) 87–90, and (*v*) 91–94 mm for Spring Creek. Aging was based on examined scales (data from 1973–1976 and 1983) and length–frequency histograms (data from 1997) of fish in East Creek (S. Hinch, K. Young, and T. Northcote, Department of Forest Sciences, University of British Columbia, Vancouver, BC V6T 1Z4, Canada, unpublished data). We attempted to match the density of fish in the enclosures to that of natural stream densities, approximately 0.49 fish·m^{-2} (Young et al. 1999). Each enclosure received a single fish of each size in East Creek and two fish of each size in Spring Creek. Initial mass ranged from 2.89 to 7.11 g in East Creek and from 3.66 to 7.55 g in Spring Creek. Fish were individually marked with unique combinations of colored latex dye injected into anal, caudal, and dorsal fins, and all adipose fins were clipped. Prior to the introduction of experimental fish, the enclosures were intensively trapped and electrofished to remove any unwanted fish.

Fish were sampled using minnow traps baited with salmon roe. Traps were set and checked daily for three consecutive days at the midpoint (East Creek only), end, and 1 week after the end of the experiment. Captured fish were anesthetized with carbon dioxide, weighed, measured, and released back into enclosures.

Relative growth rate (RGR) (percent change in body mass per day) for individuals was calculated as

$$\text{(1)}\qquad \text{RGR} = [(\text{final mass} - \text{initial mass})/(\text{initial mass} \times \text{no. of days between sampling})] \times 100$$

Most fish were in enclosures for several days before the experiment began, and some were not recaptured until several days after it had ended. We used the actual number of days between sampling in calculations rather than back-calculating initial and final mass to the start and end date of the experiment to ensure conservative growth estimates. We estimated survival as the percentage of fish from each enclosure that were caught at the end of the experiment, or at any point during winter sampling.

Emigration traps were checked daily for fish. Emigrants were weighed, measured, and then released at the center of the enclosure reach. To minimize handling stress, individuals that emigrated on two or more consecutive days were returned to the enclosure but not remeasured.

To place growth of experimental fish in a natural context, we calculated growth rates for 14 free-ranging, marked fish in East Creek. The free-range fish were within the initial size-class limits of the experimental fish. Growth rates were calculated over a minimum of 20 days during the same time period as the experiment.

Drift nets with a mesh size of 250 μm were used to collect stream invertebrates in enclosures. Two out of three replicates of each treatment in East Creek were sampled midway and at the end of the experiment, and each enclosure in Spring Creek was sampled at the end of the experiment. Drift nets were set for a total of 3 h: 2 h before sunset until 1 h after sunset. Drift density was calculated as numbers per 100 m^3.

Analyses

To test for treatment effects on mean RGR, percent survival, and emigration, we used a randomized block analysis of variance (ANOVA), where stream was the blocking variable and replicates were nested within blocks and treatments (Table 2). This design created a sampling error term that was used to test for a block effect and block by treatment interactions.

To compare condition of fish among treatment groups, we used analysis of covariance (ANCOVA) with final mass as the dependent variable and final length as the covariate (both

Table 2. Mean square estimates of ANOVA for the 2 × 2 factorial experiment, randomized block design.

Source	df	df (calculated)	Sum of square	Mean square	Mean square estimate (F value)
Block (random)	$n - 1$	$2 - 1 = 1$	SS_{BLOCK}	MS_{BLOCK}	MS_{BLOCK}/MS_{SE}
Treatment	$k - 1$	$4 - 1 = 3$	SS_{TREAT}	MS_{TREAT}	MS_{TREAT}/MS_{EE}
Food (fixed)		1	SS_{FOOD}	MS_{FOOD}	MS_{FOOD}/MS_{EE}
Cover (fixed)		1	SS_{COVER}	MS_{COVER}	MS_{COVER}/MS_{EE}
Food × Cover		1	$SS_{F \times C}$	$MS_{F \times C}$	$MS_{F \times C}/MS_{EE}$
Experimental error	$(n - 1)(k - 1)$	$(2 - 1)(4 - 1) = 3$	SS_{EE}	MS_{EE}	MS_{EE}/MS_{SE}
B × F		1	$SS_{B \times F}$	$MS_{B \times F}$	$MS_{B \times F}/MS_{SE}$
B × C		1	$SS_{B \times C}$	$MS_{B \times C}$	$MS_{B \times C}/MS_{SE}$
B × F × C		1	$SS_{B \times F \times C}$	$MS_{B \times F \times C}$	$MS_{B \times F \times C}/MS_{SE}$
Sampling error	$k\sum_{i=1}^{n}(r_i - 1)$	$4(1 - 1) + 4(3 - 1) = 8$	SS_{SE}	MS_{SE}	
Total	$\left(k\sum_{i=1}^{n} r_i\right) - 1$	$(4 \times 1 + 4 \times 3) - 1 = 15$	SS_{TOTAL}		

Note: Stream is the blocking factor, food and cover are treatments, and each treatment is replicated four times. Block (B) is a random factor, food (F) and cover (C) are fixed factors, and replicates are nested in blocks and treatments. *n*, no. of blocks; *k*, no. of treatments; *r*, no. of replicates.

variables were log transformed). This fits a regression relationship of length and mass for each treatment group and tests if length–mass relationships differ among groups.

One might ask whether individuals that survived or emigrated differed in any way from those that died or did not move. We compared the initial size-class of survivors versus nonsurvivors and fish that emigrated versus those that did not. Mann–Whitney *U* tests were used for these tests because size-class data (i.e., 1, 2, 3, 4, or 5) were ordinal and not normally distributed. We further compared final condition and RGR of fish that emigrated versus those that did not using two-factor ANCOVA (as above) and ANOVA, respectively. In both the ANCOVA and ANOVA, the second factor was food treatment. When necessary, data were transformed (and noted in the results) to meet the assumptions of ANOVA.

Young-of-the-year and a few 1-year-old cutthroat that had either not been successfully removed from enclosures or entered during a high-water event midway through the experiment in East Creek (the experiment had not yet started in Spring Creek) were present in some enclosures prior to the introduction of the experimental fish. These extra fish were taken out of enclosures when captured. Emigration, growth rate, and survival were not affected by the density of extra fish (corrected for the amount of time in enclosure), nor was emigration or growth rate affected by density of all fish in each enclosure (i.e., surviving experimental fish plus extra fish) (five analyses, ANCOVA, density covariate, all $p > 0.05$). Thus, we did not correct for density in the final analyses. No experimental fish were captured outside the enclosures during an intensive trapping session in East Creek after the high-water event.

We used the average of individual growth rates of fish in each enclosure as our response variable. However, not every fish was recaptured at the end of the experiment, and enclosures in each stream contained different numbers of fish initially. Enclosure means that are based on different numbers of fish could be biased if RGR is correlated with size of fish. Testing for this relation showed that growth rates were not related to initial mass of fish (ANCOVA on $\log x + 1$ transformed RGR, mass covariate $F_{[1,64]} = 1.48$, $p = 0.23$; slope = –0.018). We also calculated growth for East Creek over the entire 40-day period, rather than presenting data on the first and last 20 days separately, as average growth rates were not significantly different for these two time periods (repeated-measures ANOVA, time $F_{[1,8]} = 2.73$, $p = 0.14$).

Winter sampling

At the end of the summer experiment, the enclosure fences were removed, allowing the fish to disperse. We performed multiple capture–recapture sessions for the experimental fish over winter using baited minnow traps. Trapping took place in the general vicinity of, and extended beyond, where the enclosures had been located. In Spring Creek, the trapping reach (total length 113 m) was bounded upstream by a steep increase in gradient and downstream by a road culvert. Culverts set both the up- and downstream trapping limits on East Creek (total length 448 m). While deterrents to movement existed at all of the reach boundaries, the upstream culvert on East Creek was likely the only true barrier to emigration.

Traps were set 5 m apart, with an extra trap set every 15 m, along the length of the stream reach. Traps were set in the same locations for every trapping session and sampled a variety of habitat types.

Six trapping sessions were conducted after the summer experiment during October and November of 1997 and in January, February–March, April, and June of 1998. Sessions in Spring and East Creeks were separated by 0, 8, 3, 3, 1, and 0 days, respectively. To simplify analysis, the sessions were treated as if they had taken place concurrently in each stream. Sessions lasted one to three consecutive days, and traps were checked approximately every 24 h. Each captured animal was identified, measured, weighed, and returned to its point of capture. All fish had passive integrated transponder tags for individual identification implanted into the body cavity upon first capture, as some of the latex marks were fading.

Analysis

Growth

To test for differences in overwinter growth between fish that had or had not received food additions during the summer, we compared the mass of 26 experimental fish caught in September and again in April. As fish were no longer restricted to enclosures, each individual was considered a replicate. We compared mass and Fulton's condition factor (grams per cubic millimetre × 10^{-5}) (Ricker 1975) of fish in September and April by three-factor ANOVA after testing to ensure that condition did not increase or decrease as a function of fish length (Cone 1989). We did not use ANCOVA (as for condition analysis for the summer experiment) to test for differences in length–mass relationships because sample sizes were too low. Stream (East or Spring) and food treatment (fed or unfed) were fixed, between-group factors and time (September or April) was a repeated-measure factor.

Survival

We used capture data from experimental fish for which we had measures of September mass to examine the relationship between fall size and survival. For the purposes of capture–recapture analysis, the data from all days within a trapping session were pooled, with the assumption that no demographic changes had occurred over this short period. Analysis of capture–recapture data results in separate estimates of survival (Φ) and capture (P) probabilities. Here, mortality reflects losses due to both death and emigration. We estimated monthly survival by first fitting a series of biologically realistic survival–recapture models. The best model was then selected based on the principle of parsimony. The set of models was created by (1) defining a global or most parameterized model, (2) reducing the global model by alternately removing sources of variation from capture and survival model structure, and (3) modeling survival and (or) capture probabilities as logistic functions of individual fall mass.

The global model, $\Phi_{s*t}P_{s*t}$, allowed survival and capture rates to differ over time (t) and between streams (s), i.e., the time-dependent Cormack–Jolly–Seber model applied to each site. Notation follows that of Lebreton et al. (1992), where factors can be combined additively (+, parallel on the logit scale) or interactively (*). The mass-dependent models were based primarily on the structure of the best model from step 2 above, although some with a more complex or simpler structure were also fit. Covariate models were fit using the logit link, with survival or recapture expressed as a linear function of mass, i.e., probability = $b_0 + b_1$(mass).

The best model was selected according to the Akaike information criterion (AIC) (Lebreton et al. 1992). AIC selects the most parsimonious model by compromising between simple model structure with good precision but high bias and complex model structure with low bias but poor precision. The model with the lowest AIC represents the best compromise between bias and precision. We used a limited number of likelihood ratio tests to confirm results based on AIC. The overall goodness-of-fit of the global model was checked using the χ^2 statistics of Test2 + Test3 described in Burnham et al. (1987). Program MARK (White and Burnham 1999) was used for model fitting and selection (based on AICc, a modification of AIC that corrects for bias related to sample size) and goodness-of-fit testing and to calculate the final maximum likelihood survival and recapture estimates.

Fig. 1. Mean relative growth rates of cutthroat trout in enclosures with and without food and cover (n = 4 for all treatment combinations). Open bars represent no-cover treatments and solid bars represent cover treatments. Error bars are ±1 SE.

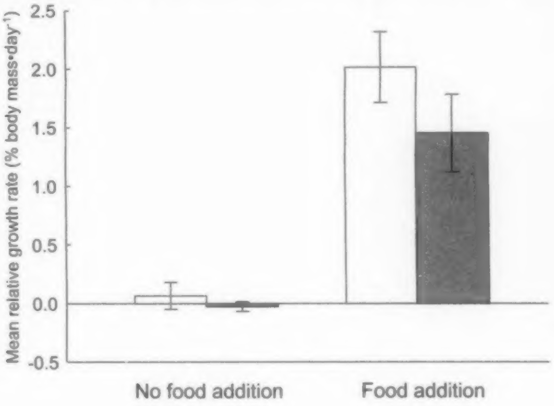

Results

Summer experiment

Our initial level of cover added and stocking densities were based on the relative wetted widths of the two streams at the time of setup and our estimation of what their widths would be at summer low flow. By the time summer low flows were reached, Spring Creek was only about 1 m wider than East Creek. This resulted in cover treatments not being proportional (percent area in cover was 6.8 and 9.4% in East and Spring creeks, respectively) in the two streams and densities (about 0.25 and 0.34 fish·m^{-2}) were below our projections. However, these differences should not be problematic because as noted earlier, growth was not related to density of fish, and stream was treated as a blocking factor and would thus control for such differences.

Growth

Growth of trout was strongly influenced by food (ANOVA, food $F_{[1,3]} = 34.76$, $p = 0.01$); based on mean growth rates per enclosure, fish receiving food addition experienced 80 times higher growth rates than fish that did not receive food (Fig. 1). By the end of the experiment, the mean mass of fed fish was 71% higher than that of unfed fish in East Creek and 30% higher in Spring Creek (Table 3). Cover did not affect growth rates (cover $F_{[1,3]} = 0.62$, $p = 0.49$) and there was no interaction between treatments (food × cover $F_{[1,3]} = 0.04$, $p = 0.85$). Growth also did not vary by stream (block $F_{[1,8]} = 0.04$, $p = 0.85$), nor were there stream by treatment interactions (all $p > 0.05$).

Table 3. Initial and final size (mean ± SE) of cutthroat trout receiving different food treatments in East and Spring creeks.

	Initial			Final		
	n	Length (mm)	Mass (g)	*n*	Length (mm)	Mass (g)
East Creek						
No food added	30	78.2±1.0	4.61±0.18	25	79.2±1.1	4.48±0.21
Food added	30	77.9±1.0	4.46±0.17	25	89.8±1.7	7.65±0.47
Spring Creek						
No food added	20	84.1±1.2	5.36±0.23	11	85.0±2.2	5.70±0.47
Food added	20	84.4±1.3	5.53±0.25	13	89.2±1.5	7.38±0.37

Note: SE, standard error.

Table 4. Numbers (mean ± 1 SE (range)) of invertebrates collected during 3-h drift net samples in experimental enclosures in East and Spring creeks.

	East Creek, Aug.	East Creek, Sept.	Spring Creek, Sept.
Aquatic			
Diptera	49±23 (7–182)	28.3±5.3 (8–69)	23±2.0 (17–26)
Plecoptera	4.1±1.0 (1–8)	3.5±0.8 (1–9)	6.5±1.0 (4–9)
Trichoptera	3.7±1.4 (1–11)	5.9±1.8 (1–23)	5±1.1 (3–8)
Ephemeroptera	0.4±0.4 (0–3)	3±0.8 (0–7)	2.5±1.4 (0–5)
Other	4.7±1.4 (1–11)	8.8±2.6 (0–34)	8±1.6 (5–12)
Terrestrial	2.4±0.6 (1- 4)	4.3±1.1 (0–12)	6±0.9 (4–8)
Drift density (no. per 100 m^3)	340±68 (200–738)	292±30 (194–519)	284±18 (251–329)
n	7	8	4

Note: SE, standard eror.

Although the RGRs of unfed fish were low and sometimes negative (mean ± 1 SE = 0.029 ± 0.05% body mass·day^{-1}, $n = 35$), they were not different from those of free-ranging trout (0.147 ± 0.04, $n = 14$, $t = -1.21$, df = 47, $p = 0.23$). Further, the minimum growth rate of unfed fish was the same as that for free-ranging fish, suggesting that growth of unfed fish was within the range of what is naturally experienced. Although not significant, the mean growth of unfed fish was five times lower than that of free-ranging fish. Any enclosure effects are likely to have been equal across all treatments, however, and thus the magnitude of growth differences between fed and unfed fish would not be affected. Growth rates of fed fish were 12 times higher than those of free-ranging trout. Drift densities were similar among enclosures (Table 4) and comparable with densities typically found in other streams (100–1000·m^{-3}) (Allan 1995).

Condition

The elevation of the length–mass regression lines was different for fed and unfed fish only (ANCOVA, food $F_{[1,3]} = 83.39$, $p < 0.01$) and the slopes of the regression lines were parallel (block × food × cover $F_{[1,58]} = 0.29$, $p = 0.96$). Thus, fed fish were in better condition, weighing 13% more than unfed fish at any given length.

Survival

Survival of trout ranged from 40 to 100%, but was generally high, with the median survival within enclosures equaling 95%. Although the main effect of cover did not indicate an effect on survival, the block (i.e., stream) by cover interaction was significant. In East Creek, survival was high regardless of treatment. Spring Creek differed, in that survival of trout in enclosures without cover was less than half that of trout with cover (ANOVA, block × cover $F_{[1,8]} = 10.32$, $p = 0.01$) (Fig. 2). There were no other treatment effects on survival (all $p > 0.05$). The initial size of fish was not related to survival (Mann–Whitney *U* test, $Z = -0.55$, $p = 0.58$).

Fig. 2. Mean survival of cutthroat trout in Spring Creek and East Creek enclosures with and without cover addition ($n = 2$ for Spring Creek treatments and $n = 6$ for East Creek treatments). Open bars represent no-cover treatments and solid bars represent cover treatments. Error bars are ±1 SE.

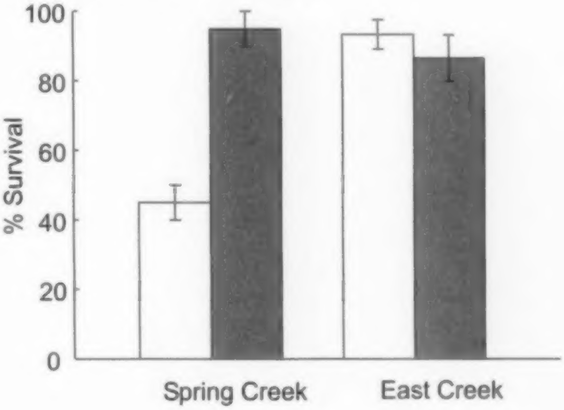

Emigration

Emigration was low during the experiment, with only 16 individuals out of 100 fish making a total of 29 moves into

Fig. 3. Comparison of mean mass of unfed (solid circles) and fed cutthroat trout (open circles) in fall and spring (n = 12 for unfed trout and n = 14 for fed trout). Error bars are ±1 SE.

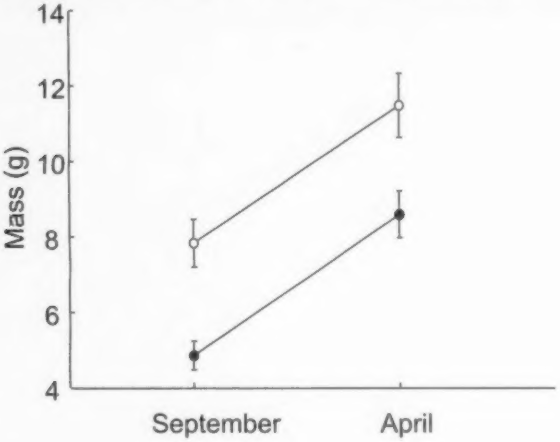

emigration traps. Of those moves, 25 were into downstream traps and four were into upstream traps. The mean number of times that fish emigrated per enclosure was not affected by either food or cover (ANOVA, food: mean ± SE = 2.75 ± 1.11, $F_{[1,3]} = 0.64$, $p = 0.49$; cover: 2.75 ± 0.63, $F_{[1,3]} = 1.34$, $p = 0.33$). Emigration decreased to an average of 0.50 ± 0.50 moves per enclosure with both food and cover present, but the decrease was not significant ($F_{[1,3]} = 3.49$, $p = 0.16$). Trends did not change when only one emigration event was counted per individual. Emigrants did not differ from nonmovers in initial size (Mann–Whitney U test, $Z = -1.13$, $p = 0.26$), final condition (ANCOVA, emigration $F_{[1,69]}$ = 0.83, $p = 0.37$), or RGRs (ANOVA on log x + 1 transformed RGR, emigration $F_{[1,69]} = 1.14$, $p = 0.29$).

Winter

Growth

Fed fish maintained their size advantage by 46% over unfed fish during winter (ANOVA, food $F_{[1,22]} = 6.27$, p = 0.02; time $F_{[1,22]} = 136.48$, $p < 0.001$; stream and all interaction terms, $p > 0.05$) (Fig. 3). By the spring, condition of fed fish (mean ± 1 SE = 0.926 ± 0.03) had decreased to that of unfed fish (0.926 ± 0.01) (ANOVA on square-root-transformed condition factor, food × time $F_{[1,22]} = 6.72$, p = 0.02).

Survival

We had measures of September mass for 74 of the 100 experimental fish and thus used capture data from these 74 individuals for survival modeling. A total of 85 recaptures were made over winter. The global Cormack–Jolly–Seber model, which estimates a unique survival and capture probability for every time period for each stream, appeared to be a good fit (East Creek: $\chi^2_{10} = 3.44$, $p = 0.97$; Spring Creek: $\chi^2_5 = 4.92$, $p = 0.43$; total $\chi^2_{15} = 8.35$, $p = 0.91$). A probability of <0.05 would indicate a poor fit. Test power was low, however, because data were sparse.

Table 5. Best fitting survival and recapture models for size–survival analysis of experimental cutthroat trout over winter.

Survival Φ	Capture P	No. parameters	AICc	ΔAICc	Deviance
•	t	**7**	**428.71**	**0.00**	**413.90**
s	t	8	430.75	2.04	413.70
•+m	t	8	430.85	2.14	413.80
•	t+m	8	430.95	2.24	413.90
s+m	t	9	432.92	4.21	413.60

Note: Notation describes the factors and covariates that affect survival and capture probability: "s" indicates that the parameter varies between streams, "t" that the parameter varies among trapping sessions, and "•" that the parameter is constant between streams or over time. "+m" indicates that the parameter was modeled as a linear function of mass (m), parameter = $b_0 + b_1(m)$, where curves are fit with common slopes but different intercepts for each stream (s+m) or at each time period (t+m). The best model is in bold. Modeling was performed using program MARK.

Fig. 4. Comparison of the cumulative minimum proportion of unfed (solid circles, solid line) and fed cutthroat trout (open circles, dotted line) present over time.

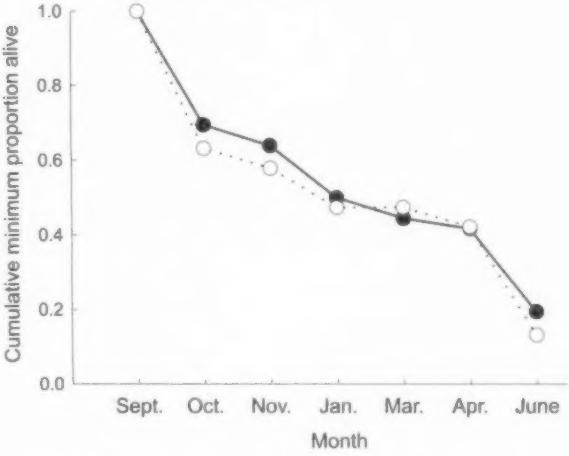

Of all of the models fit, model $\Phi_{\bullet}P_t$, had the lowest AICc, i.e., it was the most parsimonious model (Table 5). All other models had AICc values greater by at least 2.0. Selection of model $\Phi_{\bullet}$ indicates that none of the factors tested (stream, time, or the fall mass of fish) explained a significant amount of variation in survival. Likelihood ratio tests also indicated no effect of these factors. The best mass model, $\Phi_{\bullet+m}$, had a very shallow slope of –0.034 (on the logit scale), contrary to the predicted positive relationship between survival and size. Replacing the mass covariate with length or condition factor showed similar results. Under the best model, monthly recapture rates varied from 18 to 55%. Plotting the cumulative minimum proportion of unfed versus fed fish present over time illustrates no difference between the two groups (Fig. 4).

Two days of extra trapping in 140-m (East Creek) and 76-m (Spring Creek) sections immediately downstream of the study reaches during April captured no experimental fish. This suggests that emigration was minimal, although it is possible that fish had moved beyond this distance.

Discussion

As predicted, food was the dominant factor acting on trout growth, while cover acted through an effect on survival. Trout growth was clearly food limited, but there was no evidence that cover affected growth. The only cover effect was in Spring Creek, where mortality was substantially higher in the absence of cover. Although the effects of food and cover did not interact statistically, they do interact in a biological sense in that the highest biomass would occur under conditions of both high food and high cover availability. Fed fish were still larger than unfed fish by the following spring, but larger fall size did not appear to confer an advantage to fish in terms of overwinter survival.

Food and growth

Several studies have inferred that food availability limits population densities and growth of stream salmonids. These studies are often based on observations of density-dependent growth, positive correlations between food availability and fish growth or abundance, and response of fish to nutrient enhancement. Our results confirm observations from correlative and nutrient addition studies and show that food limits cutthroat trout growth in small, coastal streams. Mason (1976) also directly manipulated food supply to underyearling coho salmon (*Oncorhynchus kisutch*) in enclosed reaches of a Vancouver Island stream and increased their biomass, through both increased growth and increased survival, by 2.5 times that of controls. Stimulating primary production by adding nutrients has resulted in increased growth rates (e.g., Deegan and Peterson 1992), individual size (e.g., Slaney and Ward 1993), and possibly density (Slaney and Ward 1993) of trout and salmon. Although the scale of our experiment was not ideal for measuring a survival effect of food, the large difference in growth between treatments indicates the potential for substantial fitness consequences and thus survival and population-level changes.

The extent to which fish are limited by food likely varies seasonally and spatially. Metabolic requirements, and thus food demand, of fish increase with temperature (Ursin 1979). During summer, warm temperatures, high fish densities as a result of new recruits, and reduced water volume increase the potential for food limitation. Late summer, the period when this study was conducted, appears to be a time when growth of stream trout is naturally quite low. For example, in three small Oregon streams, growth rates of 1-year-old cutthroat trout declined steadily over the summer and by August and September had reached levels similar to rates of unfed trout in this study (Lowry 1966). In an uncontrolled field setting, it is difficult to establish food limitation as the cause of low growth, since fish may, for example, feed very little in response to decreasing temperatures, even if food is available in excess (Jonsson et al. 2001). On a basic level, our experiment shows that fish are not incapable of high growth during this period but rather that they are in fact food limited. Numerous studies report low or negative growth of stream trout during summer (e.g., Cada et al. 1987; Ensign et al. 1990), which suggests that food limitation may be common across many populations of salmonid species. Generally, the potential for food limitation may be greatest in cool, densely shaded streams, where light and low temperatures limit productivity (Hetrick et al. 1998), and (or) nutrient-poor waters. Food availability may set an upper limit on productivity (Richardson 1993), but it is important to note that other factors may curb production before food limitation occurs. Availability of spawning habitat, appropriate summer and winter habitats, predators, and temperature can all act, and potentially interact, to affect production.

Food limitation at the individual level does not necessarily mean that food is also limiting population growth. Nevertheless, a number of fitness measures, such as the number or size of eggs produced by females, age of first reproduction, and overall survivorship, can be positively correlated with body size (Wootton 1990). These factors could affect the numerical growth rate of populations. This may be particularly relevant for resident populations where population regulation can occur at adult stages (Elliott and Hurley 1998). Further, both food and cover can affect territory size of salmonids. Higher food levels tend to result in smaller territory sizes (e.g., Keeley and Grant 1995), as does cover by increasing the degree of visual isolation (Kalleberg 1958). Thus, more fish can occupy a given area. In this study, the trend for decreased emigration in the presence of both food and cover, although not significant, points to this possibility.

Cover and survival

We found no effect of cover on trout growth rates. Previous work on how cover affects growth has been equivocal. Experiments where fish have been enclosed have found increases (Sundbaum and Näslund 1998), decreases (Wilzbach et al. 1986), or no difference (Lonzarich and Quinn 1995; Spalding et al. 1995; this study) in growth in response to cover. Field manipulations where fish are free to move have generally found no effect of cover on growth (e.g., Gowan and Fausch 1996; Harvey 1998). However, density-dependent growth may confound the outcome of such studies because the habitat manipulation often results in higher numbers of fish. How cover affects fish growth may depend on whether the structure acts as velocity refuge, visual isolation, or predation refuge to fish. Cover may enhance growth by providing favorable foraging sites, for example, low-velocity positions next to swifter currents (Fausch 1984). Further, cover may reduce exposure to competitors and predators, allowing fish more time to forage and decreasing energy expenditure related to aggressive interactions (Sundbaum and Näslund 1998). There may be a negative effect on growth, however, if heavy shading reduces a fish's ability to detect or catch its own prey (Wilzbach et al. 1986). The relative importance of each function, and thus the net effect of cover, will likely vary by species, season, and state-dependent differences among fish.

We found a direct link between cover and summer survival of trout. Interestingly, the absence of cover increased mortality in one stream but had no effect in the other. All summer mortality was likely from predation, as streams were near base flow, no fish were found dead against enclosure screens, and the fish showed no signs of stress or disease during handling. This suggests that there may have been a difference in predation pressure between streams.

Variation in predation intensity among streams is undoubtedly common in nature but difficult to quantify. Predator sightings were not common, but a great blue heron (*Ardea herodias*) was observed at Spring Creek and on a few occasions a weasel (*Mustela* sp.) at East Creek. Also, larger substrate size in East Creek may have provided fish with cover from predation even in the absence of the cover treatment.

The cover effect in Spring Creek contradicts previous studies that have found no strong relation between salmonid survival and physical structure during summer. Spalding et al. (1995) found significant avian predation on juvenile coho salmon in seminatural stream channels, but mortality was not related to the complexity of brushy debris treatments. Similarly, Lonzarich and Quinn (1995) found that cover in the form of depth, rather than physical structure, was most important in determining patterns of survival for juvenile coho salmon and steelhead (*Oncorhynchus mykiss*). Rosenfeld and Boss (2001) found that energetics alone explained selection of deep habitat (i.e., pools) by 1- to 2-year-old anadromous cutthroat trout, without having to invoke greater predation risk in shallow, riffle habitats. Research based in warm-water streams demonstrates very strong predator impacts, mediated by water depth (e.g., Power 1987). The role that predation plays in structuring fish populations in more northern temperate regions is less clear. Even though predators appeared uncommon in our study area, the chance arrival of a single predator in a situation where prey are vulnerable could cause very high mortality. A study of the relation between stream size or type, predator abundance, and prey behavior would help clarify the role of predators and (or) cover.

Our results show that cover can improve survival when emigration is restricted. Under natural conditions, fish may choose to leave habitats low in cover to reduce predation risk. Indeed, in a large-scale experiment, Gowan and Fausch (1996) found that only movement, not survival, of resident trout was affected by habitat manipulation. Artificial stream channel experiments sometimes find increased emigration under low-cover conditions (Mesick 1988), although we found no evidence of this. Under high population densities, however, some individuals may be forced into suboptimal habitats by dominant conspecifics (e.g., Fausch 1984). Also, it is not uncommon for fish to become isolated in pools during summer low flow in small streams (e.g., Northcote and Hartman 1988). In situations such as these, cover could be naturally limiting to fish.

Body size and overwinter survival

Previous studies of stream-resident trout have noted a positive relation between body size and survival over winter (e.g., Hutchings 1994; Smith and Griffith 1994). Size-biased survival is thought to arise because smaller individuals are more susceptible to winter stresses (e.g., depletion of energy reserves, displacement by high water velocities, competition for limited winter habitat) or are subject to size-selective predation. We did not find that September mass of individuals was a predictor of winter survival. In fact, monthly survival rate, estimated for all 100 experimental fish using program MARK, was nearly equal for summer (excluding "no-cover" treatment in Spring Creek, 96.7%) and winter (96.6%) (Boss 1999). Fed fish did, however, maintain their size advantage over winter. That fed fish gained weight and simultaneously lost condition (i.e., grew longer) suggests that they converted energy into permanent somatic tissue rather than only using it in maintenance metabolism or temporary fat stores. Therefore, despite a lack of evidence for a survival benefit of increased size, fed individuals may have been able to allocate more energy into somatic tissue, earlier reproduction, higher fecundity, or securing the best habitats.

The magnitude of the size–survival relation, and winter survival in general, may be affected by the severity (e.g., temperature, flood events) and duration of winter (e.g., Post and Evans 1989). The winter of this study was quite mild with relatively moderate rain events and temperatures. This may have minimized size-biased mortality. In addition, the trout continued to grow from September until November and thus may have reached a threshold where survival was no longer influenced by size.

Despite a longstanding interest in identifying limiting resources for fish, basic experimental tests have rarely been performed in the field. Manipulations like those used in this study can help identify the relative importance of limiting resources and how they interact. Our study demonstrated the separate effects of food and cover on trout growth and survival and the possible implications of differences in body size for fish.

Acknowledgements

We thank Robyn Scott and Dan O'Donoghue for providing excellent field assistance; their efforts, plus those of other hard-working assistants and volunteers who gave their time, helped make this experiment possible. We appreciate helpful input and comments on an earlier version of the manuscript by Margaret Hall, Scott Hinch, Eric Parkinson, Shawna Pelech, Eric Taylor, and an anonymous reviewer. Funding was provided by the Natural Sciences and Engineering Research Council of Canada, Forest Renewal British Columbia, and the David and Mary Macaree Fellowship.

References

Allan, J.D. 1995. Stream ecology: structure and function of running waters. Chapman and Hall, London, U.K.

Bjornn, T.C., and Reiser, D.W. 1991. Habitat requirements of salmonids in streams. Am. Fish. Soc. Spec. Publ. **19**: 83–138.

Boss, S.M. 1999. Summer resource limitation and over-winter movement and survival of stream-resident coastal cutthroat trout. M.Sc. thesis, University of British Columbia, Vancouver, B.C.

Burnham, K.P., Anderson, D.R., White, G.C., Brownie, C., and Pollock, K.H. 1987. Design and analysis methods for fish survival experiments based on release–recapture. Am. Fish. Soc. Monogr. 5.

Cada, G.F., Loar, J.M., and Sale, M.J. 1987. Evidence of food limitation of rainbow and brown trout in southern Appalachian softwater streams. Trans. Am. Fish. Soc. **116**: 692–702.

Chapman, D.W. 1966. Food and space as regulators of salmonid populations in streams. Am. Nat. **100**: 345–357.

Cone, R.S. 1989. The need to reconsider the use of condition indices in fishery science. Trans. Am. Fish. Soc. **118**: 510–514.

Deegan, L.A., and Peterson, B.J. 1992. Whole-river fertilization stimulates fish production in an Arctic tundra river. Can. J. Fish. Aquat. Sci. **49**: 1890–1901.

Elliott, J.M., and Hurley, M.A. 1998. Population regulation in adult, but not juvenile, resident trout (*Salmo trutta*) in a Lake District stream. J. Anim. Ecol. **67**: 280–286.

Ensign, W.E., Strange, R.J., and Moore, S.E. 1990. Summer food limitation reduces brook and rainbow trout biomass in a southern Appalachian stream. Trans. Am. Fish. Soc. **119**: 894–901.

Fausch, K.D. 1984. Profitable stream positions for salmonids: relating specific growth rate to net energy gain. Can. J. Zool. **62**: 441–451.

Fausch, K.D., Hawks, C.L., and Parsons, M.G. 1988. Models that predict standing crop of stream fish from habitat variables. U.S. For. Serv. Gen. Tech. Rep. PNW-GTR-213.

Gowan, C., and Fausch, K.D. 1996. Long-term demographic responses of trout populations to habitat manipulation in six Colorado streams. Ecol. Appl. **6**: 931–946.

Grand, T.C., and Dill, L.M. 1997. The energetic equivalence of cover to juvenile coho salmon (*Oncorhynchus kisutch*): ideal free distribution theory applied. Behav. Ecol. **8**: 437–447.

Harvey, B.C. 1998. Influence of large woody debris on retention, immigration, and growth of coastal cutthroat trout (*Oncorhynchus clarki clarki*) in stream pools. Can. J. Fish. Aquat. Sci. **55**: 1902–1908.

Hetrick, N.J., Brusven, M.A., Meehan, W.R., and Bjornn, T.C. 1998. Changes in solar input, water temperature, periphyton accumulation, and allochthonous input and storage after canopy removal along two small salmon streams in southeast Alaska. Trans. Am. Fish. Soc. **127**: 859–875.

Hutchings, J.A. 1994. Age- and size-specific costs of reproduction within populations of brook trout, *Salvelinus fontinalis*. Oikos, **70**: 12–20.

Jenkins, T.M., Jr., Diehl, S., Kratz, K.W., and Cooper, S.D. 1999. Effects of population density on individual growth of brown trout in streams. Ecology, **80**: 941–956.

Jonsson, B., Forseth, T., Jensen, A.J., and Næsje, T.F. 2001. Thermal performance in juvenile Atlantic salmon, *Salmo salar* L. Funct. Ecol. **15**: 701–711.

Kalleberg, H. 1958. Observations in a stream tank of territoriality and competition in juvenile salmon and trout (*Salmo salar* L., and *S. trutta* L.). Inst. Freshwater Res. Drottningholm Rep. **39**: 55–98.

Keeley, E.R., and Grant, J.W.A. 1995. Allometric and environmental correlates of territory size in juvenile Atlantic salmon (*Salmo salar*). Can. J. Fish. Aquat. Sci. **52**: 186–196.

Lebreton, J.D., Burnham, K.P., Clobert, J., and Anderson, D.R. 1992. Modeling survival and testing biological hypotheses using marked animals: a unified approach with case studies. Ecol. Monogr. **62**: 67–118.

Lonzarich, D.G., and Quinn, T.P. 1995. Experimental evidence for the effect of depth and structure on the distribution, growth, and survival of stream fishes. Can. J. Zool. **73**: 223–2230.

Lowry, G.R. 1966. Production and food of cutthroat trout in three Oregon coastal streams. J. Wildl. Manage. **30**: 754–767.

Mason, J.C. 1976. Response of underyearling coho salmon to supplemental feeding in a natural stream. J. Wildl. Manage. **40**: 775–788.

Mesick, C.F. 1988. Effects of food and cover on numbers of apache and brown trout establishing residency in artificial stream channels. Trans. Am. Fish. Soc. **117**: 421–431.

Northcote, T.G., and Hartman, G.F. 1988. The biology and significance of stream trout populations (*Salmo* spp.) living above and below waterfalls. Pol. Arch. Hydrobiol. **35**: 409–442.

Poff, N.L., and Huryn, A.D. 1998. Multi-scale determinants of secondary production in Atlantic salmon (*Salmo salar*) streams. Can. J. Fish. Aquat. Sci. **55**(Suppl. 1): 201–217.

Post, J.R., and Evans, D.O. 1989. Size-dependent overwinter mortality of young-of-the-year yellow perch (*Perca flavescens*): laboratory, in situ enclosure, and field experiments. Can. J. Fish. Aquat. Sci. **46**: 1958–1968.

Power, M.E. 1987. Predator avoidance by grazing fishes in temperate and tropical streams: importance of stream depth and prey size. *In* Predation: direct and indirect impacts on aquatic communities. *Edited by* W.C. Kerfoot and A Sih. University Press of New England, Hanover, N.H. pp. 333–351.

Richardson, J.S. 1993. Limits to productivity in streams: evidence from studies of macroinvertebrates. *In* Production of juvenile Atlantic salmon, *Salmo salar*, in natural waters. *Edited by* R.J. Gibson and R.E. Cutting. Can. Spec. Publ. Fish. Aquat. Sci. No. 118. pp. 9–15.

Ricker, W.E. 1975. Computation and interpretation of biological statistics of fish populations. Bull. Fish. Res. Board Can. No. 191.

Roni, P., and Quinn, T.P. 2001. Density and size of juvenile salmonids in response to placement of large woody debris in western Oregon and Washington streams. Can. J. Fish. Aquat. Sci. **58**: 282–292.

Rosenfeld, J.S., and Boss, S. 2001. Fitness consequences of habitat use for juvenile cutthroat trout: energetic costs and benefits in pools and riffles. Can. J. Fish. Aquat. Sci. **58**: 585–593.

Slaney, P.A., and Ward, B.R. 1993. Experimental fertilization of nutrient deficient streams in British Columbia. *In* Le développement du Saumon atlantique au Québec: connaître les règles du jeu pour réussir. Colloque international de la Fédération québécoise pour le saumon atlantique, Québec, décembre 1992. *Edited by* G. Shooner and S. Asselin. Fédération québécoise pour le saumon altantique (FQSA), 42B, rue Racine, Loretteville, QC G2B 1C6. Collection *Salmo salar* No. 1. pp. 128–141.

Smith, R.W., and Griffith, J.S. 1994. Survival of rainbow trout during their first winter in the Henrys Fork of the Snake River, Idaho. Trans. Am. Fish. Soc. **123**: 747–756.

Spalding, S., Peterson, N.P., and Quinn, T.P. 1995. Summer distribution, survival, and growth of juvenile coho salmon under varying experimental conditions of brushy instream cover. Trans. Am. Fish. Soc. **124**: 124–130.

Sundbaum, K., and Näslund, I. 1998. Effects of woody debris on the growth and behaviour of brown trout in experimental stream channels. Can. J. Zool. **76**: 56–61.

Ursin, E. 1979. Principles of growth in fishes. Symp. Zool. Soc. Lond. **44**: 63–87.

White, G.C., and Burnham, K.P. 1999. Program MARK: survival estimation from populations of marked animals. Bird Study, **46**(Suppl.): 120–138.

Wilzbach, M.A. 1985. Relative roles of food abundance and cover in determining the habitat distribution of stream-dwelling cutthroat trout (*Salmo clarki*). Can. J. Fish. Aquat. Sci. **42**: 1668–1672.

Wilzbach, M.A., Cummins, K.W., and Hall, J.D. 1986. Influence of habitat manipulations on interactions between cutthroat trout and invertebrate drift. Ecology, **67**: 898–911.

Wootton, R.J. 1990. Ecology of teleost fishes. Chapman and Hall, London, U.K.

Young, K.A., Hinch, S.G., and Northcote, T.G. 1999. Status of resident coastal cutthroat trout and their habitat 25 years after riparian logging. N. Am. J. Fish. Manage. **19**: 901–911.

Estimating rates of fish movement from tag recoveries: conditioning by recapture

Richard McGarvey and John E. Feenstra

Abstract: Tag-recovery data are commonly used to estimate movement rates of fish stocks. Fishers report tagged fish found in their catch; however, not all recoveries are reported to fishery researchers and the rate of nonreporting is usually not known or is imprecisely estimated. To obviate the problem of nonreporting, an estimator of movement rates is proposed that does not use the number originally tagged but is fitted to the relative proportions recaptured in each cell in each time step subsequent to release. Rates of processes that occur in the tag-release spatial cell, such as short-term tagging mortality and survival, cancel from the predicted likelihood probabilities. Similarly, rates in the recapture cell for processes of ongoing tag loss, natural mortality, and tag nonreporting, if they can be reasonably approximated as uniform across cells, also cancel. Estimators are presented assuming one of two levels of auxiliary fishery inputs: (*i*) total mortality by cell or time step, or (*ii*) if mortality can be approximated as spatially uniform, effort totals in each cell, by time step. Yearly movement transition matrices were estimated for King George whiting (*Sillaginodes punctata*) in South Australia among 11 spatial cells from tag recoveries gathered over a period of three decades.

Résumé : Les données de recouvrement d'étiquettes de marquage sont couramment utilisées pour estimer les taux de déplacement des stocks de poissons. Les pêcheurs indiquent la présence de poissons marqués dans leurs récoltes, cependant les prises marquées ne sont pas toutes signalées aux ichtyologistes et le taux de défaut de déclaration est généralement inconnu ou alors estimé de façon imprécise. Pour contrer ce problème, nous proposons un estimateur des taux de déplacement qui n'utilise pas le nombre de poissons marqués au départ, mais qui s'ajuste aux proportions relatives de poissons recapturés dans chaque cellule dans chaque intervalle de temps depuis la remise à l'eau. Les taux des processus qui sont en opération dans la cellule spatiale de remise à l'eau, tels que la mortalité à court terme due au marquage et la survie, s'éliminent avec les probabilités prédites de vraisemblance. De même, les taux dans la cellule de recapture reliés à la perte courante d'étiquettes, à la mortalité naturelle et au défaut de déclaration des étiquettes sont aussi éliminés, si on peut assumer qu'ils sont à peu près uniformes dans les cellules. Nous présentons des estimateurs qui présupposent la disponibilité de deux niveaux de données auxiliaires sur la pêche : (*i*) la mortalité totale par cellule ou par intervalle de temps ou (*ii*) la somme des efforts de pêche dans chaque cellule pour chacun des intervalles de temps, si la mortalité peut être considérée comme uniforme dans l'espace. Des matrices de transition du déplacement annuel ont pu être dressées pour le pêche-madame moucheté (*Sillaginodes punctata*) en Australie Méridionale pour 11 cellules spatiales à partir de données de récupération d'étiquettes sur une période d'une trentaine d'années.

[Traduit par la Rédaction]

Introduction

In estimating fish-stock abundance, making explicit the movement of fish (Quinn et al. 1990; Fournier et al. 1998; Punt et al. 2000) is becoming more commonplace as spatial models become increasingly computationally feasible. Bias is reduced when migration is taken into account. For example, emigration out of a study area that is not explicitly modeled will result in overestimates of mortality, as the lower numbers in older ages are attributed by default to mortality alone.

Three forms of movement model have been postulated (for review see Quinn and Deriso 1999). Most assume a discrete time step, often yearly, and quantify movement by estimating proportions expected to move from any model cell (subregion or statistical reporting area) to all others at each model movement time.

Fish movement is modeled as diffusion when it is wholly or partly undirected to any specific destination. First developed in spatial ecological application (Okubo 1980) and adopted for fishery models (Hilborn 1987; Deriso et al. 1991; Fournier et al. 1998), diffusion estimators are applied to widely ranging oceanic stocks, notably Pacific tuna species, and fitted to tag recoveries.

The second line of movement model originated in fishery applications. Extending models by Ishii (1979) and Sibert

Received 20 February 2001. Accepted 13 June 2002. Published on the NRC Research Press Web site at http://cjfas.nrc.ca on 26 July 2002.
J16229

R. McGarvey[1] and J.E. Feenstra. South Australian Research and Development Institute, Aquatic Sciences, P.O. Box 120, Henley Beach, SA 5022, Australia.

[1] Corresponding author (e-mail: mcgarvey.richard@saugov.sa.gov.au).

Can. J. Fish. Aquat. Sci. **59**: 1054–1064 (2002) DOI: 10.1139/F02-080

(1984), the generalized movement estimation formalism of Hilborn (1990; see also Quinn and Deriso 1999) has been widely applied (Anganuzzi et al. 1994; Xiao 1996; Young et al. 1999). The tag data obtained from exploited fish stocks, denoted tag recoveries, usually depend on volunteer reporting by harvesters and anglers. Researchers capture, tag, and release a generally large number, often thousands, of animals. Notices are posted or published requesting that fishers return tags with the required information to researchers compiling the tag-recovery database. Recaptured tagged fish are voluntarily reported by commercial and recreational fishers when caught during day-to-day fishing operations. However, some or possibly many of the tagged fish that are recaptured are not reported. The rate of tag reporting is often not known, but has been estimated using a range of techniques (Sibert 1984; Xiao et al. 1999; Xiao and McShane 2000).

The third line of movement-estimation model extended mark–recapture methods originally developed for survival and abundance estimation (Seber 1982) to include populations that are spatially partitioned and moving among strata (Schaefer 1951; Chapman and Junge 1956; Darroch 1961). These methods were developed for data sets where multiple times of both tagging and simultaneous tag recovery were undertaken at regular intervals, usually yearly (Arnason 1972, 1973), notably for studies of bird migration, where research tagging and opportunistic recovery occur in the same (hunting) season (Brownie et al. 1985). Schwarz et al. (1993; see also Schweigert and Schwarz 1993) extended the model formalism of Brownie et al. (1985) to multiple strata for estimating parameters that combined movement and survival. Tag-reporting, capture, and death rates were also combined into a single estimated parameter for each year and stratum. They applied their estimator to Canadian Pacific herring (*Clupea pallasii*), into which coded metal tags were inserted and recaptured by detectors in processing plants over eight successive yearly spawning seasons.

The estimator we present below follows from and extends that of Hilborn (1990) and Schwarz et al. (1993). It is designed for the single mark–release tag-recovery data typical of commercial fish stocks where times of tagging and recapture are arbitrary or random through the year, and where only movement parameters are specifically estimated. Thus, following Hilborn (1990), it was designed for use with the usual fishery tag-recovery data, which have a lower information content than the repeated and uniformly spaced times of tag and recapture assumed by Schwarz et al. (1993), but we sought an estimator, like that of Schwarz et al. (1993), which is unbiased by (constant) tag nonreporting.

A second feature of estimating movement rates of harvested fish stocks, in addition to the disadvantage of nonreporting, is the advantage that additional information is often available. Catch- and fishing-effort totals are collected for most exploited stocks. In some fisheries, estimates of total and fishing mortality, and thereby total abundance, are produced annually, for example from virtual population analysis. Even in the absence of mortality estimates, reported effort provides a measure of relative fishing intensity.

Because many recaptured tagged fish are not reported, Peterson-style inferences based on proportions recovered from each cell as a fraction of the number originally tagged and released are biased. By implication, the number of fish tagged and released is not of direct use unless the reporting rate is known. Hilborn's (1990) estimator assumed a 100% reporting rate and was tag-conditioned in that fitted recapture proportions were of the total number released.

However, from any given tag-release source cell, information about movement is provided by the numbers recaptured and reported in each destination cell as a proportion of all reported recaptured tagged fish from the source cell. The reporting rate appears at the top and bottom in this ratio and thus cancels. The model likelihood below was fitted to these recapture proportions. In this sense it is "recapture-conditioned". Only recapture numbers are used and prior knowledge of the rate of tag reporting (assumed to be uniform among spatial cells) or of total abundance is not assumed. Similarly, using this recapture-conditioned approach we show that any other survival or process rate that can be approximated as spatially uniform will also cancel. These rates include short-term tag mortality, ongoing tag mortality and tag loss, and natural mortality. Survival in the tag-release cell also cancels when the time of movement is taken as fixed, as we assume here. This substantially reduces the data and assumed parameter inputs needed to estimate movement rates.

Four recapture-conditioned estimators are presented in Appendix A, ordered by the amount and quality of external information available about mortality by spatial cell required as input. These provide movement estimators for fishery tag recoveries applicable to most fisheries. Those with the highest quality mortality information require less or no approximation. The fourth model (eq. A4) neglects differences in overall survival rates among cells but assumes that fishing effort reported by cell and month is available. Effort data by time step and spatial cell permit correction for variation in the numbers of tags reported because of the variation in overall levels of fishing.

Fowler and March (2000) analyzed qualitative patterns of movement using tag recaptures from commercial and recreational fishers. Here we employ a subset of tag recoveries from South Australian King George whiting (*Sillaginodes punctata*) to estimate movement rates.

Materials and methods

Study site

Movement is an important aspect of the life history of South Australian King George whiting. Spawning occurs only near the mouths of the two gulfs in South Australia (Fowler et al. 1999; Fig. 1), after which eggs and larvae are transported northward up into and around the gulfs (Fowler et al. 2000). Postlarvae settle into shallow embayments, seagrass beds, and other nearshore habitats in the upper reaches. As fish reach 3 years of age, approximately the age when they become both mature and legally susceptible to harvesting, they range more widely and many undergo directed migration southward (Fowler and McGarvey 1997). By age 4 few and by age 5 nearly no fish remain in these areas. Spawning occurs only in specific areas around the southern parts of the gulfs. Thus, the population is sustained by active movement of adults southward to spawning aggregations and passive transport of larvae back to nursery areas.

Fig. 1. Map of South Australian fishery statistical reporting blocks and the reporting blocks grouped into "cells" used to aggregate tag recaptures for movement estimation. Cells 7–11 comprise Gulf St. Vincent and cells 4–6 Spencer Gulf, and the others (1–3, 12) include west-coast bays and the continental shelf of the Southern Ocean.

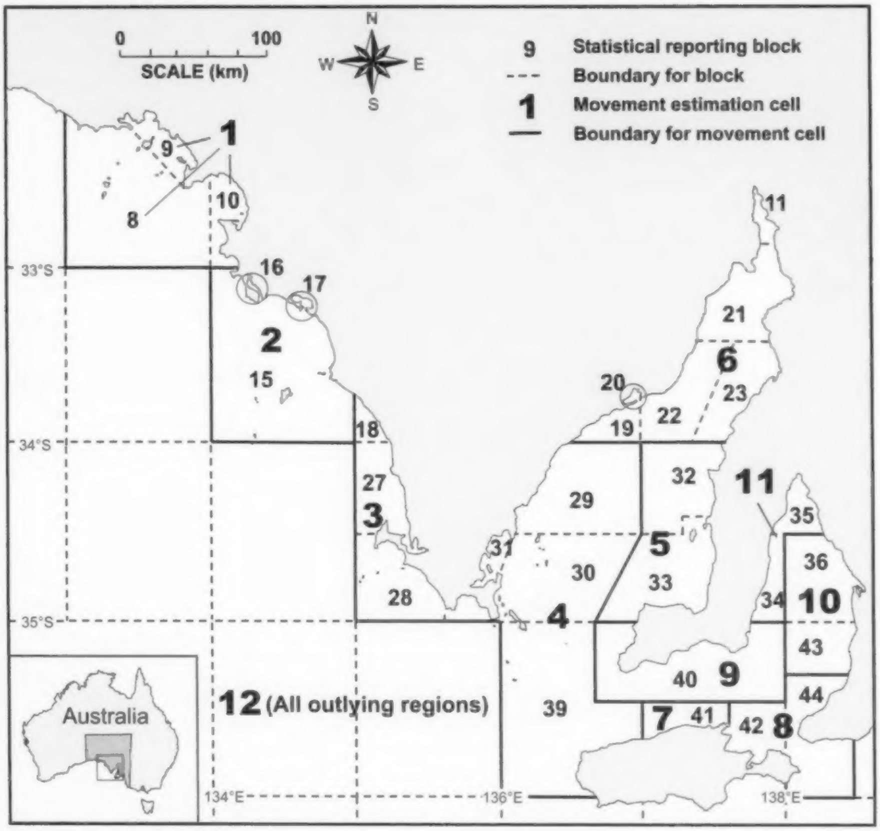

Data preprocessing

We assumed that fish move at one time each year. The sample of tag-recovery data was not large enough to subdivide into seasonal intervals. Qualitative examination of tag recaptures by season indicated that most directed movement occurred in summer (November–February), though some diffusive movement among statistical blocks, including some northward drift along shore in Gulf St. Vincent, occurred in all seasons (Fowler and McGarvey 1997). Because we sought to represent long-term directed migration, movement was assumed to occur in summer, at the beginning of January.

Effort data and tag recaptures were aggregated into 11 spatial cells (Fig. 1). Spatial cell 12 comprised all outlying, mostly offshore, blocks where reported catches of King George whiting are small (0.14%) and from which no tag recoveries were obtained.

For estimating the movement-probability parameters, only recaptured fish that had an opportunity between tagging and recapture to undertake movement (i.e., those at liberty) at the movement time in January were considered.

In addition, we excluded recaptures that were not tagged at least 2 months prior to 1 January, i.e., those that were tagged during the principal migration months, November and December, and that might have already undertaken summer migratory movement before being tagged. Three other sets of exclusion criteria were also tested, particularly those that required a 6-month time-at-large prior to May 1, but these excluded many more data points. Most importantly, using the January movement time and 2-month minimum time-at-large criteria chosen, the mean time-at-large for an average tag recapture was approximately 1 full year.

The total number of recaptures with tag and recapture locations reported was 2054, of which 453 recaptures were used in movement estimation (Table 1). Most of these recaptured fish were tagged at between about 28 and 45 months of age.

We seek steady-state (time-averaged) movement rates. With January assumed to be the time of movement, and with recaptures obtained over three decades of tag releases, we represent this movement time by the age of fish in January. Thus we effectively substitute age as a proxy for time in the data and specify the times of tag and recapture by the ages of the fish. Each data point (tagged and recaptured fish) was classified according to whether the fish was at liberty at only one January movement age of 33 or 45 months, or at both 33 and 45 months of age.

There was one cell, 7, from which no releases were recaptured and thus all input data elements in this source cell row

Table 1. Tag–recapture data used in estimating movement rates among 11 spatial cells of South Australian King George whiting (*Sillaginodes punctata*).

(A) Numbers recaptured (N_{ij}^r) for fish at large for one migration season.

	Destination spatial cell										
Source spatial cell	1	2	3	4	5	6	7	8	9	10	11
1	60	0	0	0	0	0	0	0	0	0	0
2	1	44	0	0	0	0	0	0	0	0	0
3	1	2	53	0	0	0	0	0	0	0	0
4	0	0	0	14	0	1	0	0	0	0	0
5	0	0	0	0	29	0	0	0	0	0	0
6	0	0	2	23	19	45	0	0	0	0	0
7	0	0	0	0	0	0	0	0	0	0	0
8	0	0	0	0	0	0	2	41	0	0	0
9	0	0	0	0	0	0	0	1	6	0	0
10	0	0	0	0	0	0	1	8	5	22	6
11	0	0	0	0	0	0	4	4	12	2	22

(B) Numbers recaptured (N_{ij}^r) for fish at large for two migration seasons.

	Destination spatial cell										
Source spatial cell	1	2	3	4	5	6	7	8	9	10	11
1	0	0	0	0	0	0	0	0	0	0	0
2	0	1	0	0	0	0	0	0	0	0	0
3	0	0	0	0	0	0	0	0	0	0	0
4	0	0	0	1	0	0	0	0	0	0	0
5	0	0	0	0	1	0	0	0	0	0	0
6	0	0	0	4	9	1	0	0	0	0	0
7	0	0	0	0	0	0	0	0	0	0	0
8	0	0	0	0	0	0	0	1	0	0	0
9	0	0	0	0	0	0	0	0	0	0	0
10	0	0	0	0	0	0	1	1	0	2	0
11	0	0	0	0	0	0	1	0	0	0	0

were zero (Table 1). However, prior study of South Australian King George whiting suggested that this is a sink cell for movement. Cell 7 is an important spawning area (Fowler et al. 2000) and in our analysis there is no evidence, notably from Spencer Gulf, where recaptures were obtained from releases to both spawning cells, of spawning fish returning northward to upper gulf cells. We thus assumed no movement away from spawning ground cell 7.

Model likelihood

Following previous authors (e.g., Hilborn 1990; Fournier et al. 1998), movement is represented by a transition matrix. The proportion of fish moving from any "source" cell i to any "destination" cell j on 1 January of each year is given by the matrix element, P_{ij}. Proportions remaining in any source cell i are given by the diagonal element, P_{ii}. The destination probabilities of moving to any other cell and of remaining in the source cell, i.e., all rows, must sum to 1 if, as we assume, permanent emigration out of the 11 study cells is negligible.

The likelihood is formed as the product of the predicted recapture probabilities (f_1 or f_2 below) over all individual recapture data points. The model is specified if the form of this probability (f_1 or f_2) is given for each recapture data point. The first equation in the derivation of these recapture probabilities below includes the number tagged. When proportions recovered in each destination cell (from any given source cell) are formed, the number originally tagged cancel. This predicted number recaptured in each destination cell is written in eq. 1 as a product of probabilities for tagging mortality, survival, movement, death, capture, and tag reporting.

We fitted both age-specific and age-independent models. For the age-specific model, movement rates were estimated separately for ages 33 and 45 months. The Akaike Information Criterion (AIC) corrected for small sample size (Sugiara 1978; Hurvich and Tsai 1989) was applied to compare the two models.

Because times of tag and recapture vary through the year and because survival is a strongly nonlinear (negative exponential) function of time-at-large in the periods before and after the hypothesized age(s) of movement, the ages (specified as month) of tagging (a_t) and recapture (a_r) needed to be explicit.

In eq. 1 below, the predicted absolute number reported recaptured in cell j in month a_r that were released in cell i in month a_t equals the number originally tagged and released into cell i in month a_t, times the proportion surviving tag mortality in the short time (approximately a month) following tagging, times the fraction surviving total mortality over the months from tagging to the assumed time of movement, a_m, times the probability of moving from cell i to cell j, times subsequent survival in cell j from the month of movement to the month of recapture, a_r, times the probability of dying in the month of recapture, times the probability that the cause of death was harvest, times the probability that the captured fish was reported.

Thus, the equation for the predicted number of recaptures whose time-at-large traversed the assumed time of movement (1 January) only once can be written

$$(1)\qquad \hat{N}^{r}_{ij,a_t a_r} = N^{t}_{i,a_t}(1 - m_{\mathrm{tag}})S_i[a_t, a_{\mathrm{m}}]P_{a_{\mathrm{m}},ij}S_j[a_{\mathrm{m}}, a_{\mathrm{r}}] \times (1 - \mathrm{e}^{-Z_j/12})(F_j/Z_j)f_{\mathrm{report}}$$

where $\hat{N}^{r}_{ij,a_t a_r}$ is the predicted number of fish recaptured in spatial cell j of age (in months) a_{r} that were released and tagged in spatial cell i at age a_t and N^{t}_{i,a_t} equals the number of fish tagged in spatial cell i at age a_t. Short-term mortality due to tagging, m_{tag}, is taken as a fixed proportion. Ages at month of movement (January) are denoted $a_{\mathrm{m}} \in \{a_{\mathrm{m1}} = 33, a_{\mathrm{m2}} = 45\}$; a_t is the age at which a given (data recapture) fish was tagged. $S_i[a_t, a_{\mathrm{m}}]$ is the probability of a fish tagged at age a_t in spatial cell i surviving to age a_{m} (while remaining in spatial cell i). $P_{a_{\mathrm{m}},ij}$ is the probability (to be estimated) of movement at age a_{m} from spatial cell i to spatial cell j. The age at which a given fish was recaptured is a_{r}. $S_j[a_{\mathrm{m}}, a_{\mathrm{r}}]$ is the probability that a fish alive after the time of movement at age a_{m} in spatial cell j survives to age a_{r} (while remaining in spatial cell j). F_j is the instantaneous mortality rate, for fish in spatial cell j, due to fishing from which recaptures can be obtained and f_{report} is the fraction of recaptured tagged fish that were reported (assumed to be constant over all spatial cells).

If the recapture time-at-large spans two times of movement, eq. 1 generalizes to

$$(2)\qquad \hat{N}^{r}_{ij,a_t a_r} = N^{t}_{i,a_t}(1 - m_{\mathrm{tag}})S_i[a_t, a_{\mathrm{m1}}]\left\{\sum_{k=1}^{n_{\mathrm{c}}} P_{1,ik}S_k[a_{\mathrm{m1}}, a_{\mathrm{m2}}]P_{2,kj}\right\} \times S_j[a_{\mathrm{m2}}, a_{\mathrm{r}}](1 - \mathrm{e}^{-Z_j/12})(F_j/Z_j)f_{\mathrm{report}}$$

where n_{c} is the total number of spatial cells (11). The first and second defined January ages of movement are a_{m1} and a_{m2}, specifically 33 and 45 months. Age-specific movement probabilities are given in matrix $\mathbf{P_1}$ for a_{m1} and matrix $\mathbf{P_2}$ for fish of age a_{m2}. For the age-independent model, a single $\mathbf{P}$ matrix contains all estimated movement-probability parameters, and $\mathbf{P}$ is substituted for $\mathbf{P_1}$ and for $\mathbf{P_2}$ wherever they appear.

Estimates of Z_j and F_j were obtained from an overall King George whiting fishery estimation model fitted to catch and effort totals and catch numbers at age determined from otoliths. These estimates of Z_j and F_j were derived for the final analysis of movement probabilities after iterating back between the movement estimator and the overall fishery estimator in which movement is explicit.

If Z_j can be taken as constant over time and age, the form for the survival factor, S, between any two monthly ages, a_1 and a_2 is

$$(3)\qquad S_j[a_1, a_2] = \mathrm{e}^{-Z_j(a_2 - a_1)/12}$$

The Z_j mortality rate coefficients are expressed in yearly time units (year^{-1}). Division by 12 in eq. 3 converts the monthly age difference $(a_2 - a_1)$ into yearly time.

The predicted proportions, f_1, for recaptures whose time-at-large spans a single movement season are

$$(4)\qquad f_1(j|i, a_t, a_{\mathrm{r}}) = \frac{\hat{N}^{r}_{ij,a_t a_r}}{\sum_{k=1}^{n_{\mathrm{c}}} \hat{N}^{r}_{ik,a_t a_r}}$$

When eq. 1 is substituted into eq. 4, the constant factors ($1 - m_{\mathrm{tag}}$, and f_{report}) in the model equation cancel. The number tagged, N^{t}_{i,a_t}, and the survival factor in the source cell i for the time from tagging to movement, $S_i[a_t, a_{\mathrm{m1}}]$, also cancel, since all data points in this proportion were tagged in spatial cell i and survived to reach the assumed time of migration, a_{m1}.

Substituting eqs. 1 and 3, f_1 in eq. 4 reduces to

$$(5)\qquad f_1(j|i, a_{\mathrm{r}}) = \frac{P_{1,ij}\mathrm{e}^{-Z_j\frac{a_{\mathrm{r}} - a_{\mathrm{m}}}{12}}(1 - \mathrm{e}^{-Z_j/12})\dfrac{F_j}{Z_j}}{\sum_{k=1}^{n_{\mathrm{c}}} P_{1,ik}\mathrm{e}^{-Z_k\frac{a_{\mathrm{r}} - a_{\mathrm{m}}}{12}}(1 - \mathrm{e}^{-Z_k/12})\dfrac{F_k}{Z_k}}$$

With a_t no longer explicit, this is the predicted proportion recaptured in cell j, in month a_t of those released in cell i and subsequently recaptured, for any tag month, a_t. With the age-specific model, a_{m1} or a_{m2} was substituted for a_{m}, depending on the age of recapture.

For recaptures whose time-at-large spans two movement ages (specifically, $a_{\mathrm{m1}} = 33$ months and $a_{\mathrm{m2}} = 45$ months), the predicted proportion recaptured in cell j in month a_{r} of those tagged in cell i from eq. 2 is

$$(6)\qquad f_2(j|i, a_{\mathrm{r}}) = \frac{\left\{\sum_{l=1}^{n_{\mathrm{c}}} P_{1,il}\mathrm{e}^{-Z_l\frac{a_{\mathrm{m2}} - a_{\mathrm{m1}}}{12}}P_{2,lj}\right\}\mathrm{e}^{-Z_j\frac{a_{\mathrm{r}} - a_{\mathrm{m2}}}{12}}(1 - \mathrm{e}^{-Z_j/12})\dfrac{F_j}{Z_j}}{\sum_{k=1}^{n_{\mathrm{c}}}\left\{\sum_{l=1}^{n_{\mathrm{c}}} P_{1,il}\mathrm{e}^{-Z_l\frac{a_{\mathrm{m2}} - a_{\mathrm{m1}}}{12}}P_{2,lk}\right\}\mathrm{e}^{-Z_k\frac{a_{\mathrm{r}} - a_{\mathrm{m2}}}{12}}(1 - \mathrm{e}^{-Z_k/12})\dfrac{F_k}{Z_k}}$$

The sum over l represents the possible pathways of movement starting from cell i before the first yearly movement and reaching cell j after the second. In the first movement opportunity, fish may move to any cell l and in the second they must move from that intermediary cell l to cell j. The probabilities of each pathway are (1) movement from cell of tagging i to any cell l with probability $P_{1,il}$, (2) survival in cell l over the full year from a_{m1} to a_{m2}, and (3) movement from intermediate cell l to the recapture cell, j.

In matrix multiplication formulations of the expression in braces (eq. 6), the order of movement matrix multiplications is written $\mathbf{P_1\ S\ P_2}$, where $\mathbf{S}$ is the diagonal matrix of survival over 1 full year with diagonal entries $[l, l]$ equal to $S_l[a_{\mathrm{m1}}, a_{\mathrm{m2}}]$ for each l from 1 to n_{c}. The generalization to longer times at liberty is straightforward. For example, predicted movement probabilities for recaptures with times-at-large spanning three movement seasons would be written $\mathbf{P_1\ S\ P_2\ S\ P_3}$, where $\mathbf{P_3}$ gives the movement probabilities of fish in a third age group at movement time.

Given tag-release cell i and recapture month of age a_{r}, the f's over j form a set of discrete predicted probabilities for the set of possible outcomes, namely the possible cells, j, in which a fish can be recaptured.

Given prior estimates of fishing mortality (F_j) and total mortality (Z_j) in each of the cells, j, the movement-rate probabilities, $P_{a_m,ij}$, are the sole remaining unevaluated parameters. These were obtained by maximizing the likelihood described below. When only effort data but not fishing mortalities by cell are available, spatial variation in mortality must be ignored. This approximation and the more complete list of assumptions and auxiliary data required to apply various approximate forms of eq. 5 are summarized in Appendix A.

The movement estimation joint likelihood is written as the product of the predicted probabilities of recapture for each observed outcome, the product of the f's:

$$L = \prod_{r=1}^{n_r} f[r] \tag{7}$$

where r is the index over fitted recapture data points, of which there are n_r. This likelihood is equivalent to the product of multinomials maximized by Schwarz et al. (1993). Both express the basic assumption that each recapture is an independent observation and thus that their probabilities multiply.

The minus log likelihood objective function

$$O = -\sum_{r=1}^{n_r} \log(f[r]) \tag{8}$$

was minimized by varying the movement parameters, $\{P_{s,i\,j};\ s \in \{1, 2\};\ i, j \in \{1, n_c\}\}$ that we seek to estimate.

To ensure that the probabilities all summed (over j) to 1, the parameters were constrained with the added penalty objective function term

$$\sum_{s=1}^{2}\sum_{i=1}^{n_c}\left[\log\left(\sum_{j=1}^{n_c} P_{s,ij}\right)\right]^2 \tag{9}$$

This will equal 0 if all the rows (i) in the estimated transition matrices (s) sum to 1, and increases to positive values for any row that deviates above or below a sum of 1. Additional individual constraints were imposed on the movement probability parameters to ensure that they all lie in the interval [0,1]. Weightings of 1000 and 10 000 for this penalty gave similar results, though 10 000, which we ultimately used, yielded more reasonable parameter uncertainties.

The objective function was programmed and minimized using AD Model Builder (Otter Research Ltd., Sidney, B.C., Canada), model-estimation software developed by D.A. Fournier that uses derivatives evaluated using a reverse auto-differentiation algorithm. This allowed rapid convergence to a minimum solution. We fitted to 453 recapture data points. The age-specific model had 187 parameters, while the age-independent model had 110. The negative log likelihood converged in about a minute on an 800-MHz Pentium III PC.

Results

The AIC comparison of the age-dependent model versus the age-independent model strongly favored the age-independent model. The small-sample-corrected AICs yielded a difference of greater than 400; a difference greater than 10 supports the simpler age-independent model. This simpler model, with fewer parameters, also yielded much smaller confidence intervals for some of the parameters that were poorly resolved in the age-dependent formulation.

Three overall trends are apparent in the estimated matrices (Table 2A) of movement probabilities for the age-independent model, **P**: (*i*) From a majority of cells, there is relatively little movement away, indicated by values equal to or near 1 on the diagonal of the movement-transition matrix. Estimated values of less than 5×10^{-4}, and their standard errors, were set to 0. (*ii*) Most movement occurred from spatial cells 6, 10, and 11. These are the upper cells of Spencer Gulf (6) and Gulf St. Vincent (10 and 11), respectively. Thus, nearly all significant movement was directed southward in the two gulfs. (*iii*) There is virtually no movement between the gulfs and the westerly coastal region, as anticipated from the mapped tag–recapture movements (Fowler and March 2000).

Standard errors on the model parameters were estimated in AD Model Builder from the diagonal of the variance–covariance matrix, the negative inverse of the Hessian evaluated at the likelihood maximum (Table 2B). These parameter-uncertainty estimates, given as standard errors, thus assume the standard asymptotic normal approximation about the likelihood maximum. The standard errors in each row (Table 2B) were lowest for the diagonal probabilities (of remaining in source cell), at least in part because of the larger samples of fish that did not move. The standard errors for parameters falling close to the probability bounds of 0 or 1 can be inaccurate, owing to the symmetry of the assumed normal, the Hessian being improperly estimated.

More accurate estimates of confidence intervals that do not assume normality were obtained using profile likelihood. A profile describes the exact likelihood probability density function of a parameter about its maximum-likelihood estimate. For each parameter analyzed, AD Model Builder reminimized the minus log likelihood at a range of fixed values of that parameter. The normal asymptotic confidence bounds (Table 2B) are nearly identical with those from profile likelihood for estimated probabilities that lie in the mid-range of allowed probabilities (e.g., Fig. 2*a*). However, for estimated probabilities of movement near 0 or 1, the profile-likelihood method restricts the likelihood probability density to lie within the acceptable range (e.g., Fig. 2*b*). However, for values extremely close to 0 or 1, such as P[1,1] and P[5,5], the profile-likelihood methods can also fail because optimization takes place close to a numerically imposed constraint.

The correlation matrix of parameters (not shown) showed that most correlations are 0 or small, except between (nonzero) parameters constrained to sum to 1.

Discussion

The principal advantage of movement estimation conditioned on recapture is to forego the need for all prior inputs that can be approximated as spatially uniform. This is achieved by fitting to predicted probabilities of recapture in any cell that are expressed as proportions of the number of tagged

Table 2. Estimated movement probability parameters.

(A) Matrix **P** given by elements P_{ij}, where the row (i) designates the source spatial cell and the column (j) the destination cell.

Source spatial cell	Destination spatial cell										
	1	2	3	4	5	6	7	8	9	10	11
1	1.000	0	0	0	0	0	0	0	0	0	0
2	0.025	0.975	0	0	0	0	0	0	0	0	0
3	0.016	0.033	0.951	0	0	0	0	0	0	0	0
4	0	0	0	0.940	0	0.060	0	0	0	0	0
5	0	0	0	0	1.000	0	0	0	0	0	0
6	0	0	0.003	0.208	0.252	0.537	0	0	0	0	0
7	0	0	0	0	0	0	1.000	0	0	0	0
8	0	0	0	0	0	0	0.064	0.936	0	0	0
9	0	0	0	0	0	0	0	0.130	0.870	0	0
10	0	0	0	0	0	0	0.045	0.174	0.105	0.565	0.111
11	0	0	0	0	0	0	0.135	0.087	0.278	0.048	0.452

(B) Matrix of parameter normal asymptotic confidence intervals, given as standard errors, which were estimated as the square root of diagonal elements of the variance–covariance matrix.

Source spatial cell	Destination spatial cell										
	1	2	3	4	5	6	7	8	9	10	11
1	0.005	0	0	0	0	0	0	0	0	0	0
2	0.025	0.026	0	0	0	0	0	0	0	0	0
3	0.016	0.023	0.028	0	0	0	0	0	0	0	0
4	0.001	0	0	0.058	0.001	0.058	0	0	0	0	0
5	0	0	0	0	0.005	0	0	0	0	0	0
6	0	0	0.003	0.038	0.042	0.051	0	0	0	0	0
7	0	0	0	0	0	0	0	0	0	0	0
8	0	0	0	0	0	0	0.043	0.044	0	0	0
9	0.001	0.001	0.001	0.001	0.001	0.001	0.003	0.122	0.123	0.002	0.001
10	0	0	0	0	0	0	0.033	0.054	0.045	0.071	0.043
11	0	0	0	0	0	0	0.056	0.042	0.068	0.033	0.075

fish recovered. Only recaptured fish are considered in the data set and the number of fish originally tagged is not used. Assumed spatially uniform rates of short-term (and long-term) tag mortality, survival in the source cell (up to the assumed time of movement), and nonreporting cancel from the numerator and denominator of the predicted relative probabilities of tag recovery. Also canceling is the natural survival rate.

A number of assumptions required for this movement estimator remain. These include (*i*) that movement happens once per year, (*ii*) that nonreporting (and other canceled constants) are uniform in time and spatial cell, and (*iii*) that mortality rates Z_j and F_j are known or estimated (except for the model based on eq. A4).

There are four main differences between the estimator of Schwarz et al. (1993) and the one presented here. First, the estimator of Schwarz et al. (1993) was designed for use with the standard bird-banding situation of yearly tag and recapture experiments, repeated over several years at the same time each year. This is rare in fishery tag-recovery data sets. Our estimator above accommodates the usual situation where (*i*) tagging and recapture are not spaced in yearly or other uniform time intervals, (*ii*) recaptures are not simultaneous with yearly season of tagging, and (*iii*) experiments are single mark–recapture, not repeated over successive years. This is made possible by writing the likelihood as an explicit product of the model-predicted probability of each recapture individually, and by making explicit all stages of tag loss and mortality, survival, movement, and recapture, the latter including death, capture if dead, and tag reporting if captured. In particular, we wrote the survival factors as negative exponentials over times-at-large prior to and following movement for each data recapture. Schwarz et al. (1993) combined movement and survival as a single parameter, and likewise the stages of death, capture if dead, and reporting if captured were combined. The explicit representation of these processes as separate stages of survival and movement also (*iv*) permits the inclusion of any additional information (from the fishery or otherwise) that may be available about mortality or movement individually, or about any other spatial-cell-specific inputs that do not cancel out.

For the movement and survival models fitting multiple-sample capture–recapture data of Arnason (1972, 1973) and Schwarz et al. (1993), Hestbeck (1995) showed that variation in the timing of movement during the year will bias the estimates because they implicitly assume a single survival rate referenced to the source cell. His simulations indicated that the movement, more than the survival, parameters were sensitive to this variation in movement timing. The estimator above generalizes those models to allow movement at any time during the year and differing rates of survival in source and destination cells.

The movement estimators of Schwarz et al. (1993) and a related non-Markovian model by Brownie et al. (1993) esti-

Fig. 2. Profile likelihood (—) and normal asymptotic approximations (···) of uncertainty for two parameters: (*a*) *P*[5,6] and (*b*) *P*[1,2].

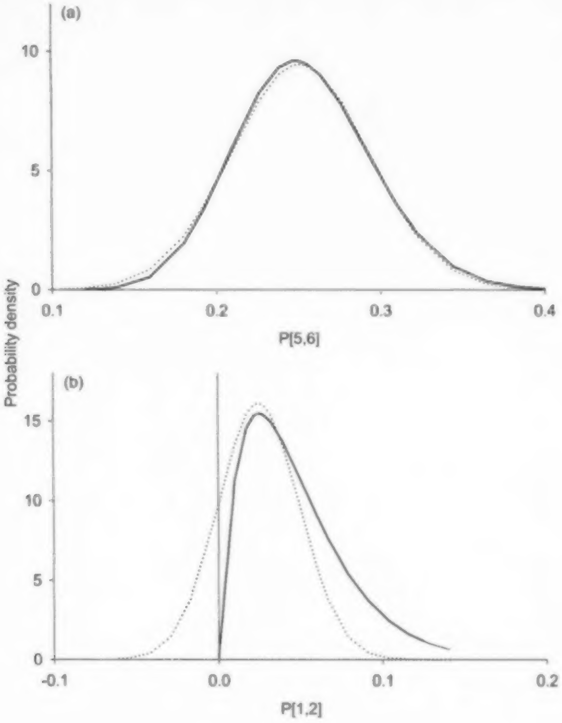

mate the recovery rate; therefore, as above, an external estimate of reporting rate is not needed. Our estimator may also claim the heuristic advantage of demonstrating more plainly how rates that are spatially constant cancel from the movement-rate estimation.

The estimator of Hilborn (1990) (*i*) assumes a 100% (or otherwise known) tag-reporting rate, often not a reasonable assumption with fishery tag recoveries. Also, because Hilborn's (1990) estimator is not recapture-conditioned, it (*ii*) does not take advantage of the fact that all spatially uniform rate inputs, including natural mortality and reporting rates, cancel from the estimation and are therefore not required.

The choice of discrete time step, upon consideration, is arbitrary. The monthly time step can be reduced to a daily one without loss of applicability, since the expected probability for each data point in the likelihood is multiplied through independently of the others, or of any identified tag group. A daily time step is feasible in practice insofar as tag and recapture times are nearly always reported by date. This offers two (generally modest) improvements in model accuracy: (1) the survival times-at-large written above in monthly time as $(a_2 - a_1)$ would then be more accurately calculated and (2) the first-order Taylor approximation in eq. A2 of $(1 - e^{-Z_j/12})$ by $Z_j/12$ would instead approximate $(1 - e^{-Z_j/365})$ by $Z_j/365$, inducing effectively negligible error. The divisors of 12 that appear throughout the predicted recapture proportions given above would then be replaced by 365 to retain the standard definition of mortality coefficients, Z and F, expressed in yearly time.

The model assumed a fixed yearly (or multiyearly) time for movement, as have most previous estimators (a notable exception being the estimators of Whitehead (2001) designed for tracked whale movements). The F_j values and total mortality rates incurred by each recaptured fish were thus taken as constant except for the discrete change at the model-assumed time of movement (1 January). In reality, the movement trajectory of fish among cells while at large and the actual time(s) when each tagged fish moved from one cell to the next, which would be needed to properly account for spatial variations in mortality, are not known, since only the beginning and end points of movement are given. Moreover the average levels of fishing to which each fish is subjected during its time-at-large may vary greatly, and in particular, the average mortality of fish that move may differ from that of fish that do not. The actual time-dependent mortality rates thus probably vary in a far more complex way during time-at-large than is assumed by any model that allows them to vary by source and recapture cells and possibly also by month (or by the source, intermediary, and recapture cells in cases where time-at-large spans two or more hypothesized yearly movement times). These models in which survival is cell-specific (eqs. 5, 6, and A1–A3) allow the best supposition to be made when it is assumed that the fishing mortality which is encountered changes discretely, once (or twice), at the model time(s) of movement. But for this reason, approximating overall mortality as constant among cells (eq. A4) is sometimes acceptable, and in some cases may be no less accurate, although in the fishery examined here, mortality is significantly higher in the upper-gulf cells. The practical advantage of the simplified model (eq. A4) is that it requires only effort data, in addition to tag recoveries, to estimate movement rates. Thus, while differences in survival between tag and recapture cells are ignored in estimator A4, these are usually less precisely known and for the reason given above are generally less accurately modeled when explicit. The remaining factor of effort over area in eq. A4 expresses the variation in tag-recovery rates due to variations in fishing effort, which is nearly always more precisely known, allowing that information, when available, to be used.

Estimates of mortality, Z_j in each cell, j, can still be obtained when only tag recoveries are available. Cell-specific mortality can be estimated as the reciprocal of mean time-at-large (Gulland 1955; Chapman 1961; Paulik 1963). This maximum-likelihood estimator of Z_j would logically use only the tag recaptures from fish that were tagged and recaptured in cell j, including those with short times-at-large that were not included in the movement estimation proper. This method of estimating cell-specific mortality has two advantages: (1) it requires no data apart from the same tag-recovery data set used to estimate movement, and (2) it maintains the objective of conditioning only on recapture, since only recaptured fish are used to calculate mean time-at-large, and thus it is not biased by nonreporting. However, this tag time-at-large estimator of mortality has a large variance (Seber 1982). Moreover, it is highly sensitive to nonrandom sampling, which is common in fisheries data sets.

Insofar as ignoring movement can bias survival, and survival is needed to estimate movement, it is natural to integrate the two into a single estimation procedure. Since the advent of powerful subroutines for objective function minimization, notably AD Model Builder, it has become feasible to integrate movement-rate estimation into the overall estimation, spatially resolved, of population abundance in a fishery. These models (Fournier et al. 1998; Punt et al. 2000) achieve greater accuracy of movement-rate estimation and a more complete description of estimate uncertainty by fitting the tag movement data in the same likelihood with other critical inputs, notably age or length composition and catch and effort totals, needed to estimate cell-specific survival. To date, many movement-integrated models have been conditioned on absolute numbers recaptured and take as input prior estimates of the tag–recapture reporting rate (Hilborn 1990; Anganuzzi et al. 1994; Punt et al. 2000) or have attempted to estimate it (Sibert 1984).

In summary, the estimator presented here eliminates the need for an externally estimated tag-reporting rate previously required by most fishery movement models using single tag–recapture random-in-time tag recoveries. Furthermore, all rate estimates for any processes that are not spatially dependent cancel from the predicted recapture proportions. However, this recapture-conditioned approach requires the use of supplementary estimates of mortality in destination cells, which do not cancel. These are needed to make up for the reduced ability to infer mortality rate from tag recoveries, which, in contrast, multiple-tag–recapture bird-banding-style experiments do afford. In this way the model we propose is optimized for use in fishery applications, making up for the lower quality of information in typical fishery tag-recovery data by employing other fishery-derived information, notably cell-specific fishing effort and if possible also mortality, that is often at hand.

Acknowledgements

We thank Keith Jones and Tony Fowler, who contributed biological insight and data. Wendy March did database processing and Gavin Wright and Janet Matthews generated figures. This work was supported by the Australian Fisheries Research and Development Corporation (Project 95/008).

References

Anganuzzi, A., Hilborn, R., and Skalski, J.R. 1994. Estimation of size selectivity and movement rates from mark–recovery data. Can. J. Fish. Aquat. Sci. **51**: 734–742.

Arnason, A.N. 1972. Parameter estimates from mark–recapture experiments on two populations subject to migration and death. Res. Popul. Ecol. (Kyoto), **13**: 97–113.

Arnason, A.N. 1973. The estimation of population size, migration rates, and survival in a stratified population. Res. Popul. Ecol. (Kyoto), **15**: 1–8.

Brownie, C., Anderson, D.R., Burnham, K.P., and Robson, D.S. 1985. Statistical inference from band-recovery data—a handbook. 2nd ed. U.S. Fish Wildl. Serv. Resour. Publ. No. 156.

Brownie, C., Hines, J.E., Nichols, J.D., Pollock, K.H., and Hestbeck, J.B. 1993. Capture–recapture studies for multiple strata including non-Markovian transitions. Biometrics, **49**: 1173–1187.

Chapman, D.G. 1961. Statistical problems in the dynamics of exploited fish populations. *In* Proceedings of the Fourth Berkeley Symposium, 1960. Vol. 4. pp. 163–168.

Chapman, D.G., and Junge, C.O. 1956. The estimation of the size of a stratified animal population. Ann. Math. Stat. **27**: 375–389.

Darroch, J.N. 1961. The two-sample capture–recapture census when tagging and sampling are stratified. Biometrika, **48**: 241–260.

Deriso, R.B., Punsly, R.G., and Bayliff, W.H. 1991. A Markov model of yellowfin tuna in the eastern Pacific Ocean and some analyses for international management. Fish. Res. **11**: 375–395.

Fournier, D.A., Hampton, J., and Sibert, J.R. 1998. MULTIFAN-CL: a length-based, age-structured model for fisheries stock assessment, with application to South Pacific albacore, *Thunnus alalunga*. Can. J. Fish. Aquat. Sci. **55**: 2105–2116.

Fowler, A.J., and March, W.A. 2000. Adult movement patterns. *In* Development of an integrated fisheries management model for King George whiting (*Sillaginodes punctata*) in South Australia. *Edited by* A.J. Fowler and R. McGarvey. Fisheries Research and Development Final Rep. 95/008, Canberra. pp. 83–104.

Fowler, A.J., and McGarvey, R. 1997. King George whiting (*Sillaginodes punctata*). South Australian Fisheries Assessment Ser. No. 97/6. South Australian Research and Development Institute, Adelaide.

Fowler, A.J., McLeay, L., and Short, D.A. 1999. Reproductive mode and spawning information based on gonad analysis for King George whiting (Percoidei: Sillaginidae) from South Australia. Mar. Freshw. Res. **50**: 1–14.

Fowler, A.J., McLeay, L., and Short, D.A. 2000. Spatial variation in size and age structures and reproductive characteristics of the King George whiting (Percoidei: Sillaginidae) in South Australian waters. Mar. Freshw. Res. **51**: 11–22.

Gulland, J.A. 1955. On the estimation of population parameters from marked members. Biometrika, **42**: 269–270.

Gulland, J.A. 1983. Fish stock assessment: a manual of basic methods. John Wiley and Sons, Chichester, U.K.

Hestbeck, J.B. 1995. Bias in transition-specific survival and movement probabilities estimated using capture–recapture data. J. Appl. Stat. **22**: 737–750.

Hilborn, R. 1987. Spatial models of tuna dynamics in the western Pacific: is international management of tuna necessary? *In* Modelling and management of resources under uncertainty. *Edited by* T.L. Vincent, Y. Cohen, W.J. Grantham, G.P. Kirkwood, and J.M. Skowronski. Lecture notes in biomathematics. No. 72. Springer-Verlag, Berlin. pp. 276–286.

Hilborn, R. 1990. Determination of fish movement patterns from tag recoveries using maximum likelihood estimators. Can. J. Fish. Aquat. Sci. **47**: 635–643.

Hurvich, C.M., and Tsai, C.-L. 1989. Regression and time series model selection in small samples. Biometrika, **76**: 297–307.

Ishii, T. 1979. Attempt to estimate migration of fish population with survival parameters from tagging experiment data by the simulation method. Investig. Pesq. **43**: 301–317.

Okubo, A. 1980. Diffusion and ecological problems: mathematical models. Springer-Verlag, Berlin.

Paulik, G.J. 1963. Estimates of mortality rates from tag recoveries. Biometrics, **19**: 28–57.

Punt, A.E., Pribac, F., Walker, T.I., Taylor, B.L., and Prince, J.D. 2000. Stock assessment of school shark, *Galeorhinus galeus*, based on a spatially explicit population dynamics model. Mar. Freshw. Res. **51**: 205–220.

Quinn, T.J., II, and Deriso, R.B. 1999. Quantitative fish dynamics. Oxford University Press, New York.

Quinn, T.J., II, Deriso, R.B., and Neal, P.R. 1990. Migratory catch-at-age analysis. Can. J. Fish. Aquat. Sci. **47**: 2315–2327.

Schaefer, M.B. 1951. Estimation of the size of animal populations by marking experiments. U.S. Fish Wildl. Serv. Fish. B, **69**: 191–203.

Schwarz, C.J., Schweigert, J.F., and Arnason, A.N. 1993. Estimating migration rates using tag recovery data. Biometrics, **49**: 177–193.

Schweigert, J.F., and Schwarz, C.J. 1993. Estimating migration rates for Pacific herring (*Clupea pallasi*) using tag-recovery data. Can. J. Fish. Aquat. Sci. **50**: 1530–1540.

Seber, G.A.F. 1982. The estimation of animal abundance and related parameters. 2nd ed. Griffin, London.

Sibert, J.R. 1984. A two-fishery tag attrition model for the analysis of mortality, recruitment, and fishery interaction. Tuna and Billfish Assessment Programme, South Pacific Commission, Noumea, New Caledonia. Tech. Rep. No. 13.

Sugiara, N. 1978. Further analysis of the data by Akaike's information criterion and the finite corrections. Commun. Stat. Theor. M, **7**: 13–26.

Whitehead, H. 2001. Analysis of animal movement using opportunistic individual identifications: application to sperm whales. Ecology, **82**: 1417–1432.

Xiao, Y. 1996. A framework for evaluating experimental designs for estimating rates of fish movement from tag recoveries. Can. J. Fish. Aquat. Sci. **53**: 1272–1280.

Xiao, Y., and McShane, P. 2000. Estimation of instantaneous rates of fishing and natural mortalities from mark–recapture data on the western king prawn *Penaeus latisulcatus* in the Gulf St. Vincent, Australia, by conditional likelihood. Trans. Am. Fish. Soc. **129**: 1005–1017.

Xiao, Y., Stevens, J.D., and West, G.J. 1999. Estimation of fishing and natural mortalities from tag experiments with exact or grouped times at liberty. Can. J. Fish. Aquat. Sci. **56**: 868–874.

Young, G.C., Wise, B.S., and Ayvazian, S.G. 1999. A tagging study on tailor (*Pomatomus saltatrix*) in Western Australian waters: their movements, exploitation, growth and mortality. Mar. Freshw. Res. **50**: 633–642.

Appendix A

Here we present a sequence of related movement models, each assuming successively increasing approximation depending on what auxiliary data are available in addition to tag recoveries. We present these successive model forms only for f_1 in eq. 4, i.e., for the predicted probabilities of recapture by cell for data recoveries that were at large over only a single movement time. The extensions to times-at-large spanning multiple movement times (f_2) and to other tag-recovery data sets are straightforward. Each f_1 equation below gives the predicted probability of each data recapture, given the date or month of recapture and spatial cell of tag and recapture. Estimators based on the various f_1 forms presented are constructed exactly as in the Methods, by multiplying the predicted f_1 probability into the overall joint likelihood of eq. 7 or eq. 8. The successive models (Table A1) are nested, so, for example, assumptions A1(*a*)–A1(*d*) continue to apply for eqs. A2–A4.

In more generalized form, eq. 4 in the Methods can be written

$$(\mathrm{A1})\quad f_1(j|i,a_\mathrm{r}) = \frac{P_{1.ij}S_j[a_{\mathrm{m1}},a_\mathrm{r}](1-\exp[-Z_{j.a_\mathrm{r}}/12])(F_{j.a_\mathrm{r}}/Z_{j.a_\mathrm{r}})}{\sum_{k=1}^{n_\mathrm{c}} P_{1.ik}S_k[a_{\mathrm{m1}},a_\mathrm{r}](1-\exp[-Z_{k.a_\mathrm{r}}/12])(F_{k.a_\mathrm{r}}/Z_{k.a_\mathrm{r}})}$$

In eq. A1, Z is understood to be an explicit function of the month of recapture, a_r, for fisheries where these mortalities have been estimated by month and year as well as spatial cell. When mortality $Z_{j.a_\mathrm{r}}$ is known to depend on time, say because effort varies by month, as well as on the age of the fish, then this dual dependence should be made explicit. Therefore, the mortality subscripts for age, in a_r for example, represent both time and age, i.e., both the month and the year for each given recaptured fish. Similarly, survival while at large in destination cell j, $S_j[a_{\mathrm{m1}}, a_\mathrm{r}]$, becomes an explicit function of monthly time step if monthly estimates are available. Writing this as a product of monthly survivals yields

$$S_j[a_{\mathrm{m1}},a_\mathrm{r}] = \prod_{a=a_{\mathrm{m1}}+1}^{a_\mathrm{r}} \exp[-Z_{j.a}/12] =$$

$$\exp\left[-\sum_{a=a_{\mathrm{m1}}+1}^{a_\mathrm{r}} Z_{j.a}/12\right] = \exp\left[-\frac{(a_\mathrm{r}-a_{\mathrm{m1}})}{12}\bar{Z}_j[a_{\mathrm{m1}},a_\mathrm{r}]\right]$$

where the first time period of survival loss occurs in the first month, from a_{m1} to $a_{\mathrm{m1}} + 1$. Thus, for survival that is both month- and cell-specific, an equally general form is obtained by using the (arithmetic) mean Z over the time-at-large of the recaptured fish in question, inside the negative exponential.

A first-order Taylor expansion approximation, $(1 - e^{-Z_j/12})(F_j/Z_j) \approx F_j/12$, simplifies eq. A1. This approximation is acceptable for total mortality rates, Z_j, of 1 or less. For example, with $Z = 1.0$, $(1 - e^{-Z/12}) = 0.080$ and $Z/12 = 0.083$. When the first-order Taylor approximation is made, this becomes

$$(\mathrm{A2})\quad f_1(j|i,a_\mathrm{r}) = \frac{P_{1.ij}\exp\left\{-\bar{Z}_j[a_{\mathrm{m1}},a_\mathrm{r}](a_\mathrm{r}-a_{\mathrm{m1}})/12\right\}F_{j.a_\mathrm{r}}}{\sum_{k=1}^{n_\mathrm{c}} P_{1.ik}\exp\left\{-\bar{Z}_k[a_{\mathrm{m1}},a_\mathrm{r}](a_\mathrm{r}-a_{\mathrm{m1}})/12\right\}F_{k.a_\mathrm{r}}}$$

If we make the common fishery stock assessment assumptions (*i*) that times-at-large extend over several months, so the monthly time and age dependence of $\bar{Z}_j[a_{\mathrm{m1}}, a_\mathrm{r}]$ can be neglected, and rename $\bar{Z}_j[a_{\mathrm{m1}}, a_\mathrm{r}] \approx Z_j$, (*ii*) set $Z_j = M + F_j$, (*iii*) take natural mortality, M, as constant in time and space, (*iv*) use effort time series data, $\{E_{j.t_\mathrm{r}}\}$, assumed to be given by cell and month of recapture (t_r), and (*v*) let $F_{j.t_\mathrm{r}} = q\,E_{j.t_\mathrm{r}}/A_j$, where catchability, q, is constant and differences in F among cells are ascribed to variation in effort per unit of fishable area, A_j (Gulland 1983, pp. 42–44), eq. A2 can be written

$$(\mathrm{A3})\quad f_1(j|i,a_\mathrm{r}) = \frac{P_{1.ij}\exp\left\{-F_j(a_\mathrm{r}-a_{\mathrm{m1}})/12\right\}E_{j.t_\mathrm{r}}/A_j}{\sum_{k=1}^{n_\mathrm{c}} P_{1.ik}\exp\left\{-F_k(a_\mathrm{r}-a_{\mathrm{m1}})/12\right\}E_{k.t_\mathrm{r}}/A_k}$$

If cell-specific Z_j estimates were available, these would remain in place of the F_j values.

Lastly, if variation in mean mortality over the time-at-large among cells is neglected, eq. A3 reduces to

Table A1. Assumptions used in sequential formulations of the movement estimator.

Number	Assumption
A1(*a*)	Movement occurs once yearly (January 1).
A1(*b*)	At each yearly movement time, fish move from the source (i.e., tag and release) cell to any one other cell without passing through intermediate cells, or they remain in the source cell.
A1(*c*)	Total mortality is uniform within source cells (but can vary by month).
A1(*d*)	Fishing mortality is uniform within source cells (but can vary by month).
A2(*a*)	The probability of death in month a_r, $(1 - \exp[-Z_{j,a_r}/12])$, can be approximated by the first-order Taylor expansion as $Z_{j,a_r}/12$.
A3(*a*)	Temporal differences in mortality averaged over months in the recapture cell (specifically, mortality rates found in the survival factors) can be neglected.
A3(*b*)	Total mortality can be written as the sum of natural and fishing mortalities, $Z_{j,t_r} = M + F_{j,t_r}$.
A3(*c*)	Natural mortality, M, is constant and uniform across cells.
A3(*d*)	Monthly fishing mortality in each cell j, F_{j,t_r}, is proportional to reported fishing effort, E_{j,t_r}, and inversely related to the area of that cell, A_j.
A4(*a*)	Fishing mortality is uniform among movement cells.

Note: The Appendix equation that is first to make use of each listed assumption is designated in the numbering of the assumptions.

$$\text{(A4)} \quad f_1(j|i, a_r) = \frac{P_{1,ij} E_{j,t_r} / A_j}{\sum_{k=1}^{n_c} P_{1,ik} E_{k,t_r} / A_k}$$

Equation A1 would be amenable for use where movement is integrated into the overall fishery estimation of fishing and total mortalities. The reduced mathematical form of eq. A2 can allow shorter computation times. Equation A3 would be applicable where accurate monthly effort data are available to account for variations in the predicted reporting rate but where fishing mortalities are less precisely known (usually the case) and not available by month.

Equation A4 approximates mortality as spatially uniform when only data for effort by cell (and optionally month) of recapture are available. Neglecting spatial differences in survival is sometimes reasonable because the underlying fish movement trajectory assumptions are likely to be poorly met. This point was taken up in the Discussion.

Species identification in deep water using multiple acoustic frequencies

R.J. Kloser, T. Ryan, P. Sakov, A. Williams, and J.A. Koslow

Abstract: Multifrequency 12, 38, and 120 kHz acoustics were used to identify the dominant fish groups around a deepwater (>600 m) seamount (a known spawning site for orange roughy, *Hoplostethus atlanticus*) by amplitude mixing of the frequencies. This method showed three distinct acoustic groupings that corresponded to three groups of fishes based on size and swimbladder type: myctophids of total length less than 10 cm, morids and macrourids with lengths >30 cm, and orange roughy with a mean standard length of 36 cm. These three groups were the dominant groups caught in the demersal and pelagic trawls in the study area. A simple model of swimbladder resonance at depth of large and small gas-filled bladder fish groups is in agreement with our experimental observations. Traditionally, demersal and pelagic trawling is used to identify fish species in acoustic records. However, orange roughy are rarely caught in mid-water owing to net avoidance. Using three frequencies, these groups could be distinguished directly over their entire vertical extent from the acoustic records. This reduces a major source of positive bias uncertainty (factor range of 2.0–6.4) in the orange roughy biomass estimates.

Résumé : Une méthode acoustique à fréquences multiples de 12, 38 et 120 Hz a servi à identifier, par le mixage des amplitudes des fréquences, les groupes dominants de poissons sur un mont sous-marin en eau profonde (>600 m), un site de fraye connu de l'hoplostète orange, *Hoplostethus atlanticus*. La méthode révèle l'existence de trois regroupements acoustiques distincts qui correspondent à trois groupes de poissons caractérisés par leur taille et leur type de vessie natatoire: les myctophidés de longueur totale inférieure à 10 cm, les moridés et les macrouridés de longueur supérieure à 30 cm et les hoplostètes de longueur standard moyenne de 36 cm. Ces trois groupes sont ceux qui dominent dans les récoltes aux chaluts démersal et pélagique dans la région. Un modèle simple de la résonance en profondeur de la vessie natatoire chez les groupes de poissons à grande et à petite vessie remplie de gaz s'accorde bien avec nos observations expérimentales. Généralement, le chalutage démersal et pélagique sert à identifier les poissons repérés dans les inventaires acoustiques. Cependant, l'hoplostète orange est rarement récolté à mi-profondeur, car il peut éviter les chaluts. L'utilisation de trois fréquences a permis de reconnaître directement les trois groupes sur toute la colonne d'eau d'après les données acoustiques. Cela réduit une source importante d'erreur d'incertitude positive (facteur variant de 2,0 à 6,4) dans les estimations de la biomasse de l'hoplostète orange.

[Traduit par la Rédaction]

Introduction

Species identification remains a critical requirement in interpreting acoustic recordings for fisheries management (Horne 2000). This is especially true in the deepwater orange roughy (*Hoplostethus atlanticus*) fisheries of Australia, New Zealand, Namibia, Chile, and the High Seas (Kloser et al. 1996 Clark 1999; Boyer and Hampton 2001). Orange roughy are a long-lived fish that have low recruitment and form large schools when spawning, making them vulnerable to over fishing. In Australian waters, the major spawning aggregation was reduced by a quarter based on acoustic snapshot surveys between 1990 and 1993 (Kloser et al. 1996). This decline in biomass combined with catch and age data led to a fishery management strategy of reduced catches to rebuild the population in future years (Bax 1999). To establish whether the orange roughy stocks are rebuilding, the acoustic echo integration method has been proposed to monitor the spawning aggregation. Orange roughy have a wax ester swimbladder and a very low target strength (TS) compared with the other dominant gas-bladdered species of deepwater communities, hence the ability to accurately monitor the spawning population becomes very sensitive to the proportion of gas-bladdered species (Kloser et al. 1997).

Trawl sampling is traditionally used to allocate species compositions to the acoustic records in mixed-species situations. Net sampling has potential biases such as variable catchability between species and spatial and temporal extrapolation of patchy demersal and pelagic trawls. Orange roughy are typically captured with demersal trawls using headline heights of 5–10 m and are not generally caught in mid-water with pelagic trawls, presumably because of their marked avoidance reaction (Koslow et al. 1995). However, acoustic measurements indicate that orange roughy schools range from the sea bed to as high as 150 m into the water column. Pelagic trawls on these acoustic marks only capture a variety of mid-water fishes, many of which have gas-filled swimbladders (Kloser et al. 1997). This avoidance of trawl

Received 5 December 2001. Accepted 30 April 2002. Published on the NRC Research Press Web site at http://cjfas.nrc.ca on 26 July 2002.
J16651

R.J. Kloser,[1] T. Ryan, P. Sakov, A. Williams, and J.A. Koslow. CSIRO Marine Research, G.P.O. Box 1538, Hobart, TAS 7001, Australia.

[1] Corresponding author (e-mail: rudy.kloser@csiro.au).

DOI: 10.1139/F02-076

sampling by orange roughy could bias the assessment of species composition allocated to the acoustic records. A method is required that uses the acoustic data to distinguish the major species groups throughout the water column.

Species identification at a single acoustic frequency was developed and used in shallow water (<200 m) using echo statistics and environmental factors (e.g., Rose and Leggett 1988; Scalabrin et al. 1996). These classification methods require a reference set of acoustic and biological data on schools that have been accurately captured and for which there have been metrics obtained. In deep water (>750 m), the resolution of the vessel-mounted surface acoustics is poor and the time required to accurately capture fishes leads to small reference data sets. The avoidance response of orange roughy to mid-water sampling gears compounds the problem, as not all fishes can be sampled equally. Fishers' observations of orange roughy schools show they aggregate and disperse over very short time frames when in a spawning aggregation, or that the observation tool is too coarse to accurately determine their true dynamics or school shapes. This makes using vessel-mounted single frequency acoustic methods for species identification difficult in deep water.

Multiple frequency acoustic methods have been used to distinguish species or groups of zooplankton and discriminate between fish and zooplankton (e.g., Holliday 1977; Greenlaw and Johnson 1983; Cochrane et al. 1991). Fish species have been discriminated or sized using broadband frequencies or a number of discrete frequencies (e.g., Holliday 1971; Trevorrow 1996). In past acoustic surveys, we observed that particular deep scattering layers at >600 m depth were sometimes more prominent on either the 12- or 38-kHz hull-mounted echosounders on our research vessel. This observation is consistent with the change in resonance of small mid-water fishes with depth (Andreeva 1964). However, we found that these echosounders and a further 12-kHz hull-mounted echosounder available on the vessel were unable to distinguish between orange roughy and other scatterers, because of either the large sampling volume or insufficient range in frequencies. We therefore placed three frequencies (12, 38, and 120 kHz) on a deep towed multifrequency towed instrument (MUFTI) and trialed the system in 1996 during our routine acoustic survey of orange roughy. The multifrequency methodology was further refined with a specific orange roughy survey in 1999. The aim of our study was to improve methods for understanding the distribution and abundance of deepwater species, and in particular, the abundance of spawning orange roughy.

Material and methods

Biological sampling

Biological samples were obtained from pelagic and demersal trawls that targeted fish concentrations that had been located acoustically. The demersal trawl net was a commercial orange roughy trawl with a 40-mm codend liner, headline length of ~35 m, and height ~4 m. Demersal trawl time (actual fishing time) varied between 5 and 15 min for target shots on marks. During target shots the gear can be almost in free-fall (moving downwards at a steep angle). A large pelagic trawl was fitted with an opening–closing, five-net cod-end system based on the multiple plankton sampler of Pearcy et al. (1977). The cross-sectional area of the net mouth when fishing, as measured by acoustic sensors, was about 105 m^2. Mesh sizes in the trawl were 100 mm in the wings, reducing to 20 mm in the body and 10 mm in the extension; cod-ends were 7 mm. Pelagic tow duration was 10–15 min in the target shots. Trawling was at a speed of 2.5–3 knots. The system could take four samples from known depths per deployment. Target trawling of fish concentrations was possible with Scanmar acoustic sensors (Åsgårdstrand, Norway) to monitor the geometry and position of the fishing gear in the water column (Williams and Koslow 1997).

The composition of each demersal catch was identified to acoustic species groups based on body size and swimbladder type (Kloser et al. 1997) and numbers, lengths, and weights obtained. Seven dominant acoustic groups were eels (2 species), morid cod (3 species), oreos (5 species), orange roughy, sharks (10 species), macrourids (14 species), and 18 species of fish and crustacea that occurred in low abundance. Macrourids have large gas-filled swimbladders, except for the dominant species, *Coryphaenoides subserrulatus*, which has a large gas-filled bladder containing a spongy matrix. Further analysis was only carried out for species groups that represented >1% of the total catch. Pelagic trawl catches were treated in the same way. Myctophids of similar size (6–10 cm) and morphology and all having gas-filled swimbladders made up the vast majority of catches; therefore, they made the greatest contribution to acoustic scattering in the water column. Small numbers of morids and macrourids were also captured in mid-water.

Acoustic equipment

The acoustic equipment consisted of a purpose-built MUFTI that housed the single-beam 12-kHz and split-beam 38- and 120-kHz transducers (Table 1). The towed body was a dead-weight type (450 kg in air) that was 2.4 m long and 0.5 m in diameter with a flat base to avoid the use of acoustic windows. The MUFTI towed body housed the transducers, transmitters, pre-amplifiers, Falmouth Scientific conductivity, temperature, and depth logger (FSI Micro CTD #1332, Cataumet, Mass.), and a monitoring pressure case. The monitoring pressure case contained equipment to measure physical parameters such as towed body pitch, roll, depth, and operating voltage, all displayed and logged continuously aboard the research vessel. The towed body was connected to the vessel by 2500 m of electromechanical cable and is further described by Kloser (1996).

Acoustic calibration

The acoustic system was calibrated at the surface and at depth with a 38.1-mm tungsten carbide sphere for all the transducers to obtain the on-axis echo integration constant (Foote et al. 1987; SIMRAD EK500 version 5.3, 1993). The TS of the sphere at a given frequency was calculated following MacLennan (1981) and checked for stability following Miyanohana et al. (1993). The equivalent beam angle is not calibrated using this method and was measured by the manufacturer of the transducer with tests on these values confirmed with a special calibration rig that rotated the transducers at the surface. The deep-tow transducers were also calibrated from 100 to 700 m to correct for changes with depth in transducer sensitivity and to test for changes in beam pattern (Kloser 1996). The seawater propagation pa-

Table 1. Specification of the transducers for the MUFTI deep-towed body and relevant calibration and instrument settings.

Transducer	12 kHz	38 kHz	120 kHz	Units
Manufacturer	MASA (single beam)	EDO Western (split beam)	SIMRAD (split beam)	
Equivalent beam width	–10	–21.1	–20.6	dB re 1 steradian
Beam width ± 3 dB	40	6.5	7	degrees
Band width	1	3.3	3.3	kHz
Pulse length	1.0	1.0	1.0	ms
Target sphere TC 38.1 mm	–42	–42.4	–39.5	dB re 1 m^2
Integrated absorption at 850-m towed body at 700 m	1.3	9.4	31.9	dB·km^{-1}

rameters of absorption and sound velocity were calculated from the formulae of Francois and Garrison (1982) and MacKenzie (1981), respectively, based upon temperature and salinity profiles obtained during the surveys with a CTD (calibration results for the relevant depths are presented in Table 1).

Acoustic sampling

Field samples were obtained from a spawning aggregation of orange roughy on St. Helens Hill (eastern Tasmania 41°14.0′S, 148°45.4′E) in July 1996 and 1999 as part of an ongoing acoustic survey for the management of the stock in the region (Kloser et al. 1996; Bax 1999). St. Helens Hill rises from 1100 to 600 m and is conical in shape (Fig. 1). The repeat surveys have used a system of straight line north–south transects at preset locations with the MUFTI towed body at a fixed depth of between 450 and 550 m (Kloser et al. 1996). To efficiently sample the fish species occurring around the hill, the MUFTI system was towed in a circle "loop" with 1800–2100 m of wire in the water at 2–5 knots, keeping the towed system a fixed 100–200 m above the seabed. For example, the ship would follow the 900-m depth contour, but owing to the long cable and vessel speed, the MUFTI towed body would be sampling in the 800- to 850-m depth contour. The vessel circled the hill in this fashion covering the 750- to 1100-m depth contours at 100-m intervals. This deployment method enabled optimal sampling of the fish species around the hill and minimized fish avoidance and down time due to turning of the vessel with long lengths of wire in the water when using traditional straight line transects.

Acoustic visualization

To manage, edit, and visualize the acoustic data, a specialized software program (ECHO) was written in C and C++ on a Sun Microsystems workstation (now Linux) using X-Windows and an Oracle database (Waring et al. 1994). This software program was upgraded to include methods for visualizing multifrequency echograms (Kloser et al. 1998). The philosophy of the program operation involved scrutinizing the individual acoustic frequencies and correcting the data by applying data modifiers and spatial restrictors. In this application, data modifiers included algorithms for noise thresholding or subtraction and applying compensation for known calibration offsets. The spatial restrictors (referenced from the surface, transducer, or sea bed) were applied to limit further computations on the particular data. Specifically, spatial restrictors were required on this data when affected by excessive platform movement and (or) electrical noise, and in redefining the start of the seabed echo. The resultant spatial offsets and data modifiers were displayed in a WYSIWYG (what you see is what you get) environment to ensure quality assurance and good user feedback for changes made. In mixing the frequencies, each frequency was allocated a separate colour palette with independent intensity start and dynamic ranges. The user could then dynamically adjust the frequencies to highlight specific differences in the echograms. Once a given presentation system was finalized, it was stored and all subsequent multifrequency echograms were viewed in the same way. The mixing algorithm used in this analysis involved displaying a particular frequency colour if it was higher in amplitude than the associated frequencies. The ability of the user to adjust the individual gains and dynamic ranges for each frequency in a dynamic fashion created an environment that greatly assisted in highlighting visual features in the frequency amplitude differences.

In total, 13 loops were carried out around St. Helens Hill in 1996 with the MUFTI deep-towed system and these were processed using the ECHO software. Each frequency was assigned a separate colour palette (12 kHz red, 38 kHz green, and 120 kHz blue) and the volume reverberation (S_v) signals adjusted for background noise, absorption, and calibration. The calibrated volume reverberation frequencies were then combined with separate colour palettes and mixed using amplitude dominance (Fig. 2). Each individual frequency and the frequency mixing highlight differences over an orange roughy aggregation (Fig. 2). This was used to train the visual classification system and to show up relative differences. The figure shows how the user adjusted the individual frequency gains to ensure that the orange roughy was an even mix of all the frequencies amplitudes seen as an even mixture of red, green, and blue pixels on the computer screen. The remaining multifrequency echogram separated into two regions of colour dominance of red (high 12-kHz signal) and green (high 38-kHz signal) (Fig. 2).

Target strength

In situ TS as derived from the SIMRAD EK500 version 5.3 were extracted from low-density regions associated with an acoustic group between frequencies at constant depth. The relevant TS selection criteria used were target threshold, –65 dB; normalized pulse length, 0.7–1.5; maximum gain compensation, 6 dB; and phase deviation, 0.5. Regions were selected where the depth was 20–30 m from the transducer face and acoustic intensity was low, targeted by pelagic trawling, and showed distinct differences in the frequency amplitudes (Fig. 3). Selection of regions based on these criteria was expected to reduce the known biases in in situ TS data

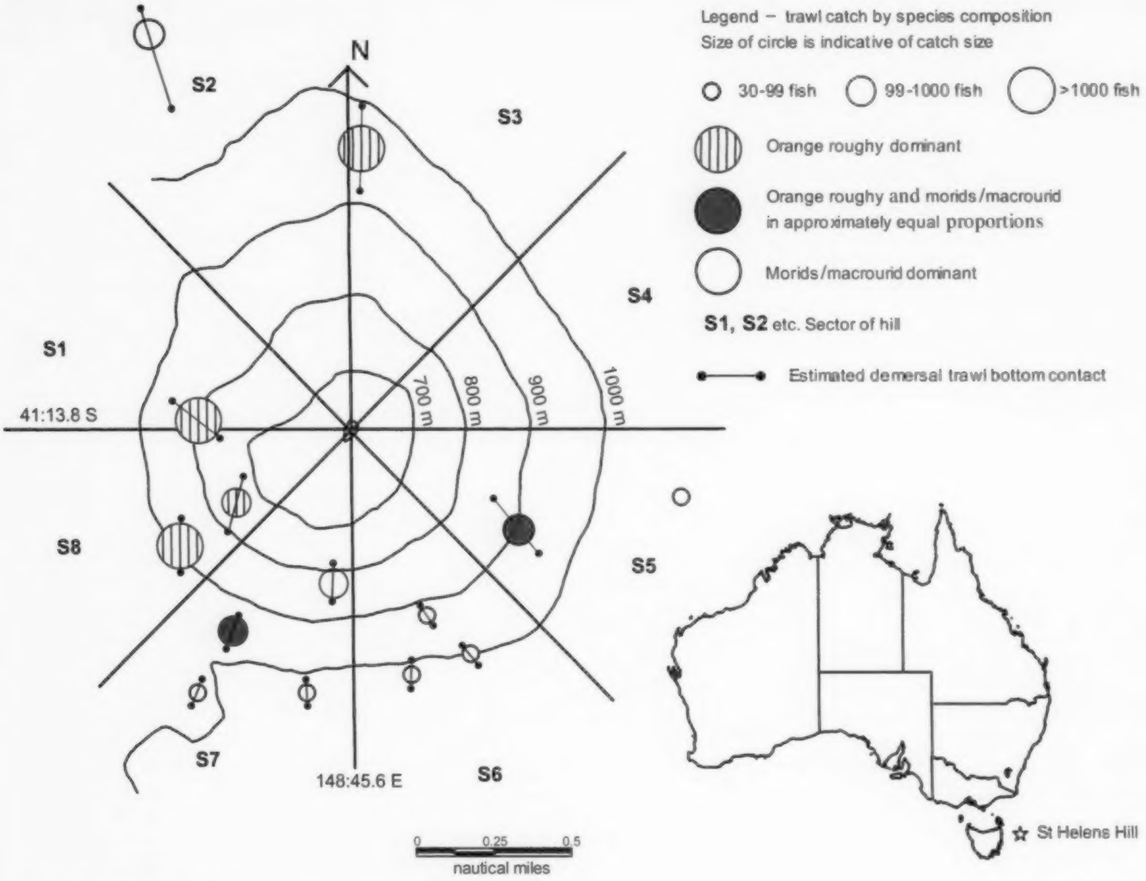
N
S1
S2
S3
S4
S5
S6
S7
S8
41:13.8 S
148:45.6 E
700 m
800 m
900 m
1000 m
0
0.25
0.5
nautical miles
Legend – trawl catch by species composition
Size of circle is indicative of catch size
30-99 fish
99-1000 fish
>1000 fish
Orange roughy dominant
Orange roughy and morids/macrourid in approximately equal proportions
Morids/macrourid dominant
S1, S2 etc. Sector of hill
Estimated demersal trawl bottom contact
St Helens Hill

Fig. 1. Demersal trawl catch positions and the relative proportions of dominant species combined by swimbladder type of orange roughy (*Hoplostethus atlanticus*) and large gas bladder (macrourids and morids) associated with the sector of the St. Helens seamount (Australia) in July 1996.

due to depth and target density (Sawada et al. 1993; Soule et al. 1995; Koslow et al. 1997). For each region the mean linear TS was calculated for the 38- and 120-kHz split beam transducers and compared to previous TS measurements following Kloser et al. (1997) (Table 2).

Simple gas bladder resonance model

To investigate the normal incident TS of gas-filled swimbladders with depth and frequency, the simple model developed for spherical spheres by Andreeva (1964), adapted for prolate spheroids by Weston (1967), and applied by Holliday (1971) was used in the following equations with minor changes in notation based on Ye (1997):

$$(1) \qquad \mathrm{TS} = 10\log_{10}(\sigma_{\mathrm{bs}})$$

$$(2) \qquad \sigma_{\mathrm{bs}} = a_{\mathrm{es}}{}^{2}\left(\left(\left(\frac{f_{\mathrm{p}}}{f}\right)^{2}-1\right)^{2}+\frac{1}{Q^{2}}\right)^{-1}$$

$$(3) \qquad f_{\mathrm{p}} = f_{\mathrm{o}}2^{\frac{1}{2}}e^{-\frac{1}{3}}(1-e^{2})^{\frac{1}{4}}\left\{\ln\left[\frac{1+(1-e^{2})^{\frac{1}{2}}}{1-(1-e^{2})^{\frac{1}{2}}}\right]\right\}^{-\frac{1}{2}}$$

$$(4) \qquad f_{\mathrm{o}} = \frac{1}{2\pi a_{\mathrm{es}}}\left(\frac{3\gamma P+4\mu_{1}}{\rho}\right)^{\frac{1}{2}}$$

$$(5) \qquad P = (1+0.103D)10^{5}$$

Here, σ_{bs} is the acoustic backscattering cross section at the incident acoustic frequency (f) of the equivalent spherical swimbladder volume of radius a_{es} with a prolate resonant frequency (f_{p}), and resonance quality factor of Q. The prolate resonant frequency is a function of the prolate spheroid roundness (e) and the spherical resonant frequency (f_{o}) at a hydrostatic pressure (P) for fish depth (D) and fish tissue density (ρ), with a ratio of specific heats for the swimbladder gas (γ) and the real part of the complex shear modulus of the

Fig. 2. Example of mixing three frequencies showing the individual calibrated volume reverberation compensated frequencies that are first quality assured removing known artefacts (*a*) red (12 kHz), (*b*) green (38 kHz), and (*c*) blue (120 kHz). A composite image (*d*) is produced where the frequencies have been optimized dynamically to highlight the amplitude differences in the echogram when there is an even mix on the region interpreted to be originating from orange roughy (*Hoplostethus atlanticus*). The dominant red (12 kHz) is interpreted to be originating from regions of species with large gas bladders (morids and macrourids), green (38 kHz) highlights the species with small gas bladders, and blue (120 kHz) highlights the orange roughy.

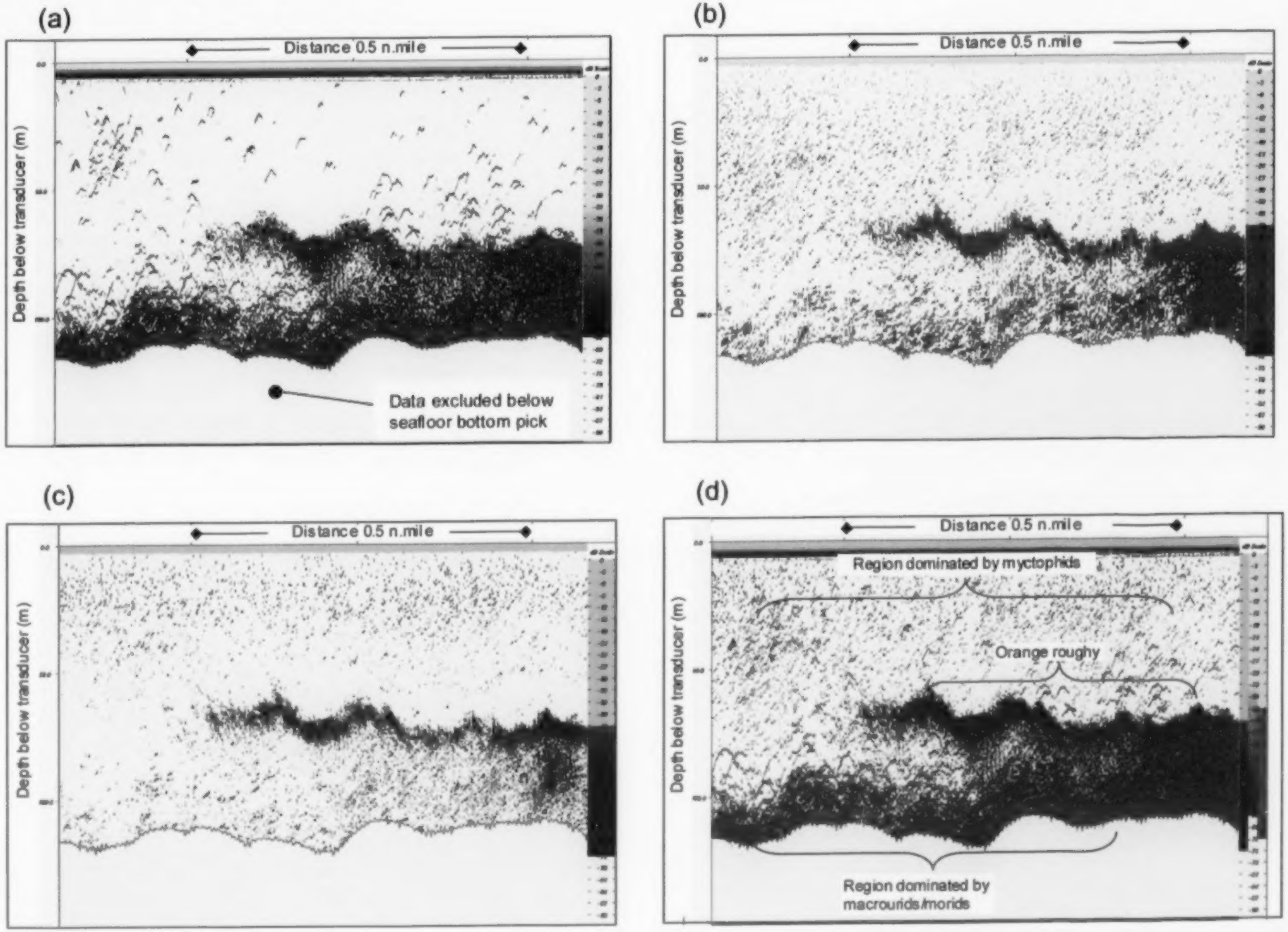

Fig. 3. Multifrequency acoustic data from a "loop" transect around St. Helens Hill, Australia, showing the dominant acoustic species group distribution as a function of sector around the hill according to the frequency mixing of Fig. 2. The towed body (MUFTI) is at a depth of ~700 m and is being towed clockwise with the vessel following the ~850-m depth contour. The five regions extracted for volume reverberation and target strength measurements are shown by enclosed polygons.

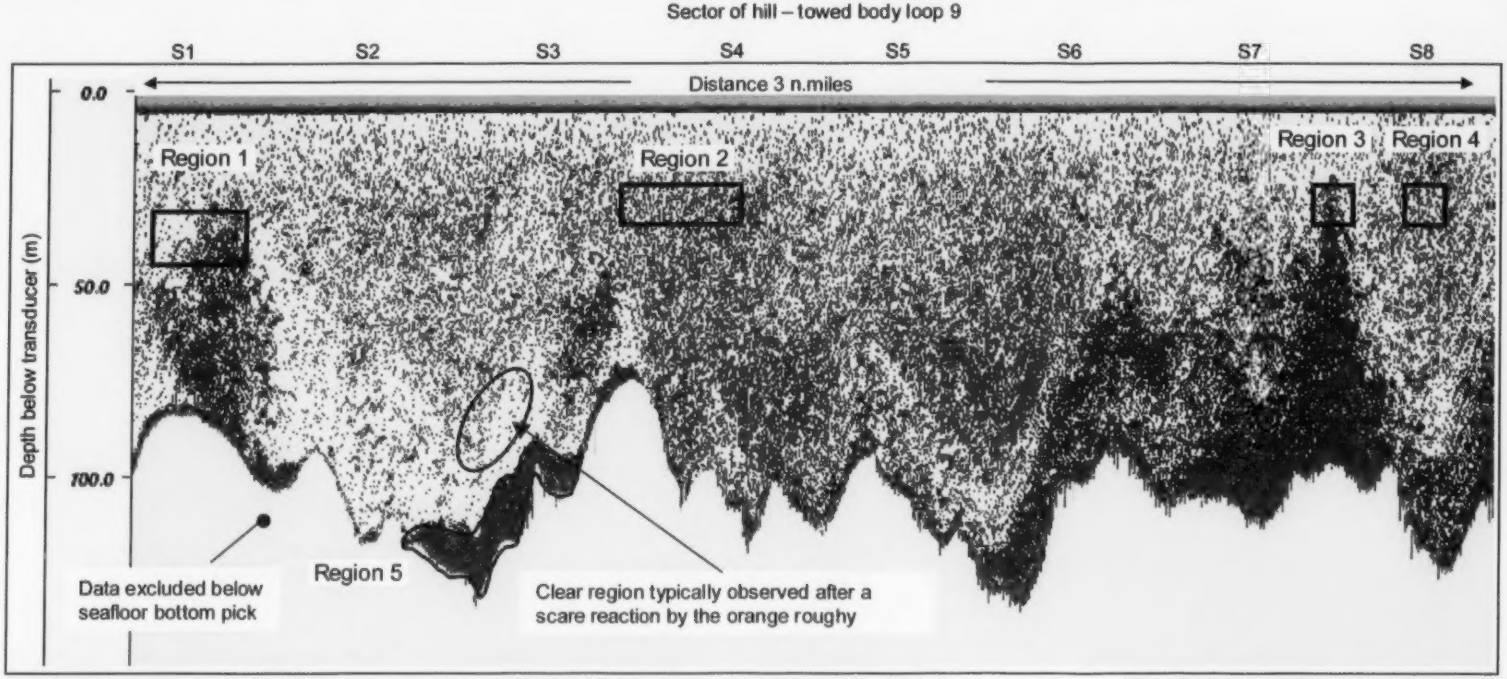

Region	Dominant species group	Dominant frequency	Colour palette
1 and 3	Macrourids/Morids	12kHz	Red
2 and 4	Myctophids	38kHz	Green
5	Orange roughy	120kHz	Blue

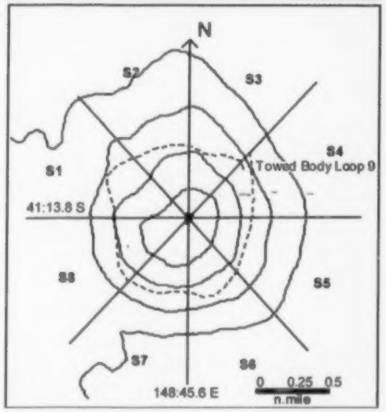

Table 2. Dominant species and species groups at St. Helens Hill, Tasmania, Australia.

Species	Swimbladder type	Length (mean, SD) (cm)	TS (dB re 1 m^2)	Acoustic category
Orange roughy	Wax ester filled	36 (4) SL	–48 to –52	Orange roughy
Myctophids (9 species with two dominant length modes)	Gas filled	5.8 (1) 9 (1)	–48 to –55	Small gas bladder
Macrourids (8 species)	Spongy tissue gas matrix or gas filled	34 (3)	–42	Large gas bladder
Morids (2 species)	Gas filled	50(8)	–32	Large gas bladder

Note: Swimbladder description and estimated target strength (TS at 38 kHz) from in situ measurements (Kloser et al. 1997). Fish length is total length unless shown otherwise as standard length (SL). SD, standard deviation.

fish tissue defined by μ_1. e is defined by the ratio of the minor semi-axis to the major semi-axis and is assumed to be 0.2.

To explore the indicative form of the model for the species encountered in this study, literature values were used from previous studies on shallower water species (Holliday 1971). Specifically, the following values were assumed: $\mu_1 = 10^5$ Pa, $\gamma = 1.4$, $\rho = 1.075\ \mathrm{kg{\cdot}m^{-3}}$, and $\delta = 5$. No measurements at depth were available for a_{es} of the gas bladders, but to best fit the experimental data, these were set to 1.4 mm for myctophids, with small gas bladders, and 5.1 mm for macrourids–morids, which have larger gas bladders. These values represent the lower end of the range of values calculated by Brooks (1977) for mid-water species, and they are consistent with the high lipid content observed in the fishes.

School size and biomass comparison

The size of orange roughy schools and associated biomass was calculated separately for both the single frequency straight line and multifrequency loop surveys. Using ECHO software, the single 38-kHz frequency north–south transect data (MUFTI towed transducer at depth 450 m) were evaluated for echo structures that originate from orange roughy based on the accumulated knowledge of trawl catches and temporal school behaviour in the region. These echo features were circled by hand using a mouse and the acoustic returns echo integrated by linearly summing the volume reverberation values vertically, automatically compensating for near-seabed shadow-zone, and averaging horizontally according to Kloser et al. (1996).

The MUFTI multifrequency loop transects circled the hill at 100-m depth contour intervals (from 750 to 1150 m depth) with the transducer 150–200 m above the seabed. The multifrequency data were used to highlight the orange roughy based on the mixing of the three frequencies and regions on the echograms were circled by hand using a mouse. The highlighted regions, on the 38-kHz frequency, were echo integrated on a per transect basis to produce an area backscatter, S_{a_l}, value for each loop representing a 100-m contour interval area, A_l, (Fig. 1). The biomass, B, of orange roughy was calculated assuming a mean weight, W, of 1.5 kg and mean TS of –50 dB re 1 m^2, where

$$B = \frac{\left(\sum_{l=1}^{n} \overline{S_{a_l}} A_l\right) W}{4\pi 10^{\frac{\mathrm{TS}}{10}}}\ \mathrm{kg}$$

Further details of the biomass calculations are outlined in Kloser et al. (2001).

Results

Biological sampling

Twenty-two demersal tows were carried out on St. Helens Hill (Fig. 1), of which 15 contained >20 fish; the total catch was 35.1 tonnes (t). The 45 species obtained were grouped into the seven acoustic categories, with four groups only contributing to <1% of the total. The three remaining groups were analysed further; orange roughy, macrourids, and morids represented 96, 2, and 1% of the total numbers, respectively. Orange roughy dominated catches on St. Helens Hill in sectors 1, 3, and 8, whereas sectors 5, 6, and 7 were dominated by macrourids and morids (Fig. 1). The difficulty of sampling all sectors and depth ranges of the hill equally resulted from seabed roughness, and lack of time availability left sectors 2, 3, 4, and 5 poorly sampled.

Three depth-stratified pelagic tows were targeted around the hill, 50–100 m above the seabed. These caught 35 species of pelagic fish, squid, and crustaceans, of which myctophids (possessing a gas-filled swimbladder) accounted for 95.5% (by numbers) of the catch. The total length of the dominant myctophids formed strong total length modes at 5.8 and 9 cm (Kloser et al. 1997). Morids and macrourids with relatively large gas bladders were also caught, but they represented less than 0.3% (by numbers) of the catch.

Acoustics

The acoustic loop survey data from the MUFTI towed system, deployed at a depth of ~150 m above the seabed, were analyzed as outlined in Materials and methods (Fig. 2) and are referenced to sectors of the hill (Fig. 3). Both the acoustics and demersal trawl distributions indicate that orange roughy were located in sectors 1, 2, and 3 and morids and macrourids are concentrated in sectors 6 and 7, as well as sectors 1 and 3, along with orange roughy (Figs. 1 and 3). It should be noted that the demersal trawling was undertaken over several days, whereas the acoustic loop transect was carried out in 1.5 h. Complete congruence between the two data sets is therefore not expected.

To directly compare volume reverberation (S_v) and in situ TS metrics between frequencies, five regions (Fig. 3) were extracted based on depth, frequency dominance, and sector on the hill associated with a particular species group (Table 3). Regions 1 and 3 are associated with species with large gas bladders dominated by the 12-kHz frequency, 4–8 dB higher

Table 3. Summary of the frequency differences in volume reverberation (S_v) and target strength (TS) for the selected regions identified in Fig. 3 with classification of dominant acoustic groups.

Region	Frequency (Hz)	Mean volume reverberation Sv (dB re 1 m)	S_v relative to dominant frequency in each region (dB re 1 m)	Mean TS (dB re 1 m^2)	No. targets	Relative TS to 38 kHz per region (dB)	Classification of dominant acoustic groups based on trawling
1	12	–63.3	0	na	na	na	Large gas bladder
1	38	–70.0	–6.7	–44.1	190	0	Large gas bladder
1	120	–71.3	–8	–42.6	48	1.5	Large gas bladder
2	12	–69.9	–5.3	na	na	na	Small gas bladder
2	38	–64.6	0	–49.3	240	0	Small gas bladder
2	120	–74.1	–9.5	–56.3	81	–7.0	Small gas bladder
3	12	–59.3	0	na	na	na	Large gas bladder
3	38	–63.4	–4.1	–39.7	206	0	Large gas bladder
3	120	–66.4	–7.1	–37.6	48	2.1	Large gas bladder
4	12	–77.1	–11.6	na	na	na	Small gas bladder
4	38	–65.5	0	–48.9	147	0	Small gas bladder
4	120	–75.5	–10	–57.6	24	–8.7	Small gas bladder
5	12	–50.6	–2.9	na	na	na	Orange roughy
5	38	–52.3	–4.6	na	na	na	Orange roughy
5	120	–47.7	0	na	na	na	Orange roughy

Note: na, not applicable.

than the S_v backscatter at 38 and 120 kHz (Fig. 4). The mean in situ TS in these regions range from –44.1 to –39.7 dB at 38 kHz and 1.5–2.1 dB higher at 120 kHz (Table 3). The higher TS at 120 kHz in these regions is unexplained and may indicate a problem with bias in the TS selection process due to the low number of targets selected at this frequency. In regions 2 and 4, which were associated with species with small gas bladders, the 38-kHz frequency was dominant with 9.5–10 dB higher S_v backscatter than the 120-kHz frequency (Fig. 4). Region 2 has a higher S_v (5.3 dB) at 12-kHz frequency owing to its larger sampling volume also including some fishes with large gas bladders, indicated in red (high 12-kHz S_v backscatter) (Fig. 3). The mean in situ TS in this region ranges from –48.9 to –49.3 dB at 38 kHz and 7–8.7 dB lower at 120 kHz (Table 3). Region 5, which we ascribe to orange roughy because of the characteristic avoidance response and trawl catch is characterized by high S_v backscatter at 120 kHz, 2.9–4.6 dB higher than at 12 or 38 kHz, respectively (Table 3). The lowest S_v backscatter for the orange roughy region 5 was from the 38-kHz frequency. No in situ TS data were obtained from region 5 because of the range from the transducer and high density of fishes.

The resonance model of small (a_{es} = 1.4 mm) and large (a_{es} = 5.1 mm) gas bladders shows the potential change in TS as a function of depth assuming constant swimbladder volume (Fig. 5). At the mean MUFTI operating depth of 750 m, the experimental TS measurements are compared to the simple model (Fig. 6). The TS values for the 12-kHz frequency have been extrapolated using the 38-kHz in situ TS values and the difference in volume backscattering strength for region 4, associated with myctophids, and region 1, associated with macrourids–morids. The simple normal incident resonance gas bladder model supports the general trend in the TS measurements with frequency; hence, our interpretation that of the three frequencies, the 38-kHz frequency has the highest S_v backscatter for small gas-filled swimbladders and the 12-kHz frequency has the highest backscatter for large gas-filled swimbladders in this example (Fig. 6).

The biomass of orange roughy on the St. Helens Hill seamount during surveys in 1999 ranged from null to 7000 t for the north–south grid surveys and 1100–2600 t for the MUFTI loop surveys (Table 4). The null value obtained from the grid survey indicates that no schooling features were observed that could be attributed to orange roughy. The lower biomass loop survey may have been due to avoidance of fish to the MUFTI towed system being closer than 100 m at times, as observed on echograms (Fig. 3). Error in the biomass calculation due to improperly assigning species composition using the north–south grid surveys could be a positive bias as high as a factor of 6.4. This error in the biomass calculation can be observed in the school areas of the echograms where they pass over the same school feature 2 h apart (Fig. 7). The estimated size of the orange roughy school defined from the grid survey based on trawl sampling and single frequency echo structure has a mean school height of 82 m, whereas the loop survey crossing the same school shows the mean school height to be 13 m. More importantly, the region allocated as orange roughy using a single frequency is shown to also contain a high mixture of fishes with large and small gas bladders using the MUFTI system (Fig. 7). No avoidance of orange roughy resulting

Fig. 4. Mean volume reverberation difference at 12 kHz (shaded) and 120 kHz (solid) frequencies relative to 38 kHz for each of the five selected regions based on Table 3. Region 5 associated with orange roughy (*Hoplostethus atlanticus*) has the lowest volume reverberation at 38 kHz.

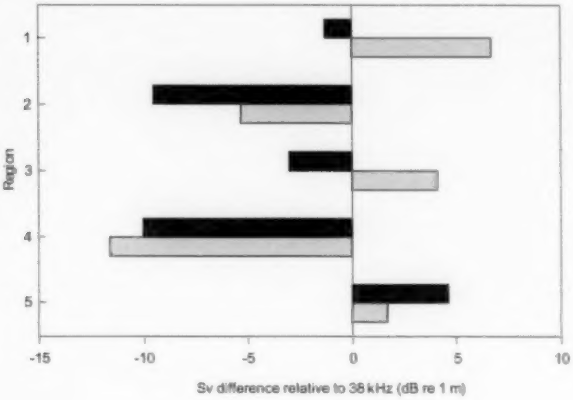

Fig. 5. Simple resonance target strength model of a spherical gas bladder for small (radius 1.4 mm) and large (radius 5.1 mm) fishes at 12 (solid line), 38 (broken line), and 120 (dotted broken line) kHz as a function of depth, assuming constant swimbladder volume.

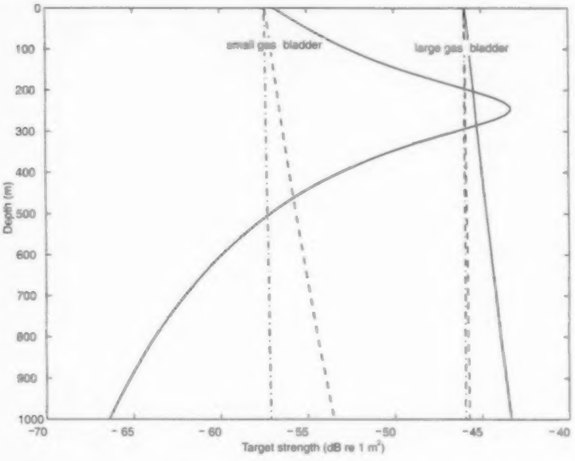

from the MUFTI transducer being 150 m above the school is evident in the echograms.

Discussion

Our acoustic system identified three acoustic groups based on the amplitude differences in the frequencies. ECHO software enabled these differences to be highlighted in a dynamic fashion that extracts the features of interest (Kloser et al. 1998). In this case, we have attributed the frequency differences to three acoustic groups of fishes as determined by their swimbladder type, size, and relative abundance. The three groups are myctophids of total length <10 cm, morids and macrourids with total lengths >30 cm, and orange roughy with a mean standard length of 36 cm. Our ability to differentiate orange roughy from other species in schools has been a major advance in interpreting single-frequency echograms and has been used in several biomass surveys of orange roughy both in Australia and New Zealand with consistent observations of species mixes in schools at orange roughy spawning sites (Kloser et al. 2000, 2001).

Fig. 6. Simple resonance target strength model at 750 m depth for a normal incident prolate spheroid (broken line, $e = 0.2$) and spheroid (solid line) swimbladder for small and large fishes (equivalent spherical radius of 1.4 and 5.1 mm, respectively) with experimental data for region 1 (○, macrourids–morids) and region 4 (*, myctophids) at the three frequencies 12, 38, and 120 kHz. The 12-kHz target strength values have been extrapolated from the ratio of S_v differences between the 38-kHz frequency in region 4 (Table 3).

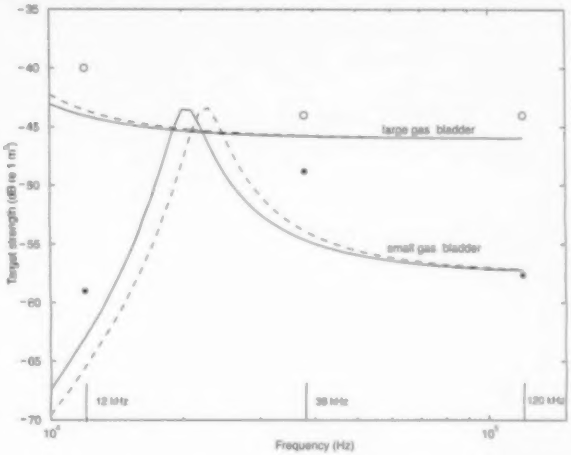

Our knowledge of orange roughy avoidance behaviour and the location of orange roughy schools on St. Helens Hill enabled us to tune the ECHO software (Koslow et al. 1995; Kloser et al. 1997). The avoidance reaction of orange roughy is evident in our echograms characterized by a low reverberation region remaining when the orange roughy school moves. The implication of this avoidance is that any remote sensing species identification system needs to be far enough away from the fish (ranges from 100 to 150 m are typical), so as not to influence their behaviour. Our use of the 120-kHz frequency is not ideal because of its high absorption in sea water for these surveys (31.9 dB·km^{-1} re 1 μPa at 1 m) reducing the effective usable range to 200 m. Other frequencies and (or) pulse transmission methods should be explored to improve this method.

Simple frequency models of the resonance from small gas bladders show a marked sensitivity to gas bladder size, eccentricity, and depth (Johnson 1977; Babailov and Kanevskii 1988). Our experimental results show that for regions dominated by fishes with small gas bladders, the backscatter measured at 38 kHz is 5 and 12 dB higher than for the 12- and 120-kHz frequencies, respectively. In this region, the mean in situ TS at 38 kHz is –49 dB and at 120 kHz is –57 dB. Based on a simple model (Weston 1967) we propose that swimbladder resonance is responsible for the high 38-kHz backscatter in this region. Conversely, the absence of a gas-

Fig. 7. Example of the difference in school size and acoustic species recognition using acoustic data from the same location in July 1999 from (*a*) the single-frequency 38-kHz north–south transects at 450 m depth and (*b*) an associated multifrequency loop transects at 750-m depth and height above bottom of 150–200 m approximately 2 h later.

Table 4. Biomass estimates of orange roughy at St. Helens Hill at 38 kHz based on north–south grid surveys with MUFTI at 450-m depth and trawl species identification, MUFTI loop surveys at 150–200 m above seabed (1999 only) using frequency mixing to highlight orange roughy (*Hoplostethus atlanticus*) schools.

Date	Survey type	Biomass estimate (tonnes)	Dominant species identification method
July 1996	North–south rid	9300*	Trawl
19 July 1999	North–south grid	Null	Trawl
31 July 1999	North–south grid	3500–7000† mean 5200	Trawl
20 July 1999	Loop	2600	Multifrequency
31 July 1999	Loop	1100	Multifrequency

Note: †Lower value indicates stricter classification of orange roughy schools using multifrequency classifications; *indicates the mean of two surveys.

filled swimbladder in orange roughy results in a relatively lower reflectance at 38 kHz, which demonstrates that this frequency is not optimal for detection of orange roughy. For regions dominated by fish with large gas bladders, the results show a high backscatter at 12 kHz, 4–7 dB higher than 38 kHz, and 7–8 dB higher than 120 kHz. For the region of aggregated orange roughy, the backscatter at 120 kHz is 2.9 and 4.6 dB higher than for 12 and 38 kHz, respectively. Thus the 120-kHz frequency has the best discrimination for orange roughy because of its lower relative response to small- and medium-sized gas bladdered fishes. The 12-kHz wide beam width is best for the fishes with large gas bladders and the 38 kHz is best for the species with small gas bladders featured in this study.

We have used a simple resonance model to explain general trends in experimental observations. Our choice of gas bladder size, and to a lesser degree, elongation, greatly alters the form of the model output. We have not measured directly the expected swimbladder size at depth or parameters such as the ratio of specific heats of the swimbladder gas and the fish tissue density and complex shear modulus over the frequency range. Measurements of swimbladder size would ideally be based on the required fish buoyancy at depth based on the fishes' lipid content. Also, we have not considered the effect of swimbladder orientation (Babailov and Kanevskii 1988). We conclude from our spherical resonance target that the general trend that we observe with the experimental data will also hold for Gaussian changes in tilt orientations. Feuillade and Nero (1998) and Ye (1997) have developed more complex gas bladder resonance scattering models. These models may be useful to explore more quantitative assessments of the multifrequency method. In this work, we have used a simple model to explore the dominant relationships in the experimental observations of fishes with gas-filled swimbladders: that excludes orange roughy.

Orange roughy represent complex scatterers with a relatively large, ossified, and cavernous head, dense backbone, and high lipid content (including a wax ester filled swimbladder) that makes accurate modelling challenging. Existing models based on overall shape and composition parameters are necessarily simplistic and there is a large disagreement between model results for this species (McClatchie and Ye 2000; Barr 2001). Our in situ TS data appears to support the model results of Barr (2001) where a 33.6-cm orange roughy has a model TS of approximately −51 dB and in situ measurements of −51 to −52.1 dB (Kloser et al. 2000). No sensitivity analysis of the model to variations in radius of curvature and (or) sound speed and density measurements of fish flesh and wax ester were performed, so the comparison may be fortuitous. The frequency response model of orange roughy proposed by Barr (2001) has many peaks for an individual fish, but we suggest that these peaks would smooth out for a range of fish sizes with more complicated composition and tilt angles, as is encountered in the ocean. The model of Barr (2001) does not explain the higher backscatter at 12 and 120 kHz experienced in this study.

A limitation of the equipment used in this trial was the wide 40-degree beam of the 12-kHz system. Unfortunately, to have a narrow beam at this low frequency, similar to the 7-degree beam width of the 38- and 120-kHz systems, would require a transducer 1.2 m in diameter. The sampling width and volume at the half power points of the 12-kHz, 1-ms pulse-length system at 100-m depth is 73 m and 3121 m^3, compared with 12 m and 112 m^3 for the 7-degree 38- and 120-kHz frequencies; the 12-kHz frequency effectively samples 28 times the water volume compared with the 38- and 120-kHz frequencies at 100-m depth. As the 12 kHz shows higher reflectance for the fishes with large gas bladders, they appear even more dominant on a multifrequency S_v compensated echogram owing to the greater sampling volume. Multifrequency echograms derived from differing beam widths complicates and limits quantitative assessment. To reduce the impact of differing sample volumes, the species mixtures need to be homogeneous over dimensions larger than the largest sampling volume, in this case 3121 m^3 at 100-m depth. Small, apparent orange roughy schools were sometimes completely absent from the 12-kHz records, making unsupervised classification based on multiple frequencies problematic. Also, the ability to ground truth our acoustic records with precisely located trawling in time and space is not possible given current technology. This limits our ability to perform rigorous statistical analyses of the data.

An obvious advantage of the multifrequency technique we have developed is the speed at which the dominant acoustic species groups can be obtained during a survey. The single-

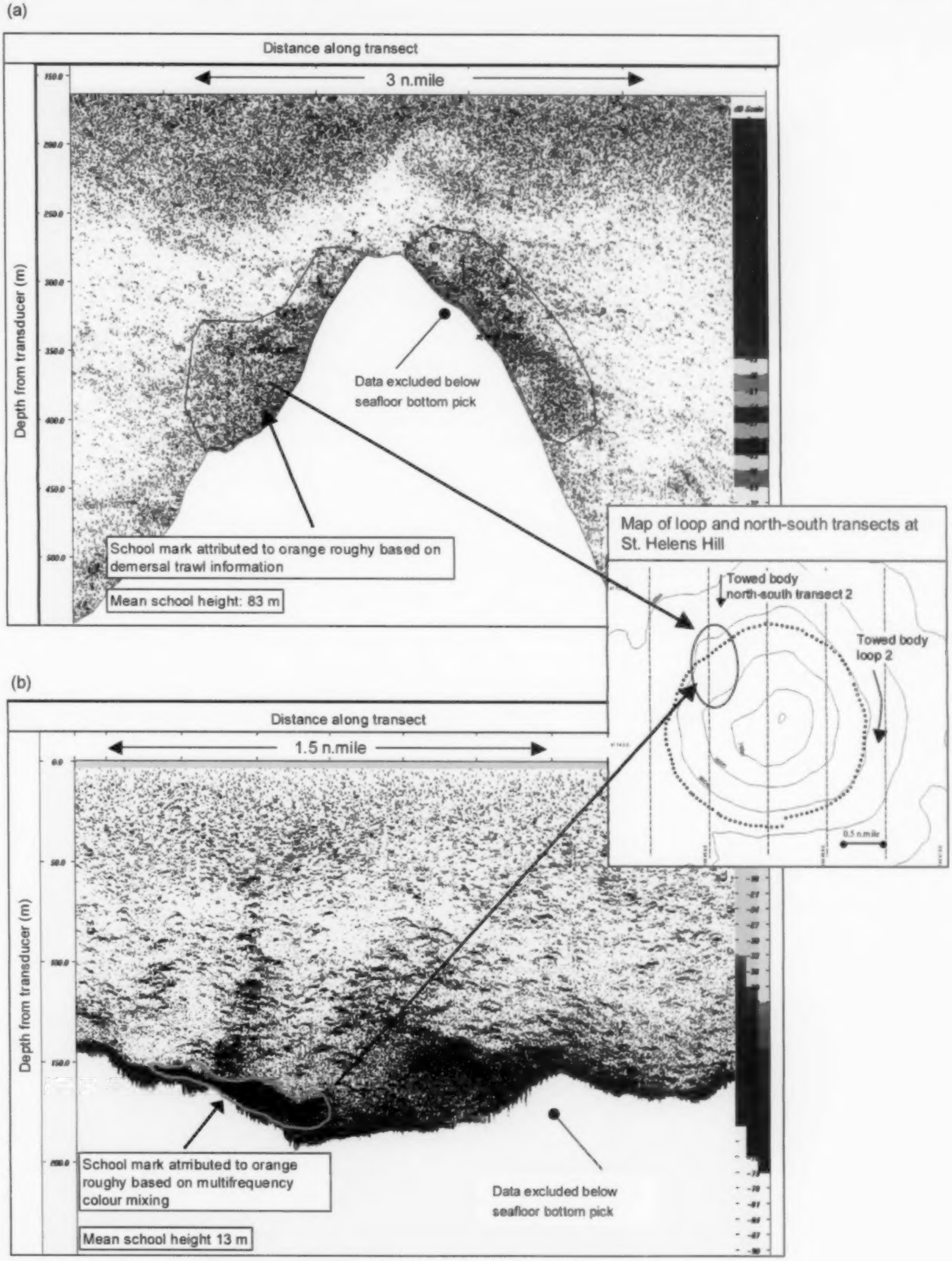
(a)
Distance along transect
3 n.mile
Depth from transducer (m)
150.0
200.0
250.0
300.0
350.0
400.0
450.0
500.0
dB Scale
Data excluded below seafloor bottom pick
School mark attributed to orange roughy based on demersal trawl information
Mean school height: 83 m
Map of loop and north-south transects at St. Helens Hill
Towed body north-south transect 2
Towed body loop 2
0.5 n.mile
(b)
Distance along transect
1.5 n.mile
Depth from transducer (m)
0.0
50.0
100.0
150.0
200.0
School mark attributed to orange roughy based on multifrequency colour mixing
Data excluded below seafloor bottom pick
Mean school height 13 m

loop survey of the hill was undertaken in 1.5 h, whereas the trawl sampling was undertaken over several days (with possible movement of fishes); also, many parts of St. Helens Hill could not be trawled. Additionally, the method of frequency mixing is relatively insensitive to calibration errors. The user can isolate a characteristic in the echo space by adjusting the colour amplitude mixing to be equal at all frequencies. Frequency amplitude differences can then be observed in other parts of the image. We have supplemented our interpretation here by both physical sampling and using a simple resonance model to explain the gross differences observed. Using this species identification technique, the snapshot biomass of orange roughy at St. Helens Hill is a factor of 2–6.4 lower than the traditional north–south grid surveys. We assume that the loop survey method is a robust relative snapshot measure of the spawning population not biased by avoidance or survey design. The 1996 and 1999 north–south grid surveys shows that the estimated biomass on the grounds has continued to decline and our new method reinforced the observed decline. This decline in biomass is occurring at a time when the assessment model is expecting an increase and has major implications for the management of the fishery (Bax 1999).

This application of multifrequency species identification has highlighted the problem of the 38-kHz frequency that is commonly used to survey orange roughy stocks. It appears that this frequency produces higher reflectance for myctophid fishes with small gas bladders at our operating depth than the 12- and 120-kHz frequencies. The 120-kHz frequency is the best of the three frequencies used for orange roughy discrimination, but has a very limited range because of its high absorption. The method of frequency mixing developed here can be used more generally to explore echo features in a wide range of multifrequency acoustic data sets. To extend this work to find optimal frequencies for particular species groups will require more refined acoustic scattering models with associated field testing. We postulate that the use of lower frequencies like commercially available 70-kHz would increase the usable range of our method and still provide the required discrimination between fishes with small gas bladders and orange roughy at 700-m depth.

Acknowledgments

We thank the many people that have contributed to this study, including Alan Poole, Ian Helmond, and Matt Sherlock, who assisted in the design and construction of the acoustic system; Jason Waring, who wrote the original ECHO software to capture and visualize the data, and Mark Lewis, who assisted in collection and processing of the biological catches; Dr. Andrew Forbes and Dr. Jock Young for reviewing an earlier draft of the manuscript; and Dr George Rose and an anonymous reviewer whose comments and suggestions improved the final manuscript. Thanks also to CSIRO Marine Research, Australian Fisheries Research and Development Corporation, Australian Fisheries Management Authority, for financial assistance under grant Nos. 99/111, 95/031, and T93/237. Additional thanks to George Clement from New Zealand Orange Roughy Management Company for supporting trials on New Zealand orange roughy.

References

Andreeva, I.B. 1964. Scattering of sound by air bladders of fish in deep sound-scattering ocean layers. Sov. Phys. Acoust. **10**: 17–20.

Babailov, E.P., and Kanevskii, V.A. 1988. Sound scattering by a gas-filled spheroidal swim bladder. Sov. Phys. Acoust. **34**(1): 11–14.

Barr, R. 2001. A design study of an acoustic system suitable for differentiating between orange roughy and other New Zealand deep-water species. J. Acoust. Soc. Am. **109**(1): 164–178.

Bax, N. 1999. Orange roughy 1999. Stock Assessment Report, South East Fishery Assessment Group. Australian Fisheries Management Authority, Canberra.

Boyer, D.C., and Hampton, I. 2001. Development of acoustic techniques for assessment of orange roughy *Hoplostethus atlanticus* biomass off Namibia, and of methods for correcting for bias. S. Afr. J. Mar. Sci. **23**: 223–240.

Brooks, A.L. 1977. A study of the swimbladders of selected mesopelagic fish species. *In* Oceanic sound scattering prediction. *Edited by* N.R. Anderson and B.J. Zahuranec. Plenum Publishing Corp., New York. pp. 565–590.

Clark, M. 1999. Fisheries for orange roughy (Hoplostethus atlanticus) on seamounts in New Zealand. Oceanol. Acta, **22**: 593–602.

Cochrane, N.A., Sameoto, D., Herman, A.W., and Neilson, J. 1991. Multiple-frequency acoustic backscattering and zooplankton aggregations in the inner Scotian Shelf basins. Can. J. Fish. Aquat. Sci. **48**: 340–355.

Feuillade, C., and Nero, R.W. 1998. A viscous-elastic swimbladder model for describing enhanced-frequency resonance scattering from fish. J. Acoust. Soc. Am. **103**: 3245–3255.

Foote, K.G., Knudsen, H.P., Vestnes, G., McLennan, D.N., and Simmonds, E.J. 1987. Calibration of acoustic instruments for fish density estimation: a practical guide. ICES Coop. Res. Rep. **144**: 69.

Francois, R.E., and Garrison, G.R. 1982. Sound absorption based on ocean measurements. II. Boric acid contribution and equation for total absorption. J. Acoust. Soc. Am. **72**: 896–907.

Greenlaw, C.F., and Johnson, R.K. 1983. Multiple-frequency acoustical estimation. Biol. Oceanogr. **2**: 227–252.

Holliday, D.V. 1971. Resonance structure in echoes from schooled pelagic fish. J. Acoust. Soc. Am. **51**: 1322–1332.

Holliday, D.V. 1977. Extracting bio-physical information from the acoustic signatures of marine organisms. *In* Oceanic sound scattering prediction. *Edited by* N.R. Anderson and B.J. Zahuranec. Plenum Publishing Corp., New York. pp. 619–624.

Horne, J.K. 2000. Acoustic approaches to remote species identification: a review. Fish. Oceanogr. **9**(4): 356–371.

Johnson, R.K. 1977. Spectral models for biological sound prediction. *In* Oceanic Sound Scattering Prediction. *Edited by* N.R. Anderson and B.J. Zahuranec. Plenum Publishing Corp., New York. pp. 625–630.

Kloser, R.J. 1996. Improved precision of acoustic surveys of benthopelagic fish by means of a deep-towed transducer. ICES J. Mar. Sci. **53**: 407–13.

Kloser, R.J., Koslow, J.A., and Williams, A. 1996. Acoustic assessment of the biomass of a spawning aggregation of orange roughy (Hoplostethus atlanticus, Collett) off southeastern Australia 1990–93. Mar. Freshw. Res. **47**: 1015–1024.

Kloser, R.J., Williams, A., and Koslow, A.J. 1997. Problems with acoustic target strength measurements of a deepwater fish, orange roughy, (*Hoplostethus atlanticus*, Collett). ICES J. Mar. Sci. **54**: 60–71.

Kloser, R.J., Sakov, P.V., Waring, J.R., Ryan, T.E., and Gordon, S.R. 1998. Development of software for use in multi-frequency acoustic biomass assessments and ecological studies. Final report to Fisheries Research and Development Corporation T93/2. CSIRO Marine Research, Hobart. *Available from* Fisheries Research and Development Corporation, P.O. Box 222, Deakin West, ACT 2600, Australia.

Kloser, R.J., Ryan, T.E., Williams, A., and Soule, M.A. 2000. Development and implementation of an acoustic survey of orange roughy in the Chatham Rise spawning box from a commercial factory trawler, FV Amaltal Explorer. Report 597.64, CSIRO Marine Research, Hobart, Australia.

Kloser, R.J., Ryan, T.E., Williams, A., and Lewis, M. 2001. Development and application of a combined industry/scientific acoustic survey of orange roughy in the eastern zone. Final report to Fisheries Research and Development Corporation 99/111. CSIRO Marine Research, Hobart. *Available from* Fisheries Research and Development Corporation, P.O. Box 222, Deakin West, ACT 2600, Australia.

Koslow, J.A., Kloser, R., and Stanley, C.A. 1995. Avoidance of a camera system by a deepwater fish, the orange roughy (*Hoplostethus atlanticus*). Deep-Sea Res. 1, **42**: 233–44.

Koslow, J.A., Kloser, R.J., and Williams, A. 1997. Pelagic biomass and community structure on the mid-continental slope off southeastern Australia based upon acoustic and midwater trawl sampling. Mar. Ecol. Prog. Ser. **146**: 21–35.

MacKenzie, K.V. 1981. A nine-term equation for sound speed in the oceans. J. Acoust. Soc. Am. **70**: 807–812.

MacLennan, D.N. 1981. The theory of solid spheres as sonar calibration targets. Scott. Fish. Res. Rep. **22**.

McClatchie, S., and Ye, Z. 2000. Target strength of an oily deepwater fish, orange roughy (*Hoplostethus atlanticus*) II. Modeling. J. Acoust. Soc. Am. **107**: 1280–1285.

Miyanohana, Y., Ishii, K., and Furusawa, M. 1993. Spheres to calibrate echo sounders at any frequency. Nippon Suisan Gakkaish, **59**: 933–942.

Pearcy, W.G., Krygier, E.E., Mesecar, R., and Ramsey, F. 1977. Vertical distribution and migration of oceanic micronekton off Oregon, Deep-Sea Res. **24**: 223–245.

Rose, G.A., and Leggett, W.C. 1988. Hydroacoustic signal classification of fish schools by species. Can. J. Fish. Aquat. Sci. **45**: 597–604.

Sawada, K., Furusawa, M., and Williamson, N.J. 1993. Conditions for precise measurement of fish target strength *in situ*. Journal of Marine Acoustical Society of Japan, **20**: 15–79.

Scalabrin, C., Diner, N., Weill, A., Hillion, A., and Mouchot, M.C. 1996. Narrowband acoustic identification of monospecific fish shoals. ICES J. Mar. Sci. **53**: 181–188.

SIMRAD Fisheries Division. 1993. SIMRAD EK500 service and technical manual. SIMRAD, Horten, Norway.

Soule, M., Barange, M., and Hampton, I. 1995. Evidence of bias in estimates of target strength obtained with a split-beam echosounder. ICES J. Mar. Sci. **52**: 139–144.

Trevorrow, M.V. 1996. Multifrequency acoustic investigations of juvenile and adult fish in Lake Biwa Japan. J. Acoust. Soc. Am. **100**: 3042–3052.

Waring, J.R., Kloser, R.J., and Pauly, T. 1994. Echo – managing fisheries acoustic data. *In* Proceedings of the International Conference on Underwater Acoustics University of New South Wales, Dec. 1994. Australian Acoustical Society, New South Wales. pp. 22–24.

Weston, D.E. 1967. Sound propagation in the presence of bladder fish. *In* Underwater acoustics. Vol. 2. Chap. 5. *Edited by* V.A. Albers. Plenum, New York. pp. 56–88.

Williams, A., and Koslow, J.A. 1997. Species composition, biomass and vertical distribution of micronekton over the mid-slope region off southern Tasmania. Mar. Biol. **130**: 259–276.

Ye, Z. 1997. Low-frequency acoustic scattering by gas-filled prolate spheroids in liquids. J. Acoust. Soc. Am. **101**: 1945–1952.

Predatory impact of the freshwater invader *Dikerogammarus villosus* (Crustacea: Amphipoda)

Jaimie T.A. Dick, Dirk Platvoet, and David W. Kelly

Abstract: To assess the increasing threats to aquatic ecosystems from invasive species, we need to elucidate the mechanisms of impacts of current and predicted future invaders. *Dikerogammarus villosus*, a Ponto–Caspian amphipod crustacean, is invading throughout Europe and predicted to invade the North American Great Lakes. European field studies show that populations of macroinvertebrates decline after *D. villosus* invasion. The mechanism of such impacts has not been addressed empirically; however, *D. villosus* is known to prey upon and replace other amphipods. Therefore, in this study, we used microcosm and mesocosm laboratory experiments, with both single and mixed prey species scenarios, to assess any predatory impact of *D. villosus* on a range of macroinvertebrate taxa, trophic groups, and body sizes. *Dikerogammarus villosus* predatory behaviour included shredding of prey and infliction of "bite" injuries on multiple victims. *Dikerogammarus villosus* killed significantly greater numbers of macroinvertebrates than did the native *Gammarus duebeni*, which is currently being replaced by *D. villosus*. This invader thus appears to impact on freshwater ecosystems through its exceptional predatory capabilities. We predict that future invasions by *D. villosus* will have serious direct and indirect effects on freshwaters, with its invasion facilitated in a larger "invasional meltdown" in regions like the North American Great Lakes.

Résumé : Pour évaluer la menace grandissante que représentent les espèces envahissantes pour les écosystèmes aquatiques, il est nécessaire d'élucider les mécanismes par lesquels les envahisseurs actuels et ceux qu'on prévoit dans le futur causent leur impact. *Dikerogammarus villosus*, un crustacé amphipode originaire de la région pontocaspienne, est en train d'envahir l'Europe et on prédit qu'il se retrouvera éventuellement dans les Grands-Lacs nord-américains. Des études sur le terrain en Europe révèlent que les populations de macroinvertébrés diminuent après une invasion de *D. villosus*. Le mécanisme qui cause un tel impact n'a pas été étudié de façon empirique, mais il est connu que *D. villosus* se nourrit d'autres amphipodes et peut les remplacer. Des expériences en laboratoire en microcosmes et en mésocosmes avec des scénarios pour une seule ou plusieurs espèces de proies nous ont permis d'évaluer l'impact de *D. villosus* en tant que prédateur d'une gamme de macroinvertébrés de taxons, de groupes trophiques et de tailles différents. Le comportement prédateur de *D. villosus* inclut le déchiquetage des proies et la morsure vulnérante de victimes multiples. *Dikerogammarus villosus* tue un nombre significativement plus grand de proies que ne le fait l'espèce indigène *Gammarus duebeni* qu'il est en voie de remplacer. L'envahisseur semble donc avoir un impact sur les écosystèmes d'eau douce à cause de ses capacités exceptionnelles de prédateur. On peut donc prédire que les invasions futures de *D. villosus* auront des effets importants, tant directs qu'indirects, sur les milieux d'eau douce et que son invasion sera facilitée par l'effondrement des communautés causé par les invasions dans des régions telles que les Grands-Lacs nord-américains.

[Traduit par la Rédaction]

Introduction

Invading aquatic species will continue to cause extensive ecological damage and economic loss (Hall and Mills 2000; Mack et al. 2000; Ricciardi and MacIsaac 2000), with invaders predicted to be the major drivers of changes in freshwater biodiversity over the next 100 years (Sala et al. 2000). Indeed, the rate of aquatic invasions may be generally increasing, with systems like the North American Great Lakes threatened with "invasional meltdown" (Ricciardi 2001). Hence, current research priorities are identification of potential new invaders together with explanations and predictions of their mode and degree of impact (Ricciardi and Rasmussen 1998; Ricciardi 2001). The Ponto–Caspian amphipod crustacean *Dikerogammarus villosus* is currently invading throughout Europe (Dick and Platvoet 2000; van der Velde et al. 2000) and is predicted to invade the North American Great Lakes (Ricciardi and Rasmussen 1998). Field surveys indicate that the ecological impact of *D. villosus* invasions may be severe, with documented declines in macroinvertebrate species coincidental with the arrival of *D. villosus* in the Dutch Lower River Rhine (van der Velde et al. 2000; G. van der Velde and M. van Riel, Laboratory of Aquatic Ecology, University of Nijmegen, The Netherlands, personal communication), the Dutch IJssel Lake (Dick and Platvoet 2000), and the French Rivers Moselle, Saone, Rhone, and the Alsace Canal (Devin et al. 2001; L. Bollache and F. Cézilly,

Received 1 March 2002. Accepted 23 May 2002. Published on the NRC Research Press Web site at http://cjfas.nrc.ca on 26 July 2002.
J16786

J.T.A. Dick[1] and D.W. Kelly. School of Biology and Biochemistry, Queen's University Belfast, MBC, 97 Lisburn Road, Belfast BT9 7BL, Northern Ireland, U.K.
D. Platvoet. Zoological Museum of Amsterdam, and Institute for Biodiversity and Ecosystem Dynamics, Faculty of Science, University of Amsterdam, P.O. Box 94766, 1090 GT, Amsterdam, The Netherlands.

[1] Corresponding author (e-mail: j.dick@qub.ac.uk).

DOI: 10.1139/F02-074

Table 1. Analysis of variance results for mean survival of prey in microcosm and mesocosm experiments (see Figs. 1 and 3).

	Microcosms			Mesocosms
Invertebrate prey	Amphipod status (none; Gd; Dv) $F_{2,12}$	Time (Days 1, 2, 3) $F_{2,24}$	Interaction $F_{4,24}$	Amphipod status (none; Gd; Dv) $F_{2,27}$
(*a*) *Caenis robusta*	86.6****	11.3***	2.9*	13.2****
(*b*) *Asellus aquaticus*	14.8***	17.9****	5.6**	51.4****
(*c*) *Ischnura elegans* (small)	60.6****	7.9**	2.2	18.6****
(*d*) *Neomysis integer* (large)	6.7**	5.3**	5.3**	0.54
(*e*) *Ischnura elegans* (large)	45.9****	10.6***	10.6****	13.7****
(*f*) *Piscicola geometra*	10.8**	4.1*	4.1*	0.49
(*g*) *Sigara* sp.	11.3**	15.2****	1.6	3.6*
(*h*) *Eurycercus lamellatus*	23.1****	27.9****	8.9****	1.6
(*i*) *Chironomus* sp.	273.9****	16.1****	5.1**	N/A
(*j*) *Neomysis integer* (small)	3.9*	17.1****	2.6*	0.06
(*k*) *Chaoborus* sp.	16.8***	50.5****	3.2*	0.26

Note: Gd, *Gammarus duebeni*; Dv, *Dikerogammarus villosus*. $^*P < 0.05$, $^{**}P < 0.01$, $^{***}P < 0.001$, $^{****}P < 0.0001$.

Laboratoire Ecologie – Evolution, Université de Bourgogne, Dijon, France, personal communication). The mechanism by which *D. villosus* impacts on macroinvertebrates has not been explicitly addressed; however, *D. villosus* has been shown to prey upon and replace populations of other amphipods, such as the North American *Gammarus tigrinus* (invasive in Europe) and a European native, *Gammarus duebeni* (Dick and Platvoet 2000). Hence, in the present study, laboratory experiments were designed to examine any predatory impact of *D. villosus*, in comparison to that of a native counterpart (*G. duebeni*), on a range of macroinvertebrate taxa and functional groups, in an attempt to elucidate the current and potential future impacts of this invader in fresh waters.

Recent studies have emphasized the utility of examining proximate behavioural mechanisms that may explain invasion success in terms of impacts on native species (see Holway and Suarez 1999). While extrapolations to the field from microcosm and mesocosm scale studies are much debated (see Huston 1999), studies of behavioural mechanisms elucidated from small-scale experiments have been successful in explaining and predicting community patterns in the field (Holway and Suarez 1999; Wilhelm and Schindler 1999; Wilhelm et al. 2000). In addition, studies carried out at multiple spatial scales improve extrapolations from individual behaviour to population and community scales (Peckarsky et al. 1997). Therefore, in this study, we conducted laboratory experiments at two spatial scales to assess any predatory impact of *D. villosus* on a suite of potential macroinvertebrate prey species. In addition, since absolute rates of predation may be inflated under laboratory conditions, we took a comparative approach, assessing *D. villosus* predation relative to that of a native counterpart, *G. duebeni*. First, we staged interactions between single amphipods and multiple individuals of each prey species at the microcosm scale. Second, we assessed changes in experimental communities of multiple amphipod individuals and multiple prey species at the mesocosm scale.

Materials and methods

Experiments 1 and 2 were conducted in July–August 2000 and 2001, respectively, at the University of Amsterdam. In both years, we collected *D. villosus* and *G. duebeni* from our previous study sites around the IJsselmeer and Markermeer (see Dick and Platvoet 2000). The amphipod species were housed separately with flora, fauna, and debris from their respective collection sites and used in experimental replicates the day following capture. In both experiments, we chose to use an abundant size class of adult males of the two species. Although *D. villosus* is on average larger than *G. duebeni* (Dick and Platvoet 2000), we used matching sizes of males in the range 16–22 mm body length, thus examining any species effect rather than any confounding size effect. If, however, as is likely, predation is size dependent, any differences in predation frequencies between the two amphipod species in the present experiments will be conservative estimates. This choice of sex and size class was also a compromise between the largest males, which may have overestimated predatory impacts, and smaller males and females, which may have underestimated predatory impacts. Macroinvertebrates were collected from freshwater sites that were as of yet not invaded by *D. villosus*; namely, the location known as "Gaslocatie N.A.M.", near Middelie, North Holland, and "Broek in Waterland", north of Amsterdam. Together, these sites provided macroinvertebrates representing typical freshwater taxonomic groups, principally, insects (nymphs and (or) larvae) and crustaceans (see Table 1 and Fig. 1). Trophic or Functional Feeding Groups (sensu Cummins and Klug 1979) were widely represented and there was a large size range of potential prey, both soft and hard bodied (see Fig. 1).

In Experiment 1, aquaria of 20 × 20 × 10 cm (L × W × H) were supplied with 3.5 L of aerated water, which was a mixture from the collection sites detailed above (17–18°C; conductivity, 800–900 $\mu S \cdot cm^{-1}$). Broken terracotta plant pots provided a diversity of three-dimensional heterogeneous surfaces and crevices for predator and prey to use. Field densities of amphipods range from less than one up to several thousand per square metre (e.g., Welton 1979; Musko 1993), with our study sites showing similar variation. In the present study, amphipods were interacting in aquaria at a density equivalent to $25 \cdot m^{-2}$, at the lower end of field densities. Macroinvertebrates were introduced into microcosms and allowed to settle for 2 h before amphipods were introduced. For each of 11 macroinvertebrate prey (see Fig. 1), five replicates each containing five individuals were monitored for three days in each of three experimental groups: (*i*) no am-

Fig. 1. Mean (+ standard error) survival of macroinvertebrates over three days in the microcosm (single prey species) experiments, with no amphipod present (open bars), *Gammarus duebeni* present (hatched bars), and *Dikerogammarus villosus* present (cross-hatched bars). Plots *a*–*k* are arranged from greatest to least difference in survival of macroinvertebrates at day 3 in microcosms with invader compared to native. Differing letters (A, B, C) indicate significant differences among experimental groups over the three days (Fisher Protected Least Significant Difference Tests). Species and trophic groups: (*a*) *Caenis robusta* (mayfly nymph, 6–8 mm), scraper; (*b*) *Asellus aquaticus* (hog louse, 8–10 mm), shredder; (*c*) *Ischnura elegans* (damselfly nymph, 8–10 mm), predator; (*d*) *Neomysis integer* (opossum shrimp, 10–12 mm), predator; (*e*) *Ischnura elegans* (damselfly nymph, 15–20 mm), predator; (*f*) *Piscicola geometra* (fish leech, 30–50 mm), parasite; (*g*) *Sigara* sp. (waterboatman, 6–8 mm), herbivore shredder–piercer; (*h*) *Eurycercus lamellatus* (waterflea, 3–4 mm), filterer; (*i*) *Chironomus* sp. (midge larva, 12–14 mm), collector–gatherer; (*j*) *Neomysis integer* (opossum shrimp, 4–5 mm), predator; (*k*) *Chaoborus* sp. (midge larva, 6–8 mm), predator.

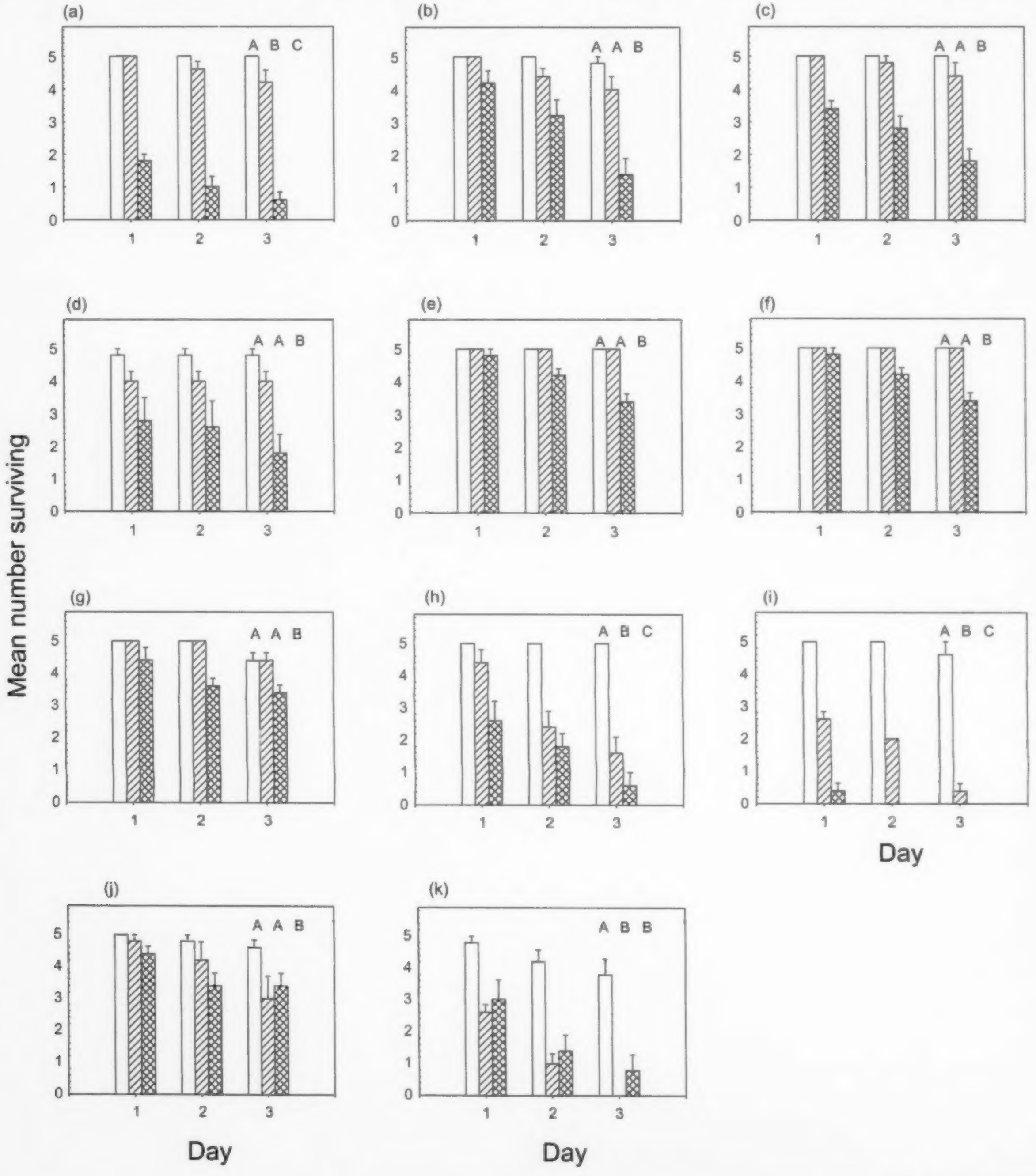

phipod present; (*ii*) a male *G. duebeni* present; (*iii*) a male *D. villosus* present. Twice daily (morning, evening), each replicate was inspected and the number and status (alive or dead) of amphipods and potential prey recorded. Any cadavers were removed and observed under binocular microscope for evidence of injury. Replicates were monitored for a further three days to examine, in groups (*ii*) and (*iii*), the survival of amphipods, thus giving an indication of their health under the laboratory conditions during the first three days, and similarly, replicates of group (*i*) were monitored to indicate the health of the macroinvertebrates.

In Experiment 2, aquaria of 60 × 40 × 20 cm (L × W × H) were supplied with 38.5 L of water and substrate as above. Each was supplied with five individuals of all 11 prey (see above) and 10 replicates monitored for three days in each of three experimental groups: (*i*) no amphipods; (*ii*) 11 male *G. duebeni*; (*iii*) 11 male *D. villosus*. Thus, amphipod–prey combinations and overall animal densities were as for microcosms, but scale was increased, amphipods had choice of prey, and all animals could interact with one another. The larger aquaria also reduced restrictions on potential distances that individuals could move vertically and horizontally. All replicates were inspected on day 3.

For each macroinvertebrate prey, data for analyses were arcsine transformations (see Sokal and Rohlf 1995) of proportions surviving. Experiment 1 data were analyzed for each prey by two-factor ANOVA (analysis of variance), Factor 1 being amphipod status (none, *G. duebeni*, *D. villosus*) and Factor 2 being time (repeated measure; days 1, 2, 3). Post-hoc tests (Fisher Protected Least Significant Difference Tests) were used to examine differences among amphipod status groups. Experiment 2 data were analyzed by a one-factor MANOVA (multiple ANOVA), the factor being amphipod status (none, *G. duebeni*, *D. villosus*), and subsequently, survival of each individual prey species by one-factor ANOVA. (For clarity, the figures associated with these analyses show mean numbers surviving.)

Results

In Experiment 1, there were no deaths of amphipods in groups (*ii*) and (*iii*) by day 3 or even day 6, indicating that the amphipod species were not differentially affected by laboratory conditions. The macroinvertebrates survived well in group (*i*) (i.e., no amphipods present) during the initial three days of the experiment (see Fig. 1), with no deaths over the subsequent three days. Thus, disappearances of macroinvertebrates in groups (*ii*) and (*iii*) could be reliably ascribed to amphipod predation of live individuals as opposed to scavenging following deaths due to some aspect of laboratory conditions. By day 3 of the experiment, and indeed mostly by day 1, *D. villosus* significantly reduced survival of all 11 species – size classes of macroinvertebrate prey tested (Fig. 1; Table 1). In addition, *D. villosus* had a significantly greater and often more rapid impact on macroinvertebrate survival than did *G. duebeni* for 10 of the 11 species – size classes and eight of the nine species tested (Fig. 1; Table 1). These differences in macroinvertebrate survival were clearly due to predation, with victims shredded and consumed. However, our observations also revealed predatory attacks that often left prey "bitten". Such individuals were removed from the microcosms, some photographed (see Fig. 2) and then isolated. Since all subsequently died within 1–3 h, these were classed as predatory kills in the data analyses.

Caenis robusta were shredded and eaten; however, we observed dead and dying specimens with bite damage to heads and bodies (Fig. 2). Indeed, in one replicate, all five nymphs sustained such bite injuries within 1.5 h, all subsequently dying within 1 h. We did not observe bite victims of *G. duebeni*, who shredded the nymphs they preyed upon. *Asellus aquaticus* and *Ischnura elegans* also suffered bite injuries (Fig. 2), the former even without having moulted and thus not yet being soft bodied. *Neomysis integer* (Leach) were killed more often in the larger than the smaller size-class, the latter appearing more capable of escape. *Piscicola geometra* appeared impervious to *G. duebeni*, but suffered significant predation and bite injuries by *D. villosus*. *Sigara* sp., despite being winged and hard-bodied, were preyed upon by *D. villosus* and often bitten (Fig. 2). *Eurycercus lamellatus* fell prey to both amphipods, but significantly more often, and generally more quickly, with *D. villosus*. Both amphipods preyed heavily on *Chironomus* sp. and *Chaoborus* sp.

In Experiment 2, two *D. villosus* and three *G. duebeni* replicates saw the death of one amphipod; however, this was considered negligible. There was a significant overall effect of "amphipod group" on the survival of macroinvertebrates ($F_{22,36} = 2.3$, $P < 0.01$; Fig. 3). Compared to the groups with no amphipods and *G. duebeni* present, *D. villosus* significantly reduced survival of *C. robusta*, *A. aquaticus*, *I. elegans* (both size classes), and *Sigara* sp. (Fig. 3; Table 1). *Neomysis integer* and *P. geometra* appeared unaffected by amphipods, whereas *E. lamellatus*, *Chironomus* sp., and *Chaoborus* sp. mostly disappeared. Mesocosms were characterized by the almost complete disappearance of victims, although we did observe predatory acts and injuries. For example, on four occasions *I. elegans* were observed being eaten alive by one or more *D. villosus*.

Discussion

Dikerogammarus villosus originates from an invasion donor "hot spot", the Ponto–Caspian region, with the ballast water of transoceanic shipping a likely invasion vector to the North American Great Lakes (see Mills et al. 1993; Ricciardi and Rasmussen 1998; Bruijs et al. 2001). Indeed, this species has already successfully invaded European regions like The Netherlands via new canals and shipping (Dick and Platvoet 2000; van der Velde et al. 2000). With many other invaders from the Ponto–Caspian established in the Great Lakes, this new invader may become part of a larger "invasional meltdown" (see Ricciardi and Rasmussen 1998; Simberloff and Von Holle 1999; Ricciardi 2001), particularly since zebra mussel (*Dreissena polymorpha*) beds, by providing substrate, may facilitate this large amphipod (see Stewart et al. 1998; Bially and MacIsaac 2000). Certainly, the arrival of *D. villosus* in western Europe has been concomitant with reductions in macroinvertebrate populations (see Introduction). Explanations and predictions of the ecological impact of *D. villosus* are therefore required, both as regards this specific case and to aid in the identification of future damaging invaders.

Fig. 2. Victims of *Dikerogammarus villosus* often suffered head bites, but legs and bodies were also often damaged.

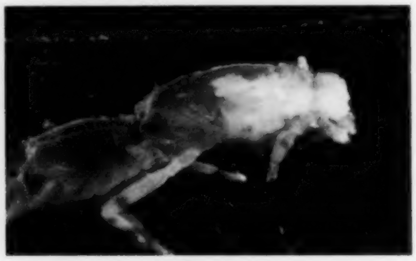

Caenis robusta

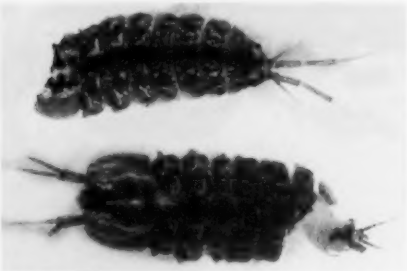

Asellus aquaticus

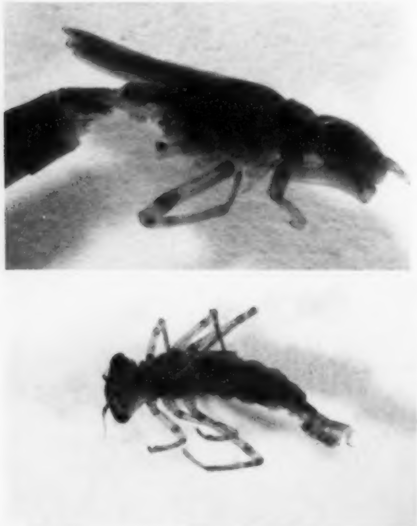

Ischnura elegans

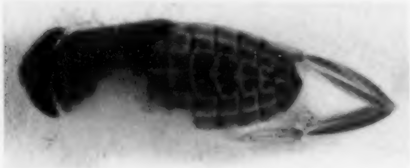

Sigara sp.

The two experiments presented here establish the exceptional predatory nature of *D. villosus*. Although animal material has been found in their guts (e.g., Hynes 1954; Ioffe 1973), amphipods such as *D. villosus* and *G. duebeni* have traditionally been viewed as principally herbivorous shredders and detritivores (Cummins and Klug 1979). More recently, however, this has been dispelled as a myth generated by over-reliance on the rigid Functional Feeding Group classification system (MacNeil et al. 1997). The predatory nature of such species concurs with the accumulated evidence of gut contents analyses, anecdotal accounts of prey capture and consumption, studies of cannibalism and intraguild predation, and most recently, demonstration of a variety of direct and indirect predatory effects of *Gammarus* spp. on macroinvertebrates (see Kelly et al. 2002). In addition, isotope analyses place *D. villosus* on the same trophic level as some fish species (Marguillier 1998). Microcosm and mesocosm studies have concurred with field surveys that predation by native *Gammarus* spp. significantly influences community composition (Anderson and Raasveldt 1974; Conlan 1994; Wilhelm and Schindler 1999). Thus, invasions into naïve communities by exotic amphipods with exceptional predatory capabilities may have profound impacts on biodiversity. Such scenarios may mirror species extinctions, both locally and globally, of naïve indigenous prey exposed to invading vertebrate predators (e.g., Zaret and Paine 1973; Diamond and Case 1986; Schoener and Spiller 1996).

Further, the present experimental approach has characterized the proximate behavioural interactions of *D. villosus* with a range of macroinvertebrate species that are likely to result during invasion. Thus, several taxonomic and trophic groups of a variety of body sizes, shapes, and structural strengths fell prey to *D. villosus*. In addition, in microcosms, *D. villosus* appeared to often simply attack and injure victims, indicating that impacts on prey may not be limited by predator satiation. On the other hand, such bite victims were not often observed at the mesocosm level, perhaps because of the increased likelihood of complete consumption of victims by multiple *D. villosus* and other predators–scavengers in the mesocosms. Whereas Experiment 1 indicates that *D. villosus* is capable of preying effectively on many such macroinvertebrate groups, Experiment 2 indicates that communities may experience differential impacts on prey species. This may arise through prey selection by *D. villosus*, since predators should take prey that is easy to catch and handle before taking more difficult prey. Indeed, species like *N. integer*, which have fast escape responses, were only significantly impacted by *D. villosus* in single-species scenarios, whereas the slow-moving *A. aquaticus* was impacted in both single- and mixed-species scenarios. Thus, *D. villosus* may switch to more difficult prey when easy prey are not present or have been depleted. In addition, declines in one species will have cascading effects on others, such that some species may increase following *D. villosus* invasion. For example, the loss of predators due to *D. villosus*, as occurred with *I. elegans* in the present study, may lessen their predatory impact and release prey species. Thus, currently and in the future, predation by *D. villosus* may have direct impacts on macroinvertebrate communities, reducing abundance and distributions of species, although indirect effects may include increases in populations of some species. Overall, a

Fig. 3. Mean (+ standard error) survival of macroinvertebrates by day 3 in the mesocosm (multiple prey species) experiment, with no amphipod present (open bars), *Gammarus duebeni* present (hatched bars), and *Dikerogammarus villosus* present (cross-hatched bars). Differing letters (A,B,C) indicate significant differences among experimental groups at day 3. Cr, *Caenis robusta*; Aa, *Asellus aquaticus*; Ie(s), *Ischnura elegans* (small); Ni(l), *Neomysis integer* (large); Ie(l), *Ischnura elegans* (large); Pg, *Piscicola geometra*; S, *Sigara* sp; El, *Eurycercus lamellatus*; Chi, *Chironomus* sp; Ni(s), *Neomysis integer* (small); Cha, *Chaoborus* sp.

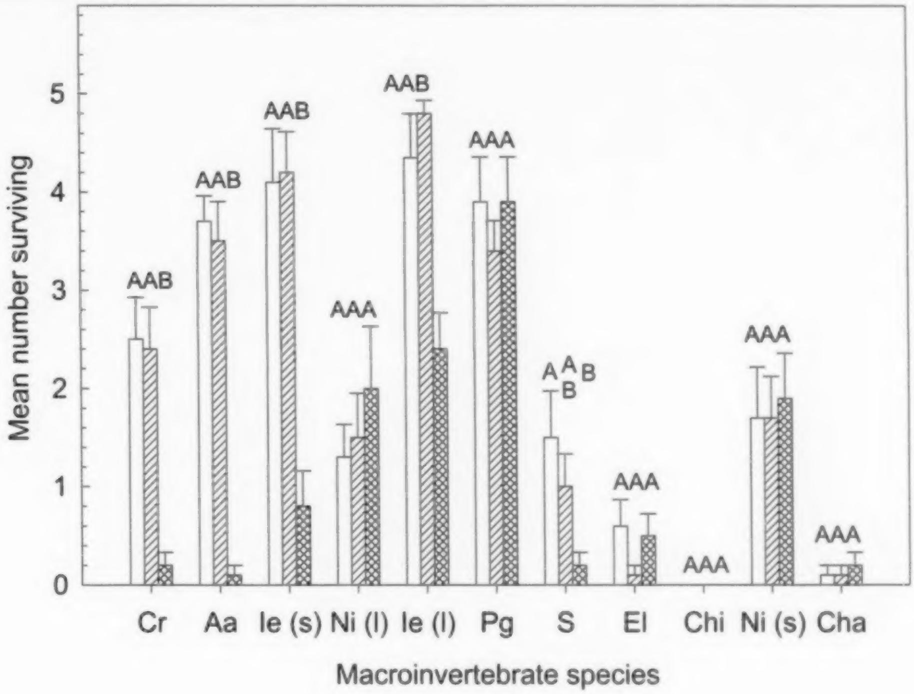

simplification of macroinvertebrate communities, in terms of species and trophic links, appears likely, a pattern that is emerging in the River Rhine (see van der Velde et al. 2000). This is a feature of other systems invaded by exceptional predators (e.g., Zaret and Paine 1973). Further, energy flow in invaded systems may be disrupted, such that higher trophic groups are affected. However, these aspects may only be addressed by monitoring pre- and post-*D. villosus* invasions in the field.

Although we used the same animal densities in our microcosm and mesocosm scales, larger experimental arenas have reduced edge effects, such that prey have more opportunity of escape from a particular predator and encounter rates may be reduced (see also Wilhelm et al. 2000). However, both of our experimental scales showed significant predation of macroinvertebrates in short time periods. This concurs with other studies whereby amphipod predation at small and intermediate laboratory scales, albeit of higher magnitude, has been shown to agree with large field scale enclosures and whole-lake patterns (Dick et al. 1999; Wilhelm and Schindler 1999; Wilhelm et al. 2000). In addition, the present experiments show that predation by the invader *D. villosus* is significantly greater than that of a native counterpart, *G. duebeni*. Thus, although laboratory enclosures may overestimate rates of predation in field situations, the relative predatory impact of *D. villosus* may be predicted to be profound in comparison to native counterparts, which themselves are likely to be replaced through predation by *D. villosus* (see Dick and Platvoet 2000).

With freshwater biodiversity over the next 100 years judged to be most influenced by species invasions (Sala et al. 2000), it is imperative that research focuses on explanations and predictions of the identities and impacts of new invaders. Such efforts must be both field and laboratory based, such that invasion patterns and the mechanisms of impacts can be linked. Such information may then be used in aquatic resource management strategies, such as the prevention and control of potentially damaging future invasions. In the present case, the clearly invasive nature of *D. villosus* and its impacts in freshwaters in Europe, in addition to its demonstrated predatory abilities, indicate this to be one such undesirable future invader.

Acknowledgements

We thank the British Council for initial financial support through their U.K.–Dutch Joint Scientific Research Programme. The University of Amsterdam also kindly provided two small research grants and David Kelly acknowledges funding from Department of Higher and Further Education, Training and Employment (DHFETE). We are grateful to Fred Schram, Rob van Soest, Ian Montgomery, Bob Elwood, Roberta Bailey, Calum MacNeil, and Ivan Ewart for a variety of helpful input.

References

Anderson, R.S., and Raasveldt, L.G. 1974. *Gammarus* predation and the possible effects of *Gammarus* and *Chaoborus* feeding on the zooplankton composition in some small lakes and ponds in western Canada. Can. Wildl. Serv. Occas. Pap. **18**: 1–23.

Bially, A., and MacIsaac, H.J. 2000. Fouling mussels (*Dreissena* spp.) colonize soft sediments in Lake Erie and facilitate benthic invertebrates. Freshwater Biol. **43**: 85–97.

Bruijs, M.C.M., Kelleher, B., van der Velde, G., and bij de Vaate, A. 2001. Oxygen consumption, temperature and salinity tolerance of the invasive amphipod *Dikerogammarus villosus*: indicators of further dispersal via ballast water transport. Arch. Hydrobiol. **152**: 633–646.

Conlan, K.E. 1994. Amphipod crustaceans and environmental disturbance: a review. J. Nat. Hist. **28**: 519–554.

Cummins, K.W., and Klug, M.J. 1979. Feeding ecology of stream invertebrates. Annu. Rev. Ecol. Syst. **10**: 147–172.

Devin, S., Beisel, J.N., Bachman, V., and Moreteau, J.C. 2001. *Dikerogammarus villosus* (Amphipoda: Gammaridae): another invasive species newly established in the Moselle river and French hydrosystems. Ann. Limnol. **37**: 21–27.

Diamond, J., and Case, T.J. 1986. Overview: introductions, extinctions, exterminations, and invasions. *In* Community ecology. *Edited by* J. Diamond and T.J. Case. Harper and Row, New York. pp. 65–79.

Dick, J.T.A., and Platvoet, D. 2000. Invading predatory crustacean *Dikerogammarus villosus* eliminates both native and exotic species. Proc. R. Soc. Lond. Ser. B Biol. Sci. **267**: 977–983.

Dick J.T.A., Montgomery, W.I., and Elwood, R.W. 1999. Intraguild predation may explain an amphipod replacement; evidence from laboratory populations. J. Zool. (London), **249**: 463–468.

Hall, S.R., and Mills, E.L. 2000. Exotic species in large lakes of the world. Aquat. Ecosyst. Health Manage. **3**: 105–135.

Holway, D.A., and Suarez, A.V. 1999. Animal behavior: an essential component of invasion biology. Trends Ecol. Evol. **14**: 328–330.

Huston, M.A. 1999. Microcosm experiments have limited relevance for community and ecosystem ecology: synthesis of comments. Ecology, **80**: 1088–1089.

Hynes, H.B.N. 1954. The ecology of *Gammarus duebeni* Lilljeborg and its occurrence in freshwater in western Britain. J. Anim. Ecol. **23**: 38–84.

Ioffe, I.I. 1973. Pool for acclimatization of invertebrates in U.S.S.R. Izv. Gos. Nauchno-Issled. Inst. Ozern. Rechn. Rybn. Khoz. **84**: 18–68.

Kelly, D.W., Dick, J.T.A., and Montgomery, W.I. 2002. Predation on mayfly nymph, *Baetis rhodani*, by native and introduced *Gammarus*: direct effects and the facilitation of salmonid predation. Freshwater Biol. **47**: 1257–1268.

Mack, R.N., Simberloff, D., Lonsdale, W.M., Evans, H., Clout, M., and Bazzaz, F.A. 2000. Biotic invasions: causes, epidemiology, global consequences, and control. Ecol. Appl. **10**: 689–710.

MacNeil, C., Dick, J.T.A., and Elwood, R.W. 1997. The trophic ecology of freshwater *Gammarus* (Crustacea: Amphipoda); problems and perspectives concerning the Functional Feeding Group concept. Biol. Rev. (Cambridge), **72**: 349–364.

Marguillier, S. 1998. Stable isotope ratios and food web structure of aquatic ecosystems. Thesis, Universiteit Brussel.

Mills, E.L., Leach, J.H., Carlton, J.T., and Secor, C.L. 1993. Exotic species in the Great Lakes: a history of biotic crises and anthropogenic introductions. J. Gt. Lakes Res. **19**: 1–54.

Musko, I. 1993. The life history of *Dikerogammarus haemobaphes* (EICHW.) (Crustacea; Amphipoda) living on macrophytes in Lake Balaton (Hungary). Arch. Hydrobiol. **127**: 227–238.

Peckarsky, B.L., Cooper, S.D., and McIntosh, A.R. 1997. Extrapolating from individual behaviour to populations and communities in streams. J. North Am. Benthol. Soc. **16**: 375–390.

Ricciardi, A. 2001. Facilitative interactions among aquatic invaders: is an "invasional meltdown" occurring in the Great Lakes? Can. J. Fish. Aquat. Sci. **58**: 2513–2525.

Ricciardi, A., and MacIsaac, H.J. 2000. Recent mass invasion of the North American Great Lakes by Ponto-Caspian species. Trends Ecol. Evol. **15**: 62–65.

Ricciardi, A., and Rasmussen, J.B. 1998. Predicting the identity and impact of future biological invaders: a priority for aquatic resource management. Can. J. Fish. Aquat. Sci. **55**: 1759–1765.

Sala, O.E., Chapin, F.S., Armesto, J.J., Berlow, E., Bloomfield, J., Dirzo, R., Huber-Sanwald, E., Huenneke, L.F., Jackson, R.B., Kinzig, A., Leemans, R., Lodge, D.M., Mooney, H.A., Oesterheld, M., Poff, N.L., Sykes, M.T., Walker, B.H., Walker, M., and Wall, D.H. 2000. Global biodiversity scenarios for the year 2100. Science (Washington, D.C.), **287**: 1770–1774.

Schoener, T.W., and Spiller, D.A. 1996. Devastation of prey diversity by experimentally introduced predators in the field. Nature (London), **381**: 691–694.

Simberloff, D., and Von Holle, B. 1999. Positive interactions of nonindigenous species: invasional meltdown? Biol. Invasions, **1**: 21–32.

Sokal, R.R., and Rohlf, F.J. 1995. Biometry. The principles and practice of statistics in biological research. 3rd ed. W.H. Freeman, New York.

Stewart, T.W., Miner, J.G., and Lowe, R.L. 1998. Macroinvertebrate communities on hard substrates in western lake Erie: structuring effects of *Dreissena*. J. Gt. Lakes Res. **24**: 868–879.

van der Velde, G., Rajagopal, S., Kelleher, B., Musko, I.B, and bij de Vaate, A. 2000. Ecological impact of crustacean invaders: general considerations and examples from the Rhine River. *In* The biodiversity crisis and Crustacea. Proceedings of the Fourth International Crustacean Congress. *Edited by* J.C. von Vaupel Klein, and F.R. Schram. Balkema, Rotterdam, The Netherlands. Crustac. Issues. Vol. 12. pp. 3–33.

Welton, J.S. 1979. Life-history and production of the amphipod *Gammarus pulex* in a Dorset chalk stream. Freshwater Biol. **9**: 263–275.

Wilhelm, F.M., and Schindler, D.W. 1999. Effects of *Gammarus lacustris* (Crustacea: Amphipoda) on plankton community structure in an alpine lake. Can. J. Fish. Aquat. Sci. **56**: 1401–1408.

Wilhelm, F.M., Schindler, D.W., and McNaught, A.S. 2000. The influence of experimental scale on estimating the predation rate of *Gammarus lacustris* (Crustacea: Amphipoda) on *Daphnia* in an alpine lake. J. Plankton Res. **22**: 1719–1734.

Zaret, T.M., and Paine, R.T. 1973. Species introductions in a tropical lake. Science (Washington, D.C.), **182**: 449–455.

Gerhard Herzberg An Illustrious Life in Science

by/par Boris Stoicheff

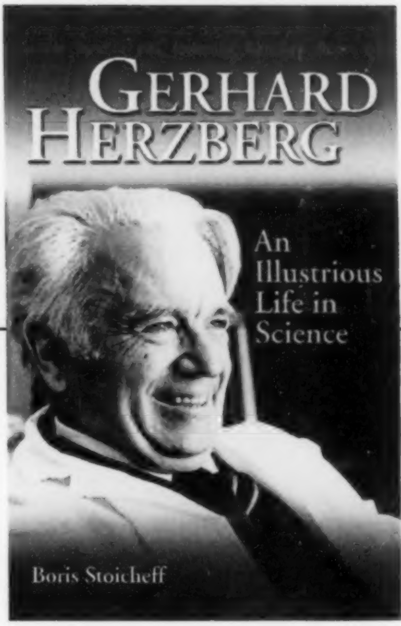

$49.95 CAN. Other countries $49.95 US
49,95 $CAN. À l'étranger 49,95 $US

Hardcover / Edition reliée
ISBN 0-660-18757-4
ISSN 1701-1833
NRC No./N° du CNRC 44462

An NRC Press Publication co-published with McGill-Queen's University Press/Une coédition des Presses du CNRC et McGill-Queen's University Press

Orders may be submitted by mail or fax to:
Les commandes peuvent être soumises par courrier ou par télécopieur à :

Order Office/Bureau des commandes

NRC Research Press/Presses scientifique du CNRC
National Research Council/Conseil national de recherches
Ottawa, ON K1A 0R6, Canada
Telephone/Téléphone : (613) 990-2254
Fax/Télécopieur : (613) 952-7656
E-mail: research.press@nrc.ca
Courriel : presses.scientifiques@cnrc.ca
Website: http://researchpress.nrc.ca
Site web : http://pressesscientifiques.cnrc.ca

PLEASE PRINT/LETTRES MOULÉES

☐ Payment enclosed / Paiement inclus ☐ Charge to/ Imputer à ☐ Visa ☐ MasterCard

Account no./N° de compte ☐☐☐☐☐☐☐☐☐☐☐☐☐☐☐☐ Expiry date/Date d'expiration ☐☐☐☐

Name/Nom
Signature
Address/Adresse
City/Ville Province
Postal code/Code postal Country/Pays
Telephone/Téléphone Fax/Télécopieur
E-mail/Courriel

Prepayment required unless order is accompanied by a purchase order number. Cheques or money orders should be made payable to: "Receiver General for Canada, Credit NRC". For all orders outside Canada, rates are in U.S. Dollars. All sales are final.
Les commandes doivent être payées d'avance à moins qu'elles ne soient accompagnées d'un numéro de bon de commandes. Les chèques ou mandats doivent être libellés au « Receveur générale du Canada, crédit du CNRC ». Toutes les vent sont finales.

Marine Protected Areas and Fisheries Closures in British Columbia

By/par Glen S. Jamieson and/et Joanne Lessard

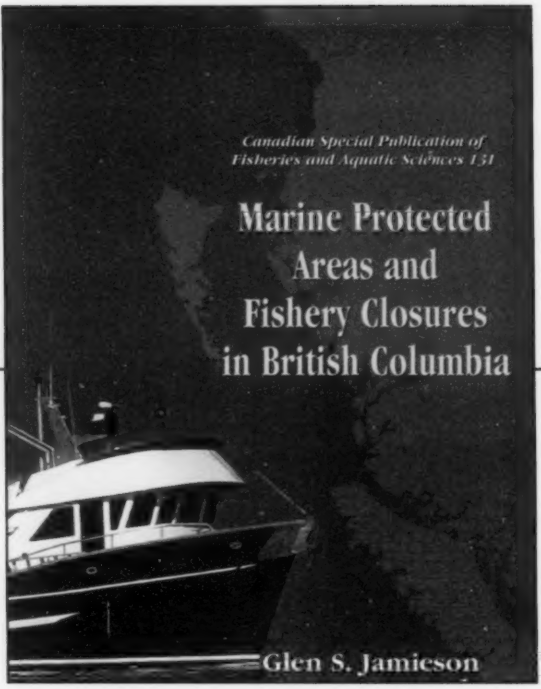
Canadian Special Publication of Fisheries and Aquatic Sciences 131
Marine Protected Areas and Fishery Closures in British Columbia
Glen S. Jamieson

$69.95/69,95 $

Other countries $69.95 US
À l'étranger 69,95 $US

Softcover / Edition brochée
414 pages
ISBN 0-660-17788-9 ISSN 0706-6481
NRC No./Nº du CNRC 42846
(Can. Spec. Publ. Fish. Aquat. Sci. No. 131)

Orders may be submitted by mail or fax to: Les commandes peuvent être soumises par courrier ou par télécopieur à :

Order Office/Bureau des commandes

NRC Research Press/Presses scientifique du CNRC
National Research Council/Conseil national de recherches
Ottawa, ON K1A 0R6, Canada
Telephone/Téléphone : (613) 990-2254
Fax/Télécopieur : (613) 952-7656
E-mail: research.press@nrc.ca
Courriel : presses.scientifiques@cnrc.ca
Website: http://researchpress.nrc.ca
Site web : http://pressesscientifiques.cnrc.ca

PLEASE PRINT/LETTRES MOULÉES

☐ Payment enclosed / Paiement inclus Charge to/ Imputer à ☐ Visa ☐ MasterCard ☐ AMEX

Account no./Nº de compte Expiry date/Date d'expiration

Name/Nom

Signature

Address/Adresse

City/Ville Province

Postal code/Code postal Country/Pays

Telephone/Téléphone Fax/Télécopieur

E-mail/courriel

Prepayment required unless order is accompanied by a purchase order number. Cheques or money orders should be made payable to : "Receiver General for Canada, Credit NRC". For all orders outside Canada, rates are in U.S. Dollars. All sales are final.
Les commandes doivent être payées d'avance à moins qu'elles ne soient accompagnées d'un numéro de bon de commande. Les chèques ou mandats doivent être libellés au « Receveur général du Canada, crédit du CNRC ». Toutes les ventes sont finales.

Culinary Herbs for Short-Season Gardeners

By/par Ernest Small and /et Grace Deutsch

Co-Published with/Co-édité par Ismant Peony Press

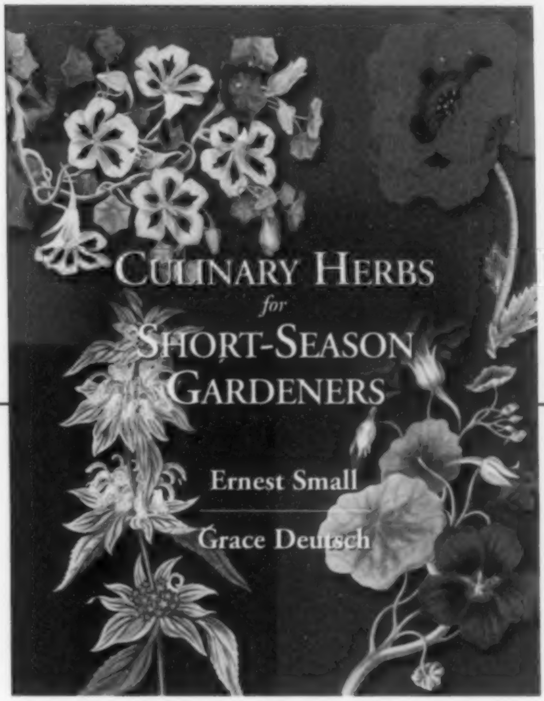

$24.95/24,95 $

Other countries $24.95 US
À l'étranger 24,95 $US

Softcover / Edition brochée
181 pages
ISBN 0-660-17785-4
NRC No./Nº du CNRC 42737

Orders may be submitted by mail or fax to: Les commandes peuvent être soumises par courrier ou par télécopieur à :

Order Office/Bureau des commandes

NRC Research Press/Presses scientifique du CNRC
National Research Council/Conseil national de recherches
Ottawa, ON K1A 0R6, Canada
Telephone/Téléphone : (613) 990-2254
Fax/Télécopieur : (613) 952-7656
E-mail: research.press@nrc.ca
Courriel : presses.scientifiques@cnrc.ca
Website: http://researchpress.nrc.ca
Site web : http://pressesscientifiques.cnrc.ca

PLEASE PRINT/LETTRES MOULÉES

☐ Payment enclosed / Paiement inclus — Charge to/ Imputer à ☐ Visa ☐ MasterCard ☐ AMEX

Account no./Nº de compte ☐☐☐☐☐☐☐☐☐☐☐☐☐☐☐☐ — Expiry date/Date d'expiration ☐☐☐☐

Name/Nom

Signature

Address/Adresse

City/Ville — Province

Postal code/Code postal — Country/Pays

Telephone/Téléphone — Fax/Télécopieur

E-mail/courriel

Prepayment required unless order is accompanied by a purchase order number. Cheques or money orders should be made payable to : "Receiver General for Canada, Credit NRC". For all orders outside Canada, rates are in U.S. Dollars. All sales are final.
Les commandes doivent être payées d'avance à moins qu'elles ne soient accompagnées d'un numéro de bon de commande. Les chèques ou mandats doivent être libellés au « Receveur général du Canada, crédit du CNRC ». Toutes les ventes sont finales.

The Canadian Conference for Fisheries Research

Ottawa, Ontario, Canada
2–5 January 2003

Where

Westin Hotel
11 Colonel By Drive, Ottawa, ON K1N 9H4
Telephone: 613-560-7000 or 800-WESTIN-1

Themes

1. Protecting Canada's aquatic resources (CCFFR/SCL)
2. Impact of invasive species (CCFFR/SCL)
3. Impacts of multiple stressor interactions on aquatic ecosystems (CCFFR/SCL)
4. Studies of aquatic biodiversity at a landscape scale (CCFFR)
5. Improvements in sampling methods (CCFFR)
6. Percid biology in a changing environment (CCFFR)

Call for papers

Abstracts in electronic form must be submitted to the program chair (jgunn@laurentian.nickel.ca) by 15 September 2002 (at the latest).

Funding

Graduate students may apply to the Clemens-Rigler Travel Fund.

Web site

For further information on the conference, registration details, program schedules, and updates, visit the CCFFR Web site (http://www. phys.ocean.dal.ca/ccffr/).

Note

The deadline for the special rate at the hotel is 3 December 2002. Early submission of abstract/poster for acceptance will ensure adequate time for hotel booking. To avoid CCFFR and SCL being charged an extra service fee, please plan to stay at the Westin Hotel while attending the conference.

La Conférences canadienne sur la recherche des pêches

Ottawa, Ontario, Canada
2 au 5 janvier 2003

Endroit

Westin Hotel
11 Colonel By Drive, Ottawa, ON K1N 9H4
Téléphone : 613-560-7000 ou 800-WESTIN-1

Thèmes

1. La protection des resources aquatiques (CCRP/SCL)
2. L'impacte des espèces non indigènes (CCRP/SCL)
3. L'impacte des stresses muliples sur les systèmes aquatiques (CCRP/SCL)
4. L'étude de la biodiversité aquatique au niveau du paysage (CCRP)
5. L'amélioration des méthodes d'échantillonege (CCRP)
6. La biologie des *Percidae* par rapport aux changements environmentaux (CCRP)

Appel pour contributions

Les résumés en format électronique doivent êtres soumis au directeur du programme (jgunn@laurentian.nickel.ca) par le 15 septembre 2002 (au dernier).

Financement

Les élèves aux études supérieures peuvent faire une demande de financement auprès des bourses de voyage Clemens-Rigler.

Site web

Pour obtenir de plus amples renseignements sur la conférence, l'inscription, l'horaire et les mises à jour, veuillez consulter le site Web de la CCRP (http://www.phys.ocean.dal.ca/ccffr/).

Nota

La date limite pour le taux spécial à l'hôtel est le 3 décembre 2002. Si l'abstrait / l'affiche est soumis à temps (avant le 15 septembre), et accepté, vous pourrez réserver une chambre à l'hôtel avant la date limite. Pour éviter que la CCRP et la SCL soient obligé de débourser des frais des services additionnels, essayez de réserver vos chambres à l'hôtel Westin.

Contents (concluded) / Table des matières (suite et fin)

J.A.E. van Oostenbrugge, E.J. Bakker, W.L.T. van Densen, M.A.M. Machiels, and P.A.M. van Zwieten **1032–1043** Characterizing catch variability in a multispecies fishery: implications for fishery management

Shelly M. Boss and John S. Richardson **1044–1053** Effects of food and cover on the growth, survival, and movement of cutthroat trout (*Oncorhynchus clarki*) in coastal streams

Richard McGarvey and John E. Feenstra **1054–1064** Estimating rates of fish movement from tag recoveries: conditioning by recapture

R.J. Kloser, T. Ryan, P. Sakov, A. Williams, and J.A. Koslow **1065–1077** Species identification in deep water using multiple acoustic frequencies

Jaimie T.A. Dick, Dirk Platvoet, and David W. Kelly **1078–1084** Predatory impact of the freshwater invader *Dikerogammarus villosus* (Crustacea: Amphipoda)

National Research Council Canada
Ottawa, Canada
K1A 0R6

Conseil national de recherches Canada
Ottawa, Canada
K1A 0R6

Postage paid at Ottawa
Publications mail
Registration No. 1240579

Port payé à Ottawa
Poste-publication
Enregistrement n° 1240579

USPS periodical postage paid at Champlain, N.Y.

Canadian Journal of Fisheries and Aquatic Sciences

Journal canadien des sciences halieutiques et aquatiques

Volume 59, Number 6, June 2002

Volume 59, numéro 6, juin 2002

---

iii Editorial / Éditorial

RAPID COMMUNICATION / COMMUNICATION RAPIDE

Brian P. Kennedy, Andrea Klaue, Joel D. Blum, Carol L. Folt, and Keith H. Nislow **925–929** Reconstructing the lives of fish using Sr isotopes in otoliths

ARTICLES / ARTICLES

Geneviève M. Carr and Antoine Morin **930–937** Sampling variability and the design of bacterial abundance and production studies in aquatic environments

Aline Philibert and Yves T. Prairie **938–951** Is the introduction of benthic species necessary for open-water chemical reconstruction in diatom-based transfer functions?

Lisa A. Eby and Larry B. Crowder **952–965** Hypoxia-based habitat compression in the Neuse River Estuary: context-dependent shifts in behavioral avoidance thresholds

Kristen D. Arkush, Alan R. Giese, Holly L. Mendonca, Anne M. McBride, Gary D. Marty, and Philip W. Hedrick **966–975** Resistance to three pathogens in the endangered winter-run chinook salmon (*Oncorhynchus tshawytscha*): effects of inbreeding and major histocompatibility complex genotypes

Geoff M. Laslett, J. Paige Eveson, and Tom Polacheck **976–986** A flexible maximum likelihood approach for fitting growth curves to tag–recapture data

Al Sosiak **987–1001** Long-term response of periphyton and macrophytes to reduced municipal nutrient loading to the Bow River (Alberta, Canada)

Arnaud Bertrand, Erwan Josse, Pascal Bach, Philippe Gros, and Laurent Dagorn **1002–1013** Hydrological and trophic characteristics of tuna habitat: consequences on tuna distribution and longline catchability

Richard A. Hinrichsen **1014–1023** The accuracy of alternative stochastic growth rate estimates for salmon populations

Mark V. Hoyer, Thomas K. Frazer, Sky K. Notestein, and Daniel E. Canfield, Jr. **1024–1031** Nutrient, chlorophyll, and water clarity relationships in Florida's nearshore coastal waters with comparisons to freshwater lakes

Continued on inside back cover / Suite au verso

Canada

Printed in Canada by / Imprimé au Canada par
University of Toronto Press Inc.
Typesetting by / Typographie par
NRC Research Press / Presses scientifiques du CNRC

0706-652X(200206)59:6;1-4